

Table of Content

TABLE OF CONTENT	ii
LIST OF FIGURES	i
LIST OF TABLES	19

2015 EXPEDITION REPORT	23
-------------------------------	-----------

PART I – OVERVIEW AND SYNOPSIS OF OPERATIONS	24
---	-----------

1 OVERVIEW OF THE 2015 ARCTICNET / AMUNDSEN EXPEDITION	24
1.1 Introduction	24
1.2 Regional settings	25
1.3 2015 Expedition Plan	27
2 LEG 1 – 17 APRIL TO 4 MAY 2015 – ST. LAWRENCE GULF AND ESTUARY AND LABRADOR SEA	30
2.1 Introduction	30
2.2 Synopsis of operations	31
2.3 Chief Scientist's comments	34
3 LEG 2 – 10 JULY TO 20 AUGUST 2015 – LABRADOR SEA, BAFFIN BAY AND THE CANADIAN ARCTIC ARCHIPELAGO	35
3.1 Introduction	35
3.2 Synopsis of Operations	36
3.3 Chief Scientist's comments	38
4 LEG 3A - 20 AUGUST TO 4 SEPTEMBER 2015 – AMUNDSEN GULF AND BEAUFORT SEA	39
4.1 Introduction	39
4.2 Synopsis of Operations	40
4.3 Chief Scientist's comments	42
5 LEG 3B – 4 SEPTEMBER TO 1 OCTOBER 2015 - AMUNDSEN GULF AND BEAUFORT SEA	43
5.1 Introduction	43
5.2 Synopsis of Operations	44
5.3 Chief Scientist's comments	45
6 LEG 4A – 1 TO 11 OCTOBER 2015 – THE CANADIAN ARCTIC ARCHIPELAGO AND BAFFIN BAY	46
6.1 Introduction	46
6.2 Synopsis of Operations	47
7 LEG 4B – 4C – 11 OCTOBER TO 1 NOVEMBER 2015 – BAFFIN BAY AND LABRADOR SEA	49
7.1 Introduction	49
7.2 Synopsis of Operations	51
7.3 Chief Scientist's comments	53

PART II – PROJECT REPORTS	55
----------------------------------	-----------

1 BIOGEOCHEMISTRY OF THE INORGANIC CARBON CYCLE, SURFACE CLIMATE, AIR-SURFACE FLUXES AND CARBON EXCHANGE DYNAMICS – LEGS 4A AND 4B	55
--	----

1.1	Introduction	55
1.2	Methodology	57
1.3	Preliminary results	58
<hr/>		
2	CHARACTERIZATION OF THE OCEAN-ICE-ATMOSPHERE SYSTEM – LEGS 1, 3A AND 3B	59
2.1	Introduction	59
2.2	Methodology – Upper atmosphere program	60
2.3	Methodology - Network of autonomous equipment	63
2.4	Preliminary results	70
2.5	Comments and recommendations	75
<hr/>		
3	AEROSOL SAMPLING: MEASUREMENT OF ATMOSPHERIC FLUXES OF TRACE ELEMENTS AND ISOTOPES (GEOTRACES) – LEGS 2 AND 3B	76
3.1	Introduction	76
3.2	Methodology	77
3.3	Preliminary results	81
3.4	Comments and recommendations	81
<hr/>		
4	BIOGEOCHEMICAL CYCLING OF METHANE – LEGS 2, 3A, 3B, 4A, 4B AND 4C	83
4.1	Introduction	83
4.2	Methodology	83
4.3	Preliminary results	85
<hr/>		
5	ICE CAMERA IMAGERY – LEG 1	88
5.1	Introduction	88
5.2	Methodology	88
5.3	Preliminary results	90
5.4	Comments and recommendations	90
<hr/>		
6	ICE ISLAND FIELD OPERATIONS – LEGS 1, 4A, 4B AND 4C	91
6.1	Introduction	91
6.2	Methodology	93
6.3	Preliminary results	99
6.4	Comments and recommendations	102
<hr/>		
7	AUV: DEPLOYMENT OF BIOARGO FLOATS IN BAFFIN BAY – LEGS 2 AND 4B	105
7.1	Introduction	105
7.2	Methodology	106
7.3	Preliminary results	107
7.4	Comments and recommendations	108
<hr/>		
8	MOORING PROGRAM – LEGS 3A AND 3B	109
8.1	Introduction	109
8.2	Methodology	110
8.3	Preliminary results	130
8.4	Comments and recommendations	131
<hr/>		
9	CTD-ROSETTE, LADCP AND UVP OPERATIONS – LEGS 2, 3A, 3B, 4A, 4B AND 4C	134
9.1	Introduction	134
9.2	Methodology – CTD-Rosette	134
9.3	Methodology – Lowered Acoustic Doppler Current Profiler (LADCP)	141
9.4	Preliminary results	141
9.5	Comments and recommendations	149
<hr/>		
10	XCTD (GEOTRACES) – LEG 2	150
10.1	Methodology	150
<hr/>		
11	TRACE METAL ROSETTE SAMPLING (GEOTRACES) – LEGS 2 AND 3B	151
11.1	Introduction	151

11.2 Methodology	152
11.3 Preliminary results	154
11.4 Comments and recommendations	157
<hr/>	
12 ²³⁰ Th, ²³¹ Pa, Nd AND CR ISOTOPES, AND REE (GEOTRACES) – LEGS 2 AND 3B	159
12.1 Introduction	159
12.2 Methodology	161
12.3 Preliminary results	169
<hr/>	
13 LARGE VOLUME <i>IN-SITU</i> OPERATIONS FOR PARTICULATE ²³⁰ Th, ²³¹ Pa, Nd ISOTOPES, CR ISOTOPES AND SI ISOTOPES (GEOTRACES) – LEGS 2 AND 3B	170
13.1 Introduction	170
13.2 Methodology	170
<hr/>	
14 ANTHROPOGENIC URANIUM, IODINE, AND CESIUM ANALYSIS IN THE ARCTIC OCEAN (GEOTRACES) – LEGS 2 AND 3B	173
14.1 Introduction	173
14.2 Methodology	173
14.3 Preliminary results	174
<hr/>	
15 NATURAL DISTRIBUTION OF STABLE N AND O ISOTOPES IN NITRATE (GEOTRACES) – LEG 2	175
15.1 Introduction	175
15.2 Methodology	176
<hr/>	
16 MEASUREMENT OF PH, ALKALINITY, $\delta^{13}\text{C}$ -DIC, $\delta^{18}\text{O}$ -WATER (GEOTRACES) – LEGS 2, 3A AND 3B	177
16.1 Introduction	177
16.2 Methodology	178
16.3 Comments and recommendations	180
<hr/>	
17 OCEAN CARBONATE CHEMISTRY AND BOUNDARY DISSOLVED INORGANIC CARBON, ALKALINITY, RADIUM ISOTOPES, AND DISSOLVED BARIUM (GEOTRACES) – LEGS 2 AND 3B	181
17.1 Introduction	181
17.2 Methodology	182
<hr/>	
18 ORGANIC CHEMISTRY OF THE BEAUFORT SEA AND ARCTIC ARCHIPELAGO (GEOTRACES) – LEGS 2 AND 3B	186
18.1 Introduction	186
18.2 Methodology	188
18.3 Preliminary results	196
18.4 Comments and recommendation	196
<hr/>	
19 RIVER SAMPLING (GEOTRACES) – LEG 2	197
19.1 Introduction	197
<hr/>	
20 MOVING VESSEL PROFILER AND CTD MESOSCALE AND MIXING SURVEY (GEOTRACES) – LEG 3B	199
20.1 Introduction	199
20.2 Methodology	200
20.3 Preliminary results	202
20.4 Comments and recommendations	203
<hr/>	
21 TURBULENT HEAT FLUXES AND DISSIPATION RATES IN THE BEAUFORT SEA – LEG 3A	205
21.1 Introduction	205
21.2 Methodology	206
21.3 Preliminary results	208
21.4 Comments and recommendations	208
<hr/>	
22 DISSOLVED GAS MEASUREMENTS (GEOTRACES) – LEG 2	209
22.1 Introduction	209

22.2 Methodology	210
22.3 Preliminary results	212
23 GENOMICS (GEOTRACES) – LEG 2	213
23.1 Methodology	213
24 MARINE PRODUCTIVITY: CARBON AND NUTRIENT FLUXES – LEGS 2, 3A, 3B, 4A, 4B AND 4C	214
24.1 Introduction	214
24.2 Methodology	215
24.3 Preliminary results – Leg 3a	218
24.4 Comments and recommendations	219
25 DISTRIBUTION AND BIODIVERSITY OF MICROORGANISMS – LEGS 3A, 4A, 4B AND 4C	220
25.1 Introduction	220
25.2 Methodology	221
25.3 Preliminary results	222
25.4 Comments and recommendations	222
26 TRACE METAL-PHYTOPLANKTON INTERACTIONS (GEOTRACES) – LEGS 2 AND 3B	223
26.1 Introduction	223
26.2 Methodology	224
27 BIOGENIC GASES, OCEAN ACIDIFICATION, PRIMARY PRODUCTION AND PHOTO-PHYSIOLOGY (GEOTRACES) – LEG 2	229
27.1 Introduction	229
27.2 Methodology	230
27.3 Preliminary results	231
27.4 Comments and recommendations	235
28 PHYTOPLANKTON PRODUCTION AND BIOMASS – LEGS 2, 3A, 4A AND 4B	236
28.1 Introduction	236
28.2 Methodology	237
28.3 Preliminary results	239
28.4 Comments and recommendations	241
29 PHYTOPLANKTON BLOOM DEVELOPMENT AND DMS PRODUCTION – LEG 2	243
29.1 Introduction	243
29.2 Methodology	243
29.3 Preliminary results	245
30 ZOOPLANKTON AND FISH ECOLOGY/ACOUSTIC – LEGS 2, 3A, 3B, 4A, 4B AND 4C	247
30.1 Introduction	247
30.2 Methodology	248
30.3 Preliminary results	251
31 CONTAMINANTS SAMPLING PROGRAM – LEGS 3A, 3B, 4A, 4B AND 4C	257
31.1 Introduction	257
31.2 Methodology	260
31.3 Preliminary results	269
31.4 Comments and recommendations	269
32 CONTAMINANTS SAMPLING PROGRAM (GEOTRACES) – LEGS 2 AND 3B	270
32.1 Introduction	270
32.2 Methodology	271
32.3 Preliminary results	273
32.4 Comments and recommendations	274
33 MARINE WILDLIFE MONITORING PROGRAM – LEG 3A	275
33.1 Methodology	275

34 SEABIRD SURVEY – LEG 4C	281	
34.1 Introduction		281
34.2 Methodology		281
34.3 Preliminary results		281
35 SEAFLOOR MAPPING, WATER COLUMN IMAGING AND SUB-BOTTOM PROFILING – LEGS 1, 2, 3A, 3B, 4A, 4B AND 4C	284	
35.1 Introduction		284
35.2 Methodology		286
35.3 Preliminary results (Leg1)		297
35.4 Preliminary results (Leg 4)		302
35.5 Comments and recommendations		313
36 BENTHIC DIVERSITY AND FUNCTIONING ACROSS THE CANADIAN ARCTIC – LEGS 3A, 3B, 4A, 4B AND 4C	315	
36.1 Introduction		315
36.2 Methodology		316
36.3 Preliminary results		320
36.4 Comments and recommendations		321
37 BENTHIC LANDER DEPLOYMENT – LEG 4B	322	
37.1 Introduction		322
37.2 Methodology		322
38 ROV CORAL AND SPONGE DIVES IN EASTERN BAFFIN BAY – LEG 4B	324	
38.1 Introduction		324
38.2 Methodology		325
38.3 Preliminary results		328
38.4 Comments and recommendations		343
39 STRATIGRAPHIC SURVEY – LEGS 4B AND 4C	345	
39.1 Introduction		345
39.2 Methodology		346
39.3 Preliminary results		346
40 GSC SEABED INSTRUMENTED LANDERS – LEG 3A	347	
40.1 Introduction		347
40.2 Methodology		349
40.3 Preliminary results		361
41 GSC PISTON CORING: GEOHAZARD AND REGIONAL GEOLOGY STUDIES – LEG 4B	367	
41.1 Introduction		367
41.2 Methodology		367
41.3 Preliminary results		369
41.4 Comments and recommendations		370
42 SEDIMENT SAMPLING – LEGS 4A, 4B AND 4C	371	
42.1 Introduction		371
42.2 Methodology		371
42.3 Comments and recommendations		372
43 PISTON CORING OF SHORELINE FEATURES – LEG 4B	373	
43.1 Introduction		373
43.2 Methodology		374
43.3 Preliminary results		374
44 SCHOOLS ON BOARD – LEG 4A	375	
44.1 Introduction		375

APPENDIX 1 – LIST OF STATIONS SAMPLED DURING THE 2014 ARCTICNET / <i>AMUNDSEN</i> EXPEDITION.....	370
APPENDIX 2 – SCIENTIFIC LOG OF THE 2014 ARCTICNET / <i>AMUNDSEN</i> EXPEDITION.....	375
APPENDIX 3 – CTD LOGBOOK OF THE 2014 ARCTICNET / <i>AMUNDSEN</i> EXPEDITION.....	407
APPENDIX 4 - LIST OF PARTICIPANTS OF THE 2014 ARCTICNET / <i>AMUNDSEN</i> EXPEDITION..	416

List of figures

Part I – Overview and synopsis of operations

Figure 2-1: Ship track and the location of stations sampled in the St. Lawrence Gulf and Estuary and in the Labrador Sea during Leg 1.....	30
Figure 3-1: Ship track and the location of stations sampled in Labrador Sea, Baffin Bay and the Canadian Arctic Archipelago during Leg 2.	35
Figure 3-2. Proposed cruise track for the 2015 CCGS <i>Amundsen</i> Expedition - Leg 2. Stations that had to be cancelled as a result of spending two weeks in Hudson Bay for escort duty are circled.	38
Figure 4-1: Ship track and the location of stations sampled in the Amundsen Gulf and Beaufort Sea during Leg 3a.....	39
Figure 5-1: Ship track and the location of stations sampled in the Amundsen Gulf and Beaufort Sea during Leg 3b.....	43
Figure 6-1. Ship track and the location of stations sampled in the Canadian Arctic Archipelago and Baffin Bay during Leg 4a.	46
Figure 7-1: Ship track and the location of stations sampled in Baffin Bay and in the Labrador Sea during Legs 4b and 4c.	50

Part II – Project reports

Figure 2-1: Ship track and the location of stations sampled in the St. Lawrence Gulf and Estuary and in the Labrador Sea during Leg 1.....	30
Figure 3-1: Ship track and the location of stations sampled in Labrador Sea, Baffin Bay and the Canadian Arctic Archipelago during Leg 2.	35
Figure 3-2. Proposed cruise track for the 2015 CCGS <i>Amundsen</i> Expedition - Leg 2. Stations that had to be cancelled as a result of spending two weeks in Hudson Bay for escort duty are circled.	38
Figure 4-1: Ship track and the location of stations sampled in the Amundsen Gulf and Beaufort Sea during Leg 3a.....	39
Figure 5-1: Ship track and the location of stations sampled in the Amundsen Gulf and Beaufort Sea during Leg 3b.....	43
Figure 6-1. Ship track and the location of stations sampled in the Canadian Arctic Archipelago and Baffin Bay during Leg 4a.	46
Figure 7-1: Ship track and the location of stations sampled in Baffin Bay and in the Labrador Sea during Legs 4b and 4c.	50
Figure 2-1. Ocean-Sea Ice-Atmosphere sampling methods during Legs 1 (upper schematic) and 3 (lower schematic).	64
Figure 2-2. The deployment of the first on ice tower via the ship.	65
Figure 2-3. Deployment of the POPS buoys.....	69
Figure 2-4. Wind speed and direction during Leg 1.....	70

Figure 2-5. Air temperature, sea surface temperature, dew point temperature and atmospheric pressure.	71
Figure 2-6. Photosynthetically active radiation (PAR), short-wave and long-wave irradiance.	72
Figure 2-7. Temperature of the ice core.	73
Figure 2-8. The air temperature, pressure and relative humidity data from the on ice met tower #8 deployed on September 9th, 2015.	73
Figure 2-9. Wind direction (red) and wind speed (green) from station #8 deployed on September 9th, 2015.	74
Figure 2-10. The trajectory from September 22 nd to September 29 th of 5 beacons deployed in the Beaufort Sea.	74
Figure 2-11. Temperature profile of the ice core taken in Penny Strait.	74
Figure 3-1. The PVC adapter plate that holds 12 – 47mm filter holders	77
Figure 3-2. The aerosol sampling locations and route in the Canadian Basin and the Canadian Arctic Archipelago during Leg 3b	78
Figure 3-3. The TISCH volume flow controlled (VFC) high volume aerosol sampler deployed on the bridge deck of the CCGS <i>Amundsen</i> during Leg 3b from September – October, 2015 (left). The anemometer, which is attached to the aerosol sampler through CR10 datalogger (right).	80
Figure 4-1. Surface water sampling (left) and samples analysis (right).	84
Figure 4-2. Locations of the sampling stations for dark incubation during Leg 3.	85
Figure 4-3. <i>In-situ</i> CH ₄ concentration in M'Clure Strait during Leg 3.	86
Figure 4-4. <i>In-situ</i> CH ₄ concentration in Queen Maud Gulf of the Canadian Archipelago during Leg 3.	86
Figure 4-5. Methane concentration vs. depth at Station 170 near Scott Inlet.	87
Figure 4-6. Methane concentration vs. depth at Station 180 near the Broughton Island.	87
Figure 5-1. Image taken at 12z on Apr 30, 2015 at 50.54N, 58.39W. It is a jpeg image (590 kB at full resolution) that provides a 45-degree view.	89
Figure 6-1. Ice island PII-A-1-f as imaged by Sentinel-1 (European Space Agency).	96
Figure 6-2. Ice penetrating radar (foreground), meteorological station (background) and row of ablation stakes between.	98
Figure 6-3. (Clockwise from top-left): Photogrammetry survey of Station 1 (wedge iceberg) after processing in Agisoft Photoscan; sidewall laser scan survey of Station 3 (small tabular iceberg); laser scan survey of the CCGS <i>Amundsen</i> illustrating the ship's drift during data collection; multi-beam keel survey data of Station 4 (saddle iceberg).	100
Figure 6-4. Image taken by the CC5MPX camera on the meteorological station showing the stripped ablation stakes and ice penetrating radar system.	101
Figure 6-5. Sample radargram from the ice penetrating radar on 22 October. The airwave is first and the bed-wave is second at approximately 170 ns (Time).	102
Figure 7-1. Deployment from the <i>Amundsen's</i> A-frame.	106
Figure 7-2. Argo float deployed.	107

Figure 7-3. Data recorded by the BioArgo float takapm003c during a test profile on 22 October (Leg 4b).....	108
Figure 8-1. Mooring locations 2014-2015-2016: BREA-iBO-ArcticNet mooring arrays.....	111
Figure 8-2. Mooring designs BS1-14, BS2-14 and BS3-13 recovered in southern Beaufort Sea during Leg 3a.....	115
Figure 8-3. Tilt and rotate calibration jig / table as utilized in Inuvik, NWT	118
Figure 8-4. Nortek ADCP Compass Verification Curve (Inuvik, Sept, 2015).....	120
Figure 8-5. ArcticNet Dragging Anchor for BS1-14.....	125
Figure 8-6. Triangulation plot from BS1-14 using Art's Acoustic Survey Matlab Script.....	129
Figure 8-7. Multibeam imagery identifying orientation and instrument depths (screenshot courtesy of ArcticNet multibeam processing team).	130
Figure 8-8. Rosette Temperature - Salinity Profile example plot (BS2-14).	130
Figure 8-9. BS2-14 CTD plot from the SBE37 moored at 152 db (162m) showing the large lay-over event on March 2 2014 (ice berg keel).	131
Figure 9-1. Top view of the SBE32 with 24x 12L Niskin bottles used on the <i>Amundsen</i> (left) and bottom view of the SBE32 showing the SBE9 CTD including additional sensors and the RDI LADCP (right). Photos: Jessy Barrette.	134
Figure 9-2. ArcticNet/GEOTRACES study region in the eastern Canadian Arctic for Leg 2.	135
Figure 9-3. ArcticNet study region in the Western Canadian Arctic, Legs 3a and b.....	135
Figure 9-4. ArcticNet study region in the eastern Canadian Arctic for Leg 4.....	136
Figure 9-5. Example of a calibration curve (left) and photo of the bottles used to collect water samples to measure salinity (right).	138
Figure 9-6. Example of oxygen calibration curve (left) and photo of the bottles used to collect water samples to measure oxygen (bottom right).	139
Figure 9-7. RDI LADCP mounted on the bottom of the SBE32 carousel on the <i>Amundsen</i>	141
Figure 9-8. Example of vertical structure (temperature and salinity – left; nitrate and fluorescence – right) for Cast 006.....	142
Figure 9-9. Evolution of the main parameters along the transect “Lancaster Sound’.....	142
Figure 9-10. Example of current velocities for the Cast 015 recorded by the LADCP.....	143
Figure 9-11. CTD casts location for Leg 3a and the beginning of 3b.	143
Figure 9-12. Example of the vertical structure (temperature and salinity – left; nitrate and fluorescence – right) for the cast 051.	144
Figure 9-13. Evolution of the main parameters along the transect “Lancaster Sound’.....	144
Figure 9-14. Example of current velocities for the cast 051 recorded by the LADCP.	145
Figure 9-15. CTD casts location for Leg 4a and the beginning of 4b.	146
Figure 9-16. Example of the vertical structure (temperature and salinity – upper graph; nitrate and fluorescence – lower graph) for the Cast 025.....	147
Figure 9-17. Evolution of the main parameters along the transect “Northern Baffin Bay” ..	147
Figure 9-18. Example of current velocities for the Cast 025 recorded by the LADCP.....	148

Figure 110-1. Map of XCTD locations along the Geotraces 2015 (Leg 2) cruise track from the Labrador Sea shelf to the Canadian Arctic Archipelago. Inset plot (red hatched lines): high resolution shelf section towards Clyde River.....	150
Figure 11-1. Location of stations where the Trace Metal Rosette was deployed on Leg 2.....	153
Figure 11-2. Sampled stations during the Canadian Arctic GEOTRACES 2015 Expedition during Leg 3b.....	154
Figure 11-3. Depth versus dissolved Zn concentration for Station BB3. Preliminary results with some indication of contamination in outlying data points.	155
Figure 12-1. Arrangement of the on-board lab bench area. Ropes hold the 20 L jerricans below the bench. On the bench, 3 samples stand in milkcrates for settling of the iron co-precipitate, in the 20 L cubitainers.....	163
Figure 19-1. Map of river sampling locations along the GEOTRACES Leg 2 cruise track through the Canadian Arctic Archipelago.	197
Figure 19-2. (Left) Roger Francois sampling from the Meham River, Cornwallis Island; (Right) Roger Francois and pilot Martin Dufor at the Tree River.	198
Figure 20-1. Bathymetry of the region studied with the moving vessel profiler (left) and MVP tracks and CTD stations during intensive sampling (right).	200
Figure 20-2. Schematic diagram of the operation of the moving vessel profiler. A 10kt boat speed, which gives approximate spacing of 1km between casts, allows observation of finescale oceanographic processes spanning distances on the order of tens to hundreds of kilometres. Oceanographic data are continuously recorded, with the freefall component being picked out during post-processing.	200
Figure 20-3. (a) Temperature (colours) and density (contours) from a long-section along Wellington Channel, through Maury Channel, and ending in Queens Channel. Note the longer mode-1 waves at approximately 0–80km. (b) Enlarged version of (a) showing the shallow area of Maury Channel and the presence of shorter internal waves, which result from flow over the rough, shallow seafloor. (c) Transect location. (d) Temperature– salinity diagram, with colours denoting distance as in panels (a) and (b).....	202
Figure 20-4. (a) Temperature (colours) and density (contours) from a cross-section across southern Wellington Channel (into the page is northward). Distances increase from a starting point not far from the eastern boundary of the channel. (b) Enlarged version of (a) showing clearly the wedge-like feature that is a buoyant coastal current enlarged in the bottom panel. (c) Transect location. (d) Temperature–salinity diagram, with colours denoting distance as in panels (a) and (b).....	203
Figure 21-1. Plot of the potential density measured by the glider over the course of the operations.	207
Figure 21-2. Approximate transects covered by the glider, as well as examples of the depth profiles and a sub-sampled temperature field from the glider CTD.	208
Figure 22-1. Preliminary oxygen concentration profiles from the 12 stations during Leg 2.	212

Figure 24-1. Cross-section of the nutrients from Station 437 (left) to Station 420 (right) during Leg 3a.	218
Figure 27-1. Spatial distribution of hydrographic parameters and biogenic gases along the cruise track. Note that horizontal lines on the $p\text{CO}_2$ and $\Delta\text{O}_2/\text{Ar}$ plots represent atmospheric saturation values. Note also that the data presented here have only received a very preliminary quality control, and do not necessarily represent the final processed values.	231
Figure 27-2. Spatial distribution of gases and hydrographic properties along the cruise track.	232
Figure 27-3. Continuous underway measurements of photoplankton photo-physiological properties were measured using fast repetition rate fluorometry (FRRF). The bottom panel shows surface irradiance cycles, while other panels show a range of other photo-physiological characteristics of surface water phytoplankton. For example, variable fluorescence (F_v/F_m), is used as a measure of the photosynthetic efficiency of electron capture in Photosystem II (PSII). This variable is often down-regulated during mid-day periods of high irradiance as a means of photo-protection. The variables P_{max} and Alpha represent the maximum (light saturated) electron transport rates and initial light-dependent slopes derived from rapid light curves.	233
Figure 27-4. Rates of gross primary productivity determined from ^{14}C bottle assays (left hand panels), and from FRRF measurements of electron transport rates (ETR). Results are from Station K1 in the southern Labrador Sea. The curves show a characteristic saturation behavior as a function of irradiance. Bottom panels show data from the deep chlorophyll max, while top panels show results from the surface mixed layer assemblages (7.5 m sampling depth). Compilation of our productivity measurements from all stations will provide valuable information on primary productivity in Arctic waters, and its light-dependency.	234
Figure 27-5. Time course of phytoplankton biomass (chlorophyll <i>a</i>) in the first CO_2 - light incubation experiment. LL and HL represent low and high light treatments, respectively, while the numbers refer to the CO_2 level (in ppm) used for each treatment. In this first experiment, we observed an initial decrease in growth rates of the high light treatment, with only a small CO_2 effect. We have a suite of other physiological and biochemical measurements that will help to understand the mechanisms underlying these responses.	234
Figure 27-6. As for Fig. 5.1.10.5, but for the second incubation experiment. In this experiment (water collected near Station BB3), no significant effects across the light or CO_2 treatments were observed.	235
Figure 28-1. Chlorophyll <i>a</i> concentrations integrated over 100 m for different size fractions, 0.7-5 μm , 5-20 μm and > 20 μm , in the Labrador Sea and southern Baffin Bay.	239
Figure 28-2. Chlorophyll <i>a</i> concentrations integrated over 100 m for different size fractions, 0.7-5 μm , 5-20 μm and > 20 μm , in Lancaster Sound, Barrow Strait and Peel Sound.	240

Figure 28-3: Chlorophyll a concentrations integrated over 100 m for different size fractions, 0.7-5 μm , 5-20 μm and > 20 μm , at all stations sampled during Leg 3a.....	240
Figure 28-4. Chlorophyll a concentrations integrated over 100 m for different size fractions, 0.7-5 μm , 5-20 μm and > 20 μm , in the Lancaster Sound and southern Baffin Bay.....	241
Figure 30-1. Flow indicated by flowmeters installed on the Double Square Net 1) in front of the 500 μm -mesh net, 2) in front of the 750 μm -mesh net, and 3) between the nets; and number of Arctic cod larvae collected by each net at each station.....	252
Figure 31-1. The 5-net vertical zooplankton sampler with LOKI (Monster net). Photo: Jessy Barrette 2013 ArcticNet Leg 1a.	260
Figure 31-2. Benthic invertebrates that were collected from the Agassiz trawl on 3 October 2015 at Station 304.....	261
Figure 31-3. SPMD cage installed on ArcticNet mooring BS-3.	268
Figure 31-4. SPMD cage installed on the line on BREA mooring BR-3.	268
Figure 32-1. Vertical distribution of total mercury in Station K1.....	273
Figure 34-1. Density of bird species observed during surveys from the CCG <i>Amundsen</i> during Leg 4c.	283
Figure 35-1. Example of periodical port side beam loss on data.....	287
Figure 35-2. Example of the data acquired in deep water conditions.....	288
Figure 35-3. Degradation of the Error Estimates Std Deviation due to correction signal loss.....	290
Figure 35-4. SIS water Column display of Mooring site BR-G before recovery. The red circle shows the buoys.....	292
Figure 35-5. Mooring BR-G added to bathymetry (purple dots) in CARIS HIPS&SIPS processing software. The exact position of the mooring is given in the lower right corner.....	292
Figure 35-6. Example of background files imported in SIS.....	293
Figure 35-7. Geographical display in SIS showing the navigation route taken to increase the bathymetric coverage; to fill the hole between two previous lines.....	293
Figure 35-8. (Left) GSC Lander; (Right) Water column display to visualize the deployment of the lander. The bright scattering in the middle of the water column. ...	294
Figure 35-9. Sound velocity profiles taken during Leg 1. From left to right: MVP transects 1501001, 1501002 and 1501003.	295
Figure 35-10. Example of the data acquire during the first MVP transect.	296
Figure 35-11. Preliminary results of the Iceberg Station 4 mapping on the barge. A) 3D point cloud view. Note that the attitude and displacement of the iceberg is not accounted for in the data. This is why the data does not match. B) First survey line of the barge around the iceberg. Yellow line shows the cross-section profile displayed in (C).....	297
Figure 35-12. Same as Figure 35.11, but with a different perspective.	298
Figure 35-13. Water Column display of A) Mooring site 1, B) Mooring site 2 and C-D) Mooring site 3.	299
Figure 35-14. Multibeam bathymetry coverage of the Natashquan delta night survey. ...	300

Figure 35-15. Example of backscatter data of the <i>Amundsen's</i> EM302 showing non-uniform level response of the transmission sectors.....	301
Figure 35-16. Graphical display of the differences in the level response of the four different transmission sectors of the EM302.....	301
Figure 35-17. Bathymetric data collected in Eclipse Sound and Navy Board Inlet during Leg 4.	302
Figure 35-18. Crescent-shaped bedforms observed in Navy Board Inlet.....	303
Figure 35-19. Location of CASQ1 site and associated bathymetric data.	303
Figure 35-20. Location of CASQ 2 site and associated bathymetric data.	304
Figure 35-21. Location of CASQ3 (AMD15-CQ3) in a sediment-filled basin in between two megascale glacial lineation in Scott Trough.....	304
Figure 35-22. Location of CASQ 4 and associated bathymetric data.....	305
Figure 35-23. New bathymetric data acquired in the Scott Inlet-Sam Ford Fjord area during Leg 4b. Positions of CASQ core-3 (AMD15-CQ3) and piston core LGM-AMU15-01 are shown by yellow dots.	306
Figure 35-24. Sam Ford Fjord bathymetry showing a grounding-line and a sediment-filled basin near the LGM-AMU15-01 piston core site. Seismic line 0026_2015_289_1015.sgy is shown by the the black line.	307
Figure 35-25. Seismic profile in Sam Ford Fjord showing the grounding-line, and a basin filled with at least 45-50 m of sediments.	307
Figure 35-26. Submerged delta/sandur at the head of Walker Arm (Sam Ford Fjord). Bathymetry shows a well-defined channel with what looks like terraces or maybe mass movement scars.	308
Figure 35-27. Bathymetry of Hecla and Gripper Trough showing mega-scale glacial lineations, mass movement scars and sediment-filled bassins.	308
Figure 35-28. Preliminary surface generated for Sam Ford Fjord ROV dive.....	309
Figure 35-29. Preliminary surface generated for Cade Dyer ROV dive.	310
Figure 35-30. Improved method for iceberg mapping and complete 3D model using combined LiDAR/photogrammetry and bathymetry project development.	312
Figure 36-1. Box core deployment and sediment cores sampling.....	316
Figure 36-2. Isotope tracing experiment set-up in the temperature controlled room and slicing of sediment cores after finishing the experiment.	317
Figure 36-3. Agassiz trawl deployment and identification of the specimens.	319
Figure 37-1. Multibeam survey of the lander deployment site (Station 177).	322
Figure 38-1. ROV dive locations for the 2015 CCGS <i>Amundsen</i> expedition. The Pond Inlet ROV dive was cancelled and replaced with the Qikiqtarjuaq dive.....	326
Figure 38-2. The SuMo ROV and the new elevator system. A) ROV and elevator, B) overall view of the elevator in the water (Scott Inlet, ~533 m), C) close-up of boxes, with a sample of the carnivorous sponge <i>Cladorhiza</i> sp. in the right arm.	327
Figure 38-3. Overview of the Navy Board ROV dive location, showing planned and accomplished ROV transect. Transect terminated early due to ROV electrical failure (see text) (left). Temperature profile at the Navy Board ROV dive site. This	

plot was generated at Ocean Data View, as the original plots from the Rosette were not available for this cast (right)..... 329

Figure 38-4. Organisms and bottom types observed during the ROV dive at Navy Board Inlet. A) Cladorhiza sp., B) Nephtheid soft coral, C) Gorgonocephalus sp. with sea tadpole, D) whelk, E) Desmospongia, F) Sea urchins and unidentified red organism, G) crinoid, H) unidentified sea cucumber and brittle stars..... 330

Figure 38-5. Overview of the Scott Inlet ROV dive location, showing surveyed area and position of the elevator (star). 331

Figure 38-6. Temperature and salinity profiles at the Scott Inlet ROV dive site. 332

Figure 38-7. Organisms and bottom types observed during the ROV dive at Scott Inlet. A) Sampling of Chondrocladia sp., B) sampling of Cladorhiza sp., C) Cladorhiza sp. sample being brought to the elevator, D) Cladorhiza sp. being put in the box, E) Chondrocladia sp., F) fan sponge, G) Polymastia sp., H) Umbellula encrinus. 333

Figure 38-8. Overview of the ROV dive near Qikiqtarjuaq, showing planned and accomplished ROV transect. 334

Figure 38-9. Temperature and salinity profiles near the Qikiqtarjuaq ROV dive site (Station 177, ~4 km from the dive site). 335

Figure 38-10. Organisms and bottom types observed during the ROV dive near Qikiqtarjuaq. A) sea anemones and unidentified white tubes, B) cluster of sea anemones, C) Gorgonocephalus sp., D) sea anemone and an stipitate sponge, E) cluster of crinoids on outcrop, F) eel-pout below curved sea anemone, G) Umbellula encrinus, H) diversity of sponges and other invertebrates, I) sea anemones and ascidian, J) ctenophore. Red lasers are 10 cm apart. 336

Figure 38-11. Overview of the ROV dive at Cape Dyer, showing planned and accomplished ROV transect, and trawl path. Transect terminated early due to ROV mechanical failure complicated by rough seas (see text)..... 337

Figure 38-12. Temperature and salinity profiles at the Cape Dyer ROV dive site..... 338

Figure 38-13. Organisms and bottom types observed during the ROV dive at Cape Dyer. A-E) diversity of sponges, F) nephtheid soft corals and octopus, G) solitary hydrozoan *Corymorpha* cf. *glacialis*, H) rockling (left) and turbot (right). Red lasers are 10 cm apart..... 339

Figure 38-14. Overview of the ROV dive at Frobisher Bay, showing planned and accomplished ROV transect. 340

Figure 38-15. Temperature and salinity profiles near the Frobisher Bay ROV dive site. ... 341

Figure 38-16. Organisms and bottom types observed during the ROV dive at Frobisher Bay. A) isopod with juveniles, B) crinoids, C) sponges, crinoids and kelp, D) large yellow sponge, E) crinoids, F-G) ascidians and sponges, H) large isopod, I-J) sponge gardens (mostly the fan sponge). Red lasers are 10 cm apart..... 342

Figure 40-1. Distribution of a shelf-break band of glacial sediment erosion (Panel A). The erosion origin and age is largely unknown. Typically, several metres of the glacial plume-deposited muds were removed but at the Mackenzie Trough mouth this exceeds 40 m (Panel B). It may be the manifestation of a catastrophic event related to glacial outburst flooding. Alternatively, oceanographic current erosion,

either modern or time-transgressive, beginning with sea-level low-stand processes. The lander deployments can address this by establishing present seabed conditions. Further understanding of this erosion phenomenon and the adjacent post-glacial mud distribution also has implications for Holocene age Mackenzie River sediment fate and the question of submarine avalanche ages. 348

Figure 40-2. Instrumented Lander configuration aboard CCGS *Amundsen* on the 2015 expedition. The “shallow” (shelf) lander (GSC Stn. 2015804-0002) in the foreground (left) differs from the “deep” (GSC Stn. 2015804-0004) only in the later generation of the MAVS (4-D) and the plate-mounted Seabird Microcat CTD compared with a MAVS 3-D and a leg-pole-mounted RBR CT (background). 350

Figure 40-3. Cartoon of Lander configuration at the seabed. 351

Figure 40-4. Instrumented Lander locations on the central Beaufort shelf-upper slope. Bathymetric contours shown on the multibeam bathymetric image. Placement is within the narrow contour-parallel zone of mud erosion shown in the previous illustration. Lander siting in the context of seismic profiles is shown in a following figure located along the thick brown line. An *Amundsen* 2015 - deployed water column oceanographic mooring site, BR-K, is also shown. Lander sites in Panels A and B are shown with greater detail in the following figure. 354

Figure 40-5. Close-up maps of Instrumented Lander locations. Subtle lines are existing 3.5 kHz sub-bottom profiler acquisitions from ArcticNet cruises. Heavier brown line is the *Amundsen* 2015 track. Panel A highlights a high-resolution Autonomous Underwater Vehicle (AUV) multibeam bathymetry rendering (courtesy C. Paull, Monterey Bay Aquarium Research Institute, MBARI). This depicts local net mud deposition (smooth) surrounding and locally overlying pingo-like features (PLFs). Placement is in “freestream” between the PLFs but locally the mounds have directed sedimentation pattern, including comet-like heads and tails manifesting the net easterly flow of the Jet. Panel B shows the much simpler topography of the uppermost slope. Anchor, CTD and box core site also shown. 355

Figure 40-6. Instrumented lander locations projected on the nearest 3.5 kHz sub-bottom profile. Profile locations in the overview map (two figures previous). 356

Figure 40-7. Multibeam acquisition screen during the shallow lander deployment. The lander is visible in the mid-water column. 357

Figure 40-8. CTD and LADCP plots from nearby the shallow Lander station (20158040002). Note the distinct body below 115 m. 358

Figure 40-9. CTD and LADCP plots from mooring Site BR-K, 485m east of the deep Lander station (20158040004). Note the distinct body below 115 m. 359

Figure 40-10. Multibeam image across a small hill-hole pair identical to newly identified features off Finnmark, Norway (King et al. in press) and in Lancaster Sound. They are attributed to an iceberg calving from the paleo-glacier’s margin whereby the plunge, roll and sediment scoop excavate a large pit (blue) and hill (red) which is generally crescentic. Curvi-linear features are iceberg scours. Depth profile and location shown. Discovery and multibeam rendering, Gabriel Joyal. 364

Figure 40-11. Multibeam image from northern Banks Island showing two canyons that are clearly deepwater correlatives with the rivers. Post-glacial uplift caused the river gullies and likely accelerated erosion. The paleo-shoreline is assumed to lie between the survey path and the land. Features identified by Gabriel Joyal and Charles DeGrandpre.....	365
Figure 41-1. Piston corer being retrieved on CCGS <i>Amundsen</i>	368
Figure 41-2. 3.5 kHz record in Pond Inlet showing the locations of the two cores collected during Leg 4b.....	369
Figure 2-1. Ocean-Sea Ice-Atmosphere sampling methods during Legs 1 (upper schematic) and 3 (lower schematic).	64
Figure 2-2. The deployment of the first on ice tower via the ship.	65
Figure 2-3. Deployment of the POPS buoys.....	69
Figure 2-4. Wind speed and direction during Leg 1.....	70
Figure 2-5. Air temperature, sea surface temperature, dew point temperature and atmospheric pressure.	71
Figure 2-6. Photosynthetically active radiation (PAR), short-wave and long-wave irradiance.	72
Figure 2-7. Temperature of the ice core.	73
Figure 2-8. The air temperature, pressure and relative humidity data from the on ice met tower #8 deployed on September 9th, 2015.....	73
Figure 2-9. Wind direction (red) and wind speed (green) from station #8 deployed on September 9th, 2015.	74
Figure 2-10. The trajectory from September 22 nd to September 29 th of 5 beacons deployed in the Beaufort Sea.	74
Figure 2-11. Temperature profile of the ice core taken in Penny Strait.	74
Figure 3-1. The PVC adapter plate that holds 12 – 47mm filter holders	77
Figure 3-2. The aerosol sampling locations and route in the Canadian Basin and the Canadian Arctic Archipelago during Leg 3b	78
Figure 3-3. The TISCH volume flow controlled (VFC) high volume aerosol sampler deployed on the bridge deck of the CCGS <i>Amundsen</i> during Leg 3b from September – October, 2015 (left). The anemometer, which is attached to the aerosol sampler through CR10 datalogger (right).	80
Figure 4-1. Surface water sampling (left) and samples analysis (right).....	84
Figure 4-2. Locations of the sampling stations for dark incubation during Leg 3.	85
Figure 4-3. <i>In-situ</i> CH ₄ concentration in M’Clure Strait during Leg 3.	86
Figure 4-4. <i>In-situ</i> CH ₄ concentration in Queen Maud Gulf of the Canadian Archipelago during Leg 3.	86
Figure 4-5. Methane concentration vs. depth at Station 170 near Scott Inlet.....	87
Figure 4-6. Methane concentration vs. depth at Station 180 near the Broughton Island.	87
Figure 5-1. Image taken at 12z on Apr 30, 2015 at 50.54N, 58.39W. It is a jpeg image (590 kB at full resolution) that provides a 45-degree view.....	89
Figure 6-1. Ice island PII-A-1-f as imaged by Sentinel-1 (European Space Agency).....	96

Figure 6-2. Ice penetrating radar (foreground), meteorological station (background) and row of ablation stakes between.	98
Figure 6-3. (Clockwise from top-left): Photogrammetry survey of Station 1 (wedge iceberg) after processing in Agisoft Photoscan; sidewall laser scan survey of Station 3 (small tabular iceberg); laser scan survey of the CCGS <i>Amundsen</i> illustrating the ship's drift during data collection; multi-beam keel survey data of Station 4 (saddle iceberg).	100
Figure 6-4. Image taken by the CC5MPX camera on the meteorological station showing the stripped ablation stakes and ice penetrating radar system.	101
Figure 6-5. Sample radargram from the ice penetrating radar on 22 October. The airwave is first and the bed-wave is second at approximately 170 ns (Time).	102
Figure 7-1. Deployment from the <i>Amundsen's</i> A-frame.	106
Figure 7-2. Argo float deployed.....	107
Figure 7-3. Data recorded by the BioArgo float takapm003c during a test profile on 22 October (Leg 4b).....	108
Figure 8-1. Mooring locations 2014-2015-2016: BREa-iBO-ArcticNet mooring arrays.....	111
Figure 8-2. Mooring designs BS1-14, BS2-14 and BS3-13 recovered in southern Beaufort Sea during Leg 3a.....	115
Figure 8-3. Tilt and rotate calibration jig / table as utilized in Inuvik, NWT	118
Figure 8-4. Nortek ADCP Compass Verification Curve (Inuvik, Sept, 2015).....	120
Figure 8-5. ArcticNet Dragging Anchor for BS1-14.....	125
Figure 8-6. Triangulation plot from BS1-14 using Art's Acoustic Survey Matlab Script.	129
Figure 8-7. Multibeam imagery identifying orientation and instrument depths (screenshot courtesy of ArcticNet multibeam processing team).	130
Figure 8-8. Rosette Temperature - Salinity Profile example plot (BS2-14).	130
Figure 8-9. BS2-14 CTD plot from the SBE37 moored at 152 db (162m) showing the large lay-over event on March 2 2014 (ice berg keel).	131
Figure 9-1. Top view of the SBE32 with 24x 12L Niskin bottles used on the <i>Amundsen</i> (left) and bottom view of the SBE32 showing the SBE9 CTD including additional sensors and the RDI LADCP (right). Photos: Jessy Barrette.	134
Figure 9-2. ArcticNet/GEOTRACES study region in the eastern Canadian Arctic for Leg 2.	135
Figure 9-3. ArcticNet study region in the Western Canadian Arctic, Legs 3a and b.....	135
Figure 9-4. ArcticNet study region in the eastern Canadian Arctic for Leg 4.....	136
Figure 9-5. Example of a calibration curve (left) and photo of the bottles used to collect water samples to measure salinity (right).	138
Figure 9-6. Example of oxygen calibration curve (left) and photo of the bottles used to collect water samples to measure oxygen (bottom right).	139
Figure 9-7. RDI LADCP mounted on the bottom of the SBE32 carousel on the <i>Amundsen</i>	141
Figure 9-8. Example of vertical structure (temperature and salinity – left; nitrate and fluorescence – right) for Cast 006.....	142
Figure 9-9. Evolution of the main parameters along the transect "Lancaster Sound'.....	142

Figure 9-10. Example of current velocities for the Cast 015 recorded by the LADCP.....	143
Figure 9-11. CTD casts location for Leg 3a and the beginning of 3b.	143
Figure 9-12. Example of the vertical structure (temperature and salinity – left; nitrate and fluorescence – right) for the cast 051.	144
Figure 9-13. Evolution of the main parameters along the transect “Lancaster Sound’.....	144
Figure 9-14. Example of current velocities for the cast 051 recorded by the LADCP.	145
Figure 9-15. CTD casts location for Leg 4a and the beginning of 4b.	146
Figure 9-16. Example of the vertical structure (temperature and salinity – upper graph; nitrate and fluorescence – lower graph) for the Cast 025.....	147
Figure 9-17. Evolution of the main parameters along the transect “Northern Baffin Bay” ..	147
Figure 9-18. Example of current velocities for the Cast 025 recorded by the LADCP.....	148
Figure 110-1. Map of XCTD locations along the Geotraces 2015 (Leg 2) cruise track from the Labrador Sea shelf to the Canadian Arctic Archipelago. Inset plot (red hatched lines): high resolution shelf section towards Clyde River.....	150
Figure 11-1. Location of stations where the Trace Metal Rosette was deployed on Leg 2.	153
Figure 11-2. Sampled stations during the Canadian Arctic GEOTRACES 2015 Expedition during Leg 3b.	154
Figure 11-3. Depth versus dissolved Zn concentration for Station BB3. Preliminary results with some indication of contamination in outlying data points.	155
Figure 12-1. Arrangement of the on-board lab bench area. Ropes hold the 20 L jerricans below the bench. On the bench, 3 samples stand in milkcrates for settling of the iron co-precipitate, in the 20 L cubitainers.....	163
Figure 19-1. Map of river sampling locations along the GEOTRACES Leg 2 cruise track through the Canadian Arctic Archipelago.	197
Figure 19-2. (Left) Roger Francois sampling from the Meham River, Cornwallis Island; (Right) Roger Francois and pilot Martin Dufor at the Tree River.	198
Figure 20-1. Bathymetry of the region studied with the moving vessel profiler (left) and MVP tracks and CTD stations during intensive sampling (right).	200
Figure 20-2. Schematic diagram of the operation of the moving vessel profiler. A 10kt boat speed, which gives approximate spacing of 1km between casts, allows observation of finescale oceanographic processes spanning distances on the order of tens to hundreds of kilometres. Oceanographic data are continuously recorded, with the freefall component being picked out during post-processing.	200
Figure 20-3. (a) Temperature (colours) and density (contours) from a long-section along Wellington Channel, through Maury Channel, and ending in Queens Channel. Note the longer mode-1 waves at approximately 0–80km. (b) Enlarged version of (a) showing the shallow area of Maury Channel and the presence of shorter internal waves, which result from flow over the rough, shallow seafloor. (c) Transect location. (d) Temperature– salinity diagram, with colours denoting distance as in panels (a) and (b).....	202
Figure 20-4. (a) Temperature (colours) and density (contours) from a cross-section across southern Wellington Channel (into the page is northward). Distances	

increase from a starting point not far from the eastern boundary of the channel. (b) Enlarged version of (a) showing clearly the wedge-like feature that is a buoyant coastal current enlarged in the bottom panel. (c) Transect location. (d) Temperature–salinity diagram, with colours denoting distance as in panels (a) and (b)..... 203

Figure 21-1. Plot of the potential density measured by the glider over the course of the operations. 207

Figure 21-2. Approximate transects covered by the glider, as well as examples of the depth profiles and a sub-sampled temperature field from the glider CTD. 208

Figure 22-1. Preliminary oxygen concentration profiles from the 12 stations during Leg 2. 212

Figure 24-1. Cross-section of the nutrients from Station 437 (left) to Station 420 (right) during Leg 3a. 218

Figure 27-1. Spatial distribution of hydrographic parameters and biogenic gases along the cruise track. Note that horizontal lines on the $p\text{CO}_2$ and $\Delta\text{O}_2/\text{Ar}$ plots represent atmospheric saturation values. Note also that the data presented here have only received a very preliminary quality control, and do not necessarily represent the final processed values. 231

Figure 27-2. Spatial distribution of gases and hydrographic properties along the cruise track. 232

Figure 27-3. Continuous underway measurements of photoplankton photo-physiological properties were measured using fast repetition rate fluorometry (FRRF). The bottom panel shows surface irradiance cycles, while other panels show a range of other photo-physiological characteristics of surface water phytoplankton. For example, variable fluorescence (F_v/F_m), is used as a measure of the photosynthetic efficiency of electron capture in Photosystem II (PSII). This variable is often down-regulated during mid-day periods of high irradiance as a means of photo-protection. The variables P_{max} and Alpha represent the maximum (light saturated) electron transport rates and initial light-dependent slopes derived from rapid light curves..... 233

Figure 27-4. Rates of gross primary productivity determined from ^{14}C bottle assays (left hand panels), and from FRRF measurements of electron transport rates (ETR). Results are from Station K1 in the southern Labrador Sea. The curves show a characteristic saturation behavior as a function of irradiance. Bottom panels show data from the deep chlorophyll max, while top panels show results from the surface mixed layer assemblages (7.5 m sampling depth). Compilation of our productivity measurements from all stations will provide valuable information on primary productivity in Arctic waters, and its light-dependency. 234

Figure 27-5. Time course of phytoplankton biomass (chlorophyll *a*) in the first CO_2 - light incubation experiment. LL and HL represent low and high light treatments, respectively, while the numbers refer to the CO_2 level (in ppm) used for each treatment. In this first experiment, we observed an initial decrease in growth rates of the high light treatment, with only a small CO_2 effect. We have a suite of other

physiological and biochemical measurements that will help to understand the mechanisms underlying these responses.....	234
Figure 27-6. As for Fig. 5.1.10.5, but for the second incubation experiment. In this experiment (water collected near Station BB3), no significant effects across the light or CO ₂ treatments were observed.....	235
Figure 28-1. Chlorophyll a concentrations integrated over 100 m for different size fractions, 0.7-5 µm, 5-20 µm and > 20 µm, in the Labrador Sea and southern Baffin Bay.....	239
Figure 28-2. Chlorophyll a concentrations integrated over 100 m for different size fractions, 0.7-5 µm, 5-20 µm and > 20 µm, in Lancaster Sound, Barrow Strait and Peel Sound.	240
Figure 28-3: Chlorophyll a concentrations integrated over 100 m for different size fractions, 0.7-5 µm, 5-20 µm and > 20 µm, at all stations sampled during Leg 3a.....	240
Figure 28-4. Chlorophyll a concentrations integrated over 100 m for different size fractions, 0.7-5 µm, 5-20 µm and > 20 µm, in the Lancaster Sound and southern Baffin Bay.....	241
Figure 30-1. Flow indicated by flowmeters installed on the Double Square Net 1) in front of the 500 µm-mesh net, 2) in front of the 750 µm-mesh net, and 3) between the nets; and number of Arctic cod larvae collected by each net at each station.....	252
Figure 31-1. The 5-net vertical zooplankton sampler with LOKI (Monster net). Photo: Jessy Barrette 2013 ArcticNet Leg 1a.	260
Figure 31-2. Benthic invertebrates that were collected from the Agassiz trawl on 3 October 2015 at Station 304.....	261
Figure 31-3. SPMD cage installed on ArcticNet mooring BS-3.	268
Figure 31-4. SPMD cage installed on the line on BREA mooring BR-3.	268
Figure 32-1. Vertical distribution of total mercury in Station K1.....	273
Figure 34-1. Density of bird species observed during surveys from the CCG <i>Amundsen</i> during Leg 4c.	283
Figure 35-1. Example of periodical port side beam loss on data.....	287
Figure 35-2. Example of the data acquired in deep water conditions.....	288
Figure 35-3. Degradation of the Error Estimates Std Deviation due to correction signal loss.....	290
Figure 35-4. SIS water Column display of Mooring site BR-G before recovery. The red circle shows the buoys.....	292
Figure 35-5. Mooring BR-G added to bathymetry (purple dots) in CARIS HIPS&SIPS processing software. The exact position of the mooring is given in the lower right corner.....	292
Figure 35-6. Example of background files imported in SIS.....	293
Figure 35-7. Geographical display in SIS showing the navigation route taken to increase the bathymetric coverage; to fill the hole between two previous lines.....	293
Figure 35-8. (Left) GSC Lander; (Right) Water column display to visualize the deployment of the lander. The bright scattering in the middle of the water column.	294

Figure 35-9. Sound velocity profiles taken during Leg 1. From left to right: MVP transects 1501001, 1501002 and 1501003.	295
Figure 35-10. Example of the data acquire during the first MVP transect.	296
Figure 35-11. Preliminary results of the Iceberg Station 4 mapping on the barge. A) 3D point cloud view. Note that the attitude and displacement of the iceberg is not accounted for in the data. This is why the data does not match. B) First survey line of the barge around the iceberg. Yellow line shows the cross-section profile displayed in (C).	297
Figure 35-12. Same as Figure 35.11, but with a different perspective.	298
Figure 35-13. Water Column display of A) Mooring site 1, B) Mooring site 2 and C-D) Mooring site 3.	299
Figure 35-14. Multibeam bathymetry coverage of the Natashquan delta night survey.	300
Figure 35-15. Example of backscatter data of the <i>Amundsen's</i> EM302 showing non-uniform level response of the transmission sectors.	301
Figure 35-16. Graphical display of the differences in the level response of the four different transmission sectors of the EM302.	301
Figure 35-17. Bathymeric data collected in Eclipse Sound and Navy Board Inlet during Leg 4.	302
Figure 35-18. Crescent-shaped bedforms observed in Navy Board Inlet.	303
Figure 35-19. Location of CASQ1 site and associated bathymetric data.	303
Figure 35-20. Location of CASQ 2 site and associated bathymetric data.	304
Figure 35-21. Location of CASQ3 (AMD15-CQ3) in a sediment-filled basin in between two megascale glacial lineation in Scott Trough.	304
Figure 35-22. Location of CASQ 4 and associated bathymetric data.	305
Figure 35-23. New bathymetric data acquired in the Scott Inlet-Sam Ford Fjord area during Leg 4b. Positions of CASQ core-3 (AMD15-CQ3) and piston core LGM-AMU15-01 are shown by yellow dots.	306
Figure 35-24. Sam Ford Fjord bathymetry showing a grounding-line and a sediment-filled basin near the LGM-AMU15-01 piston core site. Seismic line 0026_2015_289_1015.sgy is shown by the the black line.	307
Figure 35-25. Seismic profile in Sam Ford Fjord showing the grounding-line, and a basin filled with at least 45-50 m of sediments.	307
Figure 35-26. Submerged delta/sandur at the head of Walker Arm (Sam Ford Fjord). Bathymetry shows a well-defined channel with what looks like terraces or maybe mass movement scars.	308
Figure 35-27. Bathymetry of Hecla and Gripper Trough showing mega-scale glacial lineations, mass movement scars and sediment-filled bassins.	308
Figure 35-28. Preliminary surface generated for Sam Ford Fjord ROV dive.	309
Figure 35-29. Preliminary surface generated for Cade Dyer ROV dive.	310
Figure 35-30. Improved method for iceberg mapping and complete 3D model using combined LiDAR/photogrammetry and bathymetry project development.	312
Figure 36-1. Box core deployment and sediment cores sampling.	316

Figure 36-2. Isotope tracing experiment set-up in the temperature controlled room and slicing of sediment cores after finishing the experiment.	317
Figure 36-3. Agassiz trawl deployment and identification of the specimens.	319
Figure 37-1. Multibeam survey of the lander deployment site (Station 177).	322
Figure 38-1. ROV dive locations for the 2015 CCGS <i>Amundsen</i> expedition. The Pond Inlet ROV dive was cancelled and replaced with the Qikiqtarjuaq dive.....	326
Figure 38-2. The SuMo ROV and the new elevator system. A) ROV and elevator, B) overall view of the elevator in the water (Scott Inlet, ~533 m), C) close-up of boxes, with a sample of the carnivorous sponge <i>Cladorhiza</i> sp. in the right arm.	327
Figure 38-3. Overview of the Navy Board ROV dive location, showing planned and accomplished ROV transect. Transect terminated early due to ROV electrical failure (see text) (left). Temperature profile at the Navy Board ROV dive site. This plot was generated at Ocean Data View, as the original plots from the Rosette were not available for this cast (right).....	329
Figure 38-4. Organisms and bottom types observed during the ROV dive at Navy Board Inlet. A) <i>Cladorhiza</i> sp., B) Nephtheid soft coral, C) <i>Gorgonocephalus</i> sp. with sea tadpole, D) whelk, E) <i>Desmospongia</i> , F) Sea urchins and unidentified red organism, G) crinoid, H) unidentified sea cucumber and brittle stars.....	330
Figure 38-5. Overview of the Scott Inlet ROV dive location, showing surveyed area and position of the elevator (star).	331
Figure 38-6. Temperature and salinity profiles at the Scott Inlet ROV dive site.	332
Figure 38-7. Organisms and bottom types observed during the ROV dive at Scott Inlet. A) Sampling of <i>Chondrocladia</i> sp., B) sampling of <i>Cladorhiza</i> sp., C) <i>Cladorhiza</i> sp. sample being brought to the elevator, D) <i>Cladorhiza</i> sp. being put in the box, E) <i>Chondrocladia</i> sp., F) fan sponge, G) <i>Polymastia</i> sp., H) <i>Umbellula encrinus</i>	333
Figure 38-8. Overview of the ROV dive near Qikiqtarjuaq, showing planned and accomplished ROV transect.	334
Figure 38-9. Temperature and salinity profiles near the Qikiqtarjuaq ROV dive site (Station 177, ~4 km from the dive site).....	335
Figure 38-10. Organisms and bottom types observed during the ROV dive near Qikiqtarjuaq. A) sea anemones and unidentified white tubes, B) cluster of sea anemones, C) <i>Gorgonocephalus</i> sp., D) sea anemone and an stipitate sponge, E) cluster of crinoids on outcrop, F) eel-pout below curved sea anemone, G) <i>Umbellula encrinus</i> , H) diversity of sponges and other invertebrates, I) sea anemones and ascidian, J) ctenophore. Red lasers are 10 cm apart.	336
Figure 38-11. Overview of the ROV dive at Cape Dyer, showing planned and accomplished ROV transect, and trawl path. Transect terminated early due to ROV mechanical failure complicated by rough seas (see text).....	337
Figure 38-12. Temperature and salinity profiles at the Cape Dyer ROV dive site.	338
Figure 38-13. Organisms and bottom types observed during the ROV dive at Cape Dyer. A-E) diversity of sponges, F) nephtheid soft corals and octopus, G) solitary hydrozoan <i>Corymorpha</i> cf. <i>glacialis</i> , H) rockling (left) and turbot (right). Red lasers are 10 cm apart.....	339

Figure 38-14. Overview of the ROV dive at Frobisher Bay, showing planned and accomplished ROV transect.	340
Figure 38-15. Temperature and salinity profiles near the Frobisher Bay ROV dive site. ...	341
Figure 38-16. Organisms and bottom types observed during the ROV dive at Frobisher Bay. A) isopod with juveniles, B) crinoids, C) sponges, crinoids and kelp, D) large yellow sponge, E) crinoids, F-G) ascidians and sponges, H) large isopod, I-J) sponge gardens (mostly the fan sponge). Red lasers are 10 cm apart.....	342
Figure 40-1. Distribution of a shelf-break band of glacial sediment erosion (Panel A). The erosion origin and age is largely unknown. Typically, several metres of the glacial plume-deposited muds were removed but at the Mackenzie Trough mouth this exceeds 40 m (Panel B). It may be the manifestation of a catastrophic event related to glacial outburst flooding. Alternatively, oceanographic current erosion, either modern or time-transgressive, beginning with sea-level low-stand processes. The lander deployments can address this by establishing present seabed conditions. Further understanding of this erosion phenomenon and the adjacent post-glacial mud distribution also has implications for Holocene age Mackenzie River sediment fate and the question of submarine avalanche ages.....	348
Figure 40-2. Instrumented Lander configuration aboard CCGS <i>Amundsen</i> on the 2015 expedition. The “shallow” (shelf) lander (GSC Stn. 2015804-0002) in the foreground (left) differs from the “deep” (GSC Stn. 2015804-0004) only in the later generation of the MAVS (4-D) and the plate-mounted Seabird Microcat CTD compared with a MAVS 3-D and a leg-pole-mounted RBR CT (background).	350
Figure 40-3. Cartoon of Lander configuration at the seabed.....	351
Figure 40-4. Instrumented Lander locations on the central Beaufort shelf-upper slope. Bathymetric contours shown on the multibeam bathymetric image. Placement is within the narrow contour-parallel zone of mud erosion shown in the previous illustration. Lander siting in the context of seismic profiles is shown in a following figure located along the thick brown line. An <i>Amundsen</i> 2015 - deployed water column oceanographic mooring site, BR-K, is also shown. Lander sites in Panels A and B are shown with greater detail in the following figure.	354
Figure 40-5. Close-up maps of Instrumented Lander locations. Subtle lines are existing 3.5 kHz sub-bottom profiler acquisitions from ArcticNet cruises. Heavier brown line is the <i>Amundsen</i> 2015 track. Panel A highlights a high-resolution Autonomous Underwater Vehicle (AUV) multibeam bathymetry rendering (courtesy C. Paull, Monterey Bay Aquarium Research Institute, MBARI). This depicts local net mud deposition (smooth) surrounding and locally overlying pingo-like features (PLFs). Placement is in "freestream" between the PLFs but locally the mounds have directed sedimentation pattern, including comet-like heads and tails manifesting the net easterly flow of the Jet. Panel B shows the much simpler topography of the uppermost slope. Anchor, CTD and box core site also shown.....	355
Figure 40-6. Instrumented lander locations projected on the nearest 3.5 kHz sub-bottom profile. Profile locations in the overview map (two figures previous).....	356

Figure 40-7. Multibeam acquisition screen during the shallow lander deployment. The lander is visible in the mid-water column. 357

Figure 40-8. CTD and LADCP plots from nearby the shallow Lander station (20158040002). Note the distinct body below 115 m. 358

Figure 40-9. CTD and LADCP plots from mooring Site BR-K, 485m east of the deep Lander station (20158040004). Note the distinct body below 115 m. 359

Figure 40-10. Multibeam image across a small hill-hole pair identical to newly identified features off Finnmark, Norway (King et al. in press) and in Lancaster Sound. They are attributed to an iceberg calving from the paleo-glacier’s margin whereby the plunge, roll and sediment scoop excavate a large pit (blue) and hill (red) which is generally crescentic. Curvi-linear features are iceberg scours. Depth profile and location shown. Discovery and multibeam rendering, Gabriel Joyal. 364

Figure 40-11. Multibeam image from northern Banks Island showing two canyons that are clearly deepwater correlatives with the rivers. Post-glacial uplift caused the river gullies and likely accelerated erosion. The paleo-shoreline is assumed to lie between the survey path and the land. Features identified by Gabriel Joyal and Charles DeGrandpre..... 365

Figure 41-1. Piston corer being retrieved on CCGS *Amundsen*..... 368

Figure 41-2. 3.5 kHz record in Pond Inlet showing the locations of the two cores collected during Leg 4b..... 369

List of tables

Part II – Project reports

Table 1-1. Summary of variable inventory and application.....	56
Table 1-2. Stations sampled for DIC and TA during Legs 4a and 4b.	57
Table 2-1. Manual meteorological parameters recorded by the observer.	62
Table 2-2. The details of the on ice met tower deployments.	65
Table 2-3. Instruments used in the shipped based meteorological tower during Leg 1.	66
Table 2-4. Each file has the following columns, with the variable and units described.	67
Table 3-1. The table below summarizes the date, location and sampling parameters of aerosol samples and blanks on Leg 2.	79
Table 3-2. The table below summarizes the date, location and sampling parameters of aerosol samples and blanks on Leg 3b.	79
Table 3-3. A summary of aerosol samples and blanks collected during <i>Transit</i> and <i>On Station</i> on Leg 2.....	79
Table 3-4. A summary of aerosol samples and blanks collected during <i>Transit</i> and <i>On Station</i> on Leg 3b.....	80
Table 4-1. List of sampling stations for dark incubation during Leg 2.	84
Table 6-1. Iceberg mapping activities by date and location.....	95
Table 6-1: Sample data from the meteorological station.	101
Table 8-1. Description of oceanographic equipment	111
Table 8-2. Oceanographic equipment that required compass calibration, including calibration procedures.	122
Table 8-3. 2015 Short Mooring Re-Deployment Summary.....	125
Table 8-4. Mooring deployment summary 2015.	127
Table 8-5. 2015 short mooring re-deployment summary.....	127
Table 8-6. Summary table of Lessons Learned throughout the mission.	133
Table 9-1. Sensors attached to the SBE9.	136
Table 9-2. Specifications for the sensors equipped on the Rosette.	137
Table 11-1. Date and location of the TM rosette deployments on Leg 2.....	153
Table 11-2. TM Rosette sampling log summary (Leg 3b).....	156
Table 12-1. Description of the samples collected during Leg 2. The date, coordinates, station- cast, and sample ID are given. It is also reported whether the sample was filtered, whether an aliquot was taken for REE measurement, what test tube was used for the Pa and Th isotopic dilution and the associated weight of the 2 spikes (²³³ Pa and ²²⁹ Th), whether an aliquot was taken for Cr isotope measurement and any remark about the sample.	165
Table 12-2. Log of the samples collected during Leg 3b, all valid for Nd isotopes samples (PWW:Pacific Winter Water; PSW: Pacific Summer Water; SCM: Surface Chl a max).....	168
Table 13-1. Large volume pump samples for ²³⁰ Th, ²³¹ Pa, Nd isotopes, Cr isotopes and Si isotopes on Leg 2.	171

Table 13-2. Large volume pump samples for ^{230}Th , ^{231}Pa , Nd isotopes, Cr isotopes and Si isotopes on Leg 3b.	172
Table 13-3. Samples specifically taken for ^{234}Th measurements during Leg 2.	172
Table 15-1. List of water samples taken for stable nitrogen isotopes during Leg 2 of the Canadian GEOTRACES expedition.	176
Table 16-1. Sampling depths during Leg 2.	179
Table 16-2. Sampling depths during Leg 3a.	179
Table 16-3. Sampling depths during Leg 3b.	179
Table 17-1. Station locations and sample dates for dissolved inorganic carbon (DIC), alkalinity (A_T), barium, and radium isotope samples during Leg 2. DIC, A_T and Ba were sampled at every station. Radium samples were taken at the bolded stations only.	183
Table 17-2. Station locations and sample dates for dissolved inorganic carbon (DIC), alkalinity (A_T), barium, and radium isotope samples during Leg 3b. DIC, A_T and Ba were sampled at every station. Radium samples were taken at the bolded stations only.	183
Table 18-1. Samples taken and associated analysis during Leg 2.	188
Table 18-2. Samples taken for DOC (Hansell), CDOM and Thiol (Gueguen) analysis during Leg 3b. <small>[SEP]</small>	188
Table 18-3. Underway sampling during Leg 2.	189
Table 18-4. Underway samples collected during Leg 3b. Data for time sampled is correct (UTC-5) but coordinates were unavailable at the source and reflect our location 3 minutes after sampling. <small>[SEP]</small>	190
Table 18-5. List of stations where incubations were conducted, and the measurements performed during Leg 2.	192
Table 18-6. Stations and depths where $\delta^{30}\text{Si}$ samples were collected during Leg 2.	194
Table 18-7. Samples taken for bSiO_2 and $\delta^{30}\text{Si}(\text{OH})_2$ during Leg 3b.	194
Table 18-8. Samples taken for POC analysis during Leg 3b.	195
Table 18-9. Samples taken for Fe speciation during Leg 3b.	195
Table 18-10. Samples taken for ligands during Leg 3b.	196
Table 19-1. River sampling locations during the 2015 GEOTRACES (Leg 2) transit via the Canadian Arctic Archipelago.	198
Table 19-2. Geochemical parameters sampled during the 2015 GEOTRACES Leg 2 transit via the Canadian Arctic Archipelago. Analyses to be carried out at UBC, UVIC, and WHOI.	198
Table 20-1. Wellington Channel Survey Timeline.	201
Table 22-1. N_2/Ar and O_2/Ar samples collected during Leg 2.	210
Table 22-2. Oxygen samples collected during Leg 2.	211
Table 22-3. Noble gas samples collected during Leg 2.	211
Table 24-1. List of sampling stations and measurements during Leg 2.	215
Table 24-2. List of sampling stations and measurements during Leg 3a.	216
Table 24-3. List of sampling stations and measurements during Leg 3b.	216
Table 24-4. List of sampling stations and measurements during Leg 4.	217

Table 25-1. Samples collected during Leg 3a.	221
Table 25-2. Samples collected during Leg 4a.	221
Table 25-3. Samples collected during Leg 4b.	221
Table 25-4. Samples collected during the incubation experiment with seawater from Station 177 (Leg 4c).....	222
Table 26-1. List of particulate trace metal samples during Leg 2.	225
Table 26-2. List of samples for speciation during Leg 2.	227
Table 26-3. List of particulate trace metal samples during Leg 3b.	228
Table 28-1. Sampling operations during Leg 2 of the ArcticNet 2015 Expedition on board the <i>CCCS Amundsen</i>	238
Table 28-2. Sampling operations during Leg 3a of the ArcticNet 2015 Expedition on board the <i>CCCS Amundsen</i>	238
Table 28-3. Sampling operations during Legs 4a and 4b of the ArcticNet 2015 Expedition on board the <i>CCCS Amundsen</i>	239
Table 29-1. Differences between the actual pH measured after initial acidification at T1 and the targeted values calculated with CO ₂ sys.	244
Table 29-2. Variables measured during the 10 day Bioassay incubation experiment (water initially sampled at station BB3).....	246
Table 30-1. Summary of operations conducted and samples collected during Leg 2.	249
Table 30-2. Summary of operations conducted and samples collected during Leg 3a.	250
Table 30-3. Summary of operations conducted and samples collected during Leg 3b.	250
Table 30-4. Summary of operations conducted and samples collected during Leg 4.	251
Table 30-5. Mean standard length and weight of young-of-the year Polar cod at each station.	253
Table 30-6. Mean standard length and weight of adults Polar cod at each station.	253
Table 30-7. Mean standard length and weight of young-of-the year Arctic cod at each station.	254
Table 30-8. Mean standard length and weight of adults Polar cod at each station.	255
Table 30-9. Mean standard length and weight of young-of-the year Polar cod at each station.	255
Table 30-10. Mean standard length and weight of adults Polar cod at each station.	256
Table 31-1. Stations where zooplankton species were collected for contaminants during Leg 3a of ArcticNet 2015.	261
Table 31-2. Stations where zooplankton species were collected for contaminants during Leg 4 of ArcticNet 2015.	262
Table 31-3. List of benthic samples for PAH collected during Leg 3a of ArcticNet 2015.	263
Table 31-4. List of benthic samples for PAH collected during Leg 4 of ArcticNet 2015.	264
Table 31-5. Sediment and water samples collected during Leg 3b of ArcticNet 2015.	264
Table 31-6. SPMDs recovered during Leg 3a of the ArcticNet 2015 cruise.	267
Table 31-7. SPMDs deployed during Leg 3a of the ArcticNet 2015 cruise.	268
Table 32-1. Stations sampled during Leg 2.	272
Table 32-2. Stations sampled during Leg 3b.	272

Table 34-1. List of bird species observed during surveys from the CCG <i>Amundsen</i> during Leg 4c.	282
Table 35-1. MVP transects description during Leg 1.....	295
Table 35-2. MVP transects description during Leg 3b.....	295
Table 35-3. Cores data (for Etienne Brouard’s PhD study).	306
Table 36-1. Box coring stations during Leg 3.	317
Table 36-2. Box coring stations during Leg 4.	318
Table 36-3. Agassiz trawl stations during Leg 3.	319
Table 36-4. Agassiz trawl stations during Leg 4.	320
Table 38-1. List of sediment samples obtained from box cores during Leg 4b.	328
Table 38-2. Sponge samples collected using the SuMo ROV during Leg 4b.....	332
Table 38-3. Organisms sampled during the Frobisher Bay ROV dive (dive 48).....	341
Table 40-1. Summary of GSC stations sampled during Leg 3a.	352
Table 40-2. Lander anchor (train wheel) triangulation.	354
Table 41-1. Collected information for each piston core collected during Leg 4b.	370
Table 42-1. CTD, box and CASQ sampling stations.	372
Table 43-1. Locations and timings of piston core retrieval.	374
Table 43-2. Physical description of recovered samples.	374
Table 44-1. Summary of Schools on board activities provided by scientists on board Leg 4a.	375

2015 Expedition Report

The 2015 Expedition Report is a collection of all cruise reports produced by the participating research teams and assembled by the Chief Scientists at the end of Legs 1, 2, 3 and 4 of the ArcticNet Expedition onboard the CCGS *Amundsen*. The 2015 Expedition Report is divided into two parts:

Part I provides an overview of the expedition, the ship track and the stations visited, and a synopsis of operations conducted during each of the three legs.

Part II contains the reports submitted by participating science teams or researchers, with details on the specific objectives of their project, the field operations conducted and methodology used, and in some cases, preliminary results. When results are presented, they show the data as they were submitted at the end of the legs in 2015. The data presented in this report are illustrative only and have not been quality checked, thus parties interested in the results should contact the project leader or the researchers who collected the data.

The sections in Part II describing each project are organized with atmospheric, surface ocean and sea ice components first (Sections 1 to 7), followed by water column properties, which include the mooring program (Section 8), CTD-Rosette operations and physical properties (Sections 9 to 11, 20 and 21), as well as a suite of chemical and biological parameters (Sections 12 to 19 and 22 to 30). Contaminants cycling in seawater and biota are treated in Sections 31 and 32. Subsequent sections cover seabed mapping (Section 34), sediments and benthos sampling (Sections 35 and 36, 38 to 42), and ROV operations (Section 37).

The 2015 Expedition Report also includes four appendices: 1) the list of stations sampled, 2) the scientific log of activities conducted, 3) a copy of the CTD logbook and 4) the list of participants on board during each leg.

The core oceanographic data generated by the CTD-Rosette operations, as well as meteorological information (AAVOS) and data collected using the Moving Vessel Profiler (MVP), the ship-mounted current meter (SM-ADCP) and the thermosalinograph (TSG) are available in the Polar Data Catalogue (PDC) at www.polardata.ca.

Following ArcticNet's data policy, research teams must submit their metadata to the PDC and insure that their data are archived on the long-term, but it is not mandatory to use the PDC as a long-term archive as long as a link to the data is provided in the metadata (see www.arcticnet.ulaval.ca/Docs/data-policy for more details on data policy).

Part I – Overview and synopsis of operations

1 Overview of the 2015 ArcticNet / Amundsen Expedition

1.1 Introduction

Recent warming trends in the Arctic over the last several decades suggest significant future impacts to northern coastal and marine environments, including to the peoples, communities and infrastructure of these areas. ArcticNet is a Network of Centres of Excellence of Canada that brings together scientists and managers in the natural, human health and social sciences with their partners from Inuit organizations, northern communities, federal and provincial agencies and the private sector to study the impacts of climate change and modernization in the coastal Canadian Arctic.

Since 2004, ArcticNet researchers have been conducting extensive multidisciplinary sampling programs in the Canadian Arctic using the Canadian research icebreaker CCGS *Amundsen*. The overarching goal of the ArcticNet marine-based research program is to study on a long-term basis how climate induced changes are impacting the marine ecosystem, contaminant transport, biogeochemical fluxes, and exchange processes across the ocean-sea ice-atmosphere interface in the Canadian Arctic Ocean. The knowledge generated from this multi-year program is being integrated into regional impact assessments to help decision makers and stakeholders develop effective adaptation strategies for the changing coastal Canadian Arctic.

The geographic scope of the ArcticNet marine-based research program includes the Beaufort Sea in the western Canadian Arctic, the Canadian Arctic Archipelago and Baffin Bay in the eastern Arctic, and extends into Hudson Bay, Ungava Bay and along the northern Labrador coast.

In the western Arctic, northern Baffin Bay and Hudson Bay, ArcticNet has established long-term oceanic observatories. Each observatory consists of a number of moorings equipped with instruments that gather continuous records of currents, temperature, conductivity, turbidity, dissolved oxygen and the vertical flux of carbon and contaminants. Some moorings are also equipped with autonomous hydrophones to record the acoustic background and the vocalizations of marine mammals.

On Friday 17 April 2015, the *Amundsen* left its homeport of Quebec City for an initial 18-day expedition in the Labrador Sea, as a part of a collaboration between ArcticNet, Statoil Canada, the Research & Development Corporation of Newfoundland and Labrador and Husky Energy. The ship returned to Quebec City after Leg 1 and departed again on 10 July for a 115-day scientific expedition, travelling a total of 20 512 nautical miles in support of ArcticNet's annual marine-based research program (see Phase 3 projects- <http://www.arcticnet.ulaval.ca/research/phase3projects.php>) and its industry partners, the

ArcticNet ESRF program, financing research to support the decision-making process related to oil and gas exploration and development on Canada's frontier lands, GEOTRACES, an international study of the marine biogeochemical cycles of trace elements and their isotopes, and Parks Canada – The Garfield Weston Foundation Innovative, aiming at investigating the oceanographic conditions near and surrounding the shipwreck *Erebus* in the Queen Maud Gulf.

The main objective of the 2015 ArcticNet/*Amundsen* Expedition was to maintain ArcticNet's network of oceanic observatories by deploying 4 moorings and recovering 10 moorings in the Western Arctic. ArcticNet's ultimate goal was to redeploy 3 of the 10 moorings recovered in the Beaufort Sea to establish long-term marine observatories for monitoring present variability and forecasting future change in Arctic ecosystems. In addition to work conducted at the mooring stations, shipboard sampling was carried out along the ship track and at designated sampling stations, including seafloor and ice island mapping, ROV diving, meteorological measurements and the sampling of seawater, sediment, plankton, juvenile fish and sea ice.

1.2 Regional settings

1.2.1 Labrador Sea

Between Labrador and Greenland lies the Labrador Sea, a key region that includes the Labrador Current system. This strong current carries cold water down from Baffin Bay to offshore Newfoundland and, therefore, strongly influences the oceanographic conditions on the Atlantic Canadian Shelf. The Labrador Sea acts as a corridor for southward drifting icebergs and ice islands, inducing risks for activities and operations conducted offshore Newfoundland. From this perspective, gathering scientific knowledge about the area is of particular importance as to inform federal departments and the private sector about the risks associated with the exploration and exploitation of oil and gas.

1.2.2 Baffin Bay

Baffin Bay is located between Baffin Island and Greenland and connects the Arctic Ocean and the Northwest Atlantic, providing an important pathway for exchange of heat, salt and other properties between these two oceans. In the south, Davis Strait, which is over 300 km wide and 1000 m deep, connects it with the Atlantic but Baffin Bay's direct connection to the Arctic Ocean is far more restricted, consisting of three relatively narrow passages through the islands of the Canadian Arctic Archipelago (CAA). Melting ice sheets, changing sea ice conditions and changing weather also influence oceanographic conditions in Baffin Bay and Davis Strait.

Southern Baffin Bay supports concentrations of corals and sponges, inclusive of gorgonian and antipatharia species. A survey of the seafloor using the *Amundsen's* remotely operated vehicle (ROV) will be conducted to explore the area, locate and sample hotspots of corals and sponges in this unique deep and cold Arctic environment.

Baffin Bay's connection to the Arctic Ocean is far more restricted, consisting of three relatively narrow passages through the islands of the Canadian Arctic Archipelago (CAA). One of these passages, Nares Strait, is located between Ellesmere Island and Greenland and includes from south to north: Smith Sound, Kane Basin, Kennedy Channel, Hall Basin and Robeson Channel. Each winter, there is a prolonged period during which land-fast ice arches span the strait at the entrance to Robeson Channel and south of Kennedy Channel. The ice in Nares Strait then becomes land-fast and shuts down southward ice motion. In the past decade, changes to this long-standing pattern of ice conditions have been observed with weaker or absent ice arches in Nares Strait resulting in increased ice flux from the Arctic and reduced amount of ice allowed to reside in the Arctic Ocean to thicken as multi-year ice.

1.2.3 Canadian Arctic Archipelago

The Canadian Arctic Archipelago (CAA) is a vast array of islands and channels that lies between Banks Island in the west and Baffin and Ellesmere Islands in the east. While transiting through the Northwest Passage, the science teams aboard the *Amundsen* extended their time series of atmosphere, ice and ocean data. This work is aimed at better understanding how the climate, ice conditions as well as ocean currents and biogeochemistry are changing under the effects of climate change and industrialization. With ice extent and volume shrinking in the Arctic, the Northwest Passage may be ice free and open to navigation during summer in the near future. Bathymetry data and sub-bottom information were collected while transiting through the Northwest Passage to map the seafloor and identify potential geohazards and obstacles to the safe navigation of this new seaway.

1.2.4 Beaufort Sea

The Canadian Beaufort Sea/Mackenzie Shelf region of the Arctic Ocean has witnessed major changes in recent years, with decreasing sea ice cover and major shifts in sea-ice dynamics. The Beaufort Sea is characterized by a broad shelf onto which the Mackenzie River, the largest river in North America, carries large amounts of freshwater. The mixing of freshwater from the Mackenzie River and Arctic marine waters of the Beaufort Sea establishes an estuarine system over the shelf, with associated inputs of land-derived nutrients and freshwater biota. Along the Mackenzie Shelf stretches the Cape Bathurst polynya, an expanse of open water that exists year-round and is highly productive. This ecosystem is also exceptional since it provides habitat for some of the highest densities of birds and marine mammals in the Arctic.

Since 2002, extensive multidisciplinary research programs have been conducted in the Beaufort Sea area. Major oceanographic research activities were carried out as part of two major international overwintering research programs conducted onboard the CCGS *Amundsen* in 2003-2004 (CASES program) and in 2007-2008 (CFL Study). Environmental and oceanographic research activities were also conducted in the offshore region of the Mackenzie Shelf, shelf slope and Beaufort Sea since 2009, in partnership with the Oil & Gas industry and within the framework of the Beaufort Regional Environmental Assessment (BREA, www.beaufortrea.ca) program. Overall since 2004, a marine observatory of a minimum of five oceanographic annual moorings (from 5 to 17 moorings) has been deployed and maintained annually in the area by ArcticNet researchers.

1.3 2015 Expedition Plan

1.3.1 General schedule

Based on the scientific objectives, the expedition was divided into seven separate legs: Leg 1, from 17 April to 4 May 2015, took the *Amundsen* into the Labrador Sea to conduct sampling activities before coming back to Quebec City. Leg 2 took the ship to the Canadian Arctic Archipelago, and involved activities in the Labrador Sea, Baffin Bay and the Northwest Passage, from 10 July to 20 August 2015. During Legs 3a and b, the ship headed towards Resolute, between 20 August and 1 October 2015, while conducting activities in the Amundsen Gulf, Beaufort Sea, Penny Strait, Maury Channel, Queen Maud Gulf, Parry Channel and Wellington Channel. Legs 4a, 4b and 4c, from 1 October to 1 November 2015, took the ship back to Quebec City, and involved activities in the Northwest Passage, Eclipse Sound and Baffin Bay.

1.3.2 Leg 1 – ArcticNet/Industry – 17 April to 4 May 2015

Leaving Quebec City on 17 April, the *Amundsen* sailed in the St. Lawrence Gulf and Estuary and in the Labrador Sea to conduct MVP and SX90 surveys, and deploy moorings, drifters as well as underwater gliders to gather a maximum of information about the systems. The central mandate of ArcticNet during this leg was to provide federal departments and the private sector with the scientific knowledge needed to make decisions and formulate strategies regarding the oil and gas exploration and exploitation. The ship came back to Quebec City on 4 May for a full crew change at the end of Leg 1.

1.3.3 Leg 2 – GEOTRACES/ArcticNet - 10 July to 20 August 2015 – Quebec City to Kugluktuk

Leaving Quebec City on 10 July, the ship sailed towards the Labrador Sea to conduct sampling operations off the coast of Labrador. While underway to Baffin Bay to pursue its

activities, the ship was unexpectedly diverted to Hudson Bay for ice-breaking duties, which resulted in a 2 weeks hiatus, from 19 July to 3 August. This pause in operations resulted in a dramatically reduced science plan where ArcticNet cancelled nearly all its stations. The remaining expedition plan was reduced to 3 stations in Baffin Bay and 7 stations in the Canadian Arctic Archipelago, with seabed mapping being conducted between the stations. The *Amundsen* reached Kugluktuk on 20 August for a full crew change and the end of Leg 2.

1.3.4 Leg 3a – ArcticNet/Industry/GEOTRACES - 20 August to 4 September 2015 - Kugluktuk to Sachs Harbour

The *Amundsen* spent approximately 2 weeks in the Beaufort Sea/Amundsen Gulf region to service and deploy respectively 8 and 5 moorings as a part of the Integrated Beaufort Observatory (iBO) program. Operations conducted also included the deployment of 2 underwater gliders as a part of the GEOTRACES program, as well as the deployment of 2 bottom landers on the Mackenzie Shelf Slope and work at one ice station. Oceanographic sampling operations were also conducted along the ArcticNet designated transects in the Mackenzie Shelf/Southern Beaufort Sea area. The ship reached Sachs Harbour on 4 September for a science rotation and the end of Leg 3a.

1.3.5 Leg 3b – GEOTRACES/ArcticNet/Industry - 4 September to 1 October 2015 – Sachs Harbour to Resolute

After the science rotation in Sachs Harbour on 4 September, the ship spent approximately 10 days in the Canadian Basin to conduct a MVP survey, complete ice work operations and deploy a POPs buoy. The *Amundsen* then supported a suite of sampling operations while sailing towards Queen Maud Gulf, where a mooring was deployed. Following a SX90 survey, a suite of MVP transects were completed as to map the turbulent structures in Penny Strait, Queens Channel, Maury Channel and Wellington Channel. The *Amundsen* reached Resolute on 1 October for a full crew change and the end of Leg 3b.

1.3.6 Leg 4a –ArcticNet - 1 to 11 October 2015 - Resolute to Pond Inlet

After the full crew change in Resolute, the ship sailed back east through the Northwest Passage. Sampling operations were conducted in Barrow Strait until the morning of 4 October, when the ship was called for a Search and Rescue operation in Arctic Bay. The *Amundsen* then ran its sampling operations in Lancaster Sound and northern Baffin Bay until the morning of 10 October. The ship transited and reached Pond Inlet on 11 October for a scientific crew rotation to welcome Schools on Board students.

1.3.7 Leg 4b and 4c – ArcticNet - 11 to 1 November 2015 – Pond Inlet to Quebec City

Following a scientific crew change in Pond Inlet, the ship conducted operations along the coast and in the fjords of Baffin Island. Operations included ROV dives, piston and CASQ coring, ice island fragment survey, BioArgo floats deployment and oceanographic operations at designated stations. In addition to ArcticNet's sampling operations, the *Amundsen* supported the 2015 Schools on Board program from Pond Inlet to Iqaluit. A last stopover in Iqaluit on 26 October provided ArcticNet and Schools on Board participants the opportunity to disembark from the ship before the return to Quebec City. The ship then sailed south towards Quebec City while conducting limited sampling operations along the way. On 1 November, the *Amundsen* reached its homeport in Quebec City,

1.3.8 iBO program - 22 September to 7 October 2015 – Beaufort Sea and Chukchi Sea

The main objective of the 2015 iBO program was to service moorings that recorded data over the preceding 1 or 2 years for sea-ice and ocean monitoring in the Beaufort Sea and the north-eastern Chukchi Sea. Operations included the recovery of 18 oceanographic moorings at 13 sites and the deployment of 20 moorings at 14 sites, and were carried out from the CCGS *Sir Wilfrid Laurier*.

2 Leg 1 – 17 April to 4 May 2015 – St. Lawrence Gulf and Estuary and Labrador Sea

Chief Scientist: David Barber¹ (david.barber@umanitoba.ca)

¹ Centre for Earth Observation Science, University of Manitoba, 535 Wallace Building, 125 Dysart Road, Winnipeg, MB, R3T 2N2, Canada.

2.1 Introduction

Leg 1 took place from 17 April to 4 May as part of a collaboration between ArcticNet's marine-based research program, Statoil Canada, the Research & Development Corporation of Newfoundland and Labrador and Husky Energy, in the St. Lawrence Gulf and Estuary and in the Labrador Sea. This initial 18-day expedition started and ended in Quebec City (Figure 2-1)

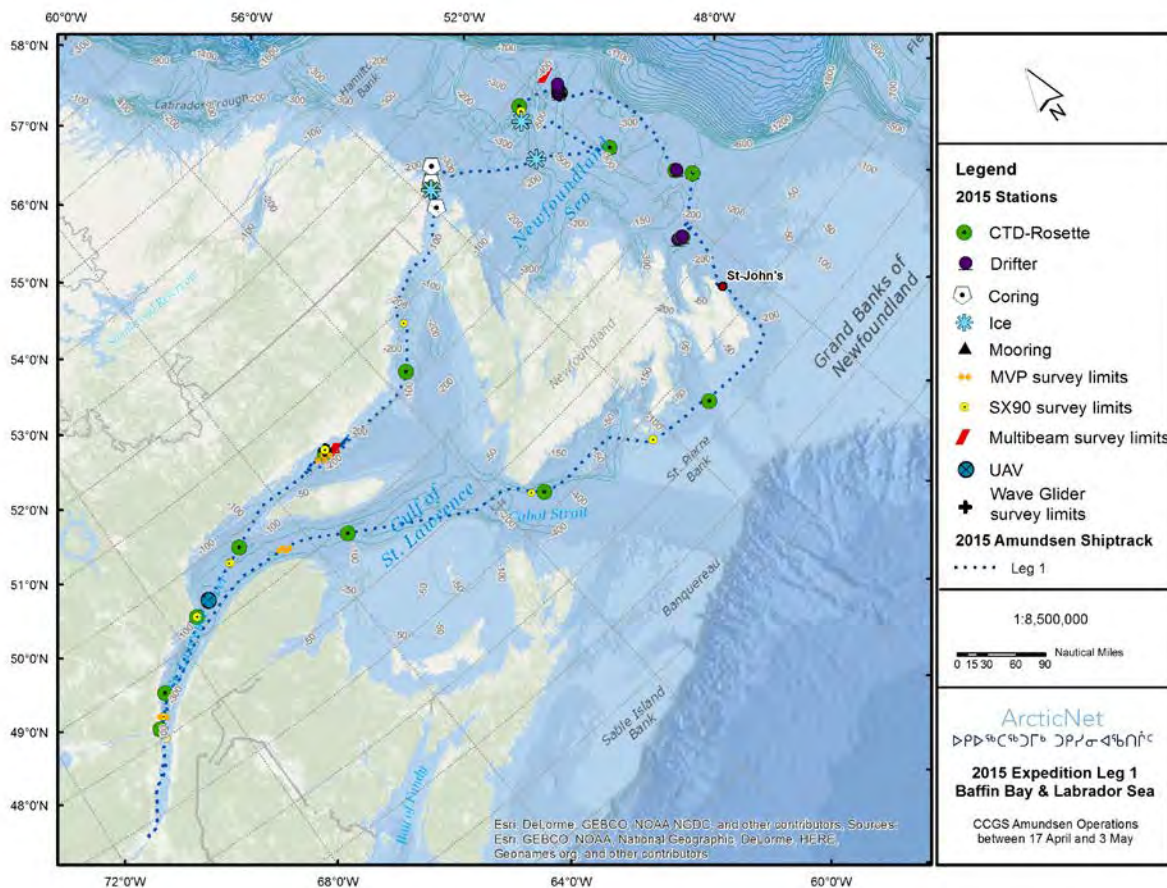


Figure 2-1: Ship track and the location of stations sampled in the St. Lawrence Gulf and Estuary and in the Labrador Sea during Leg 1.

The specific objectives of the ArcticNet and Industry field programs for Leg 1 were to:

- Conduct ice island field operations as to assess iceberg drift and deterioration;
- Conduct three MVP transects for SX90 surveys in the St. Lawrence Gulf and Estuary;
- Conduct multibeam surveys at selected sites and while transiting;
- Deploy three moorings in the Labrador Sea;
- Conduct a pilot study for ice camera imagery;
- Deploy 10 ice beacons;
- Deploy 2 weather stations;
- Deploy 2 Acoustic Doppler Current Profilers (ADCPs);
- Deploy the Wave Glider at selected stations.

2.2 Synopsis of operations

This section provides a general synopsis and timeline of operations during Leg 1. Detailed cruise reports provided by onboard participants and including specific objectives, methodology and preliminary results for projects conducted during this leg are available in Part II of this report.

During this leg, the *Amundsen* traveled from Quebec City, QC (17 April) to Labrador Sea, and came back to Quebec City (4 May), with an overall tally of operations and activities as follows:

- 21 CTD-Rosette casts;
- 3 MVP transects;
- 9 SX90 acoustic surveys;
- 3 mooring deployments;
- 2 Wave Glider deployments;
- 1 ice work station;
- 1 dedicated bathymetry / sub-bottom mapping survey;
- 1 UAV deployment.

A detailed scientific log for all sampling operations conducted during Leg 1 giving the positions and depths of the visited stations is available in Appendices 1 and 2.

2.2.1 Timeline of operations

The *Amundsen* left its homeport in Quebec City on 17 April and sailed towards St. John's, Newfoundland, while conducting sampling operations. On 20 April, the ship docked in St. John's harbour and a small science personnel change occurred during the day. The science and crew were invited to join Statoil for a social gathering before the departure of the ship in the evening. The event was well attended by both Statoil executives and science personnel from the ship.

The CCGS *Amundsen* was scheduled to depart on 21 April from St. John's harbour, however it was delayed due to weather conditions and high sea states. Wave heights were approximated at 8-12 meters with winds speeds up to 50 kts. During the day, the familiarization tour of science personnel, as well as the final mobilization, were completed.

The ship departed from St. John's early in the morning on 22 April. Operations for the day included two helicopter flights for iceberg operations and an attempt to deploy the Wave Glider. Due to ice conditions, the Wave Glider was retrieved before the ship left the vicinity to prevent any damage to the instrument.

On 23 April, the first mooring was successfully deployed at Mooring Station 1. Since the Zodiac could not be used due to mechanical problems, the mooring was deployed from the barge at 1306 UTC. The Rosette was deployed and the acoustic release was checked following the successful deployment of the mooring.

At Station #3 (Full Iceberg Station), the SX90 was deployed to conduct a survey. While circumnavigating the iceberg, the Lidar was operating on the barge (which was not deployed from the ship). The visibility cleared and the helicopter could be deployed, once for ice beacon deployment and once for photogrammetry. One additional drifter was deployed at Station #3.

On 24 April the ship arrived at the next iceberg (Station #4) at 1350 UTC and the SX90, as well as the Wave Glider, were successively deployed. The iceberg team (Derek and Anna) were able to place 4 beacons on the iceberg. The barge was deployed and a station was set up behind the iceberg to perform CTD casts for approximately 1.5 hrs, as to complement the ships' casts. On the opposite side of the iceberg, a Lidar and multibeam survey was completed with additional CTD casts. The Rosette was deployed 5 times during the day while the barge was out. The Zodiac was deployed to successfully retrieve the Wave Glider at 2150 UTC. An additional 6 drifters were deployed over a 9 nm transect west and then towards the Mooring Station #3.

On 25 April, the *Amundsen* arrived early at Mooring Station #3. The initial attempt at deploying the mooring resulted in too much ice and the mooring being stuck on a small piece of ice. The ship turned off the engines to avoid any problems with the lines getting caught in the propellers. The Zodiac had some engine troubles, which resulted in the ship needing to recover the Zodiac. Unfortunately, the lines from the mooring to the ship needed to be cut and the top of the mooring was left with the Zodiac. A second attempt at the mooring was done successfully without the deployment of the Zodiac and was followed by a triangulation and the deployment of the Rosette. The engineers have been able to repair the Zodiac, which was successfully tested in the early afternoon. The rapid core system was deployed at 2050 UTC on a small floe of ice (approx. 10-15 meters in size). The size of the floe was too small to be able to successfully retrieve a core. The ice load panel was installed at 2121 UTC in 8/10 sea ice conditions. The vessel drifted towards the ice and measured a 3 tonne load.

On 26 April, the final mooring was deployed at the updated Mooring Station #2. The original site proved to be too shallow and was moved to a deeper location at 50°16.66'N and 51°50.66'W. The mooring was successfully deployed at the new station without the use of the Zodiac. Following the mooring deployment, the triangulation as well as a CTD cast were performed. The ice load panel was installed at 2155 UTC and left for an hour while in 8/10 sea ice conditions.

April 27th was dedicated to sea ice work. The day started in the ice near Belle Isle. Ice conditions were not ideal so the *Amundsen* searched for a few thicker/larger floes. At 1310 UTC an ice team was lowered using the ice cage to deploy a beacon and take a physical core. Four helicopter flights were scheduled with Anna and Derek for pre ice management photogrammetry, iceberg beacon dropoff and iceberg photogrammetry, post ice management photogrammetry and ice beacons pickup. One ice management trial occurred from 1530 -1900 UTC – there was a focus of a 1nm by 1nm box to manage the ice. The rapid core was used on a floe at 2136 UTC.

The mornings of 28 and 29 April were dedicated to ice management trial. Each day, two beacons were deployed over the side of the ship. One rapid core was taken in the area of the ice management trial. Following the ice management trials, the ship returned to the large tabular iceberg from the previous day and did a helicopter flight to deploy an ice beacon, do some aerial photos and sample two ice cores. The Lidar mounted on the barge was used to map part of the ice island. The ice load panel was deployed before leaving the area of the ice island.

On 30 April, the ship transited back into the St. Lawrence Gulf. The SX90 was deployed at 1300 UTC, followed by a Rosette cast at 1633 UTC. The Wave Glider was deployed in the evening.

Overnight and into the early morning of May 1st, there was opportunistic mapping of the Natashquan Delta, which resulted in 7 lines, 10 nm each. Multi-beam and sub-bottom profiles were taken. The second Wave Glider, which was supposed to be deployed early in the morning, experienced some technical issues with the steering and could not be deployed. A Rosette cast was completed at 1053 UTC, followed by a SX90 deployment. A MVP transect was done for an hour from 1237 to 1334 UTC. The MMOs completed transects and surveys all day, which resulted in a few seal sightings and many birds. The UAV was tested off the helicopter deck during the morning. The manual control worked well, however the GPS control was not sufficient with a moving target. The Wave Glider deployed on 30 April was successfully recovered. The SX90 was recovered at 2222 UTC, after a full day being deployed.

MMO surveys occurred on 2 May. The MMOs spotted a blue whale and 3-4 sightings of fin whales. Lots of seabirds, bald eagles and loons were observed. American kestrels were seen on the boat and some decks. The SX90 was deployed at 1430 UTC and the 360-camera was calibrated at 1810 UTC, with the Zodiac deployed. The UAV was flown while

the Zodiac was out to get aerial photography of the ship and the Zodiac. A Rosette cast was completed at 2240 UTC for SX90 calibrations.

May 3 was dedicated to marine mammal observations in the Saguenay Marine Park Quebec. MMO surveys occurred since 4am. The SX90 was deployed at 0831 UTC, followed by a MVP transect from 0841 – 0958 UTC. The helicopter was deployed to pick up the visitors from Parks Canada and due to weather the Zodiac was used to transport the visitors back in the afternoon. At the end of the day, the Rosette was deployed. Unfortunately, the SX90 and MMOs only observed a single seal during the day. There was however lots of marine birds observed. The *Amundsen* reached its homeport in Quebec City on 4 May.

2.3 Chief Scientist's comments

Overall, Leg 1 was highly successful with productive collaborations established between teams and with the *Amundsen's* officers and crew. Despite some severe ice conditions, strong winds and bad weather, science operations were successfully conducted on a daily basis. The Chief Scientist and the science participants of Leg 1 express their gratitude to the Commanding Officer and the officers and crew of the CCGS *Amundsen* for their unrelenting support and comprehension throughout the cruise.

The initial plan (Figure 3.2) was to occupy 15 stations (2 stations in the Labrador Sea, 4 in Baffin Bay, and 9 in the Canadian Arctic Archipelago), which would satisfy the extensive sampling needs of GEOTRACES, while also providing productivity and hydrographic data for ArcticNet. Additional stations were to be occupied for ArcticNet on a section between Greenland and Devon Island, and in Kane Basin, Kennedy Channel and Petermann Fjord. Time was also allocated for additional stations in Queen Maud Gulf as part of The W. Garfield Weston Foundation - Parks Canada - ArcticNet collaborative project.

The specific objectives of the ArcticNet/GEOTRACES field programs for Leg 2 were to:

- Collect seawater with ArcticNet's Rosette;
- Collect seawater under trace metal clean conditions with GEOTRACES' Rosette;
- Sample particules with 6 McLane large volume *in-situ* pumps;
- Sample aerosols using a volumetric flow controlled high volume sampler;
- Analyze underway trace gas with a Membrane Inlet Mass Spectrometer (MIMS) and a Gas Chromatograph;
- Conduct incubations for productivity measurements with different isotopic tracers;
- Conduct 2 ocean acidification experiments;
- Sample sea ice melt ponds;
- Deploy 4 Argo floats in the Baffin Bay region;
- Sample 15 rivers in the Canadian Arctic Archipeago;
- Deploy moorings in Queen Maud Gulf;
- Conduct multibeam surveys at selected sites and while transiting;
- Sample 15 biophysical stations distributed in the Labrador Sea, Baffin Bay and Canadian Arctic Archipelago.

3.1.1 GEOTRACES program

As part of the international GEOTRACES program (www.geotraces.org), the principal mandate of the Canadian Arctic GEOTRACES project was the study input, removal and cycling of trace elements and isotopes in the water column, and to use this information to document, monitor, and predict the evolution of physical and biogeochemical processes in the Arctic Ocean. The project also included extensive biological and trace gases components of direct relevance to the long-term goals of ArcticNet, which facilitated coordination of sampling for both programs.

3.2 Synopsis of Operations

This section provides a general synopsis and timeline of operations during Leg 2. Detailed cruise reports provided by onboard participants and including specific objectives, methodology and preliminary results for projects conducted during this leg are available in Part II of this report.

During this leg, the *Amundsen* traveled from Quebec City (10 July) to Kugluktuk (20 August) and 16 stations were visited with an overall tally of operations and activities as follows:

- 31 GEOTRACES' trace metal clean CTD-Rosette casts;
- 67 ArcticNet's CTD-Rosette casts;
- 24 GEOTRACES' six large volume pumps casts
- 16 light and phytoplankton profiles, including Secchi disk and PNF;
- 29 plankton tows and trawls, including horizontal and vertical net tows, and IKMT;
- 22 XCTDs deployments;
- 1 GEOTRACES trace metal clean deck pump deployment.

A detailed scientific log for all sampling operations conducted during Leg 2 giving the positions and depths of the visited stations is available in Appendices 1 and 2.

3.2.1 Timeline of operations

The CCGS *Amundsen* left Quebec City on 10 July and completed operations at 2 Full stations (K1 and LS2) and 8 XCTD stations in the Labrador Sea. On 19 July, underway to Baffin Bay, the ship was unexpectedly diverted to Hudson Bay for ice-breaking duties. This unfortunate turn of events resulted in a 2- week hiatus (from 19 July to 3 August) and a need to dramatically reduce the science plan. To the benefit of the GEOTRACES program, ArcticNet cancelled nearly all its stations and the remaining science plan was reduced to occupying 3 of the 4 GEOTRACES Baffin Bay stations (BB1, BB2 and BB3) and 7 of the 9 Archipelago stations (CAA1, CAA2, CAA3, CAA4, CAA5, CAA6 and CAA7) (Figure 3.2). GEOTRACES sampling strategy in the CAA was also adjusted to existing ice conditions and to optimize scientific return within the remaining time. By the end of Leg 2, ArcticNet had lost most of its stations not shared with GEOTRACES (except for AN323, AN324, AN312 and AN 314), while GEOTRACES lost 3 of its 15 stations : Station BB4 in Baffin Bay and 2 stations in the CAA (Figure 3.2), the latter two were sampled during the following Leg 3b.

Seabed mapping and sub-bottom stratigraphy were conducted during transit between stations, using a multibeam sonar and a CHIRP sub-bottom profiler. The deployment of BioArgo floats in Baffin Bay was attempted but failed because of ballasting problems. The ship arrived in Kugluktuk for a full crew change on 20 August.



Figure 3-2. Proposed cruise track for the 2015 CCGS *Amundsen* Expedition - Leg 2. Stations that had to be cancelled as a result of spending two weeks in Hudson Bay for escort duty are circled.

3.3 Chief Scientist's comments

During Leg 2, the *Amundsen* two weeks reassignment to de-icing and escort operations in Hudson Strait and Hudson Bay resulted in major consequences on the science program. Although the GEOTRACES program was preserved, most of the ArcticNet's planned stations could not be sampled, which is problematic for many participants.

Despite the hiatus, 16 stations were completed, resulting in 1545 seawater or marine particle samples for multi-element and isotopic analysis, which will amount to 5336 measurements, and additional zooplankton, ichthyoplankton and fish samples.

A total of 434 incubations were conducted for carbon fixation and nutrient uptake measurements, detailed as follows:

- 156 twelve-hour ^{14}C incubations
- 88 two-hour ^{14}C incubations
- 60 ^{13}C and ^{15}N incubations
- 60 ^{32}Si incubations
- 60 ^{18}O incubations
- 10 ^{55}Fe incubations

Three CO_2 manipulation experiments and sampling operations at 15 Arctic rivers draining in the CAA were also successfully completed.

4 Leg 3a - 20 August to 4 September 2015 – Amundsen Gulf and Beaufort Sea

Chief Scientist: Keith Lévesque¹ (keith.levésque@arcticnet.ulaval.ca)

¹ ArcticNet, 1045 avenue de la Médecine, Université Laval, Québec (QC), G1V 0A6, Canada.

4.1 Introduction

Leg 3a of the 2015 Expedition took place from 20 August to 4 September and combined research programs from ArcticNet, GEOTRACES and Industry (Figure 4-1). One of the main objectives was to recover seven moorings and redeploy five new ones as part of ArcticNet's Long-Term Oceanic Observatories project and the integrated Beaufort Observatory (iBO) project funded by the Environmental Study Research Fund (ESRF).

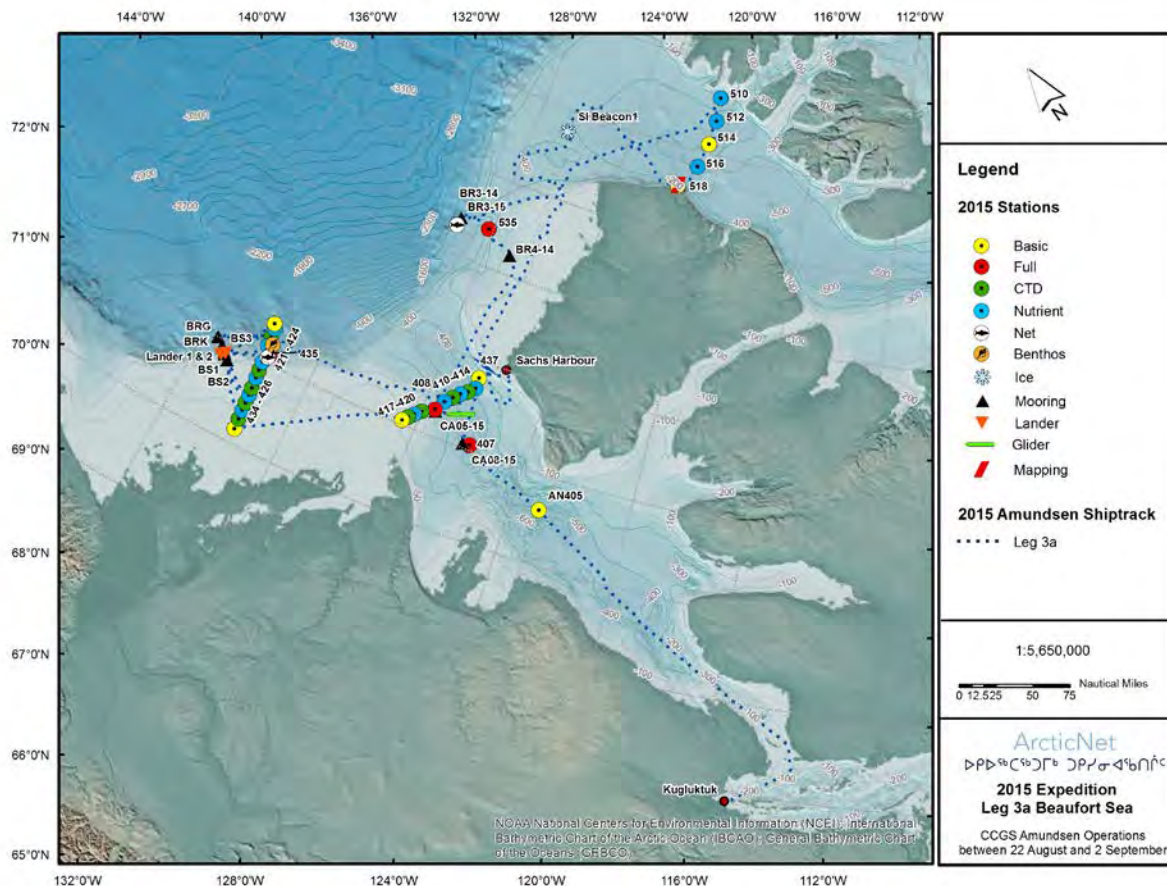


Figure 4-1: Ship track and the location of stations sampled in the Amundsen Gulf and Beaufort Sea during Leg 3a.

The specific objectives of Leg 3a were to:

- Refuel the ship in Kugluktuk on 21 August (~14 hours);
- Recover 7 oceanographic moorings in the Mackenzie Shelf/Southern Beaufort Sea area;
- Deploy 5 oceanographic moorings in the Amundsen Gulf/Mackenzie Shelf/Southern Beaufort Sea area as part of the ArcticNet Long-Term Oceanic Observatories project and the integrated Beaufort Observatory program;
- Deployment and recovery of two underwater gliders in the Beaufort Sea as part of the GEOTRACES program;
- Conduct basic sampling operations at stations along designated transects in the Mackenzie Shelf/Southern Beaufort Sea area as part of the ArcticNet program;
- Deploy four box cores at Full Stations #407 and #435 for macrobenthic biodiversity, grain size, organic content, meiofauna community structure, stable isotope signature, pigments, CNP content, contaminants and sediment surface water;
- Deploy up to four GPS position only beacons on the sea ice, each coupled with a surface meteorological station;
- Deployment of two bottom landers on the Mackenzie Shelf Slope;
- Conduct basic sampling operations at selected stations in the Beaufort Sea;
- Deployment of one POPS buoy;
- Deployment of Zodiac for surface water sampling (CH₄) in the east and west channels of the Mackenzie River estuary.
- Conduct science operations at 1 additional station within the framework of the Holocene Paleoceanography project (UQAR).

4.1.1 iBO (*Integrated Beaufort Observatory*)

This initiative establishes a regional ocean, sea ice and atmosphere observing system in the Canadian Beaufort Sea, called the integrated Beaufort Observatory (iBO). The project uses a series of integrated state-of-the-art environmental technologies deployed on ocean moorings in the Beaufort Sea to enable systematic observation of the marine environment including ice and ocean conditions. Ultimately, this information will enhance the numerical models required for planning and review of offshore activities throughout the region (see http://www.esrfunds.org/resstu_e.php for more information).

4.2 Synopsis of Operations

This section provides a general synopsis and timeline of operations during Leg 3a. Detailed cruise reports provided by onboard participants and including specific objectives, methodology and preliminary results for projects conducted during this leg are available in Part II of this report.

During this leg, the *Amundsen* traveled from Kugluktuk (20 August) to Sachs Harbour (4 September) and 50 stations were visited with an overall tally of operations and activities as follows:

- 19 CTD casts;
- 41 CTD-Rosette casts;
- 20 light and phytoplankton profiles, including Secchi disk and PNF;

- 29 plankton tows and trawls, including horizontal and vertical net tows, and Hydrobios;
- 14 Box coring stations;
- 12 Agassiz trawls;
- 1 Ice stations;
- 8 mooring recoveries;
- 2 mooring deployments and 3 re-deployments;
- 2 underwater gliders deployments;
- 2 bottom landers deployments;
- 1 dedicated bathymetry / sub-bottom mapping survey.

4.2.1 *Timeline of operations*

Leg 3a started in Kugluktuk, NU on 20 August, coinciding with a full Coast Guard crew change. Participants and Coast Guard crewmembers joined the ship using a chartered Boeing 737, which left Quebec City at 7:00 AM on 20 August and landed in Kugluktuk at 10:30 AM local time on the same day. Following the crew change, the *Amundsen's* spent a day at anchor to refuel, while Leg 3a participants prepared their laboratories and sampling equipment. A series of Safe Work Instructions Meetings also took place on 21 August to familiarize science participants and Coast Guard crew with the operations scheduled to take place during Leg 3a. The ship left Kugluktuk at 16:00 on 21 August and started its transit towards Basic Station 405 in Amundsen Gulf.

Sampling operations at Basic Station 405 were conducted on 22 August from 16:00 to midnight. The next day, operations at Full Station 407 included several deployments of the CTD-Rosette and nets and one deployment of the box core and Agassiz trawl. One autonomous glider fitted with a micro-turbulence package was also deployed as part of the GEOTRACES program. The deployment was conducted from the barge and took approximately 6 hours. Unfortunately, the glider's ballasts were not quite adapted to the water density of the area. The glider had to be recovered later during the day and brought back on board the *Amundsen* for assessment and ballast fine-tuning. Mooring CA-08-15 was successfully deployed at Full Station 407.

Sampling operations at designated stations along the ArcticNet transect between Banks Island and Cape Bathurst were conducted from 24 to 25 August. Mooring CA-05-15 was successfully deployed near Full Station 408. Another attempt was also made to deploy the autonomous glider since the ballasts of the instruments had been adjusted. The glider deployment took place on 24 August from the barge in very calm sea state. The instrument was programmed to survey part of Amundsen Gulf to collect various physico-chemical properties of the water column and then surface on 03 September in Thesiger Bay for recovery by the ship. While transiting in Amundsen Gulf, just north of Cape Bathurst, a pod of bowhead whales and seals were spotted by the Marine Wildlife Observers working from the ship's bridge.

After completing operations in Amundsen Gulf, the ship travelled west to conduct mooring and sampling operations north of Tuktoyaktuk. Moorings BR-K-14, BS-2-14 and BR-G-14 were successfully recovered on 26 August. Mooring BS-1-14 proved more difficult. The

mooring was detected with the EM302 multibeam sonar and showed to be in the normal vertical position. However, after multiple tries to release the mooring by sending an acoustic signal, it would not surface. The mooring team and Coast Guard crew later designed a grapple hook to dredge the bottom and try to dislodge the mooring. On 27 August, the mooring was dislodged and finally surfaced. When the mooring came to the surface, it was noticed that the top synthetic float and the Nortek cage had been damaged during the operation. Nevertheless, all instruments of the mooring, including the acoustic releases, were successfully recovered and in good working order. Mooring BR-K-15 was deployed on the same day as part of the integrated Beaufort Observatory project.

All science operations were cancelled from 18:00 on 27 August to 06:00 on 28 August due to a severe storm with winds gusting up to 45 knots from the northwest.

After completing a Nutrient station on the morning of 28 August, the mooring BR-G-15 was successfully deployed in the Beaufort Sea, and the ArcticNet mooring BS3-14 was successfully recovered. Two seabed-instrumented landers were deployed in the evening to investigate bottom currents and associated sediment transport. While the first deployment proved to be hassle-free at a shallow site on the Mackenzie Shelf Slope, the second one resulted in complications. In fact, after deploying the lander at a deeper site, it was noticed that several meters of line were still floating at the surface. The anchor and lander had probably not been deployed far apart enough to bring the line close to the bottom. On 29 August, an attempt to return on site to detect the orange line, was made. In growing seas, no line was detected and the attempts to retrieve the lander or sink the line was abandoned for this leg.

On 29 August, the ship completed a suite of sampling operations along a northern transect in the Beaufort Sea. A total of 8 stations were sampled, inclusive of 3 CTD, 3 Nutrient, 1 Full and 1 Basic stations. The *Amundsen* then transited north-east on 30 August to successfully recover mooring BR-4-14.

In the early morning of 31 August, Full Station 535 was completed. The rest of the day was dedicated to the recovery of mooring BR-3-14 and its immediate redeployment. On 1 September, a 9.5-hour time slot was consecrated to ice work. Operations at 2 Basic and 3 Nutrient stations were thereafter completed, drawing the leg to a close. The ship reached Sachs Harbour on 4 September for a science personnel rotation.

4.3 Chief Scientist's comments

Overall Leg 3a was successful: 50 biophysical stations were sampled and all of the mooring operations were successfully conducted. On behalf of all science personnel, our thanks and gratitude to the Commanding Officer, the officers and the crew, who accompanied us superbly during the leg.

5 Leg 3b – 4 September to 1 October 2015 - Amundsen Gulf and Beaufort Sea

Chief Scientist: Roger François¹ (rfrancoi@eos.ubc.ca)

¹ Department of Earth, Ocean and Atmospheric Sciences, University of British Columbia, 2020-2207 Main Mall, Vancouver, BC, V6T 1Z4, Canada.

5.1 Introduction

Starting on 4 September in Sachs Harbour, and ending on 1 October in Resolute, Leg 3b was a joint ArcticNet-GEOTRACES mission. On this leg, the Canadian GEOTRACES project was complemented by a 4-day process study in Penny Strait, using a Moving Vessel Profiler to study mesoscale mixing in Wellington, Maury and Perry Channels and assess the impact of these physical processes on the supply of nutrients to surface waters. The ArcticNet program included sea ice work, box coring, net casts, and a mooring deployment in Queen Maud Gulf (Figure 5-1).

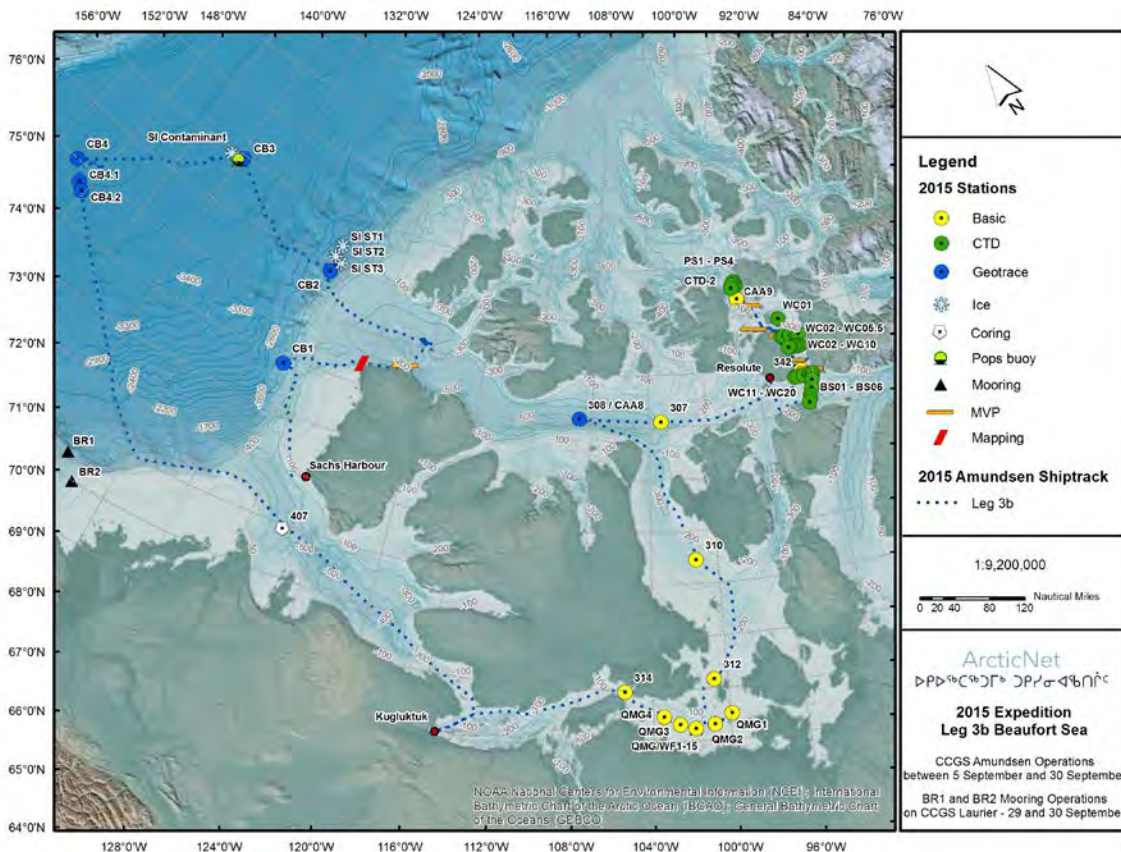


Figure 5-1: Ship track and the location of stations sampled in the Amundsen Gulf and Beaufort Sea during Leg 3b.

The specific objectives of the mission were to:

- Collect seawater with ArcticNet's Rosette;
- Collect seawater under trace metal clean conditions with GEOTRACES' Rosette;
- Sample particulates with 6 McLane large volume *in-situ* pumps;
- Sample aerosols using a volumetric flow controlled high volume sampler;
- Deploy 1 mooring in Queen Maud Gulf;
- Conduct Moving Vessel Profiler and CTD mesoscale and mixing survey in Wellington, Maury, and Perry Channels;
- Conduct multibeam surveys at selected sites and while transiting;
- Sample biophysical stations distributed in the Amundsen Gulf and Beaufort Sea.

5.2 Synopsis of Operations

This section provides a general synopsis and timeline of operations during Leg 3b. Detailed cruise reports provided by onboard participants and including specific objectives, methodology and preliminary results for projects conducted during this leg are available in Part II of this report.

During this leg, the ship traveled from Sachs Harbour (4 September) to Resolute (1 October) with 15 stations visited and an overall tally of operations and activities as follows:

- 28 CTD casts;
- 33 GEOTRACES' trace metal clean CTD-Rosette casts;
- 32 ArcticNet's CTD-Rosette casts;
- 12 GEOTRACES' six large volume pumps casts
- 44 plankton tows and trawls, including horizontal and vertical net tows, and IKMT;
- 21 box cores;
- 9 Agassiz trawls;
- 6 MVP transects;
- 4 ice work stations;
- 1 POPs buoy deployment;
- 1 mooring deployment;
- 1 SX90 survey.

A detailed scientific log of all sampling operations conducted during the leg with the positions and depths of the visited stations is available in Appendices 1 and 2.

5.2.1 Timeline of operations

The CCGS *Amundsen* sailed from Sachs Harbour on 4 September to reach the first station (CB1) in McClure Strait on 5 September, where GEOTRACES (hydrocasts and pump casts) and ArcticNet (net casts, box cores) operations were conducted until 7 September.

Operations at the dedicated station were interspersed with a mapping event and a 5.5-h MVP transect on 6 September. The ship then crossed the Canada Basin to reach Station CB4 on 8 September. The latter station was the location chosen for a cross-over station for intercalibration with the US Arctic GEOTRACES program. Operations were conducted until 10 September and included 3 ice work events, which totted up 7 hours. The US cruise occupied the same station one week after the *Amundsen* occupation. However, because of bad weather, they could not deploy their trace metal clean system and could only measure hydrography and sample the non-contamination prone key trace elements and isotopes (e.g. Nd, Th, Pa). For contamination-prone elements, our US partners have taken replicate samples at 4 depths at a nearby station (73.5N, 158.6W) that will be exchanged between relevant PIs from each cruise. In addition, they bracketed the 75°N crossover station with stations to the North and South with full water column profiles of the key TEIs that will facilitate intercalibration for the Canadian 75°N data set and the US data sets via the Carina GO-SHIP interpolation routine recently published (Lauvset and Tanhua; *Limnology and Oceanography: Methods*, in press).

After completion of the work at Station CB2, the ship transited north and conducted ice work operations on September 10. The *Amundsen* then headed north-west to reach Station CB3, where sampling operations succeeded one another until 13 September. A short ice work event as well as a POPs buoy deployment also took place on 12 September. On 14 September, sampling operations began at Station CB4. Intercalibration for aerosol sampling was performed at Stations CB4.1 and CB4.2.

Following the completion of work in Canada Basin, the ship sailed to the Amundsen Gulf to conduct benthic work at Station 407 on 18 September. On 20 and 21 September, a suite of sampling operations were completed at Stations 314, QMG4, QMG3, QMG2 and QMG1. Mooring WF1-15 was also successfully deployed in Queen Maud Gulf.

We then proceeded to McClintock and Parry channel to occupy time-series ArcticNet stations (312 and 310) and one GEOTRACES station that was missed during Leg 2 (CAA8). A suite of sampling operations were thereafter conducted at Stations 307 and 342 on 25 September.

On 26 September, two MVP surveys, totting up 17 hours, were completed around Cornwallis Island. Sampling at Station CAA9 started in the late evening of the same day. The leg ended with multiple CTD casts and two MVP surveys. The ship arrived in Resolute for a full crew change on 1 October.

5.3 Chief Scientist's comments

On behalf of all science personnel, our thanks and gratitude to the Commanding Officer, the officers and the crew, who accompanied us superbly during the leg.

6 Leg 4a – 1 to 11 October 2015 – The Canadian Arctic Archipelago and Baffin Bay

Chief Scientist: Philippe Archambault¹ (philippe.archambault@uqar.ca)

¹ Institut des sciences de la mer, UQAR, 310 Allée des Ursulines, Rimouski (QC), G5L 3A1
Canada.

6.1 Introduction

Leg 4a took place from 1 to 11 October and focused on ArcticNet's marine-based research program in the Canadian Arctic Archipelago and Baffin Bay, starting in Resolute and ending in Pond Inlet (Figure 6-1).

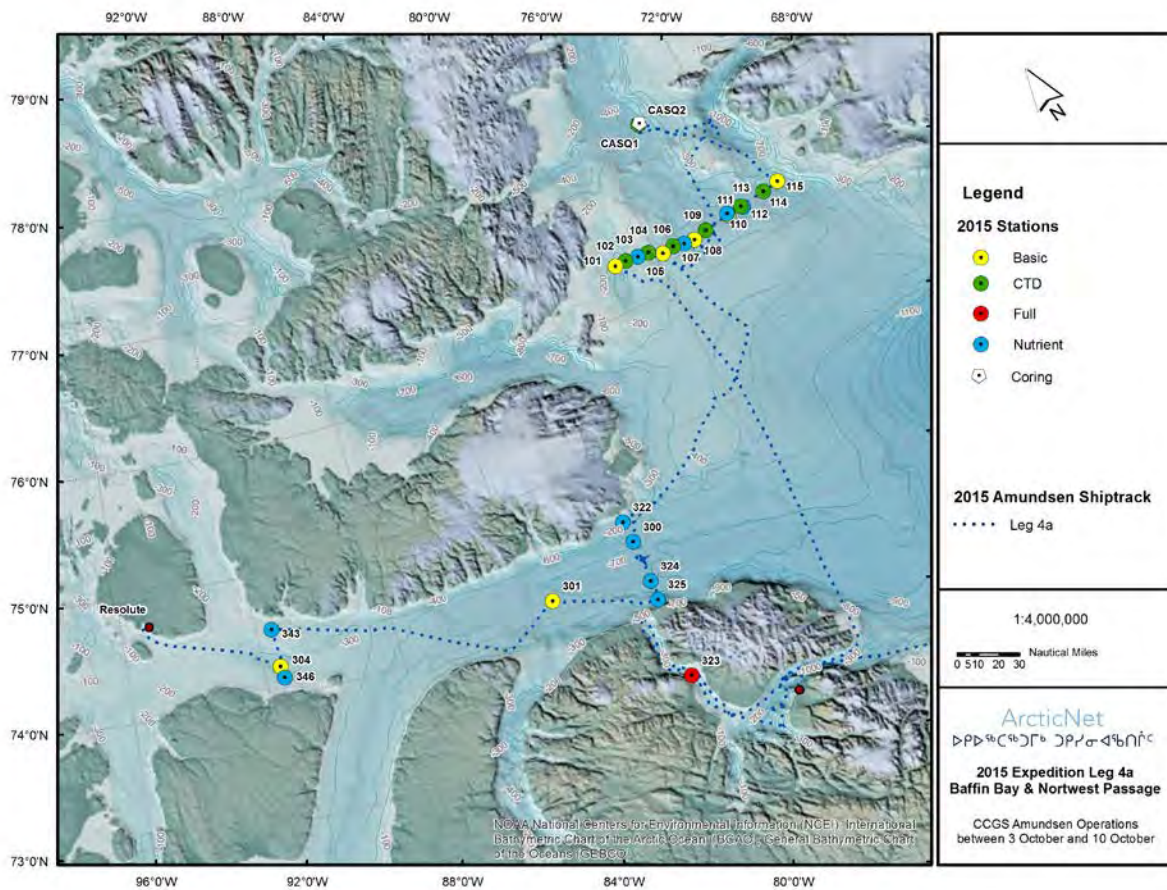


Figure 6-1. Ship track and the location of stations sampled in the Canadian Arctic Archipelago and Baffin Bay during Leg 4a.

The specific objectives and priorities of Leg 4a were to:

- Conduct sampling operations at 5 designated stations at the entrance of Lancaster Sound;
- Conduct sampling operations at Basic Station 301 in Lancaster Sound;
- Conduct sampling operations at 5 designated stations in Barrow Strait;
- Conduct sampling operations at designated stations along the Ellesmere – Greenland transect in northern Baffin Bay (76°N);
- Deploy four box cores at Full Stations 323 and 101 or 108;
- Survey the ice island fragment PII_2012_A-1_c in northern Baffin Bay;
- Conduct CASQ coring operations at two stations in northern Baffin Bay as part of a collaboration between ArcticNet, GreenEdge and ICE-ARC scientists;
- Conduct a 5h multibeam survey of an ice island scour in Northern Baffin Bay.

6.2 Synopsis of Operations

This section provides a general synopsis and timeline of operations during Leg 4a. Detailed cruise reports provided by onboard participants and including specific objectives, methodology and preliminary results for projects conducted during the leg are available in Part II of this report.

During this leg, 26 stations were visited with an overall tally of operations and activities as follows:

- 7 CTD casts;
- 29 CTD-Rosette casts;
- 12 light and phytoplankton profiles, including Secchi disk and PNF;
- 25 plankton tows and trawls, including horizontal and vertical net tows, and IKMT;
- 10 box cores;
- 8 Agassiz traws;
- 1 CASQ core.

A detailed scientific log of all sampling operations conducted during the leg with the positions and depths of the visited stations is available in Appendices 1 and 2.

6.2.1 Timeline of operations

Leg 4a started on 2 October with a slight delay due to weather conditions that prevented scientific and Coast Guard crewmembers from landing in Resolute. Following a full crew change, the ship transited towards Full Station 304, where sampling operations were conducted from 3 to 4 October. After a small transit, Nutrient Stations 346 and 343 were completed. At 11:00 AM on 4 October, the ship was called for a Search and Rescue operation at Arctic Bay. Fortunately, the people were found and the *Amundsen* resumed its transit with a detour of 125 nautical miles.

On 4 and 5 October, Basic (301, 323) and Nutrient (325, 324, 300 and 322) stations were completed before transiting to collect a Beacon belonging to the ice island mass balance project led by D. Mueller. Unfavourable ice and wind conditions (wind > 35 knots) resulted in the completion of Nutrient Station 109 on 7 October. Stations 110 to 115 were completed on the following day, and the ship reached Station CASQ-1. Once the safety meeting completed, an attempt was made to deploy the CASQ core. Unfortunately, during the deployment, the weight at the head of the device was lost. By the time a solution was found to this issue, the ship transited to Station CASQ-2. On 8 October, a CASQ operation was conducted at the station and 5.8 m of sediment were sampled.

Heavy ice conditions on 9 October prevented the deployment of horizontal samplers (e.g. Agassiz trawl and Tucker) and forced the cancellation of the ice island scour survey. However, Stations 108, 107, 106, 105 and 104 were successfully completed. In the morning of 10 October, operations at Stations 103, 102 and 101 were conducted, with the exception of horizontal sampling devices. The ship then transited towards Pond Inlet, where a scientific crew rotation was completed to welcome Schools on Board students.

The Chief Scientist's comments can be found at the end of Leg 4c, in Section 8.3 below.

7 Leg 4b – 4c – 11 October to 1 November 2015 – Baffin Bay and Labrador Sea

Leg 4b – 11 to 26 October 2015 – Baffin Bay

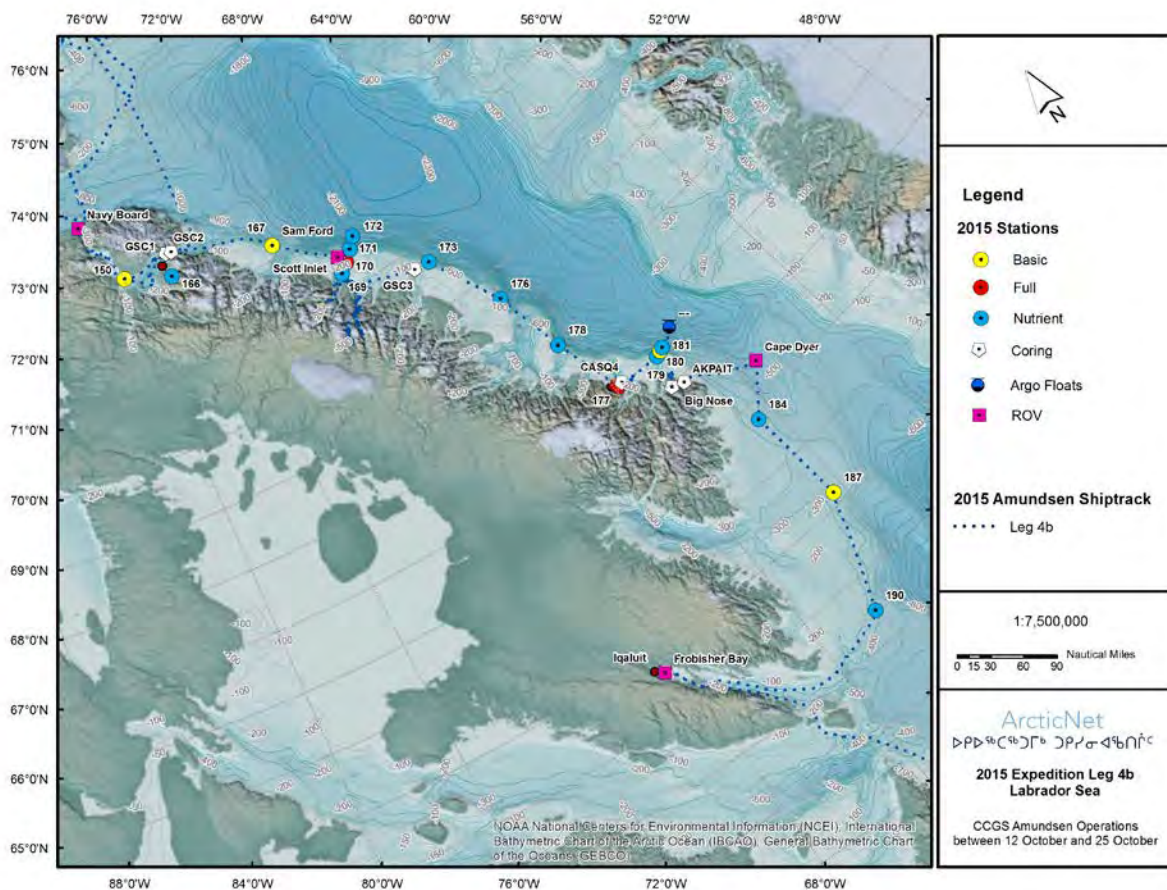
Leg 4c – 26 October to 1 November 2015 – Baffin Bay and Labrador Sea

Chief Scientist: Philippe Archambault¹ (philippe.archambault@uqar.ca)

¹ Institut des sciences de la mer, UQAR, 310 Allée des Ursulines, Rimouski (QC), G5L 3A1 Canada.

7.1 Introduction

Leg 4b-4c took place from 11 October to 1 November and focused on ArcticNet’s marine-based research program in Baffin Bay, from Pond Inlet to Iqaluit, and in the Labrador Sea (Figure 7-1).



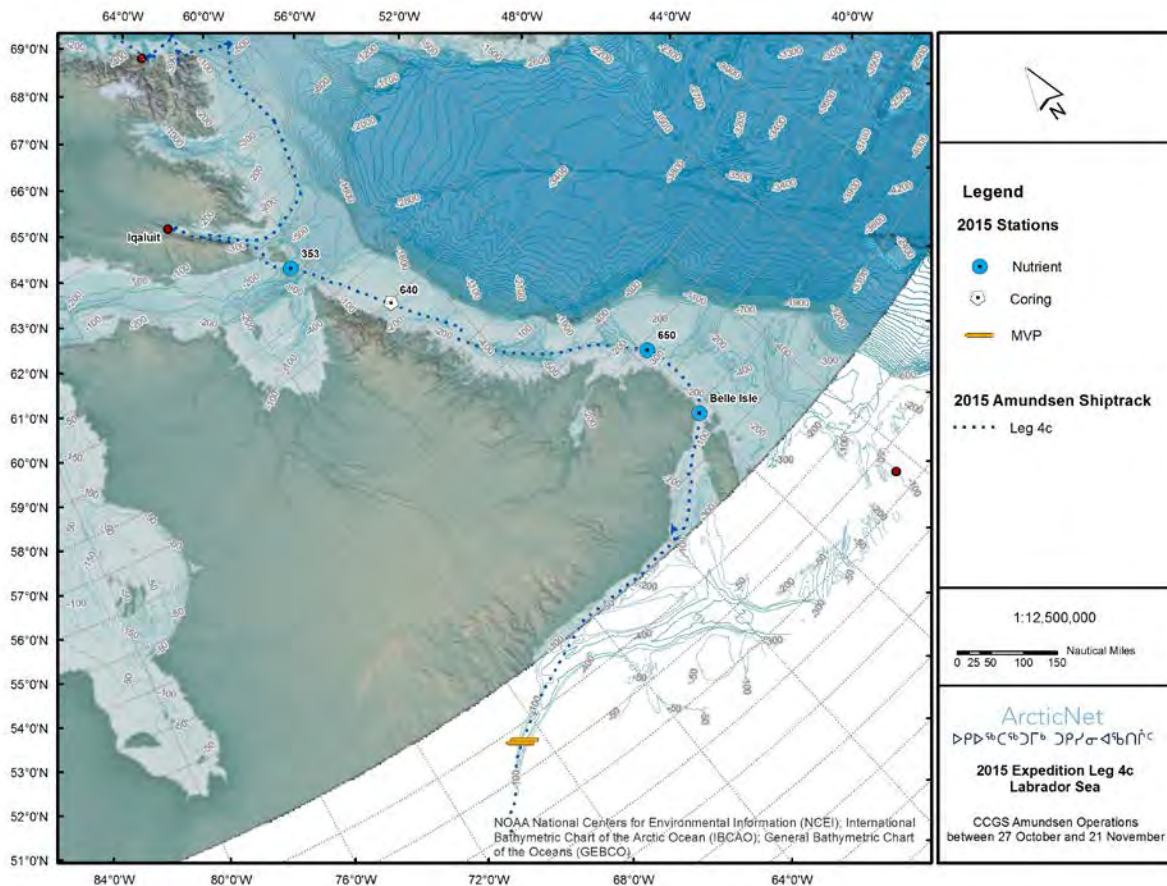


Figure 7-1: Ship track and the location of stations sampled in Baffin Bay and in the Labrador Sea during Legs 4b and 4c.

The specific objectives and priorities were to:

- Conduct ROV dives at 5 designated sites: Navy Board Inlet, Pond Inlet, Scott Inlet, Cape Dyer and Frobisher Bay (backup site for Cape Dyer is Southwind Fjord);
- Collect a piston core and box core at two designated sites near Pond Inlet for the Geological Survey of Canada (GSC);
- Conduct an 18h survey of an ice island fragment (or several fragments) along the coast of Baffin Island;
- Collect a CASQ core at a site 3nm southeast of Full Station 170 (with short multibeam survey);
- Conduct a multibeam survey of Scott Inlet fjord (~10 hrs);
- Collect a CASQ or piston core in Scott Inlet fjord;
- Conduct a multibeam survey of Sam Ford fjord (~10 hrs);
- Collect a CASQ or piston core in Sam Ford fjord;
- Conduct a multibeam survey (~3hrs) and collect one piston core and one box core at Station GSC-3;
- Conduct sampling operations at designated stations along the coast of Baffin Island;

- Collect water samples at several stations along the coast of Baffin Island at the 350m isobath;
- Collect three box cores at Full Station 170;
- Deploy a benthic lander at Full Station 177;
- Collect four box cores at Full Station 177;
- Conduct a short multibeam survey and collect a CASQ core at Full Station 177;
- Conduct short multibeam surveys in Giff's Cove, Big Nose Fjord and Akpait Fjord;
- Collect piston and box cores in Giff's Cove (2 sites), Big Nose Fjord (1 site) and Akpait Fjord (1 site);
- Collect one piston core in Frobisher Bay;
- Transfer significant amount of cargo from the community of Qikiqtarjuaq to the *Amundsen* in support of the GreenEdge program (to be carried out when at Full Station 177);
- Deploy two Argo floats east of Station 181;
- Conduct a multibeam survey in outer Frobisher Bay in 400m of water (extend existing coverage).

7.2 Synopsis of Operations

This section provides a general synopsis and timeline of operations during Leg 4b-4c. Detailed cruise reports provided by onboard participants and including specific objectives, methodology and preliminary results for projects conducted the leg are available in Part II of this report.

During this leg, 33 stations were visited with an overall tally of operations and activities as follows:

- 4 CTD casts;
- 28 CTD-Rosette casts;
- 4 light and phytoplankton profiles, including Secchi disk and PNF;
- 17 plankton tows and trawls, including horizontal and vertical net tows, and IKMT;
- 18 box cores;
- 10 piston cores;
- 6 Agassiz traws;
- 6 ROV deployments;
- 1 Lander deployment;
- 1 Argo float deployment;
- 2 MVP transects;
- 1 CASQ core.

A detailed scientific log of all sampling operations conducted during the leg with the positions and depths of the visited stations is available in Appendices 1 and 2.

7.2.1 Timeline of operations

The scientific crew change was completed by 5:30 PM on 11 October. As to fulfill the required rest time period for the CSSF team, the original schedule was modified. The ship conducted operations at Basic Station 155 in the morning of 12 October before transiting for 7.5h to reach to Navy Board Station where the Sumo was deployed. The dive was not optimal, as the thrusters of the ship seemed to interfere with the ROV navigation. Despite difficulties, a 2h video of the seafloor was successfully recorded.

The ship then transited towards Basic Station 150, where sampling activities were conducted until the morning of 13 October. On the same day, piston cores were collected at Stations GSC1 and GSC2. The ROV dive initially planned in Pond Inlet was cancelled due to adverse weather conditions and the *Amundsen* transited towards Nutrient Station 166.

On 14 October, strong winds (>35 knots) prevented the deployment of any sampling gear. As to avoid weather, the ship entered Sam Ford Fjord to perform mapping and deploy the piston core at Station LM3. A brief lull on 15 October allowed getting out of the fjord to conduct operations at Full Station 170, as well as at Nutrient Stations 171 and 172. The ship then headed back in the fjord due to adverse weather conditions. Mapping was conducted while transiting. On 16 October, the *Amundsen* reached to Scott Inlet, where the elevator and two box cores were successfully deployed. A ROV dive was also planned, but the decreasing light intensity forced the postponement of the operation. Meanwhile, the Nutrient Station 169 was completed and 2 hours of mapping were dedicated to surveying CASQ3 site.

On 17 October, the CSSF team started deploying the ROV early in the morning. However, cable issues forced once again the postponement of the dive. At 11:52 AM the ROV was launched and the team collected many coral and sponge samples in addition to recording a 2-hour video. The ROV was brought back onboard the ship at 15:00 PM.

With the night crew being uncomfortable with the deployment of the CASQ core, it was decided that the operation would be postponed until the following morning. Although this situation delayed the schedule substantially, it allowed completing the mapping of the Scott Inlet area. The CASQ core was successfully and safely deployed in the morning of 18 October. The *Amundsen* then transited southeast for 6 hours to deploy a piston core at Station GSC3. Nutrient Stations 173, 176 and 178 were thereafter successively completed.

Following a 5h transit to Qikiqtarjuaq, the crew successfully managed to upload within 2,5 hours all of the Green Edge samples and equipment to be brought back to Quebec City. The ship then transited towards Full Station 177, where sampling operations, a lander deployment and a 3h ROV dive were conducted until 20 October. Following on the ROV recovery began an ice island fragment survey. Fragment PII-A-1-f from the 2012 Petermann Glacier calving event was targeted and operations began at 7:30 AM on 20 October. Three consecutive helicopter trips were necessary as to transfer equipment and four participants on the ice island. A stationary IPR and a meteorological station were successfully installed

before 12:30 PM. Meanwhile, the *Amundsen* mapped the 2012 Petermann Glacier using the EM302 sonar and the SX90 fishing sonar.

On 21 October, Station CASQ4 was sampled using the box core, as weather conditions could not allow the deployment of the CASQ. Following a short transit, Nutrient Station 179 and Basic Station 180 were completed.

Beacon deployments and photogrammetry surveys occurred on 21 and 22 October. It was found once the helicopter departed that the tabular iceberg was a sloping one, causing the beacon to roll off the iceberg after deployment. The photogrammetry survey went on at 800 and 1200 feet aboard the helicopter. Another small ice island fragment was also visited on 22 October and a Polar iSVP beacon was successfully deployed.

One objective of the expedition was to deploy two Takuvik's BioArgo floats in the Baffin Bay region. A compromise between the time available for the operation and the minimum distance from the coast for a safe deployment was found and takapm003c was deployed on 22 October at 15:35. The float takapm010c was deployed shortly after.

Before transiting towards Big Nose and Akpait fjords, Nutrient Station 181 was completed. Three piston core operations were thereafter conducted within the fjords on 22 October. The ship transited southeast for 6.5 hours to Cape Dyer, where a bathymetric survey was completed prior to a ROV dive. This dive site was chosen based on records of sponge bycatch and high concentrations. While the initial dive plan included a 4 km transect, only 935 m could be completed due to mechanical/electrical issues with the ROV and rough seas. The ship went on with the operations at Nutrient Station 184, Basic Station 187 and Nutrient Station 190.

The *Amundsen* reached Frobisher Bay on the morning of 25 October and proceeded with a suite of piston and box core deployments. A ROV dive took also place off the coast of Hill Island in Inner Frobisher Bay. The site was selected based on the presence of two distinct slope failure scars, each with a different morphology. Due to problems from the previous dive and time constraints, 1.2 km out of the 4.2 km initially planned was surveyed in one of the landslides and on a single high-slope feature.

On the morning of 26 October, a scientific crew rotation was completed in Iqaluit. Thirteen scientists disembarked and 1 got onboard. From 27 October to 1 November, a suite of 4 Nutrient stations as well as a MVP transect were completed as the ship transited southward. On 1 November, the ship reached its homeport in Quebec City.

7.3 Chief Scientist's comments

First, I would like to congratulate and express my sincerely thank to everyone on board scientific and coast guard crew for their work and efforts in making Leg 4 a success. The ice and weather conditions were not always collaborative but everyone were willing to accept

changes and adapt their research for the benefit of all members onboard. Second, a very special thank you to Captain Gariépy, the officers and crew of the CCGS *Amundsen* for their help, professionalism and team spirit that made our time onboard the ship so special.

Part II – Project reports

1 Biogeochemistry of the inorganic carbon cycle, surface climate, air-surface fluxes and carbon exchange dynamics – Legs 4a and 4b

ArcticNet Phase 3 – Carbon Exchange Dynamics in Coastal and Marine Ecosystems.
<http://www.arcticnet.ulaval.ca/pdf/phase3/carbon-dynamics.pdf>

Project leader: Tim Papakyriakou¹ (papakyri@cc.umanitoba.ca)

Cruise participant Legs 4a and 4b: Sebastian Luque¹

¹ *University of Manitoba, Centre for Earth Observation Science (CEOS), Wallace Building, Winnipeg, MB, R3T 2N2, Canada.*

1.1 Introduction

The ocean's exchange of carbon dioxide with the atmosphere is governed by the biogeochemical cycling of carbon and physical processes throughout the water column, which determine the concentration of dissolved inorganic carbon (DIC) and total alkalinity (TA) in the surface waters. Out of the four measurable carbon system parameters (DIC, TA, pH and pCO₂), a minimum of two is needed to calculate the others and fully describe the inorganic carbon chemistry, over-determination of the system being beneficial.

Biological activity alters the chemical signatures of the water, affecting both the isotopic carbon ratio ($\delta^{13}\text{C}$) and dissolved inorganic carbon (DIC) concentrations. Phytoplankton incorporates carbon into their organic matter and preferentially selects light carbon (¹²C) over the heavier carbon isotope (¹³C). This biological fraction leads to isotopically heavy productive surface waters exhibiting low concentrations of DIC. At depth, particularly below the pycnocline, the organic carbon from sinking particulate matter is remineralized into DIC and the waters become isotopically light due to the release of ¹²C. These signals can provide powerful insight into the biological processes occurring in the water column. Further processes alter the C-isotopic signature of DIC are the uptake of isotopically lighter anthropogenic CO₂ from the atmosphere, and from terrestrial sources (runoff) revealing individual DI^{13}C characteristics. Together with further oceanographic tracers, DI^{13}C data will be used to unravel processes controlling the observed DIC distributions in the investigation area.

The surface meteorology and flux program of the *Amundsen* is designed to record basic meteorological and surface conditions, and to study exchanges of momentum, heat and mass across the atmosphere-sea ice-ocean interface.

Specific objectives of this sampling program are:

- Develop a process-level understanding of the exchange dynamics of heat, CO₂, and momentum;
- The development of tools (observations, models, remote sensing) to assist with regional budgeting of the above variables;
- Forecast how the ocean's response to climate change and variability will affect the atmosphere-ocean cycling of CO₂.

Table 1-1 lists the variables that are monitored, the location where the sensor is installed, the purpose for each variable, along with the sampling and averaging frequency (if applicable).

Table 1-1. Summary of variable inventory and application.

Variable	Instrumentation	Location	Purpose	Sample/Average Frequency (s)
Air temperature (Ta)	HMP45C-212	Foredeck tower	Meteorological parameter	1 / 60
Relative humidity (RH)	HMP45C-212	Foredeck tower	Meteorological parameter	1 / 60
Wind speed (ws-2D)	RM Young 05106-10	Foredeck tower	Meteorological parameter	1 / 60
Wind direction (wd-polar)	RM Young 05106-10	Foredeck tower	Meteorological parameter	1 / 60
Barometric pressure (Patm)	Vaisala PTB101B	Foredeck tower	Meteorological parameter	1 / 60
Sea surface temperature (T _{sf})	Apogee SI-111	Foredeck	Meteorological parameter	1 / 60
Incident solar radiation	Eppley Pyranometer	Wheel-house platform	Heat budget, microclimate	2 / 60
Incident long-wave radiation	Eppley Pyrgeometer	Wheel-house platform	Heat budget, microclimate	2 / 60
Photosynthetically active radiation (PAR)	Kipp & Zonen PARLite	Wheel-house platform	Heat budget, microclimate	2 / 60
Barometric pressure (mbar)	All Sensors BARO-A-4V-MINI-PRIME	Foredeck tower	Air-sea flux	0.1 (10 Hz)
Upper sea water temperature (T _{sw})	General Oceanics 8050 pCO ₂	Under-way system, Forward engine room	Air-sea flux, ancillary information	3 / 60
Sea water salinity (s)	General Oceanics 8050 pCO ₂	Under-way system, Forward engine room	Air-sea flux, ancillary information	3 / 60
Dissolved CO ₂ in seawater	General Oceanics 8050 pCO ₂	Under-way system, Forward engine room	Air-sea flux, ancillary information	3 / 60
pH	General Oceanics 8050 pCO ₂	Under-way system, Forward engine room	Air-sea flux, ancillary information	3 / 60
Dissolved O ₂ in seawater	General Oceanics 8050 pCO ₂	Under-way system, Forward engine room	Air-sea flux, ancillary information	3 / 60

1.2 Methodology

1.2.1 Dissolved Inorganic Carbon Sampling

During Leg 4a and 4b, a total of 529 samples were collected for analysis of DIC and TA (Table 1-2). A further 529 samples were collected for analysis of DI¹³C and 529 for ¹⁸O. All samples were collected in parallel with the Nutrient Rosette. DIC and TA samples were collected in 300 mL bottles and DI¹³C and ¹⁸O samples were collected in 10 mL vials. All samples were spiked with HgCl₂ to stop any further biological changes from taking place.

Table 1-2. Stations sampled for DIC and TA during Legs 4a and 4b.

Station	Type	N Samples	Latitude (N)	Longitude (W)	Cast #	Date
304	Full	16	74°14.819	091°30.881	001	2015-10-03
346	Nutrients	2	74°09.004	091°27.036	003	2015-10-04
343	Nutrients	2	74°32.771	091°31.450	004	2015-10-04
301	Basic	20	74°07.277	083°18.899	005	2015-10-04
325	Nutrients	2	73°49.000	080°29.221	007	2015-10-05
324	Nutrients	2	73°58.607	080°28.036	008	2015-10-05
323	Full	21	74°09.506	080°25.911	010	2015-10-05
300	Nutrients	2	74°19.037	080°29.255	011	2015-10-06
322	Nutrients	2	74°29.620	080°32.154	012	2015-10-06
110	Nutrients	2	76°18.000	073°38.721	014	2015-10-07
111	Basic	19	76°18.276	073°12.498	016	2015-10-07
113	Nutrients	2	76°19.299	072°13.105	018	2015-10-07
115	Full	20	76°20.069	071°12.058	020	2015-10-08
108	Full	18	76°16.079	074°35.144	025	2015-10-09
107	Nutrients	2	76°16.715	074°58.113	026	2015-10-09
105	Basic	16	76°17.692	075°47.968	029	2015-10-10
103	Nutrients	2	76°21.491	076°33.412	031	2015-10-10
101	Full	18	76°22.088	077°22.459	033	2015-10-10
155	Basic	16	72°29.237	078°45.131	036	2015-10-12
166	Nutrients	2	72°29.400	073°43.894	039	2015-10-14
170	Full	16	71°22.871	070°03.773	040	2015-10-15
171	Nutrients	2	71°30.812	069°35.306	042	2015-10-15
172	Nutrients	2	71°39.472	069°08.110	043	2015-10-15
169	Nutrients	2	71°16.384	070°31.726	045	2015-10-17
173	Nutrients	2	70°41.100	066°56.119	048	2015-10-19
176	Nutrients	2	69°35.772	065°21.895	049	2015-10-19
178	Nutrients	2	68°31.384	064°40.216	050	2015-10-19
177	Full	17	67°28.552	063°47.335	051	2015-10-20
179	Nutrients	2	67°26.966	061°55.421	053	2015-10-21
180	Basic	17	67°28.922	061°39.906	055	2015-10-21
181	Nutrients	2	67°30.084	061°31.640	057	2015-10-21
184	Nutrients	2	65°44.413	060°36.677	059	2015-10-23
187	Basic	9	64°10.980	060°23.005	060	2015-10-24
190	Nutrients	2	62°27.671	061°55.284	062	2015-10-24

1.2.2 *Meteorology Tower*

The meteorological tower located on the front deck of the *Amundsen* provides continuous monitoring of meteorological variables. The tower consists of slow response sensors that record bulk meteorological conditions (air temperature, humidity, wind speed/direction, surface temperature). In addition, radiation sensors were installed on the roof of the wheelhouse to provide information on incoming long-wave, shortwave and photosynthetically active radiation. All data were logged to Campbell Scientific dataloggers; a model CR1000 logger was used for the meteorology data, and a CR23X for the radiation data. All loggers were synchronized to UTC time. Ship heading and location (latitude and longitude) were measured to compensate measured apparent wind information for ship direction and motion.

Measurement of meteorological variables were done at 1-second intervals and saved as 1-minute averages. In regard to wind speed and direction, ship motion correction is applied in post-processing.

1.2.3 *Underway pCO₂ System*

A General Oceanics 8050 pCO₂ system has been installed on the ship to measure dissolved CO₂ within the upper 5 m of the sea surface in near real time. The system is located in the engine room of the *Amundsen*, and draws sample water from the ship's clean water intake. The water is passed into a sealed container through a showerhead, maintaining a constant headspace. This set up allows the air in the headspace to come into equilibrium with the CO₂ concentration of the seawater, and the air is then cycled from the container into an LI-7000 gas analyzer in a closed loop. A temperature probe is located in the equilibrator to provide the equilibration temperature. The system also passes subsample of the water stream through an Idronaut Ocean Seven CTD, which measures temperature, conductivity, pressure, dissolved oxygen, pH and redox. All data is sent directly to a computer using software customized to the instrument. The LI-7000 gas analyzer is calibrated daily using ultra-high purity N₂ as a zero gas, and a gas with known CO₂ concentration as a span gas. Spanning of the H₂O sensor is not necessary because a condenser removes H₂O from the air stream before passing into the sample cell.

1.3 **Preliminary results**

At this time, no preliminary results are available.

2 Characterization of the Ocean-Ice-Atmosphere system – Legs 1, 3a and 3b

ArcticNet Phase 3 – Sea Ice, Climate Change and the Marine Ecosystem.

<http://www.arcticnet.ulaval.ca/pdf/phase3/sea-ice.pdf>

Project leader: David Barber¹ (dbarber@cc.umanitoba.ca)

Cruise participants Leg 1: David Barber¹, Lauren Candlish¹, Kerri Warner¹, Greg McCullough¹, Geoff Gunn¹ and Shabnam Jafarikhasragh¹

Cruise participant Legs 3a and 3b: Lauren Candlish¹ and Nathalie Thériault¹

¹ *University of Manitoba, Centre for Earth Observation Science (CEOS), Department of Environment & Geography, Wallace Building, Winnipeg, MB, R3T 2N2, Canada.*

2.1 Introduction

Arctic climate has shown dramatic changes in recent decades. One of the primary indicators of the climate warming is the reduction in the extent of sea ice coverage. Through the years, a discrepancy between observed changes in the extent of the Arctic sea ice cover and the climate model predictions has been observed. Such a gap between observations and predictions can be attributable to a lack of understanding of the processes that govern sea ice melting. From this perspective, there is a need to better understand how much heat flux increases from the ocean to the atmosphere and how it influences the melting of sea ice in the Arctic region. Understanding changes in sea ice cover and surface air temperature is not only important for their direct impacts on local and global climate, but also for their societal impacts on human health, on the structure and functioning of the ecosystems and the economic activity and on new economic development (e.g. new shipping routes and excavation of oil gas in the Arctic Ocean).

This research project aimed to improve the climate predictions model and understand potential accurate climate changes by determining whether the increase of heat flux was associated with the climate variability of Canada. This project is part of an overall research initiative, dedicated to improving upon the understanding of the Arctic as a system, from the ocean, to ice features, and into the upper atmosphere. Globally, this initiative was divided into the following programs:

2.1.1 Upper atmosphere program

The upper atmosphere program was designed to monitor the atmospheric variables that can affect the Arctic atmosphere-ocean interactions. The instrumentation used provided high temporal measurements of temperature, humidity, pressure and wind for the surface up to approximately 20 km. The boundary layer is of particular importance and was monitored using a Microwave Profiling Radiometer (MWRP) at a frequency of approximately 1s.

2.1.2 Network of autonomous equipment

During Legs 1 and 3, the University of Manitoba in collaboration with Statoil and Exxon, respectively, completed an in depth study on the interactions between the ocean-sea ice-atmosphere with respect to dynamics interactions as to monitor how ice drift and the ice packs responded to external forcing mechanisms. A key objective was to define with the help of a network of autonomous equipment the point at which ice drift changed from summer conditions to winter conditions and to define the ice state that dictated when such a transition occurred.

The ice beacons and on ice towers provided spatially and temporally coincident observations on ice drift and the oceanic and atmospheric forcing mechanisms that govern ice drift. The equipment was recommended to be deployed for 24 to 48 hours to be able to determine the tidal influences versus the oceanic currents and the wind forcings. The objective was to monitor how ice drift and the ice packs respond to external forcing mechanisms.

An additional study on the validation of winds over the marine environment was performed during Leg 3. Previous studies have shown that intense storms with strong winds will break-up the ice pack (Screen et al. 2011, Long and Perrie 2012, Asplin et al. 2012), while accounts of the record minimum in the September 2012 sea ice extent attribute the loss to mechanical weakening and melting of an already thin sea ice cover due to strong winds (NSIDC 2012b, Simmonds and Rudeva 2012). In order to accurately predict the movement of sea ice and ice break-up accurate estimates of surface winds are needed. The *in-situ* data will be compared to different forecasted winds and re-analysis datasets to evaluate the current understanding and ability to correctly forecast or model winds in the high Arctic.

2.2 Methodology – Upper atmosphere program

2.2.1 Microwave Profiling Radiometer Instrumentation

A Radiometrics temperature and water vapour 3000A profiling radiometer (TP/WVP3000A) was used to measure the temperature and water vapour within the atmosphere up to 10 km using passive microwave radiometry at 22 – 29GHz, and 51 – 59GHz. The TP/WVP3000A was installed on a mount attached to the white container laboratory (the ‘Met Ocean Container’) located directly behind the ship’s wheelhouse, approximately 19 m above sea level. The instrument was suspended away from the roof of the shed to ensure that the field-of-view (approximately 15° above the horizon to the left and right to the zenith) was clear of any obstruction.

The instrument generated a vertical profile of upper-level air variables including temperature, water vapour density, relative humidity, and liquid water from the surface to an altitude of 10 km. The resolution of the measurements varied with height. The resolution of

the instrument was 50 m from the surface to an altitude of 500 m, then increased to 100 m from 500 m to 2 km altitude, and was 250 m for measurements from 2 km to 10 km (note: the height given for 50 m is actually 69 m as the instrument assumes it's at sea level when it's mounted 19 m above sea level). In addition, the instrument measured concurrent basic surface meteorology variables, including pressure, relative humidity, and ambient temperature. A skyward-looking infrared sensor measured the temperature of the sky. A rain-sensor detected the presence of any precipitation. It should be noted that the fog registered as precipitation during much of the field season. The instrument also calculated integrated column water vapour, and liquid water content. The sampling frequency for all data was approximately one complete profile per minute.

The calibration of the water vapour profiling process was continuously maintained by hourly tip curves. An external liquid-nitrogen-cooled blackbody was used to intermittently calibrate the temperature profiling process. All channels also viewed an internal black body target every 5 minutes for relative calibration. Temperature and humidity values were derived from microwave brightness temperatures using the manufacturer's neural network retrievals that had been trained using historical radiosonde measurements, and a radiative transfer model (Solheim et al. 1998). Historical radiosonde data from nearby stations were used to develop neural network coefficients for the Labrador Sea during Leg 1, while data from Inuvik N.W.T. was used to develop neural network coefficients for the Southern Beaufort Sea Region during Leg 3.

2.2.2 Vaisala CT25K Ceilometer

The Vaisala CT25K laser ceilometer measured cloud heights and vertical visibilities using pulsed diode laser LIDAR (Light Detection And Ranging) technology, where short powerful laser pulses were sent out in a vertical or near-vertical direction. The laser operates at a centre wavelength of 905 ± 5 nm, a pulse width of 100 ns, beamwidth of ± 0.53 mrad edge, ± 0.75 mrad diagonal and a peak power of 16 W. The manufacturer suggested measurement range is 0 – 25,000ft (0 – 7.5 km), however, it has been found that high, very visible cirrostratus clouds (~18-20 kft) were consistently undetected by the unit (Hanesiak 1998). The vertical resolution of the measurements was 50 ft, but decreased to 100 ft after ASCII data file conversion. The reflection of light backscatter caused by haze, fog, mist, virga, precipitation, and clouds was measured as the laser pulses traverse the sky. The resulting backscatter profile (i.e., signal strength versus height) was stored, processed and the cloud bases were detected. Knowing the speed of light, the time delay between the launch of the laser pulse and the backscatter signal indicated the cloud base height. The CT25K is designed to detect three cloud layers simultaneously, given suitable conditions. Besides cloud layers, it detected whether there was precipitation or other obstruction to vision. No adjustments in the field were needed. Output files were created hourly by the system and are in ASCII format.

2.2.3 All-Sky Camera

The all-sky camera system took images of the sky and cloud cover. The system consisted of a Nikon D-90 camera outfitted with fish-eye lenses with a viewing angle of 160 degrees, mounted in a heated weatherproof enclosure. The camera was programmed to take pictures using an external intervalometer set at 10-minute intervals, or 144 images per day. The system was mounted in a small 'crow's nest' immediately above the ship's wheelhouse.

2.2.4 Manual Meteorological Observations

Manual meteorological observations were conducted hourly throughout Leg 1 and 3-hourly throughout daytime during the entire Leg 3. Observations included current conditions with relation to precipitation type and intensity, visibility, cloud cover (octets), and sea ice coverage (tenths) (Table 2-1). Basic meteorological values were read and recorded from the onboard weather station, which is owned and operated by the Meteorological Service of Canada. Visibility, cloud octets, sea ice concentration, and precipitation type and intensity observations were subjective based on the observer. If the cloud coverage was not 100% it was not recorded as 8/8, similarly if the coverage has even 1% of clouds the cloud fraction was not recorded as 0/8.

The CCGS *Amundsen* was equipped with an AXYS Automated Voluntary Observation Ship (AVOS), with all sensors located on the roof of the wheelhouse. The AVOS is an interactive environmental reporting system that allows for the hourly transmission of current meteorological conditions to a central land station via Iridium satellite telemetry. Temperatures (air and sea surface), pressure, relative humidity (RH), wind speed, wind direction, and current GPS location were updated every ten minutes and displayed on a computer monitor located in the wheelhouse of the ship. The AVOS deploys a Rotronics MP 101A sensor for temperature and RH, with a resolution of 0.1°C and an accuracy of $\pm 0.3^\circ\text{C}$, and a $1\% \pm 1\%$ accuracy for temperature and RH, respectively. Atmospheric pressure was obtained from a Vaisala PTB210 sensor with a 0.01mb resolution and an accuracy of ± 0.15 mb. Wind speed and direction were collected from an RM Young 05103 anemometer, accurate to $\pm 3^\circ$ in direction and ± 0.3 m/s. As part of the 2013 agreement with Environment Canada, observations were inputted into the AVOS system. This was done a minimum of 4 times per day, preferably at 0000 UTC, 0600 UTC, 1200 UTC and 1800 UTC.

Table 2-1. Manual meteorological parameters recorded by the observer.

Parameter	Units
Date	UTC
Time	UTC
Latitude	decimal degrees
Longitude	decimal degrees
Temperature	°C
Relative Humidity	%
Wind Speed	kts

Parameter	Units
Wind Direction	°
Precipitation Type	snow, rain etc.
Precipitation Intensity	Heavy, moderate, light etc.
Visibility	km
Cloud Fraction	Octets
Wave Height	m
Beaufort Sea State	0-10
Sea Ice Concentration	Tenths
Sea Ice Type	MYI, FYI, rotten, icebergs

2.3 Methodology - Network of autonomous equipment

A network of autonomous equipment was deployed on multiyear sea ice floes in the Labrador Sea and Beaufort Sea, respectively during Legs 1 and 3, and left to drift with the icepack. The network utilized the Iridium satellite communications network and transmitted *in situ* data back to the University of Manitoba.

As shown in Figure 2-1, the equipment deployed during Leg 1 included:

- 10 ice beacons, deployed on multiyear ice floes and used to track ice drift;
- 2 weather stations, deployed on multiyear ice floes to collect *in situ* observations of surface winds, air temperature, humidity and air pressure;
- 2 Acoustic Doppler Current Profilers (ADCPs), deployed through multiyear ice floes to measure upper ocean currents.

Autonomous equipment deployed during Leg 3 included:

- 19 ice beacons, deployed on multiyear ice floes and used to track ice drift;
- 4 weather stations, deployed on multiyear ice floes to collect *in situ* observations of surface winds, air temperature, humidity and air pressure;
- 1 POPs buoy, deployed in the open ocean and used to measure temperature, humidity, and pressure at the surface of the ocean, with a CTD that measures from 5 to 600m deep.

Since the duration of the equipment was subject to the stability of the ice floe, equipment had to be preferentially deployed on large, thick, multiyear ice floes that were more likely to last through the end of the melt season and freeze into the ice pack during winter.

The *in situ* observations were supplemented with remotely sensed data from Radarsat that were used to calculate local ice concentrations and floe size distributions. A similar study was carried out in 2012 during the spring season as part of the Beaufort Regional Environmental Assessment (BREA), as well as in 2014 during Leg 2. The analysis focused on the seasonal change in the scaling factor and turning angle between surface winds and ice drift, the scaling factor between ocean currents and ice drift, and ice drift at inertial frequencies.

Additionally, the CCGS *Amundsen* was used during Leg 1 as a platform to test the UAV system to ascertain whether aerial imagery can be taken while flying the UAV's off of a moving vessel over mixed ice conditions.

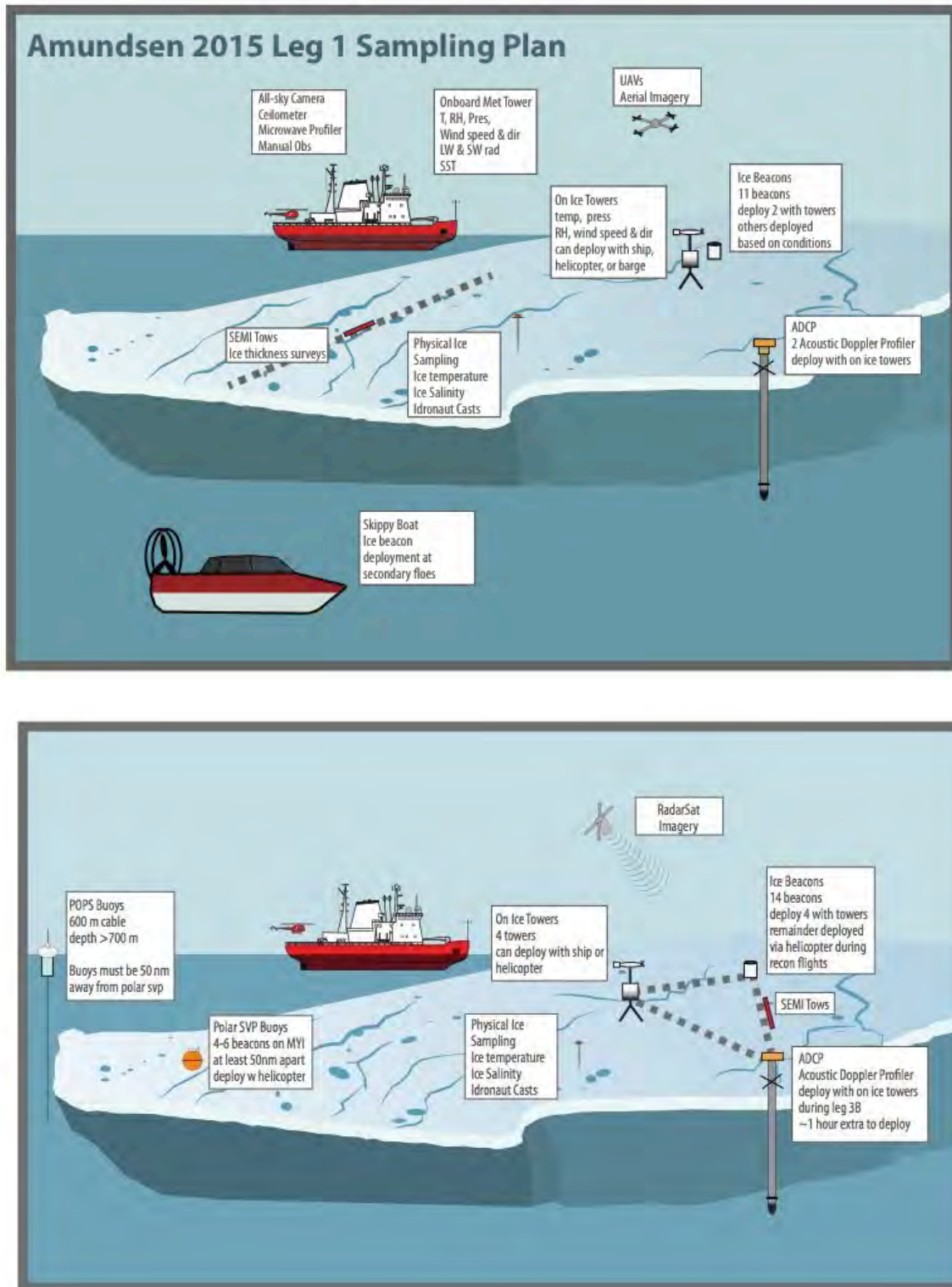


Figure 2-1. Ocean-Sea Ice-Atmosphere sampling methods during Legs 1 (upper schematic) and 3 (lower schematic).

2.3.1 On Ice Meteorological Towers

During Legs 1 and 3b, the goal was to deploy 2 and 4 on ice towers, respectively. Due to time constraints and unfavourable ice conditions, it was not possible to deploy any tower during Leg 1, while, during Leg 3, only 3 of these towers were deployed due to transmission issue with the met tower #6 (that was replaced with tower #7), and problems with the helicopter (broken during 2 weeks, and some bad weather) (Table 2-2). The deployment of each tower required finding the correct type of ice. Typically, the ice floes in the area were rotting first year ice, making finding a suitable thick piece of ice difficult. The goal was to find a piece of ice that would survive through the melt and into the fall freeze up, and possibly through to the next summer. The helicopter was used to access the correct location on the ice floe and determine how suitable and safe the ice conditions were.

Each tower has a marine grade wind anemometer and compass, a temperature and relative humidity sensor and pressure sensor. The tower has 2 deep cycle batteries connected to 3 solar panels to ensure that the batteries are fully charged going into the Arctic winter. The battery box was mounted on wooden blocks to prevent ice melt with the possible warming of the box. This will possibly increase the longevity of the on ice towers. Deployment from the ship took approximately 2-4 hours depending on the amount of physical samplings.

An Idronaut cast was also used during Leg 3 with a CTD probe that could reach 50 m from the surface of the ice.



Figure 2-2. The deployment of the first on ice tower via the ship.

Table 2-2. The details of the on ice met tower deployments.

Ice station	Deployment date	Beacon IMEI	Latitude (N)	Longitude (W)	Ice thickness (m)
7 (initially 6)	Sept 10 11:00 UTC	300234060655960	76°02.580	128°42.030	3.41
8	Sept 9 19:00 UTC	300234060652970	76°07.420	129°18.580	2.83
9	Sept 9 5:57 UTC	300234060534480	76°21.271	129°03.733	> 6

2.3.2 Ship-Based Meteorological Tower

The surface meteorology program of the *Amundsen* is designed to record basic meteorological and surface conditions, and to study exchanges of momentum, heat and mass across the atmosphere-sea ice-ocean interface. Environment Canada deployed the AAVOS system, comprising the R.M. Young (05103) anemometer, Vaisala barometer (PTB-210), and Rotronic (MP100) temperature / relative humidity sensors, while the rest of the instruments were deployed by CEOS. Meteorological data from CEOS were collected from a purpose built tower installed on the foredeck of the *Amundsen*. This location is thought to be the least affected by airflow distortion associated with the ship superstructure. Data from the AAVOS system were recorded every hour, while the rest were recorded every minute.

Table 2-3 shows the instruments deployed on the ship.

Table 2-3. Instruments used in the shipped based meteorological tower during Leg 1.

Instrument (model)	Variable	Specifications
R.M. Young Wind Monitor (05106-10)	wind speed	height: 16.4 m range: 0 – 100 m/s accuracy: ± 0.3 m/s
	wind direction	range: 0 – 360 deg accuracy: ± 3 deg
R.M. Young Wind Monitor (05103)	wind speed	height: 21.6 m range: 0 – 100 m/s accuracy: ± 0.3 m/s
	wind direction	range: 0 – 360 deg accuracy: ± 3 deg
Vaisala digital barometer (PTB-210)	atmospheric pressure	height: 21.6 m range: 50 – 110 kPa accuracy: 0.035 kPa at 20° C
Apogee infrared sensor (SI-111)	sea surface temperature	height: 8.4 m range: –55 – 80 deg C accuracy: 0.5 deg C
Rotronic Meteorological (MP100)	air temperature	height: 21.6 m range: –40 – 60 deg C accuracy: 0.2 deg C
	relative humidity accuracy: $\pm 1\%$ at 25° C	range: 0 – 100
Eppley pyranometer (PSP)	short-wave irradiance	height: 19.1 m range: 0 – 2800 W/m ² accuracy: < 5 W/m ²
Eppley pyrgeometer (PIR)	long-wave irradiance	height: 19.1 m range: 0 – 2800 W/m ² accuracy: < 5 W/m ²
Kipp & Zonen (PAR Lite)	photosynthetically active radiation	height: 19.1 m range: 0 – 3000 $\mu\text{mol}/\text{m}^2/\text{s}$

The data was processed using the following:

- One- and sixty-minute averages for navigational variables were calculated to be matched against meteorological variables.
- Data recorded at one-minute intervals were averaged every sixty minutes to be matched against data recorded at sixty-minute intervals.
- True wind direction and true wind speed were calculated for both anemometers, following equations from Smith et al. (1999).
- The sixty-minute average for wind speed and direction from the R.M. Young 05106-10 anemometer was preferred over the 05103 model, because we believe the former is subject to less flow distortion given its position on the foredeck tower. Therefore, data from the latter were selected only when data from the former were not available. Data from both anemometers were set to missing when the wind direction was aft of the ship, and therefore obstructed by the ship. The source of anemometer data is indicated by the boolean column `is_AAVOS_anemometer`, indicating whether data were measured by the 05103 model.

Three products were generated from the data:

- One-minute meteorology (CEOS);
- One-hour meteorology and radiation (CEOS);
- One-hour meteorology (Environment Canada).

Table 2-4. Each file has the following columns, with the variable and units described.

Column	Variable	Units
<code>time</code>	Time stamp (UTC)	YYYY-MM-DD HH:MM:SS
<code>longitude</code>	Longitude	deg N
<code>latitude</code>	Latitude	deg E
<code>speed over ground</code>	Speed Over Ground	<i>m/s</i>
<code>course over ground</code>	Course Over Ground	<i>m/s</i>
<code>heading</code>	Heading	deg N
<code>pitch</code>	Pitch	deg
<code>roll</code>	Roll	deg
<code>heave</code>	Heave	<i>m</i>
<code>atmospheric_pressure</code>	Atmospheric Pressure	kPa
<code>air_temperature</code>	Air Temperature	deg C
<code>dew_point</code>	Dew Point	deg C
<code>surface_temperature</code>	Sea Surface Temperature	deg C
<code>wind_speed</code>	True Wind Speed	<i>m/s</i>
<code>wind_direction</code>	True Wind Direction	deg N
<code>is_AAVOS_anemometer</code>	Missing anemometer data from 05106-10 instrument filled with 05103 instrument? (T or F)	boolean
<code>PAR</code>	Photosynthetically Active Radiation	$\mu\text{mol}/\text{m}^2/\text{s}$
<code>SW_down</code>	Short-Wave Irradiance	W/m^2
<code>LW_down</code>	Long-Wave Irradiance	W/m^2

2.3.3 *Physical Sampling*

Due to time constraints and unfavourable ice conditions, only one station was done for physical sampling during Leg 1. Station #7 occurred on April 27, 2015 at 1310 UTC at 52°13.070 N and 55°17.770 W. At this station (station #7) only one ice core was taken due to time constraints, and the ice floe was too small to deploy more than two people onto.

Physical samplings were done at 2 locations during Leg 3, one next to an on ice weather station in the Beaufort Sea, and the second in Penny Strait. Temperature profiles were taken immediately after drilling the ice. Salinity samples were brought back, melted, and analysed on the ship. One ice core will be kept in the freezer and will be scanned with the MRI of the University of Manitoba (structure analysis). All cores were taken with a 6" core barrel. Some other samples were brought back for analysis by other teams on the ship (for contamination analysis).

Sea ice physical sampling was to be conducted according to the following protocol:

- Extract two cores from the desired location, designating one for temperature and one for salinity.
- For the temperature profile, measure at surface or snow/ice interface immediately after removing snow cover. Take the temperature at intervals (5 cm for new ice, 10 cm for MYI) in the ice using temperature probe. Immediately after extracting the core, use the drill to make a hole to the center of the ice core and insert the probe to measure the temperature. Shade the sensor from direct solar radiation. Keep in mind that measuring the profile quickly is better than a high vertical resolution. Estimate the length of the ice core thickness (check if it does, in fact, match the thickness gauge observation). Additionally, if possible, measure surface water temperature from core hole.
- The FLIR camera may also be used immediately on the ice cores to determine the temperature profile.
- For the salinity profile, cut the core into 10 cm cylinders and place them into plastic containers or large whirlpack bags. Take care to identify the depth from which the sample was extracted. For example, the upper 10 cm is identified with "0-10cm," the next 10 cm is identified with "10-20cm," and so on. These samples will be brought to the ship to be melted for conductivity measurements, similar to the sampling procedure for snow.
- Use a 2-inch auger to drill through the sea ice. Identify the thickness of the sea ice using an ice thickness tape measure. If you can see the water, measure the freeboard using a ruler or the ice thickness tape measure.
- Take note of interesting features in the sea ice such as bands of dirty ice, banding, and brine channels. This can be accomplished by examination of the salinity core before it is sectioned for salinity measurements. Full microstructural analysis will not be performed on the ship.

2.3.4 *Ice Beacons*

A total of 10 ice tracking beacons were deployed during Leg 3. The beacon can be deployed

while at an ice station but also from the helicopter while doing surveys. While on the ice floe, an 8" hole was augured into the ice for the installation of the beacon. At hourly intervals, the instrument recorded its location and transmitted this information to an email server. The beacons transmitted data via an iridium satellite in the form of an email attachment. From the 5 Canatec beacons that were deployed in Beaufort Sea, 3 were at a weather station. The Oceanetics beacon was deployed in Penny Strait.

As part of the 2015 agreement with Environment Canada, CEOS deployed 4 Polar SVP beacon in Beaufort Sea. Each beacon was positioned as far away from each other as possible, however some are less than 50nm apart.

2.3.5 POPs Buoys

1 POPs buoy was deployed from the *Amundsen*, for Environment Canada, in the SE Beaufort Sea in open water conditions, somewhere off the continental shelf (Figure 2.3). The assembly of each buoy was not all that "quick." It involved attaching the individual ocean sensors along the pre-marked cable, and then attaching the cable to the floating hull in the proper way. There is a user's manual, which includes deployment instructions.

The surface unit is 397 lbs and 83" x 31" x 36 with a 600 meters long cable with a NOVA profiling unit on it. The deployment of the buoy took about 2 hours. The buoy had to be deployed weight first, unreel most of the cable into the water, attach the profiler and lower the profiler into the water, then attach and lower the surface unit in. The unit then had to be turned on using the Zodiac as the buoy must first be in the water before the unit can be activated. The location was chosen according to the depth of the ocean, far from the coast, and also far from big ice floe that would damage the instrument.



Figure 2-3. Deployment of the POPS buoys

2.3.6 UAVs

During Leg 1, the goal was to take aerial photography from a moving platform using the UAVs. Due to time constraints and unfavourable ice conditions, it was not possible to deploy the UAVs from an ice floe, however the team was not able to test the system from the helicopter deck of the CCGS *Amundsen*. Flights were conducted with a Steadidrone H6X hexcopter (flight weight of 3.8 kg) and a Steadidrone QU4D quadcopter (flight weight of 1.8 kg) carrying cameras as payload.

The flights resulted in a nadir-oriented imaging of the CCGS *Amundsen* and an oblique-oriented photography of the surrounding ocean.

2.4 Preliminary results

2.4.1 Leg 1

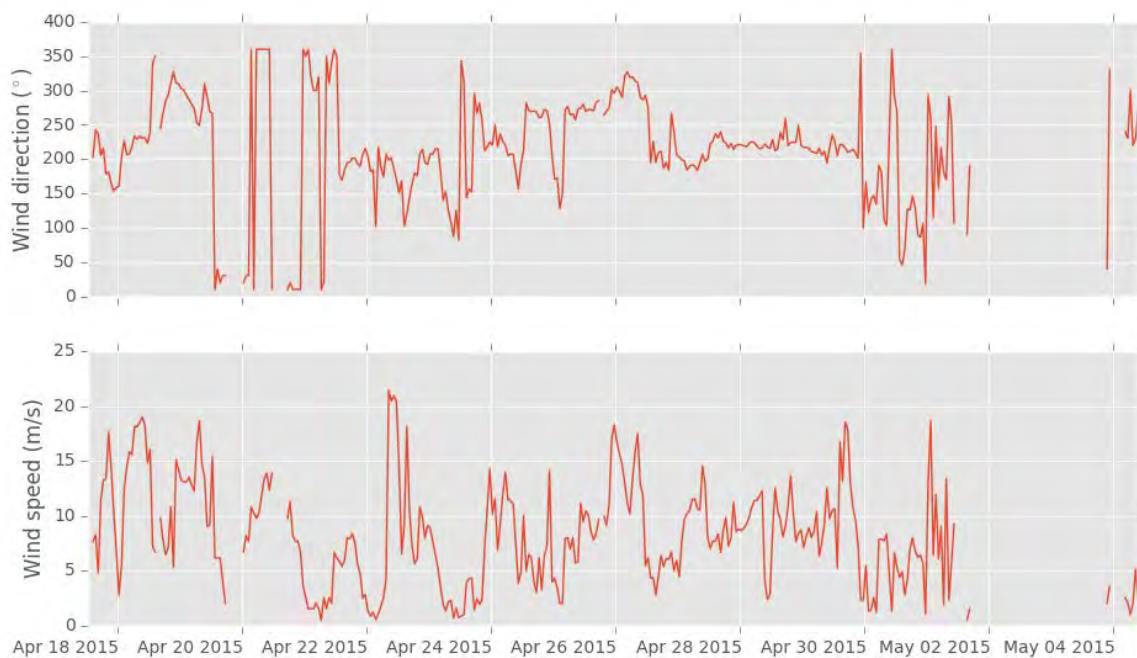


Figure 2-4. Wind speed and direction during Leg 1.

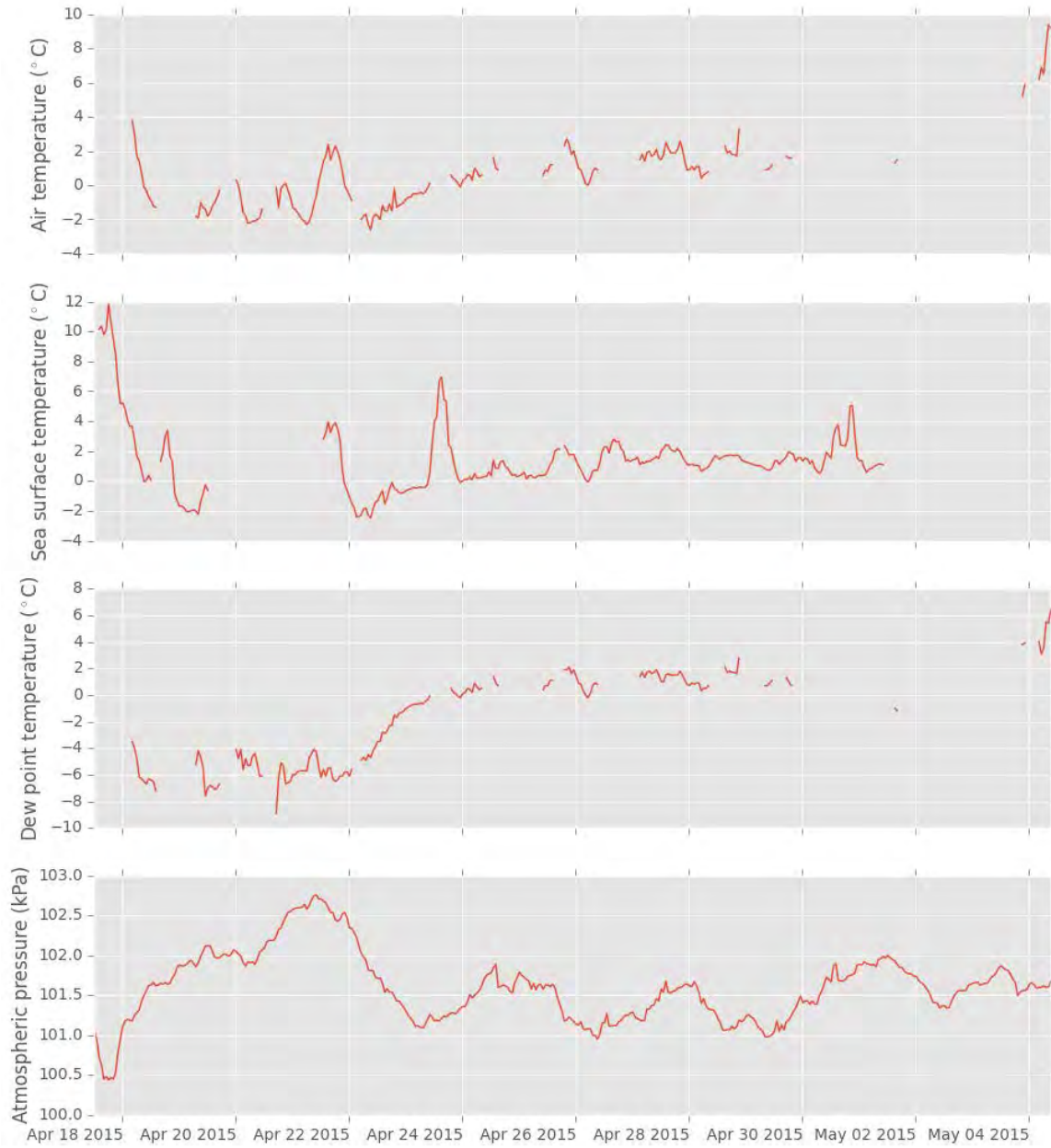


Figure 2-5. Air temperature, sea surface temperature, dew point temperature and atmospheric pressure.

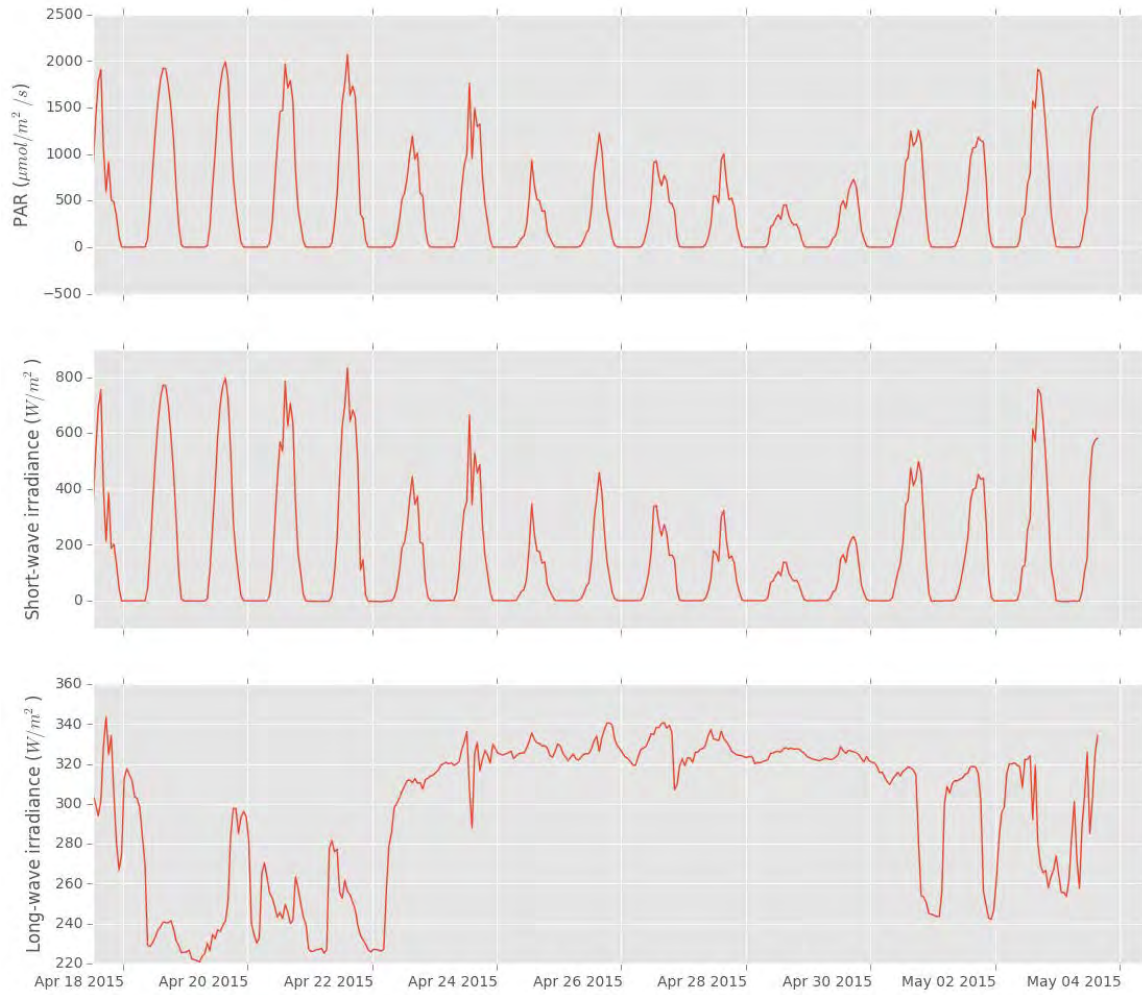


Figure 2-6. Photosynthetically active radiation (PAR), short-wave and long-wave irradiance.

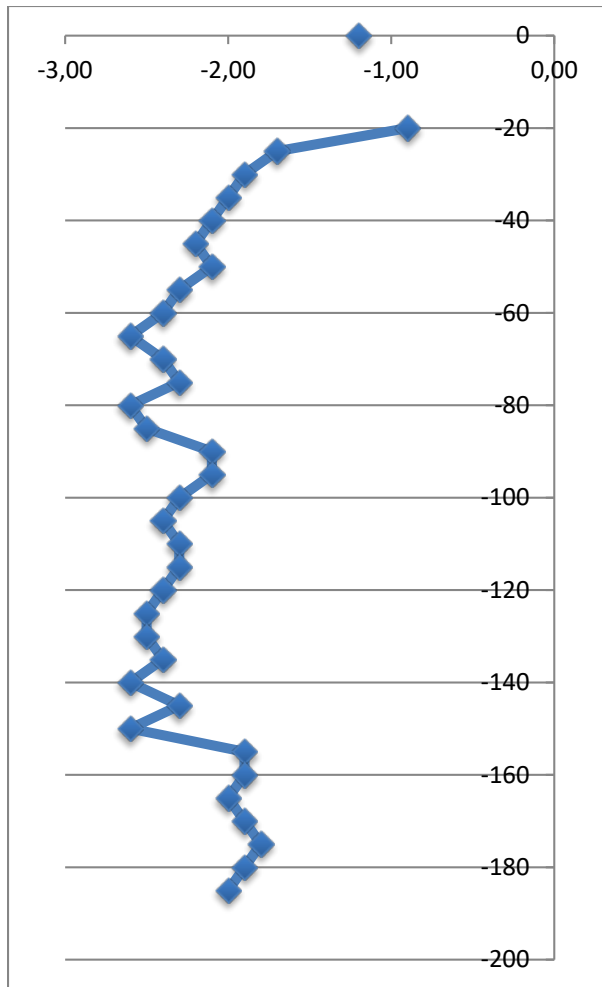


Figure 2-7. Temperature of the ice core.

2.4.2 Leg 3

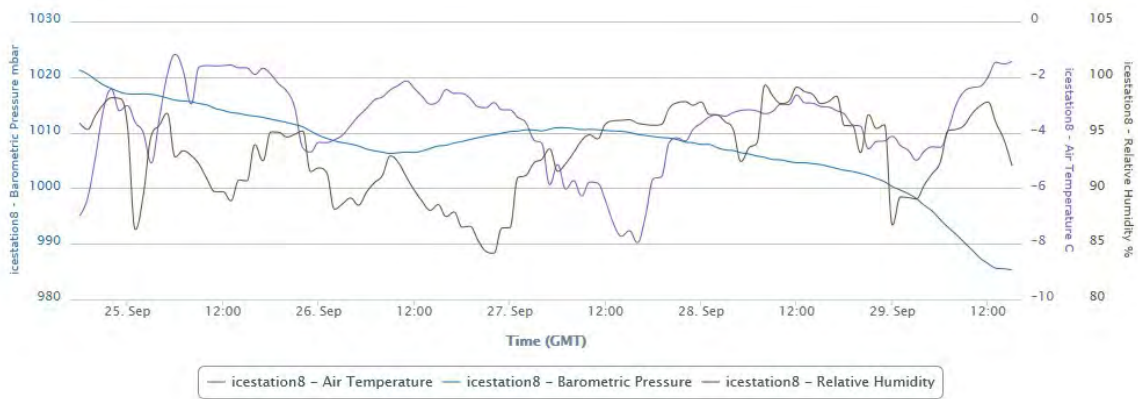


Figure 2-8. The air temperature, pressure and relative humidity data from the on ice met tower #8 deployed on September 9th, 2015.



Figure 2-9. Wind direction (red) and wind speed (green) from station #8 deployed on September 9th, 2015.



Figure 2-10. The trajectory from September 22nd to September 29th of 5 beacons deployed in the Beaufort Sea.

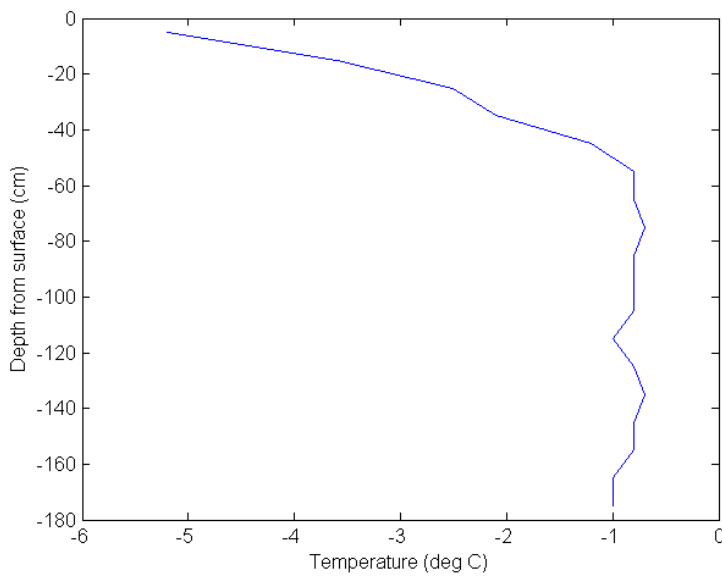


Figure 2-11. Temperature profile of the ice core taken in Penny Strait.

2.5 Comments and recommendations

During Leg 1, there were many logistical issues with the on ice work. The time of year when we were in the Labrador Sea was too late in the season for thick large homogeneous ice floes. If there was more dedicated time to work on ice, we would have needed to take the ship much further north to find ice floes that would support our team and the equipment. In future legs if there is to be on ice work it is highly recommended that the amount of transit time to find the correct type of ice be increased as well as giving a sufficient amount of time on the ice for deployments or sampling.

3 Aerosol sampling: Measurement of atmospheric fluxes of trace elements and isotopes (GEOTRACES) – Legs 2 and 3b

Project leader: Bridget Bergquist¹ (bergquist@es.utoronto.ca)

Cruise participant Leg 2: Priyanka Chandan¹

Cruise participant Leg 3b: Priyanka Chandan¹

¹ *University of Toronto, Department of Earth Sciences, 22 Russell Street, Toronto, ON, M5S 3B1, Canada.*

3.1 Introduction

Atmospheric aerosol deposition is considered an important pathway for the input of nutrients and trace metal loads to the open ocean waters via dry and wet deposition processes (Macdonald et al. 2005, Mahowald et al. 2005, Morton et al. 2013, Zhan and Gao 2014). In the atmosphere, the trace elements are associated with aerosol particles such as mineral dust, soot, volcanic ash, organic particles, sea salt crystals, bacteria and microscopic particles, from both natural and anthropogenic sources (Duce et al. 1991, Duce, 2005, Witt et al. 2006, Landing and Payton 2010). The wet and dry deposition of these aerosol particles to the open oceans can significantly impact the trace element distributions in the surface oceans, enhance the ocean primary productivity and influence the climate (Macdonald et al. 2005, Gong and Barrie 2005, Landing and Payton 2010). As such, quantifying atmospheric trace elements and isotopes (such as Al, Fe, Ti, Zn, Pb and Hg) will help gain insight into the atmospheric fluxes of key trace metals, their origin of aerosol particle sources and the biogeochemical cycling of atmospheric trace elements over the Canadian Arctic waters.

Arctic GEOTRACES Legs 2 and 3b provided an incredible opportunity to study and understand the atmospheric aerosol deposition over the Labrador Sea, Baffin Bay, Hudson Bay, Canadian Basin (CB) and the Canadian Arctic Archipelago (CAA) from the CCGS *Amundsen*. The aim of this study was to collect bulk aerosols on Whatman 41 filters to assess:

- Chemical characterization of key trace metals and isotopes;
- Quantification of atmospheric inputs of trace elements and isotopes;
- Understand the biogeochemical cycling of trace elements over the Canadian Arctic Ocean.

3.2 Methodology

The shipboard aerosol sampling during Legs 2 and 3b was conducted using a commercially available volumetric flow controlled (VFC) high volume aerosol sampler from TISCH Environmental (TE-5170V-BL). The aerosol sampler consisted of the following components :

- Aluminum frame and roof
- Brushless motor
- Elapsed time indicator (ETI)
- Flow funnel attached to the motor
- Filter holder with a PVC adapter that holds 12-47mm filters (Figure 3.1)



Figure 3-1. The PVC adapter plate that holds 12 – 47mm filter holders (courtesy of Bill Landing).

The aerosol sampler was deployed as high and forward as possible on the ship as suggested in Morton et al. (2008) to prevent contamination from the ship smoke stack. The best possible position for deployment of high volume air sampler on the *Amundsen* was on the bridge deck (Figure 3.3). The aerosol sampler was connected to an automated sector control comprising of an anemometer and a CR10 data logger. The anemometer was also mounted closer to the aerosol sampler on the bridge deck such that the cups were facing the bow and the vane was facing the stern (Figure 3.3). The sector control was controlled by Campbell Scientific software with predefined parameters for wind direction and speed. The wind direction and speed was set as $\pm 75^\circ$ either side of the bow ($105^\circ - 225^\circ$) and $> 0.2\text{m/s}$ respectively. When the wind was out of the pre-set parameters, the aerosol sampler automatically shut down. A delay time of 150s was set for the wind direction and wind speed to meet the pre-set parameters for the aerosol sampler to restart again. The aerosol samples were collected over the Labrador Sea, Baffin Bay, Hudson Bay, Canadian Basin and the Canadian Arctic Archipelago (Figure 3.2). The bulk aerosol samples were collected on acid cleaned 12 – 47mm Whatman 41 filters (Fisher Scientific 1441-047) for up to 70-hour integrated time period at a flow rate of $1\text{ m}^3/\text{min}$. The Bill Landing filter changing protocols were followed (Morton et al. 2008), where the filters were changed in a clean

bubble, located in the moon pool of the *Amundsen*. Due to large variation in transit times and station time, aerosols were strategically collected throughout Legs 2 and 3b. When the transit time and on station time was significant (>20 hours), aerosols were collected separately during *Transit* and *On Station*. For instance, Sample 12 was collected continuously from CB2 – CB3 and CB3 – CB4 over a time period of 117 hours. Based on the Elapsed time indicator installed on the sampler, the bulk aerosols were only collected for ~ 19 hours. The ETI time was significantly shorter than the run time because the ETI shut down when the wind was out of sector, which automatically shut down the aerosol sampler. However, when the transit time was minimal (4-8 hours), aerosol sampling continued on the same set of filters during *Transit* and *On Station* as shown in

Table 3-1 Table 3-2. For instance, Sample 11 was collected during transit from CB1-CB2. Due to short *Transit* times, the aerosol sampler also remained ON at Station CB2. The details of the aerosol sampling during *Transit* and *On Station* in given in Table 3-3 Table 3-4. To monitor for potential contamination, blanks were also periodically collected by exposing filters loaded onto PVC filter holder near the aerosol sampler while the wind was in sector. At the end of Leg 2 and Leg 3b, a total of 15 samples and 5 blanks were collected and stored in individual acid cleaned and pre-labeled petridishes at -20°C.



Figure 3-2. The aerosol sampling locations and route in the Canadian Basin and the Canadian Arctic Archipelago during Leg 3b

The unfortunate delays in the GEOTRACES scientific program owing to Coast Guard operations during Leg 2 in Hudson Bay opened up an opportunity to sample aerosols over Hudson Bay for two weeks in late July. Two samples (i.e. Sample 4 and Sample 5) were collected over a time period of 35-45 hours in Hudson Bay (Table 3.1). At the end of Leg 2,

a total of 9 samples and 3 blanks were collected and stored in individual acid cleaned and pre-labeled petridishes at - 20°C.

Table 3-1. The table below summarizes the date, location and sampling parameters of aerosol samples and blanks on Leg 2.

Samples	Latitude Start	Latitude Stop	Longitude Start	Longitude Stop	UTC Start	UTC Stop	Run time (hours)	ETI (hours)
Sample 1 - Sept-Iles- K1	49.36	53.81	-67.01	-54.30	2015-07-11 12:53	2015-07-13 14:48	49.9	39.8
Blank 1 - towards K1	53.81		-54.30		2015-07-13 22:00	2015-07-13 22:05	0.08	
Sample 2A - K1 - LS2	55.62	60.45	-52.37	-56.55	2015-07-15 18:09	2015-07-16 23:34	29.4	4.4
Sample 2B - LS2 - BB1	60.74	64.41	-56.67	-59.19	2015-07-19 0:15	2015-07-19 23:00	22.7	22.7
Sample 3 - LS2	60.45	60.74	-56.55	-56.67	2015-07-17 18:23	2015-07-19 0:05	29.7	8.5
Sample 4 - Hudson Bay	64.16	59.17	-59.60	-79.02	2015-07-20 0:20	2015-07-26 22:53	166.6	45.9
Sample 5 - Hudson Bay	59.19	62.40	-79.03	-77.15	2015-07-26 23:21	2015-07-31 17:18	114.0	37.7
Blank 2 - Hudson Bay	62.37		-78.05		2015-07-31 15:25	2015-07-31 15:30	0.08	
Sample 6 - BB1 - Clyde river - BB3 - BB2	69.03	72.45	-59.07	-66.58	2015-08-04 16:01	2015-08-08 22:06	102.1	67.7
Sample 7 BB3 - Lancaster Sound	72.46	73.53	-67.00	-82.20	2015-08-08 23:36	2015-08-12 9:42	82.1	54.1
Sample 8 CAA3 - CAA7	73.56	71.30	-82.17	-96.43	2015-08-12 10:20	2015-08-16 22:49	108.5	46.6
Blank 3 Lancaster Sound	73.54		-82.21		2015-08-12 10:30	2015-08-12 10:35	0.08	
Sample 9 CAA7 - Kugluktuk	71.24	67.50	-96.56	-115.1	2015-08-16 23:12	2015-08-19 23:22	72.2	17.6

Table 3-2. The table below summarizes the date, location and sampling parameters of aerosol samples and blanks on Leg 3b.

Samples	Latitude Start	Latitude Stop	Longitude Start	Longitude Stop	UTC Start	UTC Stop	Run time (hours)	ETI (hours)
Sample 10A	75.07	75.07	-120.4	-120.5	2015-09-06 23:38	2015-09-08 4:13	28.58	4
Blank 4	75.08		-120.4		2015-09-06 23:50	2015-09-06 23:55	0.08	
Sample 11	75.09	75.54	-121.0	-128.5	2015-09-08 5:02	2015-09-10 22:57	65.92	28
Sample 12A	75.52	76.59	-128.5	-139.5	2015-09-10 0:29	2015-09-11 19:06	42.61	17
Sample 10B	76.59	76.36	-139.5	-141.5	2015-09-11 19:10	2015-09-13 17:50	46.67	4
Sample 12B	76.36	74.51	-141.5	-149.3	2015-09-13 18:02	2015-09-16 20:22	74.33	2
Sample 13	74.51	70.34	-149.3	-99.22	2015-09-16 20:32	2015-09-22 12:21	135.8	74
Sample 14	70.34	75.41	-99.22	-95.02	2015-09-22 0:39	2015-09-26 20:56	116.3	61
Blank 5	70.93		-99.42		2015-09-22 1:30	2015-09-22 1:35	0.08	
Sample 15	75.41	74.59	-95.02	-92.17	2015-09-26 21:10	2015-09-29 19:00	69.83	30

Table 3-3. A summary of aerosol samples and blanks collected during *Transit* and *On Station* on Leg 2.

Samples	Transit Sampling		On Station Sampling	
Sample 1	X	Sept-Iles - K1		No sampling at Station K1
Blank 1	X	Sept-Iles - K1		
Sample 2A	X	K1 - LS2		
Sample 2B	X	LS2 - BB1		
Sample 3			X	LS2
Sample 4	X	Hudson Bay	X	Hudson Bay
Sample 5	X	Hudson Bay	X	Hudson Bay
Blank 2			X	Hudson Bay
Sample 6	X	BB1 - Clyde River - BB3 - BB2	X	Clyde River, BB3, BB2
Sample 7	X	BB2 - CAA1 - CAA3	X	CAA1, 2, 3
Sample 8	X	CAA3 - CAA7	X	CAA4, 5, 6, 7
Blank 3	X	CAA3		
Sample 9	X	CAA7 - Kugluktuk	X	CAA7, Kugluktuk

Table 3-4. A summary of aerosol samples and blanks collected during *Transit* and *On Station* on Leg 3b.

Samples	Transit Sampling		On Station Sampling	
Sample 10A			X	CB1
Blank 4			X	CB1
Sample 11	X	CB1 - CB2	X	CB2
Sample 12A	X	CB2 - CB3		
Sample 10B			X	CB3
Sample 12B	X	CB3 - CB4	X	CB4
Sample 13	X	CB4 - QMG-2 (AN)	X	QMG-2 (AN)
Sample 14	X	QMG-2 (AN) - CAA9		
Blank 5	X	QMG-2 (AN) - CAA9		
Sample 15	X	CAA9 (Penny Strait)	X	CAA9 (Penny Strait)



Figure 3-3. The TISCH volume flow controlled (VFC) high volume aerosol sampler deployed on the bridge deck of the CCGS *Amundsen* during Leg 3b from September – October, 2015 (left). The anemometer, which is attached to the aerosol sampler through CR10 datalogger (right).

3.3 Preliminary results

The aerosol filter samples were not analyzed or processed during Legs 2 and 3b. The measurement of key trace elements and isotopes on the aerosol filters will be carried out once the samples are returned back to the stable isotope laboratory at University of Toronto after CCGS *Amundsen*'s return to Quebec City in November.

3.4 Comments and recommendations

Overall, I was very satisfied with CCGS *Amundsen*'s operations on Leg 2. The Captain, Officers and the Crew of the *Amundsen* were outstanding and very helpful in successfully carrying out aerosol sampling throughout Leg 2. During Station K1, aerosol motor broke down due to sea salt spray and subsequent water damage. The ship's crew including the electrician helped me in replacing the motor and getting the aerosol sampler up and running in a short period of time. In my opinion, the TISCH aerosol sampler can be continuously deployed for an extended period of time. However, during bad weather and high waves, the sampler should be turned off and the motor must be protected from the sea salt spray and water damage. As previously mentioned, the aerosol sampling was carried out strategically to maximize the aerosol collection. This was because of short transit times and large On station times. Throughout Leg 2, the Captain and the officers accommodated my request to position the ship in forward wind on stations such that the wind remained in sector. This allowed me to collect aerosols both during *Transit* and *On Station*.

My experience in carrying out aerosol sample collection during Leg 3b was satisfactory. The Captain and the crew were very helpful in the smooth running of the high volume air sampling from September to October, just as in Leg 2. The officers of the ship were very accommodating in changing the position of the ship to allow me to change sample filters with the wind in sector. Just like in Leg 2, I was collecting aerosols both during *Transit* and *On Station*. However, unlike Leg 2, I did face some challenges in collecting aerosols while the ship was on station. Due to the position of the ship during stations (not facing forward wind), my automated sector control was not turned on and as such, the aerosol sampler was shut down throughout majority of the stations during Leg 3b.

References

- Duce, R.A., Liss, P.S., Merrill, J.T., Atlas, E.L., Buat-Menard, P., Hicks, B.B., Miller, J.M., Prospero, J.M., Arimoto, R., Church, T.M., Ellis, W., Galloway, J.N., Hansen, L., Jickells, T.D., Knap, A.H., Reinhardt, K.H., Schneider, B., Soudine, A., Tokos, J.J., Tsunogai, S., Wollast, R., Zhou, M., 1991. The atmospheric input of trace species to the world ocean. *Global Biogeochemical Cycles* 5 (3), 193–259.
- Duce, R.A., 2005. In: Oliver, J.E. (Ed.), "Aerosols", *Encyclopedia of World Climates*. Kluwer, Dordrecht, pp. 4–6.

- Gong, S.L., and L.A. Barrie, 2005. Trends of heavy metal components in the arctic aerosols and their relationship to the emissions in the Northern Hemisphere, STOTEN, in press. V342/1-3, pp 175-183.
- Landing, W. M. and Payton, A. 2010. Marine chemistry special issue: Aerosol chemistry and impacts on the ocean
- Macdonald, R.W., Harner, T., Fyfe, J. (2005) Recent climate change in the Canadian Arctic and its impact on contaminant pathways. *Science of the Total Environment* 3425–86.
- Mahowald, N.M., A.R. Baker, G. Bergametti, N. Brooks, R.A. Duce, T.D. Jickells, N. Kubilar, J.M. Prospero, and I. Tegen (2005). Atmospheric global dust cycle and iron inputs to the ocean. *Global Biogeochem. Cycles* 19, GB4025, doi:10.1029/2004GB002402.
- Morton, P.L., W.M. Landing, A. Milne, A.M. Aguilar-Islas, A.R. Baker, M.M. Baskaran, Y. Gao, C.S. Buck, et al. (2013). Methods for the sampling and analysis of marine aerosols: results from the GEOTRACES 2008 aerosol intercalibration experiment. *Limnology and Oceanography: Methods* 11, 62-78, doi:10.4319/lom.2013.11.62.
- Zhan, J., and Y. Gao (2014), Impact of summertime anthropogenic emissions on atmospheric black carbon at Ny-Ålesund in the Arctic. *Polar Research*, 33, 21821, .doi.org/10.3402/polar.v33.21821.
- Witt M., Baker A. & Jickells T.D. 2006. Atmospheric trace metals over the Atlantic and South Indian oceans: investigation of metal concentrations and lead isotope ratios in coastal and remote marine aerosols. *Atmospheric Environment* 40, 5435–5451

4 Biogeochemical cycling of methane – Legs 2, 3a, 3b, 4a, 4b and 4c

ArcticNet Phase 3 – Marine Biological Hotspots: Ecosystem Services and Susceptibility to Climate Change.

<http://www.arcticnet.ulaval.ca/pdf/phase3/marine-ecosystem-services.pdf>

Project leader: Huixiang Xie¹ (huixiang_xie@uqar.ca)

Cruise participant Leg 2: Laura Noël¹

Cruise participant Legs 3a and 3b: Lantao Geng^{1,2}

Cruise participants Legs 4a, 4b and 4c: Lantao Geng^{1,2} and Laura Noël¹

¹ *Institut des sciences de la mer de Rimouski, Université du Québec à Rimouski (UQAR), 310 Allée des Ursulines, Rimouski, Québec, QC, G5L 3A1, Canada.*

² *Key Laboratory of Tectonics and Petroleum Resources of Ministry of Education, Faculty of Earth Resources, China University of Geosciences, Wuhan 430074, China.*

4.1 Introduction

Methane (CH₄) is the second important greenhouse gas (after CO₂) in the atmosphere. The ocean has been considered as a minor source of atmospheric CH₄ as compared to anthropogenic inputs and other natural sources. However, climate warming, particularly over the Arctic region, may significantly change the CH₄ budget. The concentration of CH₄ in Arctic seawater is expected to rise substantially due to permafrost thawing, CH₄-enriched freshwater discharge, submarine hydrothermal venting, and potential CH₄ hydrate dissolution.

Currently, few data are available on CH₄ distribution and its biogeochemical cycling in Canadian Arctic seas. The objectives of 2015 Expedition were to:

- Assess methane production potentials of DMS (dimethyl sulfide), DMSO (dimethylsulphoxide) and DMSP (dimethylsulphoniopropionate), which have been hypothesized as the precursors of methane;
- Estimate the net production or consumption rate of methane in water column;
- Identify potential CH₄ hotspots related to hydrothermal activity or permafrost melting.

4.2 Methodology

During Leg 2, *in situ* concentrations of methane were measured at different depths at selected stations (Table 4-1).

Table 4-1. List of sampling stations for dark incubation during Leg 2.

Station	Latitude (N)	Longitude (W)
K1	56°33.710	052°39.390
LS-2	60°25.830	056°34.280
BB-1	66°50.540	059°02.140
BB-3	71°24.510	068°35.070
BB-2	72°45.510	066°58.720

Additionally, periodic surface water samples were collected with the pumping system. Air samples were also taken periodically and then directly analyzed.

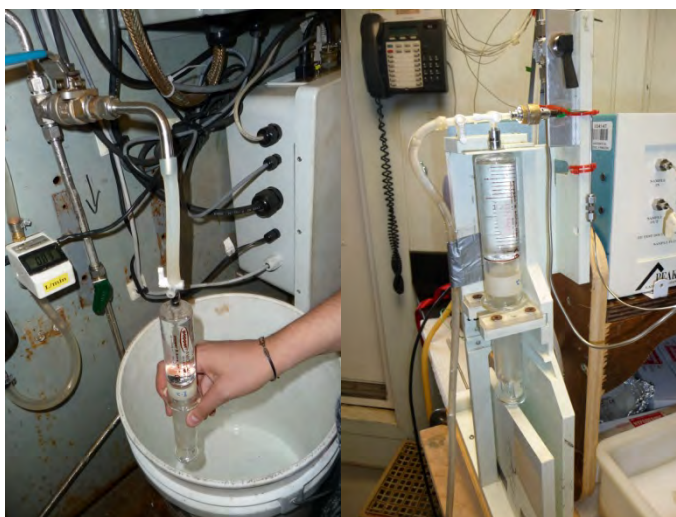


Figure 4-1. Surface water sampling (left) and samples analysis (right).

Dark incubation samples were taken at selected stations (Figure 4.2) and depths (surface, 10 m and subsurface chlorophyll maximum) during Leg 3, and analyzed immediately after sampling for the first time. Following the same protocol, Stations 107 and 101 were sampled during Leg 4. For assessing methane production potential of these precursors, those samples must be spiked with associated chemicals first before analysis. Thereafter, all dark incubation samples were stored in incubator or cold room at 4 degrees. The second and the third measurements were conducted after 10 days and 20 days, respectively.

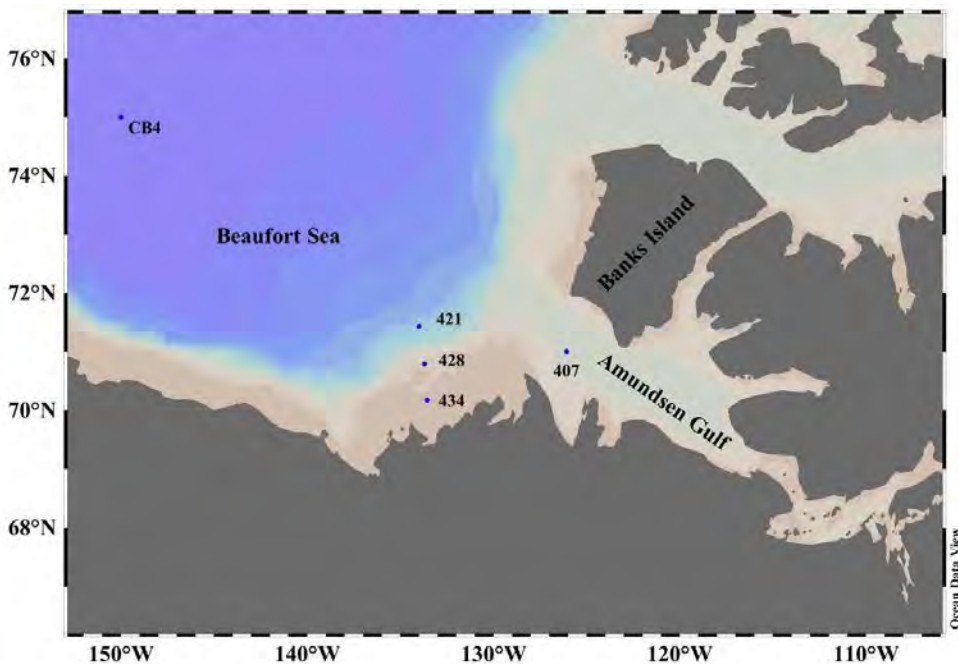


Figure 4-2. Locations of the sampling stations for dark incubation during Leg 3.

Additionally, CH₄ profiles were collected at some Basic and Full stations during Leg 3, and at each Nutrient, Basic and Full stations during Leg 4. CH₄ concentration was measured using a PP1 methane analyzer (Peak Laboratories).

4.3 Preliminary results

4.3.1 Leg 2

Methane concentrations in the Labrador Sea ranged from 1.4 nmol/L in the deepest area to 39.3 nmol/L at the surface. In the Baffin Bay, it ranged from 0.4 nmol/L to 37.4 nmol/L.

During all the leg, methane concentrations at the surface ranged between 29.5 nmol/L and 43.7 nmol/L.

4.3.2 Leg 3

No result of dark incubation is available at this moment. Below are two sections showing the distribution of CH₄ concentrations in M'Clure Strait (Figure 4.3) and Queen Maud Gulf of the Canadian Archipelago (Figure 4.4), respectively.

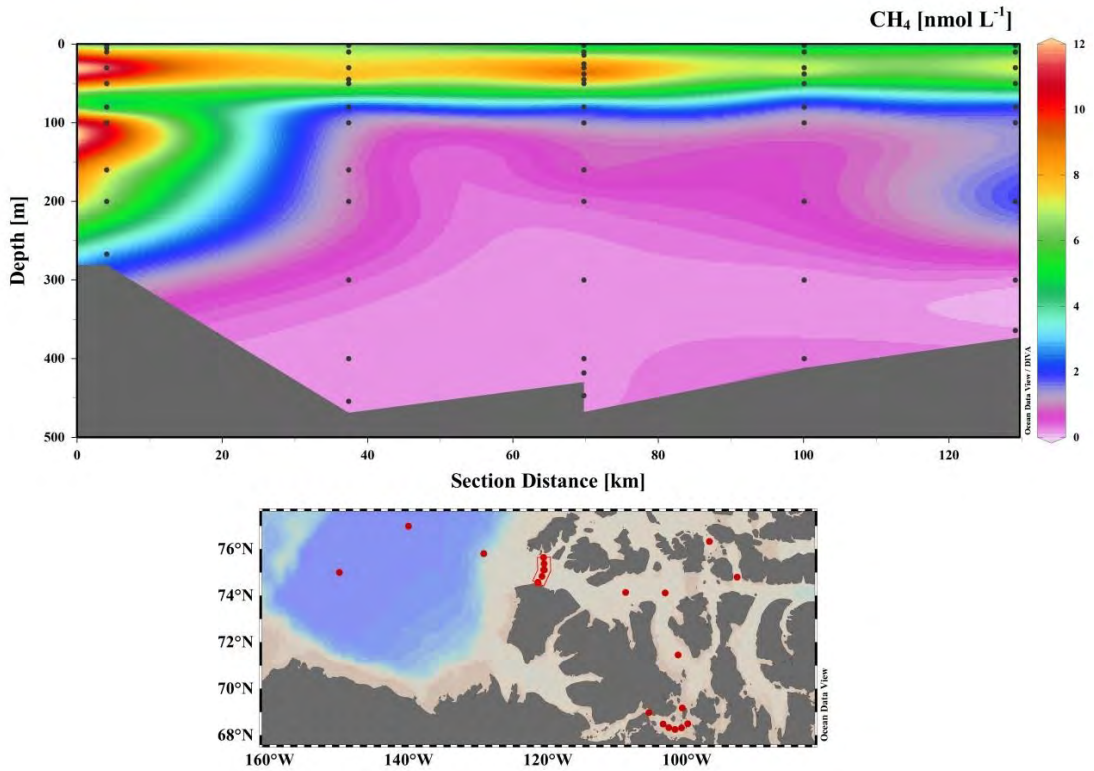


Figure 4-3. *In-situ* CH₄ concentration in M'Clure Strait during Leg 3.

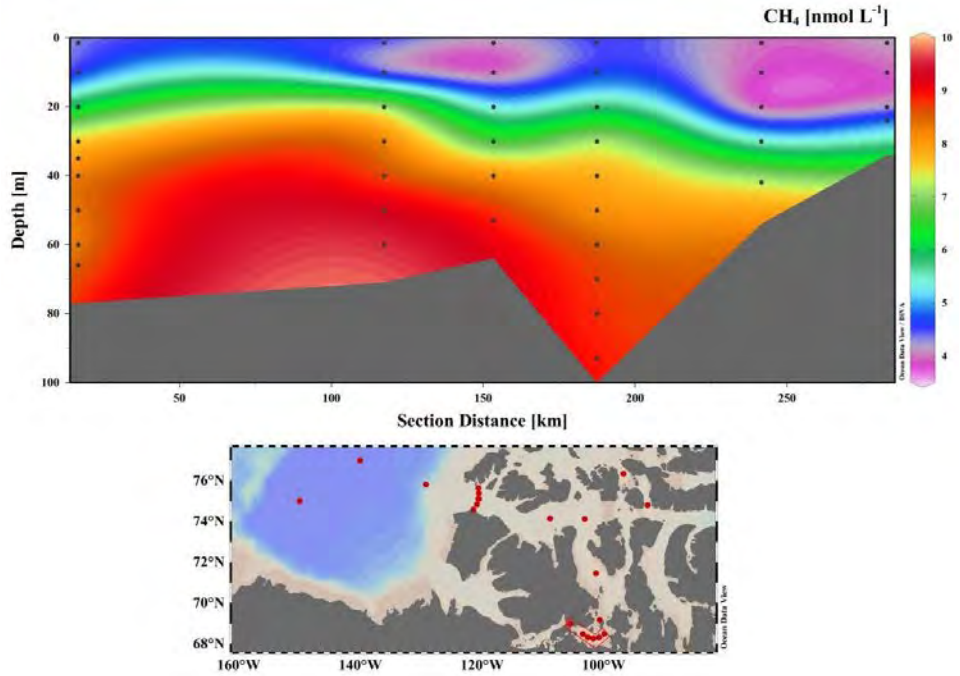


Figure 4-4. *In-situ* CH₄ concentration in Queen Maud Gulf of the Canadian Archipelago during Leg 3.

4.3.3 Leg 4

Here are two profiles showing the deep methane enrichment along the coast of Baffin Island.

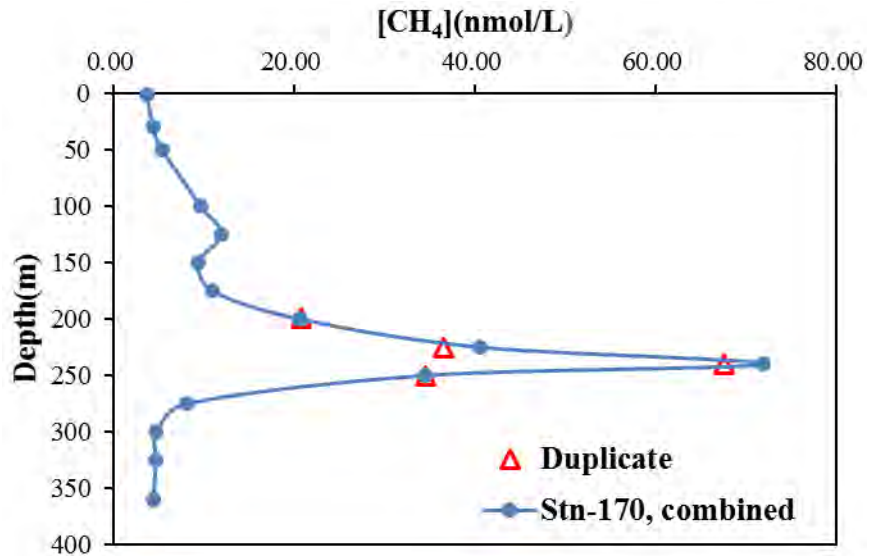


Figure 4-5. Methane concentration vs. depth at Station 170 near Scott Inlet.

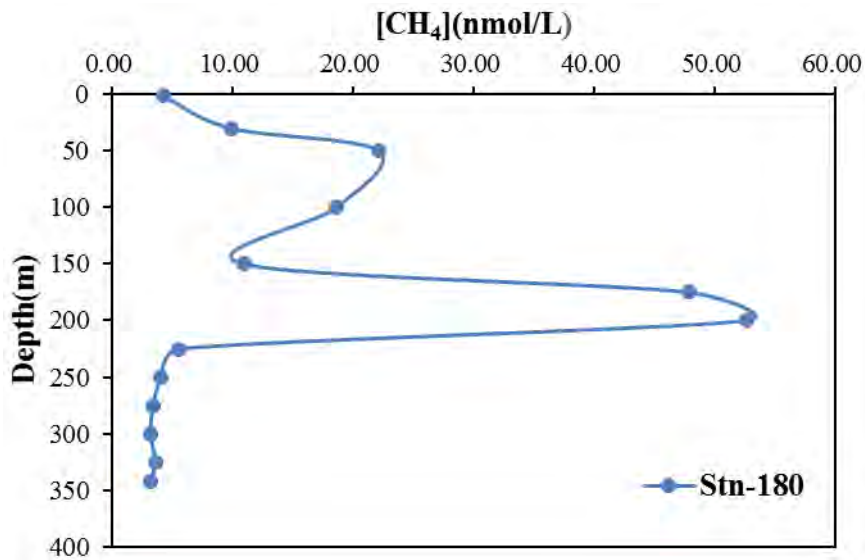


Figure 4-6. Methane concentration vs. depth at Station 180 near the Broughton Island.

5 Ice camera imagery – Leg 1

Project leader: Derek Mueller¹ (derek.mueller@carleton.ca)

Cruise participant: Hans-Martin Heyn²

¹ *Carleton University, Department of Geography and Environmental Studies, B349 Loeb, 1125 Colonel By Drive, Ottawa, ON, K1S 5B6, Canada.*

² *Trondheim University, Høgskoleringen 1, 7491 Trondheim, Norvegia.*

5.1 Introduction

In February 2015, Leah Braithwaite of the Canadian Ice Service (CIS) expressed interest in recording ice conditions surrounding Canadian Coast Guard Vessels and sending them in real time to the CIS via FTP transfer. Having imagery that was coincident with Radarsat-2 imagery was also deemed to be desirable. Derek Mueller (Carleton University) volunteered to conduct a pilot study on board Leg 1 of the Statoil / ArcticNet cruise to assess the feasibility of this concept. The following report details this progress.

5.2 Methodology

During Leg 1 of the Statoil / ArcticNet cruise, a series of cameras was mounted on the ship to provide a 360 degree view of the surrounding ice conditions. The on-ship lead on this was Hans-Martin Heyn from Trondheim University. There were 12 cameras placed in three ‘nests’ of cameras on the port, front and starboard sides of the *Amundsen*. Each nest can see 180 degrees by way of 4 x 45 degree view cameras. All images can be stitched together to make up a 360 degree view (with overlap). The cameras were not installed very high up and they were tilted downward so the amount of ice that can be seen is limited to ~80 m from the ship in places. The cameras recorded images once every 10 seconds and switched from optical to a low light mode in twilight/dark. Only one of these cameras (camera #6, forward port side) was selected for this pilot project (Figure 5.1).



Figure 5-1. Image taken at 12z on Apr 30, 2015 at 50.54N, 58.39W. It is a jpeg image (590 kB at full resolution) that provides a 45-degree view.

Computer program

A computer program was written in the scripting language Python to:

- Check the time
- Retrieve the GPS position of the ship
- Determine the need to transfer imagery (based on a set time interval, amount of daylight and anticipated Radarsat-2 passes)
- Pull the image from camera directory, rename it and add metadata such as GPS location
- Send the image via FTP to a server in Ottawa
- Occasionally look for new ACP files on the FTP site – for step #3 above

This program should be run every 5-10 minutes by a task scheduler or cron job, but the time of execution should not be on the five-minute mark (i.e., execute at 6, 11, 16... minutes past the hour) to avoid errors due to latency in the writing of GPS and camera data to network drives.

Program requirements

- Python 2.7 along with common modules
- gdal/ogr libraries and python bindings
- Exiftool
- Computer and camera set to UTC time
- Drive mapping / UNC connection to data, such as the CNAV GPS and camera data
- Internet connection
- Access to new ACP files, placed on the FTP server to receive photos coincident with Radarsat-2 imagery.

5.3 Preliminary results

The program was run successfully on a Windows machine over several days. This setup was not continually connected to the internet and the program was modified several times over this time span. This prevented a full test in a variety of conditions. However, the system appears to work well.

5.4 Comments and recommendations

- The cameras currently on board the *Amundsen* will be removed shortly. Therefore, the primary recommendation is that a weatherproof IP camera(s) with an appropriate field of view be purchased and mounted on the *Amundsen* for Leg 2.
- User needs must be identified and dealt with (file naming conventions, interval between images, other requests, etc.)
- Due consideration must be given to bandwidth limitations and cost.
- The program needs a computer to run on that will remain on at all times and be connected to the internet and the local network to get GPS position from the ship. This computer needs to have all the required software installed (all are open source). A Raspberry Pi may be a suitable candidate for this (as yet untested).
- CIS must agree to periodically supply new ACP files.
- The program needs to be modified to work with the new IP camera.
- The system must be fully tested and documented.

6 Ice island field operations – Legs1, 4a, 4b and 4c

Project leaders: Derek Mueller¹ (derek.mueller@carleton.ca) and Gregory Crocker¹ (gregory.crocker@carleton.ca)

Cruise participants Leg 1: Derek Mueller¹ and Anna Crawford¹

Cruise participant Legs 4a: Anna Crawford¹

Cruise participants Legs 4b: Anna Crawford¹ and Clark Graham¹

Cruise participant Legs 4c: Anna Crawford¹

¹ Carleton University, Department of Geography and Environmental Studies, B349 Loeb, 1125 Colonel By Drive, Ottawa, ON, K1S 5B6, Canada.

6.1 Introduction

6.1.1 Iceberg drift and deterioration (Leg 1)

The presence of icebergs (and ice islands) in areas of hydrocarbon exploration and development creates a significant impediment to safe and cost-effective operations. From a risk perspective the most important iceberg characteristics are frequency, size, and speed. These are directly controlled by iceberg *drift* and *deterioration* processes. Regarding the former, this venture aimed to collect a complete and accurate data set of iceberg drift, iceberg characteristics, and the state of the ocean in which it is drifting. Particular attention was paid to collecting conductivity/temperature profiles, which will allow assessing ocean processes that have thus far not been included in iceberg drift models or are poorly understood. Particular emphasis will be given on the influence of internal waves on an iceberg's drift. This data will allow researchers and engineers to assess the significance of these processes and serve as a basis for the improvement and calibration of iceberg forecast models.

With respect to iceberg deterioration, this field campaign was dedicated to a proof-of-concept project to map iceberg sails using a combination of laser scanning and photogrammetry (structure from motion) to develop 3D digital elevation models (DEMs). The precision and other limitations of these approaches will be determined by comparing/differencing separate DEMs created from the repeated surveys of numerous icebergs. This data is complemented by the sonar mapping of the icebergs' keels conducted by the Marine Geoscience Lab of Laval University. This will enable to plan future field campaigns effectively to measure iceberg/ice island deterioration from a small vessel using similar equipment and the tested methods of this campaign.

A description of each day of fieldwork, which was performed in conjunction with the iceberg mapping project, is provided below. This information is also given in a condensed form in Table 6-1.

6.1.2 Ice island mass balance (Leg 4)

Three large calving events, 31 km², 253 km² and 130 km² in surface area, occurred at northwest Greenland's Petermann Glacier in 2008, 2010, and 2012, respectively (Environment Canada 2012; Falkner et al. 2011; Johannessen et al. 2012). This resulted in an influx of ice islands, large and tabular icebergs, within water bodies such as Nares Strait, Baffin Bay and the Labrador Sea where they pose as hazards to shipping and natural resource extraction industries (McGonigal et al. 2011; Peterson 2011). Accessing ice islands for field data collection is strife with logistical difficulties, and this has led to a paucity of the *in-situ* data, which is necessary for the calibration and validation of drift and deterioration models as well as remote-sensing techniques for identification and deterioration detection. The CCGS *Amundsen* has provided access to numerous ice islands since 2011 (Crawford et al. 2015; Forest et al. 2012; Hamilton et al. 2012; Stern et al. 2015; Wagner et al. 2015), and it was the objective of ice island researchers from Carleton University to conduct ice island field visits with use of the vessel during Legs 4a and 4b of the 2015 ArcticNet science cruise.

The primary objective of the 2015 ice island field campaign was to deploy two systems, which would collect *in-situ* mass balance data on a drifting ice island in Baffin Bay. The first system, an ice penetrating radar, records ice thickness data and would provide information on the magnitude of thinning which the ice island will experience over 2015-2016. A meteorological station was the second system and was instrumented to collect surface melt, ice and air temperature, and location data.

This is the first deployment of an ice penetrating radar on an ice island in either hemisphere. The concurrent datasets of surface melt and ice thinning will provide the highest temporal resolution of ice island mass balance yet gathered. The ice thickness dataset will also be utilized specifically by cruise participant A. Crawford as a validation dataset in her investigations of using satellite-borne radar altimetry for detecting thickness changes of Arctic ice islands.

The study of ice island mass balance is important for industrial operations in two ways. First, the assessment of thickness, and the magnitude of thinning expected at varying latitudes and environmental conditions, can be utilized in the planning of pipeline installations and thereby mitigate pipeline or well-head ruptures due to ice island scouring of the seabed. Ice island keel depths are also an important parameter to accurately input into drift models, which provide offshore operators with predictions of their movement and thus allow for adequate planning of collision mitigation measures. Finally, the assessment of ice island mass balance during drift through decreasing latitudes can be utilized as a proxy for the deterioration of higher latitude ice features resulting from future climate change.

Secondary objectives were included for Leg 4a, where the primary deployment would not take place, as well as for Leg 4b in the event that more time was available for ice island operations. Two objectives for Leg 4a included:

- Bathymetry mapping of a site of known ice island groundings northeast of Coburg Island, NU;
- Re-surveying Petermann Ice Island (PII)-K with mobile IPR. PII-K was visited in August 2014 and a re-visit would provide information on both surface melt and thinning.

Mobile IPR was also an option for extra surveying if time allowed in Leg 4b. It was also planned to deploy three tracking beacons provided by Environment Canada for ice island drift monitoring. Aerial photogrammetry surveying would coincide with these beacon deployments during Leg 4b.

6.2 Methodology

6.2.1 Iceberg drift and deterioration (Leg 1)

Date: 16 April

Event: Boresight calibration

Personnel: Derek Mueller (DM), Anna Crawford (AC) and Josh Sampey

Event Description: The above personnel set-up the laser scanning system on a vehicle and repeatedly scanned various surfaces (e.g.: building corners, parked vehicles) to calibrate the integrated laser scanner/inertial monitoring unit (IMU)/GPS system.

Date: 17 April

Event: Barge deployment for multi-beam and laser scanner tests

Personnel (Scientific): DM, AC, Jean-Guy Nistad (JGN) and Gabriel Joyal (GJ)

Description: A 30-minute survey of the CCGS *Amundsen* was conducted to test the two barge-mounted mapping systems. This dataset will also serve as a test case for the methods which are under development to correct for target (e.g.: ship or iceberg) drift during surveying.

Date: 19 April

Event: Photogrammetry testing

Personnel (Scientific): DM, AC

Description: The helicopter flight was used to test the external camera mount (i.e.: 'the pod') and the wireless connection, which allowed the user to communicate with the nadir-directed camera. The tests were conducted on a set of small islands on which Ramey, QC is located. Two surveys were completed. Project members learned that a new lexan cover for the pod, and the removal of the camera's polarizing lens, was necessary for future iceberg photogrammetry. It was also determined that the dGPS would not obtain proper satellite signals when contained in the pod.

Date: 22 April

Iceberg: Wedge [Station 1]

Events: Beacon deployment and photogrammetry

Personnel: DM, AC, Maxim Geoffrey (MG)

Description: A Canatec beacon (IMEI 4470) was deployed on the iceberg at 14:10. The iceberg's maximum height was approximately 100 ft. One photogrammetry survey at 900 ft altitude was conducted before the helicopter returned to the ship due to poor flying conditions. Additionally, the SX90 was used to measure the iceberg's keel.

Date: 22 April

Iceberg: Dome [Station 2]

Events: Beacon deployment and photogrammetry

Personnel: DM, AC, MG

Description: A Canatec beacon (IMEI 6490) was deployed on the iceberg at 19:23 at an approximate altitude of 80 ft, as recorded by the helicopter's altimeter. One photogrammetry survey was conducted at a low altitude of 300 ft due to ceiling limitations. The SX90 was again deployed to measure the iceberg's keel.

Date: 23 April

Iceberg: Large tabular [Station 3]

Events: Beacon deployment, photogrammetry and laser scanning

Personnel: DM, AC, JGN, GJ, MG

Description: DM left at 17:19 for an ice/iceberg reconnaissance helicopter flight and successfully located the iceberg target. The SX90 again was used to locate the iceberg keel. Laser scanning was conducted from the ship by DM, AC, JGN and GJ. AC and DM left on a second helicopter flight to deploy three beacons: one Canatec (IME 91420) and two Solara units. The approximate altitude of the iceberg was 40 ft. A final helicopter flight was taken for photogrammetry surveying. Three surveys were conducted at altitudes of 1000, 1000 and 700 ft. Images were taken with the infrared camera ('FLIR') during one aerial-circumnavigation of the iceberg at 300 ft and also from the ship during laser scanning.

Date: 24 April

Iceberg: Saddle [Station 4]

Events: Beacon deployment and barge sail/keel mapping with laser scanning and multibeam sonar, respectively

Personnel: DM, AC, JGN, GJ, MG

Description: Four beacons were deployed on the iceberg: 2 Canatec (IMEI 0480 and 92490) and 2 Solara units. The maximum height of the iceberg, and also where the Canatec beacons were placed, was approximately 100 ft. The Solara units were deployed at an approximate height of 20 ft. The SX90 was used to determine the keel depth.

The barge was deployed at 16:53 and then was stationed on the east side of the iceberg (up-drift) while the *Amundsen* positioned itself approximately 500 m to the north. The first CTD cast from the barge occurred at 16:42. CTD profiling continued at this location until approximately 18:10. One additional CTD was cast closer to the iceberg for the start of the meltwater detection study; however, this data collection was cut short due to the need to recover the barge. The ADCP was deployed at 16:48 and recovered at 18:34. Five CTD casts were conducted from the CCGS *Amundsen* over a period of 4 hours and 20 minutes.

The barge circumnavigated the iceberg four times over a period of 1 hour and 8 minutes after finishing the CTD 'yo-yo' casts. The multi-beam and laser scanning systems were used to map the keel and sail of the iceberg, respectively. A problem was incurred by the laser scanning system, as it was not possible to connect to the integrated IMU. It was determined after the barge recovery that the problem was due to the power supply source.

Date: 27 April

Iceberg: Small tabular [Station 7.1]

Events: Beacon deployment, photogrammetry and laser scanning

Personnel: DM, AC, JGN, GJ

Description: Three differential GPS (dGPS) and one Canatec beacon (IMEI 95460) were deployed on the iceberg. Two photogrammetry surveys at an altitude of 1000 ft were conducted during the same helicopter flight as was used for the beacon deployment. A video was also recorded with the FLIR during a full aerial-circumnavigation of the iceberg.

The CCGS *Amundsen* circumnavigated the iceberg three times for laser scanning surveys, which were run by JGN and GJ. DM and AC took visual and infrared photos at 5 and 15-second intervals, respectively, during the laser scanning surveying. A final helicopter flight was taken by DM and AC to recover the dGPS units.

Date: 29 April

Iceberg: Ice island (grounded) [Station 12]

Events: Beacon deployment, photogrammetry, laser scanning and ice coring

Personnel: DM, AC, JG, GJ

Description: Four Canatec GPS units were deployed on the ice island in square orientation. Two ice cores, each 1 m in length, were collected from two sites in the center of the ice island. Two photogrammetry surveys were conducted by flying around the perimeter of the ice island. Infrared data was collected with the FLIR in video mode during a third circumnavigation of the ice island. JGN and GJ ran the laser scanner from the CCGS *Amundsen* while AC and DM were using the helicopter. Three laser scan surveys were conducted along one face of the ice island which was sea-ice free.

Table 6-1. Iceberg mapping activities by date and location.

Date	Site	Photogrammetry	Laser scanning	Multi-beam sonar	Ice coring	Deployed beacons
16-04-2015	CCG docks		X			
17-04-2015	CCGS Amundsen		X	X		
19-04-2015	Ramey, QC	X				
22-04-2014	Stn 1 Wedge	X				1 – Canatec
22-04-2014	Stn 2 Dome	X				1 – Canatec
23-04-2015	Stn 3 Lg tabular	X	X			2 – Solara 1 – Canatec
24-04-2015	Stn 4 Saddle		X	X		2 – Solara 2 – Canatec
27-04-2015	Stn 7.1 Sm tabular	X	X			3 – dGPS 1 - Canatec
29-04-2015	Stn 12 Ice island	X	X		X	4 – Canatec

6.2.2 Ice island mass balance (Leg 4)

Potential ice island field sites were monitored with synthetic aperture radar (SAR) imagery from the RADARSAT-2 (Canadian Space Agency) and Sentinel-1 (European Space

Agency) satellites. Positions were provided by collaborators at the Canadian Ice Service (Environment Canada) and the PolarView web interface. The objectives of Leg 4a were not realized due to: 1) high sea ice concentrations making it impossible to use the ship's sonar, and 2) the full deterioration of PII-K since field work in 2014. A beacon, which was deployed in 2014 on this small ice island was, however, recovered.

It was decided to target PII-A-1-f, a fragment of the 2012 Petermann Glacier calving event, for Leg 4b primary operations. This ice island is grounded at 67°23'N, 63°18'W—approximately 35 km southeast of Qikiqtarjuaq, NU (Figure 6.1). The 14-km² ice island was pivoting on a shoal mapped by the Amundsen's EM302 sonar and the SX90 fishing sonar on 20 October, the day of 2015 ice island field operations.

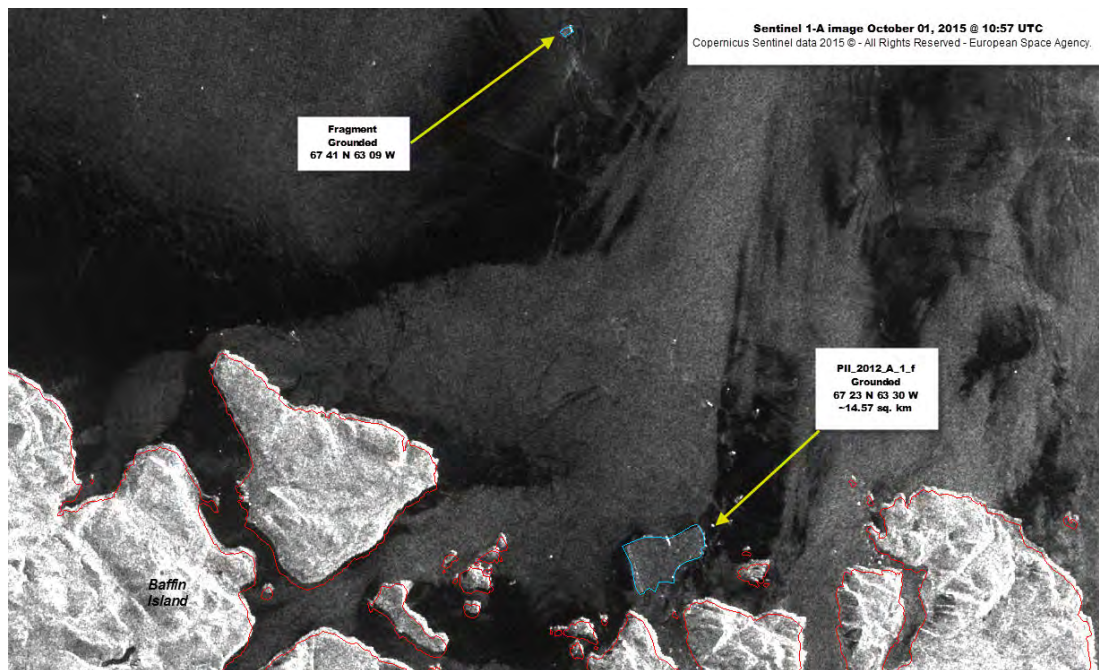


Figure 6-1. Ice island PII-A-1-f as imaged by Sentinel-1 (European Space Agency).

Team personnel consisted of Anna Crawford (team leader), Graham Clark (technician), Jonathan Gagnon (volunteer and bear monitor) and Thomas Demeules (crew member and bear monitor). The team and equipment were transferred to PII-A-1-f starting at 7:30 am EST. Three consecutive helicopter trips, one of which consisted of an equipment sling transfer, were necessary. The installation locations were decided upon, with 27 m separating the stationary IPR and weather station. A line of five stripped ablation stakes was to be installed between the two systems and 10 m from the meteorological station (Figure 6.2). A. Crawford and G. Clark led the installation of the IPR and meteorological station, respectively while Gagnon and Demeules took shifts as bear monitor and drilling 5 x 5.5 m holes with a 2" auger for the ablation stake array.

The IPR and meteorological station were secured to the ice surface by PVC stakes drilled 5.0 to 5.5 m into the ice. The installations were secured to larger diameter ABS piping, which was placed over the stakes as sleeves. Arrays of 20 W or 10 W solar panels were secured over the sleeves adjacent to the receiver and transmitter cases of the IPR as well as one of the legs of the meteorological stations tripod. A MetOcean CALIB beacon was also attached to a sleeve of the meteorological station, as was an antenna next to the IPR receiver for daily radargram transmission for remote data collection.

The meteorological station is instrumented with an SR50 sonic ranger for surface melt calculation, L109 temperature probe, ice temperature profiler (7 thermistors over 2.1 m depth), CC5MPX camera, Garmin 16X-HVS GPS, and a 9522b modem, communication block, and antenna for daily data transmission. The camera is situated as to take a weekly photo of the IPR and also the ablation stake array to give a secondary assessment of surface melt. Air and ice temperature are recorded every minute and averaged each hour, while surface ablation and location are sampled on the hour. Clark finished the meteorological station set-up before 12:30 pm EST, the time when the station is programmed to turn on the modem for data transfer over the Iridium satellite network. A radio call was made to the ship where Gabriel Joyal was able to confirm a successful data transmission by logging into Campbell Science's FTP system.

Crawford first tested the IPR and its 35 MHz antennas to ensure that a correct signal, or 'radargram', composed of a clear airwave and bed-wave (representing the ice-water interface), was captured. Once confirmed, Crawford finished the physical set-up of the IPR system (Figure 6.2). This included threading the antenna and a fiber optic cable (used to trigger the transmitter once a day by the receiver/computer system) through 2" PVC piping joined by threaded ABS connectors. The final connection used ABS cement instead of thread to avoid having to rotate either of the large Pelican cases housing the transmitter or receiver and the associated 55 Ahr and 2 x 35 Ahr batteries. In the future, a swivel connector will be used to remove this problem. Doweling and Velcro (doweling-antenna and doweling-PVC) was used to ensure that the antennas were fully elongated and located closest to the ice surface when within the 2" horizontally oriented PVC. All connections, between ABS as well as any through-connectors to the Pelican cases for the solar panels or antenna, were circled with self-amalgamating rubber tape to ensure waterproofness.



Figure 6-2. Ice penetrating radar (foreground), meteorological station (background) and row of ablation stakes between.

Once the physical set-up was complete, Crawford established the optimal settings for the IPR by interfacing with the receiver's computer through a Panasonic Toughbook and Ethernet connection and TightVNC Client software. Principle settings include the vertical range for the airwave (100 mV) and bed-wave (50 mV), trigger set (50 and 20 mV), record length ensuring that the bed-wave was captured (200 ns), pulse repetition frequency (128), stacking to average out noise (256) and the system allowed uptime – ensuring enough time for data collection and satellite transmission (6 min). Crawford used a satellite phone to call Laurent Mingo, owner of Blue Systems Integration Ltd. and maker of the stationary IPR, to confirm that the test records were correct. This was confirmed as well by Joyal on the *Amundsen*.

Gagnon and Demeules continued to drill holes for all the stakes while Crawford and Clark set up their respective systems. Issues ensued with two of the drilling options. First, the hot water drill decreased in pressure extremely quickly and caused drilling to be inadequately slow. The second option, consisting of using a power drill and 2" auger, failed due to the auger-drill adaptor failing to catch. These two issues resulted in the team needing to drill all the holes with a manual hand-crank. A final hole was drilled for the sonic ranger, which needed to be on a separate post from the meteorological station's tripod. The 6 m metal post to be inserted was composed of 3 x 2 m sections with metal coupling. This coupling was too large for the 2" auger hole. To overcome this issue, the hot water drill was inserted into the pipe to heat the surrounding ice to the necessary width. The final hole

was approximately 4 m in depth. Drilling ceased due to sunset. The team returned to the ship at 4:30 pm EST after deploying a Polar iSVP beacon on the opposing end of PII-A-1-f.

Beacon deployments and photogrammetry surveys occurred on 21 and 22 October. The tabular iceberg targeted on the 21st was realized to be greatly slopped after the helicopter departed. This caused the beacon to roll off the iceberg after deployment. Photogrammetry surveying continued at 800 and 1200 ft. The user, Crawford, sat behind the pilot and controlled the Nikon D7100 with a wireless connection provided by a CamRanger accessory and software application. All images are georeferenced with a Nikon GPS attachment. A small ice island fragment was also visited on the 22nd. A successful beacon deployment of a Polar iSVP occurred and three photogrammetry surveys were taken at 800 ft, all consisting of three flight lines while the helicopter traveled at 40 kts. The pod was transferred to the passenger side of the helicopter where Crawford sat to obtain a better viewing angle. The sun angle was continually decreasing, causing Crawford to adjust the camera settings. Shutter speed was decreased from 1/4000 to 1/3200 and the ISO was increased from 200 to 400.

6.3 Preliminary results

6.3.1 *Iceberg drift and deterioration (Leg 1)*

A large amount of aerial surveying data was collected, as presented in Table 6-1, over the 6 days of iceberg fieldwork. The CCGS *Amundsen* laser scan survey (Figure 6.3) is presently being utilized as a test case for the correction of a target's drift during surveying. The drift correction methods developed for the ship will be utilized for the 4 ice features, which were surveyed with the laser scanner (Figure 6.3). The barge was only deployed at Station 4 due to the unsuitable environmental conditions (i.e., the presence of sea ice), which were experienced at the remaining stations. Preliminary assessment of the three multi-beam surveys conducted at close range to the saddle iceberg at this location show promise for future 3D model rendering of the iceberg's keel (Figure 6.3). Initial processing of the photogrammetry surveys in Agisoft Photoscan demonstrate potential of the data collected in the field – both in regards to the spatial coverage and ability to identify the deployed GCPs (Figure 6.3) – to also create quality 3D models after further processing and analysis.

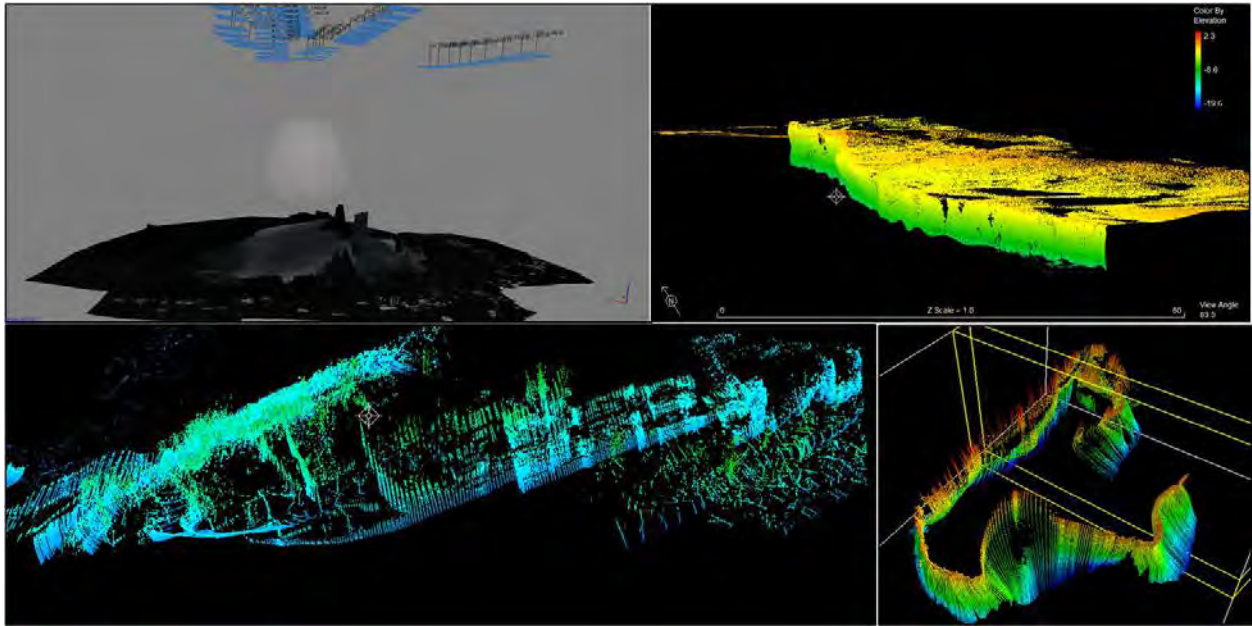


Figure 6-3. (Clockwise from top-left): Photogrammetry survey of Station 1 (wedge iceberg) after processing in Agisoft Photoscan; sidewall laser scan survey of Station 3 (small tabular iceberg); laser scan survey of the CCGS *Amundsen* illustrating the ship's drift during data collection; multi-beam keel survey data of Station 4 (saddle iceberg).

6.3.2 Ice island mass balance (Leg 4)

Data is transmitted daily by both systems, with only the camera operating at a different time frequency (weekly photo). The first image from the CC5MPX camera was taken on Wednesday, 21 October at 12:00 pm EST (Figure 6.4). It shows the IPR to be in-line and the 5 ablation stakes in the foreground. Table 6-1 shows the data that was collected and transmitted after the meteorological station had been installed for 24 hrs.

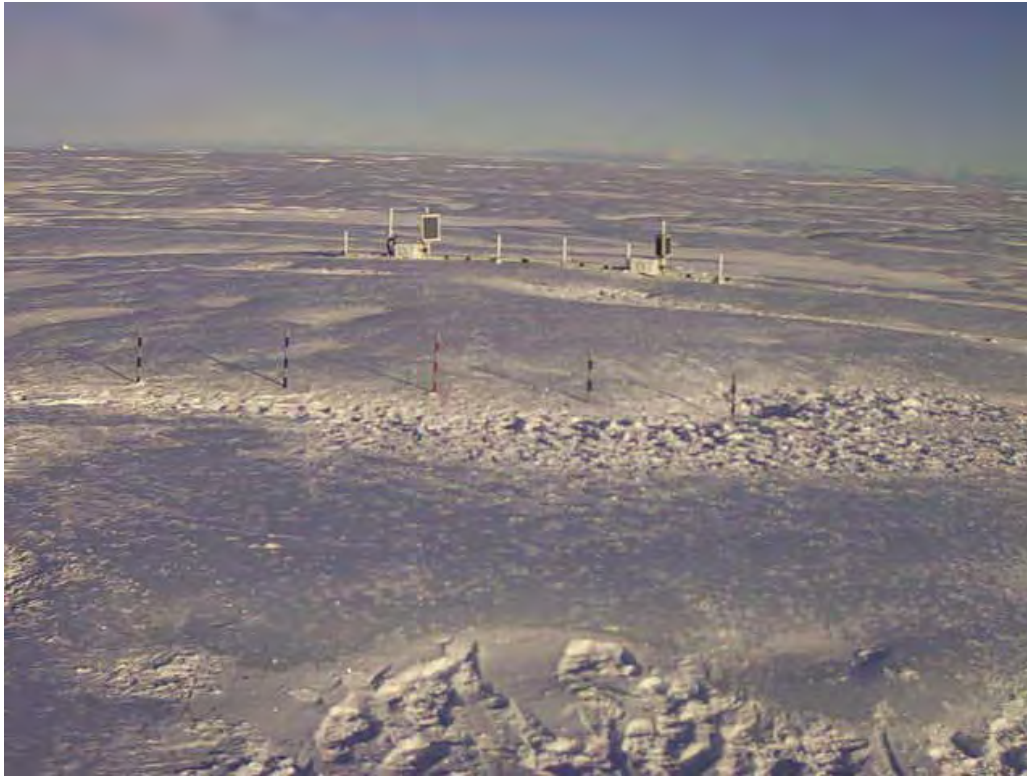


Figure 6-4. Image taken by the CC5MPX camera on the meteorological station showing the stripped ablation stakes and ice penetrating radar system.

Table 6-2: Sample data from the meteorological station.

	A	B	C	D	E	F	G	H	I	J	K	L	M	N	O	P	Q	R	S	T	U	V	W	X	Y	Z	AA	AB	J	A				
1	TOA5	2015_ice	CR1000	72392	CR1000_1	CPU1cel	64648	Hourly																										
2	TIMESTAMP	RECORD	BarV_M	PT	Temp_I	T103_C	DT	Q	Temp_C_Ai	Temp_C_C	Temp_C_D	Temp_C_E	Temp_C_F	Temp_C_G	Temp_C_H	Temp_C_I	GPGGA	Time	Latitude	Hemisp	Longitude	Hemisp	GPS_Qz	Num_Sa	HOOP	Altitude	Altitude_Geoidal	Geoidal_DGPS_A	Diff					
3	TS	RW			DegC	m	GoodK2	DegC	DegC	DegC	DegC	DegC	DegC	DegC	DegC	DegC	unitless	hhmmss	ddmm.m	N_S	ddmm.m	W_E	Smp	Smp	Smp	uu	v	v	v	Altitude	Altitude_Geoidal	Geoidal_DGPS_A	Diff	
4			Mn	Avg	Avg	Smp	Avg	Avg	Avg	Avg	Avg	Avg	Avg	Avg	Avg	Avg	Smp	Smp	Smp	Smp	Smp	Smp	Smp	Smp	Smp	Smp	Smp	Smp	Smp	Smp	Smp	Smp	Smp	Smp
5	2015/02/20 17:00	181	12.45	-3.471	-3.331	0.429	537	-3.331	-4.054	-4.088	-4.033	-4.164	-4.44	-5.019	165958	6723.4	N	6318.7	W	2	11	0.7	10.1	M	10.6	M							'6C	
6	2015/02/20 18:00	182	12.65	-3.527	-4.004	1.157	346	-4.023	-4.145	-4.173	-4.123	-4.248	-4.532	-5.035	175958	6723.4	N	6318.7	W	2	7	1.2	23.8	M	10.6	M							'6B	
7	2015/02/20 19:00	183	12.74	-3.68	-3.341	0.487	291	-4.425	-4.512	-4.547	-4.473	-4.608	-4.841	-5.107	185958	6723.4	N	6318.7	W	2	11	0.7	14.3	M	10.6	M							'6E	
8	2015/02/20 20:00	184	12.63	-3.844	-3.785	0.819	172	-5.957	-6.131	-6.085	-5.825	-5.962	-6.102	-1.047	195958	6723.4	N	6318.7	W	2	12	0.7	13.2	M	10.6	M							'6F	
9	2015/02/20 21:00	185	12.65	-4.298	-4.385	0.819	173	-6.343	-6.532	-6.364	-6.178	-6.169	-6.369	-2.449	205958	6723.4	N	6318.7	W	2	11	0.9	5.5	M	10.6	M							'58	
10	2015/02/20 22:00	186	12.63	-4.71	-4.293	0.819	175	-6.362	-6.571	-6.418	-6.236	-6.209	-6.409	-4.8	215958	6723.4	N	6318.7	W	2	11	0.7	3.4	M	10.6	M							'53	
11	2015/02/20 23:00	187	12.62	-4.9	-4.673	0.819	177	-6.537	-6.562	-6.425	-6.244	-6.22	-6.42	-6.194	225958	6723.4	N	6318.7	W	2	12	0.8	11	M	10.6	M							'6F	
12	2015/02/21 00:00	188	12.62	-5.071	-4.028	0.819	178	-6.585	-6.557	-6.431	-6.268	-6.234	-6.425	-6.489	235958	6723.4	N	6318.7	W	2	11	0.7	9	M	10.6	M							'53	
13	2015/02/21 01:00	189	12.6	-4.738	-3.393	0.819	176	-6.542	-6.553	-6.432	-6.279	-6.242	-6.429	-6.619	5858	6723.5	N	6318.8	W	2	11	0.9	6.8	M	10.6	M							'54	
14	2015/02/21 02:00	190	12.6	-4.804	-4.282	0.819	174	-6.486	-6.545	-6.425	-6.28	-6.245	-6.427	-6.689	15858	6723.5	N	6318.8	W	2	12	0.7	3.7	M	10.6	M							'5C	
15	2015/02/21 03:00	191	12.6	-4.831	-4.385	0.819	174	-6.522	-6.556	-6.438	-6.294	-6.261	-6.44	-6.75	25858	6723.5	N	6318.8	W	1	11	0.8	13	M	10.6	M							'62	
16	2015/02/21 04:00	192	12.59	-4.824	-4.163	0.819	175	-6.532	-6.55	-6.437	-6.301	-6.266	-6.441	-6.779	35858	6723.5	N	6318.8	W	2	11	0.7	13.3	M	10.6	M							'69	
17	2015/02/21 05:00	193	12.59	-4.816	-4.207	0.819	175	-6.593	-6.549	-6.437	-6.309	-6.276	-6.447	-6.807	45858	6723.5	N	6318.8	W	2	11	0.8	12.6	M	10.6	M							'6C	
18	2015/02/21 06:00	194	12.59	-5.516	-4.766	0.819	176	-6.876	-6.548	-6.439	-6.303	-6.278	-6.45	-6.83	55858	6723.5	N	6318.8	W	2	9	0.9	16.1	M	10.6	M							'68	
19	2015/02/21 07:00	195	12.59	-5.716	-4.597	0.821	174	-6.971	-6.548	-6.435	-6.32	-6.285	-6.45	-6.836	65858	6723.5	N	6318.8	W	2	10	0.8	8.1	M	10.6	M							'5E	
20	2015/02/21 08:00	196	12.58	-5.588	-4.531	0.821	175	-7.023	-6.56	-6.432	-6.325	-6.292	-6.454	-6.847	75858	6723.5	N	6318.8	W	2	11	0.8	8.8	M	10.6	M							'5C	
21	2015/02/21 09:00	197	12.58	-5.386	-5.003	0.821	176	-7.303	-6.598	-6.443	-6.329	-6.307	-6.471	-6.873	85858	6723.5	N	6318.8	W	1	11	0.8	16.8	M	10.6	M							'6A	
22	2015/02/21 10:00	198	12.58	-7.284	-5.647	0.823	178	-7.77	-6.647	-6.48	-6.351	-6.333	-6.499	-6.911	95858	6723.5	N	6318.8	W	1	12	0.6	3.4	M	10.6	M							'57	
23	2015/02/21 11:00	199	12.58	-7.84	-5.301	0.824	179	-8.14	-6.88	-6.476	-6.364	-6.34	-6.503	-6.916	105858	6723.5	N	6318.8	W	2	12	0.7	6.1	M	10.6	M							'59	
24	2015/02/21 12:00	200	12.58	-8.97	-6.739	0.826	185	-8.46	-6.726	-6.476	-6.352	-6.338	-6.506	-6.93	115858	6723.5	N	6318.8	W	1	12	0.8	26.3	M	10.6	M							'62	
25	2015/02/21 13:00	201	12.65	-8.72	-4.856	0.823	182	-8.6	-6.71	-6.429	-6.336	-6.311	-6.488	-6.322	125858	6723.5	N	6318.8	W	2	12	1	12.7	M	10.6	M							'68	
26	2015/02/21 14:00	202	12.88	-6.917	-5.136	0.825	180	-8.37	-6.599	-6.31	-6.245	-6.254	-6.462	-6.32	135858	6723.5	N	6318.8	W	2	12	0.7	10.5	M	10.6	M							'65	
27	2015/02/21 15:00	203	13.06	-5.315	-3.452	0.823	179	-7.881	-6.502	-6.222	-6.153	-6.208	-6.463	-6.955	145858	6723.5	N	6318.8	W	1	10	0.8	6.3	M	10.6	M							'56	
28	2015/02/21 16:00	204	13.38	-3.733	-4.846	0.826	185	-7.715	-6.434	-6.135	-6.082	-6.176	-6.458	-6.967	155858	6723.5	N	6318.8	W	2	9	0.9	3.1	M	10.6	M							'52	

The IPR system has recorded and transmitted daily radargrams since it was installed (Figure 6.5). Ice thickness is approximately 100 m. It is unknown why a large amount of 'ringing', or wave fluctuation after the airwave, is seen on these radargrams. This was not the case during the tests on the ice. However, the data is still usable as both the airwave and bed-wave are discernable.

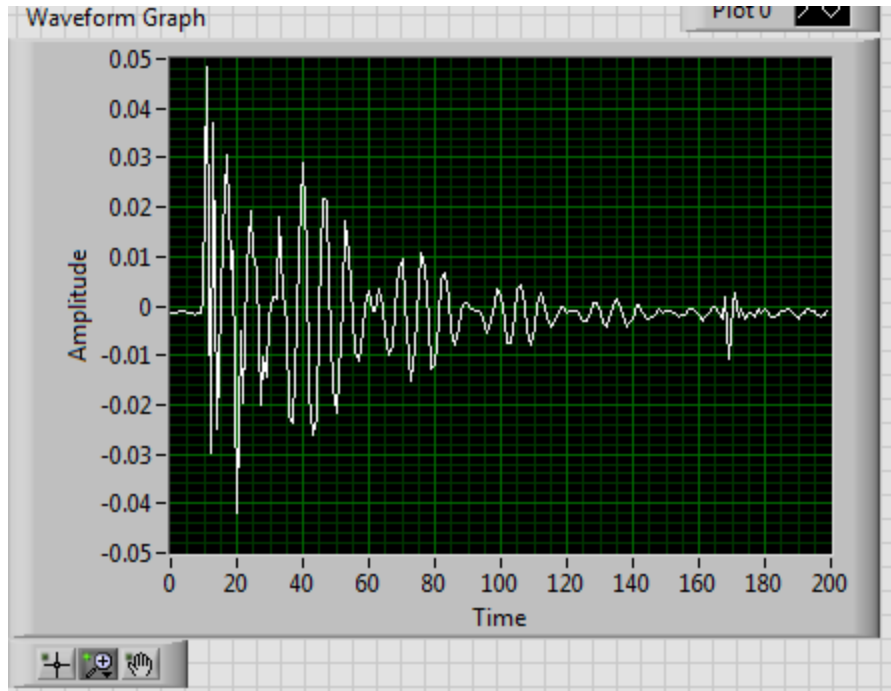


Figure 6-5. Sample radargram from the ice penetrating radar on 22 October. The airwave is first and the bed-wave is second at approximately 170 ns (Time).

6.4 Comments and recommendations

6.4.1 Iceberg drift and deterioration (Leg 1)

The data collection for the iceberg survey project during the Statoil/ArcticNet research cruise was a large success. Six icebergs were surveyed with varying combinations of methods – these being photogrammetry, laser scanning and multi-beam sonar surveying. We believe that the test days, conducted early in the campaign, were instrumental to this success. These trials allowed the users to become familiar with new equipment and software as well as improve these systems for the upcoming work on the iceberg study targets.

The iceberg survey team was never able to conduct all three surveying methods (multi-beam sonar, laser and photogrammetric surveying) on the same iceberg due to varying combinations of environmental conditions. A large issue was the presence of sea ice in the waters surrounding the ice features. It is recommended that additional time be spent on identifying/finding ice features outside of the sea ice or for the campaign to occur during a time period when sea ice is less likely to be a hindrance. We understand, however, that there are many considerations which come into play that make this difficult when organizing such a campaign.

The second large issue that the team faced was the inability to carry out a full ‘iceberg day’, which would include both surveying and oceanographic data collection. It is recommended, in the future, to begin a day of work with the iceberg surveying/sampling so that working-day

time constraints are less likely to cut sampling short. This is in the case that the iceberg project is a priority of the campaign, which should be discussed with all participants. Modification of the iceberg sampling plan, regarding duration and/or ability to work in other scientific activities while the data collection is underway, is also a possibility. Constraints were placed in the case of this project since internal waves were the subject of study and it is necessary to devote a long time period to their observation.

The next phase of the project includes post-processing the data. A large component of this step will be the correction for the iceberg drift, which occurred during surveying. Integration between the keel and sail scanning will also be undertaken in this phase. This will lead to the production of a complete 3D model of an iceberg. Analysis of the multiple models of iceberg sails will be completed to determine the precision of both the photogrammetry and laser scanning surveying methods for model creation, as well as compare the methods themselves.

6.4.2 Ice island mass balance (Leg 4)

It would be helpful, in the future, for a standard protocol to be enacted regarding ship activities and operating distance from an ice island field site. Everything has worked out fine in the years that we have conducted work from the *Amundsen*, however, there we seem to go through the same discussions and questions each year and a standard protocol would erase this need.

References

- Crawford, A.J., Mueller, D.R., Humphreys, E.R., Carrieres, T., Tran, H., 2015. Surface ablation model evaluation on a drifting ice island in the Canadian Arctic. *Cold Regions Science and Technology*, 110:170-182.
- Environment Canada. 2012. Petermann Glacier Ice Island 2012. Government of Canada. Date accessed: 15 June 2013. <http://www.ec.gc.ca/default.asp?lang=En&n=592AB94B-1&news=63B51150-B0B0438F-94CA-A1CDDFA86A25>
- Falkner, K.K., Melling, H., Münchow, A.M., Box, J., Wohlleben, T., Johnson, H.L., Gudmandsen, P., et al., 2011. Context for the recent massive Petermann Glacier Calving Event. *Eos*, 92(14):117-124.
- Forrest, A.L., Hamilton, A.K., Schmidt, V., Laval, B.E., Mueller, D., Crawford, A., Brucker, S., and Hamilton, T. 2012. Digital terrain mapping of Petermann Ice Island fragments Canadian High Arctic. Proceedings of the 21st International Symposium on Ice held 11-15 June in Dalin, China.
- Hamilton, A.K., Forrest, A.L., Crawford, A., Schmidt, V., Laval, B.E., Mueller, D.R., Brucker, S., Hamilton, T. 2012. Project ICEBERGS Final Report. Report prepared for the Canadian Ice Service, Environment Canada, Ottawa, Ontario. 36 pp.

- Johannessen, O.M., Babiker, M., Miles, M.W., 2011. Petermann Glacier, North Greenland: massive calving in 2010 and the past half century. *The Cryosphere Discussions*, 5:169-181.
- McGonigal, D., Hagen, D., Guzman, L. 2011. Extreme ice features distribution in the Canadian Arctic. *Proceedings of the 20th International Conference on Port and Ocean Engineering under Arctic Conditions held 11-14 July in Montréal, Quebec*. POAC 11-045.
- Peterson, I.K. 2011. Ice island occurrence on the Canadian East Coast. *Proceedings of the International Conference on Port and Ocean Engineering under Arctic Conditions. Held 10-14 July in Montréal, Canada*. POAC11-044.
- Stern, A.A., Johnson, E., Holland, D.M., Wagner, T.J.W., Wadhams, P., Bates, R., Abrahamsen, E.P., Nicholls, K.W., Crawford, A., Gagnon, J., Tremblay, J-E. 2015. Wind-driven upwelling around grounded tabular icebergs. *Journal of Geophysical Research: Oceans*, 120, doi:10.1002/2014JC010805.
- Wagner, T.J.W., Wadhams, P., Bates, R., Elosequi, P., Stern, A., Vella, D., Povl Abrahamsen, E., Crawford, A, Nicholls, K.W. 2014. The “footloose” mechanism: Iceberg decay from hydrostatic stresses. *Geophysical Research Letters*, 41:1-8, doi:10.1002/2014GL060832.

7 AUV: Deployment of BioArgo floats in Baffin Bay – Legs 2 and 4b

ArcticNet Phase 3 – Long-Term Observatories in Canadian Arctic Waters.

<http://www.arcticnet.ulaval.ca/pdf/phase3/marine-observatories.pdf>

Project leader: Marcel Babin¹ (marcel.babin@takuvik.ulaval.ca)

Cruise participant Leg 2: José Lagunas-Morales¹

Cruise participant Leg 4b: José Lagunas-Morales¹

¹ *Takuvik (UNI-3376), Pavillon Alexandre-Vachon, 1045 Avenue de la Médecine, Université Laval, Québec, QC, G1V 0A6, Canada.*

7.1 Introduction

It is in the scientific interest of Takuvik to understand ice-edge blooms, the physical mechanisms responsible for nutrient inputs, the propagation of sunlight (ice floe and water column), ice-edge bloom dynamics and the response of associated phytoplankton species. Ice edge blooms are systematically observed in the Baffin Bay region. In addition, observations by remote sensing of ocean color show that the spring blooms now occur 50 days earlier than in 1997.

Takuvik has launched a program for the deployment of 20 BioArgo floats in Baffin Bay and will be responsible for the follow-up of the floats together with the Laboratoire d'Océanographie de Villefranche (LOV). The latter will host the data collected by the BioArgo floats and make it accessible for public domain through their servers. Takuvik works closely with the LOV, they are both actively involved in the NAOS project, which is a french initiative for the development of the Argo network. The active payload (sensors) carried by each BioArgo float are: CTD, CDOM, PAR (400-700 nm), Oxygen, Nitrates, Chlorophyll-a, radiometer ($\lambda=380/412, 490, 555$ nm) and a transmissiometer ($\lambda=650$ nm) will produce valuable data for the scientific community.

The main objective of the activities conducted during 2015 *Amundsen's* mission was the deployment of four Takuvik's BioArgo floats in the Baffin Bay region, at Station BB2 (Leg 2). This could not be achieved due to a hydraulic fault in the conception of Argo floats for polar regions. Oil is used by the profiler to control its buoyancy, the oil used for regular Argo floats, i.e., profiling in warmer latitudes is of mineral type. The same oil was used in the Arctic version not taking into account that viscosity increases in this type of oil whenever temperatures decreases. Thus, two solutions were proposed, a) an oil change to a synthetic type or b) an adjustment of firmware parameters to account for the delay in the oil flux caused by the viscosity of the oil in cold weather. The latter was chosen and tried during the Leg 4b of the *Amundsen's* 2015 mission.

7.2 Methodology

During Leg 2, at Station BB2, (N 72°45, W 67°00), four geographical coordinates were chosen for the deployment of the BioArgo floats. The *Amundsen's* barge was used to navigate >2 nautical miles away from the ship taking into account wind and current directions. The operation was divided in two launches were two floats were to be deployed at each occasion. The coordinates of the first deployment were: N 72°44.343, W 66°54.570 and N 72°43.546, W 66°57.554. On 9 August at 5h45 the loading of the floats to the barge began. By 6h55 the first float (takapm003b) was deployed and the second one (takapm009b) at 7h30. The barge stayed for 40 minutes close to the second deployment before returning to the vessel. A mechanical problem with the barge's engine prevented this action and the ice-breaker navigated to our location to retrieve us. At this point, the LOV team had verified the status of the floats and noticed that they couldn't immerse since their density wasn't enough. The second deployment was cancelled and a recovery operation on the *Amundsen's* Zodiac was programmed to 12h00. Edouard Leymarie from the LOV, communicated the GPS points sent by the BioArgo floats, as their routine commands in abnormal situations, to the officer's deck. This information was communicated to the team in the Zodiac by VHF and the recovery of the floats was completed by 14h00.

During Leg 4b, a compromise between the time available for the operation and the minimum distance away from the coast for a safe deployment was found and the deployment point was set to 6739.39412N, 06046.91910W. Launching took place from the A-frame located in the port side of the ship. The float takapm003c was deployed on October the 22nd (2015) at 15h35 and the float takapm010c was deployed on the same day at 16h05. Figure 7.1 shows the launching operations, specifically the initialization of the profiler and Figure 7.2, shows the BioArgo float deployed. By 17h45, both floats had immersed and four hours later, they surfaced after a first test profile at a depth of 100m.

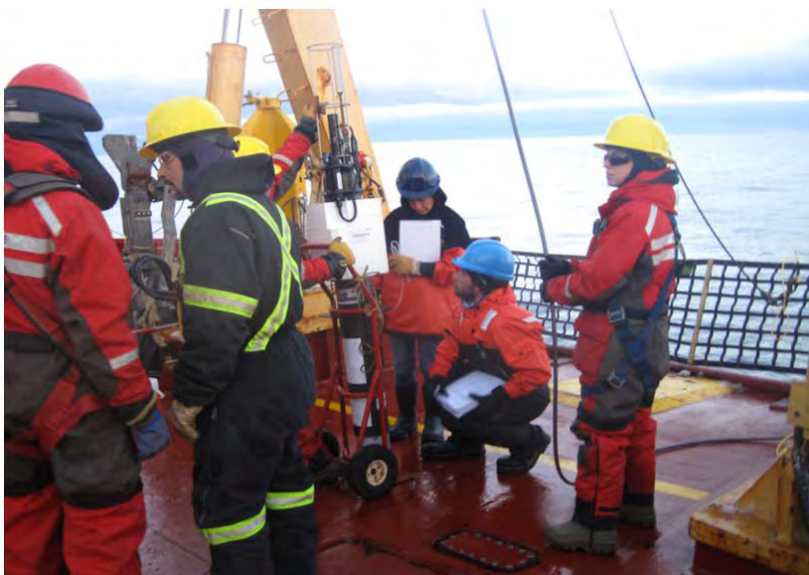


Figure 7-1. Deployment from the *Amundsen's* A-frame.



Figure 7-2. Argo float deployed.

7.3 Preliminary results

During Leg 2, a major issue regarding ballasting was found to be the cause preventing the immersion of the BioArgo floats. The BioArgo floats need to be re-ballasted accordingly to the conditions met in Baffin Bay. A thorough analysis of the conditions encountered versus the previous ballasting needs to be conducted by their manufacturer NKE in France. No preliminary results resulted from this operation.

Following their successful deployments during Leg 4b, the data gathered by both BioArgo floats is now accessible in:

<http://www.oao.obs-vlfr.fr/bioargo/PHP/takapm003c/takapm003c.html> <http://www.oao.obs-vlfr.fr/bioargo/PHP/takapm010c/takapm010c.html>

and their journey can be followed at:

<http://www.oao.obs-vlfr.fr/data-apmt/trsfrt/takapm003c/route.kml> <http://www.oao.obs-vlfr.fr/data-apmt/trsfrt/takapm010c/route.kml>

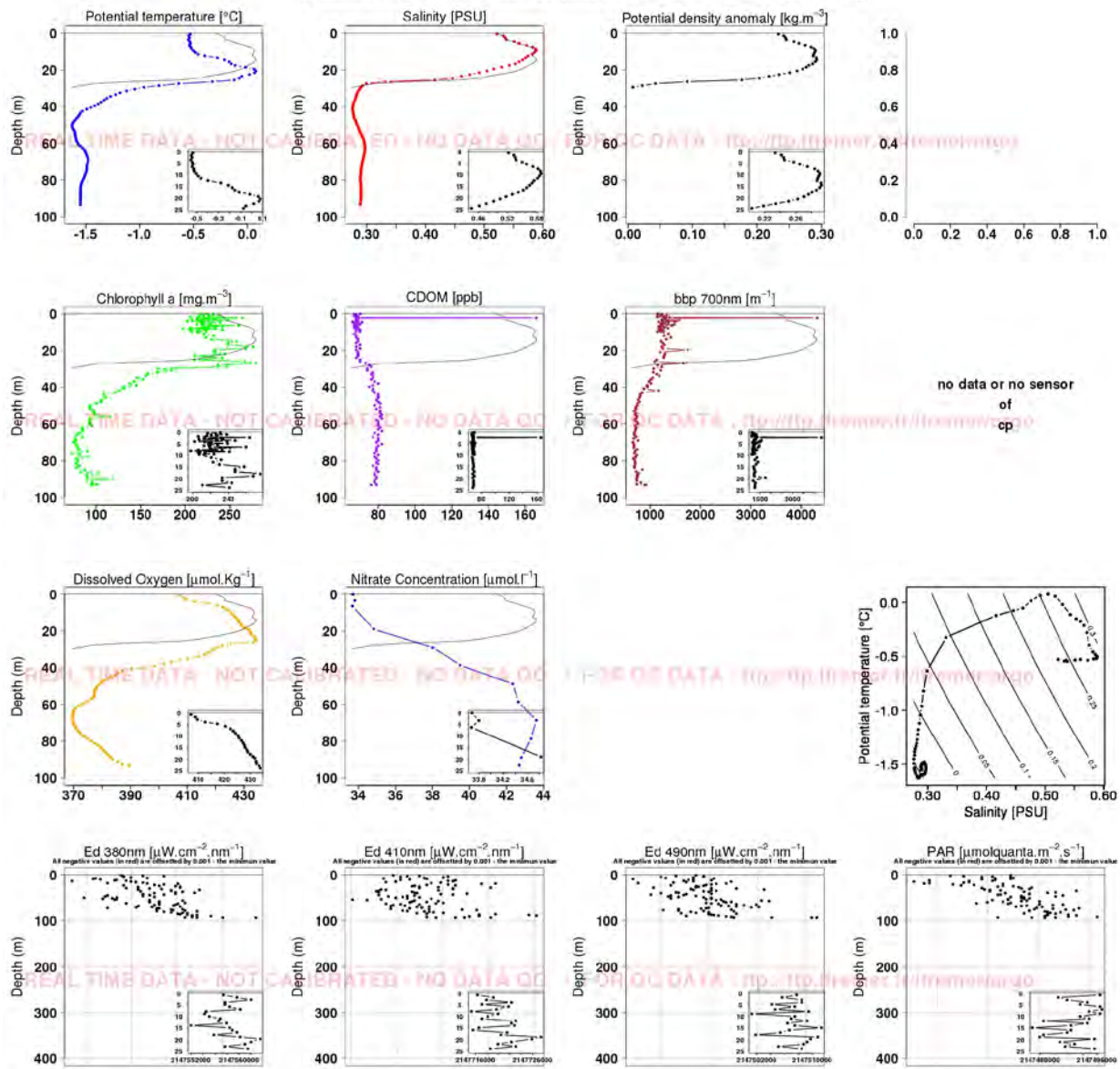


Figure 7-3. Data recorded by the BioArgo float takapm003c during a test profile on 22 October (Leg 4b).

7.4 Comments and recommendations

Internet connection was essential for this operation, since BioArgo data are sent systematically to a server and remote access was severely limited, however this is understandable due to the quality of the service available at these latitudes.

8 Mooring Program – Legs 3a and 3b

ArcticNet Phase 3 – Long-Term Observatories in Canadian Arctic Waters.

<http://www.arcticnet.ulaval.ca/pdf/phase3/marine-observatories.pdf>

Project leader: Louis Fortier¹ (louis.fortier@bio.ulaval.ca)

Cruise participants Leg 3a: Shawn Meredyk¹, Luc Michaud¹ and IMG-Golder Corporation²

Cruise participants Leg 3b: Shawn Meredyk¹ and IMG-Golder Corporation²

¹ *ArcticNet, Pavillon Alexandre-Vachon, 1045 Ave. de la Médecine, Local 4081, Université Laval, Québec, QC, G1V 0A6, Canada.*

8.1 Introduction

Sampling year 2015 was part of a summer-fall expedition studying the air-sea interactions, underwater sound ecology, ocean circulation variability and basin-shelf sediment interactions of the southern Beaufort Sea and Amundsen Gulf.

Mooring operations during Leg 3a (20 August– 4 September) were part of the ArcticNet Long-Term Ocean Observatory (LTOO) project / and Integrated Beaufort Observatory (iBO; a new program partly supported by the Environmental Study Research Fund). The iBO mooring sites are based on key locations targeted by the Southern and Northeastern Beaufort Sea Marine Observatories project funded under the former Beaufort Regional Environmental Assessment (BREA) initiative from 2011 to 2014.

Mooring operations during Leg 3b (18 September – 1 October) were part of the ArcticNet – Parks Canada – Weston Foundation innovative to investigate the oceanographic conditions near and surrounding the shipwreck *Erebus* in the Queen Maud Gulf.

In total, during Leg 3 onboard the *Amundsen*, seven moorings were recovered and seven moorings were deployed over the slope of the southeastern Beaufort Sea, Amundsen Gulf and in the Queen Maud Gulf.

Area of study

The Amundsen Gulf is an area where the air-sea interactions occurring in the ice-free sections of the southern Beaufort Sea and Amundsen Gulf were investigated. This productivity hotspot is of interest, to monitor the intermittent upwelling of cold-saline water on the eastern shelf, despite the fact that the origin of the upwelling is much closer to Cape Bathurst (e.g. CA06). In fact, ocean circulation is highly variable here, but the along-shelf flow of Pacific-derived water entering the Amundsen Gulf can be potentially monitored at depth. Mooring CA08-15 is the center of the 'Cape Bathurst polynya' as defined in Barber and Hanesiak (2004). This location is a very good candidate for the long-term monitoring of particle flux, as it has all the advantages of catching adequately both the seasonal signal and the inter-annual variability of marine productivity in the Amundsen Gulf, without having

too much of the terrigenous inputs that characterize the moorings close to the Mackenzie Shelf.

The Mackenzie Trough, a cross-shelf canyon in the Beaufort Sea shelf, has been observed to be a site of enhanced shelf-break exchange via upwelling (caused by wind- and ice-driven ocean surface stresses). The canyon provides a conduit for bringing deeper, nutrient rich water to the shelf. Shelf waters in the area are seasonally influenced by freshwater output from the Mackenzie River, both in terms of temperature-salinity properties and suspended sediments / turbidity.

Capturing the Beaufort gyre's anti-cyclonic (west) movement relative to a long-shore counter-current (east) plays an important role in understanding deep and shallow water movements relative to nutrient and particle fluxes.

Ice cover, examined by moored ice profilers and satellite imagery, plays a significant role in terms of affecting momentum transfer from wind to water, constrained (in the case of landfast ice) and enhanced (in the case of drift ice) by wind.

Hydrophone recordings on the shelf-slope area will monitor bioacoustics vocalizations throughout the year to better understand the potential impact that future operations in the Beaufort Sea could have on the marine mammals.

8.2 Methodology

8.2.1 Mooring Arrays

Over 2014-2015, the legacy BREA moorings (BRG, BR1, BR2, BRK, BR3 and BR4) accompanied by three ArcticNet moorings (BS1, BS2, BS3), formed three shelf –slope arrays that examined the spatial variability in shelf-slope processes in the southeastern Beaufort Sea (Figure 8.1). These moorings continued a long-term integrated observation of ice, water circulation and particle fluxes established in the southern Beaufort Sea since 2002. Moorings BRG, BR3 and BRK were re-deployed during Leg 3a as part of the iBO program while mooring BS1, BS2, BS3 and BR04 were recovered and not redeployed. Moorings BR1 and BR2 were recovered from the CCGS *Sir Wilfrid Laurier* on 29 September 2015 and only BR1 was redeployed on 30 September.

LTOO moorings CA08 and CA05 were deployed in the Amundsen Gulf (Figure 8.1) to extend the annual time-series collected in the area from 2002 to 2009. This region, also known as the “Cape Bathurst Polynya”, was previously identified as an area of increased biological activity due to an earlier retreat of sea ice in spring and frequent upwelling of nutrient-rich waters that develops along Cape Bathurst and near the eastern edge of the Mackenzie Shelf.

New moorings WF1 and WF2 are moorings that are part of a combined effort by the Weston Foundation, ArcticNet and Parks Canada deployed to study the oceanographic conditions near the *Erebus* and in the Queen Maud Gulf near the location of the wreck site (Figure 8.1). The Weston Foundation provided sufficient funding for oceanographic equipment and ArcticNet and Parks Canada provided technical and operations support with the vessel support from the CCGS *Amundsen / Marty Bergman*. Mooring WF1 was deployed from the *Amundsen* in 100m of water in the Queen Maud Gulf, while WF2, a benthic tripod, was deployed from the *Marty Bergman* and placed near the *Erebus* at 20m depth, with an upward looking ADCP (RDI Sentinel V) combined with an RBR CTD-Tu sensor.

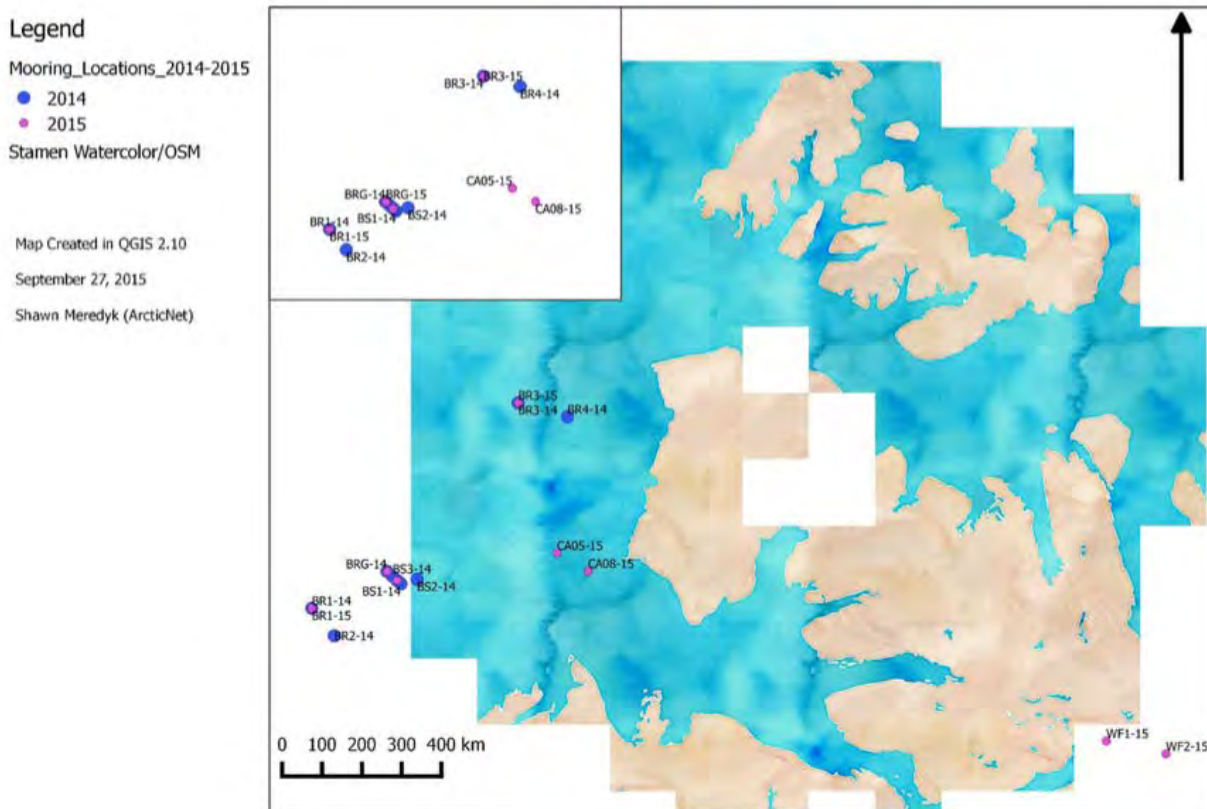


Figure 8-1. Mooring locations 2014-2015-2016: BREA-iBO-ArcticNet mooring arrays.

8.2.2 Mooring Design and Instrumentation

Table 8-1. Description of oceanographic equipment







Photo	Description and specifications
	<p>The SBE 37 was used to record the conductivity, temperature and depth (CTD) Depth 50m intervals on ArcticNet moorings</p>














Photo	Description and specifications
	<p>The AURAL M2 hydrophone from Multi- électronique was deployed to record underwater sounds at a sampling rate of 16 kHz. Depth 100-150m, on ArcticNet moorings only</p>
	<p>The Nortek 190/ 470 kHz Continental model of Acoustic Doppler Current Profiler (ADCP) was housed in stainless steel cage and six panther floats were attached to each side of the ADCP cage. The upward and downward looking profilers were designed to record 100 to 200m of water column velocity data (binning of 4m). Depth 100 and / or 300m, depending on proposed mooring depth of ArcticNet moorings only</p>
	<p>Semi-Permeable Membrane Devices (SPMDs) were designed to be installed on the ADCP cages and mooring line as well, in an effort to trap persistent organic pollutants (POPs) within a gel matrix within the traps. Deployed Depths: 50, 60, 100, 200 and 300m</p>
	<p>Satlantic In situ ultraviolet spectrophotometric (ISUS) V3 Nitrate Sensor. Deployed Depths: 60m</p>
	<p>JFE_ALEC CLW Turbidity and Chlourometer to measure the concentration of chlourophyll and gain a measure of suspended particle concentration</p>
	<p>JFE_ALEC Compact ALW Photosynthetic Active Radiation (PAR) to measure photosynthesis activity</p>
	<p>JFE_ALEC CTW device is used to measure conductivity and temperature (CT)</p>

Photo	Description and specifications
	<p>RBR XR420 CT device is used to measure conductivity and temperature (CT) along with Dissolved Oxygen (DO), Turbidity (TU) and Fluorimetry (FL) Depths: 100, 200, 300 and 400m</p>
	<p>LISST-100x particle analyzer identifies the size of particulate matter in the water column at its designated deployment depth. Depth 130-150m, BR-K, BR-2, BR-4 shallow moorings</p>
	<p>The ASL Environmental Sciences IPS (model 5) was used to measure size and thickness of ice keels and ice velocities. Deployment depth ~60m with syntactic buoy.</p>
	<p>Technicap PPS 3/3-24S 24 cup sequential sediment trap was deployed to record the annual cycle in vertical carbon flux. Depth 100 and / or 200m and / or 300m, depending on proposed mooring depth</p>
	<p>Tandem Benthos, OCEANO, CART or 8242XS acoustic releases were used as the primary recovery / release devices. Depth: 5-8m (Oceano) or 12m (CART / 8242XS) above target mooring bottom depth</p>

The ArcticNet moorings were generally designed to be of taut-line configuration consisting of

- a top float (50-60m depth),
- an ALEC CTW - Conductivity, Temperature (CT) probes to record water characteristics, ALEC CLW – Chlorophyll – Turbidity probes, ALEC ALW – Photosynthetic Active Radiation (PAR),
- two current profilers (Continental 470 kHz) with 2m vertical resolution, to record the water velocities within the water column,
- hydrophone (Aural M2) with a 16 kHz, 90min sampling rate to listen to bioacoustics signatures within the water column,
- in-line floatation (30" ORE steel float) to balance the weight/ float/ tension throughout the mooring line,
- sediment trap (Technicap PPS 3/3 with 24 sample cups – semi- monthly sampling rate) to trap descending sediment for particle flux analysis and accumulation rates,

- two 1000 kHz Nortek Aquadopp current meters (or a single- point RCM11 current meter\CTD) measuring near-bottom current speeds with associated oceanographic sensors,
- Tandem mooring releases (Benthos or Oceano) and
- An anchor (one to three train wheels).

BS2-14 Southern Beaufort Sea - Mackenzie Trough					BS3-14 Southern Beaufort Sea - Mackenzie Trough				
Proposed Position:		Longitude	Latitude	Proposed Position:		Longitude	Latitude		
Decimal Degrees (WGS84)		-135.09183	70.09485	Decimal Degrees (WGS84)		-135.23028	70.12443		
Triangulated Position:		-134.09446	70.88123667	Triangulated Position:		-135.2307857	70.92594		
Target Depth (m) :		300			Target Depth (m) :		500		
Instrument Depth (m)	Instrument	Water Weight (kg)	Other Equipment	Net weight (kg)	Instrument Depth (m)	Instrument	Water Weight (kg)	Other Equipment	Net weight (kg)
41m	 ORE 30 Buoy Buoyancy 168kg	168.0		334.2	51m	 ORE 30 Buoy Buoyancy 168kg	168.0		376.2
	50m Kevlar line 5/16"		SBE 37 #10612 and SPMD (50m)				45m Kevlar line 5/16"		
81m	<td>-14.0 -18.0 105.6</td> <td>RBR XR420 CT #15270 (100m) and SPMD</td> <td></td> <td>96m</td> <td> <td>-14.0 -18.0 105.6</td> <td></td> <td></td> </td>	-14.0 -18.0 105.6	RBR XR420 CT #15270 (100m) and SPMD		96m	<td>-14.0 -18.0 105.6</td> <td></td> <td></td>	-14.0 -18.0 105.6		
84.5m	<td>-14.0 -10.0 105.6</td> <td></td> <td></td> <td>96m</td> <td> <td>-14.0 -18.0 105.6</td> <td>RBR CT #15278 and SPMD (100m)</td> <td></td> </td>	-14.0 -10.0 105.6			96m	<td>-14.0 -18.0 105.6</td> <td>RBR CT #15278 and SPMD (100m)</td> <td></td>	-14.0 -18.0 105.6	RBR CT #15278 and SPMD (100m)	
140m	 Aural M2 hydrophone #91 (8 kHz, 120min cycle/ 10min)	-19.0	SBE 37 #10849(100m)		148m	 ORE 30 Buoy Buoyancy 168kg	-168.0		
	50m Kevlar line 5/16"					2m Kevlar line 5/16"			
199m	 Sediment trap Technicap PPS 33-24s Weight in water 18kg	-18.0	RBR XR420 CT #15258 and SPMD (200m)		160m	 Aural M2 hydrophone (8 kHz, 120min cycle/ 10min sample)	-19.0	SBE 37 #10786 (150m)	
	15m Kevlar line 5/16"		Sediment trap #30			50m Kevlar line 5/16"			
274m	 4 Benthos Buoy 17 Buoyancy 25kg	100.0			199m	 Sediment trap Technicap PPS 33-24s	-18.0	RBR XR420 CT #15259	
	5 m Kevlar Line 5/16"					100m Kevlar line 5/16"			
285m	 OCEANO acoustic releases Tandem assembly Weight in water 23kg	-44.0			209m	<td>-14.0 -18.0 105.6</td> <td>SPMD on cage (300m) and RBR XR 420 #15271</td> <td></td>	-14.0 -18.0 105.6	SPMD on cage (300m) and RBR XR 420 #15271	
	-3m polyrope line shackles -2 m chain					 4 Benthos Buoy 17 Buoyancy 25kg	100.0		
300m	 Anchor (800 lbs train wheel) 3 train wheels	-2400.0			285m	 OCEANO acoustic releases Tandem assembly Weight in water 23kg each	-44.0		
						-3m polyrope line shackles -2 m chain			220.4
					300m	 Anchor (800 lbs train wheel) 4 train wheels	-3200.0		

BS1-14

Southern Beaufort Sea - Mackenzie Trough

Proposed Position
 Decimal degrees (WGS84)
 Triangulated Position
Target Depth (m):

Longitude Latitude
 -135.50173 70.65616
 -134.85061 70.81078667
 80





~ Instr. Depth (m)	Instrument	Water	Other Equipment	Net weight (kg)
45m	 ORE 30" Buoy Buoyancy 168kg	168.0		196.6
	15m Kevlar line 5/16"		SBE 37 #10851 and SPMD (50m)	
60m	 Nortek Currentmeter #6070 Continental 470kHz Weight in water 15kg Cage (Weight in water) 6 Panther buoys Buoyancy 17.6kg Galv shackles, swivel	-15.0 -18.0 105.6		
	15m Kevlar line 5/16"		RBR XR420 CT 17113 (75m)	
75m	 OCEANO acoustic releases Tandem assembly Weight in water 22kg	-44.0		
	~3m polyrope line shackle ~2 m chain			
80m	 Anchor (800 lbs train wheel) 2 train wheels	-1600.0		

Figure 8-2. Mooring designs BS1-14, BS2-14 and BS3-13 recovered in southern Beaufort Sea during Leg 3a.

The iBO-ArcticNet moorings were designed to be of a taut-line configuration. The longer moorings (BRG, BR3, BR1) consisted of the following key components:

- ASL Ice Profiling Sonar (IPS) were used at approximately 50-60 m depth to measure ice draft. IPS were mounted in 30-inch spherical Mooring Systems International (MSI) syntactic foam floats.
- 150 kHz Teledyne RDI (TRDI) Quarter Master Acoustic Doppler Current Profiler (QM ADCP) were used at approximately 180 m water depth to profile currents with a vertical resolution of 8 m, as well as to measure ice velocity using the Bottom-Track feature. The QM ADCPs were mounted up-looking in 40-inch syntactic foam floats manufactured by Flotation Technologies.

- 75 kHz TRDI Long Ranger ADCP (LR ADCP) were used at approximately 460 m water depth to measure water velocity profile at a coarser 16 m resolution (redundancy for QM). The LR ADCPs were mounted up-looking in 40-inch syntactic foam floats manufactured by Flotation Technologies.
- In water depths greater than 500 m, high frequency short-range (<1m) Nortek Aquadopp DW (AQD) point current meters were used approximately every 100 m to measure water velocity.
- Two Technicap PPS 3/3-24S 24 cup sequential sediment traps were deployed between the IPS and LR ADCP to record the annual cycle in vertical carbon flux.
- RBR Conductivity and Temperature (CT) loggers were installed at various depths (relative to equipment that benefits from more precise CT data) to measure water temperature and salinity and to compute sound speed (used to improve IPS and ADCP processing). In some cases, Conductivity, Temperature, and Depth (CTD) loggers were used on the moorings.
- Various smaller syntactic foam floats were distributed along the mooring as required.
- Tandem EdgeTech acoustic releases were used as the primary recovery device.
- One to three train wheels were used as an anchor.

The shallow moorings (BRK, BR4, BR2) consisted of the following key components:

- IPS were used at approximately 50-60 m depth to measure ice draft. The IPS were mounted on an ASL dual cage with 8 Viny 12B3 floats.
- 300 kHz TRDI Workhorse Sentinel Acoustic Doppler Current Profiler (WHS ADCP) were used at approximately 130 to 140 m water depth to profile currents with a vertical resolution of 8 m, as well as to measure ice velocity using the Bottom-Track feature. The WHS ADCPs were mounted upward looking in 33- inch syntactic foam ellipsoid floats manufactured by MSI.
- RBR CT loggers were installed at various depths near instruments to measure water temperature and salinity and to compute sound speed (used to improve IPS and ADCP processing). In some cases, CTD loggers were used on the moorings. Additionally, a few RBR loggers also had additional sensors to measure turbidity, dissolved oxygen, fluorometry-chlorophyll.
- Sequoia LISST 100X laser diffraction systems were located 18 m above the seafloor to provide measurements of particle size distributions and associated volume concentrations in the lower water column. The LISST measurements will help to better quantify the seasonal and annual variability of vertical and horizontal fluxes of organic and inorganic solids.
- 1000 kHz Nortek Aquadopp profiling current meters (AQP) were mounted down-looking below the LISST instrument to provide details of the flow and acoustic backscatter structure near the seafloor on the continental shelf edge. The AQP's measure three-dimensional current velocities and provide a measure of acoustic backscatter intensity in 2 m range bins from the bottom to about 16 m above seabed. Combined with the velocity profile information from upward looking ADCP's the profilers provide a detailed and complete view of the water column vertical structure.
- An additional syntactic foam ellipsoid float was located above the LISST cage to provide floatation for the lower portion of the mooring.
- Tandem EdgeTech acoustic releases were used as the primary recovery device.

On 2014-2015 moorings in the cross-shelf-slope array (BRG and BRK) additional Seabird Electronics SBE37 CTD loggers were mounted at approximately 60 m for consistency with the BS1, BS2, and BS3 mooring datasets (recovered in 2015). RBR CTDs were mounted at 100 m on BRK and at 100 m and 150 m on BRG to maintain consistency with the ArcticNet moorings' recovered datasets (2015).

Semi-permeable membrane devices (SPMDs) were re-deployed on moorings BRK-15 (60m), BRG-15 (60, and 260m and 460m), BR3-15 (60 m). The SPMDs are small passive water samplers that clamp directly to the mooring line or instrument cage. The goal of the SPMDs was to monitor concentrations of persistent organic pollutants (POPs) in the mixed surface layer (Pacific water mass and the deep Atlantic waters) by Gary Stern at CEOS in Winnipeg, Manitoba (for further reference to SPMD analysis and results contact Gary Stern).

The only mooring that had a unique configuration was the benthic tripod mooring that only consisted of a 50cm tall tripod with lead weight on the tripod legs to keep the unit on the seafloor. The tripod's objective was to carry an ADCP (RDI Sentinel V) with a CTD sensor with turbidity capabilities. This new ADCP from RDI was purchased and programmed with the idea to extract wave, ice and water column velocities for an entire year near the shipwreck.

8.2.3 Field Calibrations

Compass accuracy is essential for current meters deployed near or above the Arctic Circle, due to the reduced magnitude of the horizontal component of the earth's magnetic field. Therefore, it was important to calibrate internal compasses near the approximate latitude where they were deployed and care was taken to eliminate all ferrous material in the mooring cages and in the calibration environment. A list of oceanographic equipment that contains internal compasses can be found in Table 8-2.

Calibration of the all of the RDI LR/QM/Sentinel ADCPs used for the entire 2015 mooring operations (*Amundsen* and *Laurier*) were performed in 2015 in Inuvik, NT by Golder and the post-verifications of the Nortek ADCPs was also performed in 2015 in Inuvik, NWT by Golder and ArcticNet. The calibration was conducted with a tilt and rotate jig (Figure 8.3). The calibration procedures followed standard manufacturer protocols for each instrument (see below).

RDI ADCP Field Calibration Procedure

ADCP calibrations were conducted with a leveled tilt and rotate jig / table. The calibration procedures followed standard manufacturer protocols for each instrument (Table 8-2). The general calibration procedure is briefly described below :

- Communication was established with the instrument using the manufacturer's (RDI BBtalk) calibration software over a RS- 232 serial communication line.

- Power was provided to the instrument by an external adapter powered by a portable battery pack / battery charger with a 120 VAC outlet.
- The current meters were oriented in the configuration in which they would be deployed (facing Up).
- The calibration table was rotated in 10° increments, through 360 degrees, having recorded the varying degrees of pitch, roll and heading relative to true north, until a successful (< 5° compass error) calibration was achieved.



Figure 8-3. Tilt and rotate calibration jig / table as utilized in Inuvik, NWT

A handheld Garmin GPSMap 76S was used to determine true North and the calibration table zero indicator \ mark was aligned with the table and a marker 50m away, along the same longitude. Compass calibrations and verifications were verified by rotating the current meter through 360 degrees and measuring the headings corrected for magnetic declination at each 10 degree increments and comparing these against the true north measurements from the GPS unit.

Aanderaa RCM (Recording Current Meter) Calibration Procedure (ArcticNet)

The CTD sensors on the RCM units used in the ArcticNet LTOO moorings were calibrated by ArcticNet (ULaval) in 2011. The CTD sensor compass calibration procedure was performed by the 2015 Golder mooring assistant.

The RCM11 unit was opened to verify the internal zero heading indicator, to connect the battery pack and to turn the unit onto continuous sampling (1 sensor per second) for all 8 channels (sensors connected). Deck Unit Aanderaa A-3127 was connected to the port on top of the RCM11 and to the laptop-PC, and the Hyperterm terminal program was used to look at (and during actual compass calibrations, to capture to file) the ascii output from it.

The water-current simulation Test Unit (Aanderaa A-3731) was placed over the Doppler current sensors (type DCS-3900), with transducer surfaces moistened for best acoustic contact. The RCM11 was rotated 90 degrees to verify that the acoustic sensors functioned properly and changed the simulated “direction” by about that amount (channel 3 is the compass sensor’s heading data channel). The instrument was inclined to check the built-in tilt sensor functionality.

By rotating the calibration table in 10° increments and recording the values on channel 3 (takes at least two readings before compass stabilizes), then converting the raw values (channel 3 value * 0.352) into actual headings and plotting the 6th order slope of the fitted line, compass calibration coefficients and the compass error can be calculated / recorded for post-processing of the unit’s data.

ADCP Calibration Problems / Concerns

All Nortek equipment was repaired and calibrated at the Nortek factory two weeks prior to the CCGS *Amundsen*’s departure in 2014, due to a discovery of compass calibration errors within the Nortek equipment and a deficiency¹ within Nortek’s calibration subroutine (June-July, 2014).

In 2015, all of the RDI and Aanderaa RCM11 units were calibrated in Inuvik at the BBE calibration field (June, 2015: 68.308266° N Lat, 133.4872833° W Long, IGRF Mag. Decl. 22° 52.86’ E).

Post-deployment verification of the Nortek ADCP compasses (deployed in 2014) was required to develop a corrective algorithm (post-processing QA\QC necessity) to account for any heading bias issues that the Nortek devices are not able to correct internally \ real-time (Sept 5-6, 2015: 68.308266° N Lat, 133.4872833° W Long, IGRF Mag. Decl. 22° 52.86’ E).

The results from the Nortek Compass Verifications shows that the instruments didn’t have any broken pitch\ roll sensors and that the compasses had reasonably functioned throughout the year (Figure 8.6). With that being said there were some concerns.

¹ A complete account of the 2014 Nortek calibration problems experienced by ArcticNet/ IMG-Golder mooring teams can be found in 2014 ArcticNet Mooring Report.

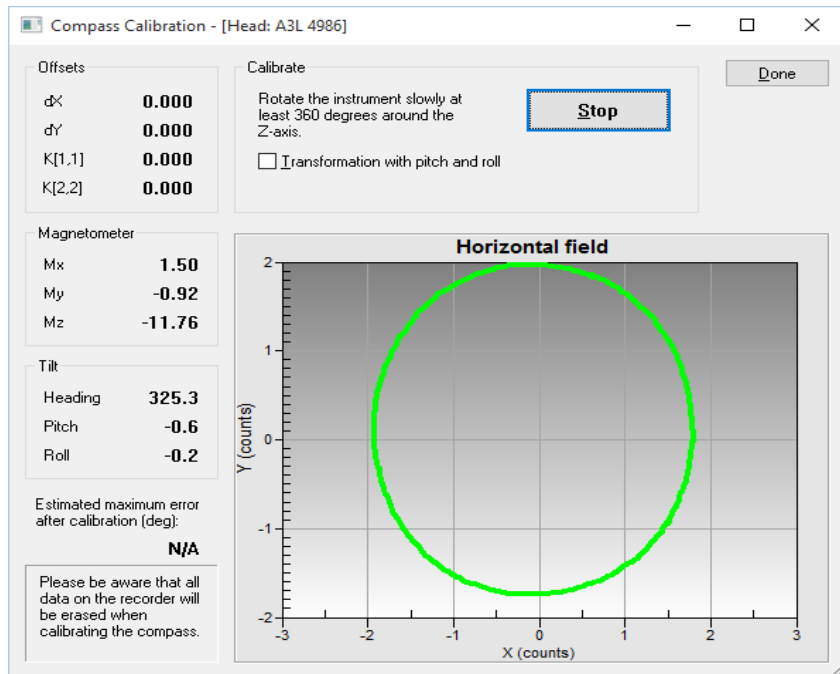


Figure 8-4. Nortek ADCP Compass Verification Curve (Inuvik, Sept, 2015).

The primary concern was that the calibration table used could be more precise when determining the heading in relation to true north. The concern is a multi-faceted problem that starts with a calibration table that despite a flat base, the inner ring of the calibration table moves slightly (< 2 deg X \ Y axis). This pitch and roll variance does affect the measured heading, though the quantitative affects to the heading are unknown, though assumed to be negligible as long as the pitch and roll don't exceed ± 2 degrees. The next concern is that the calibration table might not be exactly set to true north due to a 1 degree vs. 0.1-degree variance between handheld GPS (Garmin 76S Map) and dual antenna (ComNav G1) GPS units. Setting the calibration table to true north is not difficult as the table's 0 zero marker needs to be aligned with the same longitude as the distance marker (if using a handheld GPS unit), where as a dual antenna GPS is placed underneath the calibration table and aligned using the read-out from the antenna's NMEA stream. Both of these methods work well but are all subject to error as the table is aligned using string. The next stage of error is when the instrument is inserted into the jig apparatus. The head of the unit has a north arrow but this arrow is aligned visually and further error can also be added at this stage. Efforts to use the GPS – Compass capabilities of a handheld smartphone greatly reduce this error but again, the north arrow of the phone and of the instrument are visually aligned. Another time when heading error can present itself, is well the instrument is turning and \ or tilted, as the instrument collars are tight but do move slightly as the unit is rotated. The other factor that can also affect the heading readings is the weak vertical component of the magnetic field, due to its proximity to the pole. The matter is further complicated when the magnetic field moves, as it can and will move to give an error of several degrees, from one hour to the next. Lastly, the heading indicators marked on the outer ring of the calibration table are aligned with the best precision possible, but the table is turned by hand and the

possibility that the heading isn't exactly 0,10 ,20, etc. could also add error to the final heading reading.

The results from the verification indicate that the majority of the instruments performed within their ± 5 degrees of, acceptable polar location error (set forth by RDI). Though units AQD 8418, CNL 6107, 6112 and 6116 showed a max heading variance \ error over the acceptable recommendation of 5 degrees. Unit CNL 6107 had the greatest variance in heading and this unit will need to be inspected and repaired before re-deployment.

The good news from the verifications showed that even with all the potential true direction heading errors, that the unit was consistently approximately 10 degrees W of the true heading. This equipment offset was slightly different for each instrument but after the equipment offset and magnetic declination corrections were applied, the instrument data was plotted and a correction equation \ polynomial curve was created, reducing the heading error to 1-2 degrees.

There was also a uniform North-South bias (soft-iron). This bias was evident in the oval shape of the verification spin \ curve observed in the Nortek Calibration routine. Calibration efforts for 2016 are recommended to build \ refurbish a calibration table that integrates a dual GPS antenna to align the table to true north and the instrument head as well, throughout the calibration \ verification turn.





Current Meter Compass Calibration Summary


The pre-deployment compass calibrations of the RDI and Anderaa current meters was successfully completed in Inuvik, 2015. The instruments were returned to ArcticNet (Québec) and two RDI ADCPs (QM and LR) were also shipped to IOS to be loaded on-board the CCGS *Laurier* before its respective summer expeditions.

The results from the verification session identify that there is still good reason to perform these verifications. As the device heading offset and error was quite large in some Nortek devices and users of the data need to be aware of this and they also need to have the polynomial fit that corrects these equipment's' compass variations.

The results show that with the verification data and a polynomial fit equation we can greatly reduce the heading error and effectively correct the heading measured by the device. Unit CNL 6107 displayed a large offset and large North – South heading bias and will need to be inspected by Nortek before re-deployment. Other units AQD 8418, CNL 6112 and CNL 6116 verification data indicate that these units are less precise \ more sensitive than the other devices. Their recorded heading data is still good but the variation in these units was higher than other units, but with the verification \ calibration data, the heading data in these units is easily corrected to within less than 2 degrees of heading error.

Table 8-2. Oceanographic equipment that required compass calibration, including calibration procedures.

Equipment	Location	Purpose	Equipment Used	Calibration Procedure
<p>Nortek Aquadopp</p> 	<p>Nortek Factory, Norway (2014) * post- verification, Inuvik (2015)</p>	<p>Single-Point water velocity profiler</p>	<p>None</p>	<p>Nortek software does not correct compass bias for soft iron effects. The hard iron effects are negligible for the BREA project due to non-magnetic frame designs and lithium batteries ~50cm away from the transducer heads; thereby, negating hard-iron effects and removing the need to perform hard-iron calibrations on these devices.</p>
<p>Nortek Continental 190 / 470 kHz ADCP</p> 	<p>Nortek Factory, Norway (2014) * post- verification, Inuvik (2015)</p>	<p>3 beam - 3D water velocity profiler</p>	<p>None</p>	<p>Nortek software does not correct compass bias for soft iron effects. The hard iron effects are negligible for the BREA project due to non-magnetic frame designs and lithium batteries ~50cm away from the transducer heads; thereby, negating hard-iron effects and removing the need to perform hard-iron calibrations on these devices.</p>
<p>RDI 75 /150 kHz Long ranger / Quarter Master ADCP</p> 	<p>Inuvik, NT (2015)</p>	<p>4 beam 3D water velocity profiler, with bottom tracking</p>	<p>Calibration Table / Jig, Laptop with WinSC installed, USB to Serial adapter</p>	<p>Install into calibration table, point to 0 heading and open WinSC software, 'test' unit to verify all tests pass, set unit to zero pressure, set unit to UTC, verify compass, calibrate compass using af command, record the heading deviation by using pc2 to view the heading of the ADCP relative to the calibration table heading, measured at 10° intervals.</p>
<p>RDI 300 kHz Work Horse Sentinel ADCP</p> 	<p>Kugluktuk, NWT (2015)</p>	<p>4 beam 3D water velocity profiler, with bottom tracking</p>	<p>Calibration Table / Jig, Laptop with WinSC installed, USB to Serial adapter</p>	<p>Install into calibration table, point to 0 heading and open WinSC software, 'test' unit to verify all tests pass, set unit to zero pressure, set unit to UTC, verify compass, calibrate compass using af command, record the heading deviation by using pc2 to view the heading of the ADCP relative to the calibration table heading, measured at 10° intervals.</p>
<p>Aanderaa RCM11</p>	<p>Sensors: Université Laval (2011)</p>	<p>4-beam 2D current meter and</p>	<p>5059 Data Reading Program</p>	<p>Install into calibration table, point to 0 heading and read the data values for</p>

Equipment	Location	Purpose	Equipment Used	Calibration Procedure
1MHz 	Compass: Inuvik, 2015 (pre-deploy)	CTD-Tu-FL-DO sensors		channel 3 and convert to real heading by multiplying the raw value by 0.352. Record headings and raw values in a table and plot the values to extract the polynomial fit.

8.2.4 Health and Safety

All scientific personnel used Survitec Group immersion suits for transfers to and from the CCGS *Amundsen*. ArcticNet provided Survitec Group immersion suits for personnel transfers and advised that all mission participants needing to complete a helicopter ditching survival course provided by Survival systems (Dartmouth, NS, Canada). A safety briefing was conducted prior to boarding the helicopter in Kugluktuk, NWT and again onboard the *Amundsen* prior to transfer from the ship. The mooring team also attended the *Amundsen* safety briefing and familiarization onboard the ship and participated in the individual leg fire drill.

8.2.5 Mooring Operations Safety Documents

A Job Safety Assessment (JSA) / ÉPST (French version of JSA) concerning mooring operations was completed and made available to all crew members. The JSA identified potential risks and hazards involved in mooring operations. The JSA was approved by the ArcticNet Scientific operations supervisor (Keith Levesque). The ÉPST was also completed following the Canadian Coast Guard template and was made available to all crew members; however, it contains the same information as the JSA.

In addition to completing a JSA \ EPST, a mooring operations familiarization presentation was presented (by the Mooring Team Leader – Shawn Meredyk) to all of the relevant crew members (Captain, Boatswain, Chief Officer, deckhands) several days before mooring operations commenced.

In addition to the JSA\EPST and presentation, a ‘Toolbox’ meeting (mini meeting) was held 5 min before mooring operations began. The ‘toolbox’ meeting identified the equipment, lifting points, risks, roles and responsibilities required during mooring deployment operations. The ‘toolbox’ is an essential step within mooring operations and creates a safe working environment for all involved.

8.2.6 Mooring Operations

Mooring Recovery

All seven moorings from the Beaufort Sea (BS1, BS2, BS3, BR3, BR4, BRK and BRG) were successfully recovered using the CCGS *Amundsen* and CCGS *Sir Wilfrid Laurier* (BR1 and BR2).

Mooring BS1-14 was the only mooring that had given the mooring team any problem. The acoustic releases were interrogated (as with all of the other moorings) and returned acknowledgement; however, the mooring didn't surface. Both releases were released and the multibeam imagery showed that the mooring was still there and upright. The decision was made to retrieve BRK-14 and BS2-14 that same day, in-place of the BS1-14 and BS2-14 and BRK-14 original plan. The following day the releases gave the same response, "released", but it didn't come to the surface, and still the multibeam showed that it was there and vertical. The decision to 'drag' for the mooring was then the only remaining operation to attempt to recover the mooring. A design for a dragging device was made (Luc Michaud) and fabricated by the Chief Mechanic (Eric Dubée). The forward section of the drag anchor was three 2m sections of mooring anchor chain (in an effort to weight the leading section of the cable).

Mooring Dragging Operations

The dragging anchor was connected to the 500Hp winch and approximately 250m of cable was deployed with the dragging anchor (Figure 8.7).

The Captain then dragged the dragging anchor in diagonal passes over the mooring in an effort to dislodge the mooring. Several attempts were made and eventually the mooring was dislodged and raised to the surface. Unfortunately, it rose directly under the vessel and the propeller blades made contact with the surface float and under-lying ADCP frame, cutting the top buoy into two pieces and damaging the ADCP frame and breaking 3 out of 6 buoys off of the frame.

The recovery operation took a long time as there was a great deal of debris from the ship's damage to the mooring equipment and the operations teams were confused by the float type and colours. The covering of the floats was yellow but the interior was white and this created confusion amongst the mooring team as to whether or not the mooring was indeed BS1-14. Eventually, by visiting several debris pieces and seeing that the covers of buoys had misled us into thinking that the items at the surface were from a different mooring, they pieces were in fact debris from the damage inflicted by the vessel propellers. The damage to the equipment was not observed or heard, so it wasn't until the equipment was recovered onboard that it could be determined that the damage was in fact from the vessel propellers, which hindered or expedient recovery process. Nonetheless, the mooring was recovered and all data was recovered with no equipment damage apart from the top buoy (cut in half) and the Nortek ADCP frame (completely twisted).

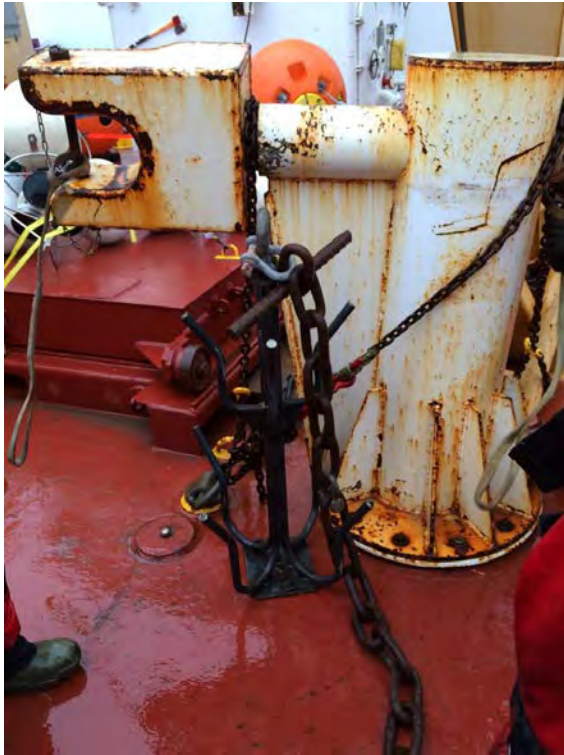


Figure 8-5. ArcticNet Dragging Anchor for BS1-14.

Mooring Data Recovery Summary

The seven moorings planned for recovery aboard the CCGS *Amundsen* between August-October 2015 were 100% successfully recovered from their original deployment locations. Table 8-3 presents a summary of the raw data recovery success, which cumulates overall at 94%.

Table 8-3. 2015 Short Mooring Re-Deployment Summary.

Mooring	Instrument	Serial number	Raw data recovery success (%)
BR-G-14	ASL Ice Profiler	51104	100
	Nortek Aquadopp DW	9743	100
	Nortek Aquadopp DW	9847	100
	RBR XR420 CT	15266	100
	RBR XR420 CT	15272	100
	RBR XR420 CT	15273	100
	RBR XR420 CT	15280	100
	RBR XR420 CTD	17352	100
	SBE 37SM Microcat	12235	100
	Technicap Trap PPS3	11_17	100
	Technicap Trap PPS3	12_18	100
	TRDI Long Ranger ADCP	13079	100
	TRDI Quarter Master ADCP	8784	100
BR-K-14	ASL Ice Profiler	51108	100

Mooring	Instrument	Serial number	Raw data recovery success (%)
	Nortek Aquadopp Profiler	11147	100
	RBR XR420 CT-FI-Tu-DO	22044	6 (failed battery)
	RBR XR420 CT-FI-Tu-DO	10419	100
	SBE 37SM Microcat	12236	100
	Sequoia LISST 100X	1473	100
	TRDI WH Sentinel ADCP	2646	100
	BR-03-14 ASL Ice Profiler	51109	100
	Nortek Aquadopp DW	2756	100
	Nortek Aquadopp DW	8418	100
	RBR XR420 CT	15263	100
	RBR XR420 CT	15264	100
	RBR XR420 CT	15275	100
	RBR XR420 CT	15281	100
	Technicap Trap PPS3	09_345	100
	Technicap Trap PPS3	12_25	100
	TRDI Long Ranger ADCP	18785	100
	TRDI Quarter Master ADCP	12823	8 (leaking connector)
BR-04-14	ASL Ice Profiler	51103	100
	Nortek Aquadopp DW	9752	100
	RBR XR420 CT	15274	100
	RBR XR420 CT-FI-Tu-DO	17114	100
	Sequoia LISST 100X	1319	100
	TRDI WH Sentinel ADCP	6320	67 (failed battery)
BS-1-14	Nortek Continental	6070	100
	RBR XR420 CT-FI-Tu-DO	17113	100
	SBE 37SM Microcat	10851	100
BS-2-14	AURAL hydrophone	22	To be determined
	Nortek Continental	6063	100
	Nortek Continental	6107	100
	RBR XR420 CT	15258	100
	RBR XR420 CT	15270	100
	SBE 37SM Microcat	10849	100
	SBE 37SM Microcat	10852	100
	Technicap Trap PPS3	05_319	100
BS-3-14	AURAL hydrophone	37	To be determined
	Nortek Continental	6112	100
	Nortek Continental	6116	100
	Nortek Continental	6064	0 (misprogramming)
	RBR XR420 CT	15269	100
	RBR XR420 CT	15271	100
	RBR XR420 CT	15268	100
	SBE 37SM Microcat	10196	100
	SBE 37SM Microcat	10850	100
	Technicap Trap PPS3	03_225	100

Data Recovery Problems

The instruments that provided less data than expected were investigated to identify the cause of failure. The following causes were identified :

- RBR XR420 CT-FI-Tu-DO #22044: the instrument stopped recording data on September 8, 2014. One of the four CR123 3V Lithium batteries failed due to a possible short-circuiting. This battery was rated at 0V at recovery (3V at deployment), when compared to ~2.6V for other batteries. Further inspection of the instrument is needed to identify the cause of the possible short-circuiting. No water was found in the instrument.
- TRDI Quarter Master ADCP #12823: the connector on the dummy plug side of the external battery housing leaked, which caused a failure in the instrument recording which stopped on September 14, 2014.
- TRDI WH Sentinel ADCP #6320: a short-circuit in one the two 45V battery packs of the external housing of this instrument resulted in the over-heating and failure of this battery pack. The instrument stopped recording data on April 14, 2015. No water was found in the instrument.
- Nortek Continental #6064: no data was recovered in this instrument (battery canister had a full charge upon recovery) due to a potential programming mix-up (the recording never started, but it was also observed that #6063 was programmed twice).

Mooring Deployment

Four moorings were deployed during Legs 3a and 3b. Two LTOO moorings CA08-15 and CA05-15 during Leg 3a and two Weston Foundation – ArcticNet – Parks Canada moorings (WF1-15 and WF2- 15) were deployed during Leg 3b (Table 8-4). Benthic Tripod Mooring WF2-15 was deployed from the CCGS *Marty Bergman* by Parks Canada submarine archeological dive team, led by Marc-Andre Bernier. The benthic tripod ADCP and CTD-Tu sensor were pre-programmed by the ArcticNet Mooring Team (Shawn Meredyk) and the tripod was assembled and equipment attached to the frame by the dive team. For more information on the WF2 deployment, please refer to Parks Canada’s report.

Table 8-4. Mooring deployment summary 2015.

Leg	Mooring ID	Latitude (N)	Longitude (W)	Depth (m)
3a	CA05-15	71°16.768	127°32.002	200
3a	CA08-15	71°00.445	126°04.719	391
3b	WF1-15	68°14.487	101°48.438	97
3b	WF2-15	68°01.130	099°00.782	20

Re-deployment Summary

All three moorings (BR3, BRK, BRG) were successfully re-deployed very near their targeted locations and very near their target depths (Table 8-5).

Table 8-5. 2015 short mooring re-deployment summary.

Leg	Mooring ID	Latitude (N)	Longitude (W)	Depth (m)
3a	BRK-15	70°51.763	135°01.706	170

3a	BRG-15	71°00.122	135°29.612	700
3a	BR3-15	73°24.566	129°21.224	690
3	iBO15-BR1*	70°25.944	139°01.235	753

*Re-deployed via the CCGS *Sir Wilfrid Laurier* (H. Melling)

Mooring Re/Deployment Procedure

- Instruments programmed and mounted into respective frames / floats;
- Verify Mooring releases function properly;
- Assemble the mooring Top-down on the fore-deck as per mooring design;
- Mooring Equipment attachments confirmed / double checked;
- Toolbox meeting with mooring and ship's mooring crew to identify roles and safety considerations (Zodiac® deployed if ice pack present);
- Launch Zodiac® (if required) ;
- Date and time are recorded for the start of mooring operations by an observing mooring team member, stationed on the bridge;
- Lower the first instrument buoy with the 500Hp winch, released at surface by SeaCatch®;
- Have the zodiac attach the tow-line to the bow horn / tack from the top instrument buoy;
- The mooring line is then tacked / secured and the zodiac is then instructed to maintain a taught-line (not tight), unless otherwise instructed by the lead mooring professional / Chief Officer;
- Raise the next instrument off of the deck and extend the A-frame, undoing the mooring line tack before the instrument reaches the deck edge;
- Descend the instrument and release the safety pin of the SeaCatch®, at deck level, then subsequently releasing the SeaCatch® and top float at the water surface.
*Depending on wave conditions, timing of SeaCatch® release may need to be timed with a high in wave period;
- The SeaCatch® is then brought back to the deck level (A-frame brought back in at the same time) and attached to the next solid structure (i.e. cage), pearl link / d-ring (added to the top-side of next device to be lifted);
- Pay-out the mooring line until there is 5-10m remaining (10m is advisable for rough seas). Then put the mooring line on-tack;
- The next instrument is then raised by the 500hp winch wire, as the mooring line in-tack is released;
- The same procedure of lowering the device to the water then putting the mooring line on tack, then attaching the SeaCatch® to the top-side of the next device follows until each device is in the water. Meanwhile, the Zodiac continues to maintain a taught-line, so as to not allow for the deployed / in- water equipment to get entangled;
- The final release of the anchor is preceded by the Zodiac releasing its tow-line of the top float (if Zodiac is in the water) and the Chief Officer confirms the tagline release from the zodiac and confirmation that the vessel is at the desired depth / position;
- The SeaCatch® on the Anchor chain shackle (located in the middle of the 2m anchor chain, just above the protective chain cylinder) was released (proceeding permission from the bridge) and the mooring free-falls into position at depth;

- The Zodiac® and 4th team member on the bridge then marks the time and mooring / target location of the last seen vertical position of the top float on- descent (if Zodiac is in the water);
- The Zodiac® returns to the vessel and the A-frame and 500hp winch are stopped and secured (if Zodiac is deployed);
- The vessel then proceeds to 3 triangulation points around the target location (distance of mooring depth away from drop location) and verification of acoustic release communications through ranging / 'pinging' allow for the anchor position to be calculated. These data were then input into a MatLab® triangulation script to determine the triangulated position of the mooring and kept within the field deployment sheets (Figure 8.8);
- Multibeam survey was performed to confirm the orientation and triangulated position of the mooring. Depending on the vessel's proximity to the mooring line, equipment and top-float depths might be visible if the vessel travels directly over-top the mooring. The multibeam images for each mooring deployment were kept within the field deployment workbook (EXCEL) and also archived at ArcticNet (Figure 8.9);
- A post-deployment CTD cast / profile was taken, though pre-deployment cast is sufficient if the CTD-Rosette is programmed to take several water samples at the same time while profiling the water column. The CTD profile plots for each mooring were kept within the field deployment workbook (EXCEL) and also archived at ArcticNet (Figure 8.10);
- The fore deck is cleaned of debris and remaining mooring equipment / cages are secured on the foredeck.

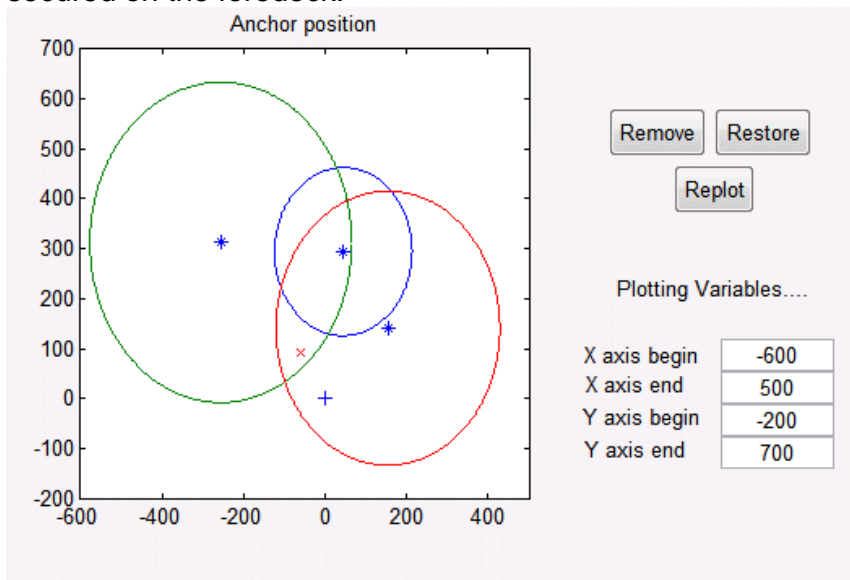


Figure 8-6. Triangulation plot from BS1-14 using Art's Acoustic Survey Matlab Script.



Figure 8-7. Multibeam imagery identifying orientation and instrument depths (screenshot courtesy of ArcticNet multibeam processing team).

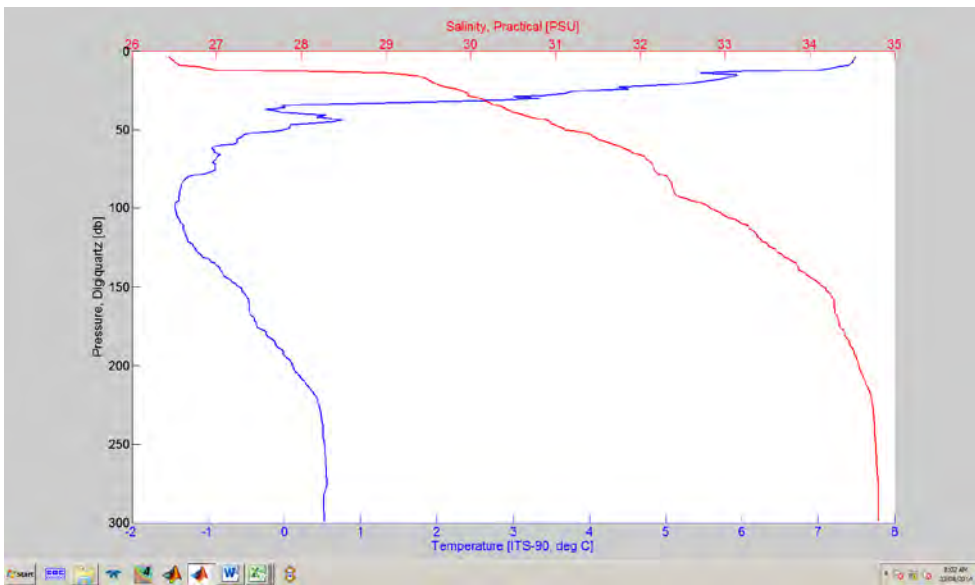


Figure 8-8. Rosette Temperature - Salinity Profile example plot (BS2-14).

8.3 Preliminary results

The preliminary look at the CTD data from the recovered moorings show a variety of benthic and pelagic currents that arrive at different times of the year. The most interesting event from a design perspective occurred on 2 March 2014 at locations BS2 and BS3. A large ice berg with an ice keel large enough to lay over the BS2-14 mooring down to at least 205m which is where the sediment trap was moored. Unfortunately, The CT on the Sediment trap didn't have pressure sensing capabilities which could identified if the traps had been pulled-down as well. Though in all the instruments that recorded the ice berg push-down a depression of 50m was only recorded. On BS3-14 CT sensors on the Nortek ADCP and

deeper sediment trap recorded a reduction by 0.5°C at the time of the lay-over, which doesn't mean that the trap or ADCP was pushed down but when the ADCP data is processed it will be evident as to whether or not the ice keel depth reached down to 300m or not.

Regardless, this was a very large piece of ice that depressed bot BS2-14 and BS3-14 for 4 days, with the largest lay-over period lasting only 12 hours (Figure 8.11).

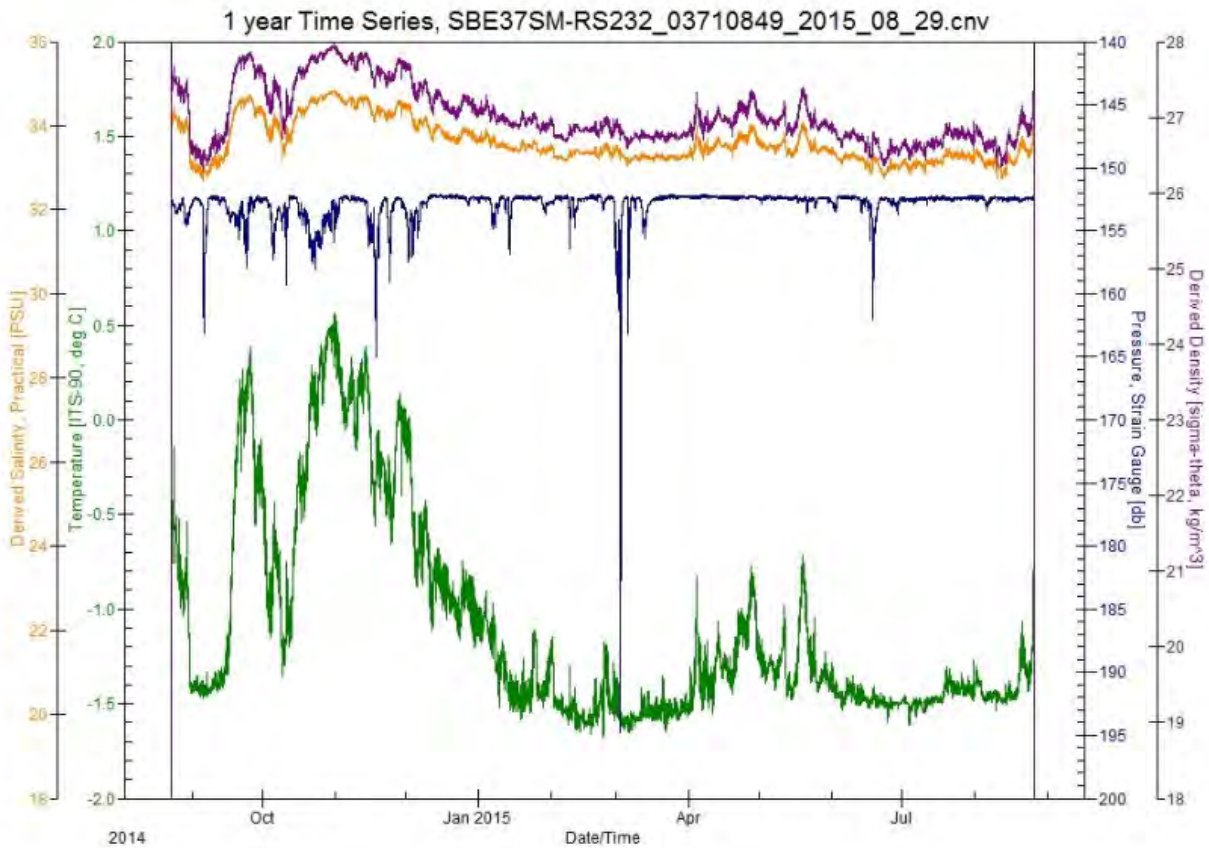


Figure 8-9. BS2-14 CTD plot from the SBE37 moored at 152 db (162m) showing the large lay-over event on March 2 2014 (ice berg keel).

8.4 Comments and recommendations

8.4.1 OCEANO Acoustic Releases

The mooring chain that is connected by tear-drop links that are shackled to the release chain could be improved to possibly reduce the chance of the release chain from getting caught on the releases or on the stretch-section ring. The needs to be a discussion with OCEANO about this and get their recommendations, as the present recommendations from

the ArcticNet mooring team are to reduce the chain length and to increase the ring size and to use slim-type shackles.

8.4.2 Battery Canister problems

On Leg 3a one of the TRDI Titanium external battery canisters (from the QM ADCP at BR-03-14) had leaked through the dummy plug connector of the bottom end cap. This issue is different than the impulse connector corrosion problem identified from 2009 and 2010. This latter problem led to the replacement of all impulse connectors (the ones connecting the ADCP to the external housing) over 2011-2012. Silicon grease was also used to cover these impulse connectors as a supplementary mitigation procedure. However, it appears that the connectors on the dummy plus side of the housings were not replaced. Silicon grease was also not applied over this connector because no signal/electricity is directed to this connector during deployment. The amount of water entering the housing was done in small doses and since the O-rings were in good condition and no signs of O-ring associated problems were seen, the problem was isolated to the connector. The energy surges caused internal connector wiring to burn-through and batteries to short-circuit and overheat. The battery canister continued to gass-off even when on deck. Following this incident, it is clear that all connectors on the dummy plug side of the TRDI titanium battery canisters need to be inspected/changed before further use and covering the dummy connector end with silicon grease would be advisable.

One of the battery packs in the plastic canister of the Workhorse Sentinel 300-kHz at BR-04-14 had experienced short-circuiting and failure. No water was found in the instrument (humidity card was OK) and the O-ring was in good condition and properly installed. It was noted that escaping gas was heard when the instrument was on-deck while additional devices such as the Novatech flashers and Benthos Pingers were being removed. Further inspection of the wiring in this battery canister is needed to identify if an incorrect wiring could be the cause of the short-circuiting.

There was one Benthos Pinger canister that had been flooded by corrosion on the conductivity screws (to activate the pinger once in water) or failing O-ring, whereby water entered the canister and caused pressure build-up, which resulted in a bystander to be hit by the top popping off. These instruments were isolated by rubber to the instrument frame and no metal contact was made. So, the reason behind the corrosion of the stainless steel screws on the pingers falls into the same oceanographic conditions problem such as the other stainless steel shackles experienced. Again, moving to using titanium screws instead of stainless steel could solve this problem, along with abandoning the acoustic pingers for XEOS satellite locator beacons.

8.4.3 Stainless Steel Shackles

2011 Mooring Report Exert :

“Extra care needs to be taken when deploying sediment traps with stainless steel shackles to replace anodes in the sediment trap. In 2011 it was decided that a safety line should be employed in combination with stainless shackles in the event that shackle corrosion results in mooring line separation. Evaluate the use of stainless shackles on sediment traps and other parts of moorings; incorporate “safety” lines between mooring line components in case of shackle failure to prevent total loss.”

The idea since 2010-2011 was that the Chinese Stainless Steel shackles were defective and not to be trusted. However, the 2014 ArcticNet moorings had used Chinese Stainless Steel shackles by accident and the BREA moorings had used shackles made in France (Wichard). During recovery of the equipment it was observed that the French Stainless Steel shackles had corroded slightly on the Stainless Steel traps, whereas the Chinese shackles showed no sign of corrosion at all, which were installed on the Titanium traps. Knowing now that stainless steel from any country could have good and bad batches of shackles and have only shown corrosion on the Stainless Steel traps, the reasons behind stainless steel corrosion on sediment traps are a combination of local oceanographic conditions and trap construction (stainless steel vs. titanium).

In terms of corrosion remediation with Stainless Steel shackles, it has been observed that Chinese shackles from batch E23 (sometimes looks like 123 on the shackle) has shown signs of corrosion and should be selected over other batches already in-stock. Another way to remedy this problem would be to purchase Titanium shackles for the stainless steel traps.

Table 8-6. Summary table of Lessons Learned throughout the mission.

Problem	Solution	Operation
Some cages and swivels have special shackle and insert sizes	Order more 3/8" and 7/16" shackles and inserts for ISUS and Nortek Cages	Deployment
Stainless Steel Shackle Corrosion	Buy Titanium Shackles	Deployment
1TB hard drive upgrade in Aural M2 could possibly need more energy than older 320 GB drives, dead batteries and no data as a result	Figure out if new battery packs or different hard drives are needed for the 1TB hard drive upgrade for the AURAL M2s; also don't use the 1TB upgrade adapters	Recovery
RDI battery case flooding through bulkhead connector	Have all RDI battery cases inspected and repaired by RDI	Recovery
Benthos Pinger SW contact corrosion	Ask Benthos recommendations	Recovery
Oceano Release chain can get caught-up on itself and prevent mooring release	Change shackles to slim model and shorten ring chain or increase the chain ring size	Recovery
Broken equipment (buoys primarily) can confuse recovery operations, by chasing false leads	Mooring design schematic images need to show exact model types with color of interior material identified	Recovery
Stainless shackles attached to stainless traps are more susceptible to corrosion than when attached to titanium traps.	Buy Titanium Shackles/traps	Recovery

9 CTD-Rosette, LADCP and UVP operations – Legs 2, 3a, 3b, 4a, 4b and 4c

Cruise participants Leg 2: Pascal Guillot² and Cris Seaton²

Cruise participants Leg 3a: Callum Mireault² and Olivier Asselin²

Cruise participants Leg 3b: Callum Mireault² and Olivier Asselin²

Cruise participants Leg 4a, 4b and 4c: Patricia DeRepentigny² and Juergen Zier²

¹ *Institut des sciences de la mer (ISMER) – Université du Québec à Rimouski, 310 Allée des Ursulines, Rimouski, QC, G5L 3A1, Canada.*

² *Université Laval, Département de biologie, Pavillon Alexandre-Vachon, 1045 avenue de la Médecine, Québec, QC, G1V 0A6, Canada.*

9.1 Introduction

The objective of this shipboard fieldwork was to characterize the water column physical and chemical properties: temperature, salinity, fluorescence, CDOM, dissolved oxygen concentration, nitrate concentration, light penetration and turbidity. A SBE 911 CTD was used in conjunction with various other sensors mounted on a cylindrical frame known as a Rosette. A 300 kHz Lowered Acoustic Doppler Current Profiler (LADCP) was attached to the frame to provide vertical profiles of the velocities on station. The Rosette was also equipped with Niskin bottles, which were used to supply water samples for biologists and chemists.

9.2 Methodology – CTD-Rosette

The Rosette frame was equipped with twenty-four (24) 12-litre bottles and the sensors described in Table 9-1 Table 9-2.

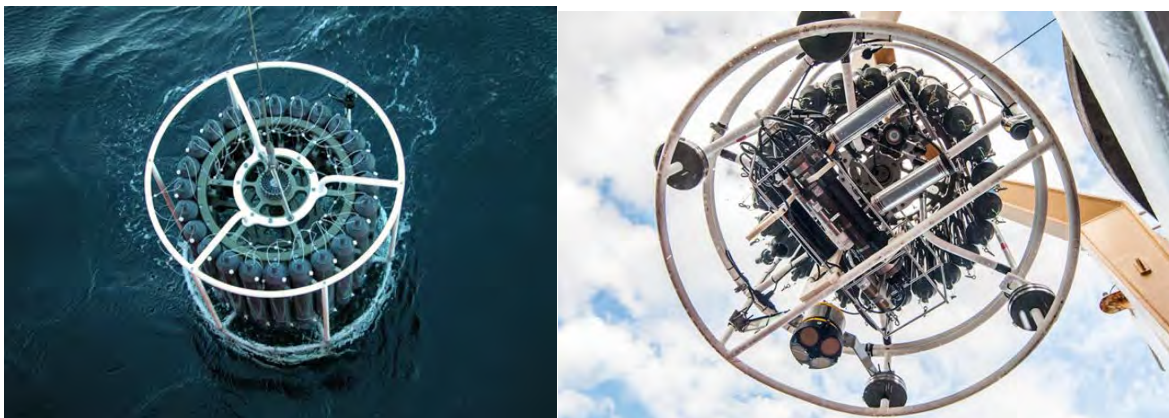


Figure 9-1. Top view of the SBE32 with 24x 12L Niskin bottles used on the *Amundsen* (left) and bottom view of the SBE32 showing the SBE9 CTD including additional sensors and the RDI LADCP (right). Photos: Jessy Barrette.

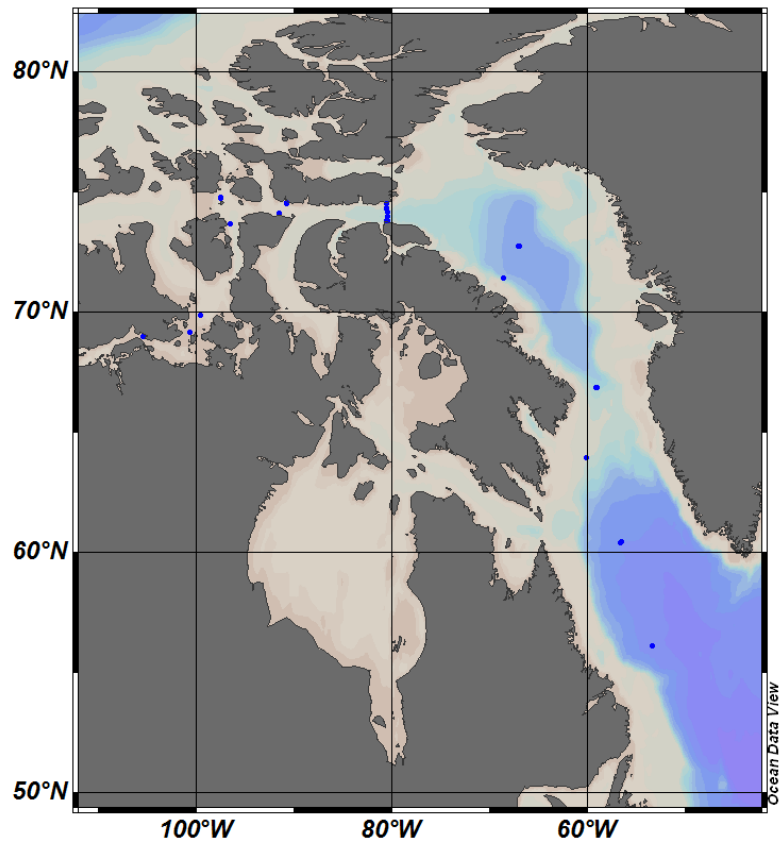


Figure 9-2. ArcticNet/GEOTRACES study region in the eastern Canadian Arctic for Leg 2.

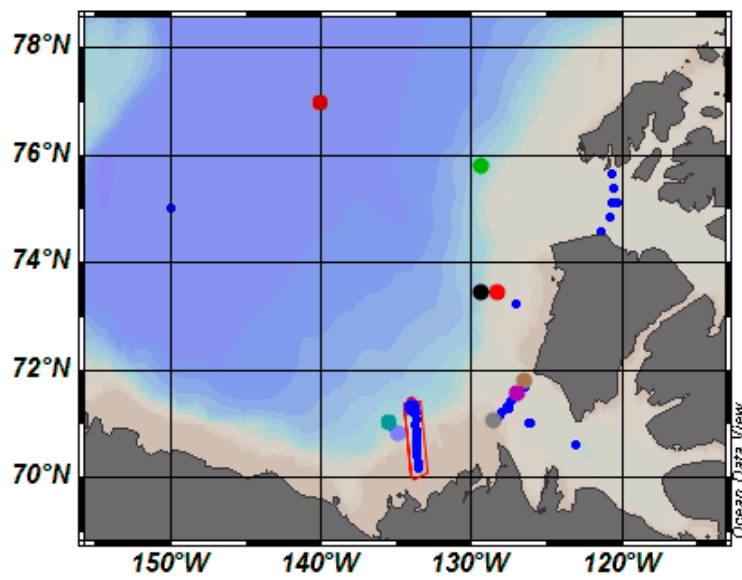


Figure 9-3. ArcticNet study region in the Western Canadian Arctic, Legs 3a and b.

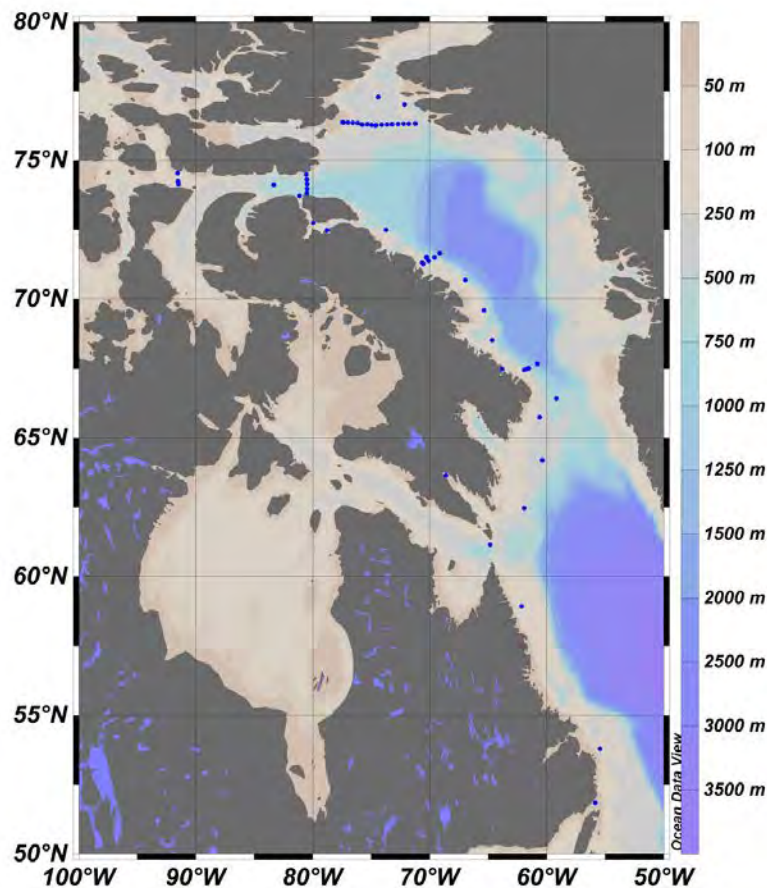


Figure 9-4. ArcticNet study region in the eastern Canadian Arctic for Leg 4.

Table 9-1. Sensors attached to the SBE9.

Instrument	Parameter	Properties	Serial Number	Calibration date
Sea-Bird SBE 911plus	CTD	Sampling rate : 24 Hz	09P24760-0679	
SBE 3plus	Temperature	Range: -5°C to + 35°C Accuracy: 0.001	03P4204	02-Dec- 2014
Paroscientific Digiquartz®	Pressure	Accuracy: 0.015% of full range	0679	26-Nov- 2014
SBE 4C	Conductivity	Range: 0 to 7 S/m Accuracy: 0.0003	042876	02-Dec- 2014
SBE 43	Dissolved Oxygen	Range: 120% of saturation Accuracy: 2% of saturation	430427	26-Nov- 2014
MBARI-ISUS Satlantic	Nitrates	Range: 0.5 to 200 M Accuracy: ± 2 M	138	12-Feb- 2015
QCP-2300 Biosherical	PAR	PAR Dynamic Range: 1.4x10 ⁻⁵ to 0.5 μE/(cm ² sec)	7270	19-Dec- 2014
QCR-2200 Biosherical	Surface PAR	PAR Spectral Response: Equal (better than ±10%) quantum response from 400 to 700nm	20147	19-Dec- 2014
Seapoint	Fluorometer	Minimum Detectable Level 0.02 μg/l Gain Sens, V/(μg/l) Range/(μg/l), 10x 0.33 15	SCT-3120	27-Jan- 2015
WetLabs C-Star	Transmissometer	Path length: 25 cm Sensitivity: 1.25 mV	CST-671DR	17-Dec- 2014
Teledyne PSA-916	Altimeter	Range: 50 m from bottom	1065	Feb 2014
WetLabs ECO	Fluorometer (CDOM)	FL(RT)DDigital output resolution : 14 bit Analog output signal: 0 -5V Range: 0.09-500ppb Ex/Em: 370/460nm	FLCDRTD-2344	16-Jun- 2015

Table 9-2. Specifications for the sensors equipped on the Rosette.

Parameter	Sensor		Range	Accuracy	Resolution
	Company	Instrument Type			
Data Logger	SeaBird	SBE-9plus ¹			
Temperature	SeaBird	SBE-03 ¹	-5°C to +35°C	0.001°C	0.0002°C
Conductivity	SeaBird	SBE-4C ¹	0-7 S/m (0-70mmho/cm)	0.0003 S/m (0.003mmho/cm)	0.00004 S/m (0.0004 mmho/cm)
Pressure	Paroscientific	410K-105	up to 10 500m (15 000 psia) ²	0.015% of full scale	0.001% of full scale
Dissolved oxygen	SeaBird	SBE-43 ³	120% of surface saturation ⁴	2% of saturation	unknown
Nitrates concentration	Satlantic	MBARI-ISUS 5T ⁶	0.5 to 2000 µM	±2 µM	±0.5 µM
Light intensity (PAR)	Biospherical	QCP-2300		□	□
sPAR	Biospherical	QCR-2200		□	
Fluorescence	Seapoint	Chlorophyll- fluorometer	0.02-150 µg/l	unknown	30
Transmissiometer	Wetlabs	C-Star	0-5 V	unknown	1.25 mV
Altimeter	Benthos	PSA-916 ⁷	0 - 100 m	unknown	0.01 m
CDOM fluorescence	Wet Labs	FL(RT)D ⁷	0.09-500 ppb	unknown	14 bit

Notes: ¹ Maximum depth of 6800m; ² Depending on the configuration; ³ Maximum depth of 7,000m; ⁴ In all natural waters, fresh and marine; ⁵ Maximum depth of 1200m; ⁶ Maximum depth of 1000m; ⁷ Maximum depth of 6000m.

9.2.1 Probe calibration

Salinity – SeaBird SBE4. Water samples were taken with 200 ml bottles on every GEOTRACES/ArcticNet casts during Leg 2 and 3b and at regular intervals (approximately every 10 casts) throughout the 2015 Leg 4 to monitor the performance of the Seabird SBE4 conductivity sensor. Samples were analyzed with a GuildLine, Autosal model 8400B which offers a range from 0.005 to 42 PSU with an accuracy better than 0.002.

An initial analysis performed on the correlation between the CTD probe and Autosal salinity values is shown in Figure 9.5. This figure was made using the unfiltered values of the average salinities of the three samples taken from the Autosal samples versus the point value of the equivalent salinity of the bottle it was sampled from. The result was a correlation of 0.9943 (R^2 value) and the data had differences (CTD probe minus Autosal) with a mean of -0.0476 and a median of -0.0158. This suggests that on average the Autosal machine calculates salinity values lower than the CTD probe. Mean difference value as well as median value is high considering the accuracy of the Autosal machine (0.002).

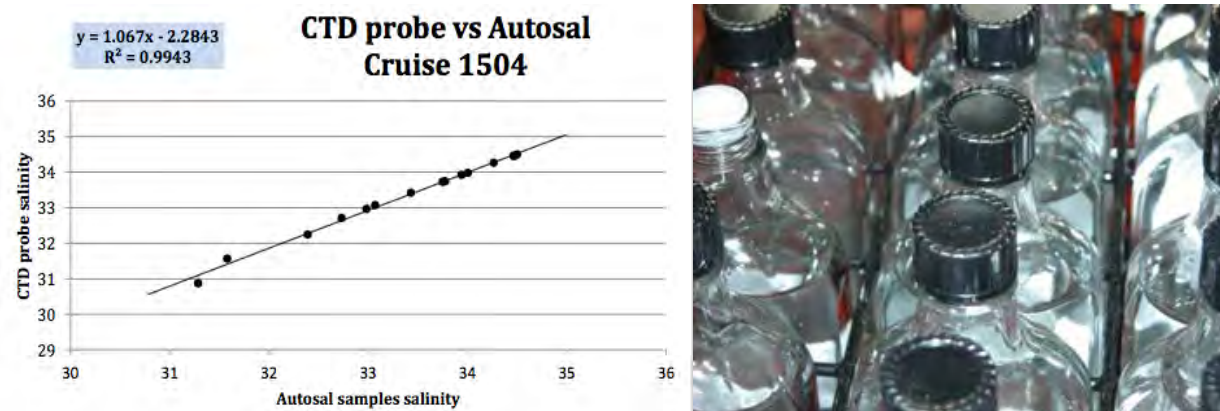


Figure 9-5. Example of a calibration curve (left) and photo of the bottles used to collect water samples to measure salinity (right).

The difference of the Autosal machine with regards to the CTD probe could be a number of different factors such as operator errors, strong salinity gradient, degradation of accuracy of the Autosal machine as well as degradation of the accuracy of the CTD probe. Unfortunately, without a further specific analysis of the data it is impossible to determine which of these factors could have led to the differences of accuracy between the actual and calculated Autosal accuracies.

Salinity – SeaBird TSG. Water samples were taken at different times during Legs 2 and 3b transit from the surface thermosalinograph to measure salinity and fluorescence. The probe is located in the engine room. The samples were also analyzed with the GuildLine. As far as the fluorescence is concerned, the samples were analyzed with a fluorometer.

Oxygen – SeaBird SBE43. The Seabird SBE43 Oxygen sensor calibration was compared to dissolved oxygen concentration measured in water samples using Winkler’s method and a Mettler Toledo titration machine (Figure 9.6). Oxygen samples were taken at regular intervals (approximately every 10 – 15 casts) and analyzed using the method stated above.

Preliminary results show a good performance of the SBE43 and values were within the manufacturer’s stated accuracy levels (2% of saturation) for the sensor. The performance of the sensor will be further assessed through a post cruise calibration performed at the manufacturer (Seabird). The graphs below show a preliminary comparison between SBE43 values and levels derived through the Winkler analysis.

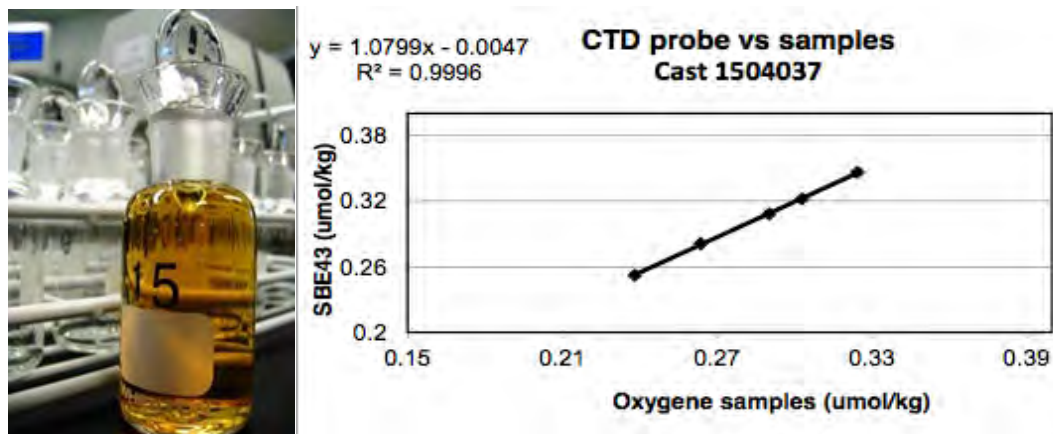


Figure 9-6. Example of oxygen calibration curve (left) and photo of the bottles used to collect water samples to measure oxygen (bottom right).

9.2.2 Water sampling

Water was sampled with the Niskin (Nansen) bottles attached to the rosette according to each team's requests. To identify each water sample, we used the term "rosette cast" to describe one CTD-rosette operation. A different cast number is associated with each cast. The cast number is incremented every time the rosette is lowered in the water. The cast number is a seven-digit number: *xyyzzz*, with

- xx*: the last two digits of the current year;
- yy* : a sequential (Québec-Océan) cruise number;
- zzz* : the sequential cast number.

For this cruise, the first cast number was 1504001. To identify the twenty-four rosette bottles on this cast we simply append the bottle number: 1504001nn, where "nn" is the bottle number (01 to 24).

All the information concerning the Rosette casts is summarized in the *CTD Logbook* (one row per cast, Appendix 3). The information includes the cast and event number and station id, date and time of sampling in UTC, latitude and longitude, bottom and cast depths, and minimalist comments concerning the casts (Table 9-3).

Table 9-3: Example of CTD logbook created for each station and cast.

Cruise ID		AJOUTER UN CAST		Québec Océan		ArcticNet						
Cruise NAME		SUPPRIMER UN CAST										
Cast	Station	Date début UTC	Heure UTC	Lat (N)	Long. (W)	Fond (m)	Prof. cast (m)	Commentaires	Type	Init		
001	304	03 / 10 / 15	22 : 31	74 ° 38.000	091 ° 30.881	314	304	Altimeter only working at 30m from bottom	Full	JZ		
002	304	04 / 10 / 15	05 : 02	74 ° 14.779	091 ° 29.418	314	304		Full	PDR		
003	346	04 / 10 / 15	06 : 51	74 ° 9.004	091 ° 27.036	272	281	Acquisition Screen blacked out for a sec close to bottom	Nuts	JZ		
004	343	04 / 10 / 15	09 : 43	74 ° 32.771	091 ° 31.450	151	140		Nuts	JZ		
005	301	04 / 10 / 15	22 : 13	74 ° 7.277	083 ° 18.899	679	669	Bottle #23 did not fire, Sal samples	Basic	PDR		
006	301	05 / 10 / 15	03 : 16	74 ° 7.268	083 ° 19.324	680	667		Basic	JZ		
007	325	05 / 10 / 15	08 : 08	73 ° 49.000	080 ° 29.221	678	668		Nuts	JZ		
008	324	05 / 10 / 15	10 : 19	73 ° 58.607	080 ° 28.036	772	762	Still no scm	Nuts	PDR		
009	323	05 / 10 / 15	13 : 00	74 ° 9.410	080 ° 28.409	790	780	No scm	Full	PDR		
010	323	05 / 10 / 15	15 : 04	74 ° 9.474	080 ° 28.228	790	780	Bottle #3 did not fire	Full	PDR		
011	300	06 / 10 / 15	04 : 12	74 ° 19.037	080 ° 29.255	701	690		Nuts	JZ		
012	322	06 / 10 / 15	07 : 03	74 ° 29.620	080 ° 32.154	662	650	encountered ice during cast, cable pinched, skipped 3 sampling depths	Nuts	JZ		
013	109	07 / 10 / 15	10 : 08	76 ° 17.381	074 ° 6.693	453	443	No scm	CTD	PDR		
014	110	07 / 10 / 15	11 : 11	76 ° 18.000	073 ° 38.721	530	520	Screen blacked out for a sec	Nuts	PDR		
015	111	07 / 10 / 15	12 : 50	76 ° 18.352	073 ° 12.980	595	585	Valve of bottle #4 open	Basic	PDR		
016	111	07 / 10 / 15	16 : 04	76 ° 18.276	073 ° 12.489	599	589		Basic	PDR		
017	112	07 / 10 / 15	19 : 00	76 ° 18.908	072 ° 42.160	564	554	Ox samples	CTD	PDR		
018	113	07 / 10 / 15	20 : 09	76 ° 19.299	072 ° 13.105	552	542	Still no scm	Nuts	PDR		
019	114	07 / 10 / 15	21 : 43	76 ° 19.511	071 ° 47.639	610	600		CTD	JZ		
020	115	08 / 10 / 15	01 : 43	76 ° 19.979	071 ° 12.097	660	650		Full	JZ		
021	115	08 / 10 / 15	07 : 37	76 ° 20.125	071 ° 14.083	665	656		Full	JZ		

An Excel® Rosette Sheet was also created for every single cast. It includes the same information as the CTD Logbook plus a table of what was actually sampled and at what depth. Weather information at the sampling time is included in each Rosette. For every cast, data from three seconds after a bottle is closed to seven seconds later is averaged and recorded in the ascii 'bottle files' (files with a btl extension). The information includes the bottle number, time and date, trip pressure, temperature, salinity, light transmission, fluorescence, dissolved oxygen, irradiance and CDOM measurements.

All those files are available in the directory "Data\Rosette" on the 'Shares' folder on the Amundsen server. There are six sub-directories in the rosette folder.

\Rosette\log\: Rosette sheets and CTD logbooks.

\Rosette\plots\: plots of every cast including salinity, temperature, oxygen, light transmission, nitrate, fluorescence and irradiance data.

\Rosette\odv\: Ocean Data Viewer file that include ctd cast files.

\Rosette\svp\: bin average files to help multibeam team to create a salinity velocity profile.

\Rosette\avg\: bin average files of every cast.

\Rosette\LADCP\: LADCP post-process data results.

9.3 Methodology – Lowered Acoustic Doppler Current Profiler (LADCP)

A 300 kHz LADCP (a RD-Instrument Workhorse[®]) was mounted on the Rosette frame (Figure 9.8). The LADCP gets its power through the rosette cable and the data is uploaded on a portable computer connected to the instrument through a RS-232 interface after each cast. The LADCP was programmed in *individual ping* mode (one every second). The horizontal velocities were averaged over thirty-two, 8 m *bins* (Legs 2 and 3b) or 4 m *bins* (Leg 4) for a total (theoretical) range of 100 to 120 m. The settings were 57600 bauds, with no parity and one stop bit. Since the LADCP is lowered with the rosette, there were several measurements for each depth interval. The processing was done in Matlab[®] according to Visbek (2002).



Figure 9-7. RDI LADCP mounted on the bottom of the SBE32 carousel on the *Amundsen*.

9.4 Preliminary results

All the preliminary results are based on raw data (not processed and not validated). Figures must not be used.

9.4.1 Leg 2

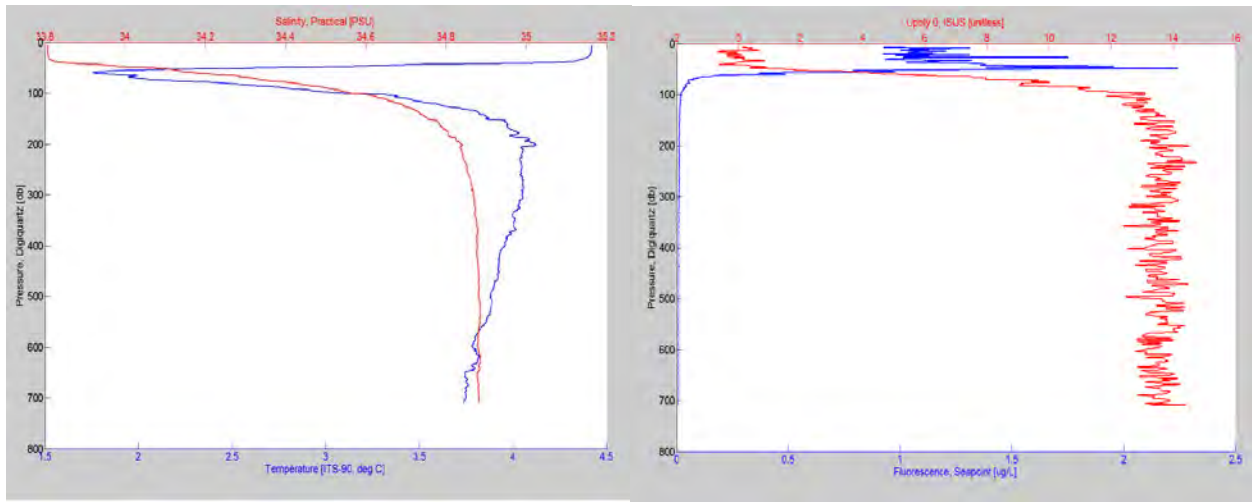


Figure 9-8. Example of vertical structure (temperature and salinity – left; nitrate and fluorescence – right) for Cast 006.

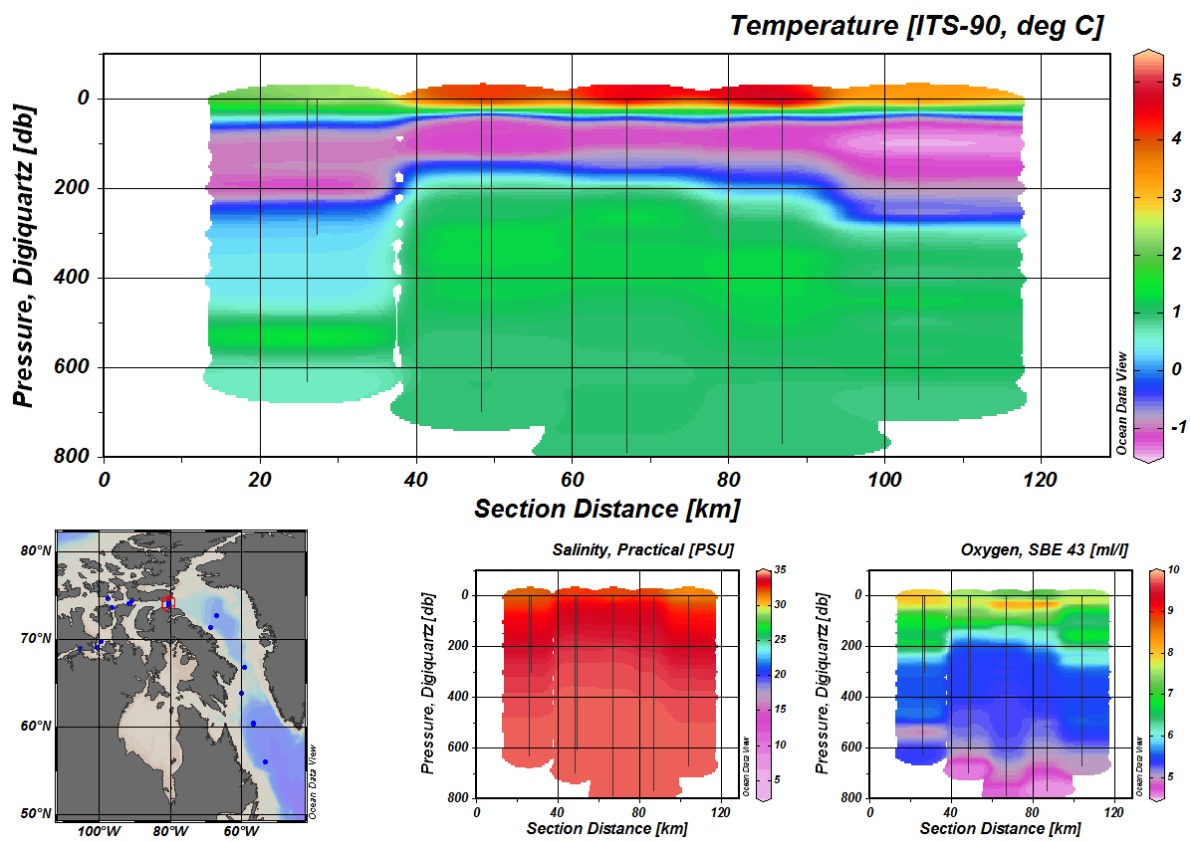


Figure 9-9. Evolution of the main parameters along the transect “Lancaster Sound”.

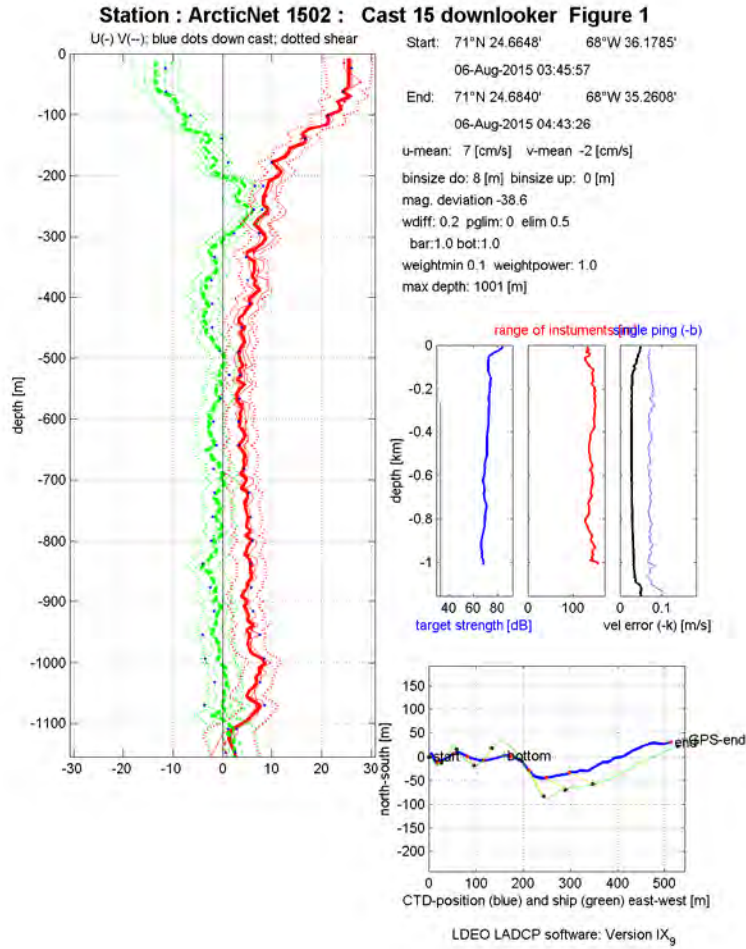


Figure 9-10. Example of current velocities for the Cast 015 recorded by the LADCP.

9.4.2 Leg 3

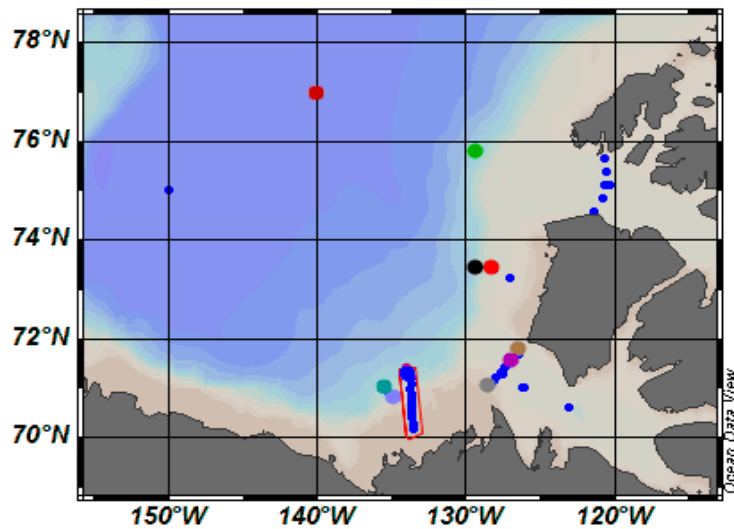


Figure 9-11. CTD casts location for Leg 3a and the beginning of 3b.

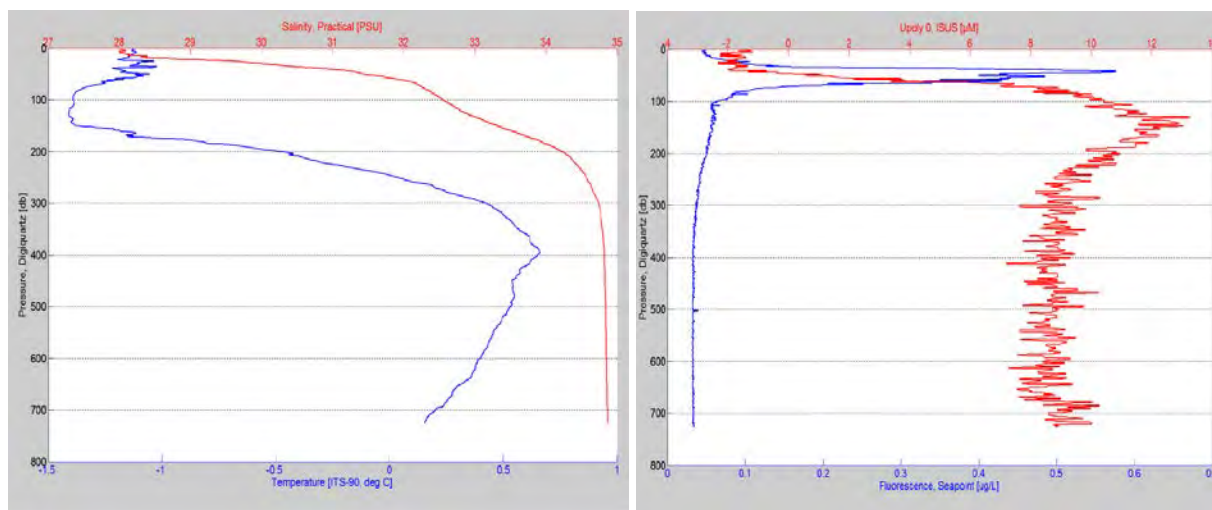


Figure 9-12. Example of the vertical structure (temperature and salinity – left; nitrate and fluorescence – right) for the cast 051.

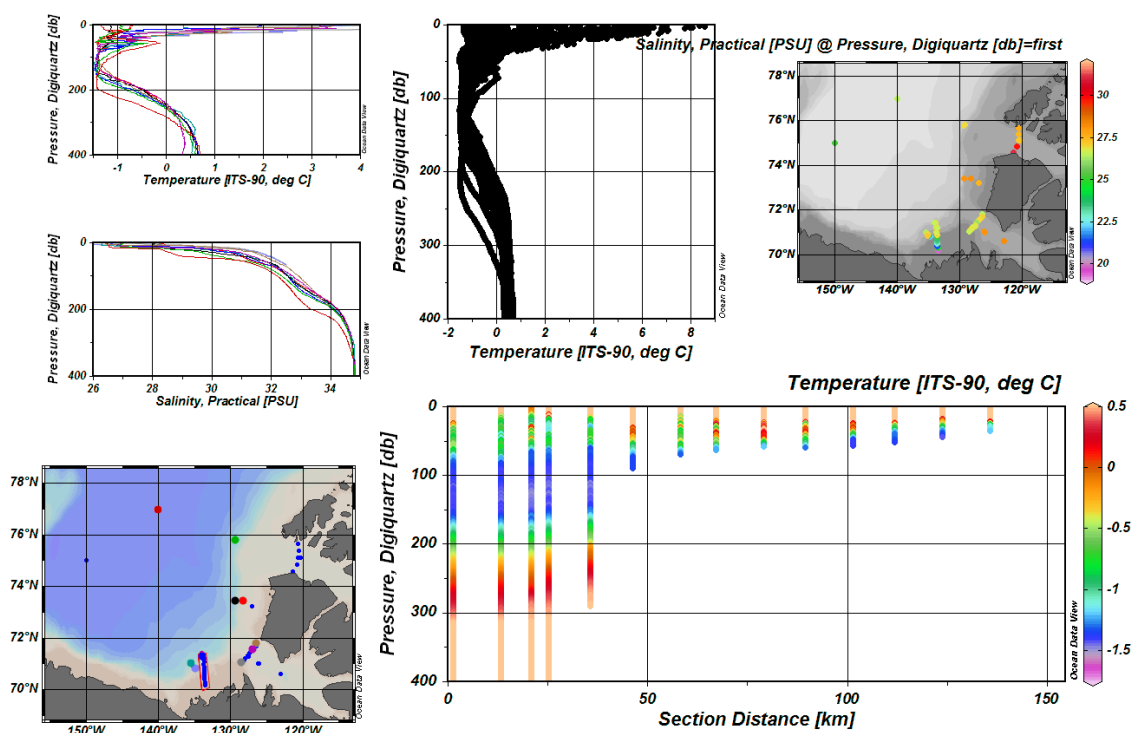


Figure 9-13. Evolution of the main parameters along the transect "Lancaster Sound".

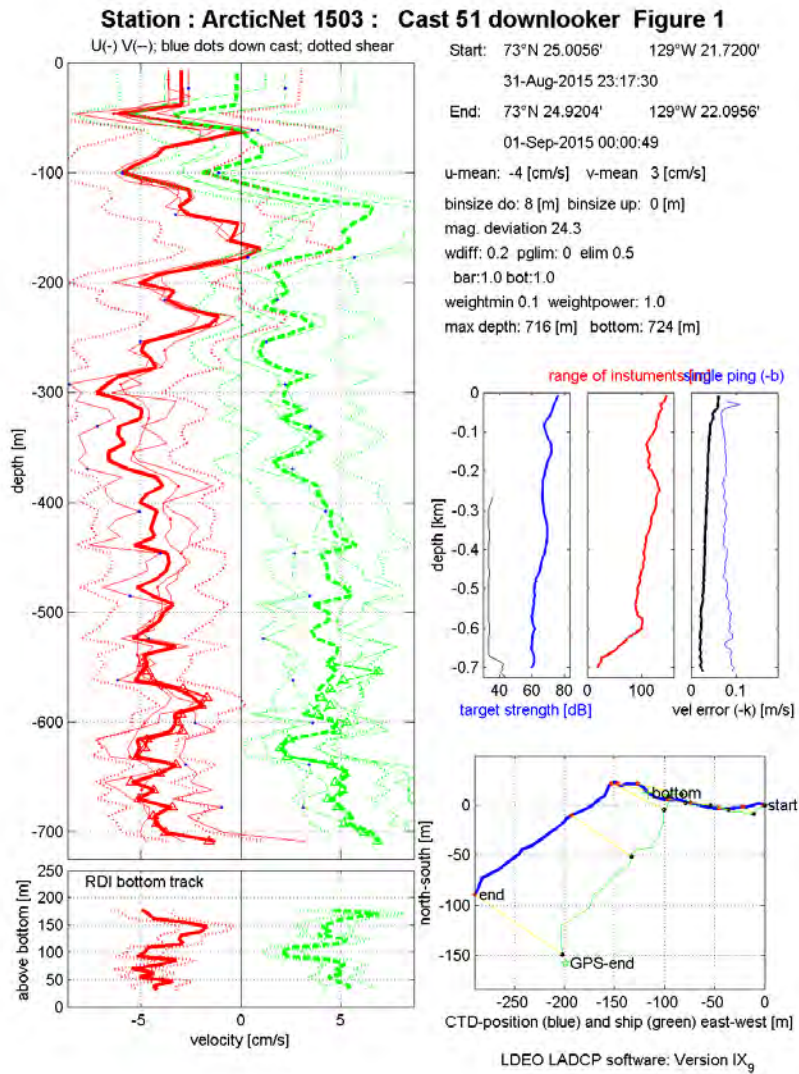


Figure 9-14. Example of current velocities for the cast 051 recorded by the LADCP.

9.4.3 Leg 4

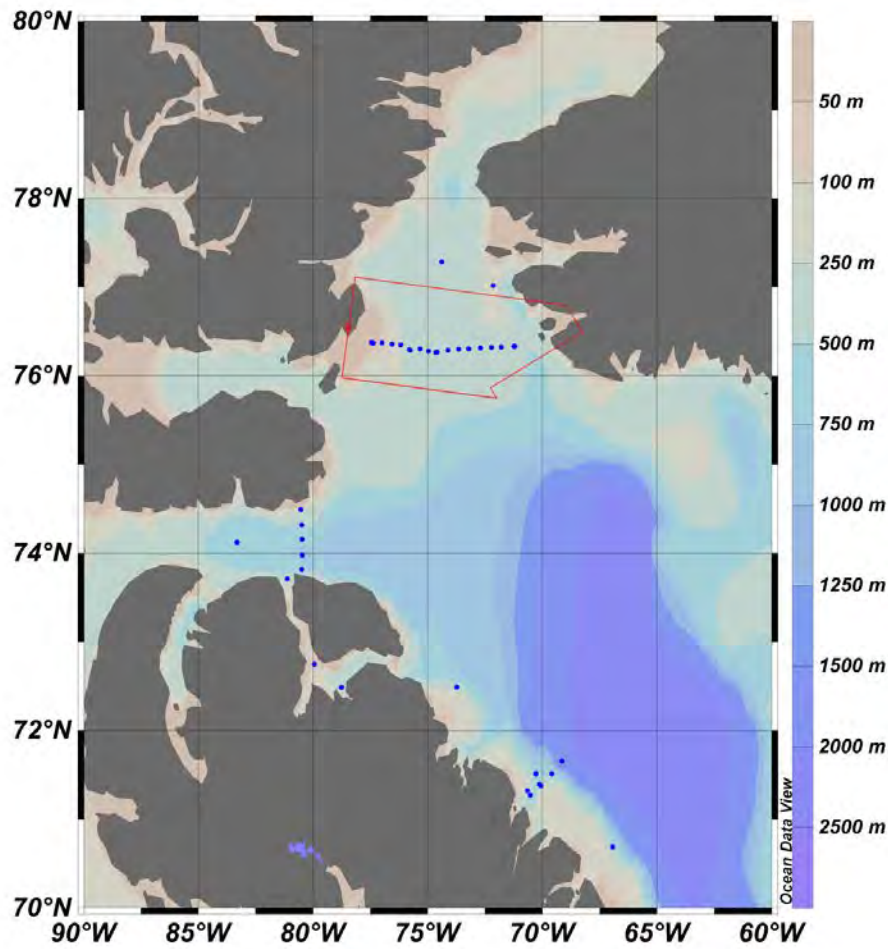
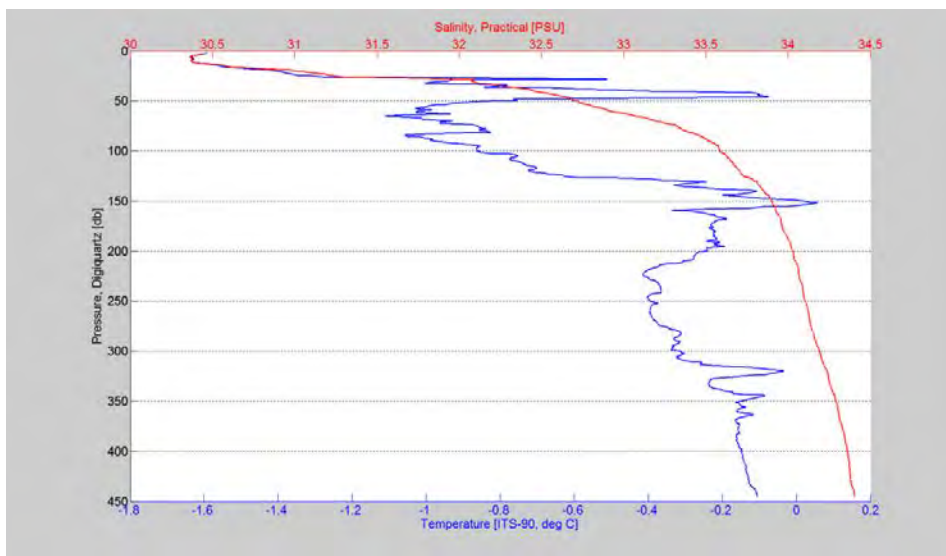


Figure 9-15. CTD casts location for Leg 4a and the beginning of 4b.



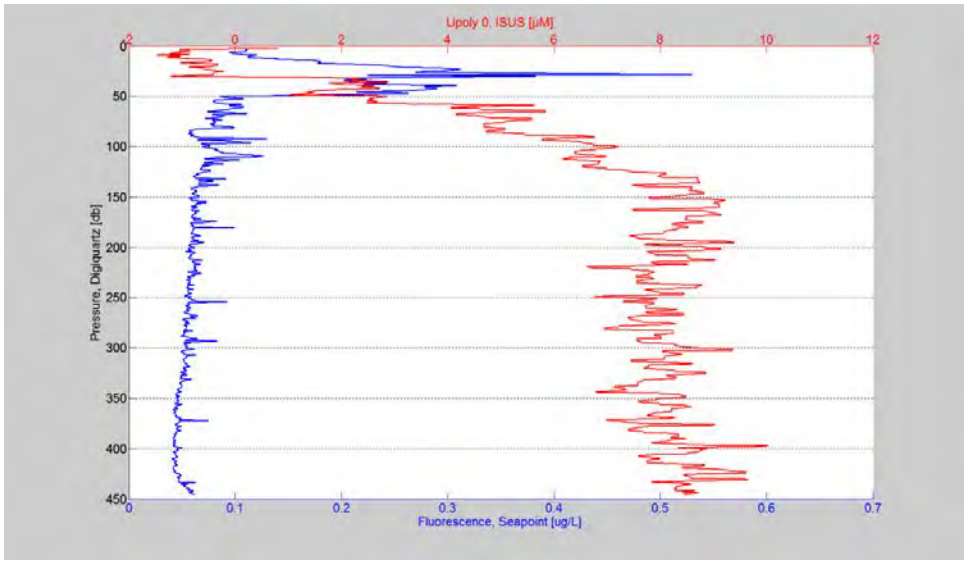


Figure 9-16. Example of the vertical structure (temperature and salinity – upper graph; nitrate and fluorescence – lower graph) for the Cast 025.

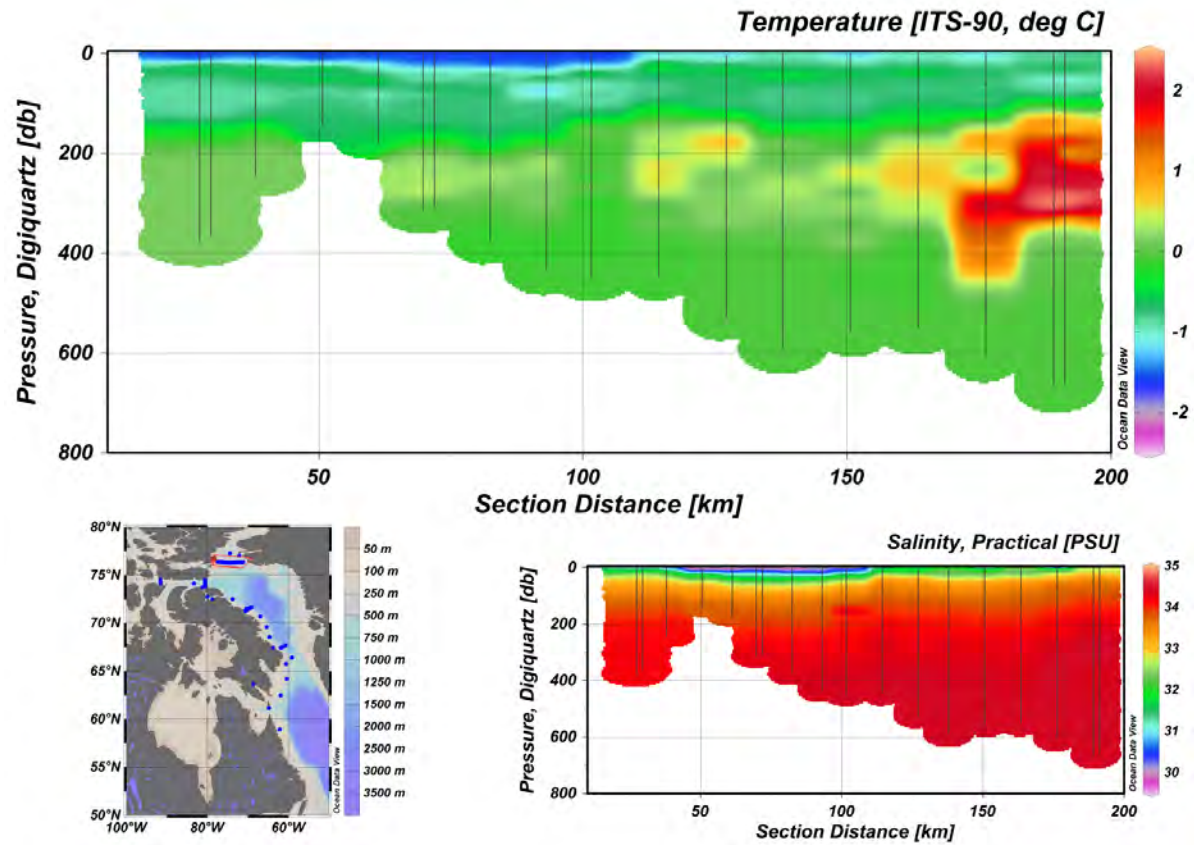


Figure 9-17. Evolution of the main parameters along the transect “Northern Baffin Bay”.

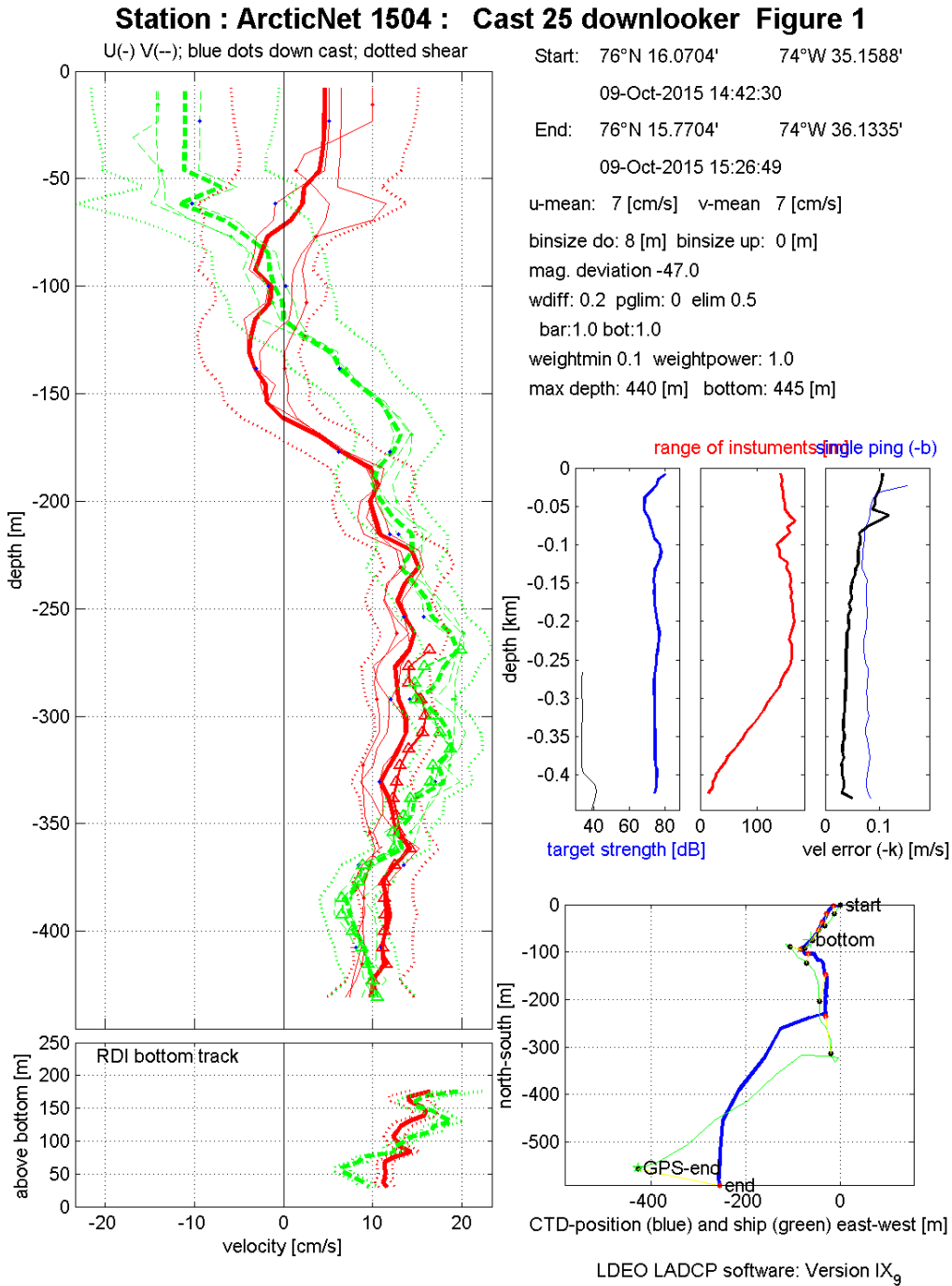


Figure 9-18. Example of current velocities for the Cast 025 recorded by the LADCP.

9.5 Comments and recommendations

A special attention has been made to keep the autosal room at an appropriate temperature (22°C). It is a crucial point to get accurate salinity values. A problem occurred at the end of the Leg 2 leading to unreliable data. The electrodes were rinsed with isopropilic alcohol (70 %).

CTD-Rosette: Several bottles were replaced during Leg 2 for spigot or leaking problems. The fluorescence Seapoint sensor sn 3114 were replaced by sensor sn 3120 after the Cast 038. The Isus nitrate sensor were replaced. A new mechanical and electrical winch termination was performed before Cast 045.

During cast 1503071 (Leg 3b), there was a communication error with the SBE 911 CTD unit that caused all data to stop transmitting from the Rosette to the deck unit. The Rosette was brought back on board and an inspection was done on the deck unit and sea cable. A problem was found in the sea cable splice where water had seeped into both the splice and the sea cable. 85m was cut from the winch in order to mitigate this seepage and the splice and mechanical support were redone to fix the problem.

During Leg 4, the cable had started to open up just above the mechanical termination. Data communication was still ok up to this point and there were no serious problems encountered (apart from unsupported modem messages in the Seasave data acquisition window during the cast). Approximately 200m of sea cable was cut from the winch in order to mitigate this seepage and the splice and mechanical support were redone to fix the problem. After 15 hours of drying time for the splice resin the Rosette was recast and worked without incident for the remainder of the leg but has shown further degradation.

The cable is due to be replaced for next year's mission. During cast 1504065 (Leg 4), the Rosette hit the sea floor and was dragged on the bottom for approximately 50m. This incident was due to many factors. First, the weather wasn't optimal and the ship was drifting at about 4 knots. Second, the water currents were strong and kept the Rosette cable at an angle during the downcast, forcing the bridge to always reposition the ship accordingly. Finally, as the rosette was stable at approximately 15m from the bottom, the sea floor started to rise, going from 424m to 317m from the beginning to the end of the cast. The Rosette frame has been damaged, bent and scratched at some places. The sea cable was damaged by the mechanical termination causing a short circuit in the sea cable and had to be redone. All instruments were tested after the incident and seem to be working fine.

LADCP: Thanks to new power supply upgrade, the ADCP intensity was sufficient even for deep cast during Legs 2 and 3b. Sometimes and probably due to the new power supply, it was difficult to communicate with the LADCP from the BBtalk software. An investigation should be done to fix the problem.

In view of the previous problems encountered with the LADCP during Leg 4, we decided to keep the LADCP on during the whole leg. By doing so, we avoided communication problems with the LADCP.

10 XCTD (GEOTRACES) – Leg 2

Project leader: Jane Eert¹ (jane.eert@dfo-mpo.gc.ca)

Cruise participants Leg 2: Kristina Brown² and Pascal Guillot³

¹ *Institute of Ocean Science, 9860 West Saanich Road, Sidney, BC, V8L 5T5, Canada.*

² *Woods Hole Oceanographic Institution, Woods Hole, MA 02543, United States.*

³ *Université Laval, Pavillon Alexandre-Vachon, Québec, QC, G1V 0A6, Canada.*

10.1 Methodology

Twenty-three expendable conductivity-temperature-depth (XCTD) probes were deployed for the Institute of Ocean Sciences (Scientist: Jane Eert) opportunistically through the Labrador Sea and Baffin Bay. The first XCTD was deployed along the 300m isotbath off the Labrador Shelf. The next 21 XCTDs were deployed at 60-70nm spacing throughout the Labrador Sea and Baffin Bay (Figure 110.1), and along 2 shelf transects at higher resolution (20-40nm; Figure 110.1, inset). The 23rd XCTD was deployed in the Canadian Arctic Archipelago at the original Station CAA-9.

The diversion of the ship to break ice in Hudson Bay occurred before an XCTD deployment entering into Davis Strait (before Station BB1). When the ship resumed operations, travel towards Davis Strait was along the coast of Baffin Bay, XCTDs were resumed again at 70nm intervals after Station BB1.

Two high resolution (20-40nm spacing) XCTD transects were carried out in an attempt to capture the southward flowing Baffin current along the western side of Baffin Bay, one crossing the shelf towards Clyde River (Figure 110.1, inset) and another approaching the north section of Lancaster Sound. Data from the XCTD deployments will be processed at the Institute of Ocean Sciences in Sidney BC.



Figure 110-1. Map of XCTD locations along the Geotraces 2015 (Leg 2) cruise track from the Labrador Sea shelf to the Canadian Arctic Archipelago. Inset plot (red hatched lines): high resolution shelf section towards Clyde River.

11 Trace metal Rosette sampling (GEOTRACES) – Legs 2 and 3b

Project leaders: Kristin J. Orians¹ (korians@eos.ubc.ca), Roger François¹ (rfrancois@eos.ubc.ca), Jay T. Cullen² (jcullen@uvic.ca), Bridget Bergquist³ (bergquist@es.utoronto.ca), Maite Maldonado¹ (mmaldonado@eos.ub.ca), Feiyue Wang⁴ (wangf@ms.umanitoba.ca), Celine Guéguen⁵ (queguen@trentu.ca), Andrew Ross⁶ (andrew.ross@dfo-mpo.gc.ca) and Chris Holmden⁷ (chris.helmden@usask.ca)

Cruise participants Leg 2: Jay T. Cullen², Priyanka Chandan³, Manuel Colombo¹, Jeff Gao⁵, David Janssen², Jingxuan Li¹, Kathleen Munson⁴, David Semeniuk¹, Kang Wang⁴ and Wen Xu⁴

Cruise participants Leg 3b: Kristin Orians¹, Manuel Colombo¹, Rowan Fox², Sarah Louise Jackson², Kathryn Purdon², Priyanka Chandan³, Ashley Elliott⁴, Kang Wang⁴, Jingxuan Li¹ and Richard Nixon⁶

¹ *University of British Columbia, Department of Earth Ocean and Atmospheric Sciences, 2020-2207 Main Mall, Vancouver BC, V6T 1Z4, Canada.*

² *University of Victoria, School of Earth and Ocean Sciences, 3800 Finnerty Road, Bob Wright Centre A405, Victoria, BC, V8P 5C2, Canada.*

³ *University of Toronto, Department of Earth Sciences, 22 Russell Street, Toronto, ON, M5S 3B1, Canada.*

⁴ *University of Manitoba, Department of Environment and Geography, 220 Sinnott Building, 70A Dysart Road, Winnipeg, MB, R3T 2N2, Canada.*

⁵ *Trent University, Department of Chemistry, 1600 West Bank Drive, Peterborough, ON, K9J 7B8, Canada.*

⁶ *Department of Fisheries and Oceans, Institute of Ocean Science, 9860 West Saanich Road, Sidney, BC, V8L 5T5, Canada.*

11.1 Introduction

The Trace Metal Rosette team was responsible for collecting trace element clean samples to characterize the distributions of dissolved and particulate trace elements, their isotopes, speciation and the ligands that bind them, in the Labrador Sea, Baffin Bay, the Canadian Basin (Beaufort Sea) and the Canadian Arctic Archipelago from the CCGS *Amundsen* during Legs 2 and 3b. These samples were collected as part of the Arctic GEOTRACES program whose stated scientific objectives were to fill critical gaps in our understanding of fundamental physical and biogeochemical processes in the Canadian Arctic Ocean and their sensitivity to projected climate change and economic development. The geochemical tracer data, in conjunction with field-based process studies and numerical models will be used to address the following specific research questions:

- How do Arctic waters flow from the Canadian Basin, through the CAA, and into the Atlantic? How are the physical, chemical and biological signatures of these water masses modified, and how might this change over the coming decades? In turn, how

can geochemical tracer distribution provide additional constraints on circulation and mixing?

- How will climate change and economic development alter the cycling of essential and toxic trace elements, and what are the likely impact upon planktonic community structure, marine productivity and contaminant fates?
- What are the potential effects of climate change on the distribution of marine productivity, biological carbon sequestration, and distributions of climate-active trace gases (e.g. CO₂, N₂O, CH₄ and dimethylsulfide - DMS) across different hydrographic regimes?
- What is the chemical buffering capacity of Arctic waters against ocean acidification, and how will acidification affect marine productivity and biogeochemical cycles?

The trace metal Rosette was used to collect samples for elements that are prone to contamination where collection with standard water sampling rosettes compromise sample integrity. These contamination prone elements include, but are not limited to:

- Dissolved trace metal concentrations: Fe, Al, Mn, Ga, Cu, Zn, Cd, Pb, Hg, Ag, Ba
- Fe and Pb isotopes
- Particulate trace elements and their isotopes
- The chemical speciation of Fe
- The organic ligands that bind Cu and Fe
- Dissolved ¹²⁹I, ²³⁰Th, ²³¹Pa concentration
- Radiogenic Pb and Nd isotopes

Underlined samples are core parameters dictated by the international GEOTRACES program (www.geotraces.org). These geochemical tracers are key towards achieving the research goals of the Arctic GEOTRACES project on Leg 2 and Leg 3b.

11.2 Methodology

Collection of seawater was performed using a trace metal Rosette system that consists of a 12 position, powder coated rosette frame equipped with 12 L, Teflon coated GO-FLO (General Oceanics, Miami, USA) bottles and a SeaBird 911 CTD/SBE 43 Oxygen sensor instrument package. In addition to the Rosette a dedicated winch with 5000 meters of non-metallic conducting sea cable and an 8ft clean sampling container were installed on the starboard foredeck. The Rosette was deployed using the winch and starboard crane over the side of the ship.

11.2.1 Leg 2

To monitor for potential contamination during sampling operations, dissolved Zn was measured immediately onboard ship using flow injection analysis (FIA) with an established

fluorescence based detection method (Nowicki et al. 1994, Janssen et al. 2015). Other samples were preserved or frozen for analysis in the PI's laboratories on shore.

The Rosette was deployed on 31 occasions and travelled almost 62 vertical kilometers during the leg (Table 11-1). The absolute number of deployments was increased to access deeper waters for general geochemical measurements in the Labrador Sea and Baffin Bay given that the ships main rosette was limited to sampling waters shallower than 1600 m.

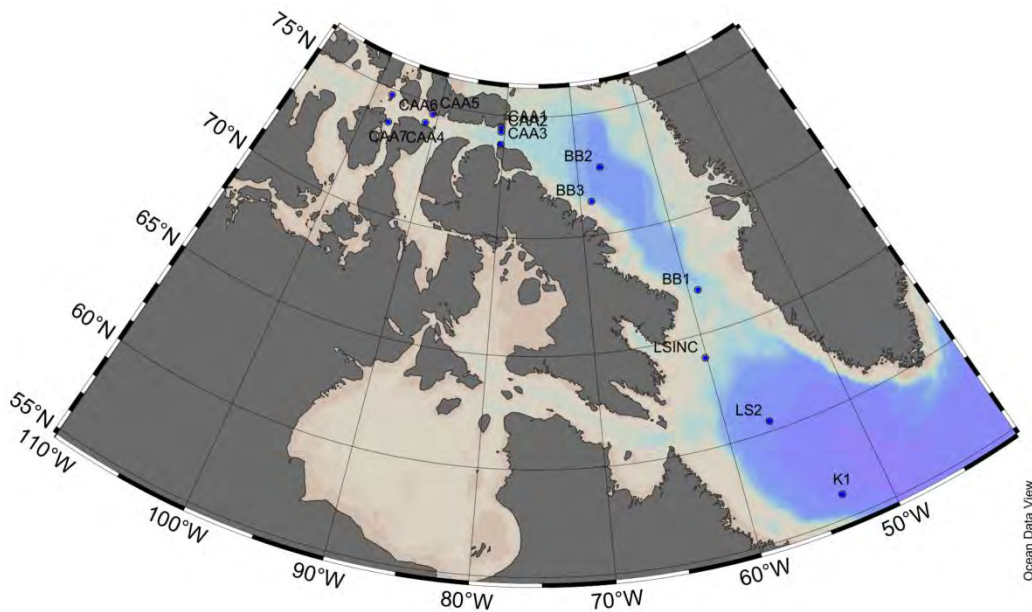


Figure 11-1. Location of stations where the Trace Metal Rosette was deployed on Leg 2.

Table 11-1. Date and location of the TM rosette deployments on Leg 2.

TMR Cast	TMR Cast at Station	Date	Station	Cruise Event Number	Latitude	Longitude	Bottom Depth (m)	Maximum Rosette Depth (m)
1	1	13/07/2015 11:42PM	K1	1	56.12017	-53.3675	3309	3010
2	2	14/07/2015 03:30AM	K1	3	56.11823	-53.3637	3311	2010
3	3	14/07/2015 08:09AM	K1	5	56.12012	-53.3667	3310	815
4	4	14/07/2015 02:37PM	K1	7	56.12087	-53.3693	3310	3015
5	1	17/07/2015 02:08AM	LS2	14	60.44933	-56.5441	3021	2400
6	2	17/07/2015 05:32AM	LS2	16	60.45237	-56.5635	3031	2800
7	3	17/07/2015 03:25PM	LS2	18	60.4534	-56.5506	3022	1215
8	4	18/07/2015 09:02AM	LS2	25	60.44635	-56.5467	3019	215
9	5	18/07/2015 05:15PM	LS2	28	60.44847	-56.5495	3022	2800
10	1	19/07/2015 10:28PM	LSINC	33	63.94828	-60.1259	481	65
11	2	19/07/2015 11:19PM	LSINC	33	63.94828	-60.1259	481	65
12	1	03/08/2015 03:43AM	BB1	34	66.85768	-59.0632	1040	1010
13	2	03/08/2015 12:40PM	BB1	40	66.85778	-59.0716	1040	210
14	1	05/08/2015 6:43PM	BB3	54	71.40887	-68.5976	1243	1010
15	2	06/08/2015 1:04AM	BB3	57	71.40748	-68.5991	1243	210
16	3	06/08/2015 7:25AM	BB3	60	71.40545	-68.601	1270	60
17	1	07/08/2015 04:40AM	BB2	69	72.7495	-66.9867	2370	810
18	2	07/08/2015 10:08PM	BB2	74	72.74973	-66.9885	2371	1010
19	3	08/08/2015 03:56AM	BB2	76	72.75105	-67	2369	2310
20	4	08/08/2015 09:07AM	BB2	79	72.75098	-66.9986	2369	160
21	5	08/08/2015 12:43PM	BB2	82	72.75037	-66.9872	2368	2337
22	1	09/08/2015 7:20PM	CAA1	92	74.52142	-80.5621	635	110
23	2	10/08/2015 0:44AM	CAA1	95	74.52197	-80.574	645	609
24	1	10/08/2015 7:04PM	CAA2	108	74.31532	-80.4993	700	600
25	1	11/08/2015 09:07AM	CAA3	117	73.80933	-80.4112	679	113
26	2	11/08/2015 7:05PM	CAA3	123	73.81622	-80.4931	676	610
27	1	12/08/2015 6:14PM	CAA5	130	74.53882	-90.8045	253	111
28	2	13/08/2015 1:41AM	CAA5	136	74.5371	-90.8078	260	252
29	1	14/08/2015 01:57AM	CAA4	149	74.1223	-91.5109	181	162
30	1	15/08/2015 04:18AM	CAA6	160	74.75433	-97.4575	260	245
31	1	15/08/2015 10:45PM	CAA7	168	73.67288	-96.5238	219	198

11.2.2 Leg 3b

Trace metal clean water samples were collected from 4 stations in the Canadian Basin (CB1, CB2, CB3 and CB4) and two stations in the Canadian Arctic Archipelago (CAA8 and CAA9). A map of the station locations is presented in Figure 11.2, and a summary of at TMR casts in Table 11-2. Station CB4 also serves as a cross-over station with the US GEOTRACES expedition, an important part of the GEOTRACES inter-calibration exercise. And lacking a cross-over station with the European groups involved in the GEOTRACES program (i.e. GEOVIDE), samples for them were collected for an inter- calibration at both CB4 and CAA8. The TM Rosette was also used for all samples collected deeper than 1500m, since the ArcticNet Rosette cable was not long enough to sample the deeper waters in the Canadian basin. The Rosette was deployed on a total of 21 occasions and travelled almost 65 vertical kilometers during Leg 3b. Samples for dissolved metals were filtered in our clean sampling van, directly from the Go Flo bottles, through Acropak Supor capsule filters (both Supor 500 or 1500) as recommended by the GEOTRACES Standard and Intercalibration Committee, Cruise and Methods Manual (CookBook, p. 53) <<http://www.geotraces.org/science/intercalibration>>. Samples were either acidified to pH \leq 1.7 within 5 days using Seastar HCl (500 μ l HCl per 250 ml sw), or frozen for later analysis (samples and speciation and/or ligand analysis).

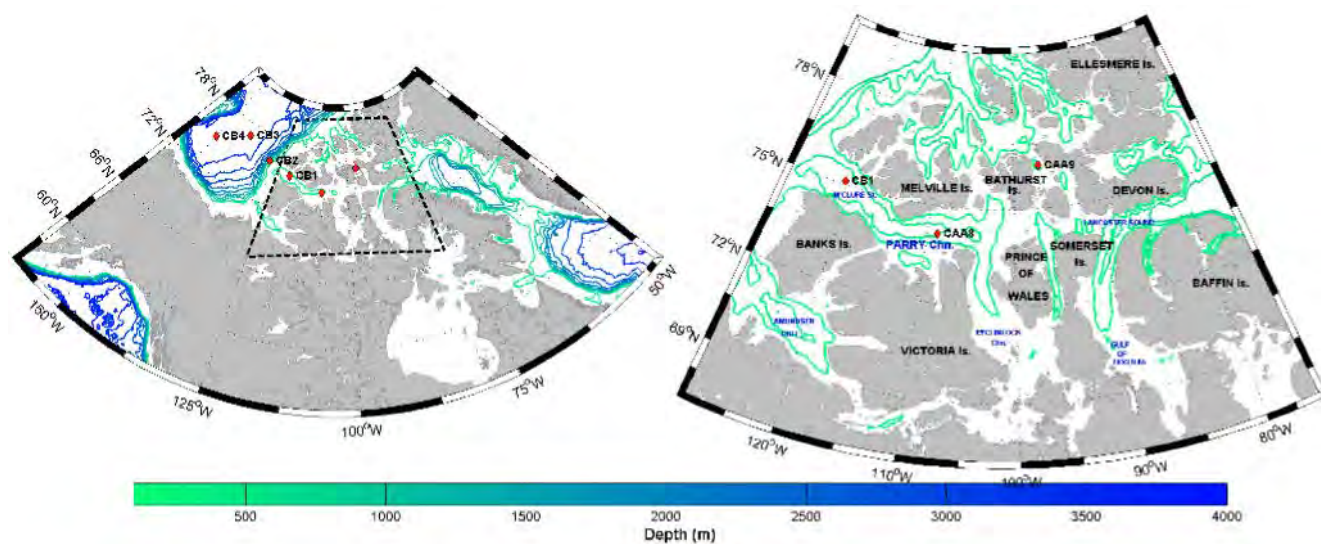


Figure 11-2. Sampled stations during the Canadian Arctic GEOTRACES 2015 Expedition during Leg 3b.

11.3 Preliminary results

11.3.1 Leg 2

The bulk of the measurements will be made on return of samples to the respective home laboratories after CCGS *Amundsen*'s return to Quebec later this year. Dissolved Zn was measured on the ship as an indicator of sample integrity given that Zn is highly prone to

contamination during sample collection and handling. These analyses were carried out by Dave Janssen in the aft Clean Lab where a trace element clean bubble was constructed during Leg 2. The onboard dissolved Zn analyses indicated the team was obtaining broadly successful trace element clean samples over the course of the leg, although initially a subset of sampling bottles showed signs of some Zn contamination. The ability to obtain clean samples improved over the course of the leg. Zinc's vertical distribution in the ocean is similar to the major algal nutrients reflecting its uptake in surface waters by phytoplankton and subsequent remineralization at depth. A characteristic profile is shown in the Figure 11.3.

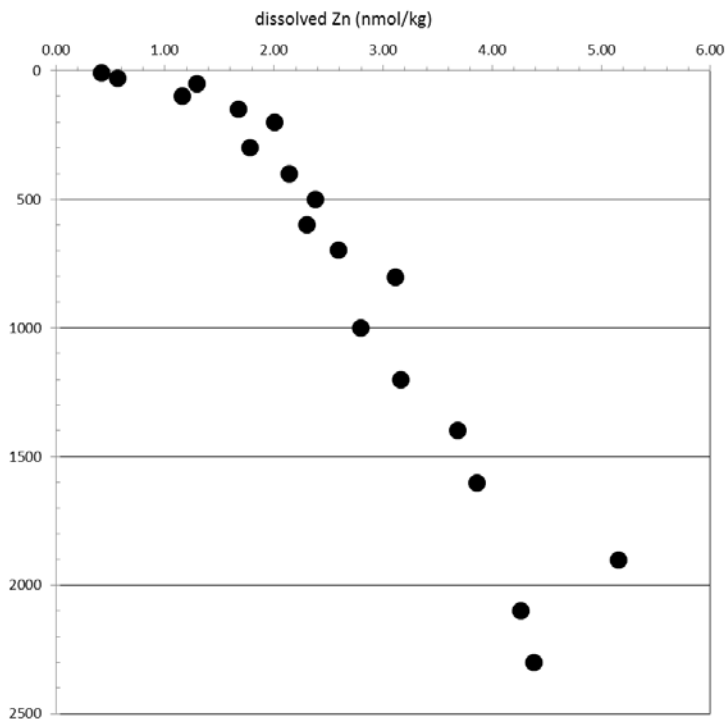


Figure 11-3. Depth versus dissolved Zn concentration for Station BB3. Preliminary results with some indication of contamination in outlying data points.

11.3.2 Leg 3b

No at sea analyses for TEI were performed on Leg 3b by the TM group (Hg analysis is covered in "Contaminants" report, Section 32). Measurements will be made upon return of samples to the respective home laboratories after CCGS *Amundsen* returns to Quebec later this year.

Table 11-2. TM Rosette sampling log summary (Leg 3b).

DATE	TIME (GMT)	TIME (UTC)	Time Code	STATION	CAST TYPE	Sampling team	EVENT No.	Lat Deg	Lat Min	Lon Deg	Lon Min	BOTTOM DEPTH	MAX DEPTH	SAMPLE NUMBERS	No. BOTTLES	WATCH	COMMENTS
5-Sep-15	13:32	18:32	IN	Test	TMROS	N/A	400	73°	51'643	N 129°	44'595	W 1226	1000	-	-	RF	TEST
7-Sep-15	17:00	22:00	IN	CB1	TMROS1	A	402	75°	06'812	N 120°	38'503	W 465	75	2019-2030	12	RF	CAST DELAYED DUE TO CABLE FAILURE
7-Sep-15	-	-	OUT	-	-	-	-	-	-	-	-	-	-	-	-	-	-
7-Sep-15	10:10	15-09-08:10	IN	CB1	TMROS2	B	406	75°	07'042	N 120°	37'998	W 460	400	2060-2071	12	RF	CAST DELAYED DUE TO CABLE FAILURE
7-Sep-15	-	-	OUT	-	-	-	-	-	-	-	-	-	-	-	-	-	-
8-Sep-15	20:27	15-09-09:27	IN	CB2	TMROS1	A	416	75°	48.88	N 129°	13.16	W 1365	200	2126-2137	12	RF	
8-Sep-15	20:56	15-09-09:56	OUT	-	-	-	-	75°	48.81	N 129°	12.92	W 1361	-	-	-	-	-
9-Sep-15	3:15	8:15	IN	CB2	TMROS2	B	419	75°	47.913	N 129°	14.821	W 1346	1200	2168-2179	12	RF	
9-Sep-15	4:13	9:13	OUT	-	-	-	-	75°	47.92	N 129°	14.84	W 1346	-	-	-	-	-
11-Sep-15	17:00	22:00	IN	CB3	TMROS-shal	B	431	76°	58.828	N 140°	2.279	W 3731	200	2248-2259	12	RF	
12-Sep-15	0:21	5:21	IN	CB3	TMROSmeso	A	434	76°	59.477	N 140°	1.901	W 3729	1400	2284-2295	12	RF	
12-Sep-15	1:25	6:25	OUT	-	-	-	-	76°	49.41	N 140°	2.187	W 3729	-	-	-	-	-
12-Sep-15	13:11	18:11	IN	CB3	TMROS1	N/A	438	76°	59.986	N 140°	5.719	W 3731	3500	2320-2331	12	RF	ORDER ID OPERATION FOR LVP AND TMROS DIFFERENT FROM IDR DEF
12-Sep-15	15:10	20:10	OUT	-	-	-	-	76°	59.942	N 140°	5.71	W ?	-	-	-	-	-
12-Sep-15	18:12	23:12	IN	CB3	TMROS2	N/A	441	77°	1.15	N 140°	2.71	W 3732	3500	2338-2349	12	RF	
12-Sep-15	20:22	15-09-13:22	OUT	-	-	-	-	77°	0.86	N 140°	2.58	W 3734	-	-	-	-	-
13-Sep-15	4:33	9:33	IN	CB3	TMROSdeep	A	444	76°	59.6	N 140°	4.26	W 3658	3500	2356-2367	12	RF	
13-Sep-15	6:43	11:43	OUT	-	-	-	-	76°	59.24	N 140°	5.75	W 3731	-	-	-	-	-
14-Sep-15	16:47	21:47	IN	CB4	TMROSshal	B	446	74°	59.81	N 150°	0.08	W 3826	220	2344-2355	12	RF	Intercal bottles (150m) and (10m)
14-Sep-15	17:12	22:12	OUT	-	-	-	-	74°	59.714	N 150°	1.196	W 3820	-	-	-	-	-
14-Sep-15	22:10	15-09-15:10	IN	CB4	TMROSmeso	A	448	75°	0.064	N 150°	0.217	W 3828	1400	2362-2373	12	RF	Intercal bottle (1400m)
14-Sep-15	23:17	15-09-15:17	OUT	-	-	-	-	74°	59.984	N 149°	59.999	W 3828	-	-	-	-	-
15-Sep-15	7:34	12:34	IN	CB4	TMROSdeep	B	451	75°	0.11	N 150°	0.01	W 3829	3500	2380-2391	12	RF	
15-Sep-15	9:51	14:51	OUT	-	-	-	-	74°	59.94	N 149°	59.63	W 3829	-	-	-	-	-
16-Sep-15	7:34	12:34	IN	CB4	TMROS1	A	455	75°	1.03	N 150°	0.81	W 3830	3500	2435-2446	12	RF	bears
16-Sep-15	9:37	13:37	OUT	-	-	-	-	75°	2.03	N 150°	0.81	W 3830	-	-	-	-	-
16-Sep-15	12:12	17:12	IN	CB4	TMROS2	B	457	75°	0.33	N 150°	0.98	W 3827	3500	2447-2458	12	RF	Part 1g
16-Sep-15	14:12	19:12	OUT	-	-	-	-	75°	0.095	N 149°	59.521	W 3827	-	-	-	-	-
16-Sep-15	17:06	22:06	IN	CB4.1	TM-Cs	A	461	74°	42.253	N 148°	46.525	W 3811	3500	2480-2491	12	RF	
16-Sep-15	19:14	15-09-17:14	OUT	-	-	-	-	74°	42.21	N 148°	45.62	W 3811	-	-	-	-	-
16-Sep-15	20:17	15-09-17:17	IN	CB4.2	TM-intercal	B	459	74°	35.578	N 148°	12.713	W 3799	1000	2465-2476	12	RF	Part 1M intercalibration
16-Sep-15	21:05	15-09-17:05	OUT	-	-	-	-	74°	35.578	N 148°	12.483	W 3800	-	-	-	-	-
23-Sep-15	22:28	15-09-24:28	IN	AN308/CAA8	TMROSshallow	B	466	74°	8.31	N 108°	50.39	W 564	120	2530-2541	12	RF	Intercal bottle (90m)
23-Sep-15	22:48	15-09-24:48	OUT	-	-	-	-	74°	8.33	N 108°	50.27	W 569	-	-	-	-	-
24-Sep-15	4:32	9:32	IN	AN308/CAA8	TMROSdeep	A	469	74°	8.34	N 108°	50.19	W 563	450	2572-2583	12	RF	Intercal bottles (450m), (250m), and (200m) (speciation only)
24-Sep-15	5:06	10:06	OUT	-	-	-	-	74°	8.38	N 108°	50.13	W 563	-	-	-	-	-
27-Sep-15	0:02	5:02	IN	CAA9	TMROSshallow	B	481	76°	20.01	N 96°	45.206	W 334	90	2638-2649	12	RF	
27-Sep-15	0:16	5:16	OUT	-	-	-	-	76°	19.98	N 96°	45.376	W 333	-	-	-	-	-
27-Sep-15	5:00	10:00	IN	CAA9	TMROSdeep	A	485	76°	19.82	N 96°	45.40	W 336	350	2669-2678	10	RF	
27-Sep-15	5:23	10:23	OUT	-	-	-	-	76°	19.83	N 96°	45.21	W 336	-	-	-	-	-

11.4 Comments and recommendations

11.4.1 Leg 2

Overall we were very satisfied with ship operations as we were on our last expedition in 2009. This level of satisfaction does not factor in the delays in the scientific program owing to Coast Guard operations in Hudson Bay, which was an unfortunate and frustrating turn of affairs outside of the ships control.

Over the course of the leg the procedure for deploying and retrieving the TMR was refined and improved with the help of the ships officers and deckhands. Given demands on the ships A-frames for other gear deployment (ArcticNet Rosette and Plankton Nets) the TMR must be deployed using the starboard foredeck crane. This requires close coordination of the crew operating the crane and the winch as the Rosette must be lifted high above the gunwale from the deck before being lowered into the water. The crane must lift the block into place, the Rosette cable placed in the block, the block raised above the deck, crane extends its arm, rotates out over the water and then the Rosette lowered into the sea. During all of these crane manipulations, the winch must manage the cable to keep tension to the block and to keep the Rosette from contacting the gunwale or the side of the ship. Even in calm conditions this a complicated procedure. This mode of deployment also puts considerable strain on our sea cable and requires the cable to bend past its specified bend radius under load. On return to the deck these operations are reversed and the cable removed from the block, the block disconnected from the crane and secured on deck. On three occasions the Rosette made significant contact with the ship and sustained minor and mostly cosmetic damage. In our opinion there is some undue risk to equipment and personnel with the current mode of deployment. A recommendation for future work (some work with the Rosette is likely to occur during the Green Edges program) would be to dedicate an existing A-frame on the ship for the TMR or to consider installing a J- or A-frame on the starboard foredeck for Rosette operations.

On two occasions the strain on our sea cable led to breaches of the cable sheath and electrical shorts in the cable requiring retermination. This was expertly and efficiently done by the ArcticNet technicians onboard. Without their efforts our sampling program would have not been nearly as successful.

11.4.2 Leg 3b

The Captain and Crew of CCGS *Amundsen* were outstanding and demonstrated considerable skill and coordination to deploy the Trace Metal Rosette, following the methods documented in a video posted from Leg 2. The video was very useful for transferring knowledge on this difficult procedure to the new teams involved in the deployment on Leg 3b. It is not an ideal method for deploying a Rosette, and we did need to re- termination on

two occasions again on Leg 3b due to kinks or water breaches (water was found to have entered the cable and travelled 75 m up the sheath). Between the UVic and ArcticNet technicians onboard, this was done with minimal down time. One suggestion, if the Rosette will be deployed off the starboard bow again in the future, is to have a block that fits the cable better, and doesn't allow the cable to rotate in the block. Ideally, it would be deployed using a dedicated A-frame on the ship.

An additional challenge we faced on Leg 3b was freezing of the sensors and trigger pins, due to the low temperatures during sampling at two of the stations (CB4 and CAA9 were both sampled at temperatures of -5 to -12 °C. Application of hot water would melt the ice, but the water would re-freeze before deployment in most cases. Some possible solutions would be a steamer or a shelter with heat lamps (the latter would be challenging in the location we deployed from on this cruise).

Additional comments from Rowan Fox and members of the *Amundsen* crew:

- the winch is not safe (operator has to sit behind drum) – order a remote pendant? Or install steel shield for operator;
- make-shift display for depth and cable rate (worked in the end, but would be good to have a better way to do this);
- level wind sensors froze sometimes – needs checking and a replacement part (needs a grease nipple, but it is too rusted for that).

12 ²³⁰Th, ²³¹Pa, Nd and Cr isotopes, and REE (GEOTRACES) – Legs 2 and 3b

Project leaders: Roger François¹ (rfrancois@eos.ubc.ca), Chris Holmden² (chris.holmden@usask.ca)

Cruise participant Leg 2: Mélanie Grenier²

Cruise participant Leg 3b: Isabelle Baconnais²

¹ *University of British Columbia, Department of Earth Ocean and Atmospheric Sciences, 2020-2207 Main Mall, Vancouver, BC, V6T 1Z4, Canada.*

² *University of Saskatchewan, Department of Geological Sciences, 114 Science Place, Saskatoon, SK, S7N 5E2, Canada.*

12.1 Introduction

Climate-driven alterations of the Arctic Ocean (e.g. sea ice cover, water masses circulation) strongly influence local biological productivity, ecosystem structure, air-sea exchange of climate-active gases, and the distribution of contaminants (e.g. Hg, Pb). At the moment, our ability to evaluate the full impact of these rapid changes and predict their future trajectory is limited by a poor understanding of the interacting chemical, physical and biological processes which shape the functional characteristics and resiliency of Arctic waters. To bridge this critical knowledge gap, a pan-Arctic field study (Arctic-GEOTRACES) is being coordinated between Canada (Legs 2 and 3b), US, Germany and France to generate a quasi-synoptic database of biogeochemical tracers of circulation, ecosystem structure and productivity, as well as a sea ice state.

The need for a basic understanding of the water masses circulation in the CAA and the adjacent need of understanding the distribution and cycle of toxic/essential trace elements in this area is a major opportunity for the development of non-traditional stable isotope tracers.

12.1.1 Chromium isotopes

Chromium in seawater is found under two oxidation states, both bearing different isotope signatures and properties: Cr(III) and Cr(VI) (Ellis et al. 2002). Cr(III) is a micronutrient for higher mammals (Mertz 1993), with concentration and isotopic composition of the Cr(III) species potentially able to trace supply fluxes from shelf sediment and groundwater (Frei et al. 2014), whereas Cr(VI) is a toxic element easily absorbed by living organisms (Richard and Bourg 1991; Standeven and Wetterhahn 1991), which species' concentration and isotopic composition are thought to trace circulation and removal fluxes to the sediment (Bonnand et al. 2013).

During the IPY-GEOTRACES cruise in 2009, the very first dataset of total Cr isotopes in these waters was determined, resulting in the identification of a unique signature for Pacific

source water (~1.5‰; Scheiderich et al. 2015, IPY Conference abstract, 2012). These measurements will add to future results for Cr isotopes and cross-parameters (e.g. Nutrients, Salinity, Pa/Th) from this cruise to potentially:

- Observe the gradual changes in Cr-isotope signature of Pacific source water as it traverses the CAA and therefore trace the evolution of the Pacific water as it moves to the Atlantic Ocean;
- Relate these changes to a range of potential addition and removal processes affecting TEIs in these waters, helping on documenting their cycle in the archipelagos.

12.1.2 Nd isotopes

Seawater acquires its Nd isotopic composition from continental sources, resulting in distinct isotopic signatures in the North Pacific and North Atlantic. The dominance of old cratons in surrounding land masses imparts a very negative (“non-radiogenic”) ϵNd to the seawater of Baffin Bay and the Labrador Sea (Stordal and Wasserburg 1986, Lacan and Jeandel 2004, Lacan and Jeandel 2005). Contrastingly, Pacific water has a less negative (“more radiogenic”) ϵNd , acquired from the young volcanic rock formations surrounding this ocean. “Boundary Exchange” (BE), i.e. the exchange of chemical elements between margin sediments and seawater, was first identified with Nd isotopes (Lacan et al. 2005b). The apparent ubiquity of BE suggests that it might add to seawater more essential bioactive metals (e.g. Mo, Fe, Cu, Zn) than what has been estimated so far (Radic et al. 2011, Slemons et al. 2012, Grenier et al. 2013, Jeandel and Oelkers – in press). Lacan and Jeandel demonstrated that Nd isotopes are particularly effective in tracing this process. In the Arctic, this approach will be particularly powerful because “radiogenic” water from the Pacific is coming into contact with margins that are very “unradiogenic”, providing an ideal setting to evaluate the extent of this process. ϵNd will also help identify Pacific Water as it transits through the Arctic, particularly through the CAA (Porcelli et al. 2009).

12.1.3 ^{230}Th and ^{231}Pa isotopes

The main purpose of ^{230}Th and ^{231}Pa measurements is to further develop these naturally occurring long-lived radioisotopes as tracers of deep and intermediate water circulation in Canada Basin, Baffin Bay and the Labrador Sea (Marchal et al. 2007, Luo et al. 2010). After formation in seawater by α -decay of uranium, they are rapidly removed by adsorption on the surface of settling particles, a process called “scavenging” (Anderson et al. 1983, Anderson et al. 1983b, Bacon 1988). ^{230}Th is more particle-reactive and has a mean residence time shorter (ca. 40 yr) than ^{231}Pa (ca. 200 yr). Consequently, ^{231}Pa is transported by ocean circulation over longer distance than ^{230}Th , which results in systematic variations in the $^{231}\text{Pa}/^{230}\text{Th}$ activity ratio in seawater in relation to water mass movement or mixing (François et al. 2007, Luo et al.). In the water column, large changes in ^{230}Th profiles were found in the Canada Basin between 1995 and 2009 (François et al. 2012, Melling et al. 2012), consistent with evidence for a recent circulation reversal of Atlantic Water in Canada Basin (Kartcher et

al. 2012). In the Labrador Sea, a significant increase in dissolved ^{230}Th concentration between 1993 and 1999 was attributed to a reduction in deep winter convection (Moran et al. 2002). In the present study, ^{230}Th and ^{231}Pa will be combined with hydrographic data and complementary tracers of circulation (^{129}I , ^{236}U) and water masses (ϵNd , N^* , Cr isotopes), in combination with numerical modelling, to further constrain changes in Atlantic Water circulation in the Canada Basin.

12.1.4 Rare Earth Elements (REE)

There are 14 naturally occurring REEs that fractionate slightly from each other in physical and chemical transformations due to small differences in ionic radius. The resulting changes in REE “patterns” provide a powerful tool for investigating environmental processes (Elferfield 1988, Byrne and Sholkovitz 1996). While ϵNd reveals the source of water masses and exchanges in the water column, the REE patterns provide complementary constraints on the processes (e.g. scavenging, lithogenic sources) that govern isotope exchanges. Thus, a likely outcome of this project will be the quantification of exchange of trace elements between waters and shelf sediments, with implications for biological productivity and contaminant dispersion.

For analytical efficiency reasons, the sampling for Cr and Nd isotopes, as well as Pa-Th and REE concentration measurements were combined during this cruise. Nd isotopes measurement's main purpose is as a water mass tracer (Pacific vs Atlantic water in the Canada Basin and CAA; Denmark Strait Overflow water vs Baffin Bay in the Labrador Sea). Another potential outcome, particularly in the CAA, is in identifying exchange of trace elements between bottom waters and shelf sediments, complementing Cr isotopes observations. The REE patterns will provide further constraints on the processes (e.g. scavenging, lithogenic sources) that govern isotope exchanges. Finally, ^{230}Th and ^{231}Pa measurements will help developing novel tracers of deep and intermediate water circulation (e.g. ^{129}I , Nd). The likely outcome of this project will be the cross-comparison of all these new tracers for the quantification of exchange of trace elements between waters and shelf sediments, with implications for biological productivity and contaminant dispersion, as well as the documentation on water masses chemical evolution in the Canadian Archipelago.

12.2 Methodology

During the Leg 2, seawater samples were collected at all stations for the measurement of the REE concentration and ϵNd , while for ^{230}Th and ^{231}Pa measurement, seawater samples were only collected at the deep stations in the Labrador Sea and Baffin Bay. Aliquots (~3-4 L) from samples dedicated to ϵNd measurements were also taken for the analysis of Cr isotopes, conducted by Isabelle Baconnais, PhD student at the University of Saskatchewan.

She was in charge of the operations related to these trace elements and isotopes (REE, ϵ Nd, ^{230}Th , ^{231}Pa , and Cr isotopes) during the Leg 3b. The operations conducted in the Leg 3b echoed the ones conducted during the Leg 2 by Mélanie Grenier (UBC).

The Canadian section done during Leg 2 was connected to the French GEOVIDE section by a common cross-over intercalibration station in the Labrador Sea (Station K1). Depth replicates were also collected at several stations for intercalibration of the measurement of ^{230}Th and ^{231}Pa with Prof. Gideon Henderson (Department of Earth Sciences, University of Oxford, Oxford, United Kingdom) and of the measurement of ϵ Nd and REE concentration with Dr. Catherine Jeandel (LEGOS, Toulouse, France).

During both legs, the *Amundsen* Rosette, which was dedicated to most of the ArcticNet samplings (AN), was used to retrieve seawater samples above 1400m, while deeper samples are collected from the Trace-Metal Rosette (University of Victoria; PI: Jay Cullen). Because of the limited volume of the Niskin/GoFlo bottles, each seawater sample was simultaneously collected from two Niskin bottles (or Go-Flo bottles when collected from the TM rosette) closed at same depths. Using Teflon tubings pre-contaminated with the sample, seawater was retrieved in acid-cleaned 20L jerricans (also pre-contaminated by three rinses with the sample) and brought back to the on-board lab in a hermetic plastic bag. There, the seawater was filtered through a one-use-only 0.45 μm -filter cartridge (AquaPrep®) mounted on an acid-cleaned tubing system connected to a peristaltic pump, operating at ~250mL/min. The filtered seawater was divided into three containers in the following order: a 1L acid-cleaned Nalgene® bottle for REE concentration measurement, a 20L acid-cleaned cubitainer for Nd isotopes determination, and a 4L trace-clean cubitainer dedicated to Cr isotopes measurement. Each container was rinsed three times with the seawater before being filled. All samples were then acidified to pH~2 using 6N HCl EG (made on-board under the fume hood of the Nutrient lab with concentrated HCl EG and milli-Q® water coming from the on-board Arctic Net system). The 1L bottles and 4L cubitainers were then stored away in UBC and Usask coolers.

Except for the Stations CB1, AN-407 and CAA9 (Leg 3b), all 20L cubitainers were spiked for the measurement of ^{230}Th and ^{231}Pa concentrations. The spike solution is a mixture of 0.5mL of ^{233}Pa at ~0.4788pmol/g, 0.2mL of ^{229}Th at ~1.5dpm, and 2mL of FeCl_3 at ~50mg/mL, prepared before the cruise and conditioned in the form of a precipitate into 15mL test tubes (one per cubitainer). The 20L cubitainers were accurately weighed empty and with the sample before the addition of the spike solution on an industrial scale. The acidification and the spiking of the seawater for Pa/Th and REE measurements were done in one shot, with the dissolution of the spike solution with ~10mL of 6N HCl EG, which was then poured into the cubitainer. The test tube containing the spike solution was then rinsed 3 times with ~10mL of 6N HCl EG to ensure a complete transfer of the spike into the sample, leading to a total use of ~40mL of 6N HCl EG to acidify the sample at pH~2. The pH was checked for every sample using pH-paper.

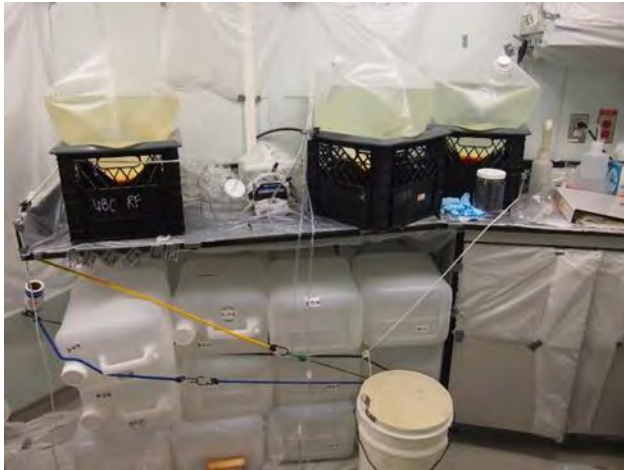


Figure 12-1. Arrangement of the on-board lab bench area. Ropes hold the 20 L jerricans below the bench. On the bench, 3 samples stand in milkcrates for settling of the iron co-precipitate, in the 20 L cubitainers.

For the 20L-samples from Stations CB1 and AN-407 (Leg 3b), ~40mL of 6N HCL EG were added for acidification, and 2mL of FeCl_3 was added separately for trace-elements' pre-concentration. For all 20L-seawater samples, they were stored ~24H to allow the equilibration of the spikes and the iron solution with the seawater. After 24H, the pH was raised to 8.0-8.5 using ~25mL of concentrated NH_4OH to engage the Fe co-precipitation. The pH was checked for every sample using pH-paper. After 48H of settling, most of the supernatant was drained using an acid-clean tubing system connected to a peristaltic pump. The remaining seawater and co-precipitate were poured into 1L acid-cleaned transparent bottles (Figure 12.1). The cubitainer was rinsed twice with Milli-Q® water 18.2M Ω to collect all the precipitate. After 12H, as the precipitate and the seawater/Milli-Q® water 18.2M Ω separated again into two phases, the supernatant was poured and discarded, and the precipitate was poured into a 50mL acid-cleaned centrifugation tube. The 1L bottle was rinsed twice with Milli-Q® water 18.2M Ω and the sample was centrifuged. The sample was finally stored in the centrifugation tubes after the removal of any remains of supernatant (i.e. seawater or Milli-Q® water 18.2M Ω).

For the Station CAA9 (Leg 3b), as the short time before the end of the leg did not allow the completion of the procedure for Pa/Th and REE measurement, and as no containers were left for the collection for Cr isotopes measurement, the seawater was filtered from one jerrican to another, with three rinses of the sample beforehand, and collection of 1L for REE concentration measurement. Jerricans and bottles were acidified with 6N HCl EG to pH~2. An aliquot of 3L will be later collected from the jerricans at UBC for Cr measurement at USask. In order to monitor any contamination from the storage of the seawater in the jerricans, a blank was done with the collection of Milli-Q® water 18.2M Ω , acidified to pH~2, into an analogue jerrican.

During the Legs 2 and 3b, 3 and 2 total procedural blanks were respectively realised. A 20L jerrican was rinsed three times with Milli-Q® water 18.2M Ω and filled directly at the on-board Millipore system. For Leg 2, the first 2 blanks were processed as samples dedicated to the measurement of REE, Pa and Th. Thus, a “spike + iron” solution was added after the

filtration and weighing. The 3rd and last total procedural blank realised during this leg was processed as a sample dedicated to the REE concentration and Nd measurement only, so 2 mL of FeCl₃ only were added after acidification. During Leg 3b, the first 20L blank was acidified with addition of 2mL of FeCl₃. The 2nd procedural blank is spiked for Pa/Th blank measurement. Both consequently followed the same procedure as described above for normal seawater samples (i.e. pH-rising, discard of supernatant, centrifugation).

During 2, samples collected for intercalibration of ²³⁰Th and ²³¹Pa measurements (with G. Henderson, UK) were filtered into a 10 L jerrican, following the method described above, acidified with 25 mL of 6 N HCl EG, and stored into G. Henderson's plastic boxes. Samples collected for intercalibration of εNd measurements (with C. Jeandel, France; ~ 10 L) were filtered into the 20 L cubitainers, following the method described above and acidified with 25 mL of 6 N HCl EG to pH = 2 while waiting for pre-concentration. Before the pre-concentration procedure on C¹⁸ SepPak cartridges loaded with a REE complexant (HDEHP/H2MEHP) (Shabani et al. 1992), pH was raised to 3.7 with ~ 12 mL of concentrated NH₄OH. Then, each of the 5 samples collected for this intercalibration were pre-concentrated on 2 C¹⁸ cartridges using 2 tubing systems and the peristaltic pump at a flow rate of 20 mL min⁻¹. The 2 cartridges were then disconnected, wrapped into parafilm, labelled and stored into small plastic bags, ready to be sent back to LEGOS (Toulouse, France).

August 5, 2015	-68.596	71.4091	BB3-AM1	B6-7 600 m	YES	YES	38	12940	0.5673	0.1956	YES	
August 5, 2015	-68.596	71.4091	BB3-AM1	B8-10 700 m	YES	YES	39	14570	0.5682	0.1956	YES	
August 5, 2015	-68.596	71.4091	BB3-AM1	B13-14 500 m	YES	YES	40	16730	0.5685	0.1963	YES	
August 5, 2015	-68.596	71.4091	BB3-AM1	B17-18 300 m - a	YES	YES	41	17360	0.5663	0.1965	YES	
August 5, 2015	-68.6034	71.4109	BB3-AM2	B9-10 100 m	YES	YES	42	17680	0.5677	0.1981	YES	
August 5, 2015	-68.6034	71.4109	BB3-AM2	B14-15 50 m	YES	YES	43	17730	0.5663	0.1869	YES	
August 5, 2015	-68.6034	71.4109	BB3-AM2	B18-19 10 m	YES	YES	44	18520	0.568	0.1954	YES	
August 7, 2015	-66.9933	72.7537	BB2-AM1	B1-2 1500 m	YES	YES	45	16490	0.5678	0.1968	YES	
August 7, 2015	-66.9933	72.7537	BB2-AM1	B7-8 1000 m	YES	YES	46	15700	0.568	0.1965	YES	
August 7, 2015	-66.9933	72.7537	BB2-AM1	B16-17 200 m - a	YES	YES	47	16270	0.5657	0.1965	YES	
August 7, 2015	-67.0218	72.7494	BB2-AM2	B2-3 600 m	YES	YES	48	16930	0.5702	0.1998	YES	
August 7, 2015	-67.0218	72.7494	BB2-AM2	B5-6 400 m	YES	YES	48	16310	0.5803	0.1964	YES	
August 8, 2015	-67.0218	72.7494	BB2-AM2	B7-8 300 m	YES	YES	50	16490	0.5687	0.2009	YES	
August 8, 2015	-67.0218	72.7494	BB2-AM2	B11-12 100 m - a	YES	YES	51	15800	0.5702	0.201	YES	
August 8, 2015			BB2-TM5	B2 2250 m	YES	YES	52	8390	0.5684	0.2	NO	
August 8, 2015			BB2-TM5	B5-6 2100 m	YES	YES	53	17160	0.5678	0.2009	YES	
August 8, 2015			BB2-TM5	B8-9 1900 m	YES	YES	54	15790	0.5666	0.2009	YES	
August 8, 2015	-66.9998	72.7507	BB2-AM4	B1-2 300 m - b	YES	YES	55	16440	0.5669	0.2006	YES	
August 8, 2015	-66.9998	72.7507	BB2-AM4	B3-4 200 m - b	YES	YES	56	16050	0.5684	0.2001	YES	
August 8, 2015	-66.9998	72.7507	BB2-AM4	B5-6 100 m - b	YES	YES	57	14950	0.5685	0.2006	YES	
August 8, 2015	-66.9998	72.7507	BB2-AM4	B7-8 50 m Intercalib	YES	YES		14730			YES	Intercalib Nd-C18 C Jeandel
August 8, 2015	-66.9998	72.7507	BB2-AM4	B9-10 60 m	YES	YES		17020			YES	Nd only
August 8, 2015	-66.9998	72.7507	BB2-AM4	B11-12 10 m Intercalib	YES	YES		15490			YES	Intercalib Nd-C18 C Jeandel
August 8, 2015	-66.9998	72.7507	BB2-AM4	B13-14 10 m	YES	YES		15990			YES	Nd only
August 10, 2015	-80.564	74.5222	CAA1-AM1	B1-2 600 m	YES	YES		17480			YES	
August 10, 2015	-80.564	74.5222	CAA1-AM1	B5-6 400 m	YES	YES		15200			YES	
August 10, 2015	-80.564	74.5222	CAA1-AM1	B11-12 200 m	YES	YES		16200			YES	
August 10, 2015	-80.5679	74.5210	CAA1-AM2	B4-5 100 m	YES	YES		17500			YES	
August 10, 2015	-80.5679	74.5210	CAA1-AM2	B15-16 scm (max chloro)	YES	YES		17400			YES	
August 10, 2015	-80.5679	74.5210	CAA1-AM2	B22-23 10 m +/-	YES	YES		17900			YES	
August 10, 2015	-80.4873	74.3159	CAA2-AM2	B4-5 100 m	YES	YES		16500			YES	
August 10, 2015	-80.4873	74.3159	CAA2-AM2	B15-16 scm (max chloro)	YES	YES		16400			YES	
August 10, 2015	-80.4873	74.3159	CAA2-AM2	B22-23 10 m +/-	YES	YES		17700			YES	
August 10, 2015	-80.5189	74.3143	CAA2-AM1	B1-2 600 m	YES	YES		17300			YES	
August 10, 2015	-80.5189	74.3143	CAA2-AM1	B5-6 400 m	YES	YES		17800			YES	
August 10, 2015	-80.5189	74.3143	CAA2-AM1	B11-12 200 m	YES	YES		17800			YES	
August 11, 2015	-80.4923	73.8186	CAA3-AM2	B4-5 100 m	YES	YES		16300			YES	
August 11, 2015	-80.4923	73.8186	CAA3-AM2	B13-14 scm (max chloro)	YES	YES		16800			YES	
August 11, 2015	-80.4923	73.8186	CAA3-AM2	B20-21 10 m +/-	YES	YES		15200			YES	
August 11, 2015	-80.4894	73.8187	CAA3-AM1	B1-2 600 m	YES	YES		17100			YES	
August 11, 2015	-80.4894	73.8187	CAA3-AM1	B5-6 400 m	YES	YES		16400			YES	
August 11, 2015	-80.4894	73.8187	CAA3-AM1	B11-12 200 m	YES	YES		16500			YES	
			River sample	#1	YES	YES		5100			YES	
			River sample	#2	YES	YES		6700			YES	
			River sample	#4	YES	YES		7900			YES	
			River sample	#5	YES	YES		6600			YES	
			River sample	#6	YES	YES		7900			YES	

August 10, 2015	-80.564	74.5222	CAA1-AM1	B1-2 600 m	YES	YES	17480		YES
August 10, 2015	-80.564	74.5222	CAA1-AM1	B5-6 400 m	YES	YES	15200		YES
August 10, 2015	-80.564	74.5222	CAA1-AM1	B11-12 200 m	YES	YES	16200		YES
August 10, 2015	-80.5679	74.5210	CAA1-AM2	B4-5 100 m	YES	YES	17500		YES
August 10, 2015	-80.5679	74.5210	CAA1-AM2	B15-16 scm (max chloro	YES	YES	17400		YES
August 10, 2015	-80.5679	74.5210	CAA1-AM2	B22-23 10 m +/-	YES	YES	17900		YES
August 10, 2015	-80.4973	74.3159	CAA2-AM2	B4-5 100 m	YES	YES	16500		YES
August 10, 2015	-80.4973	74.3159	CAA2-AM2	B15-16 scm (max chloro	YES	YES	16400		YES
August 10, 2015	-80.4973	74.3159	CAA2-AM2	B22-23 10 m +/-	YES	YES	17700		YES
August 10, 2015	-80.5199	74.3143	CAA2-AM1	B1-2 600 m	YES	YES	17300		YES
August 10, 2015	-80.5199	74.3143	CAA2-AM1	B5-6 400 m	YES	YES	17800		YES
August 10, 2015	-80.5199	74.3143	CAA2-AM1	B11-12 200 m	YES	YES	17800		YES
August 11, 2015	-80.4923	73.8186	CAA3-AM2	B4-5 100 m	YES	YES	16300		YES
August 11, 2015	-80.4923	73.8186	CAA3-AM2	B13-14 scm (max chloro	YES	YES	16800		YES
August 11, 2015	-80.4923	73.8186	CAA3-AM2	B20-21 10 m +/-	YES	YES	15200		YES
August 11, 2015	-80.4894	73.8187	CAA3-AM1	B1-2 600 m	YES	YES	17100		YES
August 11, 2015	-80.4894	73.8187	CAA3-AM1	B5-6 400 m	YES	YES	16400		YES
August 11, 2015	-80.4894	73.8187	CAA3-AM1	B11-12 200 m	YES	YES	16500		YES
			River sample	#1	YES	YES	5100		YES
			River sample	#2	YES	YES	6700		YES
			River sample	#4	YES	YES	7900		YES
			River sample	#5	YES	YES	6600		YES
			River sample	#6	YES	YES	7900		YES
August 12, 2015	-90.8018	74.5375	CAA5-AM1	B1-2 250 m	YES	YES	16600		YES
August 12, 2015	-90.8018	74.5375	CAA5-AM1	B5-6 220 m	YES	YES	15600		YES
August 12, 2015	-90.8018	74.5375	CAA5-AM1	B11-12 160 m	YES	YES	15700		YES
August 13, 2015	-90.8064	74.5387	CAA5-AM2	B4-5 100 m	YES	YES	15300		YES
August 13, 2015	-90.8064	74.5387	CAA5-AM2	B14-15 scm (max chloro	YES	YES	15200		YES
August 13, 2015	-90.8064	74.5387	CAA5-AM2	B21-22 10 m +/-	YES	YES	15100		YES
			River sample	#7	YES	YES	8000		YES
			River sample	#8	YES	YES	8200		YES
August 14, 2015	-91.5118	74.1210	CAA4-AM1	B1-2 150 m	YES	YES	5600		YES
August 14, 2015	-91.5118	74.1210	CAA4-AM1	B7-8 120 m	YES	YES	16900		YES
August 14, 2015	-91.5118	74.1210	CAA4-AM1	B15-16 60 m	YES	YES	17400		YES
August 14, 2015	-91.4933	74.1250	CAA4-AM2	B6-7 80 m	YES	YES	16000		YES
August 14, 2015	-91.4933	74.1250	CAA4-AM2	B14-15 30 m	YES	YES	16600		YES
August 14, 2015	-91.4933	74.1250	CAA4-AM2	B21-22 10 m	YES	YES	15800		YES
			River sample	#9	YES	YES	6800		YES
August 15, 2015	-97.4522	74.7596	CAA6-AM1	B1-2 250 m	YES	YES	17000		YES
August 15, 2015	-97.4522	74.7596	CAA6-AM1	B5-6 220 m	YES	YES	16600		YES
August 15, 2015	-97.4522	74.7596	CAA6-AM1	B11-12 160 m	YES	YES	17000		YES
August 15, 2015	-97.4575	74.7543	CAA6-AM2	B4-5 100 m	YES	YES	15800		YES
August 15, 2015	-97.4575	74.7543	CAA6-AM2	B14-15 scm (max chloro	YES	YES	17000		YES
August 15, 2015	-97.4575	74.7543	CAA6-AM2	B21-22 10 m +/-	YES	YES	15300		YES
August 15, 2015	-96.5236	73.6729	CAA7-AM1	B3-4 190 m	YES	YES	16100		YES
August 15, 2015	-96.5236	73.6729	CAA7-AM1	B7-8 160 m	YES	YES	17100		YES
August 15, 2015	-96.5236	73.6729	CAA7-AM1	B19-20 60 m	YES	YES	16000		YES
August 16, 2015	-96.5362	73.6639	CAA7-AM2	B4-5 100 m	YES	YES	16300		YES
August 16, 2015	-96.5362	73.6639	CAA7-AM2	B14-15 scm (max chloro	YES	YES	16500		YES
August 16, 2015	-96.5362	73.6639	CAA7-AM2	B21-22 10 m +/-	YES	YES	14000		YES
			-	Total procedural blank #3	YES	YES	15600		YES
			River sample	#10	YES	YES	7700		YES
			River sample	#11	YES	YES	7700		YES
			River sample	#12	YES	YES	7100		YES
August 17, 2015	-100.697	69.1662	AN312-AM1	B1-3 49 m	YES	YES	12100		YES
August 17, 2015	-100.697	69.1662	AN312-AM1	B8-9 20 m	YES	YES	17800		YES
August 17, 2015	-100.697	69.1662	AN312-AM1	B14-15 10 m	YES	YES	18400		YES
			River sample	#13	YES	YES	7900		YES
			River sample	#14	YES	YES	7300		YES
				Spike solution blank #1			58	0.5662	0.2003
				Spike solution blank #2			59	0.5667	0.2001
				Spike solution blank #3			60	0.5663	0.2002
				Spike solution blank #4			61	0.5659	0.2004
				Spike solution blank #5			62	0.5661	0.2002
				Spike solution blank #6			63	0.5641	0.2004
				Spike solution blank #7			64	0.5669	0.2002

CAA stations, river samples and total procedural blank #3 dedicated to the measurement of REE & Pu only (and Cr isotopes, but not for Pa/Th)

Spike solutions #58 to #64 dedicated to spike blanks

Table 12-2. Log of the samples collected during Leg 3b, all valid for Nd isotopes samples (PWW:Pacific Winter Water; PSW: Pacific Summer Water; SCM: Surface Chl a max).

Date	Latitude [°N]	Longitude [°W]	Station-Cast [#]	Event [#]	Sample Nb [#]	Niskin/Go- Flo bottle Nb [#]	Depth [m]	Filtration	REF. (LL)	²³⁰ Th- ²³¹ Pa spiking	Cr (3L)	Comments
<i>Leg 3b (Sept. 4th, 2013-Oct. 1st, 2013)</i>												
Sept. 06, 2015	75°07.35	120°38.50	CB1-AN (RADS)	401	2008-2009	B8-9	350	YES	YES	NO	YES	
Sept. 07, 2015	75°06.095	120°33.569	CB1-AN1	407	2072-2073	B1-2	Bottom	YES	YES	NO	YES	
Sept. 07, 2015	75°06.095	120°33.569	CB1-AN1	407	2077-2078	B6-7	250	YES	YES	NO	YES	
Sept. 07, 2015	75°06.095	120°33.569	CB1-AN1	407	2080-2081	B9-10	200	YES	YES	NO	YES	
Sept. 07, 2015	75°06.095	120°33.569	CB1-AN1	407	2082-2083	B11-12	150	YES	YES	NO	YES	
Sept. 07, 2015	75°06.095	120°33.569	CB1-AN1	407	2086-2087	B15-16	75	YES	YES	NO	YES	PWW (water mass)
Sept. 07, 2015	75°06.095	120°33.569	CB1-AN1	407	2088-2089	B17-18	65	YES	YES	NO	YES	PSW (water mass)
Sept. 07, 2015	75°06.095	120°33.569	CB1-AN1	407	2094-2095	B23-24	10	YES	YES	NO	YES	
Sept. 08, 2015	75°49.28	129°13.08	CB2-AN (RADS)	415	2106-2107	B5-6	700	YES	YES	YES	LOST	
Sept. 08, 2015	75°49.28	129°13.08	CB2-AN (RADS)	415	2108-2109	B7-8	500	YES	YES	YES	YES	
Sept. 08, 2015	75°49.28	129°13.08	CB2-AN (RADS)	415	2114-2115	B13-14	400	YES	YES	YES	YES	
Sept. 09, 2015	75°48.35	129°11.52	CB2-AN1	420	2180-2181	B1-2	Bottom	YES	YES	YES	YES	
Sept. 09, 2015	75°48.35	129°11.52	CB2-AN1	420	2183-2184	B4-5	1000	YES	YES	YES	YES	
Sept. 09, 2015	75°48.35	129°11.52	CB2-AN1	420	2186-2187	B7-8	800	YES	YES	YES	YES	
Sept. 09, 2015	75°48.35	129°11.52	CB2-AN1	420	2189-2190	B10-11	400	YES	YES	YES	YES	
Sept. 09, 2015	75°48.35	129°11.52	CB2-AN1	420	2191-2192	B12-13	200	YES	YES	YES	YES	
Sept. 09, 2015	75°48.35	129°11.52	CB2-AN1	420	2195-2196	B16-17	140	YES	YES	YES	YES	
Sept. 09, 2015	75°48.35	129°11.52	CB2-AN1	420	2197-2198	B18-19	65	YES	YES	YES	YES	
Sept. 09, 2015	75°48.35	129°11.52	CB2-AN1	420	2202-2203	B23-24	10	YES	YES	YES	YES	
Sept. 11, 2015	76°58.791	140°02.288	CB3-AN (RADS)	430	2224-2225	B1-2	1400	YES	YES	YES	YES	
Sept. 11, 2015	76°58.791	140°02.288	CB3-AN (RADS)	430	2226-2227	B3-4	1000	YES	YES	YES	YES	
Sept. 11, 2015	76°58.791	140°02.288	CB3-AN (RADS)	430	2240-2241	B17-18	600	YES	YES	YES	YES	
Sept. 11, 2015	76°58.791	140°02.288	CB3-AN (RADS)	430	2246-2247	B23-24	400	YES	YES	YES	YES	
Sept. 11, 2015	76°58.40	140°03.24	CB3-AN2	433	2266-2267	B1-2	1400	YES	YES	YES	YES	
Sept. 11, 2015	76°58.40	140°03.24	CB3-AN2	433	2271-2272	B6-7	250	YES	YES	YES	YES	
Sept. 11, 2015	76°58.40	140°03.24	CB3-AN2	433	2274-2275	B9-10	140	YES	YES	YES	YES	
Sept. 11, 2015	76°58.40	140°03.24	CB3-AN2	433	2277-2278	B12-13	65	YES	YES	YES	YES	
Sept. 11, 2015	76°58.40	140°03.24	CB3-AN2	433	2281-2282	B16-17	10	YES	YES	YES	YES	
Sept. 12, 2015	76°59.644	140°04.711	CB3-TM1	438	2321-2322	B2-3	3500	YES	YES	YES	YES	
Sept. 12, 2015	76°59.644	140°04.711	CB3-TM1	438	2324-2325	B5-6	3000	YES	YES	YES	YES	
Sept. 12, 2015	76°59.644	140°04.711	CB3-TM1	438	2327-2328	B8-9	2500	YES	YES	YES	YES	
Sept. 12, 2015	76°59.644	140°04.711	CB3-TM1	438	2330-2331	B11-12	2000	YES	YES	YES	YES	
Sept. 14, 2015	74°59.91	150°00.38	CB4-AN1	445	2320-2321	B1-2	1400	YES	YES	YES	YES	
Sept. 14, 2015	74°59.91	150°00.38	CB4-AN1	445	2322-2323	B3-4	1000	YES	YES	YES	YES	
Sept. 14, 2015	74°59.91	150°00.38	CB4-AN1	445	2336-2337	B17-18	600	YES	YES	YES	YES	
Sept. 14, 2015	74°59.91	150°00.38	CB4-AN1	445	2342-2343	B23-24	400	YES	YES	YES	YES	
Sept. 14, 2015	75°00.00	150°00.36	CB4-AN3	452	2392-2393	B1-2	1400	YES	YES	YES	YES	
Sept. 14, 2015	75°00.00	150°00.36	CB4-AN3	452	2397-2398	B6-7	300	YES	YES	YES	YES	
Sept. 14, 2015	75°00.00	150°00.36	CB4-AN3	452	2399-2400	B8-9	220	YES	YES	YES	YES	
Sept. 14, 2015	75°00.00	150°00.36	CB4-AN3	452	2403-2404	B12-13	71	YES	YES	YES	YES	
Sept. 14, 2015	75°00.00	150°00.36	CB4-AN3	452	2407-2408	B16-17	10	YES	YES	YES	YES	
Sept. 16, 2015	75°00.24	149°57.65	CB4-TM1	455	2436-2437	B2-3	3500	YES	YES	YES	YES	
Sept. 16, 2015	75°00.24	149°57.65	CB4-TM1	455	2439-2440	B5-6	3000	YES	YES	YES	YES	
Sept. 16, 2015	75°00.24	149°57.65	CB4-TM1	455	2442-2443	B8-9	2500	YES	YES	YES	YES	
Sept. 16, 2015	75°00.24	149°57.65	CB4-TM1	455	2445-2446	B11-12	2000	YES	YES	YES	YES	
Sept. 18, 2015	71°00.53	126°05.08	AN-407	464	2499-2500	B5-6	Bottom	YES	YES	NO	YES	
Sept. 18, 2015	71°00.53	126°05.08	AN-407	464	2502-2503	B8-9	300	YES	YES	NO	YES	
Sept. 18, 2015	71°00.53	126°05.08	AN-407	464	2505-2506	B11-12	200	YES	YES	NO	YES	Tmin
Sept. 18, 2015	71°00.53	126°05.08	AN-407	464	2508-2509	B14-15	71	YES	YES	NO	YES	SCM
Sept. 18, 2015	71°00.53	126°05.08	AN-407	464	2514-2515	B20-21	10	YES	YES	NO	YES	
Sept. 24, 2015	74°08.37	108°50.25	CAA 8-AN1	468	2549-2550	B2-3	Bottom	YES	YES	YES	NO	
Sept. 24, 2015	74°08.37	108°50.25	CAA 8-AN1	468	2552-2553	B5-6	450	YES	YES	YES	YES	
Sept. 24, 2015	74°08.37	108°50.25	CAA 8-AN1	468	2556-2557	B9-10	350	YES	YES	YES	YES	
Sept. 24, 2015	74°08.31	108°50.18	CAA 8-AN2	471	2590-2591	B1-2	Bottom	YES	YES	YES	YES	
Sept. 24, 2015	74°08.31	108°50.18	CAA 8-AN2	471	2595-2596	B6-7	250	YES	YES	YES	YES	
Sept. 24, 2015	74°08.31	108°50.18	CAA 8-AN2	471	2598-2599	B9-10	200	YES	YES	YES	YES	
Sept. 24, 2015	74°08.31	108°50.18	CAA 8-AN2	471	2600-2601	B11-12	150	YES	YES	YES	YES	
Sept. 24, 2015	74°08.31	108°50.18	CAA 8-AN2	471	2605-2606	B16-17	75	YES	YES	YES	YES	33.1/Tmin
Sept. 24, 2015	74°08.31	108°50.18	CAA 8-AN2	471	2607-2608	B18-19	60	YES	YES	YES	YES	31.8/Tmax
Sept. 24, 2015	74°08.31	108°50.18	CAA 8-AN2	471	2612-2613	B23-24	10	YES	YES	YES	YES	
Sept. 25, 2015			BLANK 1					YES	YES	NO	YES	
Sept. 25, 2015			BLANK 2					YES	YES	YES	YES	

Sept. 26, 2015	76°19.60	096°43.74	CAA 9-AN1	480	2614-2615	B1-2	Bottom	YES	YES	NO	NOT YET	
Sept. 26, 2015	76°19.60	096°43.74	CAA 9-AN1	480	2619-2620	B6-7	250	YES	YES	NO	NOT YET	
Sept. 26, 2015	76°19.60	096°43.74	CAA 9-AN1	480	2622-2623	B9-10	200	YES	YES	NO	NOT YET	
Sept. 26, 2015	76°19.60	096°43.74	CAA 9-AN1	480	2624-2625	B11-12	150	YES	YES	NO	NOT YET	
Sept. 26, 2015	76°19.60	096°43.74	CAA 9-AN1	480	2628-2629	B15-16	120	YES	YES	NO	NOT YET	
Sept. 26, 2015	76°19.60	096°43.74	CAA 9-AN1	480	2631-2632	B18-19	90	YES	YES	NO	NOT YET	33.1/Tmin
Sept. 26, 2015	76°19.60	096°43.74	CAA 9-AN1	480	2634-2635	B21-22	45	YES	YES	NO	NOT YET	SCM
Sept. 27, 2015	76°19.971	096°46.044	CAA 9-AN2	483	2658-2659	B9-10	50	YES	YES	NO	NOT YET	Tmax
Sept. 27, 2015	76°19.971	096°46.044	CAA 9-AN2	483	2662-2663	B13-14	15	YES	YES	NO	NOT YET	max part.
Sept. 27, 2015	76°19.971	096°46.044	CAA 9-AN2	483	2666-2667	B17-18	10	YES	YES	NO	NOT YET	mixed layer
Sept. 27, 2015			CAA 9-BLANK					NO	NO	NO	NOT YET	

12.3 Preliminary results

Samples were filtered and acidified on-board, and will be further processed in the on-land Stable Isotope laboratory at the University of Saskatchewan (Saskatoon, Canada) and at the University of British Columbia (Vancouver, Canada). Therefore, no results can be presented yet.

References

- Stordal, M.C., and G.J. Wasserburg, *Earth and Planetary Science Letters*, 77, 259 (Jan, 1986).
- Lacan, F., and C. Jeandel, *Geophysical Research Letters* 31, L14306 (Jul, 2004).
- Lacan, F., and C. Jeandel, *Geochemistry, Geophysics, Geosystems* 6, Q12008 (Dec, 2005).
- Lacan, F., and C. Jeandel, *Earth and Planetary Science Letters* 232, 245 (Mar, 2005b).
- Radic, A., F. Lacan, and J. W. Murray, *Earth and Planetary Science Letters* 306, 1 (Apr, 2011).
- Slemons, L., B. Paul, J. Resing, and J.W. Murray, *Marine Chemistry* 142-144, 54 (Sep, 2012).
- Grenier, M., et al., *Journal of Geophysical Research* 118(2), 592 (Jan, 2013).
- Jeandel C., and E.H. Oelkers, *Chemical Geology* (in press).
- Porcelli, D., et al., *Geochimica et Cosmochimica Acta* 73, 2645 (Feb, 2009).
- Elderfield, H., *Philos. Trans. R. Soc. London* 325, 105 (May, 1988).
- Byrne, R.H., and E.R. Sholkovitz, *The Handbook on the Physics and Chemistry of the Rare Earths* (eds. K.A. Gschneidner, Jr. and L. Eyring), pp. 497–593 (1996).
- Marchal, O., R. François, and J. Scholten, *Deep-Sea Research I* 54, 557 (Apr, 2007).
- Luo, Y., R. Francois, and S.E. Allen, *Ocean Science* 6, 381 (Mar, 2010).
- Anderson, R.F., M.P. Bacon, and P.G. Brewer, *Earth and Planetary Science Letters* 62, 7 (Jan, 1983).
- Anderson, R.F., M.P. Bacon, and P.G. Brewer, *Earth and Planetary Science Letters* 66, 73 (Dec, 1983).
- Bacon, M.P., *Philos. Trans. R. Soc. London*, 325, 147 (May, 1988).
- François, R., et al., *Paleoceanography* 22, PA1216 (Mar, 2007).
- Luo et al., op. cit.
- Francois et al., Recent incursion of deep water from the central Arctic into Canada Basin, IPY Conference abstract (2012).
- Melling, H., et al., *Climatic Change* 115, 89 (Oct, 2012).
- Kartcher, M., J.N. Smith, F. Kauker, R. Gerdes, W.M. Smethie, *Journal of Geophysical Research-Oceans* 117, C08007 (Aug, 2012).
- Moran, S.B., et al., *Earth and Planetary Science Letters* 203, 999 (Nov, 2002).
- Shabani et al., *Analytical Chemistry* 64, 7 (Apr, 1992).

13 Large volume *in-situ* operations for particulate ^{230}Th , ^{231}Pa , Nd isotopes, Cr isotopes and Si isotopes (GEOTRACES) – Legs 2 and 3b

Project leaders: Roger François¹ (rfrancois@eos.ubc.ca) and Lisa Miller¹

Cruise participants Leg 2: Maureen Soon¹ and Cheng Kuang¹

Cruise participant Leg 3b: Maureen Soon¹

¹ *University of British Columbia, Department of Earth Ocean and Atmospheric Sciences, 2020-2207 Main Mall, Vancouver, BC, V6T 1Z4, Canada.*

13.1 Introduction

Analysis of particles is essential for the interpretation of ^{230}Th , ^{231}Pa , Nd isotopes, Cr isotopes and Si isotopes measured in the water column. Particulate ^{230}Th , ^{231}Pa provide information on the mean sinking rates of particles and the influence of particle composition on $^{231}\text{Pa} / ^{230}\text{Th}$ ratio, which is used in paleoceanography to determine past changes in circulation and/or particle flux. Particulate Nd isotopes document the exchange of Nd isotopes between seawater and the lithogenic or authigenic phases of particles. Si isotopes provide information on Si isotopic fractionation during the formation of biogenic silica.

13.2 Methodology

Because of the large seawater volumes that need to be filtered to collect enough particles to make these measurements, large volume *in-situ* pumps were used to filter hundreds of liter of water at fixed depths.

The deficit of Thorium-234 in surface water has been widely used as a tracer of particle flux from surface water. Th-234 flux estimated from this deficit is converted to carbon flux using the POC/Th-234 ratio measured on particles. To limit the number of samples to be analyzed, one sample integrated over the upper 100m (by mixing five 2L samples collected at constant interval within the upper 100m) were processed on-board. Total Th-234 was obtained by MnO_2 co-precipitation on 2L of the composite samples. Particles were obtained both by filtering 6 – 8 L of the composite samples, by taking a sub-sample from the large volume pump filter deployed just under the mixed layer. A Nylon mesh was also positioned on top of the latter to capture the large sinking particles. The samples were then mounted and sent as soon as possible for Beta-counting at the Institute of Ocean Science.

Table 13-1. Large volume pump samples for ²³⁰Th, ²³¹Pa, Nd isotopes, Cr isotopes and Si isotopes on Leg 2.

Geotraces 2015 LEG 2 Large Volume In-Situ Pumps															
STN	EVENT #	Target Depth	Niskin # (LVP #)	Samp #	Th234	Si isotopes	Comments	STN	EVENT #	Target Depth	Niskin # (LVP #)	Samp #	Th234	Si isotopes	Comments
L82	17	700	1	192	x			BB2	72	400	1	193	x		
L82	17	500	2	194	x			BB2	72	300	2	194	x		
L82	17	300	3	196	x			BB2	72	200	3	196	x		
L82	17	100	4	198	x	x		BB2	72	100	4	198	x	x	
L82	17	50	5	198	x		filter missing	BB2	72	50	5	197	x		
L82	17	10	6	197	x			BB2	72	10	6	197	x		
L82	24	2800	1	263	x			BB2	75	2300	1	195	x		
L82	24	2600	2	264	x			BB2	75	2100	2	196	x		
L82	24	2400	3	265	x			BB2	75	1900	3	197	x		
L82	24	2000	4	266	x	dead board		BB2	75	1800	4	198	x		
L82	24	1500	5	267	x			BB2	75	1000	5	199	x		
L82	24	1000	6	268	x			BB2	75	600	6	200	x		
L82	27	2600	1	291			no sample	BB2	84	2300	1	200			
L82	27	2400	2	292				BB2	84	1800	2	201			
L82	27	1000	3	293		x		BB2	84	500	3	202			
L82	27	300	4	294		x		BB2	84	200	4	203			
L82	27	30	5	295		x		BB2	84	30	5	204			
L82	27	10	6	296		x		BB2	84	10	6	205			
BB1	37	700	1	247	x			CAA1	93	10	1	206	x		
BB1	37	500	2	248	x			CAA1	93	30	2	207	x		
BB1	37	300	3	249	x			CAA1	93	100	3	208	x		
BB1	37	100	4	250	x	x		CAA1	93	200	4	209	x		
BB1	37	50	5	251	x			CAA1	93	400	5	210	x		
BB1	37	10	6	252	x			CAA1	93	600	6	211	x		
BB1	41	700	1	289				CAA1	97	10	1	206			
BB1	41	500	2	290		x		CAA1	97	30	2	207			
BB1	41	300	3	291		x		CAA1	97	100	3	208			
BB1	41	200	4	292		x		CAA1	97	200	4	209			
BB1	41	100	5	293		x		CAA1	97	400	5	210			
BB1	41	10	6	294		x		CAA1	97	600	6	211			
BB3	55	700	1	455	x			CAA2	110	600	1	204			
BB3	55	500	2	456	x			CAA2	110	400	2	205			
BB3	55	300	3	457	x			CAA2	110	200	3	206			
BB3	55	100	4	458	x	x		CAA2	110	100	4	207			
BB3	55	50	5	459	x			CAA2	110	30	5	208			
BB3	55	10	6	460	x			CAA2	110	10	6	209			
BB3	59	700	1	407		x		CAA3	120	10	1	217			
BB3	59	500	2	408		x		CAA3	120	30	2	218			
BB3	59	300	3	409		x		CAA3	120	100	3	219			
BB3	59	200	4	410		x		CAA3	120	200	4	220			
BB3	59	100	5	411		x		CAA3	120	400	5	221			
BB3	59	10	6	412		x		CAA3	120	600	6	222			
CAA5	132	10	1	1107				CAA5	132	10	1	1107			
CAA5	132	30	2	1108				CAA5	132	30	2	1108			
CAA5	132	100	3	1109				CAA5	132	100	3	1109			
CAA5	132	150	4	1110				CAA5	132	150	4	1110			
CAA5	132	180	5	1111				CAA5	132	180	5	1111			
CAA5	132	250	6	1112				CAA5	132	250	6	1112			
CAA5	137	10	1	1143				CAA5	137	10	1	1143			
CAA5	137	30	2	1150				CAA5	137	30	2	1150			
CAA5	137	100	3	1151				CAA5	137	100	3	1151			
CAA5	137	150	4	1152				CAA5	137	150	4	1152			
CAA5	137	190	5	1153				CAA5	137	190	5	1153			
CAA5	137	250	6	1154				CAA5	137	250	6	1154			
CAA4	144	10	1	1185				CAA4	144	10	1	1185			
CAA4	144	30	2	1184				CAA4	144	30	2	1184			
CAA4	144	60	3	1185				CAA4	144	60	3	1185			
CAA4	144	80	4	1186				CAA4	144	80	4	1186			
CAA4	144	120	5	1187				CAA4	144	120	5	1187			
CAA4	144	160	6	1188				CAA4	144	160	6	1188			
CAA4	147	10	1	1210				CAA4	147	10	1	1210			
CAA4	147	30	2	1211				CAA4	147	30	2	1211			
CAA4	147	60	3	1212				CAA4	147	60	3	1212			
CAA4	147	80	4	1213				CAA4	147	80	4	1213			
CAA4	147	120	5	1214				CAA4	147	120	5	1214			
CAA4	147	160	6	1215				CAA4	147	160	6	1215			
CAA6	155	10	1	1279				CAA6	155	10	1	1279			
CAA6	155	30	2	1280				CAA6	155	30	2	1280			
CAA6	155	100	3	1281				CAA6	155	100	3	1281			
CAA6	155	150	4	1282				CAA6	155	150	4	1282			
CAA6	155	190	5	1283				CAA6	155	190	5	1283			
CAA6	155	240	6	1284				CAA6	155	240	6	1284			
CAA6	158	10	1	1303				CAA6	158	10	1	1303			
CAA6	158	30	2	1310				CAA6	158	30	2	1310			
CAA6	158	100	3	1311				CAA6	158	100	3	1311			
CAA6	158	150	4	1312				CAA6	158	150	4	1312			
CAA6	158	190	5	1313				CAA6	158	190	5	1313			
CAA6	158	240	6	1314				CAA6	158	240	6	1314			
CAA7	169	10	1	1379				CAA7	169	10	1	1379			
CAA7	169	30	2	1380				CAA7	169	30	2	1380			
CAA7	169	60	3	1381				CAA7	169	60	3	1381			
CAA7	169	100	4	1382				CAA7	169	100	4	1382			
CAA7	169	150	5	1383				CAA7	169	150	5	1383			
CAA7	169	190	6	1384				CAA7	169	190	6	1384			
CAA7	169	10	1	1421				CAA7	169	10	1	1421			
CAA7	169	30	2	1422				CAA7	169	30	2	1422			
CAA7	169	60	3	1423				CAA7	169	60	3	1423			
CAA7	169	100	4	1424				CAA7	169	100	4	1424			
CAA7	169	150	5	1425				CAA7	169	150	5	1425			
CAA7	169	190	6	1426				CAA7	169	190	6	1426			

Table 13-2. Large volume pump samples for ²³⁰Th, ²³¹Pa, Nd isotopes, Cr isotopes and Si isotopes on Leg 3b.

Geotraces 2015 Leg 3b LVP													
STN	EVENT #	Target Depth	LVP #	Samp #	Nd-Pa-Th (Supor)	Si isotopes	STN	EVENT #	Target Depth	LVP #	Samp #	Nd-Pa-Th (Supor)	Si isotopes
CB1	403	10	1	2031	x		CB3	442	10	1	2350		x
CB1	403	75	2	2032	x		CB3	442	58	2	2351		x
CB1	403	150	3	2033	x		CB3	442	180	3	2352		x
CB1	403	250	4	2034	x		CB3	442	400	4	2353		x
CB1	403	400	5	2035	x		CB3	442	600	5	2354	x	
CB1	403	435	6	2036	x		CB3	442	1400	6	2355		x
CB1	408	10	1	2096		x	CB4	447	15	1	2356	x	
CB1	408	40	2	2097		x	CB4	447	71	2	2357	x	
CB1	408	75	3	2098		x	CB4	447	220	3	2358	x	
CB1	408	150	4	2099		x	CB4	447	350	4	2359	x	
CB1	408	250	5	2100		x	CB4	447	500	5	2360	x	
CB1	408	400	6	2101		x	CB4	447	800	6	2361	x	
CB2	417	10	1	2138	x		CB4	450	1000	1	2374	x	
CB2	417	140	2	2139	x		CB4	450	1250	2	2375	x	
CB2	417	400	3	2140	x		CB4	450	1500	3	2376	x	
CB2	417	700	4	2141	x		CB4	450	2000	4	2377	x	
CB2	417	1000	5	2142	x		CB4	450	2500	5	2378	x	
CB2	417	bottom	6	2143	x		CB4	450	3000	6	2379	x	
CB2	421	10	1	2204			CB4	456	15	1	2459		x
CB2	421	58	2	2205		x	CB4	456	71	2	2460		x
CB2	421	140	3	2206		x	CB4	456	220	3	2461		x
CB2	421	400	4	2207		x	CB4	456	350	4	2462		x
CB2	421	800	5	2208		x	CB4	456	500	5	2463		x
CB2	421	1200	6	2209		x	CB4	456	1000	6	2464		x
CB3	432	10	1	2260	x		CB4	463	1500		2492		
CB3	432	58	2	2261	x		CB4	463	2000		2493		
CB3	432	180	3	2262	x		CB4	463	2500		2494		
CB3	432	250	4	2263	x		CAA8	467	15	1	2542	x	
CB3	432	480	5	2264	x		CAA8	467	90	2	2543	x	
CB3	432	600	6	2265	x		CAA8	467	150	3	2544	x	
CB3	439	1000	1	2332	x		CAA8	467	250	4	2545	x	
CB3	439	1400	2	2333	x		CAA8	467	450	5	2546	x	
CB3	439	2000	3	2334	x		CAA8	467	bottom	6	2547	x	
CB3	439	2000	4	2335		x	CAA8	470	15	1	764		x
CB3	439	2500	5	2336		x	CAA8	470	45	2	765		x
CB3	439	2500	6	2337		x	CAA8	470	90	3	766		x
							CAA8	470	250	4	767		x
							CAA8	470	450	5	768		x
							CAA8	470	bottom	6	769		x

Table 13-3. Samples specifically taken for ²³⁴Th measurements during Leg 2.

Station	12L sample	LVP
K1	x	
LS2	x	x
BB1	x	x
BB2	x	x
BB3	x	x
CAA1	x	x
CAA2	x	x
CAA3	x	x
CAA4	x	x
CAA5	x	x
CAA6	x	x
CAA7	x	x

14 Anthropogenic uranium, iodine, and cesium analysis in the Arctic Ocean (GEOTRACES) – Legs 2 and 3b

Project leader: Jack Cornett¹ (jack.cornett@uottawa.ca)

Cruise participant Leg 3b: Daniel Sauvé¹

¹ *University of Ottawa, Department of Earth Sciences, 120 University, Ottawa, ON, K1N 6N5, Canada.*

14.1 Introduction

There are two basic tracer applications of radionuclides ¹²⁹I and ¹³⁷Cs in the Arctic Ocean:

- Measurements of ¹²⁹I and ¹³⁷Cs, separately provide evidence for Atlantic-origin water labeled by discharges from European reprocessing plants;
- Measurements of ¹²⁹I and ¹³⁷Cs, together can be used to identify a given year of transport through the Norwegian Coastal Current (NCC) thereby permitting the determination of a transit time from the NCC to the sampling location (Smith et al. 1998).

Recently the use of ²³⁶U released from nuclear reprocessing plants in France and the UK has been proposed as a potential label for Atlantic Sea Water entering the Arctic. (Christl et al. 2012)

14.2 Methodology

14.2.1 ¹³⁷Cs samples (Leg 3b)

¹³⁷Cs sea water samples were collected from multiples depths at Stations CB 1 through 4 and placed in 20L cubitainers for further workup. Samples were acidified using 25ml of concentrated nitric acid to reduce the pH to 1 to 2 and around 4g of ammonium molybdophosphate (AMP) was added as Cesium sorbent. The supernatant was then removed and stored for later use and the AMP was collected and stored for later analysis at the University of Ottawa via gamma spectrometer.

14.2.2 ¹²⁹I samples (Legs 2 and 3b)

¹²⁹I samples were collected in 1L and 500mL Nalgene bottles based on availability and stored for transport back to the University of Ottawa where the Iodine will be extracted and analyzed on the new Accelerator Mass Spectrometer (AMS) for ¹²⁹I concentration.

14.2.3 ^{236}U samples (Leg 3b)

20L samples were collected from the same stations and depths as for ^{137}Cs and stored in 20L cubitainers. The water was then acidified using 25mL of concentrated nitric acid, after which 100 Furthermore the left over supernatant from the ^{137}Cs samples was used to extract U. As the water was already acidic from the ^{137}Cs samples, no acid was added, 1000fg of ^{233}U spike was added to the samples as a yield tracer. 10ml of 45mg/ml ferric chloride was then added to act as a sorbent for uranium. The samples were then bubbled with nitrogen gas for approximately 25 minutes to remove carbonate from the sample as ferric chloride preferentially sorbs carbonates before uranium. After bubbling 30ml of Ammonium Hydroxide was added to raise the pH of the sample to 9 to precipitate the ferric chloride and sorb the uranium to it. Samples were left to settle overnight and afterwards the supernatant was discarded and the precipitate was collected for later analysis via AMS at the University of Ottawa.

14.3 Preliminary results

On this cruise, a slightly different methodology was used in terms of using 20L cubitainers for sample storage and chemistry work. On previous cruises, plastic bag lined buckets were used for storage and chemistry work. It seemed that the method of using cubitainers for this work was much more efficient than the previously used bucket method and will continue to be used for future work as it seems much more of the precipitate can be collected much more conveniently than the previous methodology.

References

- Smith, J.N., Ellis, K.M. and Kilius, L.R. 1998. ^{129}I and ^{137}Cs tracer measurements in the Arctic Ocean. *Deep-Sea Research I*. 45(6):959-984.
- Christl, M., Lachner, J., Vockenhuber, C., Lechtenfeld, O., Stimac, I., van der Loeff, M. R., & Synal, H.-A. (2012). A depth profile of uranium-236 in the Atlantic Ocean. *Geochimica et Cosmochimica Acta*, 77, 98–107. doi:10.1016/j.gca.2011.11.009

15 Natural distribution of stable N and O isotopes in nitrate (GEOTRACES) – Leg 2

Project leader: Markus Kienast¹ (markus.kienast@dal.ca)

Cruise participant Leg 2: Nadine Lehmann¹

¹ *Dalhousie University, Department of Oceanography, 1355 Oxford Street, Life Sciences Centre, Halifax, NS, B3H 4R2, Canada.*

15.1 Introduction

The nitrogen cycle has a central role in marine biogeochemistry. Nitrogen is not only a limiting factor for biological productivity, but also has a strong influence on the cycling of other elements, such as carbon and phosphorus. One way to study nitrogen transformation is by determining the nitrogen and oxygen isotopic composition of nitrate. $\delta^{15}\text{N}$ of nitrate is mainly controlled by N_2 fixation and denitrification. The internal cycling of nitrogen (i.e. ammonification, nitrification, and NO_3^- assimilation), on the other hand, only shows little effect on nitrate $\delta^{15}\text{N}$. Those internal processes, however, strongly affect the ratio of $^{18}\text{O}/^{16}\text{O}$ in nitrate. The $\delta^{15}\text{N}$ and $\delta^{18}\text{O}$ signatures of dissolved nitrate do not only give you insights into biogeochemical cycling, but further allow you to track water masses. Water masses carry a distinct isotopic signature depending on their provenance, their circulation pattern and the transformations of oceanic fixed N occurring along their pathway. Next to salinity and temperature measurements, this isotopic signature provides a tool that allows the identification of a distinct body of water. Therefore, coupled N/O isotope measurements, on the one hand, give you information about the marine nitrogen cycle and help you distinguishing between N-cycling processes that might overlap each other and, on the other hand, can be used to elucidate the origin and history of water masses.

The Arctic Ocean plays an important role in the global oceanic nitrogen cycle. Water with a low N:P ratio enters this ocean basin from the Pacific, transits through the Bering Strait and the Beaufort Sea and eventually flows into the North Atlantic Ocean. How those waters are modified in terms of their N and O isotopic signature as they pass the Arctic throughflow has yet to be explored. The goal of was to analyze and interpret depth profiles of nitrate $\delta^{15}\text{N}$ and $\delta^{18}\text{O}$ along the transect. Those $^{15}\text{N}/^{14}\text{N}$ and $^{18}\text{O}/^{16}\text{O}$ measurements will help identifying the main water masses along the transect. They will also be used to characterize the geochemical modifications and the cycling of nitrogen within those waters as they move through the Canadian Archipelago into the Labrador Sea.

15.2 Methodology

Seawater samples for analyses of stable nitrogen and oxygen isotopes in nitrate, nitrite and nitrous oxide were obtained as outlined in Table 15-1. Samples for nitrate and nitrite analyses from below 200m depth were collected unfiltered in 60mL square Nalgene bottles. Samples from the upper 200m were filtered through a 25mm diameter 0.45µm filter and collected in 60mL Nalgene bottles. Aliquots for $\delta^{15}\text{N}/\delta^{18}\text{O}$ in nitrate were stored immediately at -20 oC. Samples for $\delta^{15}\text{N}/\delta^{18}\text{O}$ -nitrite were analyzed in terms of NO_2^- concentration using Griess reagents and measurements of absorbance at 540 nm. Nitrite concentrations at all stations were below the limit for further analyses. Stable isotope analyses will be conducted at the Granger lab in Connecticut.

Table 15-1. List of water samples taken for stable nitrogen isotopes during Leg 2 of the Canadian GEOTRACES expedition.

Station	Event	$^{15}\text{N}/^{18}\text{O}$ of NO_3^-	$^{15}\text{N}/^{18}\text{O}$ of NO_2^-	$^{15}\text{N}/^{18}\text{O}$ of N_2O
K1	1	x		
	3	x		
	6	x	x	x
LS2	14	x		
	21	x	x	
	28	x		
BB1		x	x	x
BB3	53	x	x	x
BB2	71	x	x	x
CAA1	94	x	x	x
CAA2	109	x	x	x
CAA3	124	x	x	x
CAA4		x	x	x
CAA5	131	x	x	x
CAA6		x	x	x
CAA7		x	x	x
AN312	179	x		
AN314		x		

16 Measurement of pH, alkalinity, $\delta^{13}\text{C}$ -DIC, $\delta^{18}\text{O}$ -water (GEOTRACES) – Legs 2, 3a and 3b

Project leader: Alfonso Mucci¹ (alfonso.mucci@mcgill.ca)

Cruise participant Legs 2, 3a and 3b: Constance Guignard¹

¹ *McGill University, Department of Earth & Planetary Sciences, 3450 University Street, Montreal, QC, H3A 0E8, Canada.*

16.1 Introduction

Since the beginning of the industrial period in the late 18th century, humans have emitted large quantities of CO_2 into the atmosphere, mainly as a result of fossil-fuel burning, but also because of changes in land-practices (e.g. deforestation). Whereas atmospheric concentrations oscillated between 180 and 280 ppm over much of the past 400,000 years, current atmospheric concentrations have now reached 403 ppm, diverging wildly from the very reproducible, eleven last glacial-interglacial cycles. Hence, it is hard to argue that anthropogenic activities are unrelated to this increase in atmospheric CO_2 concentration and the associated rise in global temperatures. The impact of climate change is disproportionately large in the high latitudes. Rapid warming in the northern polar region has resulted in significant glacial and sea-ice melt, affecting the fresh water budget and circulation of the Arctic Ocean and feeding back on Earth's radiation balance. Likewise, the uptake of anthropogenic CO_2 is accelerated in high latitude waters because the solubility of CO_2 in water increases with decreasing water temperature and salinity. Consequently, high latitude waters are more susceptible to ocean acidification.

A study of large-scale processes that modulate the spatial and temporal variability of the pH in surface waters, the pCO_2 gradient at the air-sea interface, and exchange of CO_2 with sub-thermocline waters and across oceanic basins. In addition to measurements of carbonate parameters (pH, TA), the stable carbon isotope composition, $\delta^{13}\text{C}$ (DIC), of dissolved inorganic carbon (DIC) will be determined to differentiate between inorganic (atmospheric CO_2 uptake, alkalinity exclusion, ikaite precipitation/ dissolution) and metabolic processes (photosynthesis, microbial degradation of allochthonous and autochthonous organic matter) in the ice and water column to CO_2 exchange. These results will be combined with historical data acquired since 2003 (i.e. CASES, IPY-CFL, IPY- Geotraces, Malina) to construct time-series of the saturation state of the waters with respect to aragonite in order to evaluate the impact of increasing atmospheric CO_2 concentrations, physical and biological processes on Arctic water acidification. In order to elucidate the role physical mixing of various source waters, the stable oxygen isotope composition, $\delta^{18}\text{O}$ (H_2O), of water will be combined to other conservative (e.g. S_P , T, TA) and non-conservative tracers (e.g. O_2 , Ba, nutrients) to quantify the relative contribution of freshwater inputs (river, sea-ice melt, snow and glacier melt) and oceanic water masses (Pacific, Atlantic) to the vertical structure of the water column and the transfer of heat, salt and carbon between the North Pacific and North

Atlantic through the Canadian Arctic Archipelago. Results of this water mass analysis will also serve as a template for the interpretation of the distribution of trace elements and their isotopes that are measured by other researchers involved in the GEOTRACES program.

16.2 Methodology

pH samples (Table 16-1 to Table 16-3) were collected from the Rosette using a rubber tube and stored in LDPE 125 ml bottles. While sampling the Niskin bottle, with a low water flow, the air was carefully removed from the sampling tube, which was held at the bottom of the bottle. The water was then allowed to overflow at about the same volume as the bottle before the tube was slowly removed from it, in order to leave enough water at the neck of the bottle to avoid having air inside while putting the cap on or having as little air as possible. The bottle was then closed air tight. The samples were, right after the sampling, equilibrated at 25°C, in a Digital One Rte 7 temperature controlled water bath, and analyzed immediately by colorimetry, using a UV-VIS spectrophotometer, model HP 8453 from Agilent Technology, using two pH indicators: phenol red and cresol purple. The sample was poured in a 50 mm quartz cell and used to measure the blank. Absorbance measurements were taken after adding the pH indicator to the sample. The method is described in Baldo, Morris and Byrne (1985) and in Clayton and Byrne (1993). TRIS buffers, prepared in the laboratory with the method described in Millero & al (1993), of salinities 35 and 25 were used to calibrate the spectrophotometer.

Alkalinity analyses were performed by titration, using an automatic titrator, model TTT865 titration manager, titralab, from Radiometer Analytical. The samples were collected from the Niskin bottles, using a rubber tube, and, stored in 250 ml glass bottles. They were poisoned, right after they were collected, with 250 microliters of a mercuric chloride saturated solution as a preservative. Apiezon grease was put on the glass stoppers before closing the bottles and they were then clipped to keep them air tight. The samples were equilibrated at 25°C in a Digital One Rte 7, controlled temperature water bath, and then, titrated with a 0.03N hydrochloric acid solution. The titrant was standardized using Dickson water, which is a reference material for oceanic CO₂ measurements, and also a reference for alkalinity measurements. The reference material was purchased from Scripps Institution of Oceanography, in La Jolla, California, USA. Samples, even though poisoned, were analyzed no more than two days after they were collected.

Samples for ¹⁸O and ¹³C were also collected. The ¹³C samples were collected in 30ml amber glass bottles and poisoned with mercuric chloride for preservation. The ¹⁸O samples were collected in 13 ml plastic test tubes with no special treatment. Those samples will be analyzed at Geotop, UQAM further in time.

Intercalibration samples for pH, alkalinity, C¹³ and O¹⁸ were collected at Station K2 (Leg 2). pH, alkalinity and C¹³ samples were poisoned with Mercuric chloride; O¹⁸ didn't undergo any

treatment. pH and alkalinity samples were stored in the refrigerated container until the return of the ship to Quebec City.

Table 16-1. Sampling depths during Leg 2.

Station	Latitude (N)	Longitude (W)	Depths sampled (m)
K1	60°27.218	056°32.884	1600, 1500, 1400, 1200, 1000, 800, 700, 600, 500, 400, 300, 200, 150, 100, 50, 30, 10
LS2	60°26.480	056°32.071	1500, 1400, 1200, 1000, 800, 700, 600, 500, 400, 300, 200, 150, 100, 50, 30, 10
BB1	66°51.502	059°04.450	1000, 800, 700, 600, 480, 300, 200, 150, 100, 50, 30, 10
BB2	72°45.396	066°59.470	2250, 2100, 1900, 1600, 1500, 1400, 1200, 1000, 800, 600, 500, 400, 300, 220, 100, 75, 71, 50, 25, 10, Surf
BB3	71°24.661	068°34.810	1000, 800, 700, 600, 500, 400, 300, 200, 150, 100, 50, 30, 10
CAA1	74°31.267	080°34.526	600, 400, 300, 200, 150, 120, 100, 80, 60, 40, 30, 10
CAA2	74°18.812	080°30.294	600, 400, 300, 200, 150, 120, 100, 80, 60, 40, 30, 10
CAA3	73°49.032	080°29.261	600, 400, 300, 200, 150, 120, 100, 80, 60, 40, 30, 10
CAA4	74°07.274	091°30.437	150, 140, 120, 100, 80, 60, 40, 30, 10
CAA5	74°32.245	090°48.094	250, 220, 190, 160, 140, 120, 100, 80, 60, 40, 30, 10
CAA6	74°45.536	097°27.078	250, 190, 140, 100, 80, 60, 40, 30, 10
CAA7	73°40.363	096°31.318	200, 140, 100, 80, 60, 40, 20, 10
AN312	69°09.896	100°41.771	Bot, 40, 30, 20, 10, 5
AN314	68°58.079	105°27.263	Bot, 60, 50, 40, 30, 20, 10, 5

Table 16-2. Sampling depths during Leg 3a.

Station	Latitude (N)	Longitude (W)	Depths sampled (m)
405	70°36.470	123°02.160	Bot, 400, 300, 200, 100, 70, 50, 40, 20, 10, Surf
407	71°00.662	126°04.918	Bot, 300, 200, 100, 70, 50, 40, 30, 20, 10, Surf
437	71°47.893	126°30.270	Bot, 200, 100, 70, 50, 30, 20, 10, Surf
408	71°18.491	127°35.917	Bot, 100, 70, 50, 30, 20, 10, Surf
420	71°03.094	128°30.680	Bot, 20, 10, Surf
434	70°10.619	133°33.259	Bot, 30, 20, 10, Surf
435	71°04.745	133°38.140	Bot, 100, 70, 50, 30, 20, 10, Surf
421	71°25.679	134°00.461	Bot, 1000, 850, 700, 600, 500, 400, 300, 200, 100, 70, 50, 30, 20, 10, Surf
535	73°24.746	128°10.567	Bot, 200, 140, 100, 70, 50, 40, 30, 20, 10, Surf
536	73°25.013	129°21.844	Bot, 500, 300, 200, 100, 70, 50, 30, 20, 10, Surf
518	74°34.320	121°26.237	Bot, 200, 100, 70, 50, 30, 20, 10, Surf
514	75°06.192	120°37.767	Bot, 300, 200, 100, 70, 50, 30, 20, 10, Surf

Table 16-3. Sampling depths during Leg 3b.

Station	Latitude (N)	Longitude (W)	Depths sampled (m)
CB1	75°06.412	120°31.113	Bot, 300, 200, 100, 75, 60, 50, 45, 25, 10, Surf
CB2	75°48.261	129°13.941	Bot, 1000, 800, 600, 400, 300, 200, 140, 100, 75, 65, 58, 40, 25, Surf
CB3	76°59.930	140°02.892	3500, 3000, 2500, 2000, 1500, 1200, 1000, 800, 600, 480, 300, 180, 100, 75, 58, 40, 25, Surf
CB4	75°00.013	149°59.838	3500, 3000, 2500, 2000, 1500, 1200, 1000, 800, 600, 500, 400, 300, 220, 100, 75, 71, 50, 25, 10, Surf
314	68°58.174	105°28.910	Bot, 60, 10, Surf

Station	Latitude (N)	Longitude (W)	Depths sampled (m)
QMG4	68°28.969	103°25.490	Bot, 60, 50, 40, 30, 20, 10, Surf
QMG	69°14.757	101°43.023	Bot, 70, 50, 30, 20, 10, Surf
QMG1	68°29.753	099°53.441	Bot, 20, 10, Surf
312	69°10.322	100°41.489	Bot, 40, 10, Surf
310	71°27.345	101°16.910	Bot, 100, 70, 50, 30, 20, 10, Surf
CAA8/308	74°08.375	108°50.358	Bot, 450, 300, 200, 100, 75, 65, 50, 40, 25, 14, 10
307	74°06.762	103°07.614	Bot, 200, 100, 70, 50, 30, 20, 10, Surf
342	74°47.653	092°46.882	Bot, 100, 70, 50, 30, 20, 10, Surf
CAA9	76°19.943	096°45.641	Bot, 200, 90, 70, 50, 40, 30, 17, 10, Surf

16.3 Comments and recommendations

16.3.1 Leg 2

As the sampling was intense due to the loss of two weeks of work, alkalinity titrations had to be conducted until the last minute before the next sampling in order to avoid building a back log in the analyses. We had to interrupt the analysis and go to the Rosette area several times to see what was going on, or, phone the people in the Rosette control room.

Therefore, we recommend the installation of a tv screen in the aft labs so the people can know when the Rosette is getting out of the water so we can avoid losing time by going up stairs several times while the Rosette is still in the water and avoid disturbing those who work in the Rosette control room by calling them.

16.3.2 Leg 3b

Since the beginning of Leg 2, a new identification system for sample, proper to this mission, has been implemented, with the adding of event numbers and a number assigned to each sample. However, this system became a source of extra work, without, at the end, proving of being of any benefit to us, and, at the same time, making the access to the needed information more difficult. Its rigidity made any correction to the pre-cast Rosette sheets quite confusing, since the sample numbers, and, sometimes event numbers, were automatically changed every time a correction was made, and the participants who had already prepared their sampling bottles had to redo it.

A file containing the correspondence between the event numbers and the actual cast numbers was supposed to be made, but, at the end, was not.

The geochem Rosette sheets final redaction, which is usually the rosette operator's task, was undertaken by someone else for the purpose of including them in a big file along with a lot of other data. However, because of the overload of work, the file stopped being updated after Station LS2 during Leg 2. Therefore, it might have been best to leave the redaction of the Rosette sheets to the Rosette operator; this would allow the participants to have access to completed Rosette sheets right away.

17 Ocean carbonate chemistry and boundary dissolved inorganic carbon, alkalinity, radium isotopes, and dissolved barium (GEOTRACES) – Legs 2 and 3b

Project leader: Helmuth Thomas¹ (helmuth.thomas@dal.ca)

Cruise participants Leg 2: Jacoba Mol¹ and Helmuth Thomas¹

Cruise participant Leg 3b: Jacoba Mol¹

¹ *Dalhousie University, Department of Oceanography, 1355 Oxford Street, Halifax, NS, B3H 4R2, Canada.*

17.1 Introduction

17.1.1 DIC and A_T

One of the primary objectives was to characterize the marine carbonate system at the stations sampled during the GEOTRACES expedition. Dissolved inorganic carbon (DIC) and Alkalinity (A_T) have been chosen, since for these two parameters certified reference materials are available, which are used internationally to warrant world class quality and comparability in time and space of the data. From these parameters, all relevant species of the carbonate system can be computed, anchored to the reference material. The data will be used to investigate carbonate system and pH conditions in dependence of water masses encountered at the various stations. In particular, attention was devoted to the spreading of the water mass, originating from the Pacific Ocean, which is channelled through the Canadian Arctic Archipelago via different routes. Furthermore, the data complement data from earlier expeditions into the region, e.g. CFL and ArcticNet, carried out by Dr Mucci's and Dr Miller's groups, which will facilitate investigations of the spatio-temporal variability of the carbonate system and ocean acidification (see for example Shadwick et al. 2013, 2011a, b).

One further objective of the work was to supply incubation experiments, carried out by Dr Tortell's and Dr Levasseur's groups (C. Hoppe, R. Husserr, M. Lizotte) with experimental conditions of the carbonate system, to verify baseline and incubation manipulations of the carbonate system and pH.

17.1.2 Radium isotopes

Radium isotopes can be used as a tracer for exchanges of matter across the sediment-water (i.e. vertical) and the land-ocean (horizontal) boundaries (e.g. Burt et al. 2013, 2014). At selected stations within the Canadian Arctic Archipelago, Ra activities were determined in the deep water column, with a spacing of 5-10m between the samples, as well as at mid-depths and in the surface waters. Lateral gradients in the surface waters, as well as vertical gradients above the seafloor and throughout the water column, if observed, will allow

establishing lateral and vertical diffusion coefficients, which in turn will be used to obtain diffusive transports of, for example, carbonate system species, nutrients or oxygen. It further will be explored, by sampling of the mid-depths water column, whether the distribution of the long-lived isotope ^{228}Ra can be used to shed light on the different spreading routes of the different water masses throughout the Canadian Arctic Archipelago.

17.1.3 Dissolved barium

Ba is mainly released from the North American continent and can therefore be used as a tracer for terrestrial freshwater input as well as a tracer for export production (e.g. Thomas et al. 2011). Together with A_T and ^{18}O , tracers for different freshwater sources (rivers, precipitation, ice melt), all freshwater sources to the Arctic can be quantified.

17.2 Methodology

17.2.1 DIC and A_T

Rosette sampling for DIC, A_T and Ba was conducted in vertical profiles at all stations as shown in Table 17-1 Table 17-2. DIC and A_T were analyzed onboard using a dual VINDTA 3C system. In case of a longer delay (>12hours) between sampling and analysis, samples were poisoned with 250 μl saturated HgCl_2 solution. DIC was determined by coulometric titration and A_T by potentiometric titration from the same sample simultaneously. Details are provided for example by Shadwick et al. (2011a).

17.2.2 Radium isotopes

Ra isotopes were collected onto MnO_2 -coated acrylic fibers from surface waters (5 m) at 14 and 1 stations during Legs 2 and 3b, respectively, as shown in Table 17-1 Table 17-2. Water column samples were taken from the Rosette at 10 stations, with near-bottom vertical profiles and mid-depths samples, four depths in total, and one surface water sample. For surface samples, the sample volume of individual samples was between 200L and 210L, for Rosette samples between 100L and 130L. ^{224}Ra and ^{223}Ra activities were obtained using the Radium Delayed Continuous Counting system (RaDeCC) system. All samples were initially counted within 2 days of sample collection to avoid significant ^{224}Ra and ^{223}Ra decay. Samples need to be recounted between 7-13 days after collection to determine activities of supported ^{228}Th and ^{227}Ac , which is then subtracted to obtain excess ^{224}Ra and ^{223}Ra activities. Following ^{224}Ra and ^{223}Ra analysis, fibers have to age for > 36 months before recounting on the RaDeCC. After this aging time, a significant amount of the original ^{228}Ra will have decayed to ^{228}Th , and the ^{228}Ra - ^{228}Th and ^{228}Th - ^{220}Rn isotope pairs will have reached secular equilibrium. Therefore, recounting fibers on the RaDeCC yields the extent of ^{228}Th in growth, which, using the various decay constants, can be used to back

calculate for the activity of ^{228}Ra at the time of sampling. More detailed methods for Ra isotope collection and analysis of ^{224}Ra and ^{223}Ra are described by Burt et al. (2013, 2014), or originally Moore (1987) and Moore and Arnold (1996).

17.2.3 Dissolved barium

Samples for dissolved Ba were taken from the Rosette parallel to samples for DIC and A_T . 30 ml nalgene bottles were rinsed three times, then filled and spiked with 15 μl concentrated HCl. Sample bottles were sealed with parafilm and taken for later analysis using isotope dilution mass spectrometry (see for details Thomas et al. 2011).

Table 17-1. Station locations and sample dates for dissolved inorganic carbon (DIC), alkalinity (A_T), barium, and radium isotope samples during Leg 2. DIC, A_T and Ba were sampled at every station. Radium samples were taken at the bolded stations only.

Station	Latitude (N)	Longitude (W)	Date
K1	56°07.444	053°22.371	14 July 2015
LS2	60°26.483	056°32.075	17 July 2015
BB1	66°51.498	059°04.451	3 August 2015
BB3	71°24.658	068°34.789	5 August 2015
BB2	72°45.401	066°59.461	7 August 2015
CAA1	74°31.262	080°34.545	10 August 2015
CAA2	74°18.811	080°30.295	10 August 2015
323	74°09.364	080°28.171	11 August 2015
324	73°58.746	080°27.562	11 August 2015
CAA3	73°49.027	080°29.255	12 August 2015
CAA5	74°32.245	090°48.088	12 August 2015
CAA4	74°7.278	091°30.347	14 August 2015
CAA6	74°45.530	097°27.067	15 August 2015
CAA7	73°40.361	096°31.315	16 August 2015
312	69°09.899	100°41.782	17 August 2015
314	68°58.105	105°27.712	18 August 2015

Table 17-2. Station locations and sample dates for dissolved inorganic carbon (DIC), alkalinity (A_T), barium, and radium isotope samples during Leg 3b. DIC, A_T and Ba were sampled at every station. Radium samples were taken at the bolded stations only.

Station	Latitude (N)	Longitude (W)	Date
405	70°36.470	123°02.134	23 August 2015
407	71°00.671	126°04.916	24 August 2015
437	71°47.896	126°30.293	24 August 2015
412	71°33.720	126°55.393	25 August 2015
408	71°18.490	127°35.929	25 August 2015
418	71°09.811	128°10.288	25 August 2015
420	71°03.157	128°30.746	25 August 2015
434	70°10.620	133°33.269	26 August 2015
432	70°23.666	133°36.130	26 August 2015
435	71°04.751	133°38.143	27 August 2015

Station	Latitude (N)	Longitude (W)	Date
428	70°47.494	133°41.242	29 August 2015
421	71°25.675	134°00.464	30 August 2015
535	73°24.742	128°10.566	31 August 2015
518	74°34.316	121°26.221	2 September 2015
514	75°06.192	120°37.766	2 September 2015
CB1	75°06.404	120°31.172	7 September 2015
CB2	75°48.250	129°13.943	9 September 2015
CB3	76°59.386	140°02.905	13 September 2015
CB4	75°00.020	149°59.708	15 September 2015
314	68°58.169	105°28.910	20 September 2015
QMG4	68°28.972	103°25.490	21 September 2015
QMG3	68°19.764	102°36.372	21 September 2015
QMG	68°14.759	101°43.018	21 September 2015
QMG2	68°18.787	100°47.986	21 September 2015
QMG1	68°29.614	099°53.434	22 September 2015
312	69°10.326	100°41.492	22 September 2015
310	71°27.347	101°16.985	23 September 2015
CAA8/308	74°08.377	108°50.350	24 September 2015
342	74°47.652	092°46.884	26 September 2015
CAA9	76°19.943	096°45.649	27 September 2015

References

- Burt, W., Thomas, H., Pätsch, J., Omar, A. M., Schrum, C., Daewel, U., Brenner, H., and deBaar, H.J.W. (2014). Radium isotopes as a tracer of sediment-water column exchange in the North Sea, *Glob. Biogeochem. Cycles*, 28, DOI:10.1002/2014GB004825.
- Burt, W. J., H. Thomas and J.-P. Auclair (2013). Short-lived radium isotopes on the Scotian Shelf: Unique distribution and tracers of cross-shelf CO₂ and nutrient transport. *Mar. Chem.*, 156, 120-129, <http://dx.doi.org/10.1016/j.marchem.2013.05.007>.
- Moore, W. S. (1987). Radium 228 in the south atlantic bight, *Journal of Geophysical Research: Oceans* (1978–2012), 92, 5177–5190.
- Moore, W. S., and R. Arnold (1996). Measurement of 223ra and 224ra in coastal waters using a delayed coincidence counter, *Journal of Geophysical Research: Oceans*, 101, 1321–1329.
- Shadwick, E. H., T. W. Trull, H. Thomas and J. Gibson (2013). Vulnerability of High Latitude Oceans to Anthropogenic Acidification: Comparison of Arctic and Antarctic Seasonal Cycles, *Nature Scientific reports*, 3, 2339, doi:10.1038/srep02339.
- Shadwick, E.H., Thomas, H., Chierici, M., Else, B., Fransson, A., Michel, C., Miller, L.A., Mucci, A., Niemi, A., Papakyriakou, T.N. and Tremblay, J.-É. (2011a). Seasonal Variability of the Inorganic Carbon System in the Amundsen Gulf Region of the Southeastern Beaufort Sea, *Limnology and Oceanography*, 56(1), 303-322, doi:10.4319/lo.2011.56.1.0303.

Shadwick, E. H., Thomas, H., Gratton, Y., Leong, D. and Moore, S., Papakyriakou, T.N., and Prowe, F. (2011b). Export of Pacific carbon through the Arctic Archipelago to the North Atlantic, *Cont. Shelf Res.*, 31, 806–816, doi:10.1016/j.csr.2011.01.014.

Thomas, H., Shadwick, E.H., Dehairs, F., Lansard, B., Mucci, A., Navez, J., Gratton, Y., Prowe, A.E.F., Chierici, M., Fransson, A., Papakyriakou, T.N., Sternberg, E., Miller, L., Tremblay, J.-É., and Monnin, C. (2011). Barium and Carbon fluxes in the Canadian Arctic Archipelago, *J. Geophys. Res.*, 116, C00G08, doi:10.1029/2011JC007120.

18 Organic chemistry of the Beaufort Sea and Arctic Archipelago (GEOTRACES) – Legs 2 and 3b

Project leaders: Andrew Ross¹ (andrew.ross@dfo-mpo.gc.ca), Diane Varela² (dvarela@uvic.ca), Maite Maldonado³ (mmaldonado@eos.ub.ca), Celine Gueguen⁴ (queguen@trentu.ca) and Dennis Hansell⁵ (dhansell@rsmas.miami.edu)

Cruise participants Leg 2: Karina Giesbrecht² and Jeff Gao⁴

Cruise participant Leg 3b: Richard L. Nixon²

¹ *Department of Fisheries and Oceans, Institute of Ocean Science, 9860 West Saanich Road, Sidney, BC, V8L 5T5, Canada.*

² *University of Victoria, School of Earth and Ocean Sciences, 3800 Finnerty Road, Bob Wright Centre A405, Victoria, BC, V8P 5C2, Canada.*

³ *University of British Columbia, Department of Earth Ocean and Atmospheric Sciences, 2020-2207 Main Mall, Vancouver, BC, V6T 1Z4, Canada.*

⁴ *Trent University, Department of Chemistry, 1600 West Bank Drive, Peterborough, ON, K9J 7B8, Canada.*

⁵ *Miami University, Department of Ocean Sciences, 4600 Rickenbacker Causeway, Miami, FL, United States.*

18.1 Introduction

18.1.1 CDOM, Humic substances and Thiol

One of the major complications in the understanding of the trace elements and isotopes (TEI) distributions is the binding with dissolved organic matter (DOM). Marine DOM contains a continuum of ligands with varying affinities for metal ions including Fe(III), Cu(II), Zn(II), Hg(II) and Al(III). Trace element distributions cannot be interpreted fully if the sources and distribution of the main ligands are not better understood. In previous studies, the similarity of vertical profiles of bioactive and potentially toxic trace metals and humic-like fluorescence suggested that the humic-like fluorophore is a major factor in controlling iron solubility and the dissolved iron concentration in deep waters (Nakabayashi 2001, 2002, Tani et al. 2003, Nakayama et al. 2009). Humic-like and fulvic-like can also function as metal complexing ligands forming stable complexes (e.g. Kogut and Voelker 2001). Similarly, the presence of glutathione-like substances in ocean waters (Le Gall and van den Berg 1998) and the high stability constants with copper (Leal and van den Berg 1998) and mercury (Han et al. 2008) suggest that thiol complexes can be important in metal solubility. To date, little is known about the source, dynamic and composition of the organic ligands in marine waters. The sampling focused on the concentrations and composition of organic ligands that are critical for interpreting the distributions of TEIs in the water column. The team proposed to employ organic tracers of rivers, *in situ* production and early diagenetic processes to the polar mixed layer, the halocline and deep waters; measurements would include colored dissolved

organic matter (CDOM), humic substances (fluorescence and electrochemistry) and thiol analysis (electrochemistry). These tracers would allow us to identify sources and processes that control the distributions of important ligands of key TEIs. The combined approach that encompasses marine DOM characterization and associated trace metal speciation (core measurements in the GEOTRACES program) will provide data needed to parameterize and conceptualize relations between the DOM cycle and the solubility of TEIs in seawater.

18.1.2 Marine biogenic silica dynamics

Diatoms, microscopic algae with siliceous cell walls, account for up to 40% of the annual marine biological carbon fixation and for a significant portion of the export of carbon from the surface to the deep ocean (Nelson et al. 1995), both important processes regulating atmospheric CO₂ concentrations. Diatoms are the largest consumers of dissolved Si (Si(OH)₄) in the oceans, generating, through the photosynthetic process, a strong coupling between the marine cycles of silicon, carbon, nitrogen and phosphorus (Si, C, N and P). However, relative to the C, N and P cycles, current knowledge of the processes affecting marine Si dynamics is limited. In order to better understand ecosystem-level responses to climate-induced oceanic changes, it is critical to evaluate the role of diatoms in the marine cycling of Si and the coupling between that cycle and other processes such as carbon fixation, transfer through the food web and export. This is especially true in the high-latitude oceans where changes in marine ecosystem from climate variability have already been documented (Li et al. 2009).

Natural variations in Si isotopes ($\delta^{30}\text{Si}$) can be used to quantify Si(OH)₄ uptake in and supply to ocean surface waters (Fripiat et al. 2011) and identify water masses (Varela et al. IPY Conference abstract, 2012). They provide a novel and powerful proxy for studying Si cycling over broad spatio-temporal scales (Varela et al. 2004), and can be used to reconstruct nutrient utilization histories (Beucher et al. 2008). During Canadian IPY-GEOTRACES, $\delta^{30}\text{Si}(\text{OH})_4$ in the Canada Basin at >1000 m depth were the heaviest ever measured in marine deep waters, and reflect the influx of relatively heavy intermediate waters from the Atlantic Ocean with some local amplification due to the biological pump (Varela et al. IPY Conference abstract, 2012).

The specific objectives of for this cruise were two-fold:

- Describe the marine biogenic silica (bSiO₂) dynamics of the upper water column and investigate the linkage between the marine cycling of Si, C and N using measurements of dissolved nutrients, particulate C, N and bSiO₂ concentrations, and uptake rates of Si(OH)₄, C, nitrate (NO₃⁻) and ammonium (NH₄⁺);
- Characterize the natural variations in the $\delta^{30}\text{Si}$ composition of both Si(OH)₄ and bSiO₂ throughout the Canadian Arctic.

18.2 Methodology

18.2.1 CDOM, Humic substances and Thiols – Gueguen and Hansell

DOC samples were collected by the TM team in amber vials (rinsed thrice with sample water) at select depths from the TM Rosette (Table 18-1 and Table 18-2); no filtration. Samples were stored at 4°C in the helideck fridge (tote 3).

All samples for CDOM, humic substances (HS) and thiol analysis were filtered through a GF/F filter and stored in 60 mL amber glass vials at 4 °C. The samples designated for humic substances and thiol analysis using voltammetry were acidified to pH around 2 using HCl immediately after filtration. Samples for DOC analysis were taken using 60 mL transparent glass vials in Leg 2 and 60 mL amber glass vials in Leg 3b.

Table 18-1. Samples taken and associated analysis during Leg 2.

Station	Targeted depths (m)	Designated Analysis
K1	1600, 1400, 1200, 1000, 800, 600, 500, 400, 300, 200, 100, 90, 70, 50, 30, 20, 10	CDOM (Gueguen)/DOC (Hansell)
LS2	2600, 1999, 1000, 800, 500, 300, 200, 150, 100, 30, 10	CDOM (Gueguen)/DOC (Hansell)
BB1	1000.5, 800, 700, 599.5, 500, 400, 300, 200.5, 149.5, 100, 47, 21.5, 11	CDOM, HS/thiol (Gueguen)/DOC (Hansell)
BB3	1000.7, 800, 699.7, 600.5, 490, 398.5, 299.6, 199.6, 148.4, 99.9, 49.9, 30.1, 10.2	CDOM, HS/thiol (Gueguen)/DOC (Hansell)
BB2	N/A	CDOM, HS/thiol (Gueguen)/DOC (Hansell)
CAA1	N/A	CDOM, HS/thiol (Gueguen)/DOC (Hansell)
CAA2	N/A	CDOM, HS/thiol (Gueguen)/DOC (Hansell)
CAA3	N/A	CDOM, HS/thiol (Gueguen)/DOC (Hansell)
CAA4	N/A	CDOM, HS/thiol (Gueguen)/DOC (Hansell)
CAA5	N/A	CDOM, HS/thiol (Gueguen)/DOC (Hansell)
CAA6	N/A	CDOM, HS/thiol (Gueguen)/DOC (Hansell)
CAA7	N/A	CDOM, HS/thiol (Gueguen)/DOC (Hansell)

Table 18-2. Samples taken for DOC (Hansell), CDOM and Thiol (Gueguen) analysis during Leg 3b.

Station	Targeted depths (m)
CB1	Tmin, Tmax, Chla max, Part max, 400, 350, 300, 250, 200, 150, 10
CB2	Tmin, Tmax, Chla max, 1200, 1000, 800, 400, 300, 200, 100, 40, 25, 10
CB3	Tmin, Tmax, Tmax ₂ , Chla max, 3500, 3000, 2500, 2000, 1600, 1400, 1200, 1000, 800, 600, 300, 250, 200, 150, 100, 40, 10
CB4	Tmin, Tmax, Tmax ₂ , Chla max, 3500, 3000, 2500, 2000, 1600, 1400, 1200, 1000, 800, 600, 300, 250, 150, 100, 40, 10
CAA8	Tmin, Tmax, Chla max, Part max, 450, 350, 300, 250, 200, 150, 120, 10
CAA9	Tmin, Tmax, Chla max, Part max, bottom, 250, 200, 150, 120, 10

Underway – Gueguen

Samples were collected approximately three times per day in vials rinsed thrice with sample water, no filtration, from the underway sampling system in the engine room (Table 18-3/ Table 18-4). Samples stored at 4°C in the helideck fridge (tote 4).

Table 18-3. Underway sampling during Leg 2.

Sample	Latitude (N)	Longitude (W)	Date	Time	Location
Loop 1	49°29.700	066°17.280	20150711	12:48	Benthic lab
Loop 2	50°48.840	065°26.760	20150711	17:49	Benthic lab
Loop 3	50°48.840	064°07.200	20150711	22:27	Benthic lab
Loop 4	49°31.560	060°32.580	20150712	8:04	Benthic lab
Loop 5	49°33.120	059°09.600	20150712	12:32	Benthic lab
Loop 6	50°27.600	057°31.020	20150712	18:27	Benthic lab
Loop 7	51°15.600	056°22.500	20150712	22:25	Benthic lab
Loop 8	53°07.260	054°21.180	20150713	8:11	Benthic lab
Loop 9	54°07.380	054°02.880	20150713	13:17	Benthic lab
Loop 10	55°12.960	053°25.260	2015071	19:06	Benthic lab
Loop 11	56°48.960	052°28.560	20150715	21:53	Benthic lab
Loop 12	58°03.960	054°20.220	20150716	9:02	Benthic lab
Loop 13	59°10.560	055°22.860	20150716	15:02	Benthic lab
Loop 14	60°07.500	056°31.860	20150716	20:08	Benthic lab
Loop 15	61°14.160	056°32.520	20150718	23:27	Benthic lab
Loop 16	63°25.260	057°26.940	20150719	11:00	Benthic lab
Loop 17	64°28.740	058°06.360	20150719	16:09	Benthic lab
Loop 18	62°01.860	065°01.320	20150720	11:01	Benthic lab
Loop 19	61°31.620	067°09.420	20150720	15:56	Benthic lab
Loop 20	62°09.360	070°05.940	20150720	21:42	Benthic lab
Loop 21	62°24.960	077°02.520	20150721	10:32	Benthic lab
Loop 22	62°06.780	078°20.160	20150721	15:11	Benthic lab
Loop 23	61°08.580	078°28.020	20150721	20:55	Benthic lab
Loop 24	60°04.980	078°15.480	20150722	11:13	Benthic lab
Loop 25	59°21.180	078°19.680	20150722	16:05	Benthic lab
Loop 26	59°12.240	078°33.060	20150722	21:23	Benthic lab
Loop 27	58°29.520	079°09.540	20150723	10:53	Benthic lab
Loop 28	59°11.280	079°05.820	20150723	15:45	Benthic lab
Loop 29	59°16.860	078°26.460	20150723	20:44	Benthic lab
Loop 30	60°03.540	078°14.880	20150730	21:24	Benthic lab
Loop 31	62°23.460	077°34.560	20150731	11:55	Benthic lab
Loop 32	62°28.320	074°26.700	20150731	17:52	Benthic lab
Loop 33	62°40.860	072°33.660	20150731	22:22	Benthic lab
Loop 34	62°01.260	069°05.820	20150801	10:58	Benthic lab
Loop 35	61°26.460	066°14.820	20150801	16:38	Benthic lab
Loop 36	62°01.260	064°34.260	20150801	21:49	Benthic lab
Loop 37	63°16.800	059°32.160	20150802	11:23	Benthic lab
Loop 38	64°07.980	059°10.320	20150802	15:34	Benthic lab
Loop 39	65°12.060	059°11.160	20150802	20:32	Benthic lab
Loop 40	67°42.420	058°26.460	20150803	23:03	Engine Room
Loop 41	69°01.860	059°03.780	20150804	11:57	Engine Room

Sample	Latitude (N)	Longitude (W)	Date	Time	Location
Loop 42	70°05.160	059°15.960	20150804	16:55	Engine Room
Loop 43	71°03.240	062°00.060	20150804	22:39	Engine Room
Loop 44	73°00.840	068°35.880	20150808	22:38	Engine Room
Loop 45	73°34.860	075°32.460	20150809	9:45	Engine Room
Loop 46	74°14.820	079°07.740	20150809	16:12	Engine Room
Loop 47	74°06.780	087°42.660	20150812	12:38	Engine Room
Loop 48	74°20.760	094°05.100	20150814	8:16	Engine Room
Loop 49	74°08.340	096°20.940	20150815	10:01	Engine Room
Loop 50	72°03.660	096°01.320	20150816	15:24	Engine Room

Table 18-4. Underway samples collected during Leg 3b. Data for time sampled is correct (UTC-5) but coordinates were unavailable at the source and reflect our location 3 minutes after sampling.

Loop	Latitude (deg N)	Longitude (deg W)	Date and time	Loop	Latitude (deg N)	Longitude (deg W)	Date and time
51	73.51.493	129.44.686	Sept 5 – 1448hrs	88	71.04.613	134.30.720	Sept 17 – 2003hrs
52	74.06.494	127.44.030	Sept 5 – 2100hrs	89	71.25.737	131.02.692	Sept 18 – 0058hrs
55	75.05.972	120.30.876	Sept 6 – 2351hrs	90	70.50.992	124.49.874	Sept 18 – 1309hrs
56	75.05.719	120.33.251	Sept 7 – 0515hrs	91	70.06.083	120.26.732	Sept 18 – 2001hrs
57	75.06.816	120.21.993	Sept 7 – 1242hrs	92	69.42.905	118.16.922	Sept 18 – 2353hrs
58	75.06.878	120.38.544	Sept 7 – 1612hrs	93	68.01.916	114.28.767	Sept 19 – 1349hrs

59	75.07.003	120.42.472	Sept 7 – 2129hrs	94	68.12.926	113.47.003	Sept 19 – 1901hrs
60	75.19.193	127.46.720	Sept 8 – 1326hrs	95	68.28.362	111.20.733	Sept 19 – 2337hrs
61	75.49.179	129.12.945	Sept 8 – 1850hrs	96	69.01.861	106.22.022	Sept 20 – 0913hrs
62	75.48.768	129.13.571	Sept 8 – 2345hrs	97	68.35.771	103.55.350	Sept 20 – 1905hrs
63	75.49.384	129.13.526	Sept 9 – 0905hrs	98	68.29.485	103.24.125	Sept 20 – 2322hrs
64	75.53.154	129.20.240	Sept 9 – 1126hrs	99	68.13.430	101.44.417	Sept 21 – 1317hrs
65	76.07.196	129.19.576	Sept 9 – 1830hrs	100	68.18.720	100.47.965	Sept 21 – 1913hrs
65	75.51.080	129.25.558	Sept 10 – 0106hrs	101	68.29.565	99.53.700	Sept 21 – 2345hrs
66	76.165.053	129.06.093	Sept 10 – 1526hrs	102	69.05.290	101.00.047	Sept 22 – 0811hrs
67	75.52.933	128.53.788	Sept 10 – 1842hrs	103	69.53.160	99.28.594	Sept 22 – 1610hrs
68	75.53.151	131.14.382	Sept 10 – 2358hrs	104	71.16.678	100.38.567	Sept 22 – 2350hrs
69	76.27.700	136.58.950	Sept 11 – 0826hrs	105	72.53.760	103.10.612	Sept 23 – 1152hrs
70	76.44.819	138.34.170	Sept 11 – 1216hrs	106	74.05.283	107.50.828	Sept 23 – 2004hrs
71	76.58.789	140.01.635	Sept 11 – 1826hrs	107	74.08.313	108.50.178	Sept 23 – 2352hrs
72	76.58.501	140.02.970	Sept 11 – 2142hrs	108	74.08.343	108.49.972	Sept 24 – 0732hrs
73	76.59.445	139.56.474	Sept 12 – 0426hrs	109	74.08.294	108.50.209	Sept 24 – 1212hrs
74	77.00.179	140.05.035	Sept 12 – 1154hrs	110	74.08.902	108.52.121	Sept 24 – 1729hrs
75	77.01.662	140.02.541	Sept 12 – 1730hrs	111	74.06.662	103.59.516	Sept 25 – 0118hrs
76	76.59.920	140.00.242	Sept 13 – 0714hrs	112	74.14.190	97.45.442	Sept 25 – 1251hrs
77	75.44.374	146.34.340	Sept 13 – 2014hrs	113	74.31.767	93.26.343	Sept 25 – 1850hrs
78	75.03.625	149.18.680	Sept 14 – 1342hrs	114	74.47.584	92.46.142	Sept 26 – 0014hrs
79	75.00.007	150.00.411	Sept 14 – 2044hrs	115	75.20.177	93.22.934	Sept 26 – 0952hrs
80	74.59.983	149.59.968	Sept 14 – 2315hrs	116	76.19.777	96.44.226	Sept 26 – 2021hrs

81	75.00.055	149.59.946	Sept 15 – 0845hrs	117	76.25.464	96.27.296	Sept 27 – 0707hrs
82	74.59.803	150.02.202	Sept 15 – 1510hrs	118	76.38.595	96.56.426	Sept 27 – 0951hrs
83	74.59.748	149.59.424	Sept 15 – 2057hrs	119	76.08.067	95.50.125	Sept 27 – 1837hrs
84	75.00.209	149.57.432	Sept 16 – 0940hrs	120	75.37.176	94.09.676	Sept 28 – 0420hrs
85	74.44.794	148.56.746	Sept 16 – 1627hrs	121	75.41.864	95.01.495	Sept 28 – 1752hrs
86	74.11.846	146.38.272	Sept 16 – 2332hrs	122	75.36.726	93.47.536	Sept 29 – 0107hrs
87	71.46.086	138.20.942	Sept 17 – 1345hrs	123	75.22.573	92.40.263	Sept 29 – 0656hrs

18.2.2 $bSiO_2$ and $\delta^{30}Si(OH)_2$ – Varela

Marine $bSiO_2$ dynamics and Si:C:N ratios - Leg 3b only

At the stations listed in Table 18-5, samples to investigate marine $bSiO_2$ dynamics and Si:C:N ratios for particles and uptake rates were collected from 12-L Niskin bottles on the CTD- Rosette. Seawater samples were collected at 6 optical depths (100, 50, 30, 15, 1 and 0.2% of surface irradiance) as determined by Marjolaine Blais (PI: Michel Gosselin) using a separate cast with a PAR sensor.

At each depth, samples were collected for the measurement of $bSiO_2$ concentrations, net $bSiO_2$ production rates and ^{32}Si , ^{13}C , and ^{15}N uptake rates. At one depth (50% irradiance), size- fractionated measurements of ^{13}C and ^{15}N uptake rates were also conducted. Samples for dissolved nutrients (NO_3^- , PO_4^{3-} and $Si(OH)_4$) and NH_4^+ were also collected and analyzed in duplicate by Isabelle Courchesne and Gabrièle Deslongchamps (PI: Jean-Éric Tremblay).

Table 18-5. List of stations where incubations were conducted, and the measurements performed during Leg 2.

Station	$bSiO_2$ collected	Incubations performed
K1		$^{13}C/^{15}NO_3$
LS2	x	^{32}Si , net $bSiO_2$, $^{13}C/^{15}NO_3$, $^{15}NH_4$.
BB1	x	^{32}Si , net $bSiO_2$, $^{13}C/^{15}NO_3$, $^{15}NH_4$.
BB2	x	^{32}Si , net $bSiO_2$, $^{13}C/^{15}NO_3$, $^{15}NH_4$.
BB3	x	^{32}Si , net $bSiO_2$, $^{13}C/^{15}NO_3$, $^{15}NH_4$.
CAA1	x	^{32}Si , net $bSiO_2$, $^{13}C/^{15}NO_3$, $^{15}NH_4$.
CAA2	-	
CAA3	x	^{32}Si , net $bSiO_2$, $^{13}C/^{15}NO_3$, $^{15}NH_4$.
CAA4	-	
CAA5	x	^{32}Si , net $bSiO_2$, $^{13}C/^{15}NO_3$, $^{15}NH_4$.
CAA6	x	^{32}Si , net $bSiO_2$, $^{13}C/^{15}NO_3$, $^{15}NH_4$.
CAA7	x	^{32}Si , net $bSiO_2$, $^{13}C/^{15}NO_3$, $^{15}NH_4$.

Seawater was collected in acid-washed 250mL, 500mL, and 2L polycarbonate bottles for ^{32}Si uptake, ^{13}C and ^{15}N uptake, and net bSiO_2 incubations respectively. Samples for ambient bSiO_2 concentrations were collected in acid-washed 2L polypropylene bottles.

Samples for gross bSiO_2 production were spiked with the radioisotope ^{32}Si (0.1 $\mu\text{Ci}/\text{mL}$ activity, Los Alamos National Laboratories) following the method of Krause et al. (2011). Samples for net bSiO_2 production were incubated for 24-48 hrs following a method similar to Demarest et al. (2011). Samples used for the determination of C assimilation rates were inoculated using $\text{NaH}^{13}\text{CO}_3$ (99% purity, Cambridge Isotopes Laboratories) isotope tracer stock with the target ^{13}C enrichment of each sample being $<10\%$ of the total ambient DIC. Samples for NO_3^- and NH_4^+ uptake rates were inoculated using $\text{Na}^{15}\text{NO}_3$ and $^{15}\text{NH}_4\text{Cl}$ (^{15}N salts were 98% purity, Cambridge Isotopes Laboratories) with the final ^{15}N enrichment target for each being approximately $\leq 10\%$. A dual-tracer method was employed for the C assimilation and NO_3^- uptake rate samples, wherein one bottle was spiked with both ^{13}C and $^{15}\text{NO}_3$.

All incubation samples were placed in a temperature-controlled on-deck incubator (cooled with surface flowing seawater) in tubes screen with blue and neutral density photographic film to simulate the in-situ irradiance and approximate wavelengths from the sampling depths. Samples were incubated for 24 hours (or up to 48 hours for net bSiO_2).

At the end of incubation, samples were terminated by gentle filtration, and the filters were dried at either room temperature for 24 hours (^{32}Si), or at $\sim 60^\circ\text{C}$ for 48 hours (net bSiO_2 , ^{13}C and ^{15}N) until further analysis on shore following the cruise.

Natural variations in $\delta^{30}\text{Si}$ of $\text{Si}(\text{OH})_4$ and bSiO_2 - Legs 2 and 3b

Seawater samples (2-4 L) for $\delta^{30}\text{Si}(\text{OH})_4$ were collected from the Rosette at discrete depths and stations listed in Table 18-6 Table 18-7. Samples were filtered through a $0.6\mu\text{m}$ polycarbonate membrane filter, and particles retained on the $0.6\mu\text{m}$ filters were dried at $\sim 60^\circ\text{C}$ for 48 hr.

Dried filter samples will be analyzed on shore for bSiO_2 concentrations. The filtered seawater was collected into acid-washed 1L filtration flasks, and stored in acid-washed 1L high-density polyethylene or 2L polypropylene bottles at 4°C . Samples will later be analyzed on shore for the $\delta^{30}\text{Si}$ composition of $\text{Si}(\text{OH})_4$.

Samples for $\delta^{30}\text{Si}$ - bSiO_2 were also collected onto $0.8\mu\text{m}$ Supor membrane filters using large volume in-situ pumps at discrete depths. Filters were dried at $\sim 60^\circ\text{C}$ for 48 hr. Dried samples will be analyzed on shore for bSiO_2 concentrations and the isotopic $\delta^{30}\text{Si}$ - bSiO_2 composition.

Table 18-6. Stations and depths where $\delta^{30}\text{Si}$ samples were collected during Leg 2.

Station	$\delta^{30}\text{Si}(\text{OH})_4$ and bSiO_2 depths (approximate depths from Rosette - m)	bSiO_2 and $\delta^{30}\text{Si}-\text{bSiO}_2$ depths (from large-volume pumps)
K1	10, 30, 100, 200, 300, 500, 1000, 1600, 2000, 2150, 2750, 3000	no samples collected
LS2	10, 30, 100, 200, 300, 500, 1000, 1600, 2000, 2500, 3000, 3500	10, 30, 300, 1000, 2500
BB1	10, 30, 100, 200, 300, 500, 700, 800, 1000	10, 30, 200, 300, 500, 700
BB2	10, 30, 100, 200, 300, 500, 1000, 1600, 2100, 2250	10, 30, 200, 500, 1600, 2300
BB3	10, 30, 100, 200, 300, 500, 700, 800, 1000	10, 30, 200, 300, 500, 700
CAA1	10, 30, 60, 100, 120, 200, 400, 600	10, 30, 100, 200, 400, 600
CAA2	10, 30, 60, 100, 120, 200, 400, 600	10, 30, 100, 200, 400, 600
CAA3	10, 30, 60, 100, 120, 200, 400, 600	10, 30, 100, 200, 400, 600
CAA4	10, 30, 40, 60, 80, 100, 120, 150	10, 30, 60, 80, 120, 150
CAA5	10, 30, 60, 100, 120, 160, 220, 250	10, 30, 100, 150, 190, 230
CAA6	10, 30, 60, 100, 120, 160, 220, 250	10, 30, 100, 150, 190, 230
CAA7	10, 30, 60, 100, 120, 140, 180, 200	10, 30, 60, 100, 160, 190

Table 18-7. Samples taken for bSiO_2 and $\delta^{30}\text{Si}(\text{OH})_2$ during Leg 3b.

Station	$\delta^{30}\text{Si}(\text{OH})_2$ and bSiO_2 depths (approximate depths from Rosette - m)
CB1	400, 350, 300, 250, 200, 150, Tmin, Tmax, Chlmax, 10
CB2	Bottom, 1200, 800, 400, 200, Tmin, Tmax, Chlmax, 25
CB3	3500, 2500, 2000, 1400, 800, 250, 200, Tmax ₂ , Tmin, 100, Chlmax, 25
CB4	3500, 2500, 2000, 1400, 800, Tmax ₂ , Tmin, 150, 100, Chlmax, 25, 10
CAA8	Bottom, 300, 250, 200, 150, 100, Tmin, Tmax, Chlmax, Partmax, 10
CAA9	Bottom, 250, 200, 150, 120, Tmin, Tmax, Chlmax, Partmax, 10

Additional sampling and collaborations

Objective 1 – Size fractionated chlorophyll a concentrations and 24 hour ^{14}C assimilation rates were measured at all of the same irradiance depths and stations by Marjolaine Blais (PI: Michel Gosselin). This will facilitate a direct comparison between the ^{13}C and ^{14}C rate measurements. Measurement of 24 hour ^{18}O production rates were performed at all of the same irradiance depths and stations by Amanda Timmerman (PI: Roberta Hamme), further expanding on the suite of productivity measurements conducted onboard. A similar set of measurements in the Antarctic resulted in a publication by Brzezinski et al. (2003).

Objective 2 – Small volume (~50mL) $\delta^{30}\text{Si}(\text{OH})_4$ samples from fifteen Arctic rivers were collected by Kristina Brown. There is currently only a single published measurement of the $\delta^{30}\text{Si}(\text{OH})_4$ composition of river water from the Canadian Arctic (Mackenzie River; Pokrovsky et al. 2013).

Ocean acidification – ^{32}Si and $^{15}\text{NO}_3$ uptake rates following a similar method described in objective 1 above were measured at the end of each of the two ocean acidification experiments run by Clara Hoppe and Nina Shuback (PI: Phillipe Tortell).

18.2.3 POC and Fe speciation – Maldonado

POC – Leg 3b only

Large volumes (~10L) of unfiltered seawater were collected in cubitainers (rinsed thrice with sample water) typically from the *Amundsen* Rosette. Pre-combusted filters were placed, using ethanol-cleaned forceps, into each funnel of a vacuum filtration system with five parallel channels. POC was collected on filters; filtrate was discarded. Filtration continued until flow rate significantly decreased and/or brown colouration appeared on filters. Sample volumes measured with calibrated bottles; listed volume accounts for small spills and leftovers. Filters folded with ethanol-cleaned forceps and placed in tinfoil. Filters were stored at -20°C, then dried at ~60°C.

Table 18-8. Samples taken for POC analysis during Leg 3b.

Station	Approximate depths from Rosette (m)
CB1	400, 350, 300, 250, 200, 150, Tmin, Tmax, Chlmax, Partmax 10
CB2	1200, 800, 400, 200, Tmin, Tmax, Chlmax, 25, 10
CB3	3500, 2500, 2000, 1400, 800, 200, Tmin, Chlmax, 25, 10
CB4	3500, 2500, 2000, 1400, 800, Tmin, 150, Chlmax, 25, 10
CAA8	Bottom, 450, 350, 300, 250, 200, 150, 100, Tmin, Partmax, Chlmax, 10
CAA9	Bottom, 250, 200, 150, 120, Tmin, Tmax, Chlmax, Partmax, 10

Fe speciation – Leg 3b only

2x500mL clean bottles (rinsed thrice with sample water) were 90% filled by the TM team with gravity-filtered seawater from the TM Rosette at each target depth. Samples stored at -20°C in the chest freezer outside the aft lab.

Table 18-9. Samples taken for Fe speciation during Leg 3b.

Station	Approximate depths from Rosette (m)
CB1	Partmax, 200, 10
CB2	Chlmax, 200, 100, 40, 10
CB3	Chlmax, 200, 100, 40, 10
CB4	Chlmax, Tmin, 100, 40, 10
CAA8	Partmax, Chlmax, 200, 10
CAA9	Chlmax, Partmax, 150, 10

18.2.4 Ligands – Ross

During Leg 3b, 4x1L clean bottles (rinsed thrice with sample water) were 90% filled by the TM team with seawater from the TM Rosette at each target depth. At least 2L for each depth were gravity-filtered; additional volume was filtered depending on flow rates. Samples stored at -20°C in the chest freezer outside the aft lab or the -20°C stand-up freezer in the aft labs.

Table 18-10. Samples taken for ligands during Leg 3b.

Station	Approximate depths from Rosette (m)
CB1	Chlmax (X2), Partmax, 200, 10 (X2)
CB2	Chlmax (X2), 200, 100, 40, 10 (X2)
CB3	Chlmax (X2), 200, 120, 100, 40, 10 (X2)
CB4	Chlmax, Tmin, 3500, 2000, 120, 100, 40, 10
CAA8	Chlmax (X2), Partmax, 200, 10 (X2)
CAA9	Chlmax (X2), Partmax, 150, 10 (X2)

18.3 Preliminary results

No analyses were performed on the ship, so no preliminary results are available at this time

18.4 Comments and recommendation

The only change I could recommend is to have water budgets flushed out sooner, although I recognize doing so may present logistical challenges which cannot be overcome.

References

- Beucher, C. B. et al. (2008). *Geochim. Cosmochim. Acta* 72: 3063-3073
- Demarest, M. S. et al. (2011). *Deep-Sea Res. II* 58: 462-476
- Fripiat, F. et al. (2011). *Mar. Chem.* 123: 11-22
- Krause, J. W. et al. (2011). *Marine Chemistry* 127: 40-47
- Li, W. K. W. et al. (2009). *Science* 326:539
- Nelson, D. M. et al. (1995). *Global Biogeochem. Cycles* 9(3): 359-372
- Varela, D.E. et al. (2004). *Global Biogeochem. Cycles* 18: GB1047

19 River sampling (GEOTRACES) – Leg 2

Project leader: Kristina Brown¹ (kbrown@whoi.edu)

Cruise participants Leg 2: Kristina Brown¹ and Roger François²

¹ Wood Hole Oceanographic Institution, 266 Woods Hole Road, Woods Hole, MA, United States.

² University of British Columbia, Department of Earth, Ocean and Atmospheric Sciences, Biological Sciences Road, Vancouver, BC, V6T 1Z4, Canada.

19.1 Introduction

River sampling was carried out using the ship's helicopter (Pilot: Martin Dufour) along the ship's cruise track as the ship transited the Canadian Arctic Archipelago (Figure 19.1). Sampling locations were chosen based on the Canadian Hydrographic Stream Network dataset (Natural Resources Canada), corresponding drainage basin geology from the Geologic Map of North America (USGS, 2005), and the proximity to the cruise track. Fifteen river stations were sampled from August 11th to 19th (Figure 19.1, Table 19-1) for the geochemical parameters listed in Table 19-2.

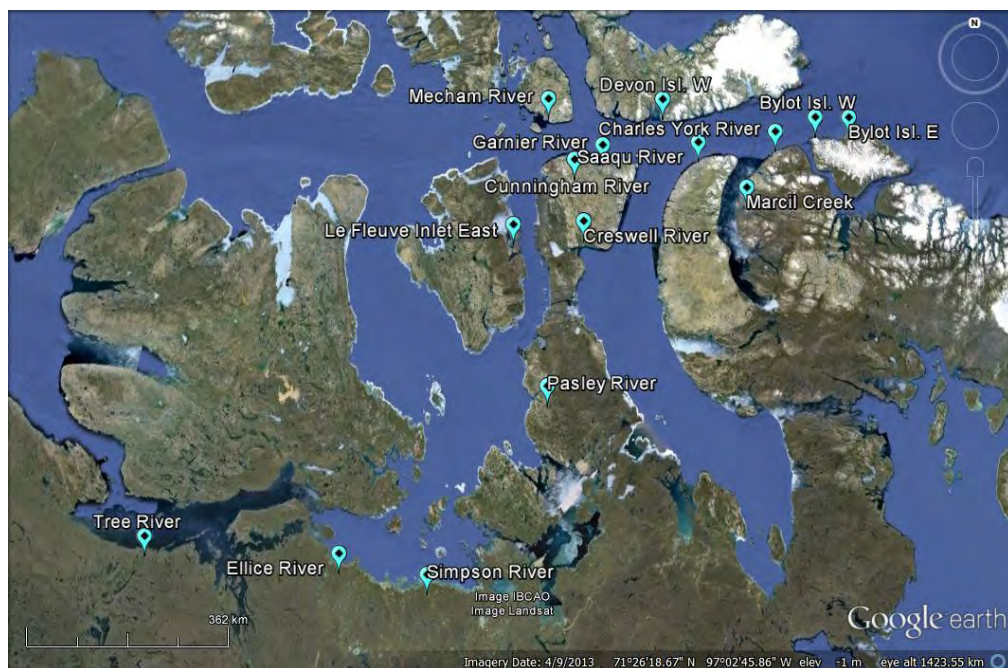


Figure 19-1. Map of river sampling locations along the GEOTRACES Leg 2 cruise track through the Canadian Arctic Archipelago.

Table 19-1. River sampling locations during the 2015 GEOTRACES (Leg 2) transit via the Canadian Arctic Archipelago.

River Number	River Name	Date Sampled	Time (local)
001	Bylot Island E	August 11, 2015	9:45
002	Bylot Island W.	August 11, 2015	15:00
003	Charles York River	August 12, 2015	5:30
004	Marcil Creek	August 12, 2015	7:21
005	Saaqu Rver	August 12, 2015	9:47
006	Devon Isl. W.	August 12, 2015	15:00
007	Cunningham River	August 13, 2015	16:01
008	Garnier River	August 13, 2015	17:55
009	Mecham River	August 14, 2015	8:45
010	Creswell River	August 16, 2015	11:40
011	Le Fleuve Inlet (East Side)	August 16, 2015	13:49
012	Pasley River	August 16, 2015	20:25
013	Simpson River	August 17, 2015	22:33
014	Ellice River	August 18, 2015	6:41
015	Tree River	August 19, 2015	7:35

Table 19-2. Geochemical parameters sampled during the 2015 GEOTRACES Leg 2 transit via the Canadian Arctic Archipelago. Analyses to be carried out at UBC, UVIC, and WHOI.

Dissolved Inorganic Carbon (DIC)	Particulate Organic Carbon (POC)	Nutrients (N, P, Si)	Dissolved Trace Metals (Fe, Mg, Pb, Ga, REE, Hg)
Total Alkalinity	14C and 13C POC	Salinity	Pb-isotopes
pH	Dissolved Organic Carbon (DOC)	Specific Density	Dissolved and particulate Nd isotopes
14C and 13C DIC	14C and 13C DOC	Si-isotopes	Sediments



Figure 19-2. (Left) Roger Francois sampling from the Mecham River, Cornwallis Island; (Right) Roger Francois and pilot Martin Dufor at the Tree River.

20 Moving Vessel Profiler and CTD mesoscale and mixing survey (GEOTRACES) – Leg 3b

Project leader: Jody Klymak¹ (jklymak@uvic.ca)

Cruise participants Leg 3b: Ken Hughes¹ and Haunt Blanken¹

¹ *University of Victoria, School of Earth and Ocean Sciences, P.O. Box 3055, Victoria, BC, V8W 3P6, Canada.*

20.1 Introduction

The central sills of the Canadian Arctic Archipelago (i.e. Penny Strait, Byam Martin Channel, Channel, Wellington Channel and the surrounding areas) are believed to be regions of large vertical mixing, the result of strong tidal currents and shallow bathymetry (Figure 20.1). As Arctic water flowing from the northwest encounters the sills in and south of Penny Strait, water properties from 70–80m depth outcrop at the surface and the water column becomes well-mixed (DeLangeBoom 1987). This not only modifies the Arctic water flowing toward the Atlantic, but also alters the baroclinic (density-driven) flow within the Archipelago.

After it leaves Wellington Channel, the water enters western Lancaster Sound, a site where moorings have been maintained for several years (Prinsenbergh, 2009) with the intention of estimating and understanding seasonal and interannual changes in heat, freshwater, and volume fluxes of water that is ultimately headed toward Baffin Bay and Labrador Sea. Fluxes through the Archipelago will be heavily influenced water mass modification in the central sills area, i.e. the region up to 300–400km upstream.

The aim was to map the turbulent structures, determine the locations of strong property fronts, and evaluate vertical mixing rates within Wellington Channel and Penny Strait using the Moving Vessel Profiler (MVP), the shipboard ADCP, and when MVP was impractical, the ship's CTD. The MVP is an ideal tool to capture the complex flow resulting from the influence of sills and islands. The high-spatial-resolution data obtained will allow to develop volume, freshwater, and heat budgets and observe changes in properties over steep topography. Further, because sampling was done as the ship traveled, it is possible to get almost-synoptic two-dimensional pictures of the ocean over scales of tens of kilometers, which is a similar to the length over which topography varies within the sampling region.

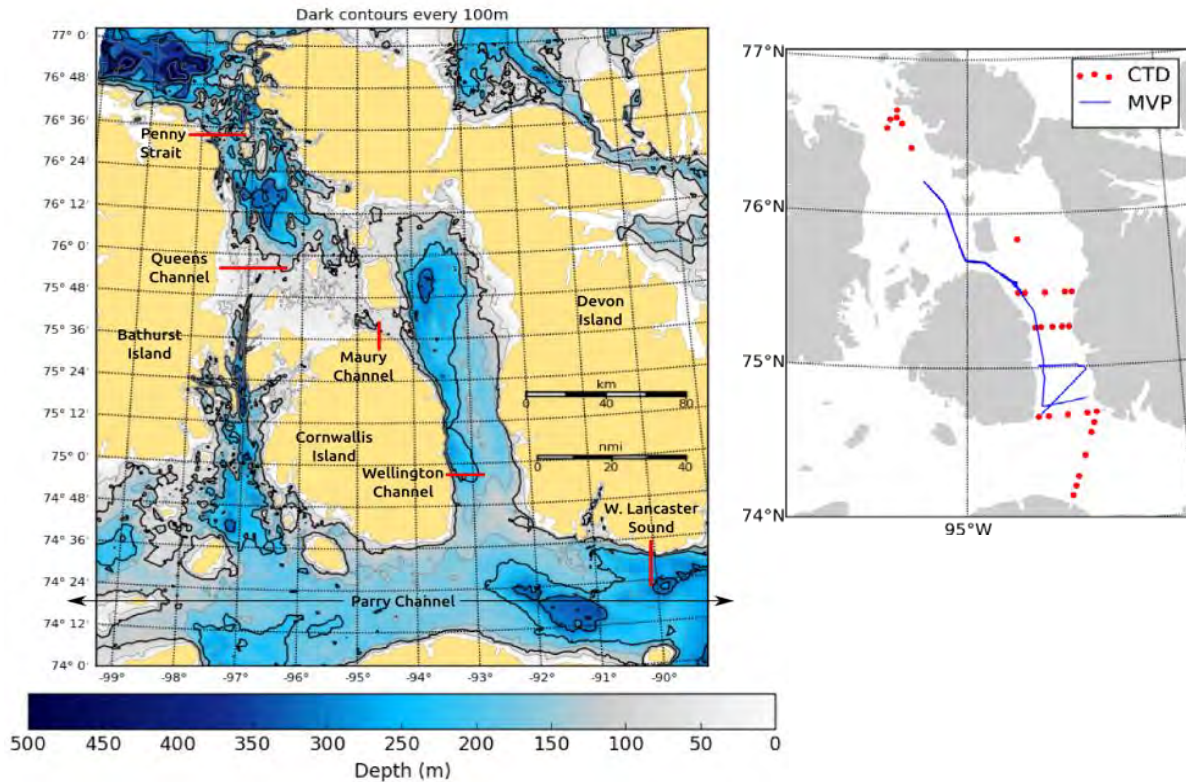


Figure 20-1. Bathymetry of the region studied with the moving vessel profiler (left) and MVP tracks and CTD stations during intensive sampling (right).

20.2 Methodology

The MVP towfish records a number of different quantities from which the following are derived: temperature, salinity, pressure, depth, sound velocity, dissolved oxygen, transmissivity, and fluorescence. With the boat travelling at approximately 8 knots and the fish freefalling, two-dimensional transects of the aforementioned properties were obtained with horizontal resolution of 1 km or less, and vertical resolution of about 1 m (Figure 20.2).

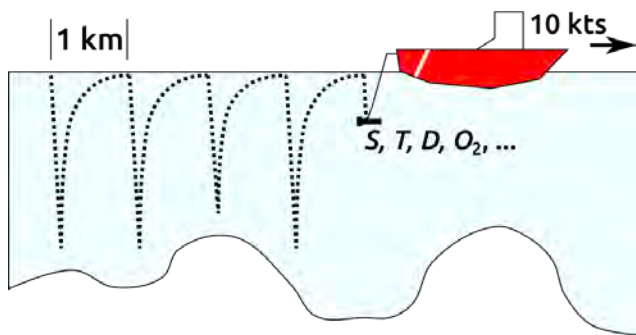


Figure 20-2. Schematic diagram of the operation of the moving vessel profiler. A 10kt boat speed, which gives approximate spacing of 1km between casts, allows observation of finescale oceanographic processes spanning distances on the order of tens to hundreds of kilometres. Oceanographic data are continuously recorded, with the freefall component being picked out during post-processing.

The timing of the sampling coincided with the approximate time of year when ice conditions within and south of Penny Strait are rapidly changing. Sea ice from the northwest episodically blows south through Penny Strait, and there is also the potential for new ice growth throughout September. The ideal plan was to take MVP observations through Penny Strait approximately 1–2 days after leaving Resolute on the 27th of September. However, by approximately mid-September, it was evident that this would not happen given that Penny Strait was already becoming blocked by sea ice (it is a danger to the towfish to sample when any ice is present). By considering changes in the ice conditions over several days, the original plan was altered to go through the constrictions north of Cornwallis Island (see Figure 20.1) and ideally over into the deeper basin south of Penny Strait. The time originally set for sampling through Penny Strait was reallocated to a focused study on changes throughout a tidal cycle in Maury Channel.

Table 20-1. Wellington Channel Survey Timeline

Survey	Time (UTC) and Date (2015)	No. of Casts
Wellington Ch. E to W (1)	08:30 26 Sep – 10:30 26 Sep	40
Wellington Ch. to Queens Ch.	10:30 26 Sep – 01:00 27 Sep	290
Penny St. rosette CTDs	11:10 27 Sep – 18:30 27 Sep	6
Maury Ch. W to E (1)	22:00 27 Sep – 06:30 28 Sep	180
Maury Ch. E to W (1)	06:30 28 Sep – 14:20 28 Sep	160
Maury Ch. W to E (2)	14:20 28 Sep – 18:30 28 Sep	125
Maury Ch. E to W (2)	18:30 28 Sep – 23:00 28 Sep	125
Maury Ch. W to E (3)	23:00 28 Sep – 00:40 29 Sep	80
Wellington Ch. rosette CTDs	03:00 29 Sep – 15:00 29 Sep	10
Wellington Ch. W to E	16:40 29 Sep – 19:20 29 Sep	55
Wellington Ch. E to W (2)	19:20 29 Sep – 22:30 29 Sep	45
Wellington Ch. rosette CTDs	00:10 30 Sep – 06:20 30 Sep	5
Lancaster Snd rosette CTDs	06:20 30 Sep – 11:10 30 Sep	7

Despite Penny Strait being blocked, the first transect was still planned between southern Wellington Channel and Queens Channel to take approximately 15 hours. During this time, the MVP data was analysed in real time, i.e. up-to-date plots of the observed properties versus depth and distance were maintained. This required existing Python scripts to be adjusted for ArcticNet’s MVP, which is a different model and has a different output format compared to this group’s own MVP. This adjusting was undertaken while onboard but before sampling started by using MVP data from the beginning of Leg 3b.

When profiling began, at least two of the four persons in the group were either monitoring the MVP’s software for any unusual signs (for example, slow cable return speed) or watching the profiler from the aft deck with radio contact to the data acquisition room. Shifts began or ended at approximately 3am and 3pm. Continual monitoring from both the acquisition room and the aft deck proved necessary as a number of problems arose, which

required coordination between both ends. A summary of the transects undertaken with the MVP is given in the Table 20-1.

20.3 Preliminary results

The initial transect down Wellington Channel, through Maury Channel, and ending in Queens Channel showed evidence of internal waves of various scales. From previous studies in the area, it was expected that water in these channels flows southeastward, which corresponds to right to left in Figure 20.3. This is consistent with what appears to be a mode-1 internal wave formed by the steep topography centred at 50km. Much shorter waves are formed by rough topography in the sill regions between 100 and 170km. These are shown zoomed in on the lower panel of Figure 20.3. It is evident from the plot that the dominant wavelengths of the internal waves in this region are correlated with the roughness scales of the bottom topography as one might expect. Other features of this long section include diverging isopycnals from right to left as water mixes after travelling over the sill and decreasing temperature moving northward. Causes of this temperature structure will be determined after further analysis.

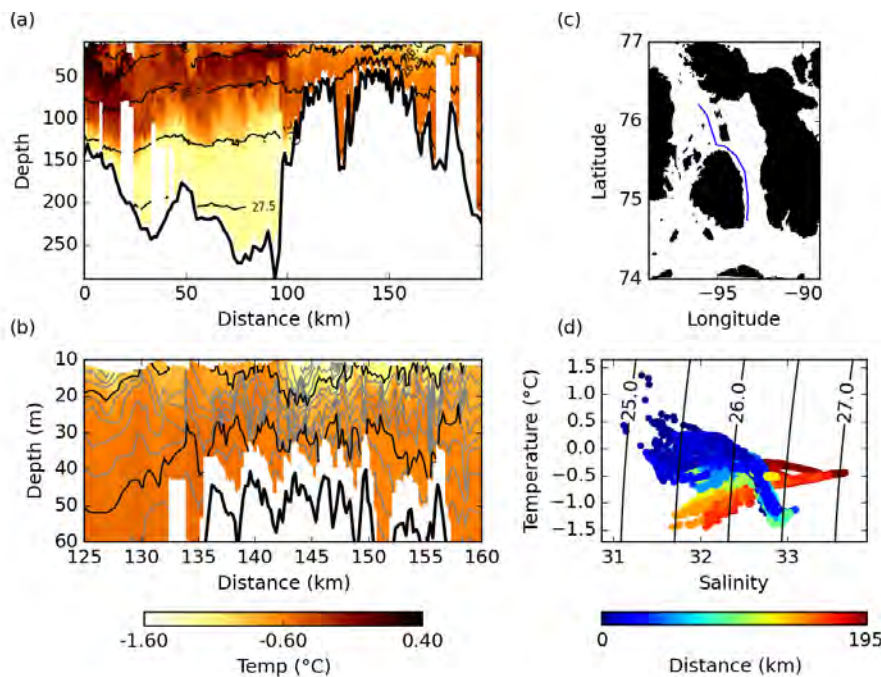


Figure 20-3. (a) Temperature (colours) and density (contours) from a long-section along Wellington Channel, through Maury Channel, and ending in Queens Channel. Note the longer mode-1 waves at approximately 0–80km. (b) Enlarged version of (a) showing the shallow area of Maury Channel and the presence of shorter internal waves, which result from flow over the rough, shallow seafloor. (c) Transect location. (d) Temperature– salinity diagram, with colours denoting distance as in panels (a) and (b).

The other initial transect, a cross-section across the southern end of Wellington Channel (Figure 20.4) shows clear evidence of a buoyant coastal current on the right hand side. Isopycnals sloping downward toward the right form a wedge-like feature like that described by Leblond (1980). These coastal currents are ubiquitous in the Canadian Archipelago and

often flow in the opposite direction to the overall southeastward flow. The team planned to use the MVP to map this coastal current at the end of the study; however, the Rosette CTD casts had to be resorted at a number of different stations in Wellington Channel.

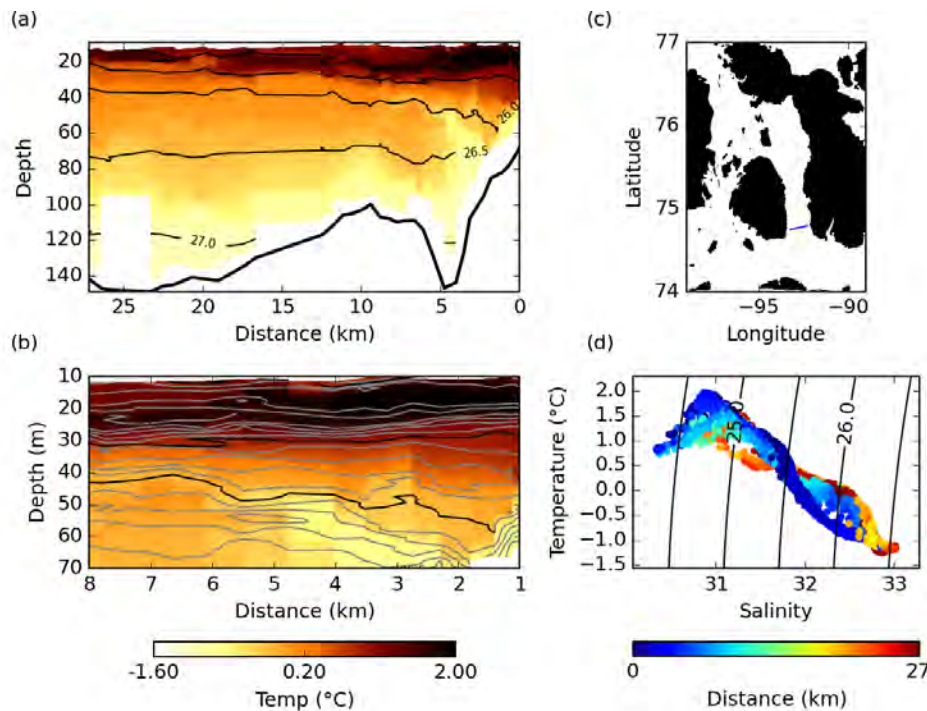


Figure 20-4. (a) Temperature (colours) and density (contours) from a cross-section across southern Wellington Channel (into the page is northward). Distances increase from a starting point not far from the eastern boundary of the channel. (b) Enlarged version of (a) showing clearly the wedge-like feature that is a buoyant coastal current enlarged in the bottom panel. (c) Transect location. (d) Temperature–salinity diagram, with colours denoting distance as in panels (a) and (b).

20.4 Comments and recommendations

The MVP was a learning experience for our group, not having worked with the system in cold weather before. Temperatures often dipped below -8 degrees C, and there were problems with ice on the cable and the moving parts. The ice on the cable is a problem because it triggers failsafe switches on the system, so we had many drops terminate prematurely, necessitating a manual recover to the surface. This was particularly challenging when making the transition from shallow topography to deep topography because the drum built up ice sheets on the deeper wraps.

The other ice issue was on the sheaves and the level wind rollers. If these seized up it greatly increased tension on the system. The motor responded appropriately, slowing the pay in speed, but the extra friction may not have been good for the cable.

There was a solution to keeping the outer sheave warm, which was to turn the installed outer-sheave heaters on. This seemed to work quite well in keeping the sheave relatively ice

free. In the future, all techs should be made aware of this feature (which is not in the manual), and be sure to turn this on.

There was a solution to terminated downcasts, which was to hold the inner sheave defeat button down during the down cast, and then release it during the upcast. This still held the possibility of aborted drops if ice made it to the outer sheave, but this was much less likely than ice in the inner sheave.

The final mechanical issue was with the brake. Its level of maintenance was very questionable. The turnbuckle adjustment appeared to back off about 6 turns the first few hours of use, causing the brake to not engage. The turnbuckle is supposed to have locking nuts and cotter pins. None were installed. The brake subsequently seized up the next day, perhaps due to ice in the brake. The brake assembly should definitely be fully reconditioned before the system is used again. It was also surprising to not have a maintenance log readily available.

An overall solution to the winch issues in such cold weather would be to enclose the winch and to heat the enclosure. Something like a tent or polyurethane freezer flaps might work well. If the winch and inner boom assembly had stayed above zero, and the outer sheave heater turned on, there would have been far fewer problems. I don't think this would be too expensive and for sustained MVP work would be helpful. The only caveat about that is that it is good for the person next to the winch to be able to see the water, so something clear at head level would be desirable. Barring that, using the *salt water* from the ship's system seemed the most effective way of clearing ice from the system. The crew found a locking spray nozzle (i.e. it could be locked to stay on so as to not freeze) and that worked very well. Another possibility is to have a compressed air nozzle dry the cable on the way in.

A couple of secondary suggestions: The physical separation of the control room and the winch was almost unmanageable. Both the winch and the control room jobs require some expertise. If there are only a few people trained to operate the MVP, it is preferable that they be in close proximity, not running from one end of the ship and up 4 flights of stairs just to help each other. For more casual MVP work this might be a good arrangement, but if there is a lot of troubleshooting going on, its quite challenging. I appreciate that lab space is tight, but a control station in the aft labs would be more ideal. One could imagine doing this via a remote desktop client to the machine in the acquisition room, the only hang up being one could not turn the deck box on and off.

The second suggestion would be that ArcticNet consider buying a smaller dual-sensor fish. The current fish is very large, and is very hard to get in and out of the water, requiring the bosun and two crew members. A smaller fish could be handled by two people without difficulty. I'm not clear on the design constraints behind the current fish, perhaps it is so large just because of weight, but I think a lot of it is hollow, so I'm not sure thats the case. If the science payload is really deemed desirable there are still smaller multi-sensor fish available.

21 Turbulent heat fluxes and dissipation rates in the Beaufort Sea – Leg 3a

ArcticNet Phase 3 – Long-Term Observatories in Canadian Arctic Waters.
<http://www.arcticnet.ulaval.ca/pdf/phase3/marine-observatories.pdf>

Project leader: Stephanie Waterman¹ (swaterman@eos.ubc.ca)

Cruise participants Leg 3a: Benjamin Scheifele¹ and Jeff Carpenter²

¹ *University of British Columbia, Department of Earth Ocean and Atmospheric Sciences, 2020-2207 Main Mall, Vancouver, BC, V6T 1Z4, Canada.*

² *Institute of Coastal Research, Helmholtz Zentrum Geesthacht, Germany.*

21.1 Introduction

This is a research project to study turbulence in the Beaufort Sea, physical processes by which heat and nutrients are transported from the deep water into the upper layers of the Beaufort Sea. The project is in collaboration with the Canadian GEOTRACES program, and its purpose is to study mixing mechanisms in the Canadian Arctic. The big-picture goals of the program are to understand regional heat fluxes in the Beaufort Sea, the modification of watermasses as they circulate along the Mackenzie Shelf and through the Amundsen Gulf, and the mechanisms that drive the distribution of trace chemicals. Results will be integrated into the modeling efforts of the GEOTRACES program.

The Arctic Ocean in the Canada Basin contains a deep layer (250-800 m depth) of warm and salty water that intrudes from the Atlantic Ocean. This water is largely isolated from the colder Pacific-origin mid-depth water by a steep density gradient that divides the two water masses and traps a large amount of heat in the Atlantic Water layer. If this heat were somehow transported to the surface, it would be sufficient to entirely melt the surface sea-ice pack in the Arctic Ocean. However, vertical fluxes through the temperature gradient are relatively small, and it is hypothesized that most of the heat that escapes the Atlantic Water layer escapes at the basin boundaries near the continental shelves. Despite the importance of understanding vertical heat fluxes in the Arctic, actual measurements of turbulent mixing and dissipation rates are sparse, and of those that do exist, most are from the Eurasian Basin. By directly measuring the distribution of dissipation rates in the Amundsen Gulf, and by making use of a ~10-year time series of CTD measurements publicly available from ArcticNet, the following specific research questions were addressed:

- Turbulent mixing (1): What is the strength and spatial distribution of turbulent mixing in the Amundsen Gulf region in late summer?
- Turbulent mixing (2): Is turbulent mixing elevated near steep topography (e.g. Rippeth et al. 2015)? Can we observe correlations to eddies, tides, wind-stress, boundary currents? If so, what does this tell us about relative importance of these mechanisms?
- Vertical fluxes: What are the implications of the observed mixing rates on heat fluxes in this region? How do these fluxes compare to previous results for the central Canada Basin?

- Larger-scale mixing: How are the Atlantic and Pacific watermasses modified as they circulate through Amundsen Gulf? How do these modifications affect vertical mixing as they moderate the strength of the stratification?

21.2 Methodology

The measurement of turbulent mixing in Amundsen Gulf was carried out using turbulent microstructure sensors (both shear and temperature) mounted to a Slocum ocean glider. The glider is an autonomous (i.e. unmanned) underwater vehicle that profiles the water column in a saw-tooth pattern. The glider propulsion is provided by a buoyancy pump that works to alter the glider volume, while the mass is kept constant, thus producing changes in the buoyancy of the glider. These buoyancy changes allow the glider to profile the water column vertically, while the wings provide the majority of the lift required for a forward trajectory. This method of propulsion requires that the glider is carefully ballasted so that it can cover the correct density change of the water column. This was the most critical aspect of performing the glider operations in Amundsen Gulf. The glider was ballasted for a target density of 1024.5 kg/m^3 , which together with its buoyancy pump range of approximately 8 kg/m^3 , allowed it to operate in water densities of 1020.5 to 1028.5 kg/m^3 .

This density limitation on the operation of the glider was critical for the mission. The figure below shows a plot of the potential density measured by the glider over the course of the operations (Figure 21.1). Attention should be drawn to the lower boundary of the density measurements. Approximately 30 hours after the deployment the surface densities dropped drastically to levels outside the operating range of the glider. This sudden drop prevented the glider from coming completely to the surface and contact with the glider was not possible for a 42-hour period. Normally under these conditions the glider would drop an emergency weight to allow it to reach the surface, however, this did not occur. The reason for this is likely that the glider did have very brief periodic surfacings during this period – enough so that the weight timer was not triggered. A passing storm on 28 August is thought to have mixed the surface layer with deeper and denser waters, causing an increase in the surface density so that communication could be reestablished.

These surfacing difficulties of the glider were also experienced during the deployment, where it was found that the glider was able to surface during the first shallow test dives, but was unable to surface for the 100 m deep test dive. This caused the glider to eject its emergency weight and required a recovery and redeployment once the weight was replaced. Using this deep test dive profile, however, allowed the glider to be accurately ballasted to within 8 g of the correct target density. Upon redeployment, the glider completed the 100 m test dive successfully.

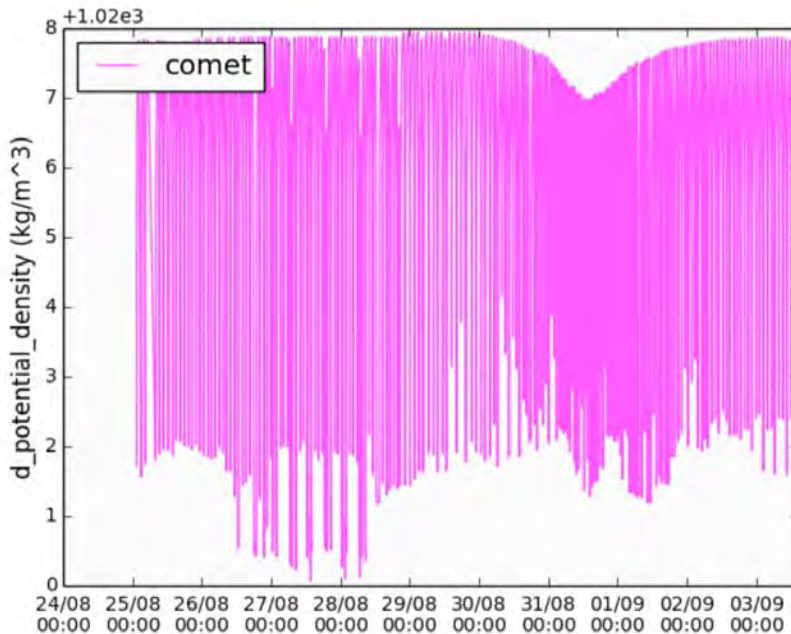


Figure 21-1. Plot of the potential density measured by the glider over the course of the operations.

The instrumentation that the glider was equipped with consisted of a CTD, microstructure sensors, as well as various navigation and communication sensors. The optical backscatter and fluorescence sensors were not used during the sampling in order to save battery power for microstructure sampling.

Figure 21.2 shows both the approximate transects covered by the glider, as well as examples of the depth profiles and a sub-sampled temperature field from the glider CTD. Using the glider echosounder to sense the location of the seabed allowed operating in a bottom tracking mode for the second half of the mission so that a fixed depth from the bottom was maintained. In order to investigate the turbulent mixing processes on the shelf slope, the glider was programmed to ascend the Amundsen slope towards Banks Island, in repeated transects (not shown in figure).

Figure 21.2 shows the type of physical data that is collected by the glider, and the distances that can be covered in a two-week deployment. During the sampling operations the turbulence microstructure data is not available, and must be downloaded and processed only after the glider is recovered.

Glider Update Aug. 30 (15:45)

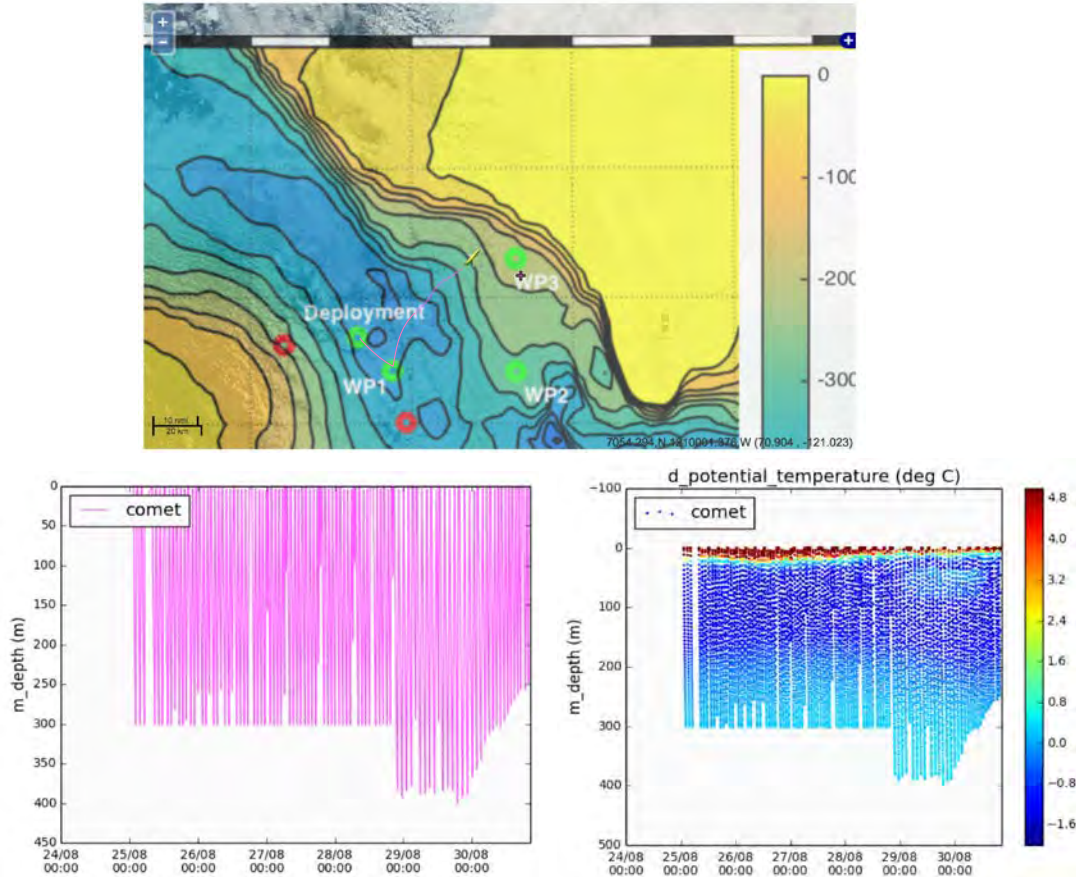


Figure 21-2. Approximate transects covered by the glider, as well as examples of the depth profiles and a sub-sampled temperature field from the glider CTD.

21.3 Preliminary results

The only results available before the recovery of the glider is made are the subsampled CTD measurements of the glider shown in the figure above. In total, approximately 300 profiles were taken over a ten-day period. These show that there is a distinct Atlantic layer water mass within Amundsen Gulf, as well as a very sharp and distinct surface mixed layer. It is also possible that the glider has transited through a mesoscale eddy on the 29 and 30 August located at 50 m depth.

21.4 Comments and recommendations

We were very happy with the planning process for mobilization. Information was communicated early enough and was clear; although receiving charter flight information (dates/times) sooner than we did would have made it a bit easier to organize international travel arrangements. We had a very positive experience onboard the *Amundsen* and using its equipment. We enjoyed working with the Coast Guard Crew and the ArcticNet staff.

22 Dissolved gas measurements (GEOTRACES) – Leg 2

Project leader: Roberta Hamme¹ (rhamme@uvic.ca)

Cruise participant Leg 2: Amanda Timmermann¹

¹ *University of Victoria, School of Earth and Ocean Sciences, P.O. Box 1700, Victoria, BC, V8W 2Y2, Canada.*

22.1 Introduction

The ocean plays a key role in controlling the atmospheric carbon dioxide concentration and thus climate change through the carbon cycle. Phytoplankton take up carbon dioxide and produce organic matter through primary production. The export of organic matter from surface waters to the deep provides a removal of carbon from the atmosphere. The high latitudes, such as the Arctic Ocean, are rapidly warming due to anthropogenic processes. However, what role warming has on the Arctic Ocean, and the ability to predict the future trajectory is still unclear due to poor understanding of the current chemical, physical and biological processes.

Three approaches were taken on this cruise to characterize the mechanisms that sequester carbon from the surface ocean and atmosphere, focusing on processes of ocean productivity, the nitrogen cycle, and the solubility pump.

22.1.1 Productivity

There are multiple standard methods to estimate primary production, and focus was given on nine methods in collaboration with other research groups. There are challenges in determining the accuracy of the methods because each measures a different “fraction” of productivity (e.g. gross, net, uptake of nutrients). The goal of this work was to look for consistent differences between the methods and uncover possible sources of bias. Samples were collected for oxygen/argon ratio (a measure of net community production), triple oxygen isotope and 24-hour ¹⁸O incubations (both measures of gross production). In collaboration with Diana Varela’s research group, 24-hour incubations were conducted for ¹³C, ¹⁵NO₃ and ¹⁵NH₄. Michel Gosselin’s research group did ¹⁴C incubations from the same casts as well. Lisa Miller (IOS) and Roger Francois (UBC) took samples for ²³⁴Th to quantify the carbon export flux. Attention will be given to satellite algorithms post-cruise to compare with all the shipboard methods.

22.1.2 Nitrogen cycle

Denitrification transforms “fixed-nitrogen” (nitrate, nitrite, ammonia, urea, etc.) to biologically inert N₂ gas. This removes biologically available nitrogen from the ocean. It has been suggested that denitrification rates are higher than inputs of fixed-nitrogen to the ocean,

leading to nitrogen further limiting primary production. To characterize denitrification in the Arctic where rates are thought to be high, we collected N₂/Ar ratio samples where a high ratio will indicate denitrification.

22.1.3 Solubility pump

The deep ocean contains more carbon than the surface due to both physical processes (the solubility pump) and biological ones. The last goal involved determining how close gases are to equilibrium with the atmosphere when water masses move into the deep ocean by making observations of noble gases which are only affected by physical processes. For this cruise, the team sought to characterize the noble gas concentrations of the major water masses in Labrador Sea and Baffin Bay.

22.2 Methodology

N₂/Ar and O₂/Ar were analyzed on the same sample. They were collected from the standard hydrography Rosette into pre-evacuated flasks through CO₂-flushed tubing to prevent atmospheric contamination. In the laboratory at University of Victoria, samples were cryogenically purified on a vacuum line and analyzed against a standard of similar composition on an isotope ratio mass spectrometer.

Table 22-1. N₂/Ar and O₂/Ar samples collected during Leg 2.

Station	Depth sampled (m)
K1	1500, 1200, 600, 50±, 30, 10±
LS2	700, 500, 300, 200, 100, 10±
BB1	700, 500, 300, 200, 100, 10±, 6
BB2	1500, 1000, 500, 300, 100, 10±
BB3	700, 500, 300, 200, 100, 10±
CAA1	600, 100, 60, 40±, 10±, 5
CAA3	600, 100, 60, 40±, 10±, 6
CAA4	100, 60, 40±, 10±
CAA5	250, 100, 60, 40±, 10±, 7
CAA6	250, 100, 40±, 10±, surface
CAA7	surface

Triple oxygen isotope samples were collected in duplicate within and below the mixed layer. Samples were collected from the standard hydrography rosette into pre-evacuated 500mL flasks through CO₂-flushed tubing to prevent atmospheric contamination. Samples will be cryogenically and chromatographically purified on a vacuum line and analyzed against a standard of similar composition on an isotope ratio mass spectrometer for the 16, 17 and 18 oxygen isotopes.

Table 22-2. Oxygen samples collected during Leg 2.

Station	Depth sampled (m)
K1	30, 10±
LS2	50±, 10±
BB1	50±, 10±
BB2	17, 6
BB3	30, 10±
CAA1	35, 5
CAA3	20, 6
CAA4	Oxygen max, 10±
CAA5	20, 7
CAA6	14, surface
CAA7	11, surface

¹⁸O incubations were collected in triplicate at 6 light depths (100, 50, 30, 15, 1 and 0.2%) at K1, LS2 BB1, BB2, BB3, CAA1, CAA3, CAA5, CAA6, CAA7. Light levels were determined on a separate PAR cast measured by Marjolaine Blais (Michel Gosselin's research group). Samples were spiked with ¹⁸O labeled water and incubated for 24 hours under a constant flow of seawater. The light levels were simulated using tubes covered in neutral density film. After 24 hours, the samples were collected into pre-evacuated flasks through CO₂-flushed tubing to prevent atmospheric contamination and will be analyzed at the University of Victoria with a similar method to the N₂/Ar and O₂/Ar samples.

Noble gas samples were to characterize deep-water masses. Samples were collected from the standard hydrography Rosette into pre-evacuated flasks through CO₂-flushed tubing to prevent atmospheric contamination. In the laboratory at University of Victoria, samples are cryogenically purified on a vacuum line and analyzed at the following stations and depths.

Table 22-3. Noble gas samples collected during Leg 2.

Station	Depth sampled (m)
K1	1500, 1200, 600
BB2	1500, 1000, 500

Dissolved oxygen samples were taken from the GEOCHEM casts at every depth and all stations. They were titrated onboard using a Mettler Toledo DM 140-Sc probe within 30 hours of collection.

22.3 Preliminary results

Results from the other analyses will not be available for a few months.

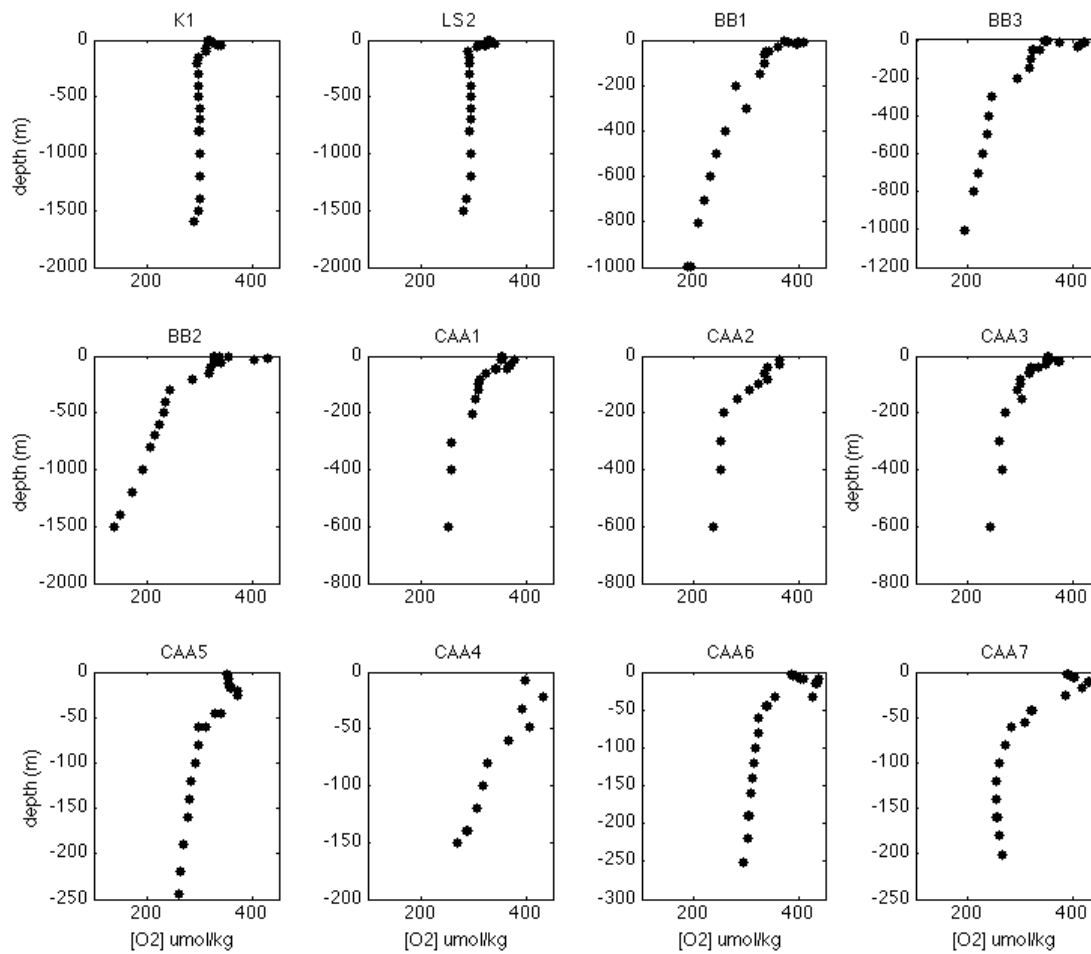


Figure 22-1. Preliminary oxygen concentration profiles from the 12 stations during Leg 2.

23 Genomics (GEOTRACES) – Leg 2

Project leader: Julie LaRoche¹ (julie.laroche@dal.ca)

Cruise participant Leg 2: Nadine Lehmann¹

¹ *Dalhousie University, Department of Oceanography, 1355 Oxford St., P.O. Box 15000, Halifax, NS, B3H 4R2, Canada.*

23.1 Methodology

Water samples for DNA/RNA analyses were collected at each GEOTRACES station. Samples were taken at ~12 depths per station, distributed over the whole water column. Approximately 4 liters of seawater per depth were collected directly from the Niskin into collapsible cubitainers. Sample water was filtered onto 3.0 and 0.2µm Durapore (Millipore) filters using low vacuum (3 kPa). Filters were immediately flash frozen using liquid nitrogen and stored at -80°C until extraction in the laboratory. Molecular analyses will be performed post-cruise at the LaRoche lab at Dalhousie University.

24 Marine productivity: Carbon and nutrient fluxes – Legs 2, 3a, 3b, 4a, 4b and 4c

ArcticNet Phase 3 – Marine Biological Hotspots: Ecosystem Services and Susceptibility to Climate Change. <http://www.arcticnet.ulaval.ca/pdf/phase3/marine-ecosystem-services.pdf>

Project leader: Jean-Éric Tremblay¹ (jean-eric.tremblay@bio.ulaval.ca)

Cruise participants Leg 2: Isabelle Courchesne¹ and Gabrièle Deslongchamps¹

Cruise participant Leg 3a: Jonathan Gagnon¹

Cruise participant Leg 3b: Gabrièle Deslongchamps¹

Cruise participant Leg 4a, 4b and 4c: Jonathan Gagnon¹

¹ *Université Laval, Département de biologie, Pavillon Alexandre-Vachon, 1045 avenue de la Médecine, Québec, QC, G1V 0A6, Canada.*

24.1 Introduction

The Arctic climate displays high inter-annual variability and decadal oscillations that modulate growth conditions for marine primary producers. Much deeper perturbations recently became evident in conjunction with globally rising CO₂ levels and temperatures (IPCC 2007). Environmental changes already observed include a decline in the volume and extent of the sea-ice cover (Johannessen et al. 1999, Comiso et al. 2008), an advance in the melt period (Overpeck et al. 1997, Comiso 2006), and an increase in river discharge to the Arctic Ocean (Peterson et al. 2002, McClelland et al. 2006) due to increasing precipitation and terrestrial ice melt (Peterson et al. 2006). Consequently a longer ice-free season was observed in both Arctic (Laxon et al. 2003) and subarctic (Stabeno & Overland 2001) environments. These changes entail a longer growth season associated with a greater penetration of light into surface waters, which is expected to favoring phytoplankton production (Rysgaard et al. 1999), food web productivity and CO₂ drawdown by the ocean. However, phytoplankton productivity is likely to be limited by light but also by allochthonous nitrogen availability. The supply of allochthonous nitrogen is influenced by climate-driven processes, mainly the large-scale circulation, river discharge, upwelling and regional mixing processes. In the global change context, it appears crucial to improve the knowledge of the environmental processes (i.e. mainly light and nutrient availability) interacting to control phytoplankton productivity in the Canadian Arctic.

The main goals of the team for Legs 2, 3a, 3b and 4 of ArcticNet 2015 were to establish the horizontal and vertical distributions of phytoplankton nutrients and to measure the primary production located at the surface of the water column using O₂/Ar ratios. During Leg 3b, secondary objectives were to quantify nitrification and regeneration processes by doing incubations with ¹⁵N tracer. In addition, natural abundance of nitrate (N isotopes) and DNA/RNA data were collected at all GEOTRACES stations. Auxiliary objective was to calibrate the *ISUS* nitrate probe attached to the Rosette.

24.2 Methodology

Samples for inorganic nutrients (ammonium, nitrite, nitrate, orthophosphate and orthosilicic acid) were taken at all Nutrient, Basic and Full stations (Table 24-1) as well as at all GEOTRACES stations (Leg 3b) to establish detailed vertical profiles. With the exception of samples collected during Leg 3b, which were frozen after sampling for later analysis, samples were stored at 4°C in the dark and analyzed for nitrate, nitrite, orthophosphate and orthosilicic acid within a few hours on a Bran+Luebbe AutoAnalyzer 3 using standard colorimetric methods adapted for the analyzer (Grasshoff et al. 1999). Additional samples for ammonium determination were taken at stations where incubations were performed and processed immediately after collection using the fluorometric method of Holmes et al. (1999).

During Leg 3b, water samples for N isotopes (natural abundance of nitrate) were collected at all GEOTRACES stations and stored at -20°C. 24h incubations with ¹⁵N tracer were accessed at 5 stations to quantify nitrification and regeneration processes. In addition, DNA and RNA data were collected at all stations where incubations were performed.

During the entire cruise, a quadrupole mass spectrometer (PrismaPlus, Pfeiffer Vacuum) was used to measure the dissolved gases (N₂, O₂, CO₂, Ar) coming for the underway seawater line located in the 610 laboratory. O₂ to Ar ratios will later be analyzed to measure primary production that occurred up to 10 days prior of the ship's passage in all the areas visited.

Table 24-1. List of sampling stations and measurements during Leg 2.

Station	NO ₃ , NO ₂ , Si, PO ₄	NH ₄
K1	X	X
LS2	X	X
BB1	X	X
BB2	X	
BB3	X	X
CAA1	X	X
CAA2	X	X
323	X	X
324	X	X
CAA4	X	X
CAA5	X	X
CAA6	X	X
CAA7	X	
312	X	
314	X	
Clara's incub.	X	
Rachel's incub.	X	

Table 24-2. List of sampling stations and measurements during Leg 3a.

Station	NO ₃ , NO ₂ , Si, PO ₄	NH ₄
405	X	X
407	X	X
437	X	X
410	X	
412	X	
414	X	
408	X	X
418	X	
420	X	X
434	X	X
432	X	
424	X	
435	X	X
422	X	
430	X	
428	X	
426	X	
421	X	X
535	X	X
536	X	X
518	X	
516	X	
514	X	X
512	X	
510	X	

Table 24-3. List of sampling stations and measurements during Leg 3b.

Station	NO ₃ , NO ₂ , Si, PO ₄	NH ₄	N Isotope	Incubation	DNA/RNA
CB1	X	X	X	X	
CB2	X	X	X	X	X
CB3	X	X	X	X	X
CB4	X	X	X	X	X
QMG	X	X			
QMG1	X	X			
QMG2	X	X			
QMG3	X	X			
QMG4	X	X			
AN 307	X	X			
AN 310	X	X			
AN 312	X	X			
AN 314	X	X			
AN 342	X	X			
AN 407	X	X	X	X	X
CAA8	X	X	X		
CAA9	X	X	X		

Table 24-4. List of sampling stations and measurements during Leg 4.

Station	NO ₃ , NO ₂ , Si, PO ₄	NH ₄
304	X	X
346	X	
343	X	
301	X	X
325	X	
324	X	
323	X	X
300	X	
322	X	
110	X	
111	X	X
113	X	
115	X	X
108	X	X
107	X	
105	X	X
103	X	
101	X	X
155	X	X
150	X	X
166	X	
170	X	X
171	X	
172	X	
169	X	
173	X	
176	X	
178	X	
177	X	
179	X	
180	X	X
181	X	
184	X	
187	X	X
190	X	
353	X	
640	X	
650	X	
Belle Isle Strait	X	

24.3 Preliminary results – Leg 3a

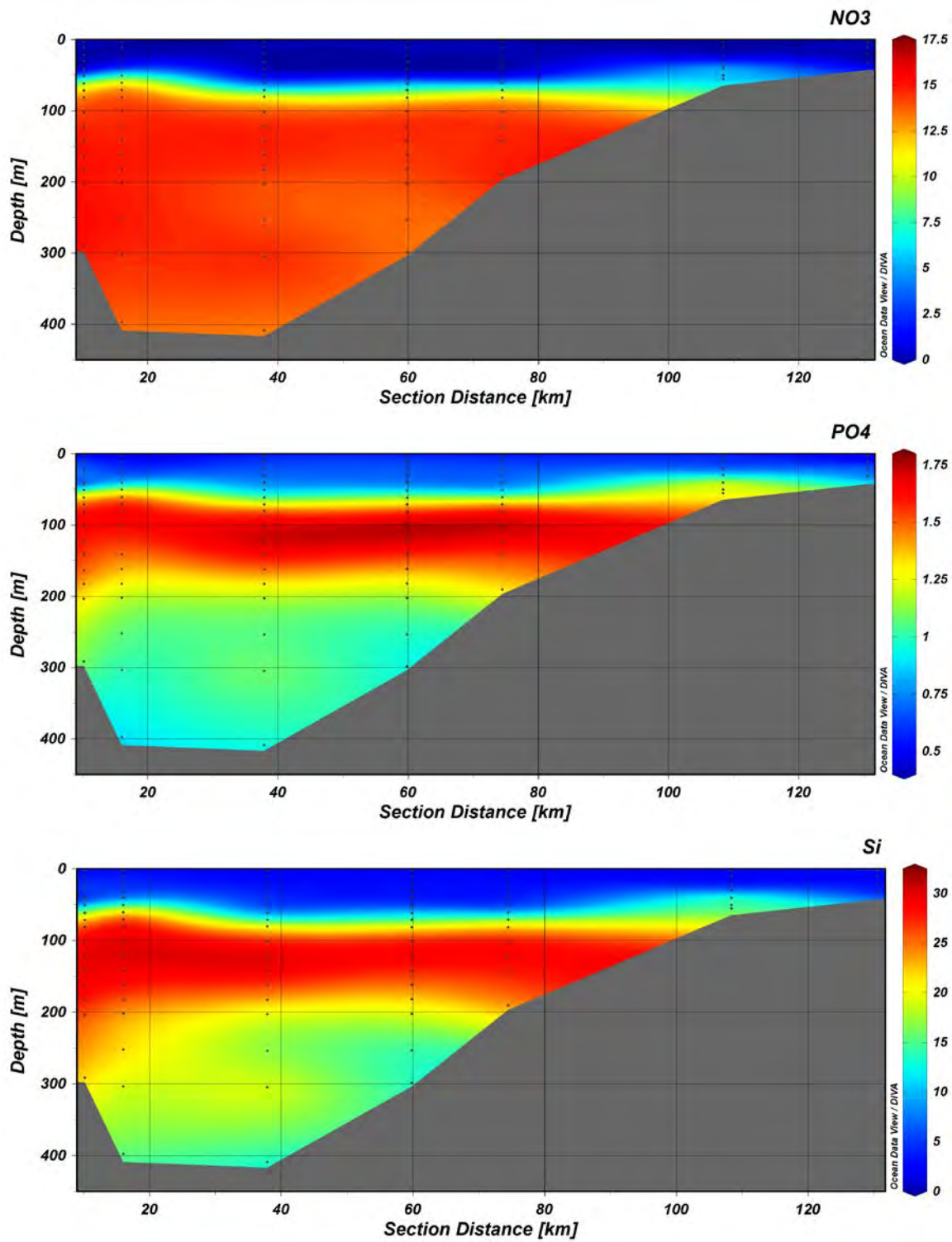


Figure 24-1. Cross-section of the nutrients from Station 437 (left) to Station 420 (right) during Leg 3a.

24.4 Comments and recommendations

Wifi network signal could be a little stronger in the 610 lab. Also, a video feed from the Rosette/CTD computer on the ship's TVs could be useful instead of going in the Rosette control room where activities can hinder the operator's work.

References

- Comiso (2006) *Geophys Res Lett* 33, L18504, doi:10.1029/2006GL027341
- Comiso et al. (2008) *Geophys Res Lett* 35, L01703, doi:10.1029/2007GL031972
- Grasshoff et al. (1999) *Methods of seawater analyses*, Weinheim, New-York
- Holmes et al. (1999) *Can J Fish Aquat Sci* 56:1801–1808
- IPCC (2007) *Climate change 2007: The physical science basis*. Cambridge University Press, Cambridge and New York
- Johannessen et al. (1999) *Science* 286:1937–1939
- Laxon et al. (2003) *Nature* 425:947–950
- McClelland et al. (2006) *Geophys Res Lett* 33, L06715, doi:10.1029/2006GL025753
- Overpeck et al. (1997) *Science* 278:1251–1256
- Peterson et al. (2002) *Science* 298:2171–2174
- Peterson et al. (2006) *Science* 313:1061–1066
- Rysgaard et al. (1999) *Mar Ecol Prog Ser* 179:13–25
- Stabeno & Overland (2001) *EOS* 82:317–321

25 Distribution and biodiversity of microorganisms – Legs 3a, 4a, 4b and 4c

ArcticNet Phase 3 – Marine Biological Hotspots: Ecosystem Services and Susceptibility to Climate Change. <http://www.arcticnet.ulaval.ca/pdf/phase3/marine-ecosystem-services.pdf>

Project leader: Connie Lovejoy¹ (Connie.lovejoy@bio.ulaval.ca)

Cruise participant Leg 3a: Pierre Galand²

Cruise participants Leg 4a, 4b and 4c: Dimitri Kalenitchenko² and Vincent Carrier¹

¹ *Université Laval, Département de biologie / Québec Océan / TAKUVIK, Pavillon Alexandre-Vachon, 1045 avenue de la Médecine, Québec, QC, G1V 0A6, Canada.*

² *Observatoire Océanologique de Banyuls, CNRS-UPMC, 66650 Banyuls sur Mer, France.*

25.1 Introduction

The research was aimed firstly at surveying and mapping the biodiversity and structure of microbial communities in the Canadian Arctic. Microbes here are considered any single celled organism that routinely cannot be observed without a microscope and therefore includes: phytoplankton, heterotrophic protists (microbial eukaryote), Bacteria and Archaea. These groups are responsible for the net production in the Arctic and their interactions within the microbial food web determine the amount of fixed carbon (lipids, sugars, proteins etc.) that is available to higher trophic levels. Microbes also mediate biogeochemical cycling including Carbon, Nitrogen and Sulfur. This work is in the context of the ArcticNet project led by Dr. J-É Tremblay and is a contribution to ArcticNet ARC3Bio program.

This program was planned to repeat sampling along planned ArcticNet Basic and Full stations to complete the time series sampling conducted by C Lovejoy during the ArcticNet program. In addition, surface and deep samples will contribute to an ongoing collaboration between C. Lovejoy and P. Galand and other researchers at CNRS Banyuls sur Mer, on identifying biogeochemical processes mediated by Euryarchaeota. This is part of the project EUREKA led by P. Galand that aims at revealing the diversity and function of marine Euryarchaeota, an important phyla of the domain Archaea. Euryarchaeota account for up to 10% of prokaryotes in the ocean and have not been cultivated. For this reason, genomic approaches will be used to characterize this group from different water masses. Finally, incubations were conducted to test the effect of freshwater on Arctic microbial communities. The experiments aimed at testing if dormant cells are able to start growing when environmental conditions change in the ocean. The project was conducted in the context of melting ice.

25.2 Methodology

Water samples were collected directly from the Niskin-type bottle mounted on Rosette. Depths for sampling were identified on the downward cast based on specific features and a goal of collecting water from a variety of water masses. Samples were collected from Basic and Full stations (Table 25-1 to Table 25-3). For this mission, samples were taken for microbial DNA and RNA, Flow Cytometry, DAPI Eukaryota, FNU and FISH for Bacteria and Eukarya. Flow cytometry samples were preserved in gluaradehyde for biomass estimation and in a Glycine-TE buffer for eventual single amplified genome (SAG) work. Using this technique, single cells were sorted into multiwall plates and their whole genome amplified by random primers then sequenced. Part of the SAG work is financed by the EUREKA project and the rest is contingents on additional funding.

Table 25-1. Samples collected during Leg 3a.

Date	Latitude (N)	Longitude (W)	Station	Cast #	# Depths sampled
22/08/2015	70°36.581	123°02.014	405	1	6
24/08/2015	71°48.000	126°29.000	437	7	6
25/08/2015	71°18.735	127°34.865	408	14	6
25/08/2015	71°03.058	128°30.662	420	20	2
26/08/2015	70°10.614	133°33.233	434	21	2
27/08/2015	71°04.763	133°37.824	435	31	6
29/08/2015	71°25.806	133°59.582	421	44	6
31/08/2015	71°04.763	133°37.824	435	48	6
02/09/2015	75°06.904	120°34.802	514	55	6

Table 25-2. Samples collected during Leg 4a.

Date	Latitude (N)	Longitude (W)	Station	Cast #	# Depths sampled
03/10/2015	74°14.781	091°31.078	304	2	5
04/10/2015	74°07.307	083°19.183	301	6	5
05/10/2015	74°09.382	080°28.449	323	9	5
07/10/2015	76°18.414	073°12.916	111	15	6
08/10/2015	76°19.932	071°11.951	115	21	6
09/10/2015	76°16.232	074°36.012	108	24	5
09/10/2015	76°19.054	075°45.539	105	28	5
10/10/2015	76°23.004	077°24.007	101	34	5

Table 25-3. Samples collected during Leg 4b.

Date	Latitude (N)	Longitude (W)	Station	Cast #	# Depths sampled
11/10/2015	72°29.200	078°45.914	155	35	5
15/10/2015	71°22.788	070°04.273	170	41	5
20/10/2015	71°18.735	127°34.865	177	52	4
21/10/2015	67°28.665	061°45.772	180	54	4
23/10/2015	64°08.971	061°55.454	187	60	5

Table 25-4. Samples collected during the incubation experiment with seawater from Station 177 (Leg 4c).

Date	Flux cytometry	Nutrients	DNA/RNA
23/10/15	18 samples	18 samples	0 samples
25/10/15	18 samples	18 samples	0 samples
26/10/15	0 samples	0 samples	18 samples
27/10/15	18 samples	18 samples	0 samples
29/10/15	18 samples	18 samples	0 samples
31/10/15	18 samples	18 samples	18 samples

25.3 Preliminary results

No preliminary results can be generated, samples will be analysed at Laval University and Banyuls sur Mer.

25.4 Comments and recommendations

We had good weather and all sampling operation went well. During Leg 3a, the extra time we gained gave us the opportunity to sample stations in the M'Clure strait The lab space allocated allowed good working conditions. We thank the Chief Scientist for a well-organised cruise and Captain and crew for their professionalism and support. We just notice it may be a good thing to have a designated person on board for the chemical waste procedure.

26 Trace metal-phytoplankton interactions (GEOTRACES) – Legs 2 and 3b

Project leaders: Maite Maldonado¹ (mmaldonado@eos.ub.ca), Andrew Ross² (andrew.ross@dfo-mpo.gc.ca)

Cruise participants Leg 2: David Semeniuk¹ and Jingxuan Li¹

Cruise participant Leg 3b: Jingxuan Li¹

¹ *University of British Columbia, Department of Earth, Ocean and Atmospheric Sciences, 2020-2207 Main Mall, Vancouver, BC, V6T 1Z4, Canada.*

² *Fisheries and Oceans Canada, Institute of Ocean Science, 9860 West Saanich Road, Sydney, BC, V8L 4B2, Canada.*

26.1 Introduction

Bioactive metals, such as Fe, Cu and Zn, are essential for phytoplankton growth and may potentially limit primary productivity in the sea. Indeed, Fe availability controls primary productivity in 30-40% of the global ocean. Phytoplankton may, in turn, influence trace metal concentrations and speciation in the ocean by; (a) taking up trace elements to fulfill their growth requirements, (b) releasing organic complexes to enhance or prevent metal acquisition, and (c) altering trace metal redox speciation through enzymatic activity (reductases & oxidases) at their cell surface. To gain a better understanding of the biogeochemical cycles of essential trace elements in the global ocean, it is therefore imperative to investigate the interactions between primary producers and the distribution and speciation of bioactive trace elements. During the 2 Arctic cruises in the summer of 2015, the team aimed to investigate how micronutrient supply and speciation affects primary productivity, photosynthetic efficiency (in collaboration with Dr. Tortell), species composition and trace metal elemental composition of phytoplankton. In order to achieve this, samples were collected to determine vertical profiles of particulate bioactive metals at all the stations, as well as samples to determine trace metal speciation (in collaboration with Andrew Ross at IOS). In the euphotic zone and the chlorophyll maximum, the speciation data and the particulate metal data will be combined with HPLC pigment data (which we collected also) to determine how phytoplankton community composition affects particulate metals in the water column. Data will also be examined in the context of dissolved metals data (J. Cullen and K. Orians) to establish how dissolved metals affect the trace metal composition of particles in the water column.

Moreover, during Leg 2 in the CAA, pCO₂ / pH manipulation experiments were conducted at 2 stations (in collaboration with Tortell) as to investigate how changes in pH affect Fe bioavailability to polar plankton communities, using short-term Fe uptake assays. These data will also be combined with the dissolved and speciation trace metal data. The project also aimed at establishing what controls Fe transport in indigenous Arctic plankton communities. To do so, Fe transport kinetic parameters (using short-term Fe uptake) were

determined for 2 plankton size fractions at 5 stations in the first cruise along the CAA. These data will be examined along the particulate trace metal data, the dissolved metals and the Fe speciation data.

To achieve the objectives, the followings were determined during Leg 2:

- Phytoplankton biomass (size-fractionated chlorophyll *a*) and species composition (by microscopic examination / HPLC analysis of accessory pigments (Maldonado/Tortell) and flow cytometry (Varela/Maldonado)) were determined;
- Trace metal quotas of size- fractionated particles (using HR-ICPMS, as well as radiotracers);
- Phytoplankton photosynthetic efficiency and photosynthesis-irradiance curves using active fluorescence;
- Size-fractionated rates of trace metal uptake at saturating and sub-saturating concentrations, as well as micronutrient uptake kinetics using radiotracers.

These physiological and ecological data will be complemented with differential proteomic analyses of samples collected from regions with distinct trace metal characteristics, and will enable us to elucidate how trace elements control protein expression. Various shipboard incubations will be set up to test whether phytoplankton communities are limited by one or various trace elements, or co-limited by trace metals/light/macronutrients.

26.2 Methodology

After collecting sample for salinity and nutrients (if applicable), the GOFLO bottle (approximately 10 L water remaining) was drained to a cubitainer through a piece of masterflex tubing and a spigot, which replaced the cap of cubitainer. Then the water was filtered off-line through 0.45 micrometer poresize SUPOR filter, which was dried afterwards. Filtrate was collected for volume measurement. Filtration was done in a clean 'bubble' built in Aft lab in Leg 2 and forward filtration lab during Leg 3b.

For Leg 2 Fe speciation operations, 2x500mL bottles (rinsed thrice with sample water) were 90% filled by the TM team with gravity-filtered seawater from the TM rosette at each target depth. Samples stored at -20°C.

Table 26-1. List of particulate trace metal samples during Leg 2.

Depth	Goffo	Sample	Station	Event info (UTC)	Depth	Goffo	Sample	Station	Event info (UTC)
3000m	2	2		1 – July 13	40	5	712		92 – Aug 9
2750m	4	4		TM rosette	LL=0.2	6	713		TM rosette
2600m	6	6		2342h	LL=1	7	714		1920h
2450m	8	8		56.12017N	Chlmax	9	716		74.52142N
2450m	9	9		53.3615W	LL=30	10	717		80.5621W
2300m	10	10			LL=50	11	718		
2300m	11	11			600m	1	750		95 – Aug 10
2150m	12	12	K1	3 – July 14	400m	3	752	CAA1	TM rosette
200m	6	18		TM rosette	300m	5	754		0044h
				0330h	200m	7	756		74.52197N
				56.11823N					80.574W
				53.3637W					
800m	1	49		5 – July 14	150m	9	758		
600m	3	51		TM rosette	100m	12	761		
				0809h					
				56.12012N					
				53.3667W					
2400m	4	148		14 – July 17	40m	4	985		117 – Aug 11
2000m	6	150		TM rosette	Chlmax	7	988		TM rosette
2000m	7	151		0208h	20m	9	990		0907h
2000m	9	153		60.44933N	10m	11	992		73.80933N
				56.5441W					80.4112W
1800m	10	154			600m	2	1026	CAA3	123 – Aug 11
1600m	11	155			400m	4	1028		TM rosette
2700m	3	182	LS2	16 – July 17	300m	6	1030		1905h
2600m	4	183		TM rosette	200m	7	1031		73.81622N
2200m	8	187		0532h	150m	10	1034		80.4931W
1600m	11	190		60.45237N	100m	12	1036		
				56.5635W					
700m	6	203		18 – July 13	150m	1	1240		149 – Aug 14
				TM rosette				CAA4	TM rosette
				1525h					0157h
				60.4534N					74.1223N
				56.5506W					91.5109W
2000m	12	308		28 – July 18	40m	7	1246		
				TM rosette	Chlmax	10	1249		
				1715h					
				60.44847N					
				56.5495W					
1000m	2	312		34 – Aug 3	10m	11	1250		
700m	4	314		TM rosette	220m	3	1074		130 – Aug 12
500m	7	317		0343h	100m	12	1082		TM rosette
				66.85768N					1814h
				59.0632W					74.53882N
									90.8045W
300m	10	320			LL=1	7	1143		136 – Aug 13
150m	2	378	BB1	40 – Aug 3	Chlmax	9	1145		TM rosette
LL=0.2	5	381		TM rosette	LL=50	11	1147	CAA 5	0141h
				1240h					74.5371N
				66.85778N					90.8078W
				59.0716W					

LL-1	7	383			240	1	1339		160 – Aug 15
Chlmax	9	384			190	3	1341		TM rosette
LL-30	10	386			150	5	1343		0418h
LL-50	12	388			75	7	1345	CAA6	74.75433N
1000m	1	603		74 – Aug 7	Chlmax	10	1348		97.4575W
600m	5	607		TM rosette	10	11	1349		
300m	7	609		2208h	190m	1	1409		168 – Aug 15
				72.74973N					TM rosette
				66.9885W					2245h
2250m	1	657		79 – Aug 8	160m	3	1411		73.67288N
2100m	5	661		TM rosette	120m	4	1412	CAA7	96.5238W
1600m	6	662		0907h	75m	7	1415		
150m	7	663	BB2	72.75098N	Chlmax	10	1418		
LL-0.2	9	665		66.9986W	10m	11	1419		
LL-1	11	667							
Chlmax	2	689		82 – Aug 8					
LL-30	4	691		TM rosette					
LL-10	9	696		1243h					
				72.750378N					
				66.9872W					
1000m	2	444		54 – Aug 5					
700m	4	446		TM rosette					
500m	7	449		1843h					
300m	12	454		71.40887N					
				68.5976W					
150m	2	486	BB3	57 – Aug 6					
LL-0.2	5	489		TM rosette					
LL-1	7	491		0104h					
Chlmax	9	493		71.40748N					
15m	10	494		68.5991W					
10m	12	496							

Table 26-2. List of samples for speciation during Leg 2.

Depth	Station	Event info (UTC)
1000m	LS2	18–July13 TM rosette, 1525h 60.4534N, 56.5506W
500m		34–Aug3 TM rosette, 0343h 66.85768N, 59.0632W
50m	BB1	40–Aug3 TM rosette, 1240h 66.85778N, 59.0716W
10m		
50m	BB2	69–Aug7 TM rosette, 0440h 72.7495N, 66.9867W
10m		
1000m		74–Aug7 TM rosette, 2208h 72.74973N, 66.9885W
50m	BB3	57–Aug6 TM rosette, 0104h 71.40748N, 68.5991W
10m		
43m	CAA1	92–Aug9 TM rosette, 1920h 74.52142N, 80.5621W
10m		
40m	CAA2	108–Aug10 TM rosette, 1904h 74.31532N, 80.4993W
10m		
40m	CAA3	117–Aug11 TM rosette, 0907h 73.80933N, 80.4112W
15m (4)		
10m		
40m	CAA4	149–Aug14 TM rosette, 0157h 74.1223N, 91.5109W
Chlmax		
10m		
40m	CAA5	136–Aug13 TM rosette, 0141h 74.5371N, 90.8078W
10m		
75m	CAA6	160–Aug15 TM rosette, 0418h 74.75433N, 97.4575W
Chlmax		
10m		
75m	CAA7	168–Aug15 TM rosette, 2245h, 73.67288N, 96.5238W
Chlmax		
Chlmax		
10m		

Table 26-3. List of particulate trace metal samples during Leg 3b.

Depth	Gofl	Sampl	Statio	Event info	Depth	Gofl	Sampl	Statio	Event info
Tmin	2	2020		402 – Sept 7	Tmin	2	2345		446 – Sept 14
Tmax	4	2022		TM rosette	150m	4	2347		TM rosette
Chlma	7	2025		2200h	Chlma	7	2350		TM rosette
Partma	9	2027		75.06.80N	25m	11	2354		2147h - 2212h
10m	11	2029		120.38.51W	1400	2	2363		448 – Sept 15
400m	2	2060		406 – Sept 8	800m	4	2365		TM rosette
350m	4	2062	CB-1	TM rosette	Tmax2	7	2368	CB-4	TM rosette
300m	6	2064		0310h	10m	11	2372		0310h - 0417h
				75.07.04N					74.00.160N
250m	7	2067		120.37.89W	2500m	4	2383		451 – Sept 15
200m	10	2068			2000m	7	2386		TM rosette
150m	12	2070			3500m	11	2381		1234h - 1451h
200m	2	2127		416 – Sept 9	1000m	1	2465		459 – Sept 17
Tmin	4	2129		TM rosette	1000m	2	2466		TM rosette
Tmax	6	2131			300m	3	2467		TM rosette
Chlma	7	2132		01h - 0156h	300m	4	2468		0014h - 0117h
10m	11	2136		75.48.88N	71m	5	2469		74.35.57N
1200m	2	2169		419 – Sept 10	71m	6	2470	CB 4.2	148.12.60W
800m	4	2171		TM rosette	10m	11	2475	pMe	
400m	7	2174			10m	12	2476	interc	
25m	12	2179	CB-2	0815h - 0913h	90m	3	2532		466 – Sept 24
200m	2	2249		431 – Sept 11	Chlma	7	2536		TM rosette
Tmin	4	2251		TM rosette	Partma	9	2538		TM rosette
Chlma	7	2254			Mld	11	2540		0328h - 0348h
25m	9	2256		2200h - 2219h	450m	2	2573		469 – Sept 24
1400m	2	2285		434 – Sept 12	350m	4	2575		TM rosette
800m	4	2287		TM rosette	250m	6	2577		TM rosette
480m	7	2290			200m	9	2580	CAA 8	0932h - 1006h
Mld	11	2294	CB-3	0521h - 0625h	150m	11	2582		74.08.36N
2500m	5	2360		444 – Sept 13	120m	12	2583		108.50.16W
3500m	11	2357		TM rosette	90m	2			481 – Sept 27
2000m	7	2362			70m	3			TM rosette
				0933h -	Chlma	9			TM rosette
				01143h	Mld	11			0512h - 0516h
				76.59.60N		4	2672		485 – Sept 27
				140.04.26W		6	2674		
						9	2676	CAA 9	TM rosette
						10	2677		1000h - 1023h
									76.19.82N
									96.45.30W

27 Biogenic gases, ocean acidification, primary production and photo-physiology (GEOTRACES) – Leg 2

Project leader: Philippe Tortell¹ (ptortell@eos.ubc.ca)

Cruise participants Leg 2: Philippe Tortell¹, Nina Schuback¹, Clara Hoppe², Tereza Jarnikova¹ and Dave Seminiuk¹

¹ *University of British Columbia, Department of Earth, Ocean and Atmospheric Sciences, 2020-2207 Main Mall, Vancouver, BC, V6T 1Z4, Canada.*

² *Alfred Wegener Institute, Am Alten Hafen 26, 27568, Bremerhaven, Germany.*

27.1 Introduction

Marine phytoplankton play a vital role in the global biogeochemical cycles of nutrients and climate-active gases. Primary production removes CO₂ from surface waters, and leads to the accumulation of O₂ and dimethylsulfide (DMS), while bacterial respiration in sub-surface waters leads to the production of methane (CH₄) and nitrous oxide (N₂O). These gases (CO₂, DMS, CH₄ and N₂O, in particular) influence the atmospheric radiative balance, thereby affecting global climate. It is thus important to understand the biogeochemical controls on primary productivity and CO₂, DMS, CH₄ and N₂O cycling in marine waters. To date, there have been relatively few studies of these gases in high Arctic marine waters, and it is presently unclear how primary productivity and gas cycling may respond to future changes in surface ocean conditions, including increased acidity and temperature, reduced sea ice cover and changing light levels and surface water stratification. The research project was designed to examine these questions. In particular, the work was designed to address the following specific objectives:

- Generate high spatial resolution maps of surface water concentrations and sea-air fluxes of CO₂ and DMS across different hydrographic domains in Subarctic and Arctic waters. Relate variability in surface water gases to other environmental conditions (e.g. chlorophyll a, sea ice cover, mixed layer depths, etc.);
- Use high resolution $\Delta\text{O}_2/\text{Ar}$ (biological oxygen saturation) measurements to map the spatial distribution of net community production (NCP). Couple these NCP estimates with continuous measurements of phytoplankton photo-physiology derived from Fast Repetition Rate Chla Fluorometry (FRRF);
- Map the distribution of surface water concentrations of DMSP and DMSO (reduced sulfur compounds derived from DMS);
- Quantify gross primary productivity in surface waters, based on measured rates of carbon uptake and photosynthetic electron transport, and examine the light-dependency of these rates. Use the results to examine the electron requirements for carbon fixation ($\phi_{e,c}$);
- Conduct CO₂ and light controlled manipulation experiments to examine phytoplankton physiological and ecological responses to altered seawater CO₂ concentrations and irradiance levels.

27.2 Methodology

A wide range of analytical and experimental techniques were used to conduct the work. Surface gas measurements were conducted using automated purge and trap gas chromatography (PT-GC; for DMS/P/O), and membrane inlet mass spectrometry (MIMS; for CO₂, ΔO₂/Ar, and DMS). These instruments were set up in the forward filtration lab, and programmed to operate autonomously, sampling from the ship's seawater intake, with automated calibration sequences. Photo-physiological measurements (e.g. variable Chla fluorescence, F_v/F_m , and cross sectional absorption area, σ) were also measured from the ship's seawater intake (forward filtration lab) using an FRRF equipped with a flow-through measurement cuvette. Discrete depth profile samples for CH₄ and N₂O measurements were collected from the *Amundsen* Rossette, for subsequent mass spectrometric analysis at UBC.

Primary productivity was assessed at all of the major stations using short-term (2 hour) ¹⁴C incubation assays, and with FRRF measurements of photosynthetic electron transport rates. Samples were collected from several depths in the upper water column and processed immediately. For both of these assays, measurements were conducted over a range of light levels to generate photosynthetic light curves. A variety of other samples (e.g. total and size fractionated chla, HPLC analysis of photosynthetic pigments) were collected to support the productivity measurements.

Two CO₂ and light manipulation experiments were conducted using deck-board incubations. Water for these experiments was collected using the Trace Metal Clean Rosette or from a surface water pump. Water for incubations was collect near Stations K1 and BB3. Phytoplankton were allowed to grow in 8L bottles placed in incubators with different light screening (~ 50% and 20% of surface irradiance levels), with continuous bubbling with either 400 or 1200 ppm CO₂ gas mixtures. Phytoplankton growth rates were followed by daily measurements of chla and nutrient concentrations, and additional photo-physiological measurements were made using FRRF. When phytoplankton had consumed ~ 75% of the nutrients in bottles, most of the volume was removed (for use in a variety of physiological assays), and replaced with 0.2 μm filtered water. This dilution approach was used to prolong the incubation experiments and observe subtler ecological changes (e.g. species shifts) across the different treatments. Water removed from the incubation bottles was sampled for measurements of Chla (total and size fractionated), POC, accessory photosynthetic pigments (via HPLC), DNA/RNA, flow cytometry, and iron uptake rates (using ⁵⁵Fe) and primary productivity (using ¹⁴C and FRRF).

27.3 Preliminary results

Figure 27.1 and Figure 27.2 below show the distribution of various hydrographic properties and biogenic gases across the cruise track. As shown in these figures, large gradients in all surface water properties were observed. Over much of the cruise track, surface waters were under-saturated in CO₂ (creating a favourable gradient for oceanic CO₂ uptake) and exhibited biologically- induced O₂ supersaturation ($\Delta O_2/Ar > 0$). NCP estimates will be derived from these data using information on surface wind speeds and mixed layer depth estimate, as will estimates of sea-air CO₂ and DMS fluxes. DMS concentrations varied by a factor of ~ 10 , with sharp gradients often coinciding with rapid changes in pCO₂ and $\Delta O_2/Ar$. Across the cruise track, strong hydrographic fronts (i.e. rapid changes in salinity or surface temperature), were often associated with productivity hot-spots, suggesting a potential role for physical nutrient supply in stimulating surface water productivity.

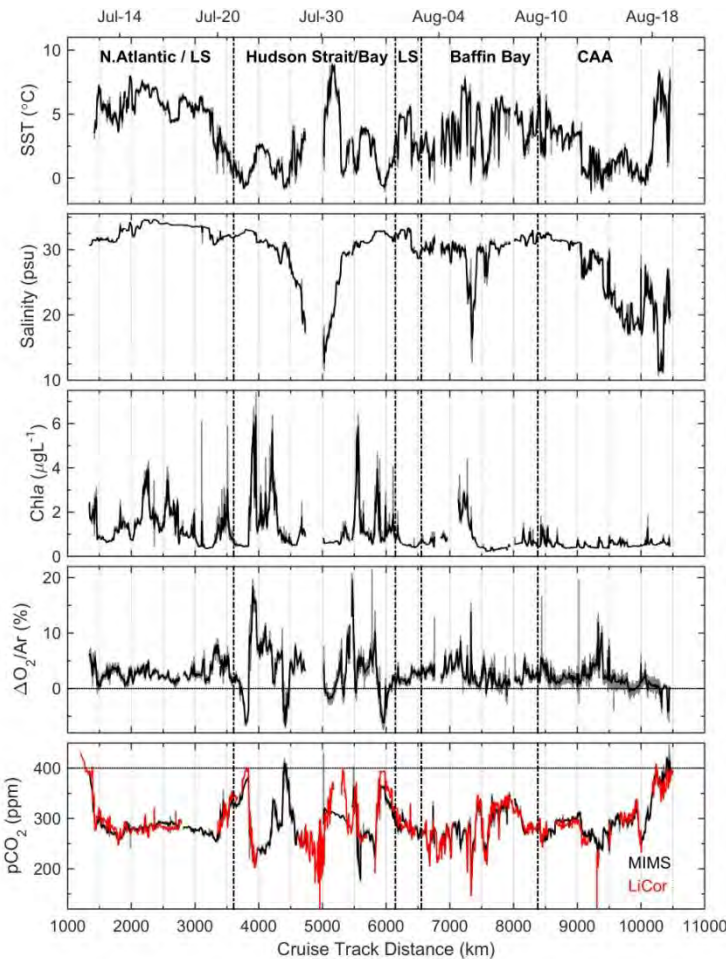


Figure 27-1. Spatial distribution of hydrographic parameters and biogenic gases along the cruise track. Note that horizontal lines on the pCO₂ and $\Delta O_2/Ar$ plots represent atmospheric saturation values. Note also that the data presented here have only received a very preliminary quality control, and do not necessarily represent the final processed values.

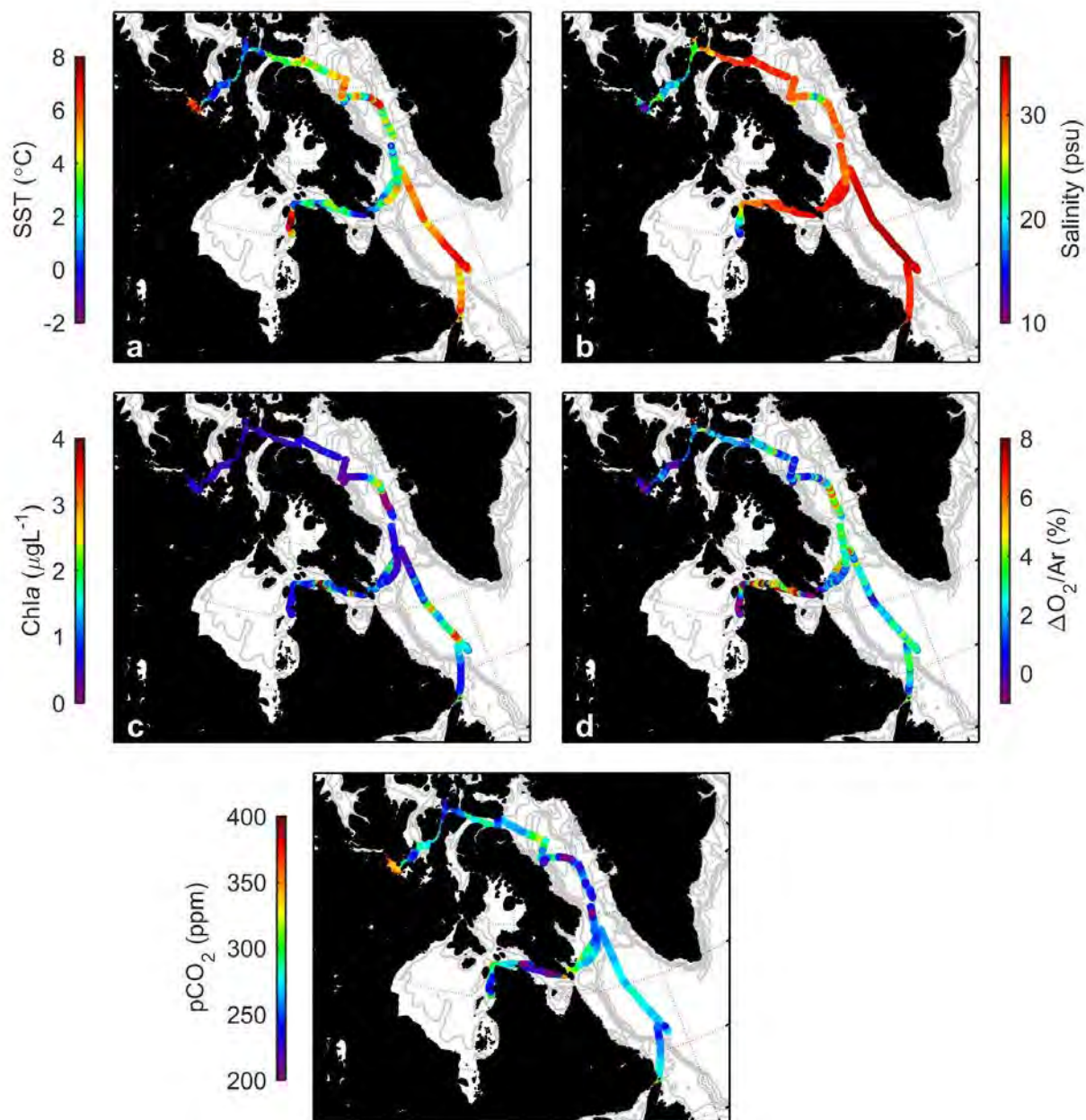


Figure 27-2. Spatial distribution of gases and hydrographic properties along the cruise track.

Figure 27.3 shows the distribution of various photo-physiological properties (measured by FRRF) along the cruise track. Over much of the cruise track, strong diel (day-night) cycles in phytoplankton photo-physiology were observed. For example, the mid-day decrease in variable chlorophyll fluorescence (F_v/F_m), is indicative of a down-regulation of photosynthetic light harvesting capacity during periods of high light. This is a mechanism used for photo-protection.

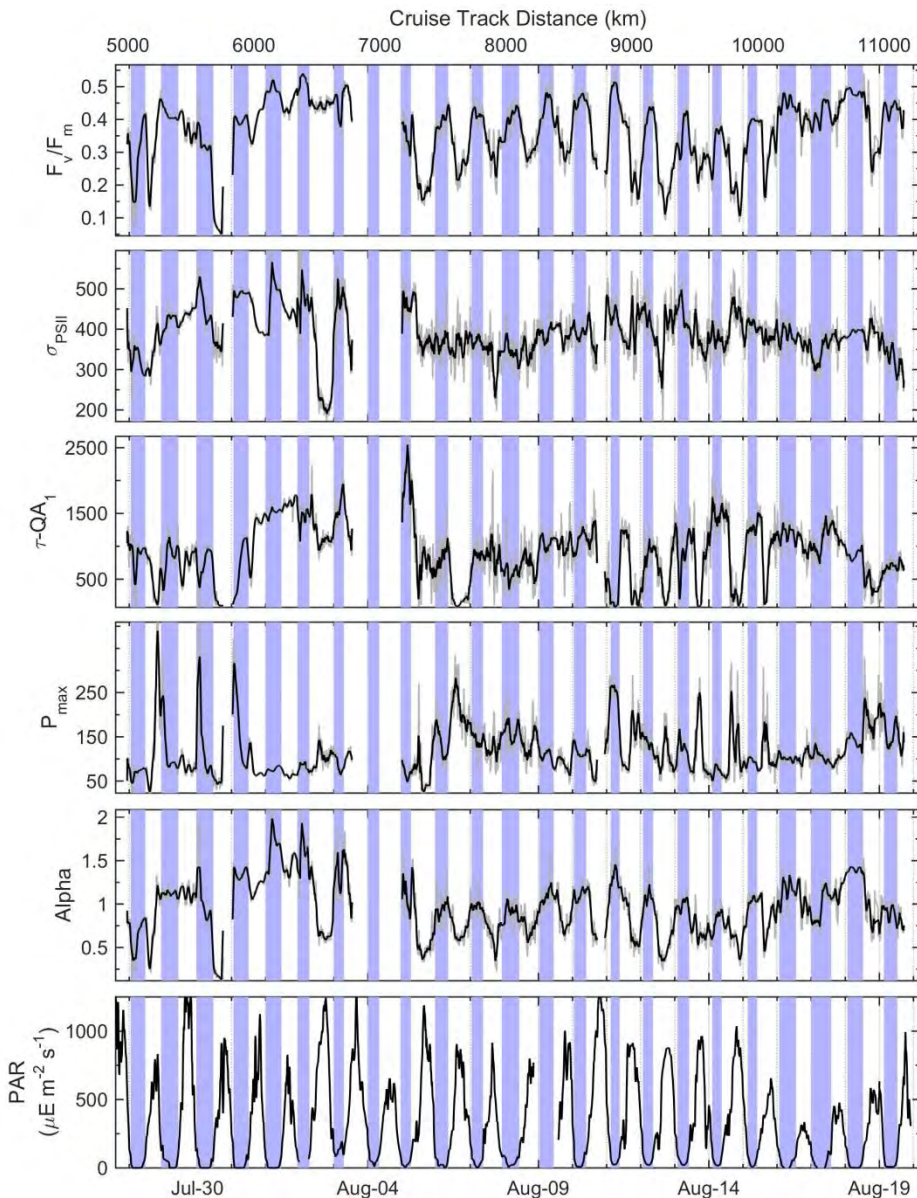


Figure 27-3. Continuous underway measurements of photoplankton photo-physiological properties were measured using fast repetition rate fluorometry (FRRF). The bottom panel shows surface irradiance cycles, while other panels show a range of other photo-physiological characteristics of surface water phytoplankton. For example, variable fluorescence (F_v/F_m), is used as a measure of the photosynthetic efficiency of electron capture in Photosystem II (PSII). This variable is often down-regulated during mid-day periods of high irradiance as a means of photo-protection. The variables P_{max} and Alpha represent the maximum (light saturated) electron transport rates and initial light-dependent slopes derived from rapid light curves.

Primary productivity measurements (Figure 27.4) enabled to further characterize the photosynthetic light dependency of phytoplankton assemblages. Excellent results with both ^{14}C assays were obtained, and with FRRF measurements of electron transport rates (ETR).

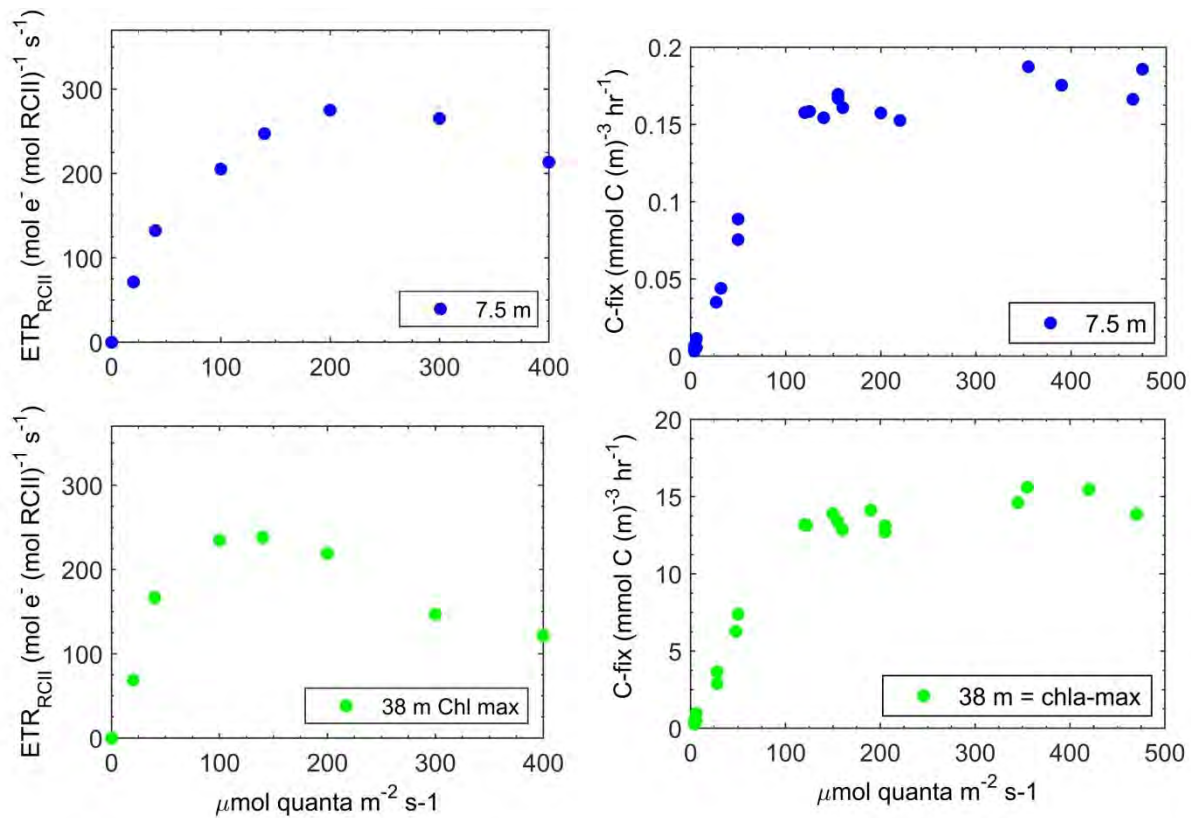


Figure 27-4. Rates of gross primary productivity determined from ^{14}C bottle assays (left hand panels), and from FRRF measurements of electron transport rates (ETR). Results are from Station K1 in the southern Labrador Sea. The curves show a characteristic saturation behavior as a function of irradiance. Bottom panels show data from the deep chlorophyll max, while top panels show results from the surface mixed layer assemblages (7.5 m sampling depth). Compilation of our productivity measurements from all stations will provide valuable information on primary productivity in Arctic waters, and its light-dependency.

Finally, preliminary results from the two deck-board incubation experiments (Figure 27.5 and Figure 27.6) demonstrated clear effects of CO_2 and light manipulations in one experiment, with much smaller effects in the second experiment.

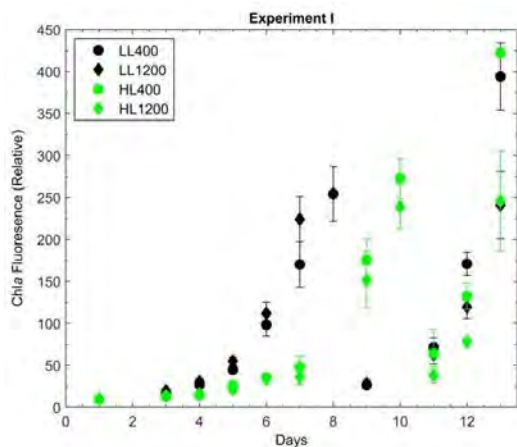


Figure 27-5. Time course of phytoplankton biomass (chlorophyll a) in the first CO_2 - light incubation experiment. LL and HL represent low and high light treatments, respectively, while the numbers refer to the CO_2 level (in ppm) used for each treatment. In this first experiment, we observed an initial decrease in

growth rates of the high light treatment, with only a small CO₂ effect. We have a suite of other physiological and biochemical measurements that will help to understand the mechanisms underlying these responses.

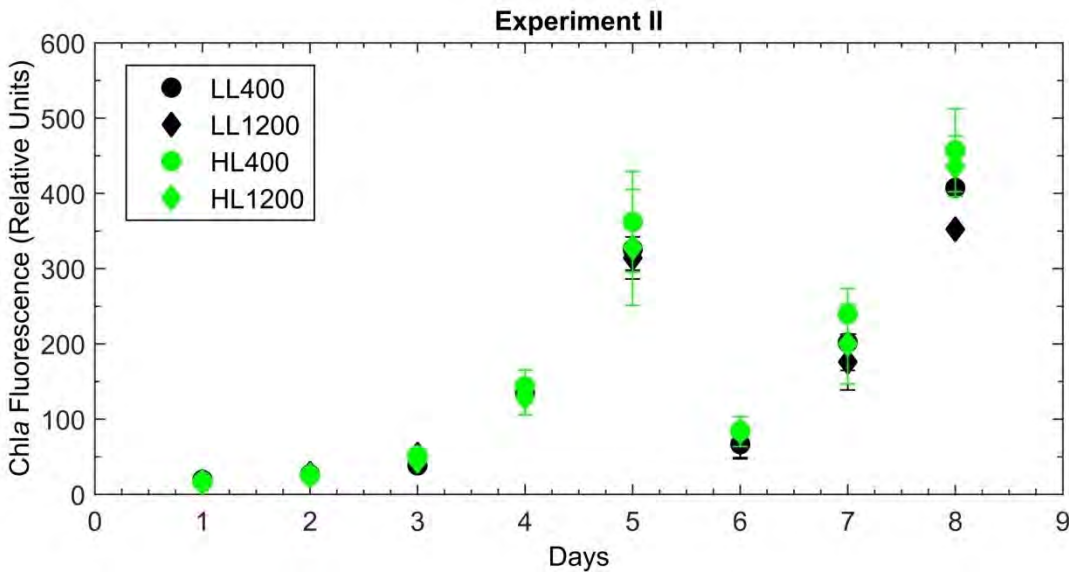


Figure 27-6. As for Fig. 5.1.10.5, but for the second incubation experiment. In this experiment (water collected near Station BB3), no significant effects across the light or CO₂ treatments were observed.

27.4 Comments and recommendations

We experienced a range of technical issues with a variety of ship-board equipment (winches, cranes, moon pool hydraulics etc.). These presented some minor delays, but were all quickly rectified by the excellent engineering staff. On at least one occasion, crew were asked to put in over-time hours to resolve time-sensitive problems. We did find it rather cumbersome to run gas lines from the containers on the foredeck to the forward filtration lab. Perhaps some kind of sleeve could be put in place to make it easier to slide gas lines through. I also found that the seawater supply to the forward filtration lab (and other parts of the ship) has a lot of rust coming through. I'm not sure how this could be addressed in the future.

28 Phytoplankton production and biomass – Legs 2, 3a, 4a and 4b

ArcticNet Phase 3 – Marine Biological Hotspots: Ecosystem Services and Susceptibility to Climate Change. <http://www.arcticnet.ulaval.ca/pdf/phase3/marine-ecosystem-services.pdf>

Project leaders: Michel Gosselin¹ (michel_gosselin@uqar.ca) and Michel Poulin² (mpoulin@mus-nature.ca)

Cruise participant Leg 2: Marjolaine Blais¹

Cruise participants Leg 3a: Joannie Charette¹ and Michèle Pelletier-Rousseau¹

Cruise participants Leg 4a: Marjolaine Blais¹ and Virginie Galindo³

Cruise participant Leg 4b: Virginie Galindo³

¹ *Université du Québec à Rimouski (UQAR), Institut des sciences de la mer (ISMER), 310 allée des Ursulines, Rimouski, QC, G5L 3A1, Canada.*

² *Canadian Museum of Nature, P.O. Box 3443, Station D, Ottawa, ON, K1P 6P4, Canada.*

³ *Centre for Earth Observation Science, University of Manitoba, 463 Wallace Building, Winnipeg, MB, R3T 2N2, Canada.*

28.1 Introduction

Primary production plays a central role in the oceans as it supplies organic matter to the higher trophic levels, including zooplankton, fish larvae and marine mammals and birds. Marine polar ecosystems are particularly sensitive to any changes in primary production due to their low number of trophic links (Grebmeier et al. 2006; Moline et al. 2008; Post et al. 2009). The Arctic Ocean is changing as evidenced by the decrease in sea ice thickness and extent (Stroeve et al. 2007; Kwok et al. 2009), the early melt and late freeze-up of sea ice (Markus et al. 2009) and the enhancement of the hydrological cycle (Peterson et al. 2006; Serreze et al. 2006). These environmental changes have already altered the phytoplankton biomass distribution in the Arctic Ocean (Arrigo et al. 2008; Pabi et al. 2008). In this context, the general objectives of the research project were to:

- Determine the spatial and temporal variability in production, biomass, abundance and taxonomic composition of the phytoplankton communities;
- Determine the role of environmental factors on the phytoplankton dynamics and its variability in Baffin Bay, in the Canadian Arctic Archipelago and in the Beaufort Sea.

To avoid duplication of measurements with the ones done by GEOTRACES team, specific objectives for Leg 2 were reduced to determine:

- downwelling incident irradiance, every 10 minutes, with a Li-COR 2 pi sensor;
- transparency of the upper water column with a Secchi disk;
- underwater irradiance profile with a PNF-300 probe;
- chlorophyll *a* and pheopigment concentrations with a Turner Designs fluorometer (3 size- classes: >0.7 µm, >5 µm, >20 µm);
- phytoplankton production using the ¹⁴C assimilation method (2 size-fractions: >0.7 µm, >5 µm).

In addition to the specific objectives listed above, objectives for Legs 3a and 4 included:

- concentrations of dissolved organic carbon (DOC), total organic carbon (TOC), total dissolved nitrogen (TDN) and total nitrogen (TN) with a Shimadzu TOC-V_{CPN} analyzer;
- abundance and taxonomic composition of phytoplankton using the inverted microscopy method;

An additional objective for Leg 3a was to determine the abundance of pico- and nanophytoplankton and heterotrophic bacteria by flow cytometry

28.2 Methodology

At each water column station, water samples were collected with 12 L Niskin-type bottles attached to the CTD-Rosette. During the daytime, the depth of the euphotic zone was determined with the Secchi disk and the PNF-300 probe. Size-fractionated (3 size-classes: >0.7 μm , >5 μm and >20 μm) chlorophyll *a* concentrations were measured onboard the ship at each sampling depth with a Turner Designs fluorometer (model 10-AU). Size-fractionated (2 size-classes: >0.7 μm and >5 μm) primary production was estimated at 7 optical depths in the water column (i.e. 100%, 50%, 30%, 15%, 5%, 1%, and 0.2% of the surface irradiance) following JGOFS protocol for simulated *in situ* incubation. The other samples collected during this expedition will be analyzed at ISMER. Detailed sampling activities are summarized in Table 28-1 to Table 28-3. Chlorophyll *a* data will be used for the calibration of the chlorophyll *a* fluorescence sensor. During Leg 2, PAR data, downwelling incident irradiance and underwater irradiance profiles, were also shared with GEOTRACES.

Table 28-1. Sampling operations during Leg 2 of the ArcticNet 2015 Expedition on board the CCCS *Amundsen*.

Station	Cast	Date	Position		Total	Chlorophyll <i>a</i>		Primary production	
			Lat (°N)	Long (°W)		> 5µm	> 20µm	Total	> 5 µm
K1	1	14-Jul-14	56°7.342	53°22.385	X	X	X	X	X
LS-2	6	17-Jul-14	60°27.218	56°32.884	X	X	X	X	X
BB-1	11	3-Aug-14	66°51.397	59°03.544	X	X	X	X	X
BB-3	17	6-Aug-14	71°24.494	68°35.684	X	X	X	X	X
BB-2	20	8-Aug-14	72°45.100	66°59.568	X	X	X	X	X
St 322 (CAA-1)	25	10-Aug-14	74°31.067	80°34.331	X	X	X	X	X
St 300 (CAA-2)	28	10-Aug-14	73°19.288	79°29.603	X	X	X	X	X
St 325 (CAA-3)	35	11-Aug-14	73°48.862	80°28.684	X	X	X	X	X
StCAA-5	45	13-Aug-14	74°32.004	90°48.119	X	X	X	X	X
StCAA-4	50	14-Aug-14	74°7.480	90°30.055	X	X	X	X	X
CAA-6 (Ice edge)	55	15-Aug-14	74°45.431	97°27.461	X	X	X	X	X
CAA-7	59	16-Aug-14	73°39.611	96°32.130	X	X	X	X	X
VS (Ice edge)	61	17-Aug-14	69°52.607	99°32.488	X	X	X		
312	64	17-Aug-14	69°09.896	100°41.771	X	X			
314	65	18-Aug-14	68°58.102	105°27.697	X	X	X	X	X

Table 28-2. Sampling operations during Leg 3a of the ArcticNet 2015 Expedition on board the CCCS *Amundsen*.

Station	Cast	Date (yy-mm-ii)	Position (min)		Chlorophyll <i>a</i>			POC/ PON	DOC/DN TOC/TN	HPLC	Taxo	Cyto. flux	Primary production	
			Lat (°N)	Long (°W)	> 0.7µm	>5µm	>20µm						>0.7µm	>5µm
405	1	15-08-23	70°36.581	123°2.014	X	X	X	X	X	X	X	X	X	X
407	3	15-08-23	71°1.150	126°9.170	X	X	X	X	X	X	X	X	X	X
437	6	15-08-24	71°47.848	126°30.140	X	X	X	X	X	X	X	X	X	X
408	15	15-08-25	71°18.534	127°35.892	X	X	X	X	X	X	X	X	X	X
420	20	15-08-25	71°3.058	128°30.662	X	X	X	X	X	X	X	X	X	X
434	21	15-08-26	70°10.614	133°33.233	X	X	X	X	X	X	X			
435	30	15-08-27	71°4.745	133°37.859	X	X	X	X	X	X	X	X	X	X
421	44	15-08-29	71°25.819	133°59.393	X	X	X	X	X	X	X	X	X	X
535	48	15-08-31	73°24.939	128°11.799	X	X	X	X	X	X	X	X		
536	51	15-08-31	73°25.012	129°21.677	X	X	X	X	X	X	X	X	X	X
518	52	15-09-02	74°33.880	121°27.104	X	X	X	X	X	X	X	X	X	X
514	55	15-09-02	75°6.904	120°38.504	X	X	X	X	X	X	X	X	X	X
510	58	15-09-02	75°38.332	120°38.381	X	X	X	X	X	X	X			

Table 28-3. Sampling operations during Legs 4a and 4b of the ArcticNet 2015 Expedition on board the CCCS *Amundsen*.

Station	Cast	Date (yy-mm-jj)	Position (min)		Chlorophyll a			POC/ PON	DOC/DN TOC/TN	HPLC	Taxo	Cyto. flux	Primary production	
			Lat (°N)	Long (°W)	> 0.7µm	>5µm	>20µm						>0.7µm	>5µm
304	2	15-10-04	74°14.779	91°29.418	X	X	X	X	X	X	X	X	X	X
301	6	15-10-04	74°7.268	83°19.324	X	X	X	X	X	X	X	X	X	X
323	9	15-10-05	74°9.410	80°28.409	X	X	X	X	X	X	X	X	X	X
111	15	15-10-07	76°18.352	73°12.980	X	X	X	X	X	X	X	X		
115	21	15-10-08	76°20.125	71°14.620	X	X	X	X	X	X	X	X	X	X
108	24	15-10-09	76°15.912	74°38.826	X	X	X	X	X	X	X	X	X	X
105	28	15-10-09	76°17.380	75°45.318	X	X	X	X	X	X	X	X		
101	34	15-10-10	76°22.572	77°27.040	X	X	X	X	X	X	X	X	X	X
155	35	15-10-11	72°29.213	78°45.856	X	X	X	X	X	X	X	X		
170	41	15-10-15	71°23.447	70°07.418	X	X	X	X	X	X	X	X	X	X
177	52	15-10-20	67°28.525	63°47.336	X	X	X	X	X	X	X	X	X	X
180	54	15-10-21	67°28.884	61°40.009	X	X	X	X	X	X	X	X		
187	60	15-10-24	64°10.991	60°22.920	X	X	X	X	X	X	X	X		

28.3 Preliminary results

During Leg 2, chlorophyll *a* concentrations varied from about 25 to 120 mg m⁻² in the Labrador Sea and southern Baffin Bay. Large cells (> 5 µm) composed between 20 and 95% of the total biomass (Figure 28.1).

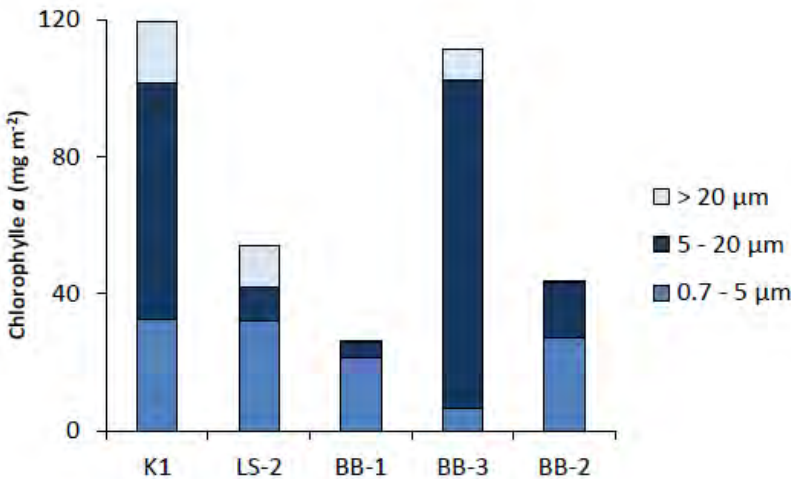


Figure 28-1. Chlorophyll *a* concentrations integrated over 100 m for different size fractions, 0.7-5 µm, 5-20 µm and > 20 µm, in the Labrador Sea and southern Baffin Bay.

Chlorophyll *a* concentrations varied from about 15 to 175 mg m⁻² in the Canadian Arctic Archipelago. Large cells (> 5 µm) dominated biomass at all stations (Figure 28.2). The Station CAA- 6 had highest biomass and was close to an ice edge.

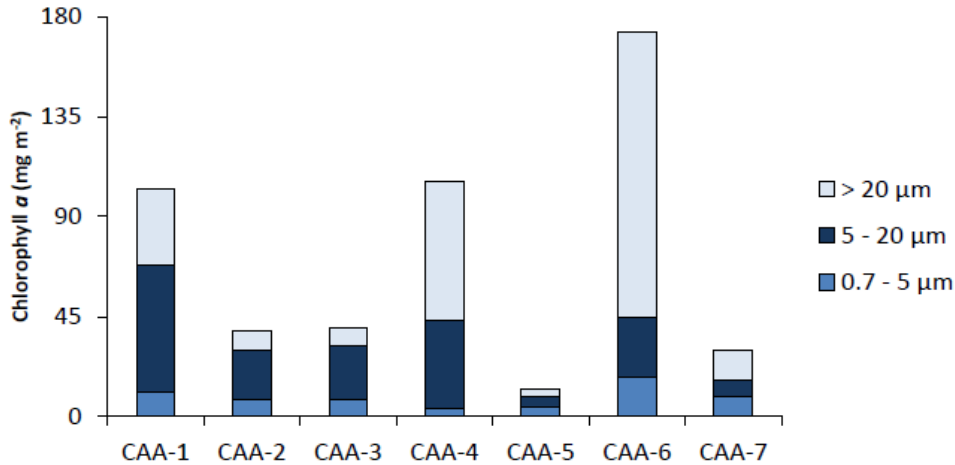


Figure 28-2. Chlorophyll *a* concentrations integrated over 100 m for different size fractions, 0.7-5 μm , 5-20 μm and > 20 μm , in Lancaster Sound, Barrow Strait and Peel Sound.

During Leg 3a, chlorophyll *a* concentrations varied from about 8 to 52 mg m^{-2} . Small cells dominated the biomass in the Beaufort Sea, while they accounted for less than 20% of the biomass in the Amundsen Gulf. The highest biomass was found in the Amundsen Gulf (Figure 28.3).

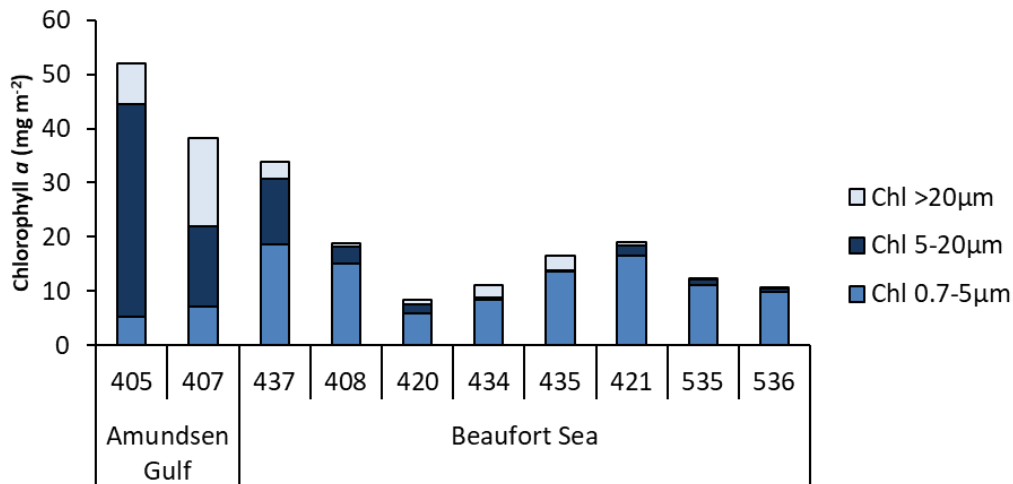


Figure 28-3: Chlorophyll *a* concentrations integrated over 100 m for different size fractions, 0.7-5 μm , 5-20 μm and > 20 μm , at all stations sampled during Leg 3a.

Chlorophyll *a* concentrations varied from about 9 to 180 mg m^{-2} in the Lancaster Sound and southern Baffin Bay. Large cells (> 5 μm) composed between 58 and 95% of the total biomass (Figure 28.4).

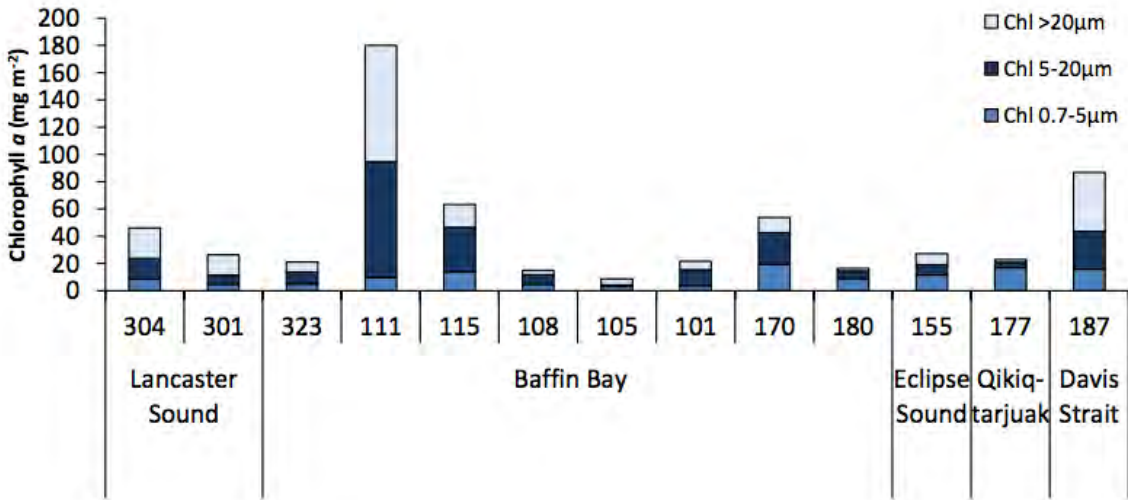


Figure 28-4. Chlorophyll *a* concentrations integrated over 100 m for different size fractions, 0.7-5 μm, 5-20 μm and > 20 μm, in the Lancaster Sound and southern Baffin Bay.

28.4 Comments and recommendations

A speaker could improve the security in the Radvan to hear all important messages from the Captain or other calls.

References

- Arrigo KR, van Dijken G, Pabi S (2008) Impact of a shrinking Arctic ice cover on marine primary production. *Geophys Res Lett* 35:L19603, doi:10.1029/2008GL035028
- Grebmeier JM, Overland JE, Moore SE, Farley EV, Carmack EC, Cooper LW, Frey KE, Helle JH, McLaughlin FA, McNutt SL (2006) A major ecosystem shift in the northern Bering Sea. *Science* 311:1461-1464
- Kwok R, Cunningham GF, Wensnahan M, Rigor I, Zwally HJ, Yi D (2009) Thinning and volume loss of the Arctic Ocean sea ice cover: 2003-2008. *J Geophys Res* 114:C07005, doi:10.1029/2009JC005312
- Landry, M.R., Brown, S.L., Yoshimi M.R., Selph, K.E., Bidigare, R.R., Yang, E.J., & Simmons, M.P. (2008). Depth-stratified phytoplankton dynamics in Cyclone Opal, a subtropical mesoscale eddy. *Deep-Sea Research II* 55: 1348– 1359
- Markus T, Stroeve JC, Miller J (2009) Recent changes in Arctic sea ice melt onset, freezeup, and melt season length. *J Geophys Res* 114:C12024, doi:10.1029/2009JC005436
- Moline MA, Karnovsky NJ, Brown Z, Divoky GJ, Frazer TK, Jacoby CA, Torrese JJ, Fraser WR (2008) High latitude changes in ice dynamics and their impact on polar marine ecosystems. *Ann N Y Acad Sci* 1134:267-319
- Pabi S, van Dijken GL, Arrigo KR (2008) Primary production in the Arctic Ocean, 1998-2006. *J Geophys Res* 113, C08005, doi:10.1029/2007JC004578
- Peterson BJ, McClelland J, Curry R, Holmes RM, Walsh JE, Aagaard K (2006) Trajectory Shifts in the Arctic and Subarctic Freshwater Cycle. *Science* 313:1061-1066

- Post E, Forchhammer MC, Bret-Harte MS, Callaghan TV, Christensen TR, Elberling B, Fox AD, Gilg O, Hik DS, Høye TT, Ims RA, Jeppesen E, Klein DR, Madsen J, McGuire AD, Rysgaard S, Schindler DE, Stirling I, Tamstorf MP, Tyler NJC, van der Wal R, Welker J, Wookey PA, Schmidt NM, Aastrup P (2009) Ecological Dynamics Across the Arctic Associated with Recent Climate Change. *Science* 325:1355-1358
- Serreze MC, Barrett AP, Slater AG, Woodgate RA, Aagaard K, Lammers RB, Steele M, Moritz R, Meredith M, Lee CM (2006) The large-scale freshwater cycle of the Arctic. *J Geophys Res* 111:C11010, doi:10.1029/2005JC003424
- Stroeve J, Holland MM, Meier W, Scambos T, Serreze M (2007) Arctic sea ice decline: Faster than forecast. *Geophys Res Lett* 34: L0950, doi:10.1029/2007GL029703

29 Phytoplankton bloom development and DMS production – Leg 2

ArcticNet Phase 3 – Marine Biological Hotspots: Ecosystem Services and Susceptibility to Climate Change. <http://www.arcticnet.ulaval.ca/pdf/phase3/marine-ecosystem-services.pdf>

Project leaders: Maurice Levasseur¹ (maurice.levasseur@bio.ulaval.ca) and Jean-Éric Tremblay¹ (jean-eric.tremblay@bio.ulaval.ca)

Cruise participants Leg 2: Martine Lizotte¹ and Rachel Husserr¹

¹ *Université Laval, Québec-Océan, Pavillon Alexandre-Vachon room 2078, 1045 avenue de la Médecine, Québec, QC, G1V 0A6, Canada.*

29.1 Introduction

Conspicuous alterations in the Arctic Ocean are underway and include reductions in snow cover as well as sea ice extent and thickness, the occurrence of which is linked to profound modifications in light availability in surface waters below the ice and at its margin. In conjunction, ocean acidification, a phenomenon dubbed “the other CO₂ problem”, is amplified in polar oceans due to the increased solubility of CO₂ in cold water. This study aims to assess the impact of both pH modifications and shifts in light regime on arctic microbial communities and their biosynthesis of the climate-relevant compound dimethylsulfide (DMS) and its algal precursor dimethylsulfoniopropionate.

29.2 Methodology

Two Bioassay incubations of 10 days were planned in Southern Baffin Bay and Northern Baffin Bay in summer 2015 with the intent on simulating conditions encountered by blooming phytoplankton in a progressively acidified Arctic Ocean (6 levels of decreasing pH) submitted to light fields typical of either under-ice (low-light) or open ocean (high-light).

Due to complications with ship time allocation, the team was in the obligation to conduct a first experiment in Davis Strait. For reasons still unknown, this experiment was unsuccessful: phytoplankton biomass (proxied by chlorophyll *a* concentrations) progressively decreased during the 4 days we sampled and FRRF measurements (conducted by Nina Schuback) confirmed the cellular death of the phytoplankton community. As no signs of recovery were seen after 4 days, even in our control bags, it was decided to stop the experiment. A possible explanation for this result could be attributed to light shock as microbial communities were sampled from 55 m depth, approximately 10 m below the deep chlorophyll maximum. Initially, this depth was chosen in order to start the incubations with high concentrations of nutrients (7 μmol of nitrates). Unfortunately, this may have been too deep for the phytoplankton subsequently (and rapidly) exposed to ambient surface light. A suite of tests was also undertaken to improve the methodological procedures related to the acidification protocol. The team would like to thank Constance Guignard (Al Mucci team) for her help with alkalinity measurements during this period of troubleshooting.

A second experiment was conducted at Station BB-3 (71°24.373'N - 70°11.269'W) on August 6th 2015. The initial acidification was conducted following procedures described in Guide to best practices for ocean acidification research and data reporting adding strong acid (HCl 0.02N) and bicarbonate (NaHCO₃ 0.3N) in the bags. Added volumes of bicarbonate and acid were calculated by manipulating the carbonate system with the software CO₂sys in order to fully mimic “natural” ocean acidification: rise of the total inorganic carbon with constant alkalinity. Although alkanities after initial acidification were not entirely similar due to manipulation biases and the difficulty in properly controlling the concentration of added solutions of NaHCO₃ and HCl, target pH's were achieved, as demonstrated in Table 29-1 (note however that these data are not corrected for m-cresol purple dye bias and alkalinity).

Table 29-1. Differences between the actual pH measured after initial acidification at T1 and the targeted values calculated with CO₂sys.

Treatment	Duplicate	pH measured at 4.84°C	pH targeted, calculated at 4.84°C
1L (control)	a	7.915	7.944
	b	7.915	
1H (control)	a	7.935	7.944
	b	7.928	
2L	a	7.780	7.785
	b	7.767	
2H	a	7.754	7.771
	b	7.742	
3L	a	7.638	7.643
	b	7.641	
3H	a	7.620	7.644
	b	7.618	
4L	a	7.445	7.486
	b	7.444	
4H	a	7.390	7.486
	b	7.444	
5L	a	7.336	7.336
	b	7.324	
5H	a	7.291	7.336
	b	7.287	
6L	a	7.141	7.186
	b	7.142	
6H	a	7.162	7.186
	b	7.157	

In order to avoid similar problems encountered during the first experiment, the experimental design was changed by adding a mesh on the incubator thereby reducing the incident light. Moreover, a second 300µm nitex mesh was added on the bags assigned to the low light treatment: those were already covered with one Mylar D film (which cuts UV-B radiation) and one 300µm nitex mesh which allowed approximately 40% of incident light to pass. The transmittance for the high light treatment was 80%: these bags were not covered by neither mesh nor mylar.

Furthermore, the initial water was taken a bit shallower to prevent any light shock (38 meters) although the team had to deal with lower concentrations of nutrients (approximately

5 μmol of nitrates). After filtering the AN rosette water with a 200 μm nitex mesh in order to remove mesozooplankton grazers, 12 bags of 10 liters were filled and the evolution of each bag was followed by subsampling every day during 10 days.

Finally, another core objective of this cruise was the monitoring of ArcticNet stations for water column budgets of sulfur compounds (DMS, DMSP and DMSO). Unfortunately, this part of the scientific goals was greatly reduced through both equipment failures and reduction in ship time allocated to science. The team did however manage to sample a selection of ArcticNet/Geotraces Rosette stations located in Lancaster Sound, Baffin Bay and Peel Sound. The following stations were sampled for total DMSP and dissolved DMSP: CAA1-CAA2-CAA3-CAA4-CAA5-CAA6-CAA7 and 314. Full vertical light profiles (100%, 50%, 30%, 15%, 5%, 1%, 0.2%, sub- chlorophyll maximum (SCM), and 100m) were taken at each of these stations. One of the greatest challenges met during the cruise was the malfunctioning of an injection valve allowing the transfer of gaseous DMS from a purge and trap system towards a Pulsed Flame Photometric Detector (PFPD) Gas Chromatograph. After having worked very well during the first two weeks of the cruise, it then failed entirely following icebreaking maneuvers in Hudson Bay, making it impossible to analyze samples of oceanic DMS.

29.3 Preliminary results

Despite numerous challenges faced during the cruise, the second incubation experiment met with success. This success was in great part due to incredible collaborations fostered before and during the cruise.

An uptake of nitrate was indeed mirrored by an exponential increase in Chl *a* between T1 and T5, reaching a plateau until T8, then decreasing thereafter. The physiological state of the phytoplankton cells was followed through FRRF measurements, which showed a similar trend as that observed for concentrations of Chl *a*. Furthermore, the team was able to make DMS measurements on their underway PFPD Gas Chromatograph while remaining put on various stations between BB3 and CAA7. Initially low concentrations of DMS (ca. 0.5nM) increased steadily during the course of the experiment, especially in the control bags, to reach levels of ca. 20nM. A core variable measured during the incubations was pH. Alkalinity measurements were conducted onboard and will be further examined in the coming weeks. Several other variables were sub-sampled and will be analyzed post-cruise in Laval University laboratories: total DMSP, dissolved DMSP, total DMSO, bacterial abundance, flow cytometry, HPLC, phytoplankton taxonomy (Table 29-2).

Table 29-2. Variables measured during the 10-day Bioassay incubation experiment (water initially sampled at station BB3)

	T0	T1	T2	T3	T4	T5	T6	T7	T8	T9
pH	X	X	X		X		X			
DIC	X	X			X					
Alkalinity	X	X			X					
Salinity	X									X
Chl a	X	X	X	X	X	X	X	X	X	X
Nutrients	X	X	X	X	X	X	X	X	X	X
Taxonomy	X					X				X
Cytometry	X	X	X	X	X	X	X	X	X	X
HPLC	X							X		X
DMSPt	X	X	X	X	X	X	X	X	X	X
DMSPd	X	X	X	X	X	X	X	X	X	X
DMSO	X	X	X	X	X	X	X	X	X	X
DMS	X		X		X	X		X	X	X
FR/RF		X		X	X		X	X		X

30 Zooplankton and fish ecology/acoustic – Legs 2, 3a, 3b, 4a, 4b and 4c

ArcticNet Phase 3 – The Arctic cod (*Boreogadus saida*) ecosystem under the double pressure of climate change and industrialization. <http://www.arcticnet.ulaval.ca/pdf/phase3/arctic-cod.pdf>

ArcticNet Phase 3 – Long-Term Observatories in Canadian Arctic Waters.

<http://www.arcticnet.ulaval.ca/pdf/phase3/marine-observatories.pdf>

Project leader: Louis Fortier¹ (Louis.fortier@bio.ulaval.ca)

Cruise participants Leg 2: Caroline Bouchard¹ and Mathieu LeBlanc¹

Cruise participants Leg 3a: Mathieu LeBlanc¹, Gabrielle Nadaï¹ and Charlotte Lafleur¹

Cruise participants Leg 3b: Cyril Aubry¹, Marie Parenteau¹, Thibaud Dezutter¹ and Maxime Geoffroy¹

Cruise participants Leg 4a, 4b and 4c: Cyril Aubry¹, Marie Parenteau¹ and Thibaud Dezutter¹

¹ Université Laval, Québec-Océan, Pavillon Alexandre-Vachon room 2078, 1045 avenue de la Médecine, Québec, QC, G1V 0A6, Canada.

30.1 Introduction

The main objective during these legs was the monitoring of zooplankton and fish key parameters (abundance, diversity, biomass and distribution) using various sampling nets and the echosounder EK60.

During Leg 2, specific objectives included the collection of zooplankton and fish samples, acoustic data to:

- Document the composition, abundance and biomass of the pelagic fish communities in the North and the West of Baffin Bay (M. LeBlanc, U. Laval)
- Provide new and key information on the biodiversity and ecosystem function in the marine waters of the Kitikmeot region, considered a *mare incognita* for which information on marine ecosystems is acutely wanting (C. Bouchard, U. Laval)
- Assess food web structure and dynamics in the Queen Maud Gulf / Victoria Strait region using stable isotopes ($\delta^{13}\text{C}$ and $\delta^{15}\text{N}$) analysis (M. Falardeau, McGill U.)
- Study the population genetics of the dominant species (J. Nelson, U. Victoria)

During Leg 3b, specific objectives included the collection of zooplankton and fish samples, acoustic data and marine mammals' observation using a fisheries sonar to:

- Provide new and key information on the biodiversity and ecosystem function in the marine waters of the Kitikmeot region, considered a *mare incognita* for which information on marine ecosystems is acutely wanting (C. Bouchard, U. Laval);
- Study the population genetics of the dominant species (J. Nelson, U. Victoria).

The 2-weeks rerouting of the *Amundsen* during Leg 2 to escort commercial ships in Hudson Bay and subsequent changes in the original mission plan precluded our team to fulfill entirely their objectives. Specific objective 1 was only partly reached since all stations in the North of Baffin Bay were not visited during Leg 2. Specific objectives 2 and 3 were not

entirely reached as many stations planned in the area concerned were cut from the original plan. As the *Amundsen* mission plan includes several stations in the Kitikmeot region during Leg 3b, these objectives may be partly fulfilled by the end of 2015. Samples were collected in some areas of high importance for the study of genetic population and therefore can consider objective 4 as fulfilled.

30.2 Methodology

5 Nets Vertical Sampler (5NVS) (2 × 200µm, 1 × 500µm, 1 × 50µm, LOKI). Zooplankton sampler. Four 1-m² metal frames attached together and rigged with either three 6-m long (Legs 2 and 3a) or 4-m long (Legs 3b and 4), conical-square plankton nets, an external 10-cm diameter, 50-µm mesh net, and a LOKI (Lightframe Onsite Keyspecies Investigation system). Deployed vertically from 10 meters off the bottom to the surface, or less at deep station as the maximum depth recommended for the LOKI is 1000 m. The 5NVS was equipped with three TSK® flowmeters. After removal of fish larvae/juveniles (kept separately in 95% ethanol + 1% glycerol), zooplankton samples from one 200-µm, one 500-µm mesh, and the LOKI nets were preserved in 4% formaldehyde solution for abundance measurements while samples from the other 200-µm mesh net were either provided to Gary Stern for the assessment of contaminant levels (Leg 3a) or frozen at -20°C for dry weight measurements (Legs 2, 3b and 4).

Double Square Net (DSN) (1 × 500µm, 1 × 750µm, 1 × 50µm). Ichthyoplankton Net. Rectangular frame carrying either two 6-m long (Legs 2 and 3a) or 4,5-m long (Legs 3b and 4), 1-m² mouth aperture, square-conical nets and an external 10-cm diameter, 50-µm mesh net (to collect microzooplanktonic prey of the fish larvae). The sampler was towed obliquely from the side of the ship at a speed of ca. 2-3 knots to a maximum depth of 90 m (depth estimated during deployment from cable length and angle; real depth obtained afterward from a Star-Oddi® mini-CTD attached to the frame). The DSN was equipped with three KC® flowmeters. Fish larvae collected with the DSN were measured and preserved individually in 95% ethanol + 1% glycerol. Zooplankton samples from the 500-µm mesh net were preserved in 4% formaldehyde solution for further taxonomic identification while those from the 750-µm mesh net were either provided to Gary Stern's team for the assessment of contaminant levels (Leg 3a) or preserved in 95% ethanol for genetic analyses (Legs 2, 3b and 4).

Hydrobios (9× 200µm) – Leg 3a only. Multi-nets plankton sampler. Square device carrying nine nets opened sequentially with 0.5-m² mouth aperture and mesh size of 200 µm. The sampler was deployed vertically from 20 meters off the bottom to the surface and the nets were opened at different depths that were set before the deployment. After removal of fish larvae/juveniles (kept separately in 95% ethanol + 1% glycerol), zooplankton samples from the nine nets were preserved in 4% formaldehyde solution for abundance measurements.

Isaac-Kidd Midwater Trawl (IKMT) – Legs 2, 3b and 4 only. Pelagic juvenile and adult fish sampler. Rectangular net with a 9-m² mouth aperture and mesh size of 11 mm in the first section, 5 mm in the last section. The net was lowered to a depth where a fish aggregation has been detected by the echosounder and towed at that depth for 20 minutes at a speed of 2-3 knots (depth estimated during deployment from cable length and angle; real depth obtained afterward from a Star-Oddi® mini-CTD attached to the frame). Fish collected with this sampler were measured and stored at -80°C.

Benthic Beam Trawl. Demersal fish sampler. Rectangular net with a 3-m² mouth aperture, 32-mm mesh size in the first section, 16 mm in the last section, and a 10-mm mesh liner. The net was lowered to the bottom when fish aggregation was detected by the echosounder and towed for 20 minutes at a speed of 3 knots. Fishes collected with this sampler were measured and stored at -80°C.

Acoustic monitoring. The Simrad® EK60 echosounder of the *Amundsen* allowed to continuously monitor the spatial and vertical distribution of zooplankton and fish, the later mostly represented by Arctic cod (*Boreogadus saida*). The hull-mounted transducers are in operation 24h a day thus providing an extensive mapping of where the fishes are along the ship track.

Sonar observation – Leg 3b only. The Kongsberg® SX90 fish sonar allowed to detect the presence of marine mammals and possible near surface schools of fish. Marine mammal observations were validated by a wildlife observer working at the bridge from 08:00 to 20:00 (local time).

Table 30-1. Summary of operations conducted and samples collected during Leg 2.

Station	Date	5NVS	DSN	IKMT	Beam Trawl
K1	14-07-2015		x		
LS2	17-07-2015	x	x		
BB1	03-08-2015	x	x		
BB3	06-08-2015		x	x	
BB2	07-08-2015		x		
OPP1	09-08-2015		x		
CAA1	10-08-2015		x	x	
CAA2	10-08-2015	x	x		
CAA3	11-08-2015		x	x	
CAA5	13-08-2015		x		x
CAA4	13-08-2015		x		x
CAA6	14-08-2015		x		x
CAA7	15-08-2015	x	x		
312	17-08-2015	x	x		x
314	19-08-2015	x	x		x

Table 30-2. Summary of operations conducted and samples collected during Leg 3a.

Station	Date	5NVS	DSN	Hydrobios	Beam Trawl	Fish Samples
405	23-08-2015	x	x			4 Polar cod 3 unknown specie
407	23-08-2015	x	x	x	x	90 Polar cod; 9 unknown specie
437	24-08-2015	x	x			6 Polar cod
408	25-08-2015	x	x	x		9 Polar cod
420	25-08-2015	x	x			2 Polar cod; 5 unknown specie
434	26-08-2015	x	x			
435	27-08-2015	x	x	x	x	25 Polar cod; 6 unknown specie
421	30-08-2015	x	x			2 Polar cod
535	31-08-2015	x	x	x		4 Polar cod
Opp. 2	01-09-2015				x	2 Polar cod; 74 unknown specie
518	02-09-2015	x	x			7 Polar cod; 2 unknown specie

Table 30-3. Summary of operations conducted and samples collected during Leg 3b.

Station	Date	5NVS	DSN	Hydrobios	IKMT	Beam Trawl
CB1	07 09 15	X	X	X		X
CB2	10 09 15	X	X	X		
CB3	12 09 15	X	X	X		
CB4	14 09 15	X	X	X		
314	20 09 15	X	X			X
QMG4	21 09 15	X	X			X
QMG3	21 09 15	X	X			X
QMG-mooring	21 09 15	X	X		X	X
QMG2	21 09 15	X	X			X
QMG1	22 09 15	X				
312	22 09 15	X	X			X
310	23 09 15	X	X			
308	24 09 15	X	X	X		X
307	25 09 15	X				
342	26 09 15	X	X			X
CAA9	27 09 15	X				

Table 30-4. Summary of operations conducted and samples collected during Leg 4.

Station	Date	5NVS	DSN	Hydrobios	IKMT	Beam Trawl
304	03-10-15	X	X	X		X
301	05-10-15	X	X			
323	05-10-15	X	X	X	X	X
111	07-10-15	X	X			
115	08-10-15	X	X	X		X
108	09-10-15	X		X		X
105	09-10-15	X				
101	10-10-15	X		X		
155	12-10-15	X	X			
150	13-10-15	X	X			X
170	15-10-15	X	X	X		X
177	20-10-15	X	X	X	X	X
180	21-10-15	X	X			X
187	24-10-15	X	X			X

30.3 Preliminary results

30.3.1 Leg 2

Beside the zooplankton and fish samples collected (Table 30-1), Leg 2 has been an opportunity for to test some aspects of our sampling methods. These tests will result in helpful recommendations for the team in the future. Here are three questions to which the team started to provide an answer (investigations will continue during Legs 3 and 4):

Is there a clogging problem with the DSN?

Zooplankton nets, especially when towed, can get clogged by different organisms (e.g phytoplankton, jellyfish). Net clogging reduces filtering efficiency and thus may resulted in biased abundance estimates. To verify if the DSN get clogged during deployment, the flow indicated by two flowmeters inside the nets was compared to one installed between the nets. As indicated by higher flows given by the flowmeter installed outside the nets than those installed inside the nets, clogging occurred at Stations CAA-3 to CAA-7 and 314; and as expected, the clogging was more important in the 500 μm -mesh net than in the 750 μm -mesh net, exepcted for Station 314 where flow were equal (Figure 30.1). Intense phytoplankton blooms characterized these six stations and surely caused the clogging. To investigate if net clogging may result in biased abundance estimations, the number of Arctic cod larvae collected in the 500 μm -mesh net and the 750 μm -mesh were compared for five stations, in which the clogging was more important in the former than in the the latter. Consistently higher larval abundances in the 750 μm -mesh net would indicate a bias. Among the five stations concerned, two had more larvae in the 750 μm -mesh net, one had more larvae in the 500 μm -mesh net, and two had approximatly the same number in both nets (Figure 30.1). As such, it is not possible for now to conclude on the effect of net clogging on abundance data.

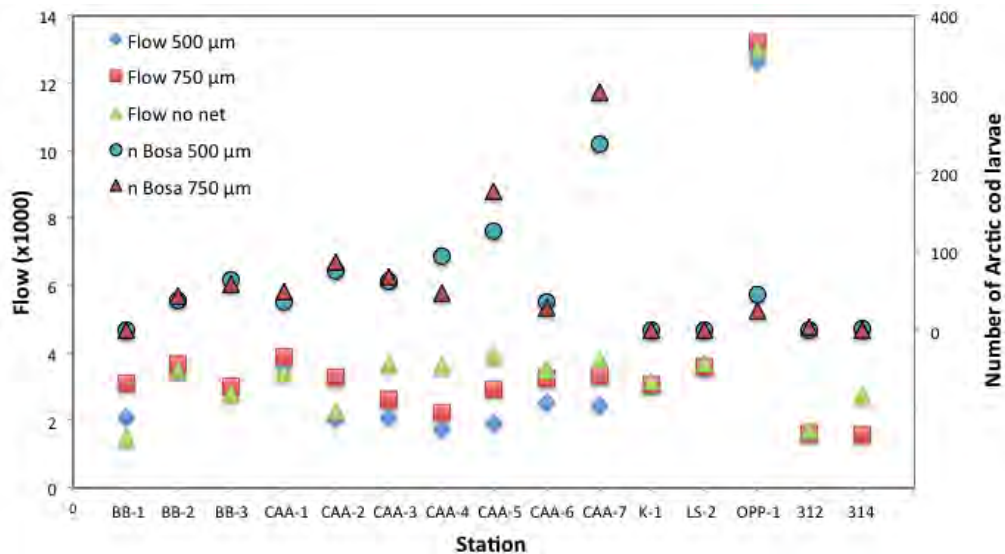


Figure 30-1. Flow indicated by flowmeters installed on the Double Square Net 1) in front of the 500 μm-mesh net, 2) in front of the 750 μm-mesh net, and 3) between the nets; and number of Arctic cod larvae collected by each net at each station.

Is cable length/angle a reliable method to estimate sampling depth?

During DSN and IKMT deployments, the cable length and its angle were used relative to the horizon to send the sampler at the desired depth. For example, a fish aggregation is targeted at 300 m and have an angle of 60°, 600 m of cable (the cosinus of 60° being 0.5) will be unrolled. However, it was discovered that this method tends to overestimate the sampling depth. Indeed, the maximum depth indicated by the mini-CTD (installed on the sampler frame) was often shallower than the depth estimated from the cable length and angle. For example, at Stations BB-2 and CAA-1, a cable length of 180 m combined with a 60° angle should have brought the DSN to a 90 m depth but the mini-CTD indicated maximum depth for these casts of 68 m and 67 m, respectively. The team first tested the possibility that the mini-CTDs were not accurate (or not correctly calibrated) by attaching two of those on the ArcticNet CTD-Rosette for a 300-m cast and compared the maximum depths given by the instruments. One mini-CTD was accurate while the other underestimated the maximum depth by 6 m, which was not enough to contribute significantly to the differences observed with the cable/angle method. The difference probably arise from curving of the cable in the water column and, for deeper casts (with the IKMT especially), from the large difference in depth a small difference in angle estimation can cause.

What's the best way to collect mesopelagic Arctic cod?

Young adult Arctic cod are often found aggregated in a mesopelagic layer from 200 to 400 m. To sample these small individuals, the IKMT was deployed a first time at Station BB-3 in a low-density aggregation visible on the echosounder and collected only one 81-mm Arctic cod. As acoustic data (target strength analysis) indicated a mean fish size in the aggregation of 55 mm, the team hypothesized that the IKMT mesh size was too large to efficiently

sample these small fish. Hence at Station OPP-1 the DSN was deployed in a mesopelagic aggregation of similar density than that of Station BB-3, and collected two Arctic cod (80 and 84 mm standard length). At Station CAA-1, the IKMT was deployed in a series of four 5-minutes steps separated by ca. 10 m depth (instead of 20 min trawl at the same depth) in a relatively dense aggregation and collected 49 Arctic cod (standard length 81 ± 11 mm). From these preliminary observations, the team concluded that the IKMT is effective at sampling the mesopelagic Arctic cod, that its deployment by consecutive steps is a good way to cope with the difficulty in estimating the trawling depth with the cable length/angle method, and that acoustic density values (Sv) greater than -70 dB (at least yellow or green on the echogram) should be detected in order to have a successful IKMT cast

30.3.2 Leg 3a

29 net deployments were done during Leg 3a (Table 30-2) in which a total of 277 fish were caught. 90 individuals were young-of-the-year (87% of Polar cod) and 187 were adults (53% of Polar cod). Mean standard length (SL) and mean weight (W) of the young Polar cod were 2.52 cm and 0.1053 g (n=78) (Table 30-5), and were 9.31 cm and 6.7839 g (n=72) for the adults (Table 30-6). Standard lengths of the fish were measured onboard, while mean weight was estimated using weight-standard length relationship of Geoffroy et al. (in review)¹.

Table 30-5. Mean standard length and weight of young-of-the year Polar cod at each station.

Station	Mean SL (cm)	Mean W (g)	n
405	2.83	0.1510	4
407	3.29	0.2446	10
437	2.70	0.1300	6
408	2.83	0.1522	9
420	2.57	0.1119	2
434	-	-	-
435	3.24	0.2329	8
421	2.83	0.1517	2
535	2.05	0.0546	4
518	2.26	0.0738	6
514	1.95	0.0460	27
All	2.52	0.1053	78

Table 30-6. Mean standard length and weight of adult Polar cod at each station.

Station	Mean SL (cm)	Mean W (g)	n
407	9.79	7.9569	52
435	8.24	4.5854	17
Opp. 2	7.70	3.7006	2
518	6.00	1.6698	1
All	9.31	6.7839	72

30.3.3 Leg 3b

Forty-four net deployments were conducted during Leg 3b (Table 30-3) in which a total of 577 fish were caught. Two hundred and eighty-two individuals were young-of-the-year (61% Arctic cod) and 295 were adults (33.9% Arctic cod). Mean standard length (SL) and mean weight (W) of the young Arctic cod were 2.9 cm and 0.247 g (n=85) (Table 30-7), and 15.9 cm and 40.44 g (n=100) for the adults (Table 30-8). SL of the fish was measured onboard, while mean weight was estimated using a W to SL model ($W(g)=0.0055*SL(cm)^{3.19}$) from Geoffroy *et al.* (in review).

Eight and a half hours of SX90 survey were completed in the Mc'Lintock Channel from 17h (UTC) on September 22 to 1h30 on September 23. The marine wildlife observer identified 20 seals, 1 polar bear and many different bird species from September 20-30.

Table 30-7. Mean standard length and weight of young-of-the year Arctic cod at each station.

Station	Mean SL (cm)	Mean W (g)	n	Total Polar cod sampled	% of Polar cod
CB1	2.43	0.120	7	7	87.5%
CB2	1.39	0.016	1	1	100%
CB3			0	0	
CB4			0	0	
314	2.8	0.147	1	1	33.3%
QMG4	3.11	0.258	4	4	30.77%
QMG3	3.2	0.225	1	1	6.66%
QMG-mooring	4.15	0.528	2	2	22.22%
QMG2	3.7	0.358	2	2	8%
QMG1			Not sampled		
312	2.16	0.075	20	20	69%
310	1.88	0.046	14	14	93.33%
308	2.34	0.084	6	6	85.71%
307			Not sampled		
342	4.07	0.494	27	114	72.61%
CAA9			Not sampled		
All	2.90	0.247	85	172	61%

Table 30-8. Mean standard length and weight of adult Polar cod at each station.

Station	Mean SL (cm)	Mean W (g)	n	Total fish sampled	% of Polar cod
CB1	15.05	36.26	11	35	31,4%
CB2			Not sampled		
CB3			Not sampled		
CB4			Not sampled		
314			0	2	0%
QMG4			0	0	
QMG3	6.4	2.05	1	6	16.66%
QMG-mooring			0	2	0%
QMG2			0	5	0%
QMG1			Not sampled		
312			0	3	0%
310			Not sampled		
308	16.33	42.71	84	92	91.3%
307			Not sampled		
342	11.55	13.89	4	150	2.66%
CAA9			Not sampled		
All	15.9	40.44	100	295	33.9%

30.3.4 Leg 4

36 net deployments were done during Leg 4 (Table 30-4) in which a total of 609 fish were caught. 244 individuals were young-of-the-year (85.25% of Polar cod) and 295 were adults (31.67% of Polar cod). Mean standard length (SL) and mean weight (W) of the young Polar cod were 3.55 cm and 0.351 g (n=172) (Table 30-9), and 11.47 cm and 14.93 g (n=127) for the adults (Table 30-10). Standard lengths (SL) of the fish were measured onboard, while mean weight was estimated using weight-standard length relationship ($W(g)=0,0055*SL(cm)^{3,19}$) from Geoffroy et al. (in review).

Table 30-9. Mean standard length and weight of young-of-the year Polar cod at each station.

Station	Mean SL (cm)	Mean W (g)	n	Total Polar cod sampled	% of Polar cod
304	3,35	0,29	35	41	76,09%
301	3,34	0,272	25	25	100%
323	3,25	0,275	25	31	96,88%
111	3,54	0,318	5	5	83,33%
115	3,8	0,405	13	13	92,86%
108			Not sampled		
105			Not sampled		
101			Not sampled		
155	3,93	0,488	25	49	100%
150	3,40	0,303	24	24	92,31%
170	4,08	0,513	18	18	64,29%
177	4,70	0,766	1	1	16,67%
180			0	0	0%
187	2,60	0,116	1	1	33,33%
All	3,55	0,351	172	208	85,25%

Table 30-10. Mean standard length and weight of adult Polar cod at each station.

Station	Mean SL (cm)	Mean W (g)	n	Total fish sampled	% of Polar cod
304	9,01	6,19	11	34	32,35%
301			0	1	0%
323	9,63	7,80	4	35	11,43%
111				Not sampled	
115	11,53	14,28	30	36	83,33%
108	12,49	19,24	38	71	53,52%
105				Not sampled	
101				Not sampled	
155				Not sampled	
150			0	17	0%
170	12,57	19,03	26	71	36,62%
177	9,63	8,68	8	41	19,51%
180	9,49	7,36	10	82	12,20%
187			0	13	0%
All	11,47	14,93	127	401	31,67%

References

Geoffroy M, Majewski A, LeBlanc M, Gauthier S, Walkusz W, Reist J, Fortier L (in review)
 Vertical segregation of age-0 and age-1+ polar cod (*Boreogadus saida*) over the annual cycle in the Canadian Beaufort Sea.

31 Contaminants sampling program – Legs 3a, 3b, 4a, 4b and 4c

Project leaders: Gary A. Stern^{1,2} (gary.stern@dfm-mpo.gc.ca), Feiyue Wang² (feiyue.wang@umanitoba.ca), Casey Hubert³ (chubert@ucalgary.ca), Liisa Jantunen⁴ (liisa.jantunen@ec.gc.ca), Brendan Hickie⁵ (bhickie@trentu.ca)

Cruise participants Leg 3a: Alexis Burt², Amy Noel³, Oscar Montoya³ and Wen Xu²

Cruise participants Leg 3b: Amy Noel³ and Xiaoxu Sun⁶

Cruise participants Leg 4a: Alexis Burt² and Michelle Kamula²

Cruise participants Leg 4b and 4c: Alexis Burt² and Margaret Cramm³

¹ Fisheries and Oceans Canada, 501 University Crescent, Winnipeg, MB, R3T 2N6, Canada.

² Centre for Earth Observation Science, Department of Environment and Geography, Clayton H. Riddell Faculty of Environment, Earth and Resources, University of Manitoba, 460 Wallace Building, Winnipeg, MB, R3T 2N2, Canada.

³ Department of Biological Sciences, University of Calgary, 2500 University Drive NW, Calgary, AB, T2N 1N4, Canada.

⁴ Environment Canada / CARE, Air Quality Processes Research Section, Air Quality Research Division, Science and Technology Branch, Centre for Atmospheric Research Experiments, 6248 Eighth Line, Egbert, ON, L0L 1N0, Canada.

⁵ Environmental & Resource Studies Program, Trent University, 1600 West Bank Drive, Peterborough, ON, K9J 7B8, Canada.

⁶ Department of Earth and Atmospheric Science, Georgia Institute of Technology, Atlanta, Georgia, 30332, USA.

31.1 Introduction

31.1.1 Hydrocarbon, Mercury and Methyl Mercury

Oil reserves are currently being studied for extraction in Baffin Bay (including the North Water polynya, Davis Strait, Lancaster Sound and Jones Sound) and in the Beaufort Sea by major oil companies; with some potential reservoirs estimated to contain billions of barrels of oil. Global warming and reduced ice coverage has made these reserves more accessible and the exploration/exploitation of offshore oil in the region more feasible. With declining ice conditions oil exploration and shipping traffic through the North West Passage will only increase; both of these activities have the potential to increase petroleum hydrocarbon concentrations in Baffin Bay and in the Southern Beaufort Sea and Amundsen Gulf. However, hydrocarbons are also naturally present as a result of natural oil seeps, fossil fuel combustion, and terrestrial run-off. The purpose of this study is to measure baseline concentrations of hydrocarbons in the Baffin Bay and in the Southern Beaufort Sea and Amundsen Gulf marine environment in advance of future oil exploration/exploitation and increased shipping.

31.1.2 Benthic microbial diversity

Marine sediment environments are high in microbial diversity and abundance with a cubic centimeter of seabed typically containing billions of microbial cells – about a thousand fold more than in overlying seawater. The theme of the research in the Canadian Arctic Archipelago was to establish baseline data for the diversity and activity of microorganisms in Arctic sediments, and experimentally investigate how short and long term changes in environmental parameters (e.g. temperature; pulses of organic compounds such as hydrocarbons) may affect the community composition, metabolic rates and cycling of carbon and other nutrients. This work will determine the impact of permanently cold temperatures on the rates of biogeochemical processes such as sulfate reduction, which is responsible for up to half of organic carbon mineralization in coastal sediments (Jørgensen 1982).

The occurrence and locations of marine hydrocarbon seeps in Canada's Arctic are important to assess the ability of microbiota in Arctic seawater and sediments to biodegrade accidentally released crude oil or other pollutants. A rapid natural response may depend on a region's microbiota being 'primed' for such biodegradation by the slow natural release of hydrocarbons from seabed seeps (Hazen et al. 2011). Given that industrial activity and traffic in the Northwest Passage is poised to increase, the inherent biodegradative capacity of marine microorganisms was tested experimentally on samples obtained. Sediment associated microbial communities were also compared to microbial communities in the water column to elucidate possible relationships of hydrocarbon degrading communities between the two environments. This data will be used to help develop a predictive measure of how different regions of the Arctic could respond to various pollution scenarios. In addition, since polyaromatic hydrocarbons (PAH) are naturally present in the Beaufort Sea, especially in the Mackenzie River delta, it would be expected that the naturally present archaea and bacteria possess metabolic abilities biodegradation. The microbial communities isolated from these sediments may be potentially suitable for bioremediation of Alberta's tailings ponds. Samples collected during Leg 3b will also be compared to Gulf of Mexico (GoM) sediment samples to measure any differences in the potential for biodegradation (microbial communities, rates of hydrocarbon oxidation).

Another goal of the work was targeted diversity studies to explore the abundance and function of spore-forming thermophilic sulfate-reducing bacteria in permanently cold sediments, extending biogeography analyses that have been performed in other Arctic sediments (Hubert et al. 2009). Arctic thermophiles are thought to derive from warm deep sediments and get transported up into the cold ocean via seabed hydrocarbon seepage.

This data will be used to help develop a predictive measure of how different regions of the Arctic could respond to various pollution scenarios.

31.1.3 Contaminants in a changing Arctic - Mercury in the atmosphere and seawater

Mercury is one of the primary contaminants of concern in the Arctic marine ecosystem. It can be transported and deposited to the Arctic via long-range atmospheric transport. Gaseous elementary mercury (GEM) is the main mercury species in the atmosphere since it has a long residence time (up to two years) and is relatively stable (Stephen et al. 2008). In the presence of strong oxidants in the air (e.g. halogen atoms), GEM can be rapidly oxidized into reactive gaseous mercury (RGM), which then can be adsorbed onto aerosols to become particulate mercury (PHg). Both RGM and PHg are much more reactive than GEM, and can readily deposit onto the surface environment (e.g. snow, ice and seawater).

In the springtime Arctic, the oxidation and deposition processes are accelerated by photolytically produced reactive halogens, resulting in the so-called mercury depletion events. In the summer time, on the other hand, the open ocean can be a source of atmospheric mercury and release mercury into the air. Previous model studies suggest that 30-40% mercury deposited to the ocean is re-emitted. Much less is known about the oxidation process of GEM during the Arctic summer.

Furthermore, monomethylmercury (MMHg) in the seawater has arisen attention in recent years due to its high toxicity and its key role in biomagnification in the food web. Though release of sediment produced methylated Hg (MeHg, sum of MMHg and dimethylmercury) was postulated as the primary seawater MeHg source (Hammerschmidt and Fitzgerald 2006), sub-surface peak of MeHg recently observed in different oceans suggest water column Hg methylation is a more important source in seawater. So far, the source and distribution of mercury species, especially MMHg, remain unclear.

The objective of this project were to:

- Analyze three different species of mercury in the air: GEM, RGM and PHg;
- Measure total Hg and MeHg concentrations in the seawater.

The results of atmospheric mercury measurement will improve the understanding of Hg redox reactions and exchange between the atmosphere and the ocean in the Arctic summer. Mercury species in the seawater measurement will help to determine the distribution of total Hg (Hg_T) and MeHg as well as particulate Hg (Hg_P) in the Canadian Arctic seawater and identify the mechanisms of Hg methylation in water column.

31.1.4 SPMD deployments

The goal with the SPMDs was to monitor concentrations of persistent organic pollutants (POPs) in the mixed surface layer, the Pacific water mass and the deep Atlantic waters. The SPMDs were placed close to CTDs and/or ADCPs located in each of these layers to allow the team to relate results to information gathered from them and confirm which water mass they were sampling. For more mooring information please see the mooring team's cruise report (Section 8).

31.2 Methodology

31.2.1 Hydrocarbon, mercury and methyl mercury

While on board the *CCGS Amundsen*, invertebrates (benthic and pelagic), surface sediment and sediment cores were collected for this research.

Pelagic Invertebrates: Zooplankton were sampled from the whole water column using the 5-net vertical sampler (Monster Net with LOKI: 1 m² 200 µm mesh; Figure 31-1), and from the surface 60m (Leg 3a) and 90 m (Leg 4) using the oblique net tow (Tucker Net: 1 m² 750 µm mesh) at respectively 12 and 8 stations during Legs 3a and 4a, and at 6 stations during Leg 4b (Table 31-1 and Table 31-2). Species of interest included: *Calanus hyperboreus*, *C. glacialis*, *Paraeuchaeta glacialis*, *Metridia longa*, Chaetognaths (including *Parasagitta elegans*, *Pseudosagitta maxima*, and *Eukrohnia* sp.), *Themisto libellula*, *T. abyssorum*, *Hyperia galba*, *Clione limacina*, *Limacina helicina*, Ostracoda, Ctenophora and Hydromedusae.

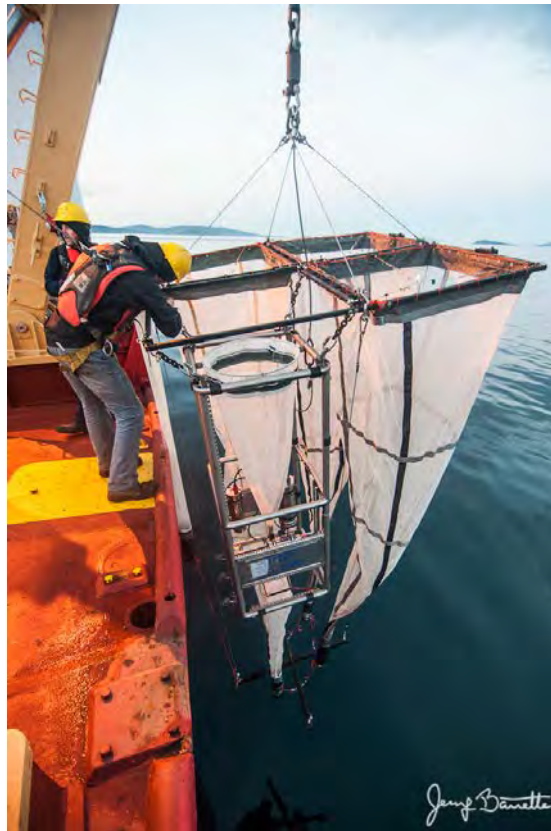


Figure 31-1. The 5-net vertical zooplankton sampler with LOKI (Monster net). Photo: Jessy Barrette 2013 ArcticNet Leg 1a.

Benthic Invertebrates: Benthic animals were collected using the Agassiz trawl, as well as opportunistically from the Beam trawl during Legs 3a and 4. Samples were identified as best as possible and set aside by the members of the Archambault team (Figure 31-2). They

were subsequently labelled and frozen at -20°C. Groups of interest included: Asterozoidea (sea stars), Ophiurozoidea (brittle stars), decapods, molluscs, isopods, amphipods, and polychaete worms. Stations sampled are noted in Table 31-3 and Table 31-4.



Figure 31-2. Benthic invertebrates that were collected from the Agassiz trawl on 3 October 2015 at Station 304.

Push coring: Samples destined for hydrocarbon analysis were collected during Legs 3a, 3b and 4 using 10 cm diameter plastic push cores from the box core (Table 31-5). The sediment core was subsequently placed on a manual extruder and sectioned by 0.5 cm intervals for the first 10 cm, and then 1.0 cm for the balance of the core (approximately 30 cm total). Sediment was stored in Whirl-pak plastic bags, and stored at -20°C. Surface sediments (0-5 cm) were collected for this research as well as for PCB analysis.

Table 31-1. Stations where zooplankton species were collected for contaminants during Leg 3a of ArcticNet 2015.

Leg	Station	Location	Date	Latitude (N)	Longitude (W)	Tow	Bottom Depth (m)	Sampler Depth (m)
3A	405	Amundsen Gulf	23 Aug	70°36.538	123°02.181	Vertical Tow (1m ² , 200um mesh)	609	600
3A	407	Amundsen Gulf	23 Aug	71°00.531	126°04.733	Vertical Tow (1m ² , 200um mesh)	393	383
3A	407	Amundsen Gulf	24 Aug	71°00.469	126°05.917	Oblique Tow (1m ² , 750um mesh)	393	59,26
3A	437	Amunds Transect	24 Aug	71°47.647	126°31.307	Oblique Tow (1m ² , 750um mesh)	315	71,78
3A	437	Amunds Transect	24 Aug	71°48.155	126°30.251	Vertical Tow (1m ² , 200um mesh)	294	281
3A	408	Amunds Transect	25 Aug	71°17.000	127°33.000	Oblique Tow (1m ² , 750um mesh)	204	86,14
3A	408	Amunds Transect	25 Aug	71°18.000	127°35.000	Vertical Tow (1m ² , 200um mesh)	202	192

3A	420	Amunds Transect	25 Aug	71°03.000	128°32.000	Oblique Tow (1m2, 750um mesh)	42	12,73
3A	420	Amunds Transect	25 Aug	71°03.000	128°33.000	Vertical Tow (1m2, 200um mesh)	44	30
3A	434	Mackenzie Transect	26 Aug	70°10.000	133°34.000	Oblique Tow (1m2, 750um mesh)	47	27,93
3A	434	Mackenzie Transect	26 Aug	70°10.000	133°32.000	Vertical Tow (1m2, 200um mesh)	47	37
3A	435	Mackenzie Transect	27 Aug	71°04.000	133°40.000	Oblique Tow (1m2, 750um mesh)	245	75,19
3A	435	Mackenzie Transect	27 Aug	71°04.000	133°38.000	Vertical Tow (1m2, 200um mesh)	301	290
3A	421	Mackenzie Transect	30 Aug	71°25.730	133°59.000	Oblique Tow (1m2, 750um mesh)	1212	75,37
3A	421	Mackenzie Transect	30 Aug	71°25.730	133°00.250	Vertical Tow (1m2, 200um mesh)	1207	700
3A	535	East Banks Island	31 Aug	73°24.115	128°09.881	Oblique Tow (1m2, 750um mesh)	275	73,54
3A	535	East Banks Island	31 Aug	73°24.520	128°13.962	Vertical Tow (1m2, 200um mesh)	300	290
3A	518	M'Clure Strait	2 Sep	74°33.690	121°27.550	Oblique Tow (1m2, 750um mesh)	220	76,23
3A	518	M'Clure Strait	2 Sep	74°34.366	121°26.496	Vertical Tow (1m2, 200um mesh)	260	250
3A	514	M'Clure Strait	2 Sep	75°07.460	120°41.410	Oblique Tow (1m2, 750um mesh)	467	80,72
3A	514	M'Clure Strait	2 Sep	75°07.600	120°41.360	Vertical Tow (1m2, 200um mesh)	466	453

Table 31-2. Stations where zooplankton species were collected for contaminants during Leg 4 of ArcticNet 2015.

Leg	Station	Location	Date	Latitude (N)	Longitude (W)	Tow	Bottom Depth (m)	Sampler Depth (m)
4A	304	Lancaster Sound	3 Oct	74°14.858	091°29.319	Oblique Tow (1m2, 750um mesh)	316	111.27
4A	304	Lancaster Sound	3 Oct	74°15.019	091°30.369	Vertical Tow (1m2, 200um mesh)	314	304
4A	301	Lancaster Sound	4 Oct	74°07.321	083°18.854	Oblique Tow (1m2, 750um mesh)	675	
4A	301	Lancaster Sound	4 Oct	74°07.107	083°19.221	Vertical Tow (1m2, 200um mesh)	674	664
4A	323	Lancaster Sound	5 Oct	74°10.208	080°25.593	Oblique Tow (1m2, 750um mesh)	785	74.5
4A	323	Lancaster Sound	5 Oct	74°09.780	080°27.210	Vertical Tow (1m2, 200um mesh)	790	780
4A	111	Northwater Transect	7 Oct	76°18.514	073°13.382	Oblique Tow (1m2, 750um mesh)	595	77.3
4A	111	Northwater Transect	7 Oct	76°18.335	073°12.349	Vertical Tow (1m2, 200um mesh)	597	587
4A	115	Northwater Transect	7 Oct	76°19.810	071°14.860	Oblique Tow (1m2, 750um mesh)	673	87.2
4A	115	Northwater Transect	7 Oct	76°19.980	071°13.033	Vertical Tow (1m2, 200um mesh)	660	650
4A	108	Northwater Transect	9 Oct	76°15.587	074°36.442	Vertical Tow (1m2, 200um mesh)	449	439
4A	105	Northwater Transect	9 Oct	76°17.569	075°46.899	Vertical Tow (1m2, 200um mesh)	312	302
4A	101	Northwater Transect	10 Oct	76°21.402	077°23.288	Vertical Tow (1m2, 200um mesh)	378	368
4B	155	Near Pond	11-12	72°28.762	078°46.728	Oblique Tow (1m2, 750um mesh)	388	80.7

Leg	Station	Location	Date	Latitude (N)	Longitude (W)	Tow	Bottom Depth (m)	Sampler Depth (m)
		Inlet	Oct			750um mesh)		
4B	155	Near Pond Inlet	11-12 Oct	72°29.260	078°45.610	Vertical Tow (1m ² , 200um mesh)	299	289
4B	150	Eclipse Sound	13 Oct	72°44.516	079°55.454	Oblique Tow (1m ² , 750um mesh)	126	63.8
4B	150	Eclipse Sound	13 Oct	72°44.940	079°56.160	Vertical Tow (1m ² , 200um mesh)	128	118
4B	170	Scott Inlet	14-15 Oct	71°22.560	070°03.686	Oblique Tow (1m ² , 750um mesh)	258	105
4B	170	Scott Inlet	14-15 Oct	71°22.778	070°04.034	Vertical Tow (1m ² , 200um mesh)	258	248
4B	177	Qikitarjuaq	20 Oct	67°28.315	063°47.572	Oblique Tow (1m ² , 750um mesh)	373	83.5
4B	177	Qikitarjuaq	20 Oct	67°28.603	063°47.379	Vertical Tow (1m ² , 200um mesh)	371	361
4B	180	Baffin Bay	21 Oct	67°28.785	061°39.990	Oblique Tow (1m ² , 750um mesh)	315	71.8
4B	180	Baffin Bay	21 Oct	67°28.681	061°39.534	Vertical Tow (1m ² , 200um mesh)	344	334
4B	187	Baffin Bay	23-24 Oct	64°11.225	060°21.699	Oblique Tow (1m ² , 750um mesh)	355	103.2
4B	187	Baffin Bay	23-24 Oct	64°10.896	060°23.179	Vertical Tow (1m ² , 200um mesh)	354	344

Table 31-3. List of benthic samples for PAH collected during Leg 3a of ArcticNet 2015.

Leg	Station	Location	Date	Operation	Latitude (N)	Longitude (W)	Bottom Depth (m)
3A	405	Amundsen Gulf	23-Aug-15	Boxcore	70°36.501	123°01.786	628
3A	405	Amundsen Gulf	23-Aug-15	Agassiz	70°36.645	123°02.756	628-602
3A	407	Amundsen Gulf	24-Aug-15	Boxcore	71°00.651	126°06.006	393
3A	407	Amundsen Gulf	24-Aug-15	Agassiz	71°00.000	126°80.000	393
3A	407-437	Amundsen Gulf	24-Aug-15	Beam Trawl	71°02.760	126°17.460	386-382
3A	437	Amunds Transect	24-Aug-15	Boxcore	71°48.273	126°29.796	276
3A	437	Amunds Transect	24-Aug-15	Agassiz	71°47.741	126°29.897	393-398
3A	408	Amunds Transect	25-Aug-15	Boxcore	71°18.784	127°35.677	202
3A	408	Amunds Transect	25-Aug-15	Agassiz	71°18.574	127°35.968	202-200
3A	420	Amunds Transect	25-Aug-15	Agassiz	71°02.000	128°31.000	40-43
3A	434	Mackenzie Transect	26-Aug-15	Boxcore	70°10.000	133°33.000	47
3A	434	Mackenzie Transect	26-Aug-15	Agassiz	70°11.000	133°34.000	46-47
3A	435	Mackenzie Transect	27-Aug-15	Boxcore	71°04.770	133°38.150	302
3A	435	Mackenzie Transect	27-Aug-15	Agassiz	71°04.500	133°40.320	298
3A	435	Mackenzie Transect	29-Aug-15	Beam Trawl	71°02.384	133°42.192	240-225
3A	Benthos	700 m target depth	29-Aug-15	Agassiz	71°11.290	133°44.407	716-648
3A	421	Mackenzie Transect	30-Aug-15	Boxcore	71°25.589	134°00.038	1203
3A	535	East Banks Island	31-Aug-15	Boxcore	73°25.010	128°11.760	290
3A	535	East Banks Island	31-Aug-15	Agassiz	73°24.220	128°14.000	291-304
3A	518	M'Clure Strait	2-Sep-15	Boxcore	74°34.311	121°26.567	269
3A	518	M'Clure Strait	2-Sep-15	Agassiz	74°34.200	121°28.700	308-227
3A	514	M'Clure Strait	2-Sep-15	Boxcore	75°06.226	120°37.679	474
3A	514	M'Clure Strait	2-Sep-15	Agassiz	75°06.110	120°35.427	451-440

Table 31-4. List of benthic samples for PAH collected during Leg 4 of ArcticNet 2015.

Leg	Station	Location	Date	Operation	Depth (m)	Latitude (N)	Longitude (W)
4A	304	Lancaster Sound	3-Oct-15	Agassiz	322	74°15.644	091°27.888
4A	304	Lancaster Sound	3-Oct-15	Beam Trawl	316	74°15.666	091°32.020
4A	304	Lancaster Sound	3-Oct-15	Box core	313	74°14.795	091°31.181
4A	301	Lancaster Sound	4-Oct-15	Agassiz	676	74°08.235	083°18.485
4A	301	Lancaster Sound	4-Oct-15	Box core	677	74°07.127	083°18.136
4A	323	Lancaster Sound	5-Oct-15	Agassiz	789	74°10.840	080°28.065
4A	323	Lancaster Sound	5-Oct-15	Beam Trawl	793	74°11.500	080°35.487
4A	111	Northwater	7-Oct-15	Agassiz	592	76°18.340	073°12.890
4A	115	Northwater	7-Oct-15	Agassiz	664-676	76°20.370	071°18.140
4A	CASQ1	Baffin Bay	8-Oct-15	Box core	702	77°16.746	074°21.428
4A	108	Northwater	9-Oct-15	Agassiz	449-445	76°15.510	074°38.700
4A	108	Northwater	9-Oct-15	Beam Trawl	447	76°13.690	074°44.150
4A	101	Baffin Bay	10-Oct-15	Box core	399	76°22.435	077°26.468
4B	155	Pond Inlet	12-Oct-15	Agassiz	346-397	72°29.640	078°47.450
4B	150	Eclipse Sound	12-Oct-15	Agassiz	127-126	72°45.020	079°56.630
4B	150	Eclipse Sound	12-Oct-15	Beam Trawl	133-147	72°43.980	079°53.050
4B	155	Pond Inlet	12-Oct-15	Box core	376	72° 29.290	078°46.860
4B	170	Scott Inlet	14-Oct-15	Box core	259	71°22.761	070°04.153
4B	170	Scott Inlet	15-Oct-15	Agassiz	264-245	71°22.684	070°03.631
4B	170	Scott Inlet	15-Oct-15	Beam Trawl	265-271	71°23.660	070°03.260
4B	CASQ3	Scott Inlet	16-Oct-15	Box core 1 of 2	832	71°19.314	070°38.975
4B	CASQ3	Scott Inlet	16-Oct-15	Box core 2 of 2	833	71°19.316	070°38.966
4B	CASQ3-2	Scott Inlet	17-Oct-15	Box core	607	71°30.786	070°16.327
4B	ROV	Scott Inlet	17-Oct-15	Box core	607	71°30.786	070°16.327
4B	177	Qikitarjuaq	20-Oct-15	Beam Trawl	418	67°28.300	063°46.930
4B	177	Qikitarjuaq	20-Oct-15	Agassiz	653-677	67°28.381	063°41.631
4B	177	Qikitarjuaq	20-Oct-15	Box core 1 of 3	371	67°28.577	063°47.389
4B	177	Qikitarjuaq	20-Oct-15	Box core 2 of 3	373	67°28.579	063°47.407
4B	177	Qikitarjuaq	20-Oct-15	Box core 3 of 3	374	67°28.580	063°47.510
4B	180	Baffin Bay	21-Oct-15	Agassiz	345-361	67°28.937	061°39.756
4B	180	Baffin Bay	21-Oct-15	Beam Trawl	349-400	67°29.280	061°41.170
4B	187	Baffin Bay	24-Oct-15	Agassiz	350-352	64°10.970	060°24.090
4B	187	Baffin Bay	24-Oct-15	Beam Trawl	357	64°12.170	060°25.790
4B	Frobisher Bay	Baffin Bay	25-Oct-15	Box core 1 of 2	121	63°38.410	068°36.731
4B	Frobisher Bay	Baffin Bay	25-Oct-15	Box core 2 of 2	128	63°38.646	068°36.638
4C	640	Baffin Bay	27-Oct-15	Box core 1 of 3	145	58°55.621	062°09.321
4C	640	Baffin Bay	27-Oct-15	Box core 2 of 3	141	58°55.710	062°09.430
4C	640	Baffin Bay	27-Oct-15	Box core 3 of 3	141	58°55.923	062°09.429

Table 31-5. Sediment and water samples collected during Leg 3b of ArcticNet 2015.

Leg	Station	Location	Date	Operation	Depth	Latitude (N)	Longitude (W)
3B	CB1	McClure Strait	06-Sep-15	CTD Rosette	465	75°07.350	120°38.500
3B	CB1	McClure Strait	07-Sep-15	Box Core	409	75°06.750	120°21.400
3B	CB2	Beaufort Sea	10-Sep-15	CTD Rosette	1344	75°47.108	129°17.443
3B	CB2	Beaufort Sea	10-Sep-15	Box Core	1350	75°47.030	129°17.080
3B	CB3	Beaufort Sea	11-Sep-15	CTD Rosette	3735	76°58.510	140°03.090

3B	CB3	Beaufort Sea	12-Sep-15	TM Rosette	3731	76°59.938	140°05.702
3B	CB3	Beaufort Sea	12-Sep-15	TM Rosette	3732	77°01.150	140°02.710
3B	CB4	Beaufort Sea	14-Sep-15	CTD Rosette	3829	75°00.030	149°59.600
3B	CB4	Beaufort Sea	15-Sep-15	TM Rosette	3829	75°00.030	149°59.600
3B	407	Beaufort Sea	18-Sep-15	CTD Rosette	390	71°00.330	126°04.560
3B	407	Beaufort Sea	18-Sep-15	Box Core	398	70°59.600	126°03.280
3B	314	NW Passage	20-Sep-15	CTD Rosette	77	68°58.200	105°28.890
3B	314	NW Passage	20-Sep-15	Box Core	81	68°58.256	105°28.251
3B	314	NW Passage	20-Sep-15	Box Core	80	68°58.193	105°28.505
3B	314	NW Passage	20-Sep-15	Box Core	81	68°58.208	105°28.348
3B	QMG4	NW Passage	20-Sep-15	CTD Rosette	71	68°29.000	103°25.480
3B	QMG4	NW Passage	20-Sep-15	Box Core	67	68°29.060	103°25.660
3B	QMG3	NW Passage	21-Sep-15	CTD Rosette	64	68°19.770	102°36.398
3B	QMG3	NW Passage	21-Sep-15	Box Core	67	---	---
3B	QMG	NW Passage	21-Sep-15	CTD Rosette	107	68°14.803	101°43.057
3B	QMG	NW Passage	21-Sep-15	Box Core	100	---	---
3B	QMG2	NW Passage	21-Sep-15	CTD Rosette	54	68°18.810	100°47.990
3B	QMG2	NW Passage	21-Sep-15	Box Core	59	68°18.720	100°47.890
3B	QMG1	NW Passage	21-Sep-15	CTD Rosette	35	68°29.630	099°53.440
3B	QMG1	NW Passage	22-Sep-15	Box Core	48	68°29.469	099°54.091
3B	312	NW Passage	22-Sep-15	CTD Rosette	65	69°10.330	100°41.600
3B	312	NW Passage	22-Sep-15	Box Core	64	69°10.220	100°41.700
3B	310	NW Passage	23-Sep-15	CTD Rosette	163	71°27.411	101°16.734
3B	310	NW Passage	23-Sep-15	Box Core	158	71°27.411	101°16.734
3B	308	NW Passage	24-Sep-15	CTD Rosette	565	74°08.320	108°50.080
3B	308	NW Passage	24-Sep-15	Box Core	564	74°08.356	108°50.193
3B	308	NW Passage	24-Sep-15	Box Core	---	---	---
3B	308	NW Passage	24-Sep-15	Box Core	---	---	---
3B	307	NW Passage	25-Sep-15	CTD Rosette	357	74°06.675	103°07.454
3B	307	NW Passage	25-Sep-15	Box Core	350	74°06.980	103°06.000
3B	342	NW Passage	25-Sep-15	CTD Rosette	137	74°47.670	092°46.860
3B	342	NW Passage	25-Sep-15	Box Core	138	74°47.650	092°46.880

31.2.2 Benthic microbial diversity

During Legs 3a, 3b and 4, sediment was collected using the box core. During Legs 3a and 3b, water was collected using the CTD-Rosette.

Surface sediment sampling: Samples collected for microorganism incubation experiments were scraped from the top 5 cm of the box core using a plastic spatula, stored in 2L heat sealed plastic bags and then kept at 4°C. An effort was made to eliminate all headspace from the plastic bags.

Surface samples destined for microorganism diversity analysis were scraped from the top 5 cm of the box core using a stainless steel pallet knife into 15ml plastic cryovials, spiked with 5 ml of 95% ethanol and stored at -80°C. 2mL headspace was kept for freezing expansion. Triplicate sample vials were collected whenever possible.

Sediment push coring: Cores for microorganism incubations and diversity were collected using the same equipment the hydrocarbon study. These cores were sectioned by 2.0 cm intervals for the first 10 cm and then 5.0 cm intervals for the balance. At each interval, duplicate subsamples were collected for microorganism diversity using the same 15 ml vials and methods described earlier. The bulk of the remaining section was kept in Whirl-pak plastic bags and stored at 4°C.

Sediment push coring for GoM comparison – Leg 3b only: Push cores from the box core Full stations were sectioned at 1cm intervals and stored at - 80°C for DNA extraction in Whirl-pak plastic bags.

Water sampling – Legs 3a and 3b only: Water was requested for microbial community analysis to compare to sediment microbial communities (collected as previously described). 4L each of surface and bottom water was requested and sampled from Niskin bottles into rinsed and bleached Nalgene carboys at each of the Full and Basic stations. 2L of water from each depth was successively filtered over 0.8µm, 0.45µm, and 0.2µm Pall filters. Filters were stored in Whirl-pack bags at -20°C for future DNA extraction and sequencing of the 16s rRNA genes.

Water sampling for GoM comparison – Leg 3b only: Water samples were collected at the surface and bottom depths from the CTD Rosette Niskin bottles. For each depth, 1L of the water sample was passed through a 0.22µm filter tower and preserved in -80°C freezer for DNA extraction. Approximately 100ml of additional water was filtered through 0.22µm-syringe filter for future nutrient analysis.

Diesel biodegradation experiments – Legs 3a and 3b only: Surface sediment from Stations 405 (negative seep station) and 435 (positive seep station) (Leg 3a), as well as CB1, CB2 and 314 (Leg 3b) were used to inoculate anaerobic diesel biodegradation incubations. Inoculated bottles used 10g of sediment, 40mL of artificial seawater with 20mM sulphate, and 50µL of diesel or crude oil. Unamended and sediment-free controls were set up in line. Incubations from Leg 3a will be sampled monthly, while incubations from Leg 3b will be sampled every two months; sulfate reduction, diesel removal, and microbial community composition will be monitored.

GoM crude oil incubations – Leg 3b only: 2.5mL of surface sediment collected at Full stations was mixed with 7.5 volumes of filtered bottom water from the same station and incubated with 0.1% v/v crude oil. For water incubations, 10mL of seawater was also incubated with 0.1% v/v crude oil. For both types of incubations, additional triplicate enrichments with no oil addition were included as controls. To simulate *in situ* conditions and prevent any photochemical processes, incubations were stored at 4°C and in the dark. No obvious oxygen consumption has been observed yet.

PAH biodegradation experiments – Leg 3a only: Sediment cores from the Beaufort Sea seabed retrieved from Stations 407, 435, and 535 were divided in two sections, from 0-15 cm and 15-30 cm. The first section was assigned for aerobic experiments and the second

for anaerobic. Aerobic and anaerobic treatments and controls were set up in quintuplicates by the addition of 40 mL of the respective homogenized sediments and 30 mL of artificial seawater. The headspaces of the anaerobic incubations were replaced by a nitrogen and carbon dioxide gas mix (N₂/CO₂ 90:10). The aerobic incubations will be used as an inocula source for future experiments, while the anaerobic incubations will be monitored for sulfate reduction, methane production, and PAH removal. Subsamples from each core were taken from 0 cm, 15 cm, and 30 cm, for 16S rRNA gene sequencing and sulfate quantification purposes.

31.2.3 Contaminants in a changing Arctic - Mercury in the atmosphere and seawater

An automated Tekran atmospheric mercury speciation system measured mercury continuously throughout Legs 3a and 4. An outdoor atmospheric sampler was installed on the starboard bow on a stand. The outdoor sampling unit was fed into the starboard dry lab container, where two additional units, the pump module and the 2537B mercury detector unit, measured real-time GEM during the ship transects in the Canadian Arctic. Discrete GEM measurements were obtained every 5 minutes. The placement of the atmospheric sampling unit was selected in order to obtain air samples that were not contaminated by exhaust from the ship engines and to measure as close to the water surface as possible to best determine exchange between the atmosphere and ocean.

At Portable In-Situ Laboratory for Mercury Speciation (PILMS) on the ship, seawater samples taken from Trace Metal Rosette on Leg 2 were analyzed during Leg 3a by Tekran 2600 for total mercury concentration.

During Leg 3a, the ArcticNet Rosette was planned to wash out for mercury sampling. However, as it has been washed by Triton (a detergent) for three times, the test for MQ water from the Rosette is still not clean enough for mercury sampling.

31.2.4 SPMD deployments – Leg 3a only

10 SPMD cages were recovered on 3 ArcticNet (BS) and 2 BREA (BR) moorings as outlined below (Table 31-6). At some depths it was possible to fix the SPMD cages directly to the instrument cages (Figure 31.3), and at some depths the cages were fixed to the mooring line (Figure 31.4). All cages were recovered and only 2 were damaged during the recovery operation. Damages were not terribly concerning; all the cages will be able to be used again in the future.

Table 31-6. SPMDs recovered during Leg 3a of the ArcticNet 2015 cruise.

SPMD Depth (m)	BS-1 (80m)	BS-2 (300m)	BS-3 (500m)	BR-04 (155m)	BR-03 (700m)
50-60m surf mixed layer	SPMD 50m	SPMD 50m	SPMD 50m	SPMD 60m	SPMD 60m
50-200m Pacific water		SPMD 100m	SPMD 100m		SPMD 200m
>200 m Atlantic water		SPMD 200m	SPMD 300m		



Figure 31-3. SPMD cage installed on ArcticNet mooring BS-3.



Figure 31-4. SPMD cage installed on the line on BREA mooring BR-3.

3 BREA (BR) moorings in 2015 were deployed with SPMDs as outlined in Table 31-7 below.

Table 31-7. SPMDs deployed during Leg 3a of the ArcticNet 2015 cruise.

SPMD Depth (m)	BR-K (170m)	BR-G (700m)	BR-03 (700m)
50-60m surf mixed layer	SPMD 145m	SPMD 60m	SPMD 60m
50-200m Pacific water		SPMD 180m	SPMD 180m
>200 m Atlantic water		SPMD 460m	

31.3 Preliminary results

No analyses were performed on the ship for hydrocarbon, mercury and methyl mercury as well as benthic microbial diversity and SPDM deployments. Analysis of the collected data on the atmospheric mercury instrument is ongoing. However, initial review of the data show that GEM concentrations in the air ranged from 0.9 to 1.3 ng m⁻³ during Legs 3a and 4. The concentration of total mercury measured in the seawater during Leg 2 is 0.1-0.5 pM. However, some samples have higher values of mercury ~1.2 pM. These high values could be a result of particle mercury scavenging from the air and then it deposits in the surface seawater.

31.4 Comments and recommendations

31.4.1 Leg 3a

Station 514 is the same as Station 2010, which was sampled during CFL Leg 9 in 2008! It was such a great opportunity to go back to sample the benthic and pelagic invertebrate communities – thanks Keith and Commandant Lacerte. The boxcore failed to collect sediment samples a few times due to rocky bottom, thus samples should be collected opportunistically at nearby stations as a backup. The Agassiz trawl was not deployed at Station 421, as it was too deep (1200m).

31.4.2 Leg 3b

We were unable to collect samples at the deep stations (CB3 and CB4) due to insufficient winch cable length for both the CTD Rosette and the boxcore. Sediment samples from these depths could be very interesting to compare to shelf and slope samples in the future; therefore, a longer cable for both could be useful.

31.4.3 Leg 4

The box core failed to collect sediment samples a few times due to rocky bottom. When this occurs, we would like if samples could be collected opportunistically at nearby stations as a backup. This did occur for Station 170, where we also obtained box cores at the nearby ROV dive site and the CASQ3 core site. Station 170 (Scott Inlet) was so different this year, compared to the past two seasons of sampling. It would be something to discuss with the bottom-mapping group, whether we should continue to sample at the exact location of Station 170, or should we move it around to find proper sediments. Sample analysis should be performed before any decisions will be taken on this subject.

References

Hazen et al. 2011, Science 330: 204.
Hubert et al. 2009, Science 325: 1541.
Jørgensen 1982, Nature 296: 643.

32 Contaminants sampling program (GEOTRACES) – Legs 2 and 3b

Project leader: Feiyue Wang¹ (feiyue.wang@umanitoba.ca)

Cruise participants Leg 2: Kathleen Munson¹, Kang Wang¹ and Wen Xu¹

Cruise participants Leg 3b: Kang Wang¹ and Ashley Elliott¹

¹ *Centre for Earth Observation Science, Department of Environment and Geography, Clayton H. Riddell Faculty of Environment, Earth and Resources, University of Manitoba, 460 Wallace Building, Winnipeg, MB, R3T 2N2, Canada.*

32.1 Introduction

32.1.1 Total and Methylated Mercury in Seawater

Mercury (Hg) in the Arctic marine ecosystem is a hot topic due to its high toxicity and biomagnification in the food web, and the main culprit of both features is monomethylmercury (MMHg). While major progress has been made with respect to the Hg distribution and speciation in the atmosphere and biota, much less is known about the source and distribution of Hg species (MMHg in particular) in the Arctic seawater, which is the primary Hg exposure pathway to marine biota.

Though release of sediment produced methylated Hg (MeHg, sum of MMHg and dimethylmercury) was postulated as the primary seawater MeHg source (Hammerschmidt and Fitzgerald 2006), sub-surface peak of MeHg recently observed in different oceans suggest water column Hg methylation is a more important source in seawater. In addition, the subsurface MeHg peak always shows up in the depth where nutrients are high and dissolved oxygen is low, suggesting the association of in-situ MeHg production and organic matter (OM) remineralization.

Considering the knowledge gap in distribution and source of MeHg in the Arctic Ocean, the objectives of this project are set as:

- To map the distribution of total Hg (Hg_T) and MeHg as well as particulate Hg (Hg_p) in the Canadian Arctic seawater;
- To identify the mechanisms of Hg methylation in water column, and how it is associated with OM remineralization.

32.1.2 Atmospheric Mercury

Mercury is one of the primary contaminants of concern in the Arctic marine ecosystem. It can be transported to the Arctic via long-range atmospheric transport. Gaseous elementary mercury (GEM) is the main mercury species in the atmosphere since it has a long residence time (up to two years) and is relatively stable (Stephen et al. 2008). In the presence of strong oxidants in the air (e.g. halogen atoms), GEM can be rapidly oxidized into reactive

gaseous mercury (RGM), which then can be adsorbed onto aerosols to become to particulate mercury (PHg). Both RGM and PHg are much more reactive than GEM, and can readily deposit onto the surface environment (e.g. snow, ice and seawater). In the springtime Arctic, the oxidation and deposition processes are accelerated by photolytically produced reactive halogens, resulting in the so-called mercury depletion events. In the summer time, on the other hand, the open ocean can be a source of atmospheric mercury and release mercury into the air. Previous model studies suggest that 30-40% mercury deposited to the ocean is re-emitted. Much less is known about the oxidation process of GEM during the Arctic summer.

The objective of the atmospheric mercury project was to analyze three different species of mercury in the air: GEM, RGM and PHg. Together with the complementary project measuring mercury species in seawater, the results of this project will improve our understanding of Hg redox reactions and exchange between the atmosphere and the ocean in the Arctic summer.

32.2 Methodology

32.2.1 Total and Methylated Mercury in Seawater

Seawater samples were collected via Trace metal Rosette from all the GEOTRACES stations along the route of *Amundsen* during Legs 2 (except LS2) and 3b (Table 32-1 and Table 32-2). Samples of Hg_T and MeHg were included in all the stations, while large volume (up to 11L) of seawater were filtered to get the data of particulate Hg (Hg_P) in Stations K1, BB2 (Leg 2) and CB4 (Leg 3b). At Station BB2, extra samples of Hg_T and MeHg were collected for inter-calibration.

Both Hg_T and MeHg were acidified immediately upon collection, and refrigerated before being analyzed onboard the ship at the Portable In-Situ Laboratory for Mercury Speciation (PILMS). The instrument used was a Tekran 2600 for Hg_T analysis and a Brooks Rand MERX for MeHg. On the other hand, the filters for Hg_P were frozen for shipment to Winnipeg for analysis at University of Manitoba.

To study the mechanism of Hg methylation in water column, incubation experiments were carried out onboard. Isotopic enriched Hg and MMHg were spiked to newly collected seawater to start the incubation, which were stopped after certain period of time by acidification. The samples for incubation will be shipped to University of Manitoba for analysis.

Table 32-1. Stations sampled during Leg 2.

Station	Location	Samples collected
K1	Labrador Sea	HgT, HgP, MeHg
BB1	Baffin Bay	HgT, MeHg
BB3	Baffin Bay	HgT, MeHg
BB2	Baffin Bay	HgT, HgP, MeHg inter-calibration
CAA1	Northwest Passage	HgT, MeHg
CAA2	Northwest Passage	HgT, MeHg
CAA3	Northwest Passage	HgT, MeHg
CAA5	Northwest Passage	HgT, MeHg
CAA4	Northwest Passage	HgT, MeHg
CAA6	Northwest Passage	HgT, MeHg
CAA7	Northwest Passage	HgT, MeHg

Table 32-2. Stations sampled during Leg 3b.

Station	Location	Coordinates	Bottom Depth (m)	Samples collected
CB1	Beaufort Sea	75°N, 120°W	465	HgT, MeHg
CB2	Beaufort Sea	75°N, 129°W	1365	HgT, MeHg
CB3	Beaufort Sea	76°N, 140°W	3500	HgT, MeHg
CB4	Beaufort Sea	75°N, 150°W	3830	HgT, HgP, MeHg inter-calibration
CAA8	Parry Channel	74°N, 108°W	560	HgT, MeHg
CAA9	Penny Strait	76°N, 096°W	340	HgT, MeHg

32.2.2 Atmospheric Mercury

An automated Tekran atmospheric mercury speciation system measured mercury throughout the Legs 2 and 3 transects. Two outdoor atmospheric samplers, the 1130 and 1135 modules, were installed on the starboard bow on a stand fabricated by the *Amundsen* engineers during mobilization in Quebec City. The outdoor sampling units fed into the starboard dry lab container, where two additional units, the pump module and the 2537B mercury detector unit, measured real-time GEM, RGM and PHg during the ship transects in the Canadian Arctic. The placement of the atmospheric sampling units was selected in order to obtain air samples that were not contaminated by exhaust from the ship engines and to measure as close to the water surface as possible to best determine exchange between the atmosphere and ocean. Discrete GEM measurements were obtained every 5 minutes. Analysis of PHg and RGM samples occurred after 2-hour collection periods.

During the first week of sampling in Leg 3a the two outdoor sampling units were exposed to water and were damaged. Following this event, it was only possible to sample GEM throughout the remaining transects. Continuous monitoring of GEM was carried out with measurements every 5 minutes.

32.3 Preliminary results

32.3.1 Total and Methylated Mercury in Seawater

During Leg 2, with most of Hg_T and MeHg data in process, the distribution of Hg_T in Station K1 is presented in Figure 32.1. Vertical distribution of total mercury in Station K1. The average Hg_T concentration in this station was 0.67 ± 0.14 pM, comparable with the recent published data in North Atlantic Ocean (Bowman et al. 2014). The low Hg_T in surface water might be resulted from particle scavenging, while the increasing concentrations in deep water are probably reflecting the release of Hg during remineralization.

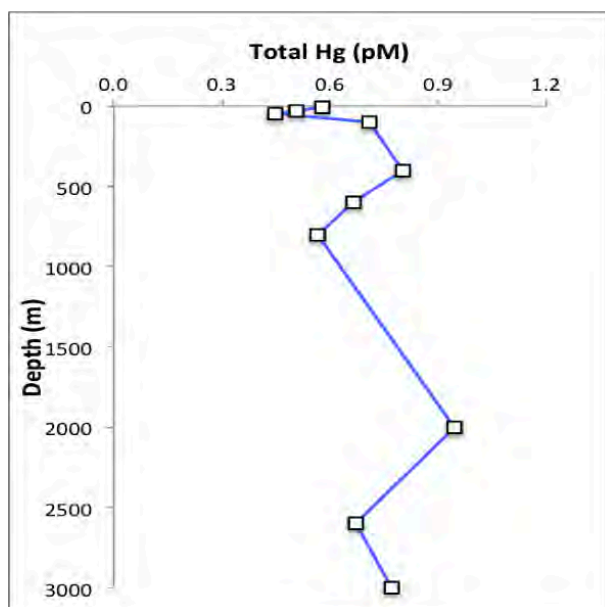


Figure 32-1. Vertical distribution of total mercury in Station K1.

On Leg 3b, while Hg_T concentrations in most of the seawater samples were in the range of 0.4-2.0 pM, some samples in mixed layer are showing value as high as ~4pM, which might be reflecting the atmospheric Hg deposition in surface seawater.

32.3.2 Atmospheric Mercury

Analysis of the collected data is ongoing. However, initial review of the data show that GEM concentrations in the air range from 0.8 to 1.2 $ng\ m^{-3}$ during Leg 2 and 0.8 to 1.6 $ng\ m^{-3}$ during Leg 3b.

32.4 Comments and recommendations

Because the atmospheric sampling was continuous throughout the cruise, we were able to collect atmospheric data during the diversion in the Hudson Bay. As a result, the atmospheric sampling was not hindered to the extent that our seawater sampling was during the icebreaking diversion.

The expedition was well planned and involved the cooperation of many. We were fortunate to execute sampling at all stations in the original plan as well as adding an additional station at the end to use up extra ship time available during Leg 3b. This extra station is of interest and we believe it was a good use of ship time. We are thankful that the chief scientist and ship captain were flexible in allowing opportunistic sampling of sea ice and water when time was available and conditions were suitable.

33 Marine Wildlife Monitoring Program – Leg 3a

ArcticNet Phase 3 – Marine Biological Hotspots: Ecosystem Services and Susceptibility to Climate Change.

<http://www.arcticnet.ulaval.ca/pdf/phase3/marine-ecosystem-services.pdf>

Cruise Participant Leg 3a: KAVIK Stantec

33.1 Methodology

The Marine Wildlife Observer (MWO) watch begins at sunrise and is completed at sunset. A new schedule has been applied for two observers on board the CCGS *Amundsen* to have at minimum, one observer on watch (on the bridge) during all daylight hours.

33.1.1 August 21st, 2015 – Friday

Operational updates

- MWO watch began at approximately 16:15² after refueling operations were complete near Kugluktuk

Marine mammal and seabird sightings

- No marine mammal sightings; glaucous gulls recorded during transit

HSE Updates/Issues

- Rangyn Lim and Trevor Lucas attended the Vessel Safety orientation tour at 13:30
- Three toolbox meetings (RMS1) were conducted and the RMS2 (Fit for duty assessment) was reviewed and signed off:
 - Morning - before the helicopter flight. Helicopter safety video and survival suit videos were watched. Reminders to wear warm clothing, close-toed shoes, no hoodies or jewelry.
 - Afternoon - when boarded the *Amundsen* and assigned rooms. Kavik-Stantec safe work practices were reviewed with Trevor. Reminders to be aware of our room location (starboard) and emergency exits.
 - Evening - after the end of the first shift. Watched the life on board presentation at the science team meeting presented by Keith. Reminders to be aware and not distracting during deck operations and bridge operations.

33.1.2 August 22nd, 2015 – Saturday

Marine mammal and seabird sightings

² Time reported is in Central Standard Time (CST) or `ship time`.

- No marine mammal sightings; loons, tundra swans and glaucous gulls were recorded during transit and while on station (*total sighting counts and individual numbers will be provided in the final report*)

HSE Updates/Issues

- Fire drill at 15:10 – both Trevor Lucas and Rangyn Lim participated. Completed at approximately 16:00.
- Three toolbox meetings (RMS1) were conducted and the RMS2 (Fit for duty assessment) was reviewed and signed off:
 - Morning – first full day shift. Reminder to self-assess for the Fit for Duty (RMS2 form) and bring up any issues if feeling ill to crew lead or chief scientist.
 - Afternoon – Reminder to bring personal life jacket to muster station and be aware of mustering at Starboard side
 - Evening – Reminder to understand the mustering bell and wear the life jackets tied appropriately with rope slings under the arm and collar velcro attached.

33.1.3 August 23rd, 2015 – Sunday

Marine mammal and seabird sightings

- A ringed seal was spotted today during slowed transit to search for the glider. The one seal was seen close to the port side of the bow looking towards the vessel. Common eiders, snow geese, parasitic and long-tailed jaegers were recorded at station and during transit.

HSE Updates/Issues

- Three toolbox meetings (RMS1) were conducted and the RMS2 (Fit for duty assessment) was reviewed and signed off:
 - Morning – Reminder to wear steel toed boots while on bow and front deck. Do not go on the deck during station operations.
 - Afternoon – In rough weather, reminder to stay hydrated and let crew lead or someone else know if feeling ill.
 - Evening – Reminder to secure personal items and equipment on bridge at the end of shift in case of rough weather.

33.1.4 August 24th, 2015 – Monday

Marine mammal and seabird sightings

- Two separate sightings of ringed seals (2 individuals in total) were observed during transit east towards the barge and glider deployment site.
- Glaucous gulls and parasitic jaegers were recorded during transit and at stations.

HSE Updates/Issues

- CCGS medical forms for Rangyn Lim and Trevor Lucas were completed and submitted to the nurse.
- Three toolbox meetings (RMS1) were conducted and the RMS2 (Fit for duty assessment) was reviewed and signed off:
 - Morning – Reminder to complete the medical form for the *Amundsen* nurse.
 - Afternoon – Reminder to wear warm layers and closed toed shoes on the bridge.
 - Evening – Reminder that the decks will be slippery after rough weather and to always maintain 3 points of contact.

33.1.5 August 25th, 2015 – Tuesday

Marine mammal and seabird sightings

- Bowhead whales were recorded on transit from Station 420 to 434 in shallow depths at approximately 35 – 40 m. There were six sightings of bowhead whale individuals and 3 sightings of bowhead whales in pairs. A total of 12 bowhead whales were recorded in total. Three sightings of ringed seals (3 individuals in total) were observed at Station #420 and during transit towards Station 434. Glaucous gulls, and yellow-billed loons were also identified at station.

HSE Updates/Issues

Three toolbox meetings (RMS1) were conducted and the RMS2 (Fit for duty assessment) was reviewed and signed off:

- Reminder to raise any issues to crew lead or chief scientist if any hazards or near misses are observed.
- Reminder to take visual breaks during long observations with binoculars.

33.1.6 August 26th, 2015 – Wednesday

Marine mammal and seabird sightings

- Two bowhead whales were recorded in the morning at approximately 7:50 am during transit towards mooring station BS 1 in ~70 m water depth.
- A Sabine gull, yellow-billed loon and glaucous gulls were also recorded during transit and at stations.

HSE Updates/Issues

Three toolbox meetings (RMS1) were conducted and the RMS2 (Fit for duty assessment) was reviewed and signed off:

- Reminder to exercise and stretch between shifts for muscle cramps from sitting for long periods of observation.

33.1.7 August 27th, 2015 – Thursday

MWO watch ended at approximately 17:30 due to high Beaufort Sea states (6-7) and wind (> 40 knots).

Marine mammal and seabird sightings

- Common eiders were recorded flying SE while on station.

HSE Updates/Issues

- Two toolbox meetings (RMS1) were conducted and the RMS2 (Fit for duty assessment) was reviewed and signed off:
 - Reminder to secure all equipment on the bridge and personal items in cabin for weather warning in the evening.
 - Trevor was feeling slightly seasick after the shift during the rough weather.

33.1.8 August 28th, 2015 – Friday

Marine mammal and seabird sightings

- An individual bowhead whale was sighted in the evening during transit to the GSC Lander 2 deployment.
- A sighting of 6 ringed seals feeding, was recorded in the late evening on transit towards Station 431.
- Arctic terns, Sabine's gulls, long tailed jaeger, northern fulmar and glaucous gulls were recorded

HSE Updates/Issues

- Three toolbox meetings (RMS1) were conducted and the RMS2 (Fit for duty assessment) was reviewed and signed off:
 - Reminder to stay hydrated and drink water throughout the day.

33.1.9 August 29th, 2015 – Saturday

Marine mammal and seabird sightings

- Arctic tern, yellow-billed loons, common eiders and glaucous gulls were recorded during transit and at stations.

HSE Updates/Issues

- Three toolbox meetings (RMS1) were conducted and the RMS2 (Fit for duty assessment) was reviewed and signed off:
 - Reminder to wash hands and use hand sanitizer regularly.

33.1.10 August 30th, 2015 – Sunday

Marine mammal and seabird sightings

- Three bowhead whale sightings were recorded, two of an individual and one sighting of a pair during transit to mooring station BR4 in shallow water depths at approximately 55 m.
- One polar bear sighting observed on an ice floe. Trevor Lucas considered it as a likely female after looking at photos from the shape of its head and body.
- A ringed seal was recorded near an ice floe edge in the water during the late evening.
- Common eiders and glaucous gulls were also recorded while on transit.

HSE Updates/Issues

- Three toolbox meetings (RMS1) were conducted and the RMS2 (Fit for duty assessment) was reviewed and signed off:
 - Reminder to secure items as the vessel approaches and transits through larger ice floes. Vessel vibrates much more.
 - Earplugs are provided in case they are needed during the night as well.

33.1.11 August 30st, 2015 – Monday

Marine mammal and seabird sightings

- Common eiders and glaucous gulls were recorded during transit and near mooring stations.

HSE Updates/Issues

- Three toolbox meetings (RMS1) were conducted and the RMS2 (Fit for duty assessment) was reviewed and signed off:
 - Reminder to clean binoculars with alcohol wipes to prevent eye infections from sharing.

33.1.12 September 1st, 2015 – Tuesday

Marine mammal and seabird sightings

- One sighting of a polar bear mother and two cubs

HSE Updates/Issues

- Three toolbox meetings (RMS1) were conducted and the RMS2 (Fit for duty assessment) was reviewed and signed off:
 - Watched the helicopter safety video completed the tour with the pilot.
 - Reminder to know how to use the seatbelts and exit handles in the helicopter

33.1.13 September 2nd, 2015 – Wednesday

Marine mammal and seabird sightings

- Two sightings of ringed seals during transit and at station.
- One sighting a northern fulmar.

HSE Updates/Issues

- Three toolbox meetings (RMS1) were conducted and the RMS2 (Fit for duty assessment) was reviewed and signed off:
 - Reminders to pack equipment securely for demobilization
 - Check helicopter schedule for flight into Sachs Harbour

34 Seabird survey – Leg 4c

ArcticNet Phase 3 – Marine Biological Hotspots: Ecosystem Services and Susceptibility to Climate Change.

<http://www.arcticnet.ulaval.ca/pdf/phase3/marine-ecosystem-services.pdf>

Cruise Participant Leg 4c: Liam E. Peck¹

¹ *Canadian Wildlife Service, Environment Canada, Canada.*

34.1 Introduction

The east coast of Canada supports millions of breeding marine birds as well as migrants from the southern hemisphere and northeastern Atlantic. In 2005, the Canadian Wildlife Service (CWS) of Environment Canada initiated the Eastern Canada Seabirds at Sea (ECSAS) program with the goal of identifying and minimizing the impacts of human activities on birds in the marine environment. Since that time, a scientifically rigorous protocol for collecting data at sea and a sophisticated geodatabase have been developed, relationships with industry and DFO to support offshore seabird observers have been established, and over 100,000 km of ocean track have been surveyed by CWS-trained observers. These data are now being used to identify and address threats to birds in their marine environment. In addition, data are collected on marine mammals, sea turtles, sharks, and other marine organisms when they are encountered.

34.2 Methodology

Seabird surveys were conducted from the port side of the bridge of the CCG *Amundsen* from 26 Oct – 1 Nov, 2015. Surveys were conducted while the ship was moving at speeds greater than 4 knots, looking forward and scanning a 90° arc to one side of the ship. All birds observed on the water within a 300m-wide transect were recorded, and the snapshot approach for flying birds (intermittent sampling based on the speed of the ship) was used to avoid overestimating abundance of birds flying in and out of transect. Distance sampling methods were incorporated to address the variation in bird detectability. Details of the methods used can be found in the CWS standardized protocol for pelagic seabird surveys from moving platforms (Gjerdrum 2012).

34.3 Preliminary results

In total, 607.5 km of ocean were surveyed from 26 Oct – 1 Nov, 2015. A total of 272 birds were observed in transect (489 birds in total) from 7 families (Table 34-1). Bird densities averaged 1.3 birds/km² (ranging from 0 – 33.4 birds/km²). The highest densities of birds (>

10 birds/km²) were observed off the coast of southern Labrador, along the north coast of the Gulf of St. Lawrence, and in the St. Lawrence estuary (Figure 34.1).

Alcids accounted for 60% of the sightings (Table 34-1), which were primarily Dovekie. The Dovekie are considered the most numerous bird in the North Atlantic, the majority of which breed in Greenland and winter in Atlantic Canada. Gulls made up a combined 30% of the birds observed, primarily Herring Gulls, Black-legged Kittiwakes, and Glaucous Gulls, all of which breed along the Atlantic coast.

Table 34-1. List of bird species observed during surveys from the CCG *Amundsen* during Leg 4c.

Family	Species	Latin	Number observed in transect	Total number observed
Procellariidae	Northern Fulmar	<i>Fulmarus glacialis</i>	16	32
	Great Shearwater	<i>Ardenna gravis</i>	1	1
	Sooty Shearwater	<i>Ardenna griseus</i>	0	2
Hydrobatidae	Leach's Storm-Petrel	<i>Oceanodroma leucorhoa</i>	0	5
Anatidae	Common Eider	<i>Somateria mollissima</i>	5	5
	Greater Scaup	<i>Aythya marila</i>	0	2
	Genus: Goldeneye and Bufflehead	<i>Bucephala</i>	2	2
	Long-tailed Duck	<i>Clangula hyemalis</i>	1	1
	Unidentified Ducks	All duck genera	0	3
Scolopacidae	Unidentified Shorebirds	<i>Numenius</i>	0	32
	Unidentified Phalaropes	<i>Phalaropus</i>	0	1
Laridae	Herring Gull	<i>Larus argentatus</i>	35	43
	Black-legged Kittiwake	<i>Rissa tridactyla</i>	26	38
	Glaucous Gull	<i>Larus hyperboreus</i>	13	20
	Great Black-backed Gull	<i>Larus marinus</i>	6	11
	Bonaparte's Gull	<i>Larus philadelphia</i>	2	2
	Iceland Gull	<i>Larus glaucoides</i>	1	1
	Bonaparte's Gull	<i>Larus philadelphia</i>	0	1
	Unidentified Gulls	<i>Larus</i>	0	14
	Pomarine Jaeger	<i>Stercorarius pomarinus</i>	0	1
Alcidae	Dovekie	<i>Alle alle</i>	75	114
	Thick-billed Murre	<i>Uria lomvia</i>	44	51
	Black Guillemot	<i>Cephus grylle</i>	6	6
	Common Murre	<i>Uria aalge</i>	3	7
	Razorbill	<i>Alca torda</i>	0	1
	Unidentified Murres	<i>Uria</i>	11	31
	Unidentified Auks	Alcidae	0	36
Passeriformes	Unknown Songbird	Passeriformes	25	26
TOTAL			272	489



Figure 34-1. Density of bird species observed during surveys from the CCG Amundsen during Leg 4c.

References

Gjerdrum, C., D.A. Fifield, and S.I. Wilhelm. 2012. Eastern Canada Seabirds at Sea (ECSAS) standardized protocol for pelagic seabird surveys from moving and stationary platforms. Canadian Wildlife Service Technical Report Series. No. 515. Atlantic Region. vi + 36 pp.

35 Seafloor mapping, water column imaging and sub-bottom profiling – Legs 1, 2, 3a, 3b, 4a, 4b and 4c

ArcticNet Phase 3 – The Canadian Arctic Seabed: Navigation and Resource Mapping.
<http://www.arcticnet.ulaval.ca/pdf/phase1/16.pdf>

Project leader: Patrick Lajeunesse¹ (patrick.lajeunesse@ggr.ulaval.ca)

Cruise participants Leg 1: Gabriel Joyal¹, Jean-Guy Nistad¹ and Annie-Pier Trottier¹

Cruise participants Leg 2: Étienne Brouard¹ and Glenn Toldi²

Cruise participants Leg 3a: Gabriel Joyal¹ and Charles De Grandpré¹

Cruise participants Leg 3b: Charles De Grandpré¹ and Heidi Yu²

Cruise participants Leg 4a, 4b and 4c: Gabriel Joyal¹ and Étienne Brouard¹

¹ *Université Laval, Département de géographie, Pavillon Abitibi-Price, 2405 rue de la Terrasse, Québec, QC, G1V 0A6, Canada.*

² *Canadian Hydrographic Service – Central and Arctic Region, 867 Lakeshore Rd., Burlington, ON, L7R 4A6, Canada.*

35.1 Introduction

35.1.1 Leg 1 – 17 April to 4 May 2015

Three members of the *Marine Geoscience Lab.* (MGL – Université Laval, Québec) were onboard and responsible for multibeam data acquisition. The main objective of the mission was to acquire data on sea ice and icebergs, as well as water mass properties and meteorology in the NE Newfoundland Shelf. The MGL has been involved mainly in the iceberg mapping, in collaboration with the *Water and Ice Research Lab.* (WIRL – Carlton University, Ottawa), but also collected data on the seabed morphology and sub-bottom stratigraphy of the studied area during transits. The MGL was also responsible for surveying and identifying moorings after their deployment.

During this oceanographic mission, the MGL has taken part into four main projects:

- Iceberg Mapping on the Barge (Statoil and Carleton University);
- Mooring Deployment and Validation of Instrument Depths (Statoil, ASL and ArcticNet);
- Transit Mapping (Université Laval and ArcticNet);
- MVP (Moving Vessel Profiler) deployment for SX90 surveys.

The participants on the cruise also used “free” time (free time during night during the Wave glider trials) in the Natashquan area to map the submarine portion of the delta. Finally, a calibration test for backscatter was conducted during the transit from Natashquan to Pointe-des-Monts.

35.1.2 Leg 2 – 10 July to 20 August 2015

The Marine Geoscience Lab. (MGL – Université Laval, Québec) and the Canadian Hydrographic Service (CHS) were onboard and responsible for multibeam data acquisition. The main objective of the mission was to acquire data on water properties in Baffin Bay and in the Canadian Archipelago as part of a ArcticNet-GEOTRACES cruise. The MGL-CHS team has been mainly involved in mapping the seabed morphology and in acquiring sub-bottom stratigraphy during transits.

35.1.3 Leg 3 – 20 August to 1 October 2015

The Marine Geoscience Lab. (MGL – Université Laval, Québec; Legs 3a and 3b) and the Canadian Hydrographic Service (CHS; Leg 3b) were onboard and responsible for multibeam data acquisition.

Leg 3a was dedicated mainly to mooring operations. Two landers (tripods with ADCP) were deployed by the Geological Survey of Canada. Two transects were also sampled. All the transits between stations were mapped.

Leg 3b was dedicated mainly to sampling operation for the GEOTRACES program. A mooring has also been deployed during the second half of the leg and a station transect has been sampled. Finally, a Moving Vessel Profiler transect has been performed during the last four days of the leg. Most of the transit between stations has been mapped. Because of a hardware problem on the multibeam during the deep water station in the Beaufort Sea (which will be discussed more in detail in a later section), some of the transit did not get mapped, or the resolution of the mapping was very low.

The MGL-CHS has been involved mainly in the acquisition of data on the seabed morphology and sub-bottom stratigraphy during transits. The team was also responsible for surveying and identifying moorings before their recovery and after their deployment. This cruise report presents the instruments, methods and preliminary results from Leg 3:

- Mooring recovery and deployment for validation of instrument depths
- Transit mapping
- GSC landers deployment assistance
- Moving Vessel Profiler (MVP)

35.1.4 Leg 4 – 1 October to 1 November 2015

The *Marine Geoscience Lab.* (MGL – Université Laval, Québec); was onboard and responsible for multibeam data acquisition.

The MGL has been involved mainly in the acquisition of data on the seabed morphology and sub-bottom stratigraphy during transits and for dedicated mapping surveys. This cruise report presents the instruments, methods and preliminary results from Leg 4:

- Transit mapping
- Dedicated mapping surveys
 - Sam Ford Fjord and Scott Inlet
 - ROV dive sites
 - CASQ coring sites
 - 3 GSC coring sites
 - Merchants Bay – piston coring

35.2 Methodology

35.2.1 Equipment

Kongsberg EM302 Multibeam Sonar. The *Amundsen* is equipped with an EM302 multibeam sonar operated with the Seafloor Information System (SIS). Attitude is given by an Applanix POS-MV receiving RTCM 1-9 corrections from a CNAV 3050 GPS receiver. Position accuracies were approximately $< 0.6\text{m}$ (0.8m during Legs 1 and 2) in planimetry and $< 1\text{m}$ in altimetry. Beam forming at the transducer head is done by using an AML probe. CTD-Rosette casts, when available, were used for sound speed corrections. During long periods without CTD casts, the WOA09 model was used. The processing of bathymetric point cloud and data integration is made in the CARIS HIPS&SIPS v9.0.1 software. Final grids will be generated with MB-System and distributed soon on a web interface at Université Laval's library. A new Hydrographic Working Station (HWS) was installed by Kongsberg in June 2014³.

There were some issues with the echosounder during the Leg 2. First, an electrical problem was detected in the electric circuit between the PU and the transducer head. There was too much current intensity going through the circuit. BIST tests of the systems were ran to get some information on what was going on and an email was sent to Kongsberg for them analyze the test results. Kongsberg replied that the intensity wasn't that much problematic but that there were issues with some TX boards. From looking over the BIST results they saw that in TX slots we had errors on board 5, 18, 19, 20, and 21. The team did to figure if the errors lied in the boards or in the transducer. The tests revealed that the errors come from the transducer. The errors are probably due to physic problem such as rust or bad connections. Although this problem does not seem to affect data, it is something that should be looked at after the summer mission.

Another problem was the periodical loss of port side beams on data (Figure 35-1). It didn't show any logical periodicity as it happened sometime here and then. This problem was probably due to degradation of the port side beams transducers. This problem had no link with the electrical problem as it occurred before the electrical problem.

³ The SIS for EM302 was upgraded to version 4.1.5 and the PU firmware was upgraded to version 1.0.4. Two third-party softwares were installed: Applanix MV-POS View and Hyperterminal.

The other problem was the length of the period needed for emitting and receiving in greater depths (> 1000m). The echosounder needed ~6 – 8 seconds to emit and receive its signal. It looks too much as it should take between 2 and 4 seconds depending on depths. K-sync configurations were checked and the problem did not seem to come from there. The team also tried to figure out if it was a parameter issue in SIS software. These tests didn't bring any clue on what could delay the system. Still this problem wasn't linked with the electrical problem as it happened before it.

During Leg 3, the team tried to assess the issues raised during the previous leg about electrical problems between the PU and the transducers

According to discussion Gabriel had with the Kongsberg technician when he came in June, this problem could have been due to the incompatibility problem between the EM302 Processing Unit and the older EM300 transducers. Alexis Cardenas, the Kongsberg technician, also raised the hypothesis that the ice window in front of the transducer head could have affected the quality of the BIST tests. After installing the new HWS in June, the BIST tests were ran and same results as in Leg 2 were obtained. Kongsberg's Technical Support team told the team that the problem was "normal" and should not affect data quality. These failures in the BIST tests were also noted by Doug Cartwright in 2008 when the old EM300 PU was replaced by the newer EM302 PU⁴.

For the electrical problem, this issue was also raised by the CCG Senior Electrician. This must be checked in further details.

The loss of the port side beam was also noted. Kongsberg was contacted.

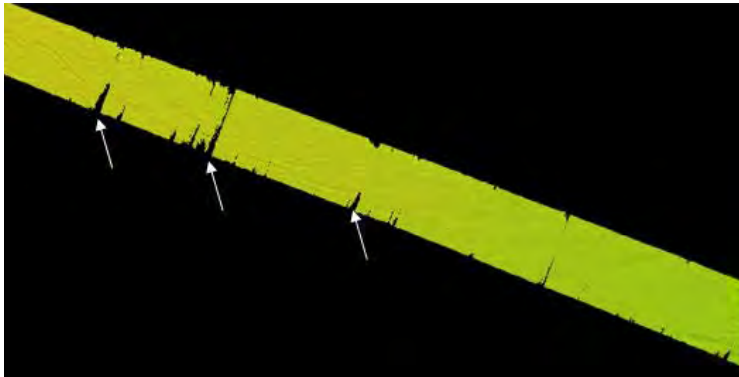


Figure 35-1. Example of periodical port side beam loss on data.

In accordance with what was said before, some issues occurred with the multibeam during Leg 3b. During deep water operations, the ping rate was very low causing a very poor resolution (about 170 meters between each swath, Figure 35-2).

⁴ (<http://www.omg.unb.ca/people/cartd/em302.html>)

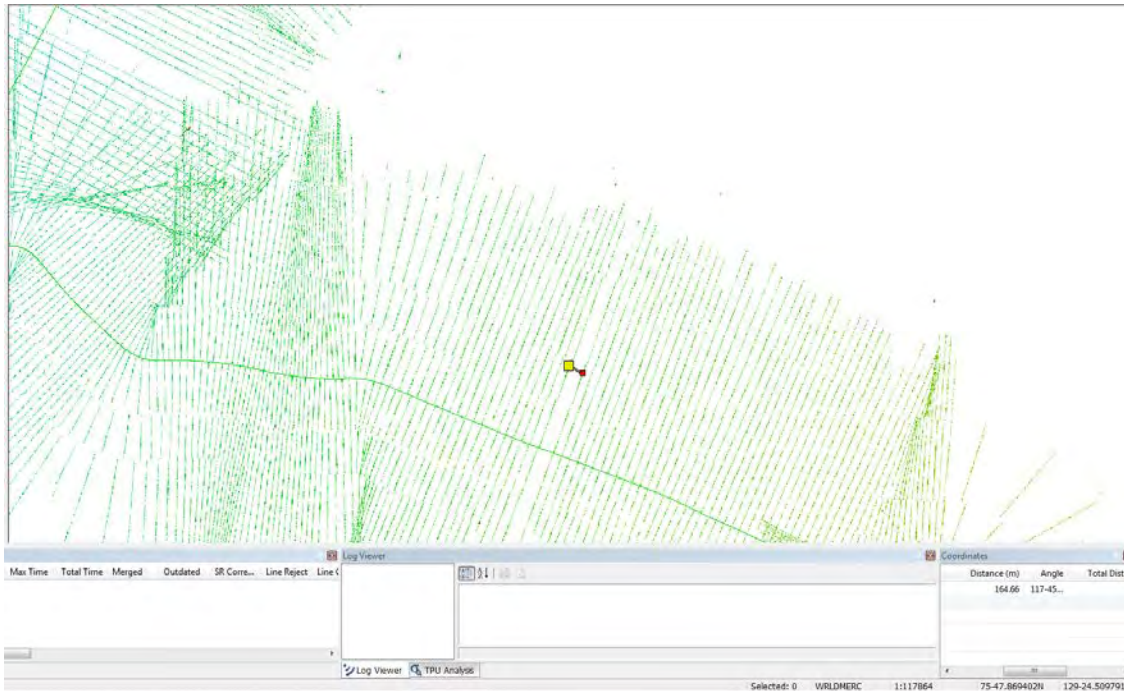


Figure 35-2. Example of the data acquired in deep water conditions.

At first the team tried to change some options in SIS to see if it could solve the problem. The “external trigger” option was turned off in the runtime menu, to make sure that the K-Sync was not limiting the EM302 but no difference was observed. After that, the Dual swath mode was changed from Fixed to Dynamic, though still it did not make any difference.

So in order to know what the problem was, the team communicated with Kongsberg, which asked us to run a telnet session to log the message from the multibeam. After Kongsberg analyzed the results from the telnet session, they told us that the issue was probably related to the BSP boards, the RX boards or the Ethernet connector. In accordance with those results, the team first tried to make a new Ethernet connector, the one in place being in very bad condition, though it didn’t change the quality of the data. It was then decided to remove the BSP and RX boards and clean them with a compressed air duster. Finally, this last operation did make a difference. The ping rate increased and so did the data resolution.

During Leg 4, the problems with the multibeam sonar noted during Legs 2 and 3 were assessed and taken into account. The electronic boards of the EM302 processing unit have been cleaned. The EM302 has also been removed from the K-Sync trigger system in order to increase the ping rate at its maximum. This modification did not change anything to the other sonars because the EM302 was in both groups in the *Shallow Water Survey (<750m)* settings, which was the most used one.

It seems that the multibeam is running better in deep waters (>700m), although a complete maintenance should be done on electronic components before the 2016 cruise.

Knudsen 320BR CHIRP Sub-bottom Profiler. Sub-bottom profiles were acquired by a 3.5 kHz Knudsen 320-BR CHIRP. This single beam sonar is capable of imaging sub-bottom

stratigraphic profiles of the seafloor. The sub-bottom profiler worked as expected during Leg 3a and 4. GSC representative onboard during both legs were very interested in getting the .sgy files every day. Edward (Ned) King brought a portable hard drive to get all the 2014 and 2015 (up to the end of Leg 3a) Knudsen data to bring it to GSC, as they will host the *Amundsen's* sub-bottom data distribution service.

However, at the end of Leg 3b, the computer of the sub-bottom profiler started to shut down for no reason. After some investigations, the team noticed that the problem was related to SCSI board, which is a device that makes the connection between the sub-bottom profiler and the computer. Because it was a hardware problem and no spare component was available, the team was not able to solve the problem. The sub-bottom profiler was operated for the last four days of the leg knowing that the computer would intermittently shut down. For this reason, the sub-bottom profiler data for the last four days are intermittent. Though, to be sure that the sub-bottom profiler would work properly for the Leg 4, Gabriel was contacted and asked to bring a brand new computer and a new SCSI adaptor on board.

Moving Vessel Profiler (MVP) 300. Along track profiles of sound velocity were performed using a Moving Vessel Profiler (MVP 300) towed behind the ship at 8 kts.

Reson 8101 Multibeam Sonar. – Leg 1 only. For this dedicated mission, the barge was equipped with a *Reson 8101* multibeam sonar operating at a frequency of 250 kHz. The transducer was tilted 30° to the port side of the vessel in order to map the submerged portion of icebergs. An *IXSEA Octans III* motion sensor was used, as well as a *Hemisphere VS131* GPS receiver.

CNAV 3050 GNSS receiver. Since the beginning of Leg 3a, the team noticed that they were having problems receiving the CNAV corrections they purchased (yearly plan to improve the positioning quality from ~30cm to ~3cm). The receiver had a problem with fixing the corrections (the indicator light on the front panel of the receiver was flashing green and red). The corrections would fix for a few minutes and then the receiver would restart the initialization phase. The effects of this error on the systems were not noticed right away. The main effect was noticed on the position Error Estimates Std Deviation (Figure 35-3).

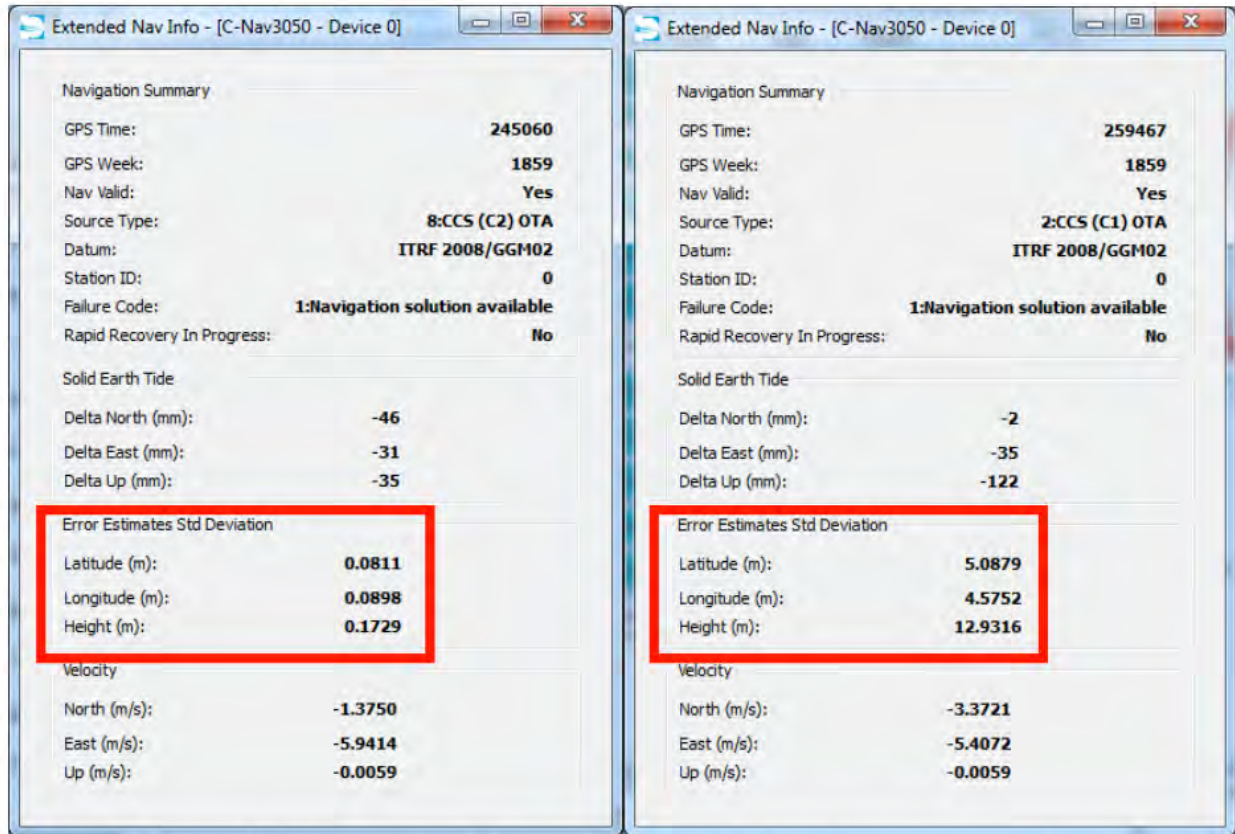


Figure 35-3. Degradation of the Error Estimates Std Deviation due to correction signal loss.

Another effect was observed by Simon Morisset, the ArcticNet technician who uses the GPS GGA string to feed the hull-mounted ADCP. He was having the following error messages saying that the VTG/GGA data was now unavailable. Since the CNAV was the primary GPS source for the ADCP, it was decided that the GGA source would be changed for the POS MV, which looked more stable.

CNAV Technical Support was contacted and many possible answers were raised:

- Inappropriate cable type and length (max. 63m); This explanation seemed unlikely as this problem did not appear last year, while the exact same setup (antenna, cable type, cable length and receiver) was used.
- Power failure (too much resistance) in the cable / on the antenna connector / on the receiver; Even if the resistance in the cable was not tested (because the team did not want to shut down the GPS), the CCG was asked to send someone up on the mast to verify possible antenna degradation or rust on the connectors. According to a picture and the deckhand, the connector and the antenna were in good shape. The deckhand was also asked to clean the antenna (as well as the POS MV antennas)
- Antenna not high enough: Once again, the mounting is the same as last year and the antenna is located on the highest mast of the ship. In fact, the CNAV antenna is the highest point of the ship!
- Elevation angle too low: After a discussion with the CCG Electronic Officer, it was found that the elevation angle of the correction satellites was too low to be able to track it.

Nevertheless, despite degraded positioning accuracies and warning messages in the ADCP acquisition software, no changes on the Position Accuracies on the POS MV between fixed or unfixed stage of the CNAV were observed. For many hours, the team did not have the corrections and the POSMV would still be able to be accurate to about 50 cm planimetric resolution and 1.4m in vertical resolution. The team is now starting to think that the corrections do not affect the quality of the RTCM feed to the POS MV.

As the ship was heading south during Leg 4, the problem seemed to have resolved. This means that the issues were due to the relative position of the ship's receiver and the corrections satellites. The need of this correction will have to be reassessed in the future, as it did not improve significantly the quality of the final positioning accuracies.

35.2.2 Field work procedures

All the data acquired during the cruise were pre-processed in real-time using the CARIS HIPS&SIPS 8.1.5 software. This pre-processing phase is essential to rapidly detect any anomaly in the data collection.

Mooring recovery and deployment

The role of the mapping team during mooring deployment and recovery was to

- Ensure the mooring was still in its position (identify the buoys and the exact position);
- Validate the depths of the deployment sites;
- Map the surface morphology of the sites;
- Determine the verticality of the moorings after deployment (Figure 35-4).

The team logging the lines over the mooring. The lines were processed in CARIS HIPS&SIPS right after to find the exact position (Figure 35-5). The procedure started with the visualization of the water column data to find the buoys. The buoys scattering was added to bathymetry (Figure 35-5). The exact position was given to the bridge to ensure exact and safe recovery.

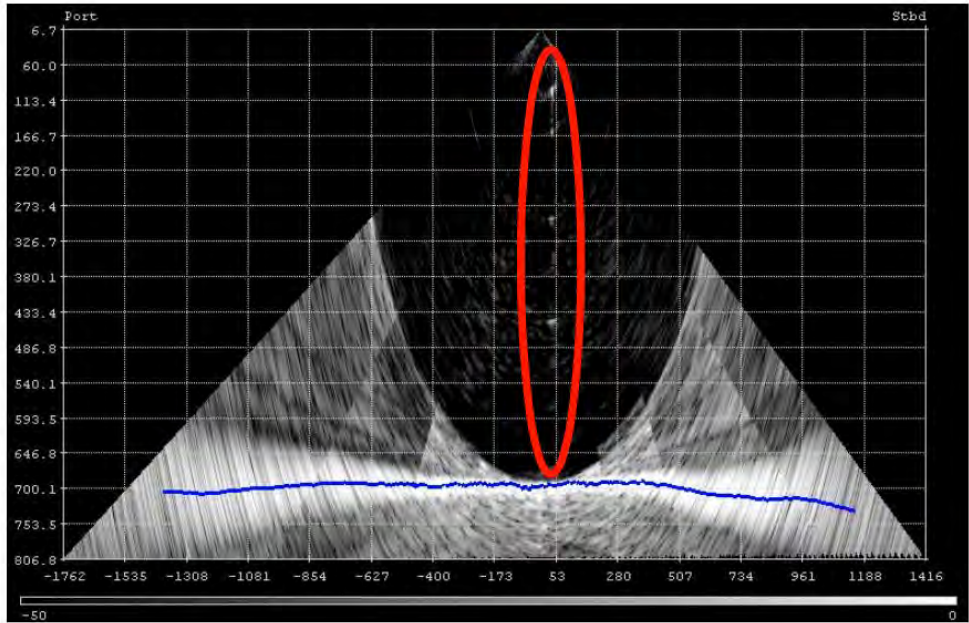


Figure 35-4. SIS water Column display of Mooring site BR-G before recovery. The red circle shows the buoys.

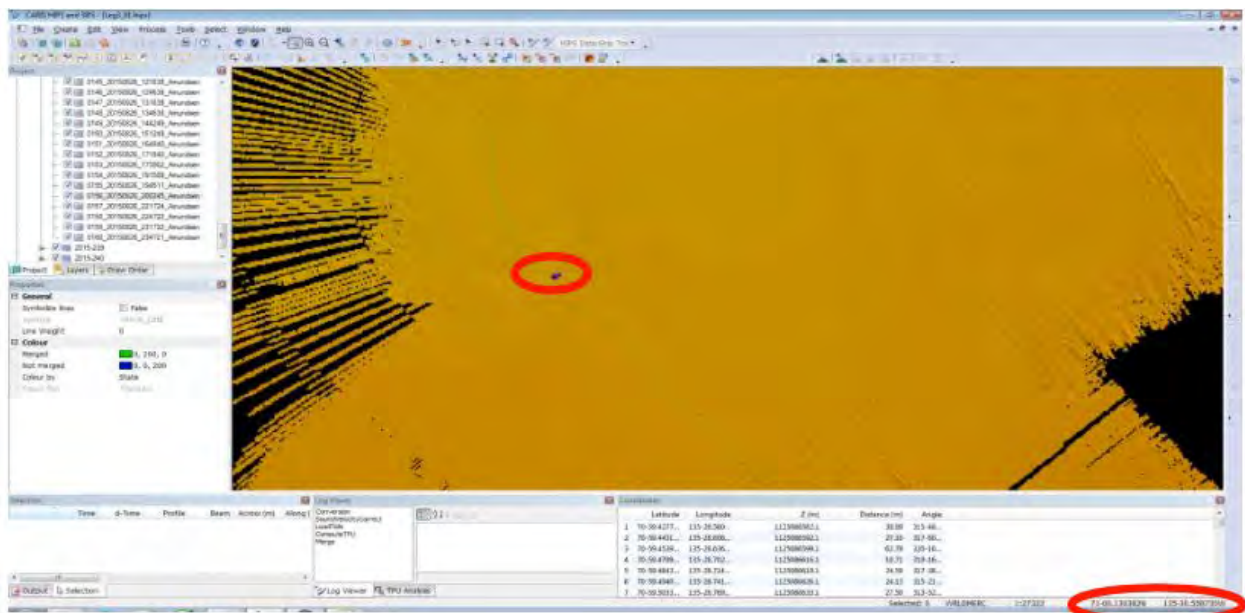


Figure 35-5. Mooring BR-G added to bathymetry (purple dots) in CARIS HIPS&SIPS processing software. The exact position of the mooring is given in the lower right corner.

The team was able to identify all the moorings during Legs 3a and 3b. The resolved positioning precision was around 10 meters.

Transit Mapping

Transit routes were surveyed systematically during all the legs in order to increase the multibeam dataset. The discussions the team had last year with the commanding officers

led to a major improvement of the navigation interface displayed on the bridge. Since the team has a new HWS, it is now possible to load multiple background files. Those background files include the CHS chart and the multibeam coverage (Figure 35-6). Glenn Toldi, a CHS representative who was onboard during Leg 2, brought the CHS Arctic multibeam database. The bathymetric coverage was very useful to create navigation maps that were imported into SIS to improve the seabed coverage.

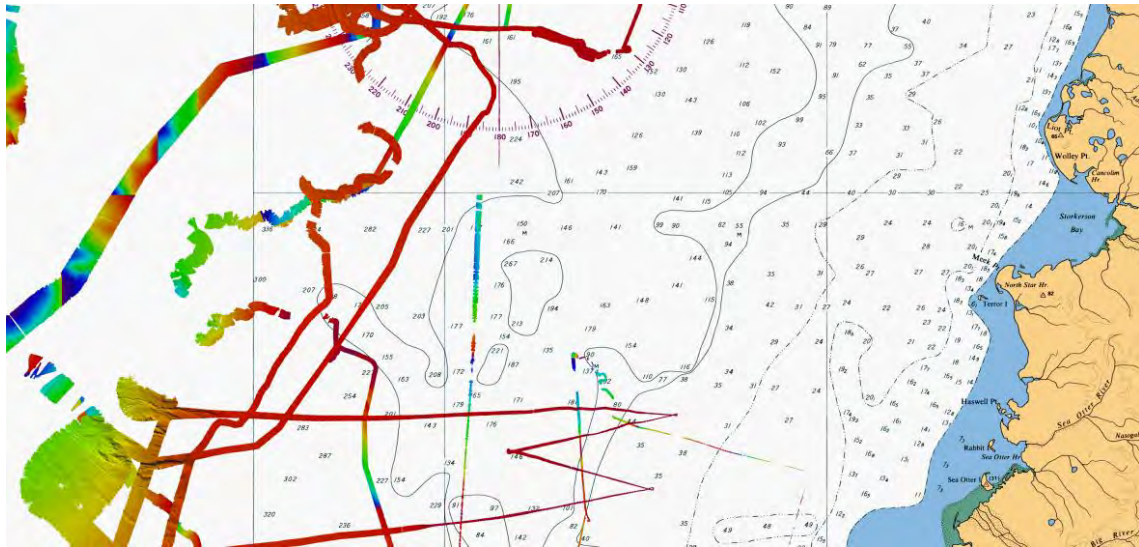


Figure 35-6. Example of background files imported in SIS.

This improvement greatly helped the planning of the transit lines. The helmsmen were able to follow new routes along existing coverage. They were doing their best to increase the coverage and keeping an overlap of at least 15-25% (Figure 35-7). They were very happy with the SIS display. Moreover, there is now a UHF radio in the acquisition room that really increases the ability to start logging after stations and to be constantly in contact with the bridge.

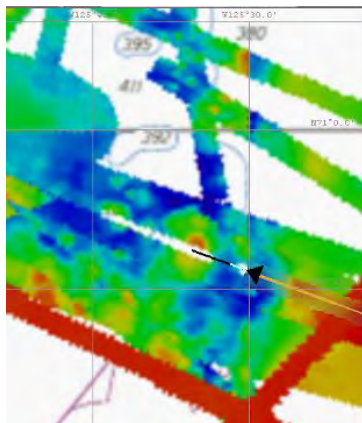


Figure 35-7. Geographical display in SIS showing the navigation route taken to increase the bathymetric coverage; to fill the hole between two previous lines.

All the data will be shared with the Canadian Hydrographic Service (CHS) to update marine charts and might be useful for future work within the ArcticNet program. During Leg 1, all the raw multibeam and sub-bottom lines logged at the East of Newfoundland were given to Statoil on a hard drive.

GSC Landers

During Leg 3, the seabed mapping team helped the GSC landers deployment (Figure 35-8). During the deployment, the water column display was used to assess the depth of the lander as it was going down to the seabed (Figure 35-8). This technique was useful only for the deployment. As the landers approached the seabed (<5-10m off bottom), the team was not able to identify the scattering of the lander alone.

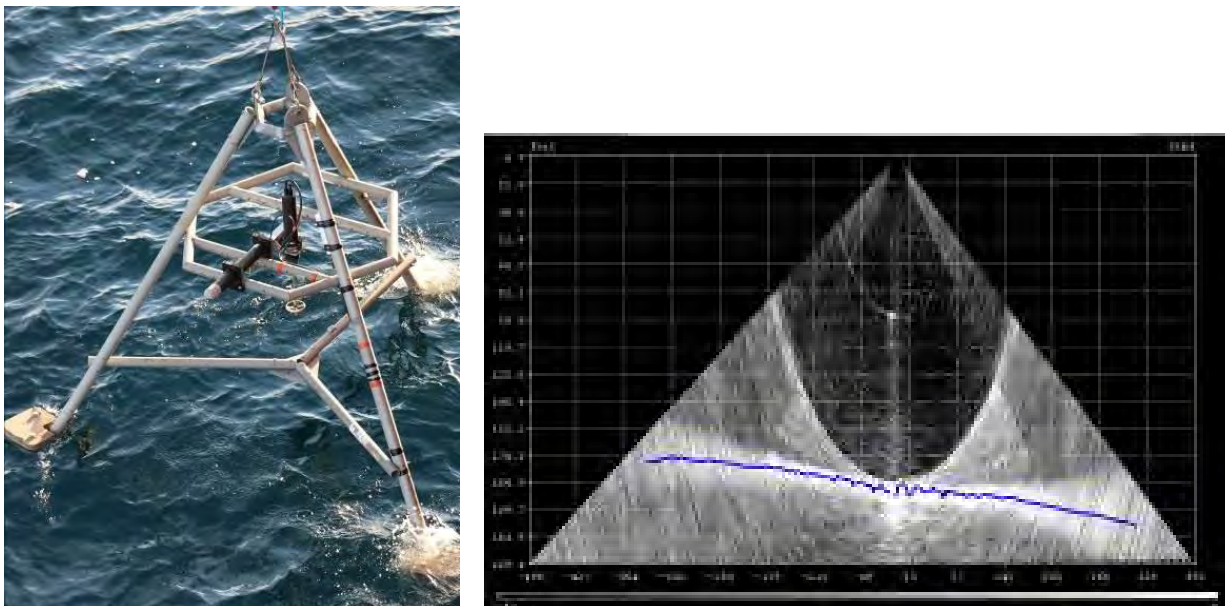


Figure 35-8. (Left) GSC Lander; (Right) Water column display to visualize the deployment of the lander. The bright scattering in the middle of the water column.

Moving Vessel Profiler (MVP) 300

Three MVP transects were carried in the St. Lawrence Gulf and Estuary as requested by Maxime Geoffroy (SX90 operator; Table 35-1). Those transects are going to be used to model the water column properties along transects. Table 35-1 describes the MVP transects. Both the down and up casts were logged.

Table 35-1. MVP transects description during Leg 1.

Name of Transect	Location	Nb. of casts	Maximum depths (m)	Description
1501001	St. Lawrence Gulf (Grande-Rivière)	4	225	Sea Trials
1501002	St. Lawrence Gulf (Natasquan-Aguanish)	12	80	SX 90 Survey off Natashquan
1501003	St. Lawrence Estuary (Escoumins – Bergeronnes)	9	300	SX 90 Survey off Escoumins – Tadoussac

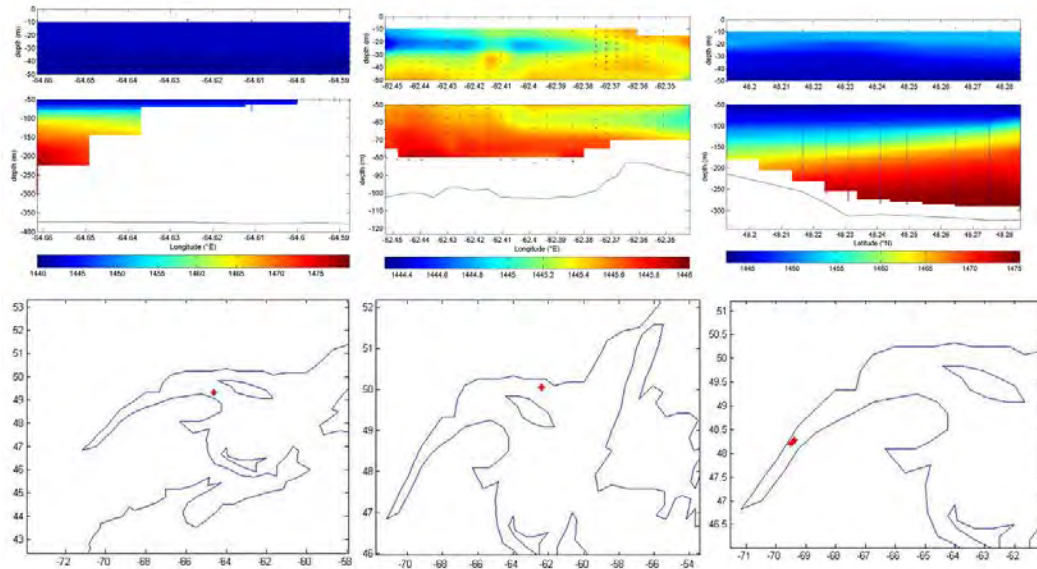


Figure 35-9. Sound velocity profiles taken during Leg 1. From left to right: MVP transects 1501001, 1501002 and 1501003.

One MVP transect was done at the beginning of the Leg 3b in the McClure Strait. Four days were dedicated to MVP data acquisition at the end of the Leg 3b in the Wellington Channel, Maury Channel and in the Penny Strait, though the team haven't been involved with those operations (see Section 20 for further details). The Table 35-2 shows the detail for the MVP transect that has been done in McClure Strait.

Table 35-2. MVP transects description during Leg 3b.

Name of transect	Location	# of casts	Maximum depths (m)	Description
15030001	McClure Strait	36	500	Cross section of the McClure Strait

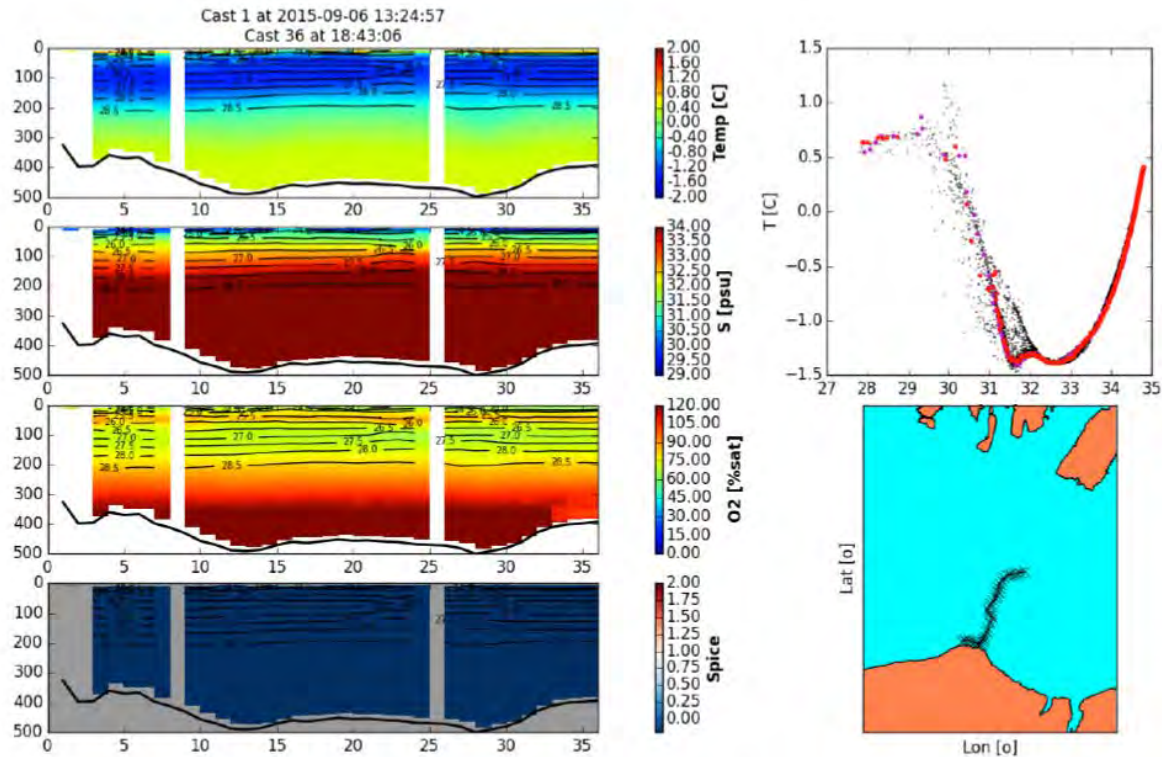


Figure 35-10. Example of the data acquired during the first MVP transect.

The MVP data will also be used by the seabed mapping team for sound velocity corrections in the post-processing phase of the multibeam data.

Reson 8101 Multibeam Sonar

Health and Safety:

- A SWI was held for the barge deployment and the MVP deployment.
- Every preparation work on the barge was announced to the officer in charge on the bridge.
- Immersion suits and life jackets were worn at all time during the deployment.
- The barge survey has followed all the safety recommendations from the SWI.

The barge has been deployed once for dedicated iceberg survey (April 27th). The *Reson 8101* multibeam sonar worked perfectly fine and has been able to map the submerged portion of the iceberg. Three circum-navigations of the iceberg were done in order to improve the point coverage and to perform statistical analysis of the method capability.

Field Procedure writing

Since last year, the team has been working on a document that would include all of the procedures and installation parameters of the system ran on board the *Amundsen*. During Leg 3a, a preliminary version (still in progress) was written, which was upgraded during Leg 4. This field procedure guide is very important to ensure proper documentation of the operations the team needs to do while onboard and to keep track of any changes in the networking or the acquisition/processing workflows.

During Leg 4, the team got in contact with Ian Church, a former UNB responsible for multibeam acquisition and processing on the *Amundsen*, and he will try to send all the guides and procedures they had concerning the EM302 and the pool of equipment related to multibeam data acquisition. This will greatly help understanding old troubleshooting procedures to improve the team's capacity to resolve problems in the future.

35.3 Preliminary results (Leg1)

35.3.1 Reson 8101 Multibeam Sonar

In general, the survey went very well, excepted for the LiDAR portion. The team was not able to connect the Novatel IMU via the network. They later found that the problem was coming from the lack of output power from the barge's inverter. It was still not possible to log the raw laser data, keeping in mind that the attitude from the multibeam system data could be post-processed and added to the raw laser point clouds.

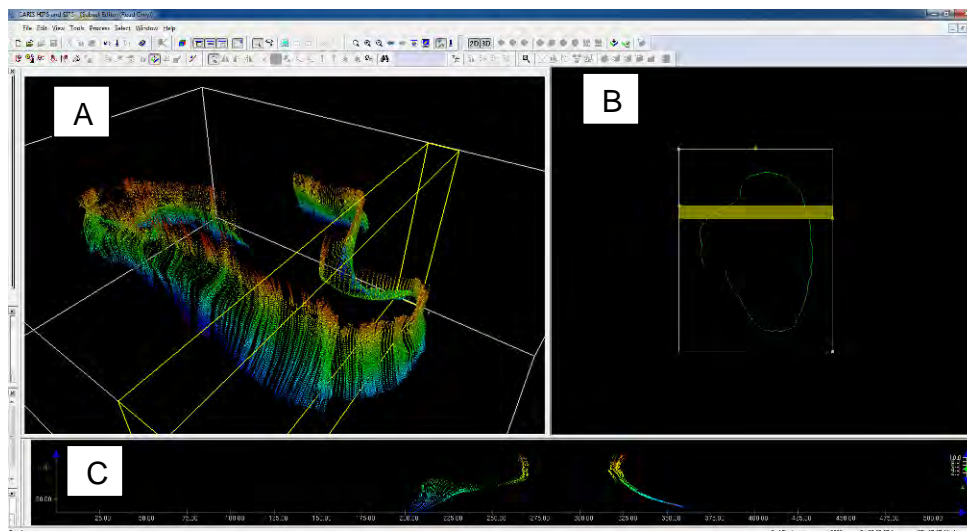


Figure 35-11. Preliminary results of the Iceberg Station 4 mapping on the barge. A) 3D point cloud view. Note that the attitude and displacement of the iceberg is not accounted for in the data. This is why the data does not match. B) First survey line of the barge around the iceberg. Yellow line shows the cross-section profile displayed in (C).

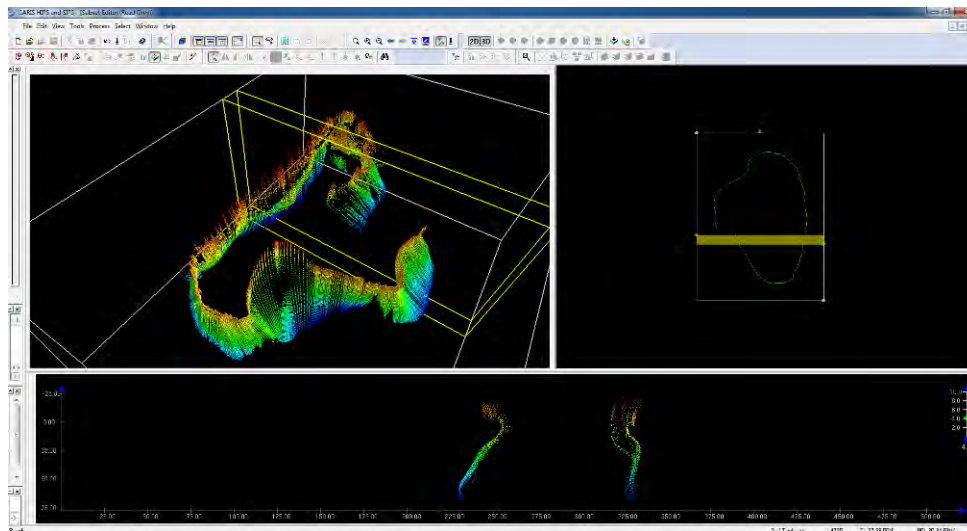


Figure 35-12. Same as Figure 35.11, but with a different perspective.

On the multibeam side, it was not possible to clearly track the keel of the iceberg. As the first images show, the data quality seems to be very interesting. The post-processing phase has been largely discussed with the WIRL and the Statoil representatives. The team managed to put in place a plan for the work to come. Here are the main roles/responsibilities of each group:

- WIRL (main research group for the project):
 - Record the iceberg drift and movement (post-processing of the beacons data);
 - Identify a method for tide correction and vertical datum of the survey (to match with the multibeam data);
 - Develop *Python* codes for modelling the iceberg drift during the survey;
 - Literature review to find similar studies and methods (data publishing?);
- MGL:
 - Correct for sound velocity profiles in order to reduce ray tracing artifacts around the iceberg;
 - Identify a method for tide correction and vertical datum of the survey (to match with the LiDAR data);
 - Develop partnerships with the *Département de géomatique* of Laval University (Sylvie Daniel and Rock Santerre) to gather information about the corrections that need to be applied for mapping moving objects (LiDAR and multibeam);
 - Literature review to find similar studies and methods (data publishing?);
- Statoil:
 - Weekly/monthly emails to keep in touch with the advances.

It would have been very important to have a complete survey site (i.e. LiDAR, multibeam, photogrammetry and high resolution beacons deployments) in order to compare different methods for 3D iceberg imaging. However, the team was not able to get as many data as the weather and ice conditions allowed for safe and reasonable work.

35.3.2 Mooring deployment and imaging

At Mooring Sites 1 and 3, differences of + 10-20m water depth differences were found between the Statoil depths (300m) and the real-time depths (310-320m). For Mooring Site 3, a difference of - 50 m was found and the Mooring team had to find a new site for the deployment.

All the processed surfaces and the raw data of the mooring sites were given to Statoil on their backup drive. Screengrabs of the real-time wedge display of the water column were also taken in order to validate the buoys depths and the upright positions of the moorings (Figure 35-13).

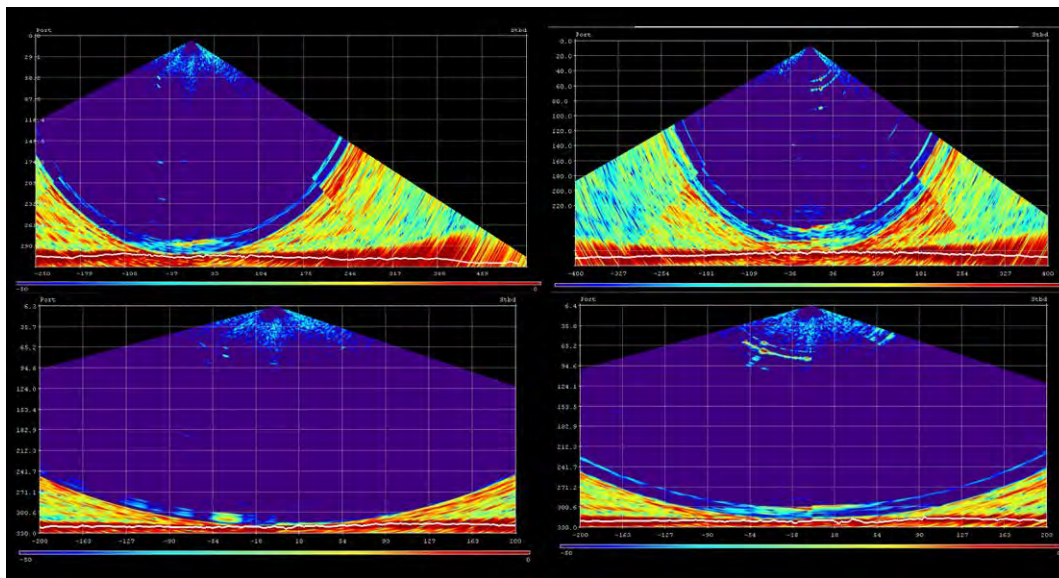


Figure 35-13. Water Column display of A) Mooring site 1, B) Mooring site 2 and C-D) Mooring site 3.

35.3.3 Transit Mapping

In the Belle Isle Strait, an immense ice island has been studied during almost 2 days. The SX90 survey around it showed that its westernmost part was grounded. According to the RADARSAT imagery and the currents in the area, this ice island is drifting toward the SW. The team was able to map the seabed morphology in front of the ice island. This survey represents pre-scouring conditions. Future surveys in the area should include on mapping few lines to see the effect of a partially grounded ice island on the seabed morphology.

35.3.4 Natashquan Delta

During wave glider tests, the ship had to stay within a 10 nm buffer distance from the glider. Since the deployment site was near the Natashquan river delta⁵, Gabriel Joyal proposed to use the available time during the night to survey a portion of the delta. A total of 70 nm of multibeam and sub-bottom lines were acquired (Figure 35-14). The data are very exciting and revealed rich information of the sedimentary processes on the delta submarine channels.

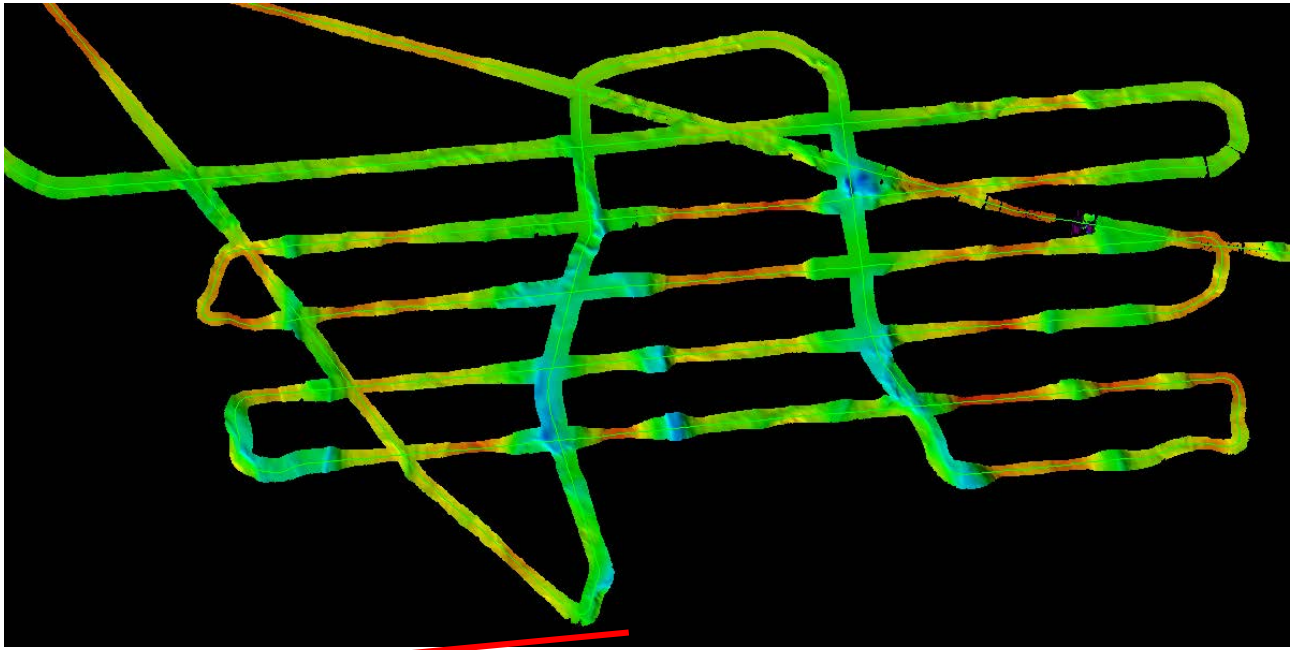


Figure 35-14. Multibeam bathymetry coverage of the Natashquan delta night survey.

35.3.5 Calibration lines for the EM302 Backscatter Data

On May 1st 2015, from 04h15 to 06h30, the *Amundsen* conducted EM302 multibeam data collection that will serve to partially calibrate the backscatter response of the echosounder. Figure 35.15 shows a sample of the backscatter data obtained from one survey line of completed. The level response of the transmission sectors is not uniform across-track. This is further evidence by generating the angular backscatter response curve of Figure 35-16 where the response level (in dB) is plotted against the beam-pointing angle with transmission sectors separately color-coded.

⁵ This site has been in the scope of the Marine Geoscience Laboratory, as part of a large research project on understanding the edification of the paleo-deltas of the North Shore of the St. Lawrence and the recent dynamics of the submarine fans. The Natashquan delta has been surveyed very few times and only a little amount of literature had documented its Quaternary evolution (e.g. Sala and Long 1989). This opportunity was of great value for the laboratory and will certainly result in future dedicated mapping surveys in the area using the R/V *Louis-Edmond-Hamelin* (CEN).

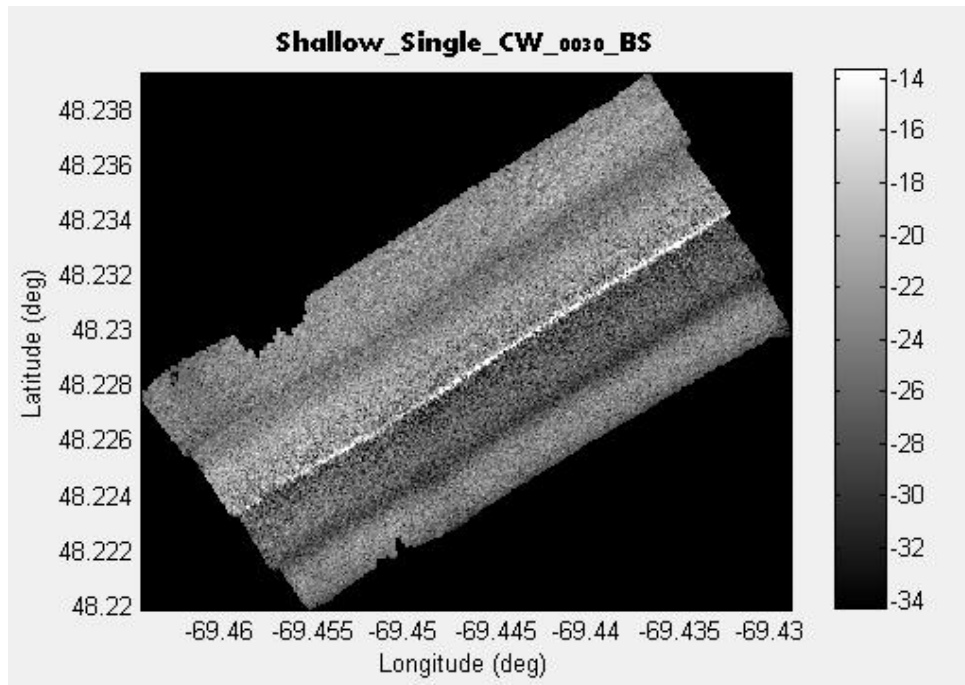


Figure 35-15. Example of backscatter data of the *Amundsen's* EM302 showing non-uniform level response of the transmission sectors.

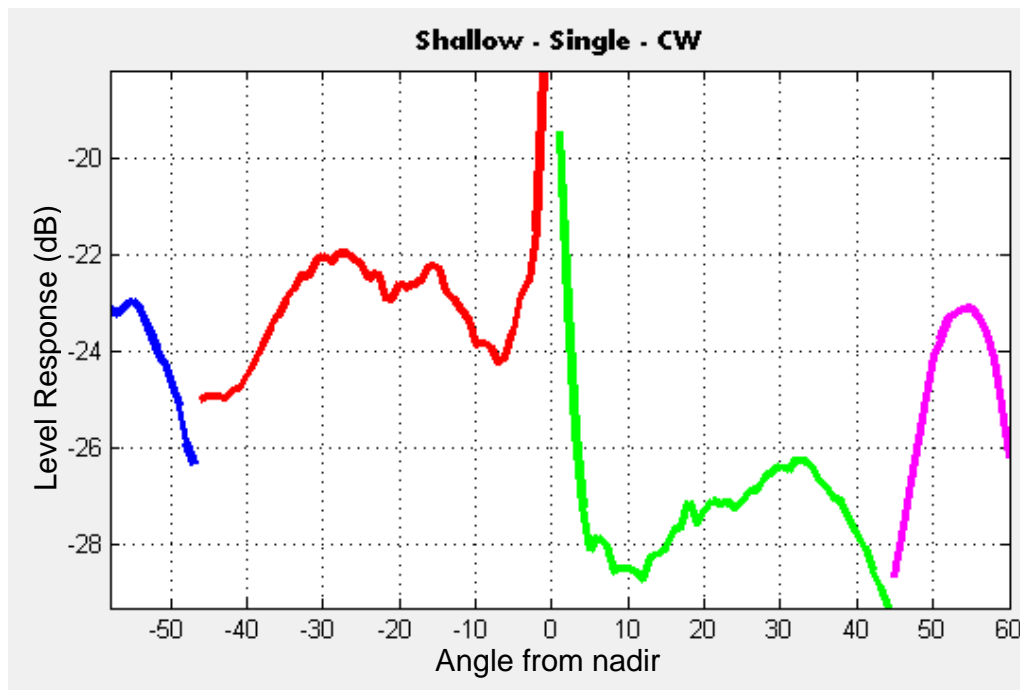


Figure 35-16. Graphical display of the differences in the level response of the four different transmission sectors of the EM302.

A report on the calibration of the *Amundsen* EM302 backscatter response will be completed during the fall of 2015 and will be provided to ArcticNet.

35.4 Preliminary results (Leg 4)

35.4.1 Navy Board Inlet and Eclipse Sound

At the beginning of the leg, all the transits between stations were used to add new data to the coverage of Eclipse Sound and Navy Board Inlet (Figure 35-17). During a transit line in Navy Board Inlet, crescent-shaped bedforms off an alluvial fan were found (Figure 35-18). This feature, also called cyclic step, is associated to supercritical shallow flow, often in response to turbidity currents (Kostic et al. 2010). Repetitive surveys over this type of submarine feature can give a lot of information about sedimentary processes from the coast to marine environments.

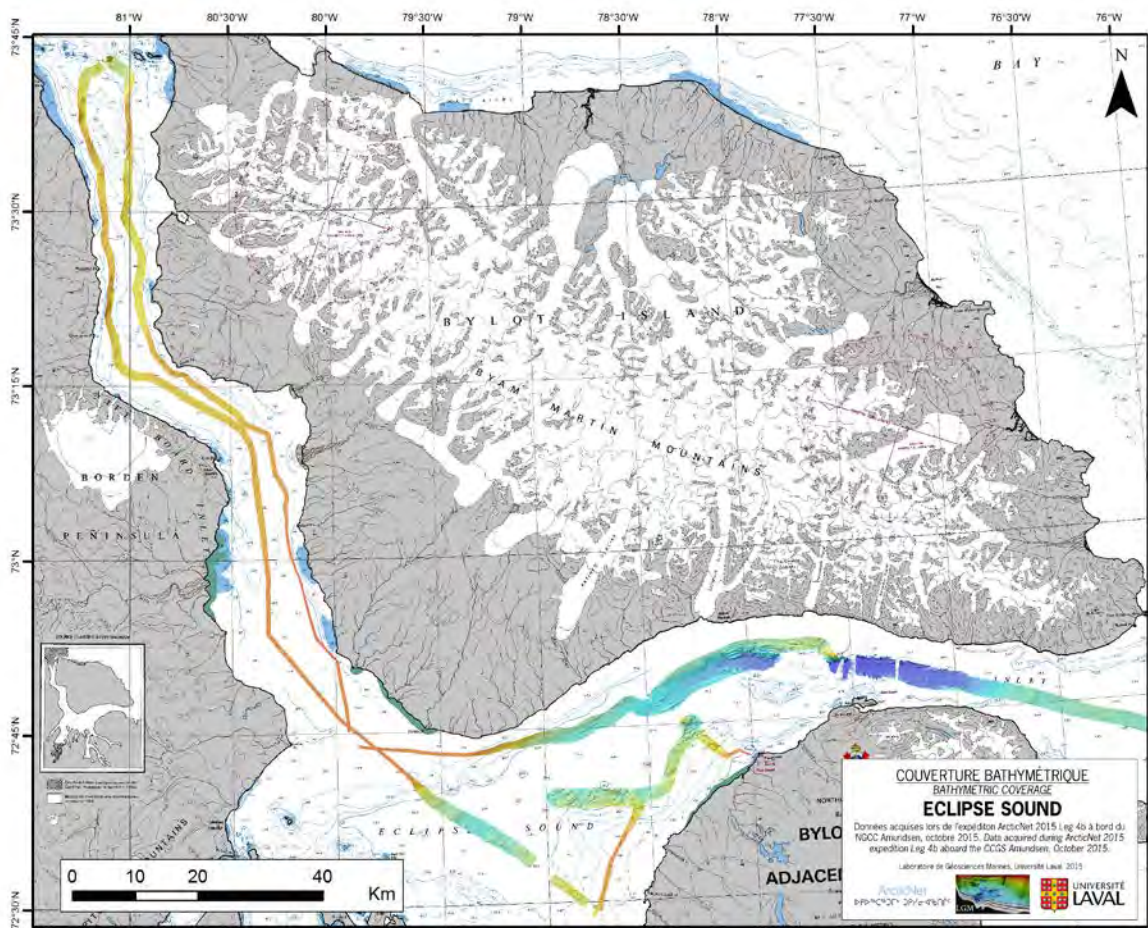


Figure 35-17. Bathymetric data collected in Eclipse Sound and Navy Board Inlet during Leg 4.

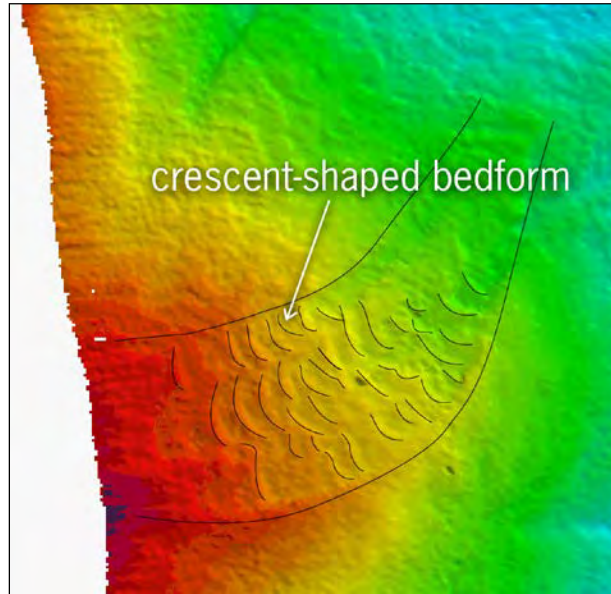


Figure 35-18. Crescent-shaped bedforms observed in Navy Board Inlet.

35.4.2 CASQ core sites

The mapping team helped the CASQ core team in selecting the best coring sites for Legs 4a and 4b, based on 3.5 KHz sub-bottom profiling and mapping during the cruise. Here are presented the new bathymetric data for each CASQ site and some subbottom profiles acquired at those sites.

CASQ1 – Smith Sound

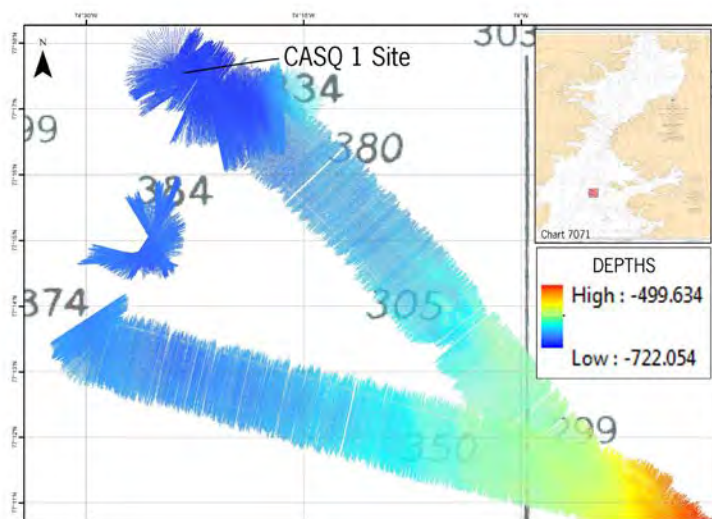


Figure 35-19. Location of CASQ1 site and associated bathymetric data.

CASQ2 – Qaanak Trough, Greenland

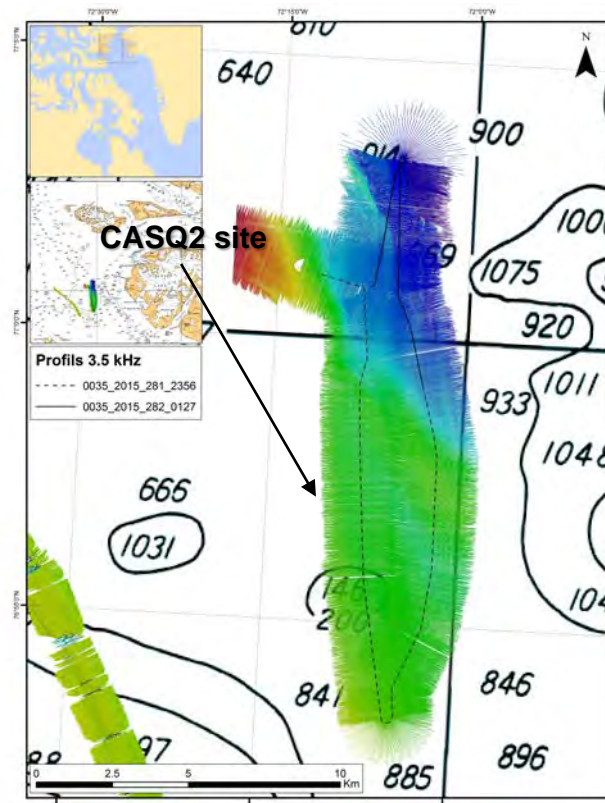


Figure 35-20. Location of CASQ 2 site and associated bathymetric data.

CASQ3 – Scott Inlet

This core was sampled for Etienne's PhD study and in collaboration with G. Massé, P. Lajeunesse and J. Giraudeau.

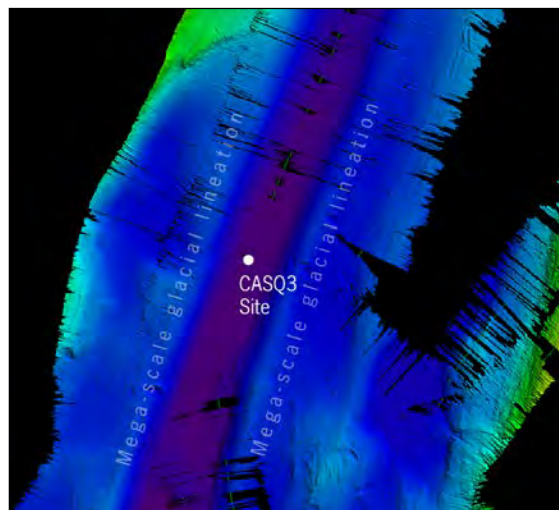


Figure 35-21. Location of CASQ3 (AMD15-CQ3) in a sediment-filled basin in between two megascale glacial lineation in Scott Trough.

CASQ4 – Qikiqtarjuag

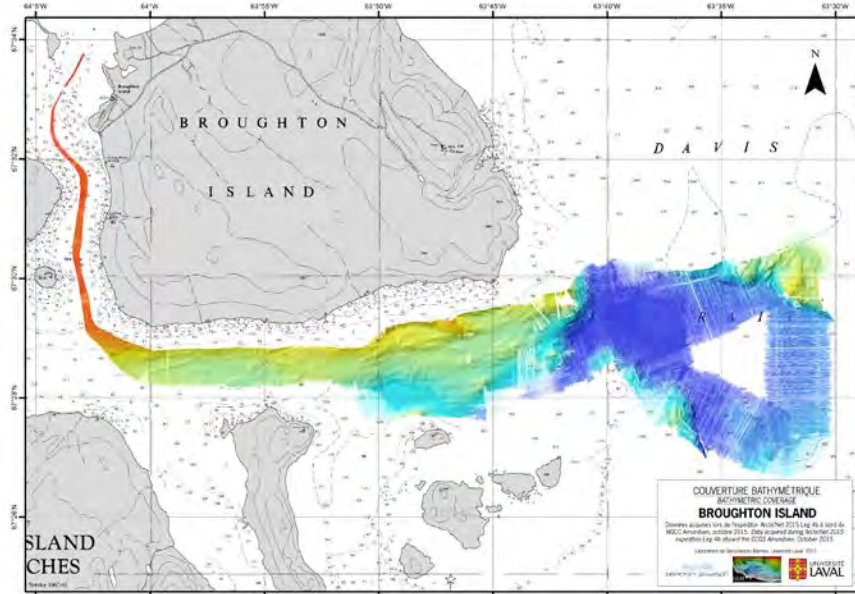


Figure 35-22. Location of CASQ 4 and associated bathymetric data.

35.4.3 Sam Ford Fjord & Scott Inlet Mapping and coring operations

24 hours were dedicated for multibeam mapping of Scott Inlet and Sam Ford Fjord. Most part of the dedicated time was used to map Sam Ford Fjord since sea conditions were not good enough for mapping purpose. However, the team managed to use all transits between stations in the area to increase the coverage in the area of Scott Inlet. The mapping conducted in the area was also used to get useful data for other operations like piston coring at Station LGM-AMU15-01, CASQ coring Station 3 and for ROV dives. The mapping resulted in a near complete coverage of Sam Ford Fjord (except for the head of the fjord, which wasn't accessible because of a shallow sill) and in an extension of already mapped area in Clarke Fjord and Scott Inlet. Some interesting features were observed in Hecla and Gripper Trough and in Sam Ford Fjord. In Hecla and Gripper Trough, a basin linking Sam Ford Fjord to Scott Inlet, the team observed what is thought to be a mega-scale glacial lineations and mass movement scars (Figure 35-27). In Sam Ford Fjord, some grounding-lines, sediment-filled bassins, moraines, a submerged-delta/sandur, channels and mass movement scars were observed (Figure 35-23 and Figure 35-26).

Where coring sites were planned, sub-bottom surveys were conducted to validate the choice of the coring sites. Sub-bottom profile from Sam Ford Fjord showed a long (~45 – 50 m) sediment sequence in front of a grounding-line, where the piston core LGM-AMU15-01 was conducted (Figure 35-25). In Scott Inlet a ~10 m (Holocene?) sediments sequence was observed where the AMD-CQ3 CASQ core was done. At the coring sites, the team helped the coring crew since two of the cores were for Etienne Brouard PhD study.

Piston coring at site LGM-AMU15-01 data is shown in Table 35-3. Coring was successful as 4,59 m of sediments were recuperated.

CASQ core data is shown in Table 35-3. Coring wasn't as good as expected; the team only recuperated 3,98 m. Maybe the weight on the corer wasn't heavy enough since the weights were lost during previous CASQ coring operations.

Table 35-3. Cores data (for Etienne Brouard's PhD study).

Site	Date	Latitude (N)	Longitude (W)	Geo-region	Water depth (m)	Depth method	Corer	Core length (cm)	Trigger core total length (cm)
LGM-AMU15-01	14 October	70°42.310	070°47.750	Baffin Bay – Sam Ford Fjord	781	32 kHz	Piston AGC-Large	459	97
AMD-CQ3	17 October	71°19.321	070°38.748	Baffin Bay – Scott Inlet	832	32 kHz	CASQ	398	n/a

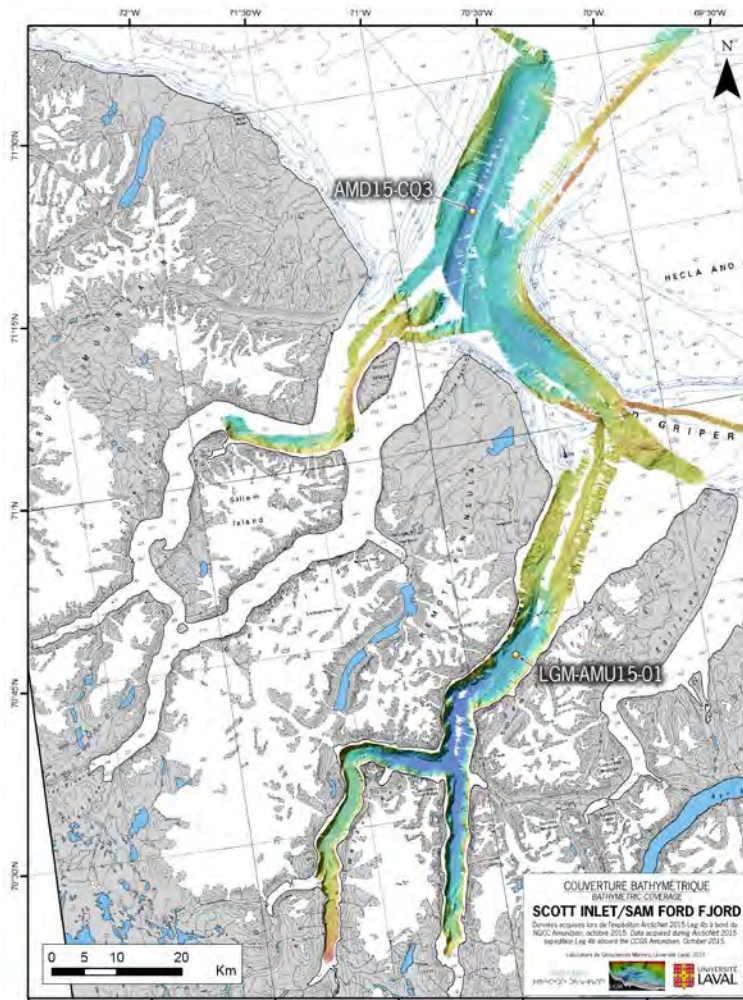


Figure 35-23. New bathymetric data acquired in the Scott Inlet-Sam Ford Fjord area during Leg 4b. Positions of CASQ core-3 (AMD15-CQ3) and piston core LGM-AMU15-01 are shown by yellow dots.

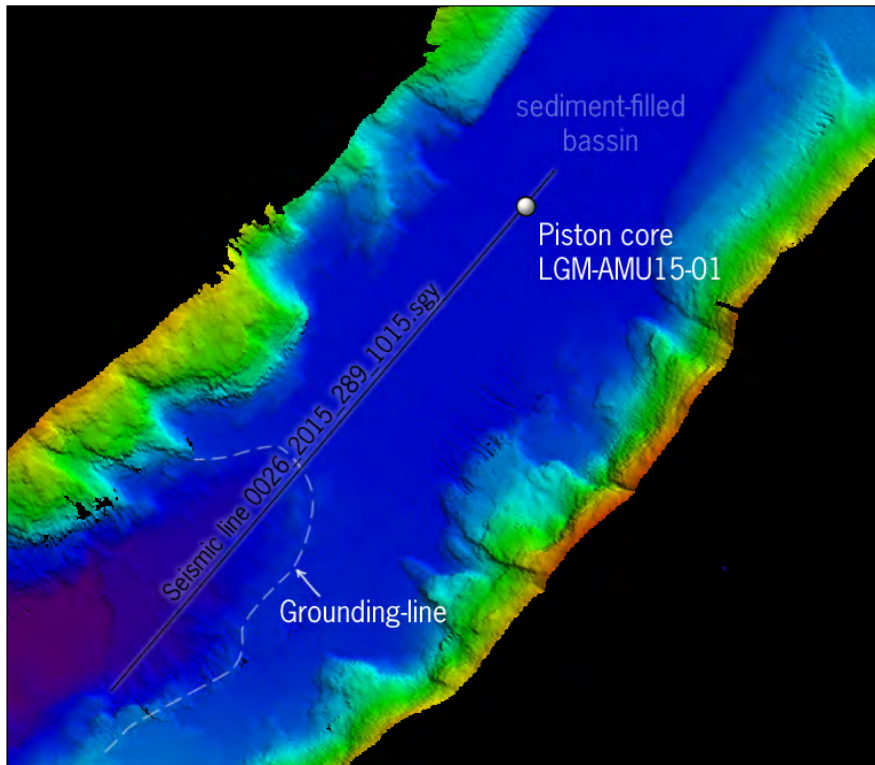


Figure 35-24. Sam Ford Fjord bathymetry showing a grounding-line and a sediment-filled basin near the LGM-AMU15-01 piston core site. Seismic line 0026_2015_289_1015.sgy is shown by the the black line.

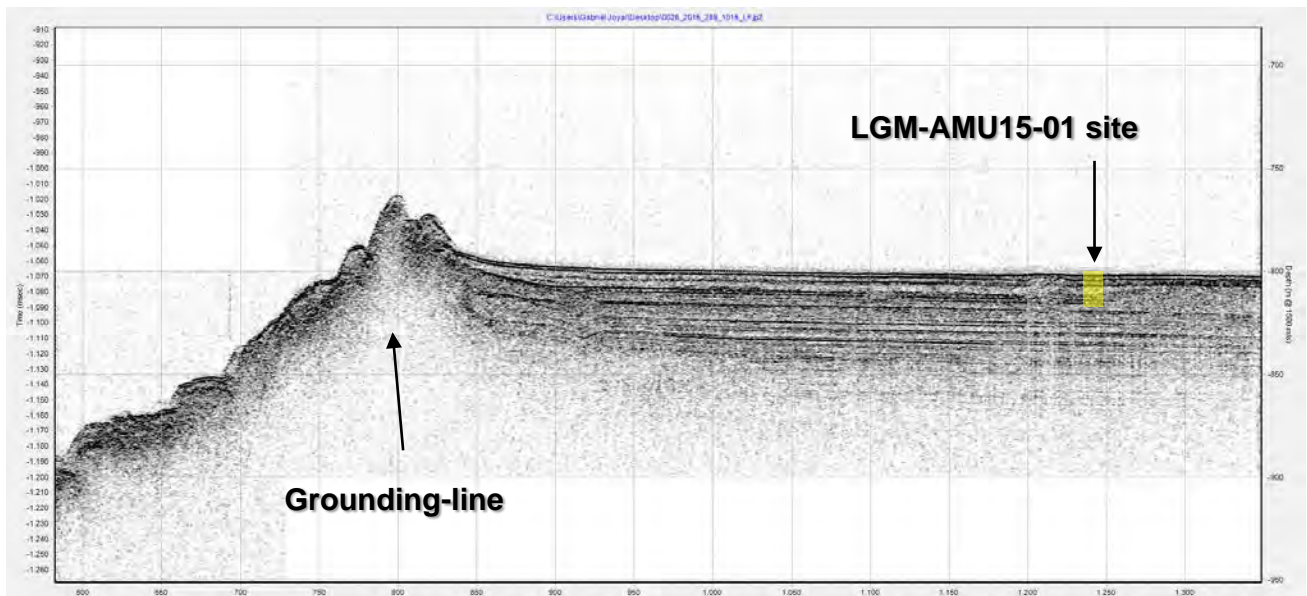


Figure 35-25. Seismic profile in Sam Ford Fjord showing the grounding-line, and a basin filled with at least 45-50 m of sediments.

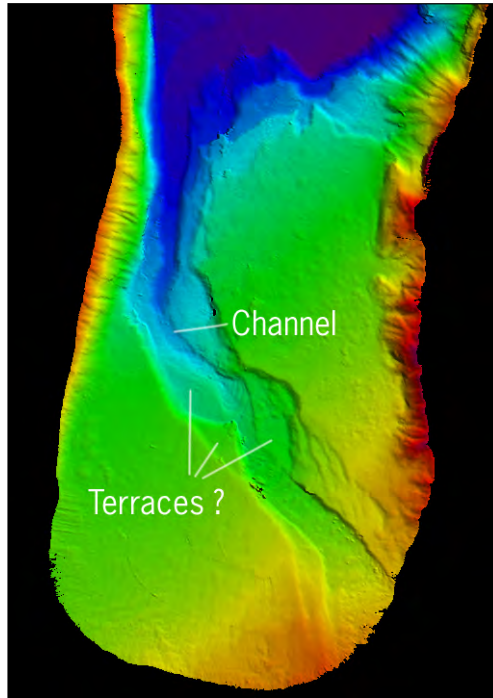


Figure 35-26. Submerged delta/sandur at the head of Walker Arm (Sam Ford Fjord). Bathymetry shows a well-defined channel with what looks like terraces or maybe mass movement scars.

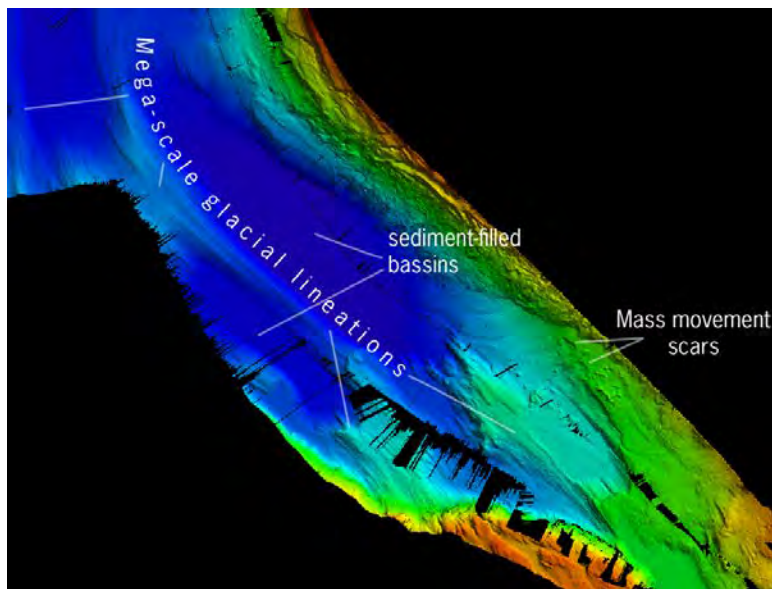


Figure 35-27. Bathymetry of Hecla and Gripper Trough showing mega-scale glacial lineations, mass movement scars and sediment-filled bassins.

35.4.4 ROV sites mapping

The MGL team has been involved with the ROV team to perform a bathymetric survey over planned ROV dive sites in Sam Ford Fjord and Cape Dyer.

Sam Ford Fjord

Due to problem the ROV team had with the ROV, the mapping team was asked to do a survey over steep sections at the entrance of Sam Ford Fjord. The mapping team provided them with the preliminary surface generated prior to the piston core deployment (Figure 35.28).

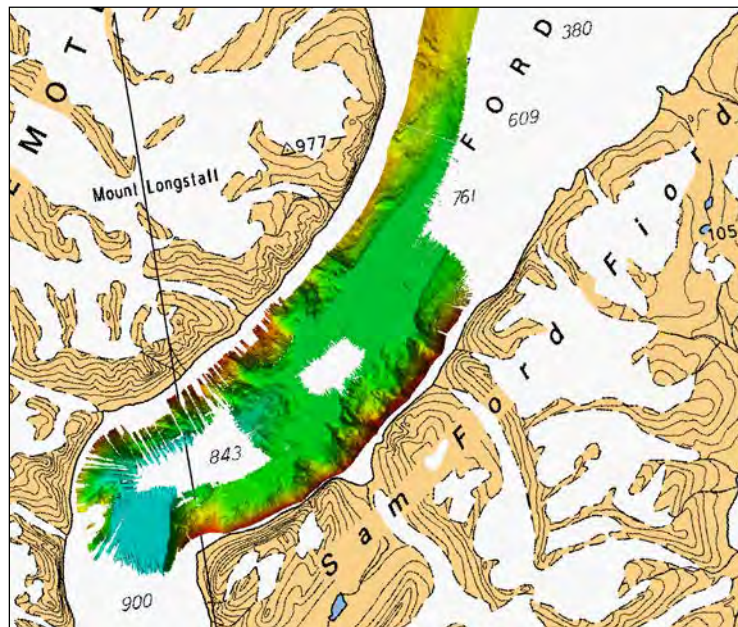


Figure 35-28. Preliminary surface generated for Sam Ford Fjord ROV dive.

Cape Dyer

At the Cape Dyer site, the team was given >5-7 hours (4-5 hours before dive; 1-2 after the dive) to perform a bathymetric survey over a planned dive. The mapping team was very impressed by the level of preparation of the ROV team of the survey, as they already had planned line to optimize the coverage (50% overlap) at the survey depth (± 730 m). Although the wave conditions were not optimal, the team was able to generate a 20-m resolution grid; which is acceptable for the ROV team's planning.



Figure 35-29. Preliminary surface generated for Cade Dyer ROV dive.

35.4.5 Piston core sites

Eclipse Sound and Clyde River (GSC)

GSC1 and GSC2 core sites were very much well mapped and known by the Geological Survey of Canada. The mapping team played a larger role in mapping an area in Clyde River Trough. Although there was not a lot of acoustic penetration on the 3.5 kHz, R. Bennett was able to identify a proper coring site.

Merchants Bay area (MUN)

The team was also implicated in the mapping of the Big Nose and Akpait Fjords. One piston core in each fjord was planned. The main challenge for was to deal with the poor amount of bathymetric data available in these fjords. The team worked with the navigation officers to gather all the available information (mainly from the CHS, the R/V *Nuliajuk* – provided by the MUN students and the 2014 *Amundsen* cruise). It was possible to plan approaches lines based on previous years' data. However, the team was not able to perform the requested bathymetric survey the MUN team asked because of lack of data. After suggestions made by the Commanding Officer, the survey plan was changed and a sector off Durban Island was mapped (4-5hrs). The coverage now connects Merchants Bay to Durban Strait.

Even if the 3.5 kHz showed coarse sediments at the Big Nose site, the MUN team decided to core away from their original site. After unsuccessful core, a better sedimentary sequence, located nearby the original coring site, was found.

In Akpait fjord, a piston core was deployed at the planned site. Although the MUN team provided the bathymetric data⁶, the team would have liked them to be more implicated during the planning of approaches and dedicated bathymetric surveys. This implication is very important since this region is not well charted and even the charts are poor quality (high coastline position offsets, bad depths on the chart, etc.). Getting track lines of the R/V *Nuliajuk* would have allowed to verify if the unknown depths on the region were due to sonar incapacity to track the bottom (the EM2040 sonar mounted on the R/V *Nuliajuk* has a depth range limited to 300-350m in sea water). This would have helped a lot the planning of the dedicated mapping in the area.

35.4.6 Ice Island Survey

In collaboration with the WIRL, the mapping team has been involved in the mapping of an ice island. A circum navigation of the big tabular iceberg was first done at a distance of < 0.3 nm in order to map the keel of the iceberg using the EM302 multibeam echosounder. It was possible to track the keel for most of the iceberg in the water column display. In the post-processing software (CARIS HIPS&SIPS), the water column scattering of the ice island was added to bathymetry to obtain a 3D model of its submerged part (Figure 35-30). The second circum navigation of the iceberg was performed to scan the iceberg using the SX90 sonar. This fishery sonar is capable of imaging water column scattering up to a distance of 2.2km. In collaboration with M. Geoffroy (written procedure), the SX90 was used properly. As opposed to the EM302 sonar, the SX90 was not accurate enough to image the shape of the iceberg, but was able to track the keel over the whole perimeter. The grounding area of the iceberg was found with the SX90.

The team is still working on the development of the processing method, but preliminary results so far have shown great potential for determining keel depths and submerged morphology.

Ongoing collaborative work with the WIRL will lead to the development of an improved method for iceberg mapping and complete 3D model using combined LiDAR/photogrammetry and bathymetry (Figure 35-30– Lajeunesse et al. *submitted*).

⁶ As for last year, the data the MUN team provided had a georeferencing problem. The 2015 R/V *Nuliajuk* singlebeam data was projected in a custom projection and did not displayed properly with the previous' years data

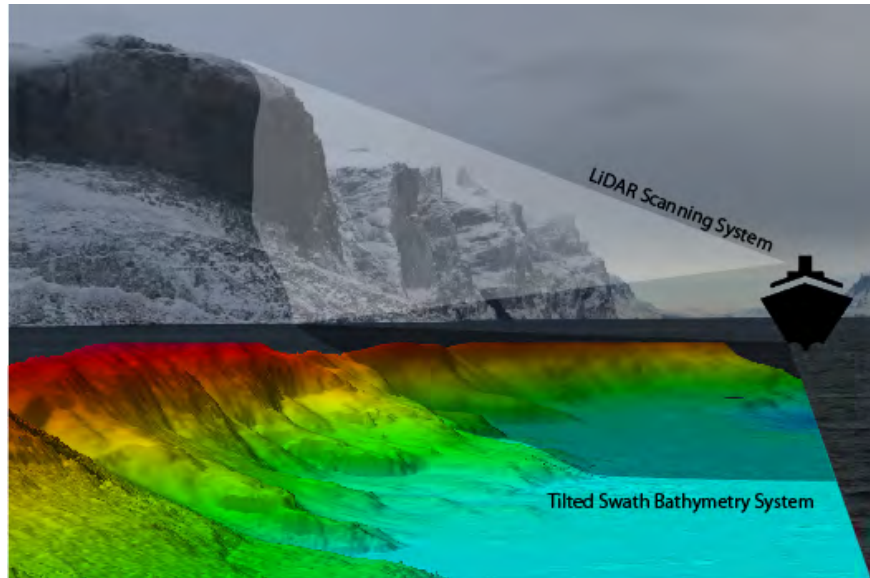


Figure 35-30. Improved method for iceberg mapping and complete 3D model using combined LiDAR/photogrammetry and bathymetry project development.

35.4.7 Perform BIST tests during transit

It was not possible to perform a BIST test in transit conditions in order to evaluate the noise levels on the receivers during normal transit speeds.

35.4.8 Other interesting bottom features

Hills and holes caused by iceberg calving and rotation

In Lancaster Sound, at least 2 hills and holes were identified. These features have recently been documented by King et al. (*In Press*). In the past, these features were thought to be pockmarks, but the most recent analysis has shown that they might have a glacial origin. They might have formed at the ice margin during deglaciation as icebergs and ice islands were calving off the glaciers.

Further work will be undertaken in collaboration with the Geological Survey of Canada (GSC) to better document the location of these features in the Canadian Arctic, as well as to assess their geotechnical properties

35.5 Comments and recommendations

Although Leg 1 was a complete success, some issues occurred and the following measures should be taken in order to improve the different surveys:

- Improve communication prior to survey with the WIRL: We think that a better planning of the cruise with the WIRL would have helped the deployment. Discussions and meetings could have led to a better cooperation between the two teams and improvement of the survey design. Future work in collaboration must include preparation meetings and detailed methodology from each group to avoid working in double;
- Survey more than one iceberg in order to have replicates and improve the statistical significance of the methodological approach;
- Make sure that the power supply on the barge is outputting enough power for the instruments: During the LiDAR and multibeam survey on the barge, we had some issues with power supply to the LiDAR IMU (Novatel SPAN-SE). After testing different connexions, we found that the 1000W inverter recently mounted on the barge was not powerful enough for some of the instruments (in terms of output A). For future surveys, we should plan on using the Honda generator instead of the inverter.
- Install a *Kongsberg 2040c* on the barge: This sonar has narrower beams ($0.5 \times 0.5^\circ$), higher frequency (200-400 kHz) and longer range (up to 350 m), that can greatly improve the resolution of the survey. Moreover, a new GPS device (capable of L1 and L2 bands recording) should be installed to reduce inaccuracies in positioning;
- Re-survey the “grounded” ice island area north of Belle Isle Island: the first survey we did during this cruise represents pre iceberg scouring conditions. Knowing precisely the drift of the tabular iceberg with the beacons deployed during the cruise and the remote sensing observations, it could be of great interest to re-survey the area where the ice island might have drifted to see the effects of ice drifting on the seabed morphology. A survey line will be prepared for the transit north of the 2015 *Amundsen* summer cruise. Leg 2 participants should ask the bridge/chief scientist to deviate the ship if needed to at least have one line over the area.
- Develop a method to monitor iceberg displacement during mapping operations: During the pre-processing of the LiDAR and multibeam data, we found it hard to account for iceberg displacement, but mainly for changes rotation angles during the survey, just by using the beacons deployed on the iceberg. We were thinking of developing a low-cost motion sensor (home made using *Arduino* and *Raspberry-Pi* devices connected to an *Iridium* data broadcast system) that could improve our monitoring capabilities of the iceberg motion in the three dimensions (roll, pitch and yaw);
- Change the Hydrographic Working Station (HWS): Since the 2014 cruise, the main multibeam acquisition computer is showing heavy signs of degradation. The Canadian Hydrographic Service (CHS) has already ordered a new HWS and should be delivered in June 2015. The new HWS will (or, at least, should) be installed by a Kongsberg technician before or during the 2015 Sea Trials;

Since the Leg 2 was modified due to Coast Guard duties, no special project was achieved during this leg. Although the cruise was a success in its transit mapping duties, some issues occurred and the following measures should be taken in order to improve the different surveys:

- Monitor the electrical problem: it will need an inspection of the transducers at the end of the summer mission.

In accordance with the issues that occurred during the Leg 3b, the following measures should be taken in order to improve the different surveys:

- Assess the real need for the CNAV correction plan we purchase every year.
- Purchase portable hard drives to do a 3rd backup of the data. By the end of Leg 3a, we realized that the Alienware's (CARIS processing computer) hard drive was almost full (only 15 Gb available). Even if the CARIS folder is backed up automatically on the NAS server, we think that a 2nd backup could be needed before deleting data on the processing computer. The same situation stands for the SIS acquisition software. The local disk where the bathymetric data are stored was almost full by the end of Leg 3a. For now, Gabriel has backed up the SIS data on his personal hard drive. The HIPS and SIPS projects of Leg 2 have been stored on the CHS hard drive. In the future (starting on Leg 4), we will bring a portable hard drive to bring data at the office after each leg. We should also think about adding a new drive in the Alienware computer (or change the processing computer).
- Further investigations should be done in order to better understand what is causing the decrease of ping rate when we are in deep water.
- Upgrade our Sub-bottom Profiler system since because it is an old system other similar troubles (to those describe in the previous section) could happen in the legs to come.

During heavy winds conditions (>40 knots), we noticed that the mast where the CNAV and POS MV antennas are located was shaking a lot. Even if there is nothing to do with this, it is good to know that possible accuracy degradation can be caused by the vibration of the antennas during strong wind events.

References

- King, E. L., Rise, L., Bellec, V. *Submitted*. Crescentic submarine hills and holes produced by iceberg calving and rotation. In Dowdelwell, J.A., Canals, J.A., Jakobsson, M., Tood, B., Dowdswell, E.K., Hogan, K. A. (eds) *Atlas of Submarine Glacial Landforms: Modern, Quaternary and Ancient*. Geological Society, London, Memoirs.
- Kostic, A., Sequeiros, O., Spinewine, B., Parker, G. 2010. Cyclic steps: A phenomenon of supercritical shallow flow from the high mountains to the bottom of the ocean. *Journal of Hydro-environment Research*, 3(4), 167-172. DOI: 10.1016/j.jher.2009.10.002
- Sala, M., Long, B., 1989. Évolution des structures deltaïques de la rivière Natashquan, Québec. *Géographie Physique et Quaternaire*, 43(3), 311-323.

36 Benthic diversity and functioning across the Canadian Arctic – Legs 3a, 3b, 4a, 4b and 4c

ArcticNet Phase 3 – Marine Biological Hotspots: Ecosystem Services and Susceptibility to Climate Change.

<http://www.arcticnet.ulaval.ca/pdf/phase3/marine-ecosystem-services.pdf>

Project leaders: Philippe Archambault¹ (philippe_archambault@uqar.ca), Christian Nozais² (christian_nozais@uqar.ca) and Ursula Witte³ (u.witte@abdn.ac.uk)

Cruise participants Leg 3a: Solveig Bourgeois³ and Christian Nozais²

Cruise participants Leg 3b: Solveig Bourgeois³ and Laure de Montety¹

Cruise participants Leg 4a: Cindy Grant¹

Cruise participants Leg 4b: Cindy Grant¹ and Frédéric Olivier⁴

Cruise participants Leg 4c: Cindy Grant¹

¹ *Institut des sciences de la mer (ISMER) – Université du Québec à Rimouski, 310 Allée des Ursulines, Rimouski, QC, G5L 3A1, Canada.*

² *Université du Québec à Rimouski, 300 Allée des Ursulines, Rimouski, QC, G5L 3A1, Canada.*

³ *Oceanlab, Main Street, Newburgh, ELLON, Aberdeenshire, AB41 6AA, Scotland.*

⁴ *Muséum National d'Histoire Naturelle de Paris, 57 rue Cuvier, 75005 Paris, France.*

36.1 Introduction

Ecosystem functions and services are linked to the diversity of active microbes, algae and consumers that compose the lower food web. Ongoing changes in the physical Arctic environment alter biodiversity in several ways, including shifts in species dominance and community structure, extinctions and invasions that affect major biogeochemical functions, including N cycling, PP, pelagic-benthic coupling and carbon storage. We have no certitude yet about how these changes will impact the food web. Arctic zooplankton is dominated by a handful of highly adapted, large copepod species that convert pulsed PP into lipid stores that are crucial for the survival of top predators (Darnis et al. 2012), but we do not know how this dominance will respond to change. By affecting both the quantity and the quality of sinking OM, shifts in PP, PFTs and zooplankton will presumably impact the diversity, community structure and function of the benthic fauna. Benthic consumers have been shown to depend more closely on ice algae than on phytoplankton (MacMahon et al. 2006, Sun et al. 2009, Roy et al. 2014), but with the scarce knowledge available for the Canadian Arctic it is difficult to quantify and predict the cumulative impact of diverse factors of change on benthic biodiversity and function.

The main objectives were to

- Describe and compare the biodiversity (using a variety of different diversity indices) in different locations of the Canadian Arctic in relation to environmental variables;
- Describe the relative importance of phytoplankton and ice algae as a food source to benthic organisms by looking at compound specific isotopes in faunal tissues, sediments and water column particulate organic matter;

- Track pathways of particulate organic carbon processing and uptake by the benthic community during isotope tracing experiment.

36.2 Methodology

The box core (Figure 36-1) was deployed to quantitatively sample diversity, abundance and biomass of endobenthic fauna and to obtain sediment cores for sediment analyses and incubations. From 28 (Leg 3) and 11 (Leg 4) box cores, sediments of usually a surface area of 0.125 m² and 10-15 cm in depth were collected and passed through a 0.5 mm mesh sieve and preserved in a 4 % formaldehyde solution for further identification in the laboratory (Table 36-1 and Table 36-2). Sub-cores of sediments were collected for sediment pigment content (with 10 mL truncated syringes of an area of 1.5 cm² each), organic carbon content, sediment grain size and compound specific isotopes (with 60 mL truncated syringes of an area of 5 cm² each); for sediment pigments, organic carbon content and compound specific isotopes, the top 1 cm was collected, although for sediment grain size, the top 5 cm was collected. Sediment pigment and compound specific isotope samples were frozen at -80°C, and organic carbon samples, porosity and sediment grain size samples were frozen at -20°C. All samples will be transported off the ship for analyses in the lab at the Université du Québec à Rimouski and University of Aberdeen (for compound specific isotope analysis).



Figure 36-1. Box core deployment and sediment cores sampling.

For the isotope tracing experiment (Figure 36-2), incubations of 15 sediment cores were performed at two stations (Leg 3) Station 177 (Leg 4) (Table 36-1 and Table 36-2) in a dark and temperature controlled room (ca 4°C). Five cores acted as controls; ¹³C, ¹⁵N labelled ice algae or phytoplankton was added to five cores each. The oxygen concentrations in the water column overlying the sediment (bottom water collected from Rosette water samples obtained at the same station) in the incubation cores were measured periodically (about 24h intervals) over 4 days to examine sediment community oxygen consumption. To examine

carbon remineralization rates, water samples for $DI^{13}C$ analysis were collected at 24-hour intervals. Additional water samples for nutrient and $DO^{13}C$ (bacterial breakdown of organic matter) analysis were taken at days 0, 2 and 4. At the end of the incubations, the top 10 centimeters of sediment in the cores was sliced. Half of each slice was frozen in $-80^{\circ}C$ for phospholipid fatty acid analysis whereas the other half was sieved on a 0.5 mm mesh sieve to obtain macrofauna, which was preserved in a 4% seawater-formalin solution for later isotope tracer uptake analysis.

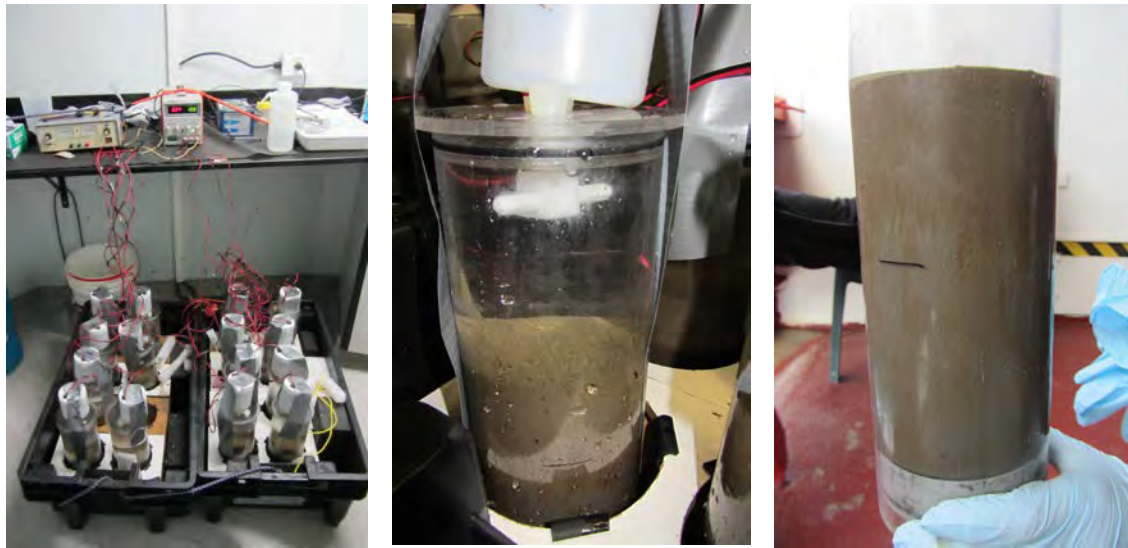


Figure 36-2. Isotope tracing experiment set-up in the temperature controlled room and slicing of sediment cores after finishing the experiment.

Table 36-1. Box coring stations during Leg 3.

Station ID	Local Date	Latitude (N)	Longitude (W)	Depth (m)	Diversity	Grain size	Pigments	Organic content	Isotopes - Sed	Incubation	Comments
405	Aug 22 2015	70°36.501	123°01.786	628	X	X	X	X	X		
407	Aug 23 2015	71°00.651	126°06.006	393	X	X	X	X			
437	Aug 24 2015	71°48.273	126°29.796	274	X	X	X	X			
408	Aug 25 2015	71°18.784	127°35.677	202	X	X	X	X			
434	Aug 26 2015	70°10.000	133°33.000	47	X	X	X	X	X		
435	Aug 27 2015	71°04.770	133°38.150	302	X	X	X	X	X		
435	Aug 27 2015	71°04.740	133°37.960	307						X	
435	Aug 27 2015	71°04.750	133°37.790	302						X	
421	Aug 29 2015	71°25.589	134°00.038	1203	X	X	X	X			
535	Aug 31 2015	73°25.010	128°11.760	291	X	X	X	X			

Station ID	Local Date	Latitude (N)	Longitude (W)	Depth (m)	Diversity	Grain size	Pigments	Organic content	Isotopes - Sed	Incubation	Comments
518	Sep 02 2015	74°34.341	121°26.567	269	X	X	X	X	X		
514	Sep 02 2015	75°06.226	120°37.679	457	X	X	X	X			
CB1/4 Miles East	Sep 07 2015	75°06.730	120°21.340	409	X	X	X	X			
CB2	Sep 10 2015	75°47.130	129°17.450	1355	X	X	X	X	X		
407	Sep 18 2015	70°59.620	126°03.390	395						X	
407	Sep 18 2015	70°59.680	126°03.770	398						X	
314	Sep 20 2015	68°58.291	105°28.415	78	X	X	X	X			
QMG4	Sep 20 2015	68°29.060	103°25.710	69	X	X	X	X			
QMG3	Sep 21 2015	68°19.801	102°36.545	67	X	X	X	X			
QMG-Mooring	Sep 21 2015	68°14.654	101°43.039	100	X	X	X	X			
QMG-2	Sep 21 2015	68°18.720	100°47.910	59	X	X	X	X			
QMG-1	Sep 22 2015	68°29.497	99°54.276	45	X	X	X	X			
312	Sep 22 2015	69°10.230	100°41.590	63	X	X	X	X			
310	Sep 23 2015	71°26.980	101°17.540	158	X	X	X	X			gravels
308	Sep 24 2015	74°08.356	108°50.193	564	X	X	X	X			
307	Sep 27 2015	74°07.100	103°05.540	349	X	X	X	X			
342	Sep 25 2015	74°47.630	092°47.010	138	X		X	X			sediment with rocks
CAA9	Sep 27 2015	76°19.810	096°45.350	336	X	X	X	X	X		sediment with rocks

Table 36-2. Box coring stations during Leg 4.

Station ID	Date	Latitude (N)	Longitude (W)	Depth (m)	Diversity	Grain size	Pigments	Organic content	Isotopes Sediments	Incubation	Comments
Full-304	2015-10-03	74°14.795	091°31.181	313	x	x	x	x			
Basic-301	2015-10-04	74°07.127	083°18.136	677	x	x	x	x			
Full-323	2015-10-05	74°09.450	080°28.588	794	x	x	x	x			
Basic-111	2015-10-07	76°18.410	073°12.910	595	x	x	x	x			
Full-115			No box core, too rocky								
Full-108	2015-10-09	76°15.880	074°36.740	448	x	x	x	x			
Basic-105	2015-10-09	76°17.655	075°50.482	330	x	x	x	x			

Full-101	2015-10-10	76°22.435	077°26.468	399	x	x	x	x	
Basic-155	2015-10-12	72°29.290	078°46.860	376	x	x	x	x	
Basic-150					No box core, too rocky				
Full-170					No box core, too rocky				
Full-177	2015-10-20	67°28.430	063°41.526	680					x x
Full-177	2015-10-20	67°28.441	063°41.555	679	x	x	x	x	x x
Basic-180	2015-10-21	67°28.986	061°39.996	360	x	x	x	x	
Basic-187					No box core, too rocky				

At 20 (Leg 3) and 12 stations (Leg 4), the Agassiz trawl (Figure 36.3) was deployed to collect epibenthic fauna (Table 36-3 Table 36-4). Catches were passed through a 2 mm mesh sieve. When possible, specimens were identified to the lowest taxonomic level, then count and weigh. The unidentified specimens were preserved in a 4% seawater-formalin solution or frozen at -20°C for later identification. At 11 stations (Leg 3) and at Station 177 (Leg 4), some specimens were frozen at -80°C for compound specific isotope analysis.



Figure 36-3. Agassiz trawl deployment and identification of the specimens.

At stations where the megafauna was kept for further analysis, water samples (10 m above bottom and chlorophyll maximum) were taken from the CTD Rosette, filtered on GF/F filters and kept at -80°C for particulate organic matter compound specific isotope analysis.

Table 36-3. Agassiz trawl stations during Leg 3.

Station ID	Local Date	Start			End			Duration (min)	Comments
		Latitude (N)	Longitude (W)	Depth (m)	Latitude (N)	Longitude (W)	Depth (m)		
405	Aug 22 2015	70°36.670	123°01.840	628	70°36.645	123°02.756	602	3	
407	Aug 23 2015	71°00.840	126°06.930	393	71°00.000	126°08.000	393	3	
437	Aug 24 2015	71°48.167	126°30.477	293	71°47.741	126°29.897	298	3	rocks
408	Aug 25 2015	71°18.794	127°35.816	202	71°18.514	127°35.968	200	3	
420	Aug 25 2015	71°03.000	128°31.000	40	71°02.000	128°31.000	43	5	hard bottom
434	Aug 26 2015	70°10.990	133°34.000	46	70°11.000	133°34.000	47	5	1st trawl didn't work
435	Aug 27 2015	71°04.730	133°38.050	298	71°04.500	133°40.320	300	5	
435	Aug 29 2015	71°12.490	133°41.840	716	71°11.290	133°44.407	648	8	
535	Aug 31 2015	73°25.010	128°11.840	291	73°24.220	128°14.000	304		net empty

Station ID	Local Date	Start			End			Duration (min)	Comments
		Latitude (N)	Longitude (W)	Depth (m)	Latitude (N)	Longitude (W)	Depth (m)		
518	Sep 02 2015	74°34.372	121°25.955	308	74°34.200	121°28.700	227	5	
514	Sep 02 2015	75°06.098	120°37.186	451	75°06.110	120°35.427	440	5	
CB1/ 4 miles east	Sep 07 2015	75°06.810	120°21.446	408	75°07.693	120°20.910	408	3	
314	Sep 20 2015	68°58.154	105°28.634	75	68°58.366	105°28.886	74	3	
QMG4	Sep 20 2015	68°29.080	103°25.670	68	68°28.660	103°26.390	76	3	
QMG3	Sep 21 2015	68°19.750	102°36.470	63	68°19.460	102°36.470	62	3	
QMG-	Sep 21 2015	68°14.583	101°43.347	105	68°14.176	101°42.732	98	3	
QMG-2	Sep 21 2015	68°18.770	100°47.880	59	68°18.560	100°47.900	74	3	
312	Sep 22 2015	69°10.110	100°42.250	64	69°09.940	100°41.780	60	03:15	
310	Sep 23 2015	71°27.530	101°16.200	166	71°26.750	101°17.640	158		Cancelled, strong
308	Sep 24 2015	74°08.242	108°49.705	563	74°08.890	108°52.480	561		gravel

Table 36-4. Agassiz trawl stations during Leg 4.

Station ID	Date	Start			End			Duration (min)
		Latitude (N)	Longitude (W)	Depth (m)	Latitude (N)	Longitude (W)	Depth (m)	
Full-304	2015-10-03	74°15.282	091°28.848	321	74°15.644	091°27.888	322	3
Basic-301	2015-10-04	74°07.189	083°18.808	676	74°08.235	083°18.485	678	3
Full-323	2015-10-05	74°09.487	080°27.702	789	74°10.840	080°28.065	789	3
Basic-111	2015-10-07	76°18.530	073°13.270	590	76°18.340	073°12.890	592	3
Full-115	2015-10-08	76°20.510	071°14.020	664	76°20.370	071°18.140	676	3
Full-108	2015-10-09	76°15.830	074°47.410	449	76°15.510	074°38.700	445	3
Basic-105				No trawl, too much ice				
Full-101				No trawl, too much ice				
Basic-155	2015-10-12	72°29.410	078°46.600	346	72°29.640	078°47.450	397	3
Basic-150	2015-10-13	72°44.960	079°56.290	127	72°45.020	079°56.630	126	3
Full-170	2015-10-14	71°22.816	070°04.265	264	71°22.684	070°03.631	245	3
Full-177	2015-10-20	67°27.934	063°44.082	653	67°28.381	063°41.631	677	3
Basic-180	2015-10-21	67°28.812	061°39.726	345	67°28.937	061°39.756	361	3
Basic-187	2015-10-24	64°10.380	060°24.020	350	64°10.970	060°24.090	352	3

36.3 Preliminary results

At this point, we do not know exactly if spatial and temporal variability of benthic diversity is governed by sediment type, food availability or other environmental variables. Samples collected for compound specific isotope analysis and during the incubation experiment also require further analysis. For detailed results, identification of organisms and sediment analyses will be carried on in home labs.

However, some striking comments can be made at this point: Stations CB-2 and 308 exhibited very lower benthic diversity, abundance and biomass than all the other stations sampled.

36.4 Comments and recommendations

36.4.1 Leg 3

We did not deploy the box core and the Agassiz trawl at Stations 420 and 342 respectively because the bottom was too rocky; using a benthic camera might be a good alternative to get data at those stations.

We did not deploy the box core at the deepest Stations CB-3 and CB-4 because the cable was not long enough to reach the seafloor.

We did not deploy the Agassiz trawl at the Stations 310, 307 and CAA9 because of ice or weather conditions.

36.4.2 Leg 4

We did not deploy the box core at Stations 115,150 and 170 because the bottom was too rocky; using a benthic camera and/or the ROV might be a good alternative to get data at those stations. We did not deploy the Agassiz trawl at the Stations 105 and 101 because of ice conditions.

37 Benthic lander deployment – Leg 4b

ArcticNet Phase 3 – The Canadian Arctic Seabed: Navigation and Resource Mapping.
<http://www.arcticnet.ulaval.ca/pdf/phase3/seabed-mapping.pdf>

Project leaders: Ursula Witte¹ (u.witte@abdn.ac.uk) and Philippe Archambault² (philippe.archambault@uqar.ca)

Cruise participants Leg 4b: Keith Jackson

¹ University of Aberdeen, Oceanlab, Main Street, Newburgh, AB41 6AA, Scotland.

² UQAR-ISMER, 310 Allée des Ursulines, C.P. 3300, Rimouski, QC, G5L 3A1, Canada.

37.1 Introduction

The objective was to deploy a benthic lander fitted with a camera pointing at the sediment surface as to monitor the sedimentation process, especially of algae descending from sea ice during the melt season.

37.2 Methodology

Following the completion of preliminary tests, the lander was deployed at Station 177 at 6:30pm on 20 October 2015. The deployment comprised two distinct phases, including lowering it to a few meters above the seabed and then releasing it. No detailed information on the seabed at the point of deployment was available, as the ROV dive and coring operations were conducted some distance away. However, the lander was confirmed to have landed in the correct orientation at 280m depth. A multibeam survey suggested the site was a broad and level shelf (Figure 37-1).

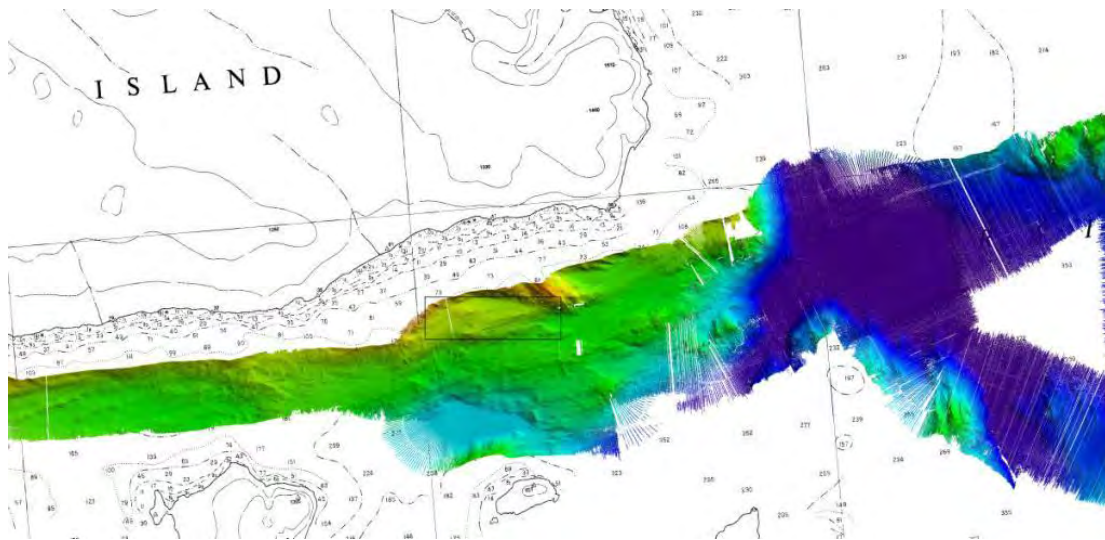


Figure 37-1. Multibeam survey of the lander deployment site (Station 177).

The lander was ballasted with approximately 90Kg of steel plates. The buoyancy of 35Kg in water corresponded to approximately 55Kg holding the lander down. It was suggested that more ballast would be desirable but as the frame of the lander had not been tested with heavier loads, concerns over its structural integrity limited the ballast used. It was noted that the site had a small tidal range (about 1.4m max from tide tables) and no discernable currents were reported by the ROV pilot during its 6-hour dive.

The lander was fitted with two IXYS RT 661 BS1-DDL acoustic releases. These can be released using a TT301B deck box using codes 2939 or 2854. The position on the ships log at time of release was 67°29.183 N 63°48.393W.

It should be noted that due to time constraints regarding the preparation and shipping of the lander, it was a necessary to use lightweight affair with an operating depth of 200m, as originally specified. However, the deployment site turned out to be somewhat deeper (i.e. 280m). As to allow a large margin of safety, recovery should take place at the earliest opportunity to minimize the risk of corrosion, compression or failure of the floatation.

38 ROV coral and sponge dives in Eastern Baffin Bay – Leg 4b

ArcticNet Phase 3 – The Canadian Arctic Seabed: Navigation and Resource Mapping.
<http://www.arcticnet.ulaval.ca/pdf/phase3/seabed-mapping.pdf>

Project leaders: Evan Edinger^{1,2} (eedinger@mun.ca), Philippe Archambault³ (philippe.archambault@uqar.ca), Kent Gilkinson⁴ (kent.gilkinson@dfo-mpo.gc.ca), Paul Snelgrove^{2,5} (psnelgro@mun.ca), Suzanne Dufour² (sdufour@mun.ca) and Vonda Wareham⁴ (vonda.wareham@dfo-mpo.gc.ca)

ROV pilots: Vincent Auger⁶ and Peter Lockhart⁶

Cruise participants Leg 4b: Philippe Archambault³, Suzanne Dufour², Paul Snelgrove^{2,5}, Bárbara de Moura Neves², Vonda Wareham⁴, Joost Verhoeven², Robert Deering¹ and Rebecca Steinhart²

¹*Department of Geography, Memorial University of Newfoundland, Elizabeth Avenue, A1B 3X9, St. John's, NL, Canada.*

²*Department of Biology, Memorial University of Newfoundland, Elizabeth Avenue, A1B 3X9, St. John's, NL, Canada.*

³*Institut des sciences de la mer, Université du Québec à Rimouski, 310 allée des Ursulines, G5L 3A1, QC, Canada.*

⁴*Department of Fisheries and Oceans Canada, Northwest Atlantic Fisheries Centre, 80 East White Hills Road, A1C5X1, St. John's, NL, Canada.*

⁵*Department of Ocean Sciences, Memorial University of Newfoundland, Elizabeth Avenue, A1B 3X9, St. John's, NL, Canada.*

⁶*Canadian Scientific Submersible Facility, 110-9865 West Saanich Road, North Saanich, BC, V8L 5X8, Canada.*

38.1 Introduction

The Super Mohawk (SuMo) ROV program aboard the CCGS *Amundsen* during its 2015 mission is sponsored jointly by ArcticNet, the *Amundsen program* and by Fisheries and Oceans Canada. The major goals of the DFO-funded program to study coral and sponge habitats in the Canadian Arctic and the ArcticNet HiBio (Hidden biodiversity and vulnerability of hard-bottom and surrounding environments in the Canadian Arctic) project are to discover previously unknown coral and sponge biodiversity, other invertebrate and fish biodiversity, and previously under-sampled habitat types in the Canadian Arctic, especially the Eastern Arctic including Baffin Bay. Particular emphasis is placed on steep and deep hard-bottom habitats that cannot be sampled effectively using traditional oceanographic sampling methods such as box cores.

Many of the dive targets were selected on the basis of their bathymetry, slope, and surficial geology. Other sites were chosen based on previously identified sponge diversity and abundance hotspots (Cape Dyer), presence of carnivorous sponges (Scott Inlet), or

previously identified natural disturbance events in the form of submarine landslides (Hill Island, Frobisher Bay). At Scott Inlet, carnivorous sponges belonging to the genera *Chondrocladia* and *Cladorhiza* were observed during the 2014 ROV-*Amundsen* expedition. Although these sponges have a potential in natural product bioprospecting, the microbiomes of *Chondrocladia* (from any region) and of *Cladorhiza* from shallower, polar regions have not yet been explored, and for this reason Scott Inlet was also chosen as one of the targets for the 2015 expedition.

Finally, one of the goals of the project was to identify and characterize corals and sponges in areas of the Arctic that have not previously been impacted by commercial fishing activities.

The specific objectives were to:

- Determine which invertebrate and fish species are present in the various sites;
- Determine how different steep/deep areas are from gravelly bottom sites described in Roy et al. (2014);
- Measure the size-frequency distribution of cold-water corals especially the prominent and common Arctic sea pen *Umbellula encrinus*, and of the most prominent sponge species occurring at the various sites;
- Sample corals and sponges in order to assess their associated microbial and invertebrate faunas, and sampling for verifying identification of sponges. Specifically, to sample carnivorous sponges (*Cladorhiza* and *Chondrocladia*) from the Scott Inlet ROV dive site (and opportunistically from other locations) to determine their species identity and perform a metagenomic analysis of the microbial communities associated with various morphological features of these unique sponges;
- Take box core samples from most of the dive sites to describe resident microbial communities using metagenomic approaches and culture Actinobacteria, which are known antibiotics producers (this research will be done in collaboration with Dr. Kapil Tahlan at Memorial University).

38.2 Methodology

A total of five locations in Baffin Bay were chosen to be surveyed using the SuMo ROV during the *Amundsen* 2015 expedition: Navy Board Inlet, Pond Inlet, Scott Inlet, Cape Dyer, and Frobisher Bay (Figure 38.1). The dive at the Pond Inlet site was cancelled due to a combination of issues with the ROV and scheduling. As a result, a site near Qikiqtarjuaq (near Station 177) was later added to the plan.

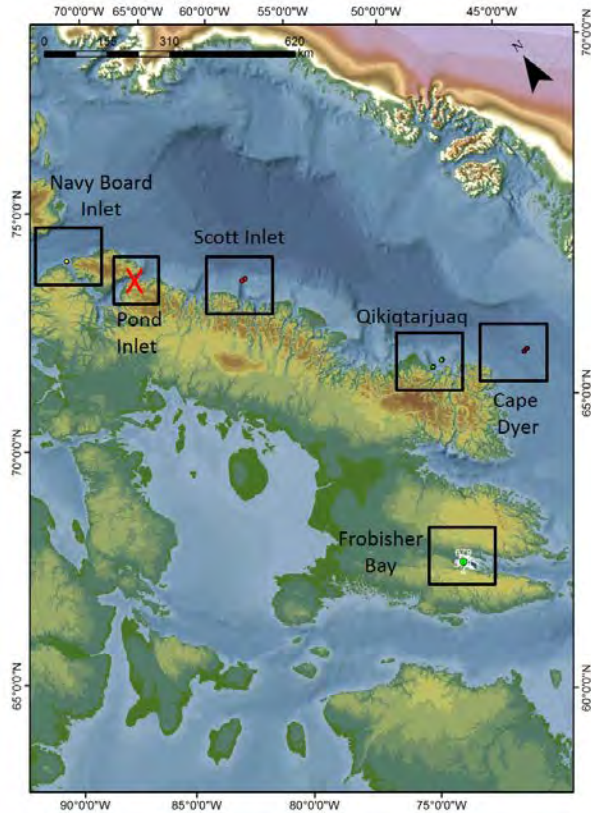


Figure 38-1. ROV dive locations for the 2015 CCGS *Amundsen* expedition. The Pond Inlet ROV dive was cancelled and replaced with the Qikiqtarjuaq dive.

The ROV (Figure 38-2) has a high definition (HD) camera (1Cam Alpha, Sub C Imaging, 24.1 megapixels) and two red lasers 10 cm apart for size indication. We used the FH video recording mode (second best resolution), since using the best resolution would reduce the camera storage capacity.

An elevator built to be used with this ROV was planned to be deployed during three of the five dives: Pond Inlet, Scott Inlet, and Frobisher Bay. However, it was only deployed in Scott Inlet due to time limitations. The elevator consisted of a platform holding seven polycarbonate boxes of mixed sizes at its base, and five floats at the top of the platform (Figure 38-2).

A multibeam survey was conducted in the Qikiqtarjuaq and in the Cape Dyer dive sites, from where multibeam data was not previously available. Before each dive a CTD was also deployed, recording temperature, salinity, density, dissolved oxygen, sound velocity, and current speed using an ADCP on the rosette. However, in Cape Dyer the CTD was deployed after the dive, in order to have more time available for the dive.

The primary activity during all dives was the acquisition of video data, except in Scott Inlet where sampling of sponges using the elevator was the main objective of the dive. Pre-established video-transects were followed at each location, with stops for photographs and

sampling. The Integrated Real-Time Logging System (IRLS) was used for logging observations and activities during each dive.

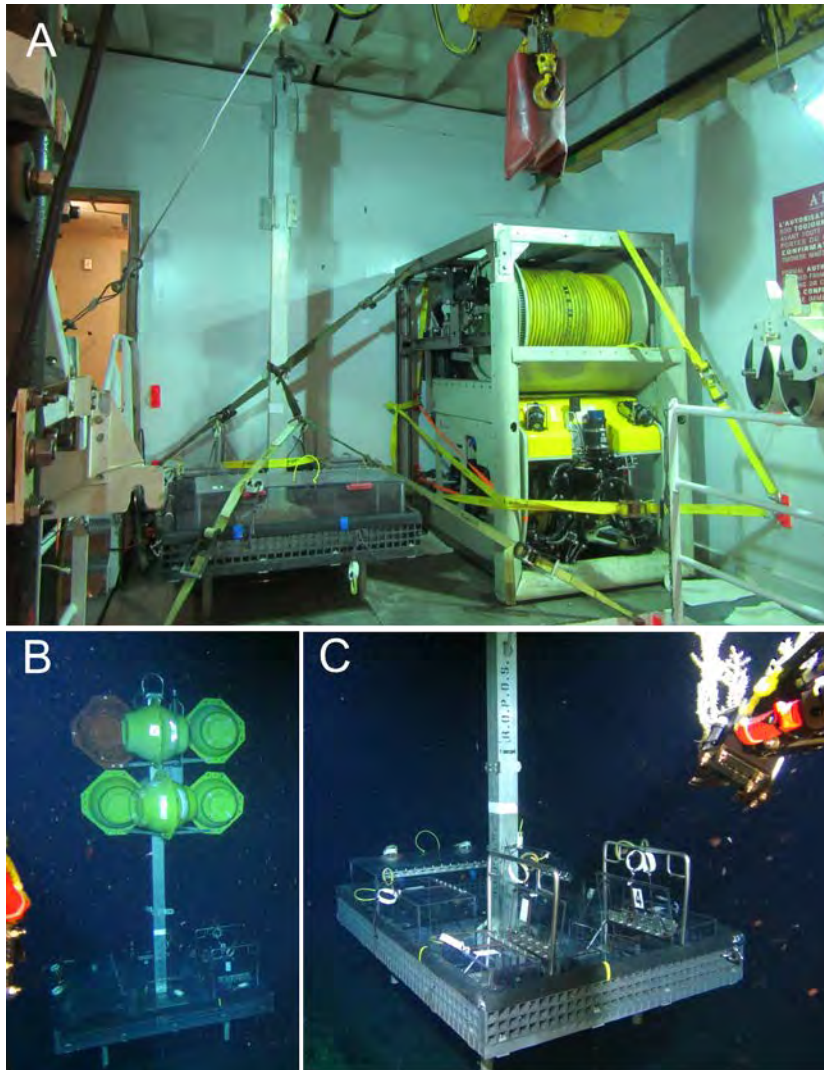


Figure 38-2. The SuMo ROV and the new elevator system. A) ROV and elevator, B) overall view of the elevator in the water (Scott Inlet, ~533 m), C) close-up of boxes, with a sample of the carnivorous sponge *Cladorhiza* sp. in the right arm.

Once aboard, samples of carnivorous sponges were photographed, immediately dissected and processed for DNA (freezing at -80°C , fixation in 100% ethanol) and histological analyses (fixation in buffered 2.5% glutaraldehyde). Additional samples (i.e. other sponges and ascidian) were photographed and frozen at -20°C , and sponge fragments were also fixed in RNAlater. Over the course of Leg 4b, a total of 20 sediment samples were collected from box cores obtained at Full stations. Sediment samples (Table 38-1) were frozen at -80°C for later processing.

Table 38-1. List of sediment samples obtained from box cores during Leg 4b.

Date	Station	Latitude (N)	Longitude (N)	Depth (m)	Sediment volume (ml)
12.10.15	155B	72°29.200	078°45.914	295	20
12.10.15	155B	72°29.200	078°45.914	295	5
14.10.15	170	71°22.788	070°04.273	385	20
14.10.15	170	71°22.788	070°04.273	385	5
14.10.15	170	71°22.788	070°04.273	385	20
14.10.15	170	71°22.788	070°04.273	385	5
16.10.15	CASQ3	71°19.314	070°38.975	832	20
16.10.15	CASQ3	71°19.314	070°38.975	832	5
16.10.15	CASQ3	71°19.314	070°38.975	832	20
16.10.15	CASQ3	71°19.314	070°38.975	832	5
16.10.15	CASQ3	71°19.314	070°38.975	832	20
16.10.15	CASQ3	71°19.314	070°38.975	832	5
17.10.15	CASQ3-2	71°19.314	070°38.975	832	20
17.10.15	CASQ3-2	71°19.314	070°38.975	832	5
20.10.15	177	67°29.138	063°48.393	282	20
20.10.15	177	67°29.138	063°48.393	282	5
20.10.15	177-2	67°29.138	063°48.393	282	20
20.10.15	177-2	67°29.138	063°48.393	282	5
21.10.15	180	67°28.665	061°45.772	185	20
21.10.15	180	67°28.665	061°45.772	185	5

38.3 Preliminary results

Dive 43: Navy Board Inlet (73.7149963 N, -81.1238022 W) - October 15th 2015

At this site, the planned transect length was 2 km, but only ~450 m were surveyed (Figure 38-3) due to electrical problems with the ROV. The surveyed line depth ranged between 434-453 m. Bottom temperature (452.8 m) at this site was -0.7 °C, and salinity was 33.63 PSU (Figure 38-3).

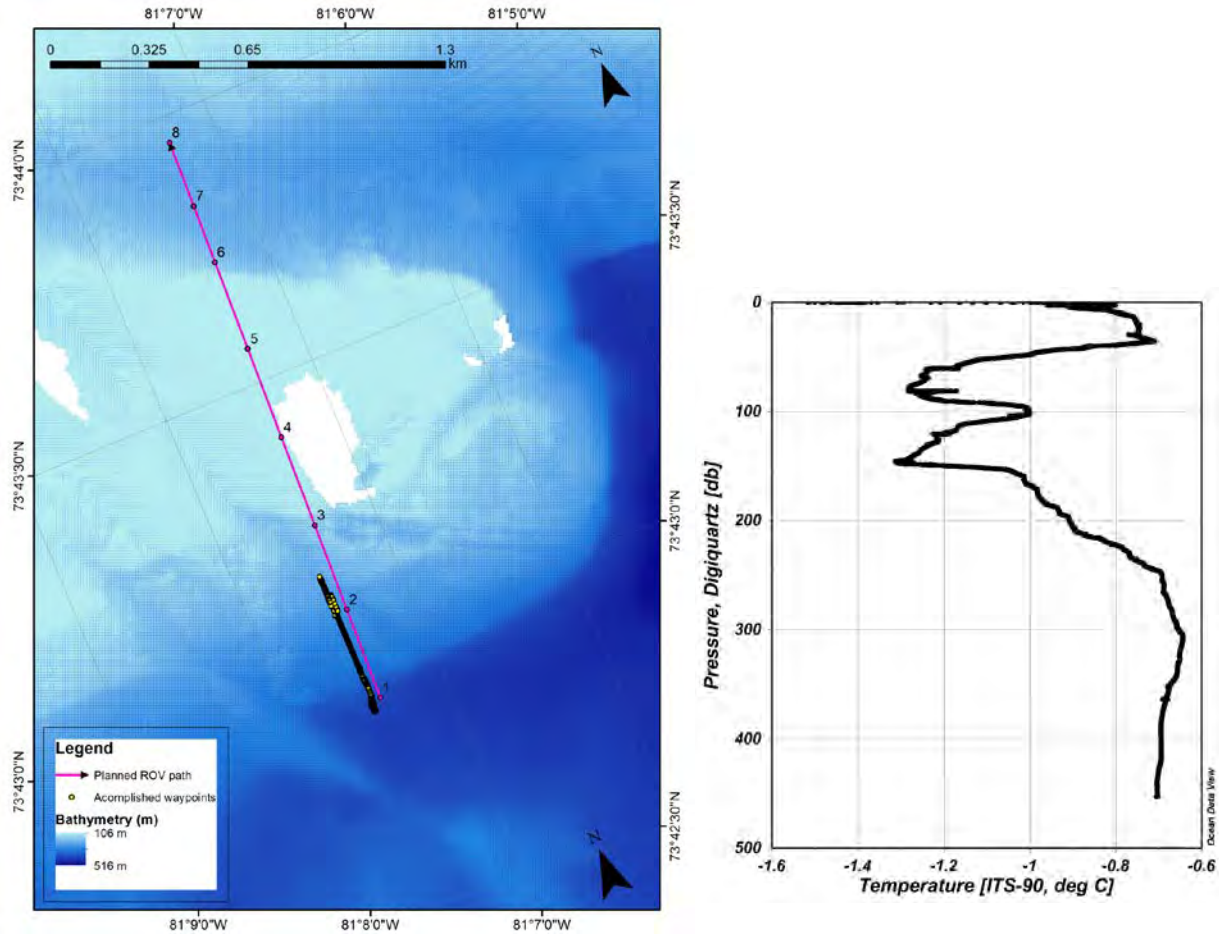


Figure 38-3. Overview of the Navy Board ROV dive location, showing planned and accomplished ROV transect. Transect terminated early due to ROV electrical failure (see text) (left). Temperature profile at the Navy Board ROV dive site. This plot was generated at Ocean Data View, as the original plots from the Rosette were not available for this cast (right).

Echinoderms were the most commonly observed organisms, with brittle stars being the most abundant taxa observed during the dive. Other commonly observed echinoderms include the basket star *Gorgonocephalus* sp., the sea urchin *Strongylocentrotus* sp., sea cucumbers, the feather star *Poliometra* sp., the sea star *Crossaster papposus* and others. Sea anemones and ceriantharians were also frequently observed. Shrimps were also very conspicuous at this site (Figure 38-4).

Soft corals (Family Nephtheidae) were also observed, but not very frequently. Whelks and the jellyfish *Ptychogastria polaris* were also seen near the bottom during the dive. The carnivorous sponge *Cladorhiza* sp. was observed only once during this dive, but additional sponges were also seen, such as *Mycale* sp. and other undetermined species. Fish such as sculpins, Cottidae fish, and a sea tadpole *Careproctus reinhardi* were also observed (Figure 38-4).

In terms of bottom type, the surveyed site was mainly rocky. At certain areas the bottom was dominated by gravel, while in others it was dominated by cobbles and pebbles (Figure 38.4). Bedrock outcrops were also surveyed during this dive, being covered with polychaete tubes, sea urchins, and sponges.

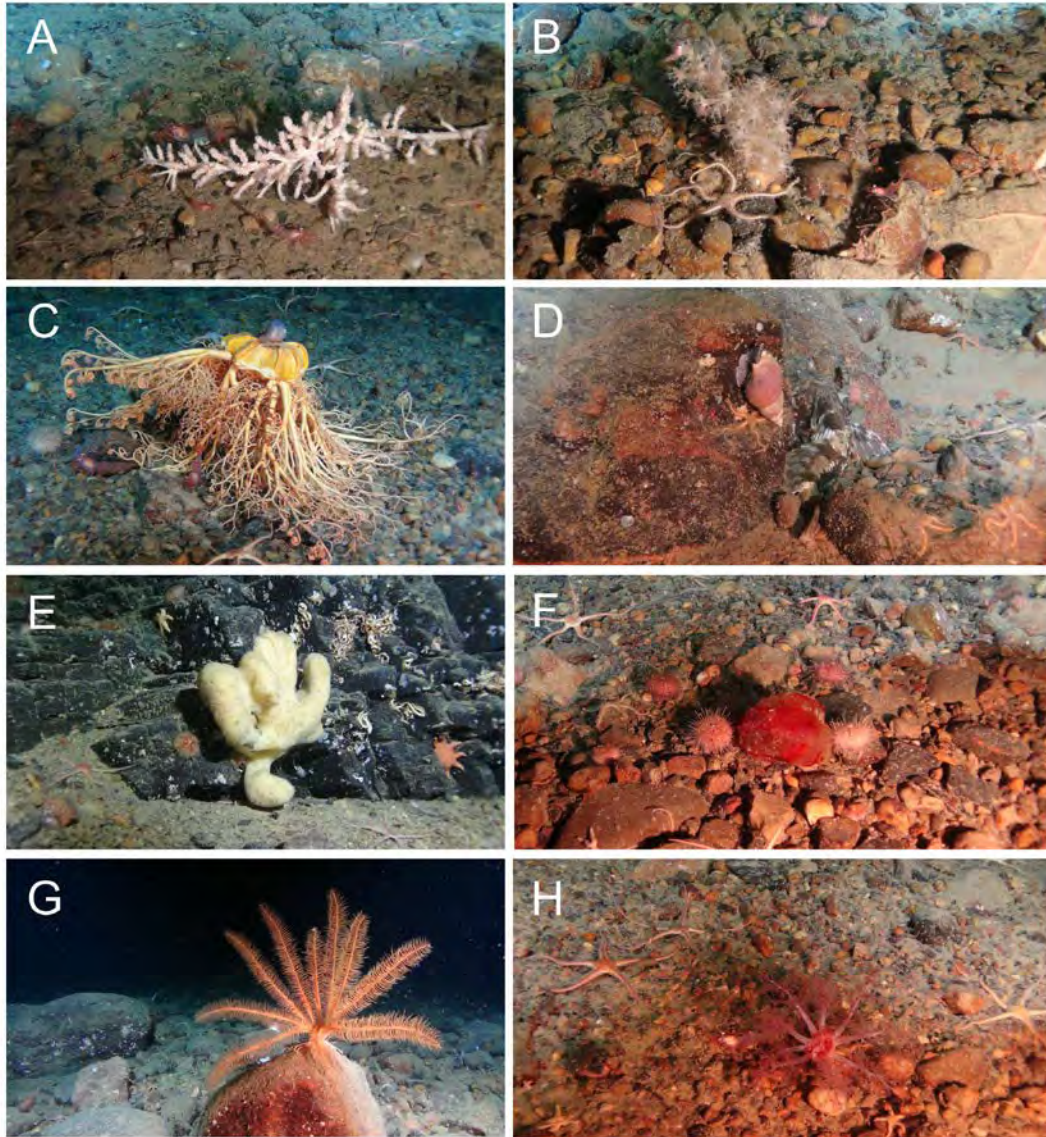


Figure 38-4. Organisms and bottom types observed during the ROV dive at Navy Board Inlet. A) *Cladorhiza* sp., B) Neptheid soft coral, C) *Gorgonocephalus* sp. with sea tadpole, D) whelk, E) *Desmospongia*, F) Sea urchins and unidentified red organism, G) crinoid, H) unidentified sea cucumber and brittle stars.

Dive 44-45: Scott Inlet (71.5162964 N, -70.2777023 W) - October 17th 2015

At this site, there was no pre-established transect to be followed, as the objective was the sampling of carnivorous sponges. The surveyed area was ~3428 m², ranging depths between 520-533 m (Figure 38-5). Bottom temperature (595 m) near the dive site was ~1.3 °C, and salinity was ~34.4 PSU (Figure 38-6).

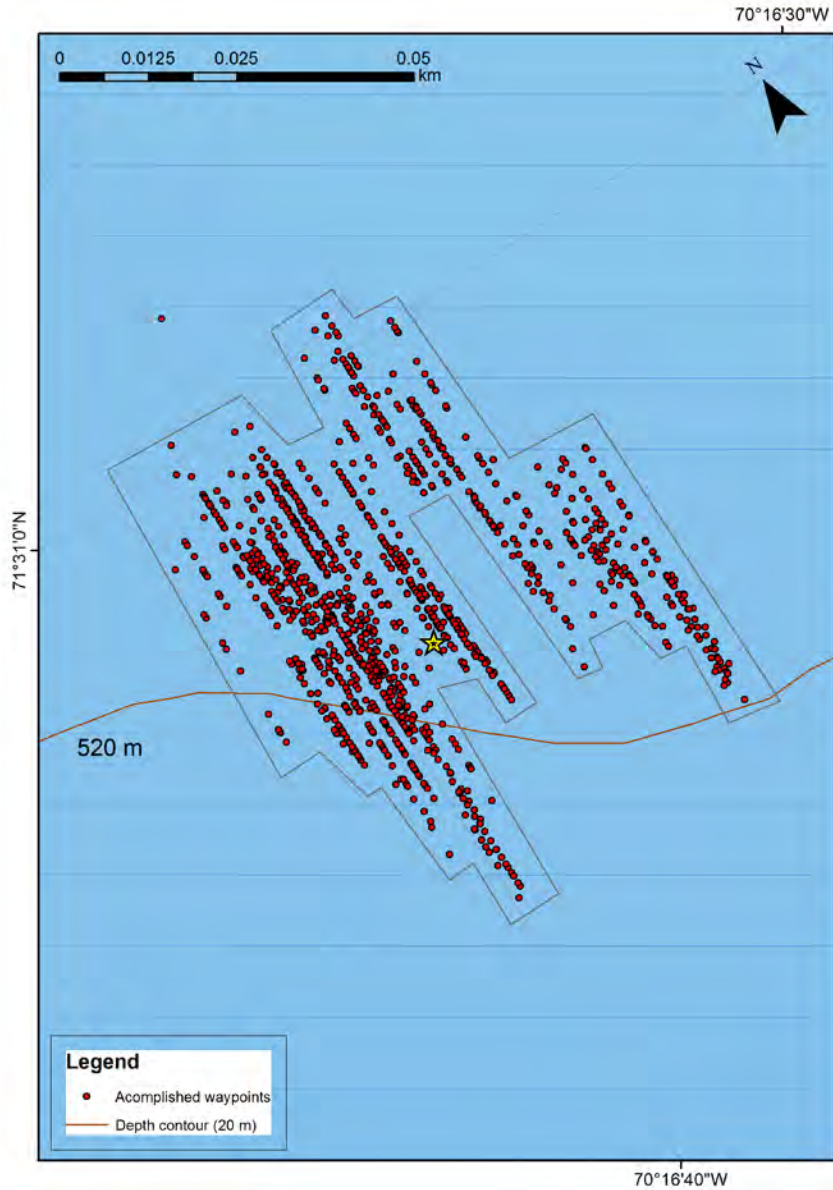


Figure 38-5. Overview of the Scott Inlet ROV dive location, showing surveyed area and position of the elevator (star).

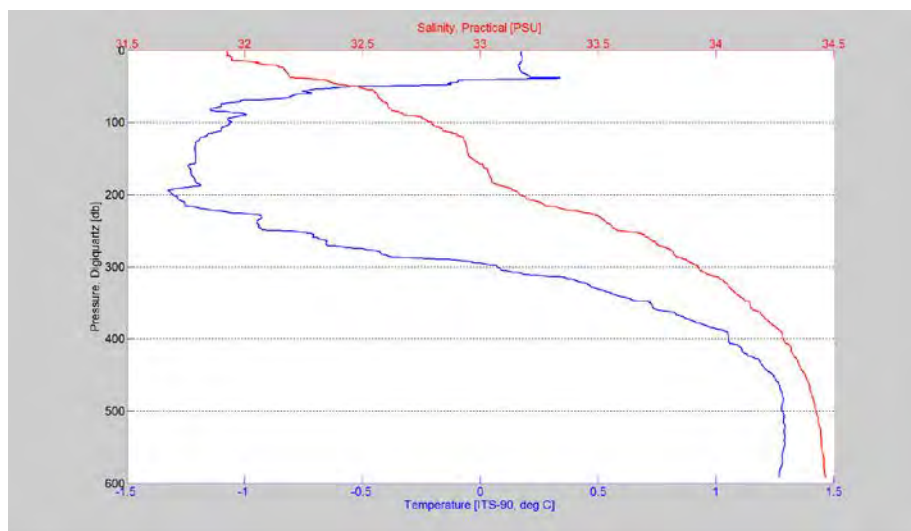


Figure 38-6. Temperature and salinity profiles at the Scott Inlet ROV dive site.

The new sampling elevator was deployed at the evening of October 16th at a site where carnivorous sponges had been observed during the 2014 *Amundsen* expedition (elevator location: 71°31.0031'N, 70°16.6786'W; depth of 533 m) (refer to Figure 38-2). Total deployment time was 3 hours. On October 17th, we used the ROV and the sample elevator to successfully collect three carnivorous sponges from Scott Inlet during dives 44 and 45. During dive 44, one sample (44-1; Table 38-2) of *Chondrocladia* sp. was collected and placed in a sample box on the elevator. Due to technical issues with the ROV, dive 44 was aborted and a second dive (45) was undertaken a few hours later after ROV problems were resolved.

Table 38-2. Sponge samples collected using the SuMo ROV during Leg 4b.

Genus	Dive	Date	Sample	Latitude (N)	Longitude (W)	Depth (m)	Size (cm)
<i>Chondrocladia</i>	44	17.10.15	44-1	71°30.9911'	70°16.0464'	523	37
<i>Cladorhiza</i>	45	17.10.15	45-1	71°30.9889'	70°16.6472'	521	30
<i>Chondrocladia</i>	45	17.10.15	45-3	71°30.9627'	70°16.6843'	525	30
<i>Chondrocladia</i>	46	20.10.15	46-1	67°28.6089'	63°41.0648'	684	12
<i>Cladorhiza</i>	46	20.10.15	46-2	67°28.6539'	63°40.8323'	660	4

During dive 45, a specimen of *Cladorhiza* sp. (sample 45-1; Table 38-2) and a second specimen of *Chondrocladia* sp. (sample 45-3) were collected. Other organisms observed during dives 44 and 45 include sea anemones, the sea pen *Umbellula encrinus*, brittle stars, and additional sponges including vase sponges, whelks, as well as abundant copepods (and marine snow) in the water column. The bottom consisted of sand, mud, and abundant cobble (Figure 38-7). The elevator was successfully retrieved, and recovery time was 1 hour.

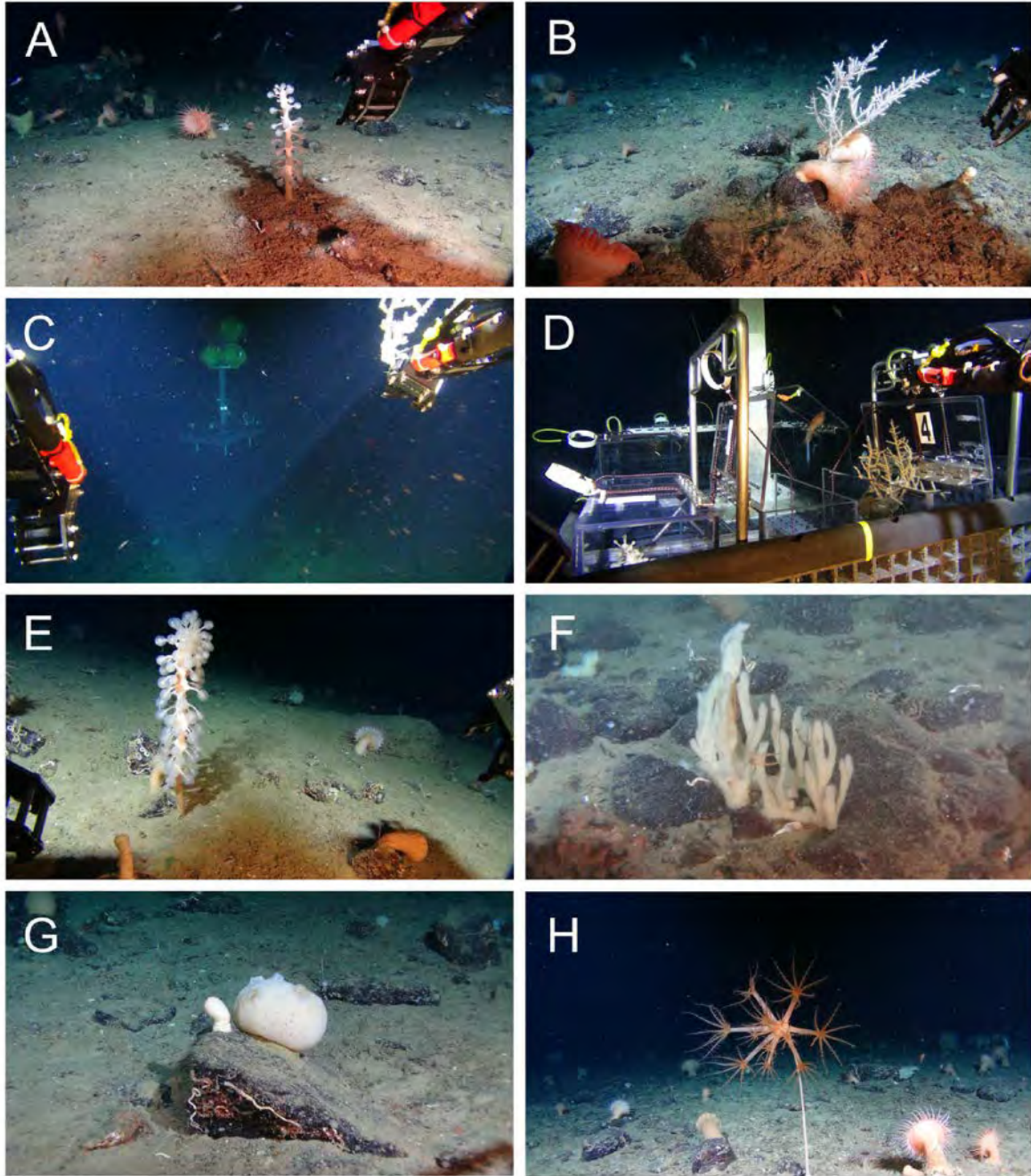


Figure 38-7. Organisms and bottom types observed during the ROV dive at Scott Inlet. A) Sampling of *Chondrocladia* sp., B) sampling of *Cladorhiza* sp., C) *Cladorhiza* sp. sample being brought to the elevator, D) *Cladorhiza* sp. being put in the box, E) *Chondrocladia* sp., F) fan sponge, G) *Polymastia* sp., H) *Umbellula encrinus*.

Dive 46: Qikiqtarjuaq (67.4741974 N, -63.6929016 W) - October 20th 2015

A ROV dive near Qikiqtarjuaq (~4 km from Station 177) was added to the plan, as a replacement to the dive that could not take place in Pond Inlet (Figure 38.8). A multibeam survey was conducted in the area before the dive, and the specific site was chosen based on high slope features. The original dive transect was planned to follow a line 1.5 km in length, but only 954 m could be completed due to time limitations (Figure 38.8). The transect path crossed depths ranging 620-680 m. Bottom temperature (370 m) was 0.8 °C (Station 177), and salinity was ~34 PSU (Figure 38.9).

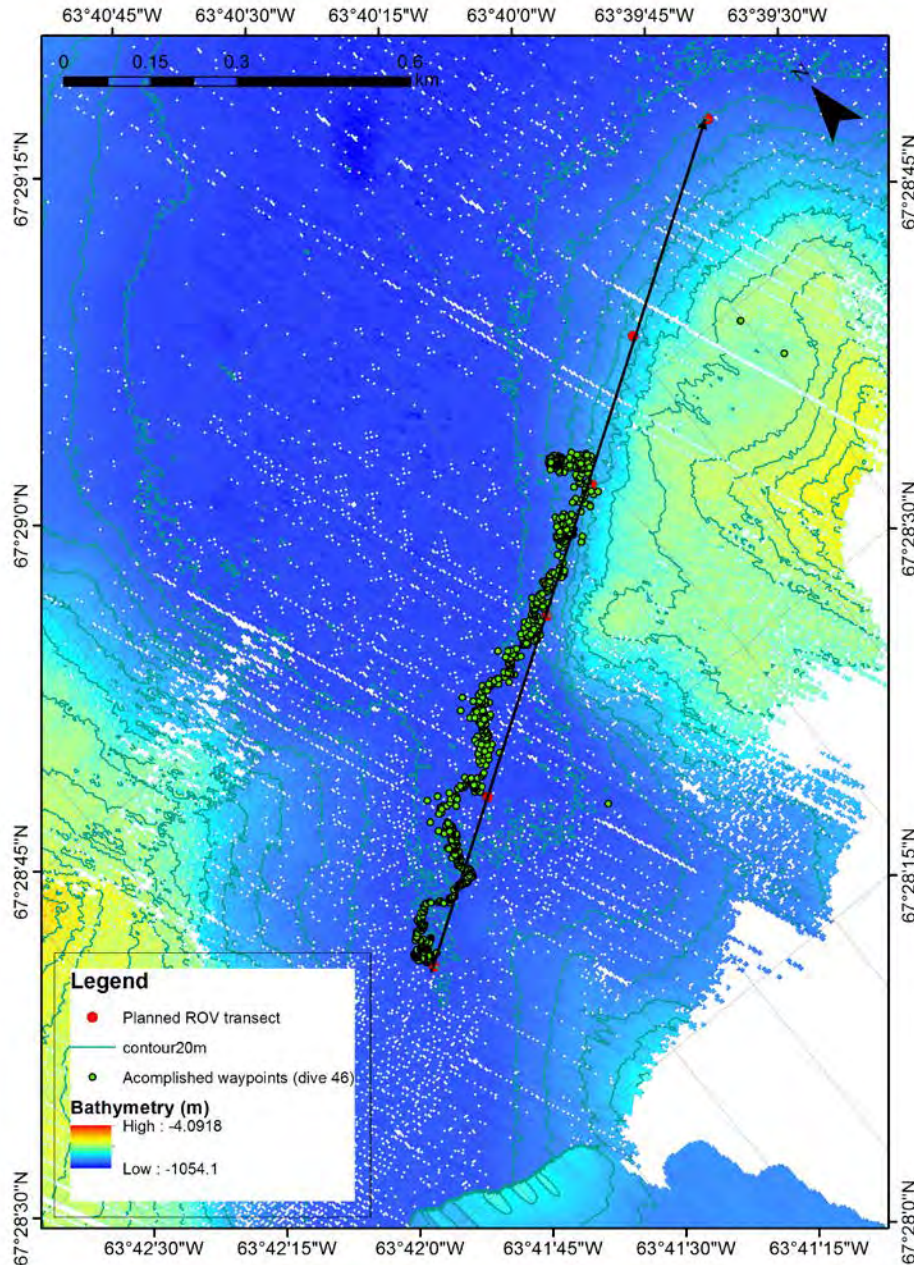


Figure 38-8. Overview of the ROV dive near Qikiqtarjuaq, showing planned and accomplished ROV transect.

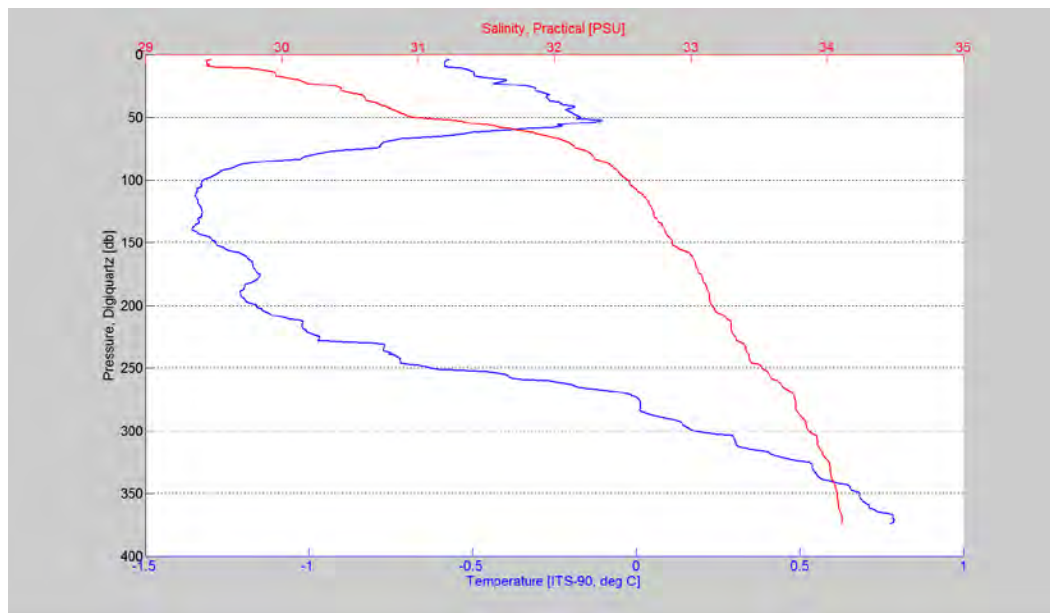


Figure 38-9. Temperature and salinity profiles near the Qikiqtarjuaq ROV dive site (Station 177, ~4 km from the dive site).

The dive transitioned from a flat slope area with muddy substrate (680 m), into a gentle slope with scattered boulders, concluding with rocky outcrops (620 m).

Sea anemones (*Actinauge* sp.) were the dominant organisms in the first part of the dive, forming dense fields (e.g. 2.8 individuals/m²) in the soft mud substrate. Other notable species included giant *Umbellula* sp. sea pens, with one individual reaching ~ 230 cm height, 75 cm width and having 56 polyps. Other organisms observed in the muddy substrate included: ascidians (?*Ciona intestinalis*), ophiuroids (brittle stars, the basket star - *Gorgonocephalus* sp.), at least two species of decapods (shrimps), cnidarians (tube-dwelling sea anemones and solitary stalked hydrozoans - *Corymorpha* sp.), fish (skate sp., eelpout-*Lycodes* sp., Arctic alligator fish), whelk sp., sponges, and an unidentified cluster of small white tubes (Figure 38-10).

Towards the latter portion of the transect, larger boulders and rock outcrops were observed colonized by sponges (*Polymastia* spp., fan sponges), sea anemones, nephtheid soft corals, bryozoans, and crinoids. The community structure of the surrounding muds also transitioned with fewer sea anemones but with stalked hydroids and more sponge observations such as *Chondrocladia* sp., *Cladoriza* sp., and stipitate/stalked sponges) (Figure 38.10). The dive transect concluded at the base of a steep outcrop dominated by crinoids at 614 m.

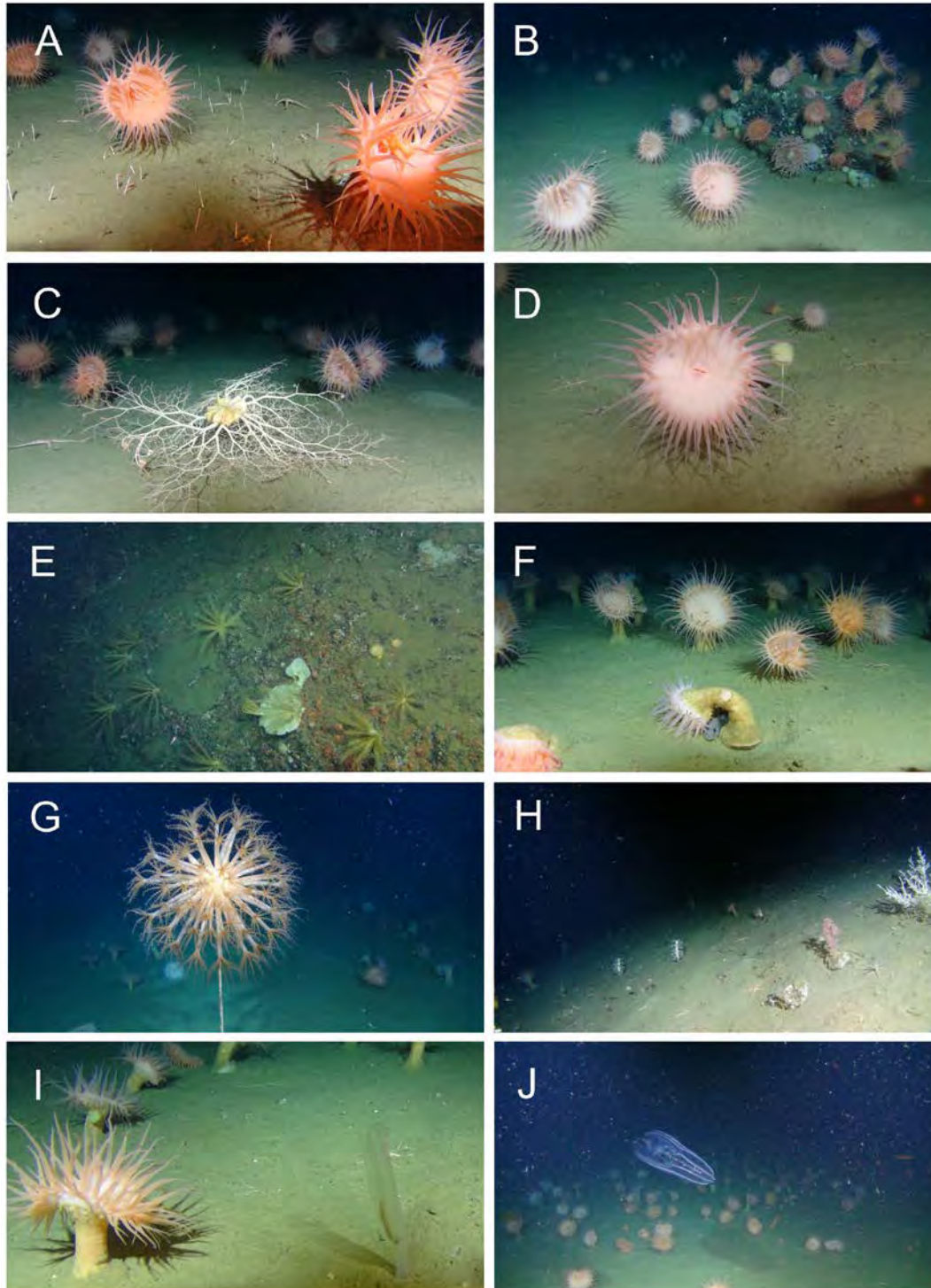


Figure 38-10. Organisms and bottom types observed during the ROV dive near Qikiqtarjuaq. A) sea anemones and unidentified white tubes, B) cluster of sea anemones, C) *Gorgonocephalus* sp., D) sea anemone and an stipitate sponge, E) cluster of crinoids on outcrop, F) eel-pout below curved sea anemone, G) *Umbellula encrinus*, H) diversity of sponges and other invertebrates, I) sea anemones and ascidian, J) ctenophore. Red lasers are 10 cm apart.

Dive 47: Cape Dyer (66.4132996 N, -59.2184982 W) - October 23th 2015

This site was chosen based on records of sponge bycatch and areas identified as having high sponge concentrations (Kenchington et al. 2010), with the dive transect crossing a trawl path from a 2006 DFO survey set. A multibeam survey was conducted over the site but in two parts; the majority completed before the dive and the remainder after the dive.

The original dive transect was planned to follow a line 4 km in length, but only 935 m could be completed due to mechanical/electrical issues with the ROV (Figure 38-11). The transect path crossed depths ranging 746-750 m. Bottom temperature (718 m) was ~1.5 °C, and salinity was ~34.5 PSU (Figure 38.12).

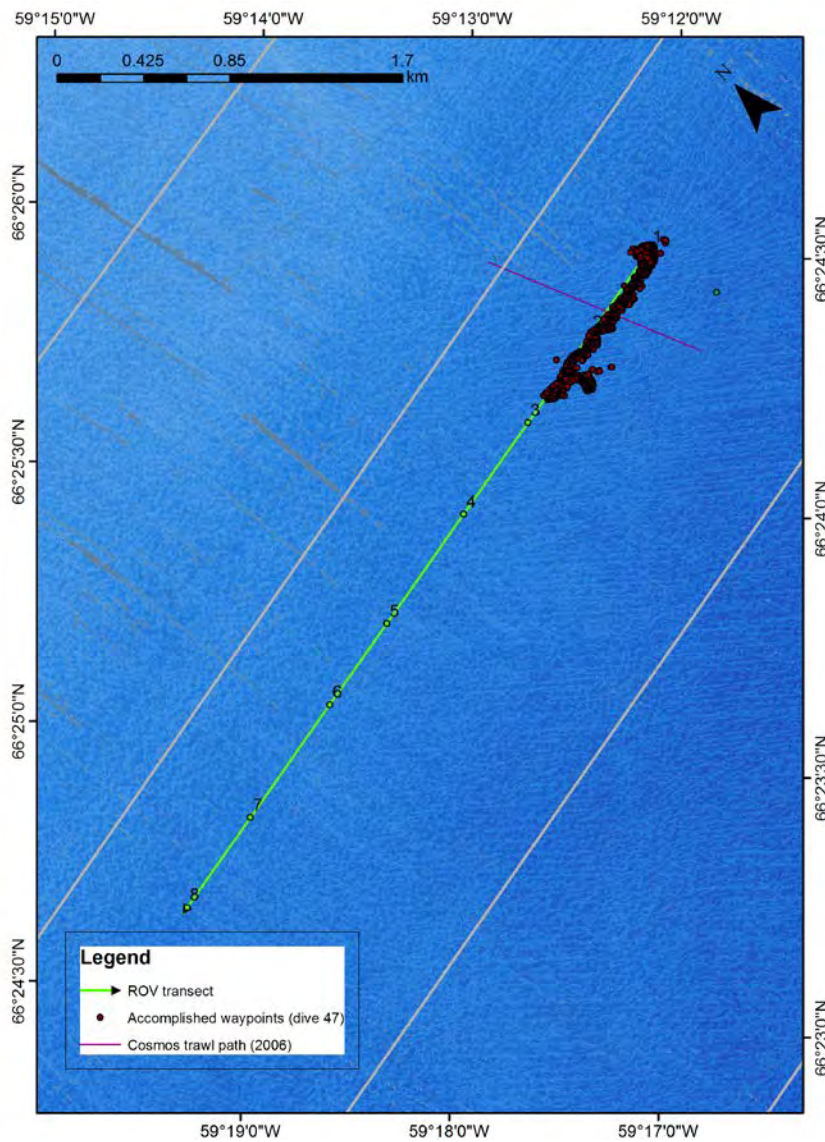


Figure 38-11. Overview of the ROV dive at Cape Dyer, showing planned and accomplished ROV transect, and trawl path. Transect terminated early due to ROV mechanical failure complicated by rough seas (see text).

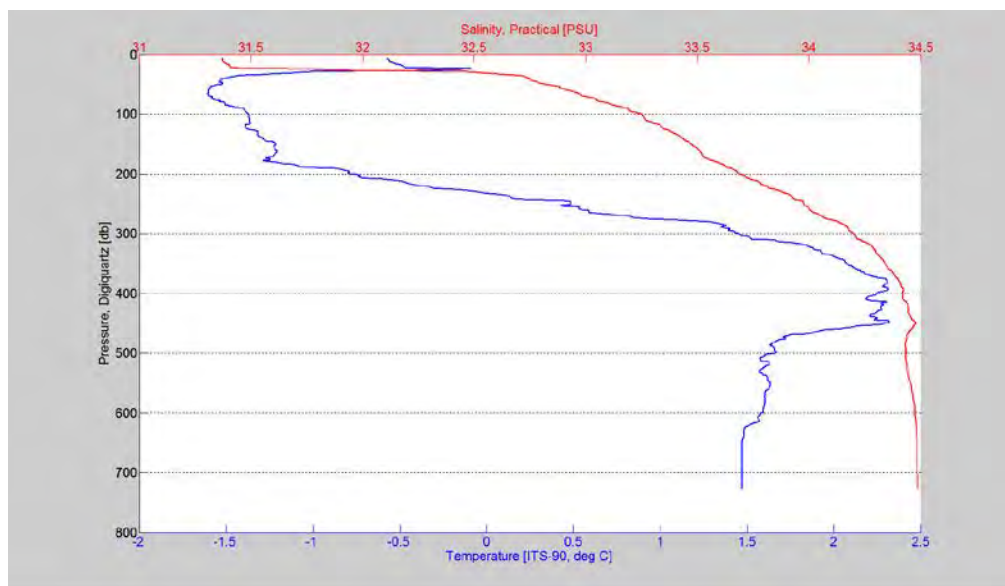


Figure 38-12. Temperature and salinity profiles at the Cape Dyer ROV dive site.

At this site, the bottom was flat and dominated by soft mud with sporadic boulders. Sponges were the dominant organism found on both substrate types, and were composed of species from two classes: Demospongiae (*Geodia* spp., *Stryphnus-Aplysilla* spp., *Craniella* sp., *Polymastia* spp.) and Hexactinellida (*Asconoma* sp.) (Figure 38-13). In many cases sponge species could not be determined due to thick layers of epifauna encrusting individuals. No samples were collected due to mechanical failure of the ROV arms.

Corals were also abundant at this site, with soft corals (nephtheid corals) observed on hard substrates, and the sea pen *Umbellula encrinus* in soft muds. Other notable groups observed during transect included: ascidians, echinoderms, arthropods (pycnogonids), decapods (shrimps), other cnidarians (sea anemones and solitary stalked hydrozoans - *Corymorpha* cf. *glacialis*), cephalopods (octopus and squid), and numerous fish species (Greenland halibut - *Reinhardtius hippoglossoides*, eelpout (*Lycodes* sp.), rockling - *Gaidropsarus* sp., sea tadpole – *Careproctus reinhardti*, and grenadier – Family Macrouidae) (Figure 38-13).

Assessment of the impact of the single trawl from 2006 DFO Cosmos Trawl survey could not be confirmed in the preliminary results. However, upon review of processed multibeam data, linear features were observed and may indicate the site was exposed to more anthropogenic disturbances (e.g. bottom contact fishing gear) than originally thought, and would explain the relatively small size of many individual sponges (e.g. *Chondrocladia*) and overall low sponge biomass.

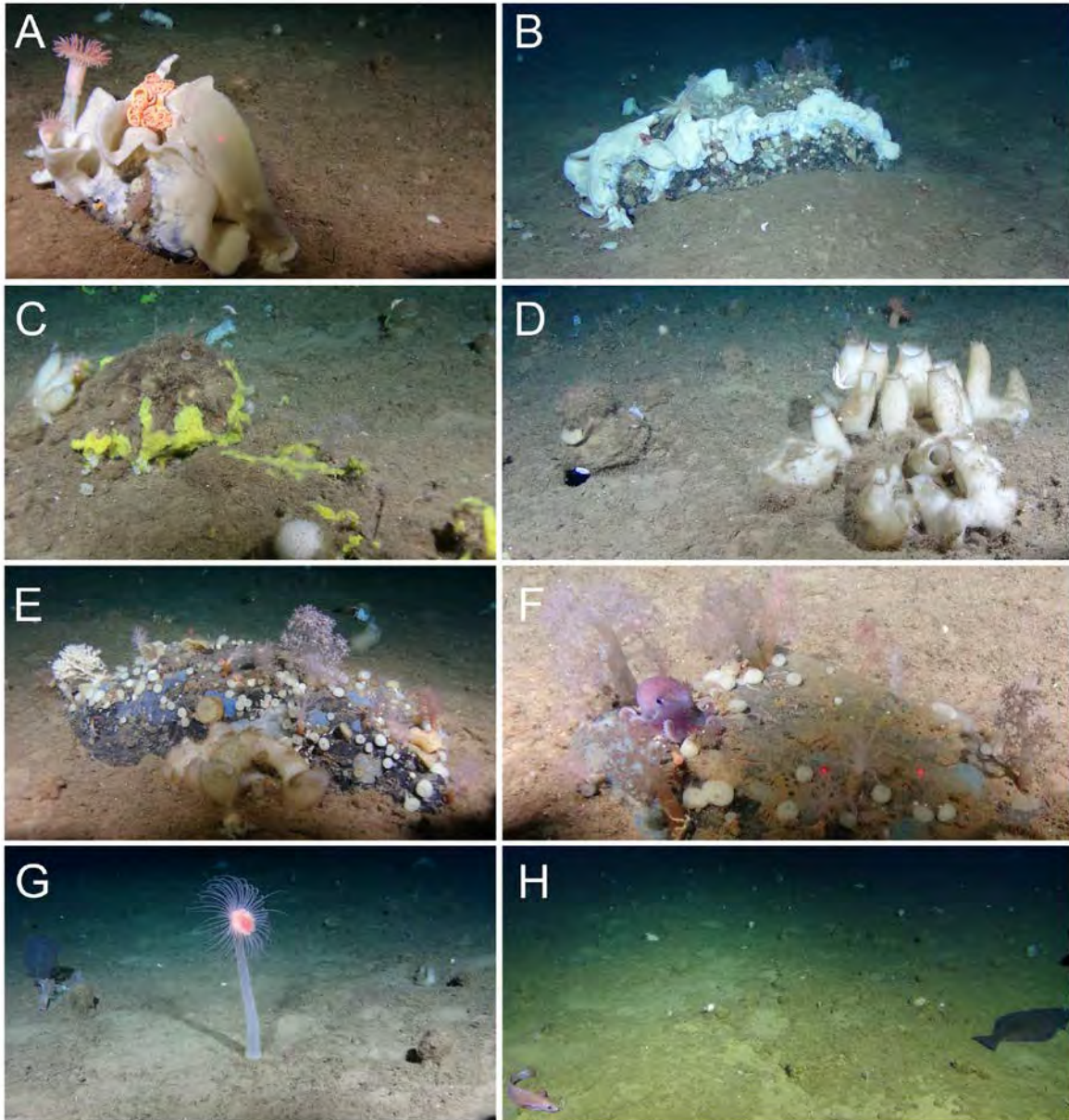


Figure 38-13. Organisms and bottom types observed during the ROV dive at Cape Dyer. A-E) diversity of sponges, F) nephtheid soft corals and octopus, G) solitary hydrozoan *Corymorpha* cf. *glacialis*, H) rockling (left) and turbot (right). Red lasers are 10 cm apart.

Dive 48: Frobisher Bay (63.6385994 N, -68.6306992 W) - October 25th 2015

This dive took place off the coast of Hill Island in Inner Frobisher Bay. The site was selected because of the presence of two distinct slope failure scars, each with a different morphology. The original dive transect was planned to be 4.2 km in length, but the dive plan was adjusted, as the ROV had shown problems in the previous dives. Focus was given on only one of the landslides and on a single high-slope feature. Furthermore, the elevator was not deployed in this dive due to time constraints.

Total planned and accomplished transect lengths were 1.2 km (Figure 38-14), crossing depths ranging 59-139 m. Bottom temperature (at 115 m) was -0.59 °C, and salinity was ~32.57 PSU (Figure 38-15). The dive started at 139 m depth in a soft bottom area outside of the landslide, where ascidians (?*Ciona intestinalis*) were very abundant, forming fields (Figure 38-16). Echinoderms and isopods were frequently seen, including isopods with juveniles clustered on the front appendages of the adults (Figure 38-16). Large concentrations of kelp were observed, although it is undetermined whether the kelp is resident to the site or from shallower depths.

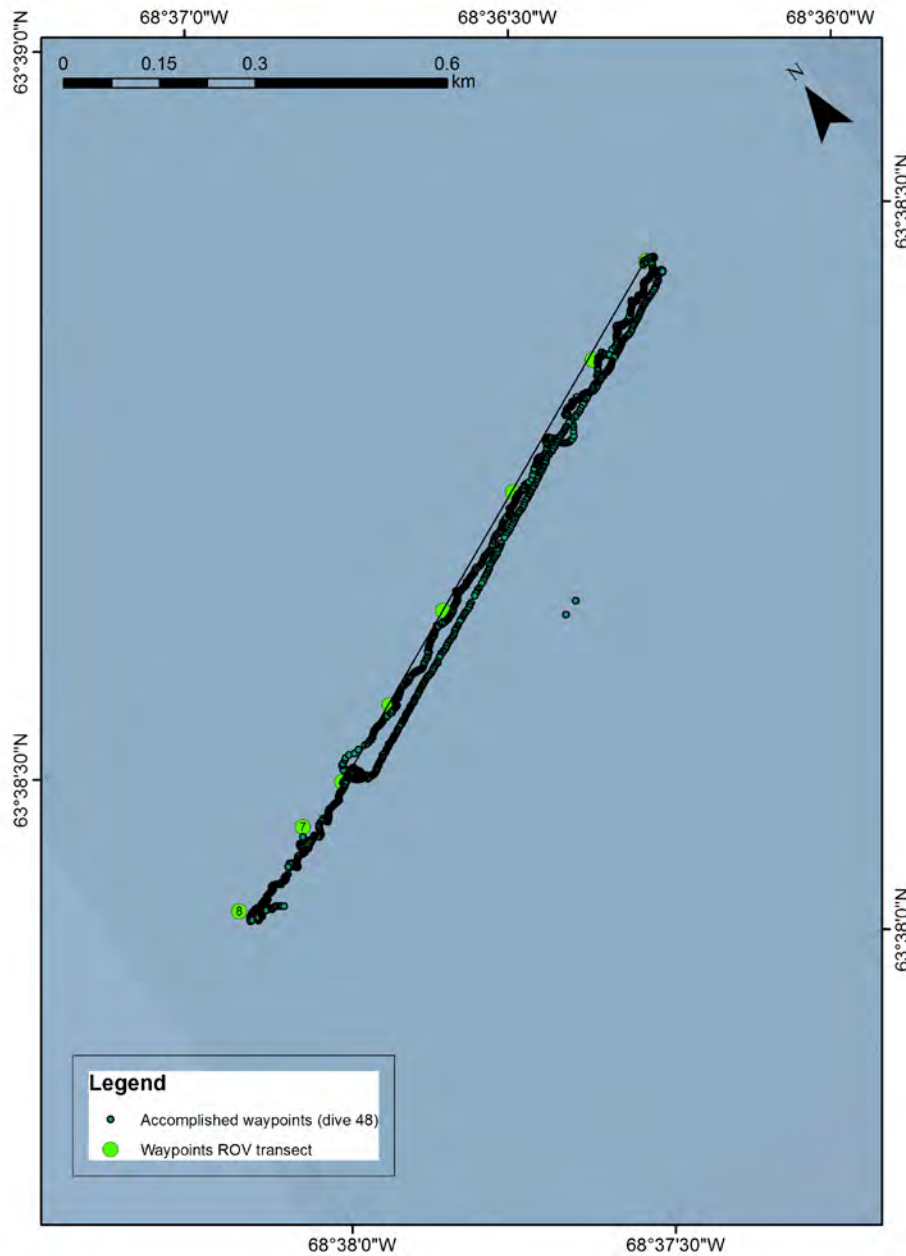


Figure 38-14. Overview of the ROV dive at Frobisher Bay, showing planned and accomplished ROV transect.

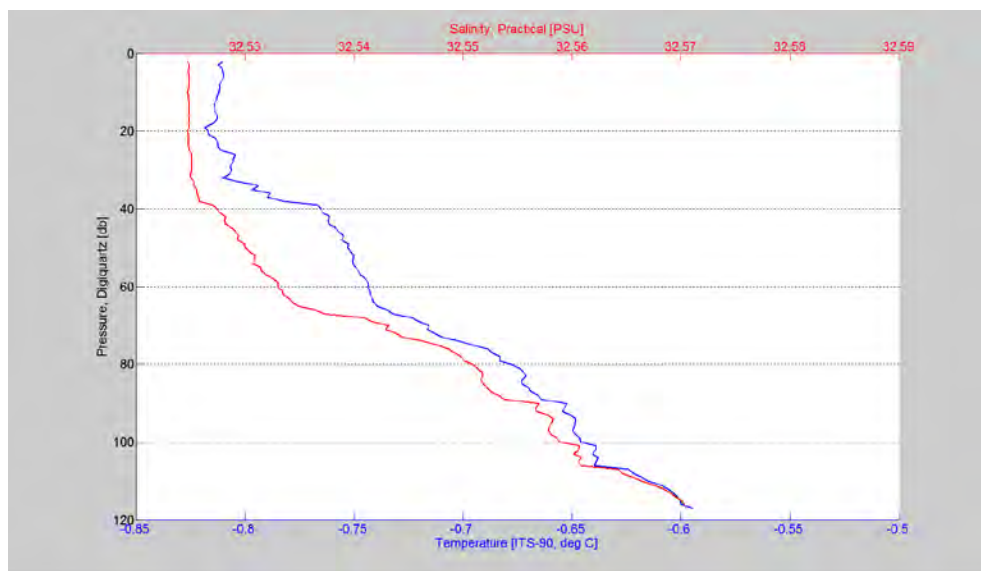


Figure 38-15. Temperature and salinity profiles near the Frobisher Bay ROV dive site.

Brittle stars and feather stars were the dominant organisms in the landslide area, along with sponges (*Desmospongia*), while ascidians were much less abundant (Figure 38-16). In the landslide area crinoids were more abundant where slope was higher. The sea star *Solaster* cf. *endeca* was also observed in this part of the dive. The landslide ridges observed in the bathymetry could be identified during the transect as changes in the slope. Sporadic boulders encrusted with soft corals (few), sponges, crinoids and tube polychaetes. Fish (eel pout, sea tadpoles, and sculpins) were also observed. Juvenile scallops were also abundant in this part of the transect, with densities of at least 24 individuals/m². Picnogonids were also conspicuous in the landslide area.

After surveying the landslide area, we went back to the beginning of the dive in order to sample ascidians, and to give continuity to the transect in a high slope area. One globular sponge (sample 48-1), one ascidian (sample 48-2), and one arborescent sponge (sample 48-3) were successfully sampled using the ROV arms (Table 38-3). Because the samples were kept in the ROV arm, only fragments of the arborescent sponge could be retrieved. The globular sponge (sample 48-1) had a peculiar garlic smell.

Table 38-3. Organisms sampled during the Frobisher Bay ROV dive (dive 48)

Taxon	Sample	Latitude (N)	Longitude (W)	Depth (m)	Size (cm)
<i>Desmospongia</i>	48-1	63°38.575	068°36.527	65	13 (diam)
Asciacea	48-2	n/a	n/a	88	13 (dead)
<i>Desmospongia</i>	48-3	n/a	n/a	88	fragments

n/a = not available at the moment

In the second part of the transect we surveyed the transition zone between a flat bottom environment and a rocky outcrop. A high concentration of ascidians and sponge gardens (dominated by arborescent sponges) were observed in this part of the dive, as well as crustaceans (isopods), sea cucumbers (probably *Psolus fabrici*), crinoids, ophiuroids, sea stars, sea anemones, and tube polychaetes (Figure 38-16). Fish were also seen throughout the dive, including a juvenile flatfish, alligator fish, and sea tadpoles.

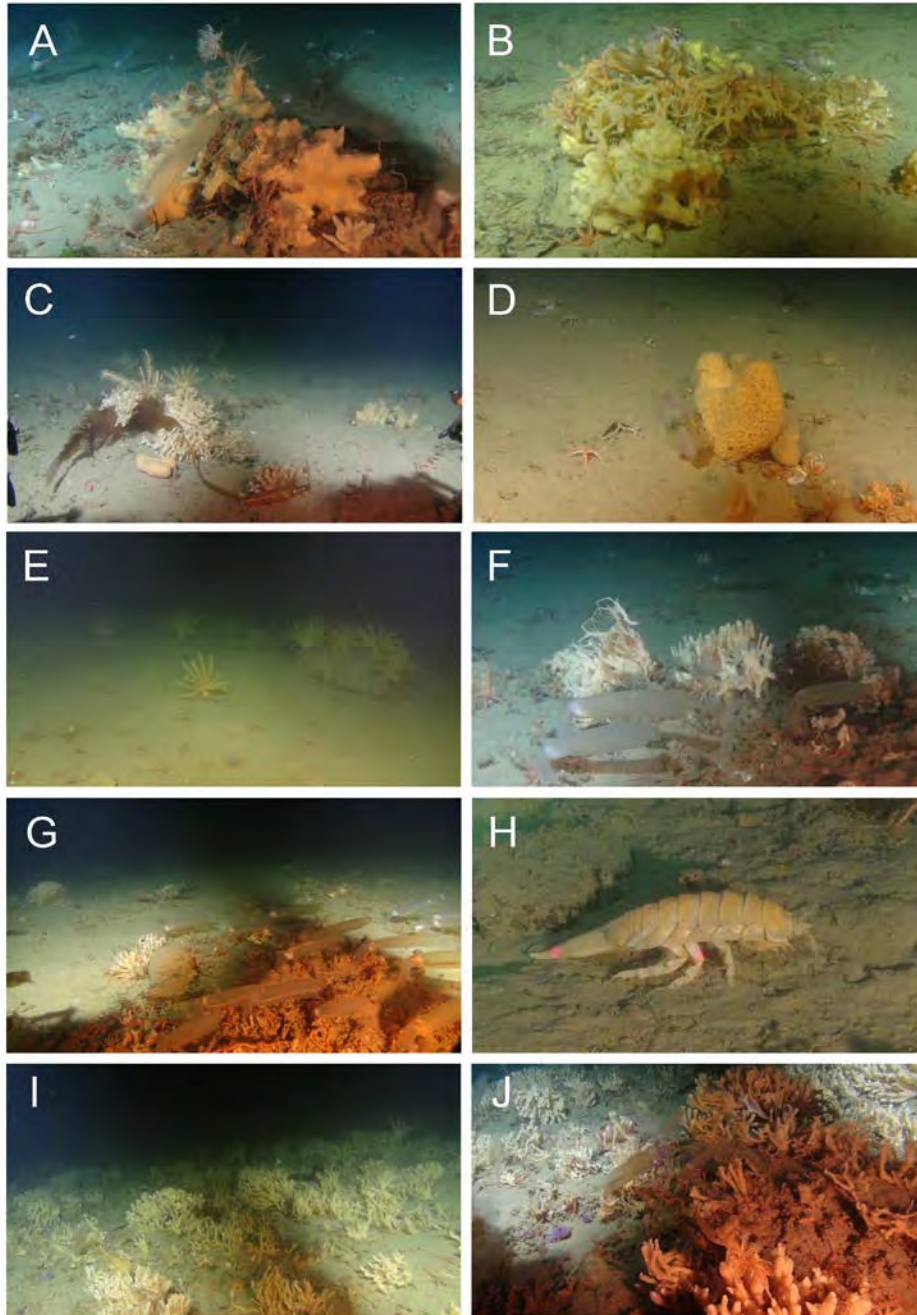


Figure 38-16. Organisms and bottom types observed during the ROV dive at Frobisher Bay. A) isopod with juveniles, B) crinoids, C) sponges, crinoids and kelp, D) large yellow sponge, E) crinoids, F-G) ascidians and sponges, H) large isopod, I-J) sponge gardens (mostly the fan sponge). Red lasers are 10 cm apart.

38.4 Comments and recommendations

38.4.1 Conclusions and future directions

These preliminary results indicate that the dives were successful, based on objectives specified in the original dive plan:

Invertebrates and fish diversity

The diversity of sponges, corals, other invertebrates and fish was documented at all surveyed sites. These observations indicate high sponge concentrations and species richness in Cape Dyer and Frobisher Bay. Although biomass in Cape Dyer appears to be much lower than expected, dense sponge gardens were identified in the Frobisher Bay area (refer to Figure 38-16). Future ROV investigation in Frobisher Bay is highly recommended in order to better assess the ecological significance of this area.

The presence of anemone fields and giant colonies of the sea pen *Umbellula* in the Qikiqtarjuaq area highlight the ecological importance of this site, where further ROV investigation is also recommended.

Observations show corals co-occur with sponges as well as other benthic animals (e.g. fish, octopus, shrimp, hydroids, brittle stars, sea anemones, and bryozoans).

Steep/deep versus gravelly bottom sites

The ROV survey at Navy Board showed pebbles, boulders and bedrock dominated the substrate. As a result, this site would be unsuitable for traditional sampling methods such as box coring and trawling, and highlights the importance of ROV technology.

An array of bottom types was observed in all five sites, from muddy bottoms to bedrock outcrops. The benthic fauna associated to the different bottom types was also distinct and dominated by different organisms, indicating the need to sample both types of habitats (e.g. soft and hard bottoms).

Size-frequency distribution of *Umbellula encrinus*

Colonies of *U. encrinus* were observed in three of the five dive sites (Scott Inlet, Qikiqtarjuaq, and Cape Dyer). Based on our current knowledge on this species, substrates in Navy Board were inhospitable, and Frobisher Bay was too shallow. Size-frequency distribution will be determined by analyzing the videos, with the assistance of the red lasers 10 cm apart.

New elevator system

Collections using the new elevator system in Scott Inlet were successful, with several carnivorous sponges being obtained. Although the elevator could not be deployed at all three planned sites, samples were still collected utilizing SuMo's arms as an alternative.

Box cores

Box cores planned in association with most of the dive sites were successfully collected, and samples will be analyzed later for microbial and invertebrate fauna studies.

38.4.2 Difficulties encountered and suggestions of improvement

Dives were terminated early in three of the five dive sites (Navy Board Inlet, Scott Inlet, Cape Dyer) due to electrical shortages causing visual black-out, hydraulic failure, mechanical failure, or a combination of two or more factors. In the case of SuMo, infrequent use and associated maintenance, combined with overdue upgrades are the source of the failures previously stated; the ROV team aboard (Vincent Auger and Peter Lockhart, Canadian Scientific Submersible Facility) will submit detailed recommendations. Considering the logistics and resources required to conduct ROV surveys, maximizing chances of success is paramount. Based on discussions between the ROV team and scientists aboard the 2015 expedition, sufficient time and resources should be allocated to SuMo prior to the 2016 *Amundsen* expedition.

Furthermore, it is recommended that commercial fishing footprint data from Vessel Monitoring Systems be available prior to the 2016 expedition, in order to assist with dive sites selection. The addition of these data will help to focus the ROV dives in areas that have not been impacted by bottom-contact fishing gear (e.g. Cape Dyer).

39 Stratigraphic survey – Legs 4b and 4c

Project leaders: Robert Deering¹ (robert.deering@mun.ca), Trevor Bell¹ (tbell@mun.ca), Don Forbes^{1,2} (dforbes@nrcan.gc.ca), Evan Edinger¹ (eedinger@mun.ca) and Calvin Campbell² (calvin.campbell@canada.ca)

Cruise participants Leg 4b: Robert Deering¹, Jonathan Carter¹, Robbie Bennett² and Robert Murphy²

Cruise participants Leg 4c: Jonathan Carter¹

¹*Department of Geography, Memorial University of Newfoundland, St. John's, Newfoundland, A1B 3X9, Canada.*

²*Geological Survey of Canada (Atlantic), Bedford Institute of Oceanography, 1 Challenger Drive, Dartmouth, NS, B2Y 4A2, Canada.*

39.1 Introduction

Inner Frobisher Bay is an area in which marine geohazards and future infrastructure projects intersect. From extensive multibeam echosounding surveys carried out in the area aboard CCGS *Amundsen* and MV *Nulijuk* over the past two years a particular type of marine geohazard, submarine slope failures, have been found in abundance. With more than 250 of these submarine slope failure features being found in the inner bay they present a challenge to future seabed development in the region. The aim of this project was to better understand why these events occur where they do and how they are triggered, in support of future infrastructure development in the area. Given the large number of the seabed features in inner Frobisher Bay, a number of them were selected to complete more intensive work on. The focus was primarily on the Hill Island site. At this site, two large submarine slope failure features are present, both with unique characteristics meant to represent different types of slope failure found in the bay. Last year a piston core was collected from one of the lobes of the larger more complex event off of Hill Island, providing insight into the stratigraphic context in which this event occurred and constraining the date of occurrence to sometime after 5600 Cal BP. This year three piston cores were planned for the area with the main focus being on this large, complex event. The first priority was a site outside of the footprint of the slope failure feature on undisturbed seabed. This is meant to be a witness core for the cores collected inside the slope failure with an aim to better constrain dates by comparing stratigraphy. The second priority target was a site inside the toe of the secondary lobe of the complex event, with the purpose of providing a date for this second slope failure originating inside the same footprint. The third priority was from a second discrete slope failure event proximal to the complex event. As mentioned, this feature has characteristics that differ substantially from the complex event, with the purpose of this core being to provide a date of occurrence as well as insight into the stratigraphic context in which the event occurred. On top of this, box cores were to be collected at priorities 1 and 2 in order to analyze near-seabed sediments to determine how much sedimentation has occurred at these sites since the slope failure occurred.

39.2 Methodology

For piston coring methodology refer to the section on piston coring for marine geohazards research by the GSC (Section 40). Samples from box cores were collected by pushing the same plastic core liner as is used in piston coring into the sediments to extract an intact stratigraphic sequence. These push cores were then treated with the same methods as piston cores following extraction.

Two piston cores were collected at the first and second priority sites. At our first priority site (63° 38.271' N 68° 36.670' W) approximately 5 m of sediments were collected as a witness core outside the footprint of the slope failure feature in the area. At our second priority site (63° 38.386' N 68° 36.705' W) approximately 6 m of sediments were collected from the secondary lobe of the Hill Island Slide Complex. On board they were sealed with wax and packed away for shipment to the Bedford Institute of Oceanography for further analysis. They will complement the piston core collected from the primary lobe of the complex in 2014.

39.3 Preliminary results

With no analysis having been done onboard, there are no preliminary results to report..

40 GSC seabed instrumented landers – Leg 3a

ArcticNet Phase 3 – The Canadian Arctic Seabed: Navigation and Resource Mapping.
<http://www.arcticnet.ulaval.ca/pdf/phase3/seabed-mapping.pdf>

Project leaders: Edward L. King¹ (edward.king@canada.gc.ca) and Michael Li¹ (Michael.li@canada.gc.ca)

Cruise participants Leg 3a: Edward L. King¹ and Angus Robertson¹

¹*Geological Survey of Canada (Atlantic), Bedford Institute of Oceanography, 1 Challenger Drive, Dartmouth, NS, B2Y 4A2, Canada.*

40.1 Introduction

There were two main objectives to the GSC participation on *Amundsen* 2015, Leg 3a. These were directed towards goals of the University of Laval/ArcticNet seabed mapping project (Patrick Lajeunesse, lead) and the ongoing Beaufort Sea Geohazards Activity of the NRCan Public Safety Program.

The first was to perform the first seabed-situated current and related sediment behavior and the second was to utilize opportunistically collected multibeam and sub-bottom profiler acoustic data and possibly influence some site and geo-feature focused collection. These data contribute significantly towards the University of Laval ArcticNet seabed mapping project and to development of a GSC-focused shallow geologic framework which is necessary for glacial and post-glacial seabed processes and history to provide a spatial and temporal context for geohazards.

More specifically, the goal was to deploy two seabed instrumented landers to investigate bottom currents and related sediment behavior. Newly identified and mapped sediment deposition and erosion phenomena, determined from acoustic survey data, combined with indications of moderate water column current events from Golder/ArcticNet mooring data near the central Beaufort Shelf break are the rationale for the lander deployments (Figure 40-1). The placement was strongly influenced by the 2015 and historical mooring locations which can provide conditions of the full water column, into which the measured seabed currents can be placed in a broader context. This will strengthen process interpretations from the landers. The mooring data indicated winter events; this strongly influenced the GSC plan for a one-year deployment time span, thus determining a somewhat unique lander configuration. First time deepwater deployments under the sea ice and limitations of lander size, complexity and battery life necessitated a rather modest instrument package selection.

Figure 40-1 shows a preliminary map of the distribution of an erosional surface, cut into stratified glacially derived sediments, which were deposited under “rain-out” conditions, likely from distant ice streams at the mouth of Mackenzie and/or Amundsen Gulf troughs.

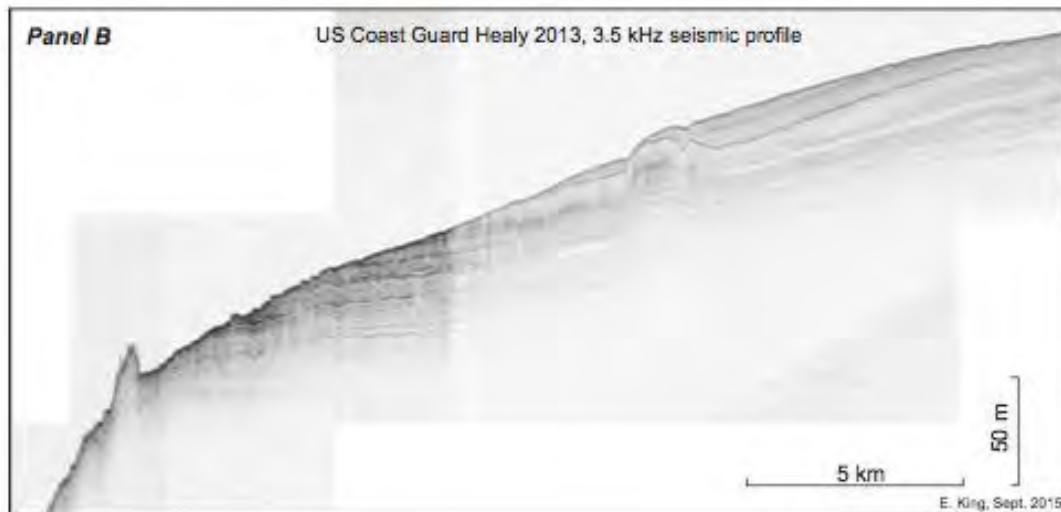
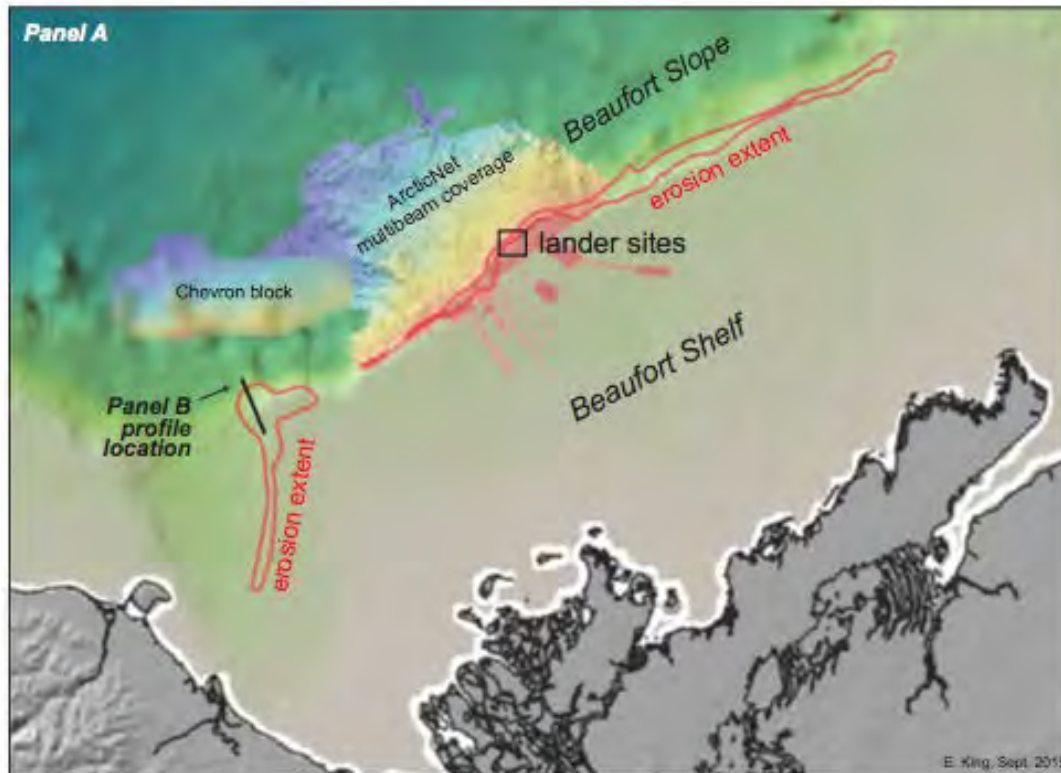


Figure 40-1. Distribution of a shelf-break band of glacial sediment erosion (Panel A). The erosion origin and age is largely unknown. Typically, several metres of the glacial plume-deposited muds were removed but at the Mackenzie Trough mouth this exceeds 40 m (Panel B). It may be the manifestation of a catastrophic event related to glacial outburst flooding. Alternatively, oceanographic current erosion, either modern or time-transgressive, beginning with sea-level low-stand processes. The lander deployments can address this by establishing present seabed conditions. Further understanding of this erosion phenomenon and the adjacent post-glacial mud distribution also has implications for Holocene age Mackenzie River sediment fate and the question of submarine avalanche ages.

40.2 Methodology

Two lander sites were selected. The aim at the shallow site was to capture outermost shelf conditions where existing AUV-collected very high-resolution multibeam coverage identified the lee and stoss deposition. This site allows a precise placement of the lander with respect to the PLFs in addition to planned further (coring) investigation of the muds to help establish conditions and long-term rates of degradation (local melting?) of the PLFs. The deeper site as nearby as possible to the existing BR-K mooring, while simultaneously sited on the erosion surface where maximum currents might be expected. The present interpretation of the erosion surface has multiple hypotheses ranging from early post-glacial current erosion under a different hydrological regime than the present, to episodic current erosion that is still maintained in the present.

Legacy data from Golder Associates-ArcticNet water column moorings near the Lander sites showed that sediment events occur seasonally, necessitating a deployment crossing fall and winter seasons. Recovery is planned for summer 2016.

40.2.1 Lander Preparation and Deployments

After discussions with the Chief Scientist, a strategy and sequence of accessing the frame and setup space was set. At several follow-up sessions (Chief Scientist, Captain, Chief Officer and deck crew) deployment techniques were agreed upon. Ship's crew built a spool stand to enable feeding the orange ½ inch poly mooring to the A-frame via the capstan. Ongoing deep mooring recoveries and deployments on the foredeck prevented immediate assembly.

On August 26th (ship's time) foredeck assembly of the tripods began and Robertson finished programming the sensors. Instruments and other components were added over the next two days and deployment commenced early evening of August 28th following a final planning/toolbox while a CTD Rosette was launched followed by a box core. The train wheel anchor was positioned under the A-frame, mooring line spool, capstan and A-frame snatch block arranged and the lander was then slowly lowered to the seabed. Under slow drift of the ship the mooring line was hand-guided and finally the end hard-eye shackled to the top of the float package. The train wheel, acoustic release, chain and floats package was then lowered to the water surface. This was released using a sea-catch after the ship reached approximately 300 m from the lander tripod site. An identical procedure was executed for the second lander deployment (deeper site), which immediately followed a box core, which was set aside for processing following lander deployment.

Unfortunately, this time it was more difficult to trace the progress of the floating line following tripod deployment (it lead under the bow) and there was some concern about drawing the line taut and tipping the tripod. The anchor package was again dropped at approximately 300 m from the tripod, but short of the planned radius mark of 400m. While completing push core / box core processing and anchor triangulation several tens of metres of floating line

were noticed on the sea surface. Discussion with the Chief Scientist the following day led to a plan of returning to the site by helicopter to first detect the orange rope and then launch the FRC and attempt to weight the line with a shackle-chain combination. A minor problem required cancellation of the flight but the FRC search and weight plan was executed despite growing wind and seas. Bridge and the FRC searching for well over an hour was unsuccessful and the rope was deemed submerged due to the current. The operation was abandoned. A further site investigation was planned for the following *Amundsen* leg and, failing success then, from the CCGS *Sir Wilfred Laurier* (Humfrey Melling, Chief Scientist, DFO-IO).

40.2.2 Instrument and Programming Specifications

Figure 40-2 shows the Landers with the 2015 deployment instruments and Figure 40-3 presents a cartoon of the seabed-situated arrangement of anchor, release, floats and tripod with groundline.

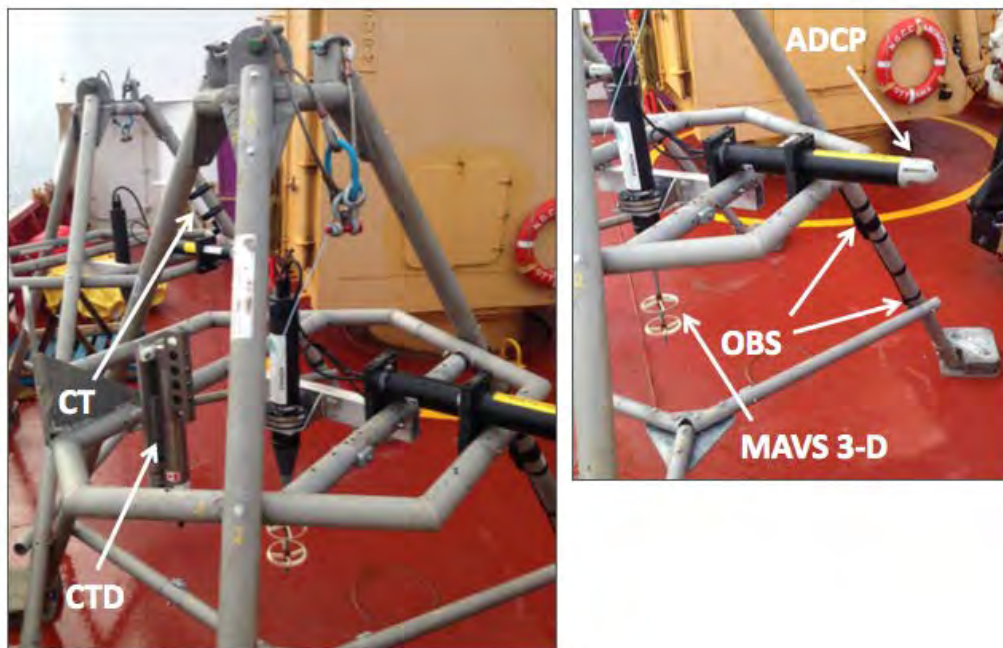


Figure 40-2. Instrumented Lander configuration aboard CCGS *Amundsen* on the 2015 expedition. The “shallow” (shelf) lander (GSC Stn. 2015804-0002) in the foreground (left) differs from the “deep” (GSC Stn. 2015804-0004) only in the later generation of the MAVS (4-D) and the plate-mounted Seabird Microcat CTD compared with a MAVS 3-D and a leg-pole-mounted RBR CT (background).

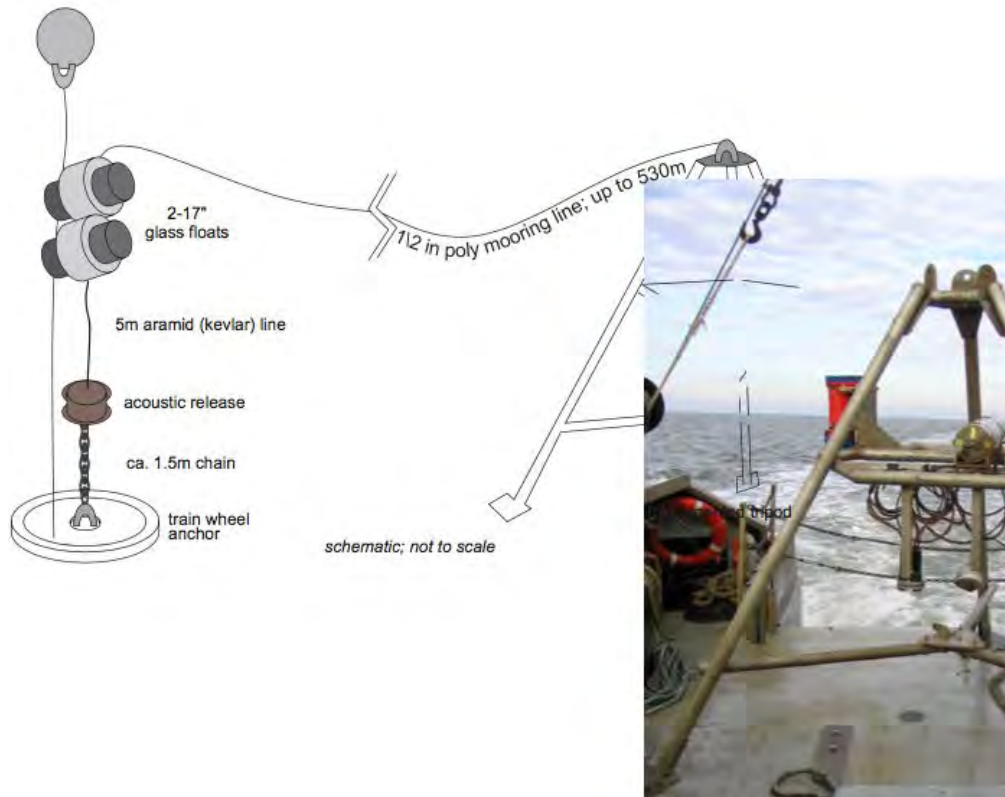


Figure 40-3. Cartoon of Lander configuration at the seabed.

First Deployment

The first lander deployment (GSC Station20158040002) was on the outermost shelf in 165 m water depth (Table 40-1). A Nobska MAVS-4D (S/N: 10292) travel time current meter was centrally located on the frame in a downward orientation with a probe height of 100 cm from the seabed. A Seapoint optical back scatterance sensor (S/N: 12774) was attached to the MAVS and secured to the inside of a leg at 100 cm height. A Nortek AquaDopp 2 MHz acoustic Doppler current profiler with right angle head and 200 m pressure transducer (S/N: AQD6706/ASP4061) was positioned horizontally looking in a downward direction at a height of 155 cm from the seabed. A D&A optical back scatterance sensor (S/N: 8524) was attached to the AquaDopp and secured to the inside of a leg at 50 cm height. A SeaBird MicroCat Conductivity/Temperature/Depth sensor (S/N: 375M40415-5341) was mounted at a height of 160 cm above the bed.

The MAVS-4D and associated OBS were programmed to run for 2.5 mins every 2.0 hrs at 2 Hz storing 300 samples. With a double lithium pack installed the MAVS-4D would run for well over a year on power and would be limited to approximately 11 months on memory. The AquaDopp and associated OBS were programmed to run for 1.0 min every 1.0hr internally averaging to log 1 profile every hour using 10 cm cells and a 20 cm blanking zone. The AquaDopp would have no memory issues running for up to 1 year and with a double

Table 40-1. Summary of GSC stations sampled during Leg 3a.

GSCA Station No.	Sample Type	ArcticNet Station No.	Day / Time (local)	Latitude (N)	Longitude (W)	Target Seismic Record		Water Depth (m)	Corer Length (cm)	App. Penn. (cm)	Core Length (cm)	No. of Sections	Comments
						Day/Time	Instrument						
un-numbered	Rosette CTD		240/1830	70°50.150	135°07.800	-	-	164	-	-	-	-	Rosette duration (sea surface to sea surface) was 10 min; stated time is deployment time. Recovery position: N 70° 50.10; W 135°07.86, W.D 171m
0001	Box Core	un-numbered	240/1858	70°50.140	135°07.830	256/1001	3.5kHz	167	-	-	-	-	GSC Box Core. 2/3 full. Sub-samples: Bulk (ca. 5 kg) and surface (one vial, 0-3 cm depth); Drop position is not corrected for A-Frame-GPS antenna offset (about 50m); water depth from ship's sounder
0001A	Push								60	40	32.0	1	GSC Push Core from 0001 (one only)
0002	Sediment Transport	Lander-2	240/2008	70°50.140	135°07.748	256/1001	3.5kHz and high res. AUV multibeam	168	-	-	-	-	Target - flat seabd area about 150 m by 150 m among pingo-like features; PLFs have lee and stoss sediment accumulation from contour currents. Drop position is not corrected for A-Frame-GPS antenna offset (about 50 m)
70°50.166				135°07.763	165			-	-	-	-	Position with approximate offset from ship's GPS antenna correction; Water depth from 2013 MBARI AUV multibeam coverage. This is final Lander position	
0002		Lander-2 anchor; from antenna	240/2017	70°50.031	135°07.889	-	-	166	-	-	-	-	Drop position; neither depth or position corrected for A-Frame-antenna offset
0002		Lander-2 anchor; from triangulation	240/2035 to 240/2050	70°50.008	135°07.789	-	-	155	-	-	-	-	Triangulation solution yielded intersections within 9 metres for anchor position. Water depth from 2013 MBARI AUV multibeam coverage.
0003	Box Core	un-numbered	240/2112	70°52.217	135°01.649	255/1017	3.5kHz	206	-	-	-	-	GSC Box Core. 2/3 full. Sub-samples: Bulk (ca. 5 kg) and surface (one vial, 0-3 cm depth); Drop position is not corrected for A-Frame-GPS antenna offset (about 50m); water depth from ship's sounder
0003A	Push								60	40	35.0	1	GSC Push Core from 0003 (one only)
0004	Sediment Transport	Lander-1	240/2151	70°52.160	135°01.127	255/1017	3.5kHz	187	-	-	-	-	Drop position is not corrected for A-Frame-GPS antenna offset (about 50m)
70°52.135				135°01.147	-	-	185	-	-	-	-	Position with approximate offset from ship's GPS antenna correction; Water depth from 2009-10 ArcticNet multibeam coverage. This is final Lander position	
0004		Lander-1 anchor; from antenna	240/2202	70°52.217	135°00.670	-	-	183	-	-	-	-	Drop position is not corrected for A-Frame-GPS antenna offset (about 50m)
0004		Lander-1 anchor; from triangulation	240/2205 to 240/2219	70°52.184	135°00.684	-	-	180	-	-	-	-	Triangulation solution yielded intersections within 6 metres for anchor position. Water depth from 2009-10 multibeam coverage.

lithium pack the estimated battery usage for this period would be approximately 21 % not including the OBS drain.

The SeaBird CTD was programmed to burst every 10 min and average four samples to log 1 measurement.

Second Deployment

The second lander deployment (GSC Station20158040004) was at the shelf break (Lander-1) while the second is located just below the shelf break in 185 m water depth (Table 40-1). Both consisted in identical frames and mooring bridle. A Nobska MAVS-3D (S/N: 10209) travel time current meter was centrally located on the frame in a downward orientation with a probe height of 100 cm from the seabed. A Seapoint optical back scatterance sensor (S/N: 11067) was attached to the MAVS and secured to the inside of a leg at 100 cm height. A Nortek AquaDopp 2 MHz acoustic Doppler current profiler with right angle head and 500 m pressure transducer (S/N: AQD2666ASP2349) was positioned horizontally looking in a downward direction at a height of 155 cm from the seabed. A D&A optical back scatterance sensor (S/N: 8148) was attached to the AquaDopp and secured to the inside of a leg at 50 cm height. A RBR Conductivity/Temperature sensor model XR-420 (S/N: 15222) was mounted at a height of 160 cm above the bed.

The MAVS-3D and associated OBS were programmed to run for 2.5 mins every 2.0 hrs at 1 Hz storing 150 samples. With a double lithium pack installed the MAVS-4D would run for well over a year on power and would be limited to approximately 11 months on memory. The AquaDopp and associated OBS were programmed to run for 1.0 min every 1.0 hr internally averaging to log 1 profile every hour using 10 cm cells and a 20 cm blanking zone. The AquaDopp would have no memory issues running for up to 1 year and with a single lithium pack the estimated battery usage for this period would be approximately 43 % not including the OBS drain. The RBR CT was programmed in burst mode and log one sample every 30 min.

40.2.3 Station Summary

Lander Instrument Locations

Table 40-1 summarizes the Lander and associated CTD and box core stations. Table 40-2 shows the triangulation coordinates and ranges from which precise location of the anchors was derived.

An overview map of the general topographic and geo-features of both landers is provided in Figure 40-4. More detailed views of each site are shown in Figure 40-5.

Table 40-2. Lander anchor (train wheel) triangulation.

Identification		Deployment time		Transducer position*				Triangulated position**		
ArcticNet Station No.	GSC Station	Acoustic Interrogator or site number	Day / Time (local)	Latitude (N)	Longitude (W)	Water Depth (m)	Slant range (m)	True range (m)	Latitude (N)	Longitude (W)
Lander-2	20158040002	1	240/2035	70°50.176	135°07.277	169	437	403	70°50.008	135°07.769
		2	240/2044	70°50.157	135°08.258	176	412	376		
		3	240/2050	70°50.357	135°07.727	179	643	621		
Lander-1	20158040004	1	240/2205	70°52.229	135°00.573	186	205	92.3	70°52.184	135°00.664
		2	240/2212	70°52.299	135°01.787	217	735	711		
		3	240/2219	70°52.034	135°01.661	187	692	667		

*interrogator transducer deployed from port foredeck forward of the A-Frame; not offset-corrected for GPS antenna

**graphically constructed from true ranges (in ArcMap)

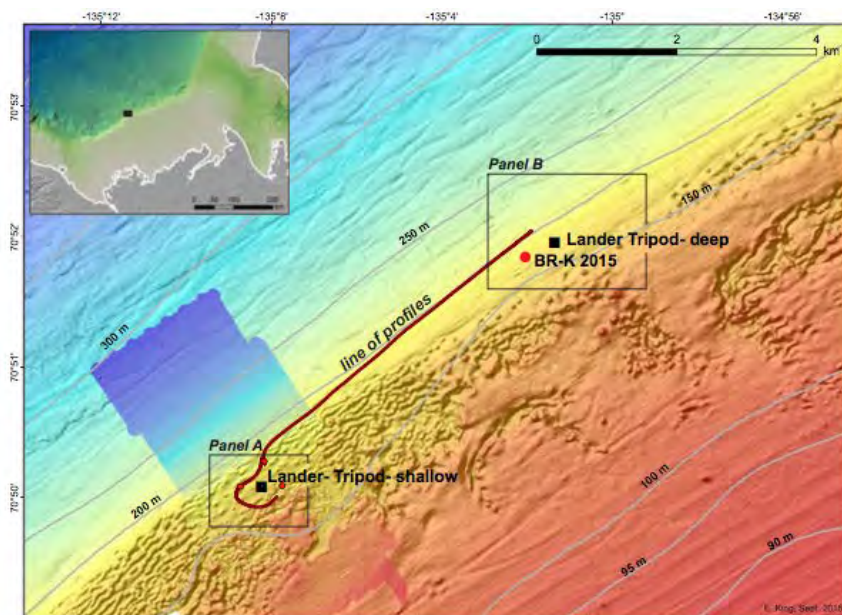


Figure 40-4. Instrumented Lander locations on the central Beaufort shelf-upper slope. Bathymetric contours shown on the multibeam bathymetric image. Placement is within the narrow contour-parallel zone of mud erosion shown in the previous illustration. Lander siting in the context of seismic profiles is shown in a following figure located along the thick brown line. An *Amundsen* 2015 - deployed water column oceanographic mooring site, BR-K, is also shown. Lander sites in Panels A and B are shown with greater detail in the following figure.

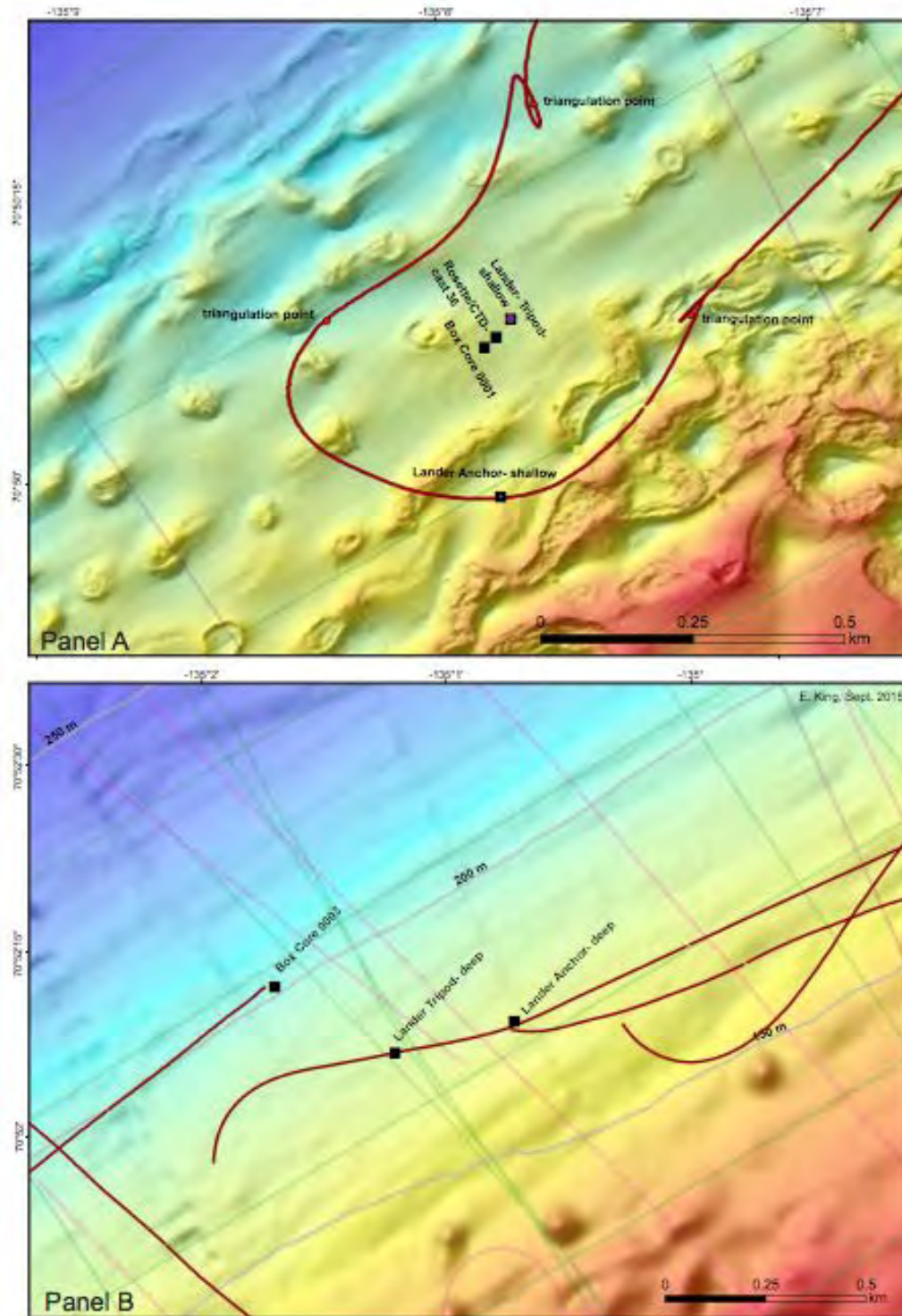


Figure 40-5. Close-up maps of Instrumented Lander locations. Subtle lines are existing 3.5 kHz sub-bottom profiler acquisitions from ArcticNet cruises. Heavier brown line is the *Amundsen* 2015 track. Panel A highlights a high-resolution Autonomous Underwater Vehicle (AUV) multibeam bathymetry rendering (courtesy C. Paull, Monterey Bay Aquarium Research Institute, MBARI). This depicts local net mud deposition (smooth) surrounding and locally overlying pingo-like features (PLFs). Placement is in "freestream" between the PLFs but locally the mounds have directed sedimentation pattern, including comet-like heads and tails manifesting the net easterly flow of the Jet. Panel B shows the much simpler topography of the uppermost slope. Anchor, CTD and box core site also shown.

A further geological sense of the sites is provided through sub-bottom profiler illustrations in Figure 40.6. The shallow site likely has more than 1 metre of post-glacial muds while the deeper lies on the erosional unconformity in glacial marine muds. Figure 40.7 is a real-time representation of the Lander at the deep site during deployment, when the tripod was visible in the water column.

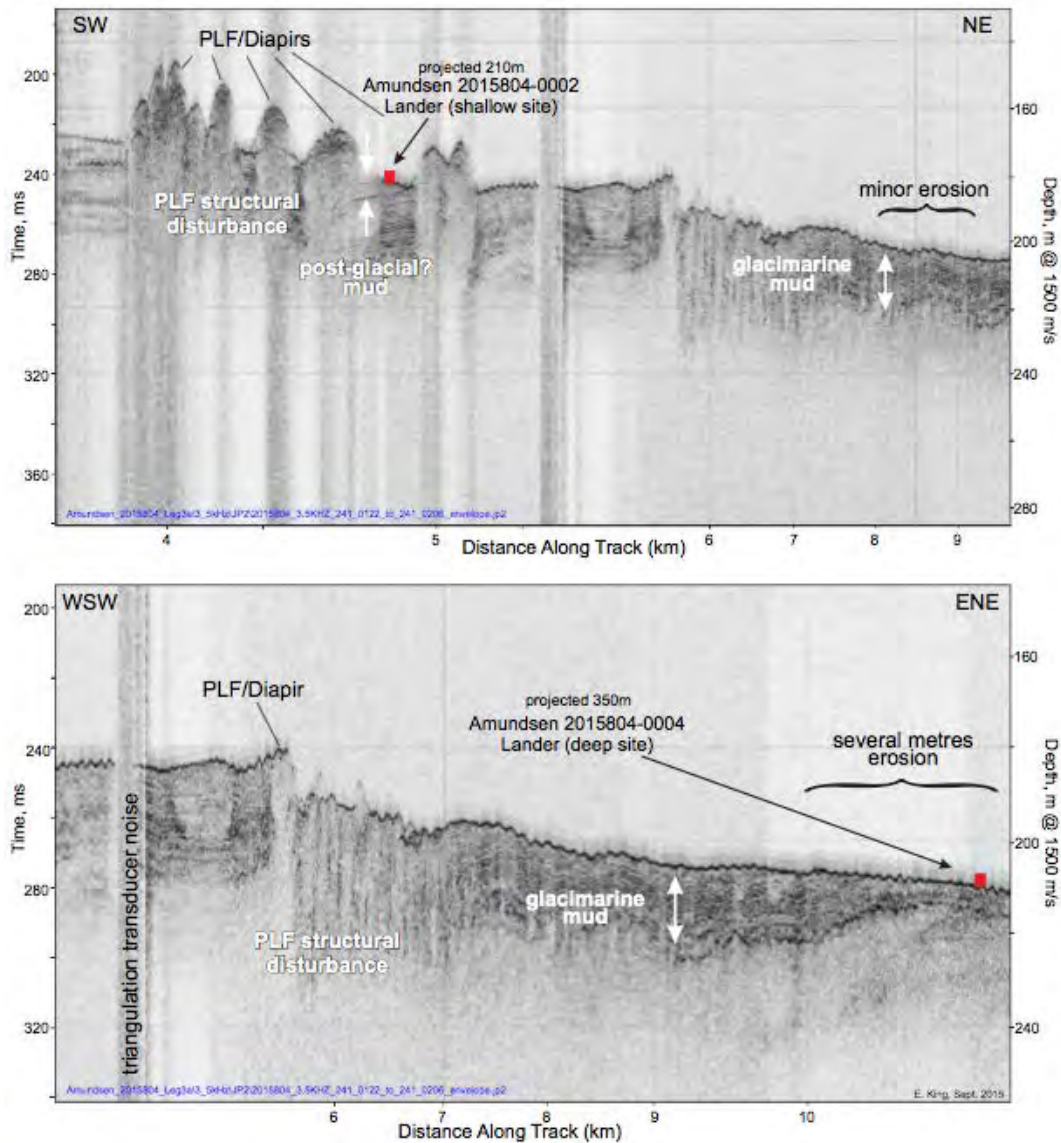


Figure 40-6. Instrumented lander locations projected on the nearest 3.5 kHz sub-bottom profile. Profile locations in the overview map (two figures previous).

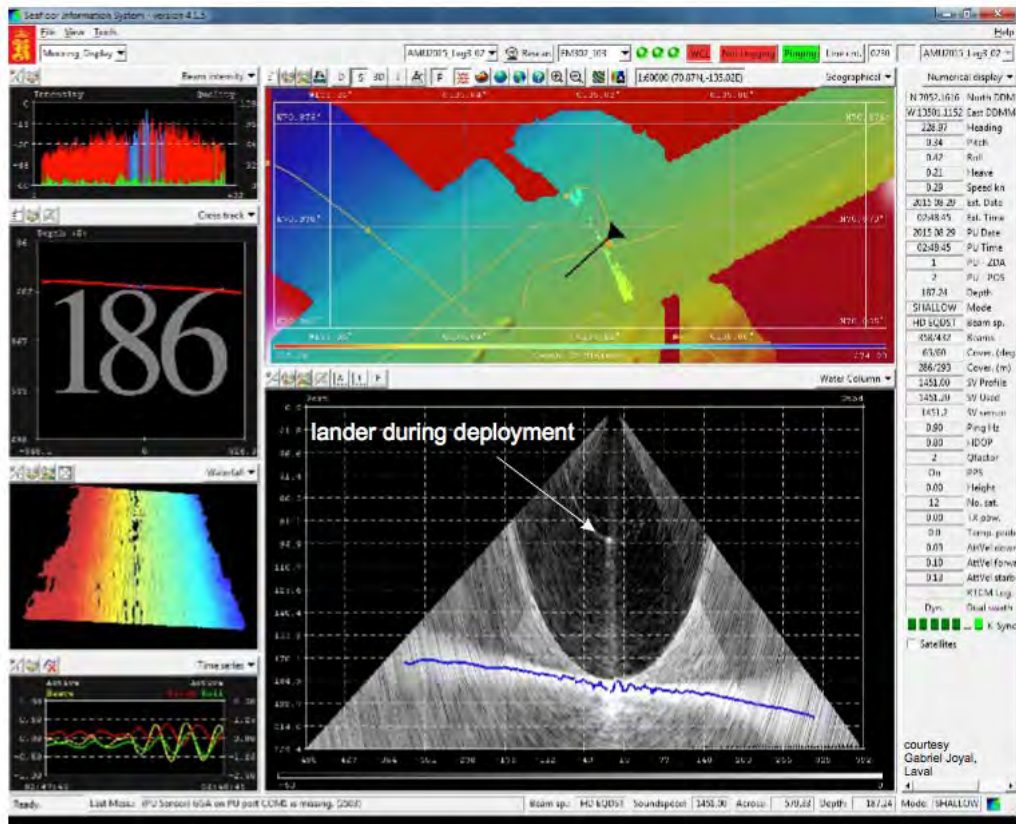


Figure 40-7. Multibeam acquisition screen during the shallow lander deployment. The lander is visible in the mid-water column.

CTD

A CTD and LADCP (lowered Acoustic Doppler Current Profile) cast (Cast 36) was conducted near the shallow lander deployment site (GSC stn. 20158040002). Figure 40.8 Figure 40.9 illustrate shipboard generated plots for the two sites. The cast from 2 days previous serves to characterize the water column at the deep site, using the 2015 Golder Associates-ArcticNet BR-K mooring cast.

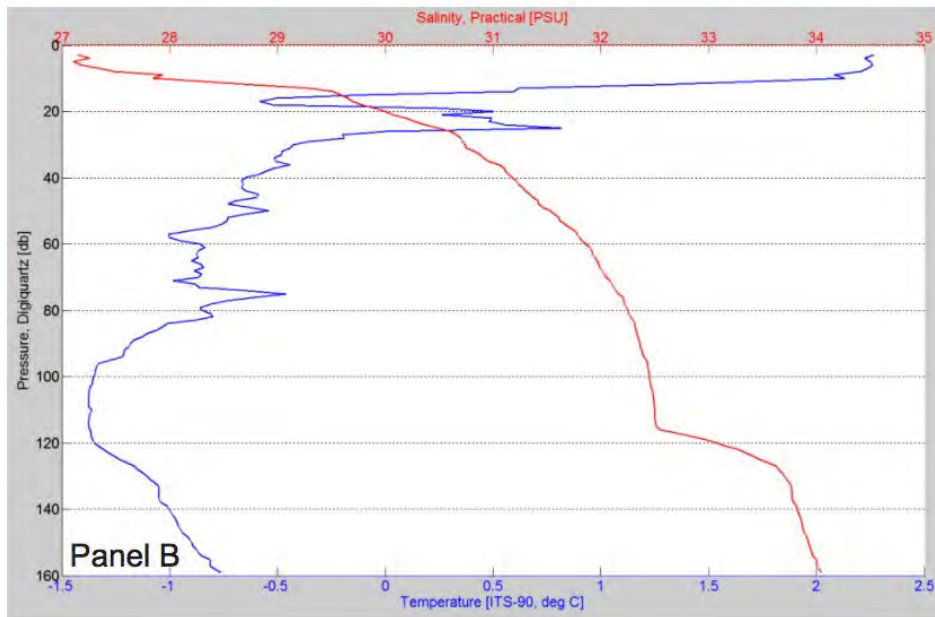
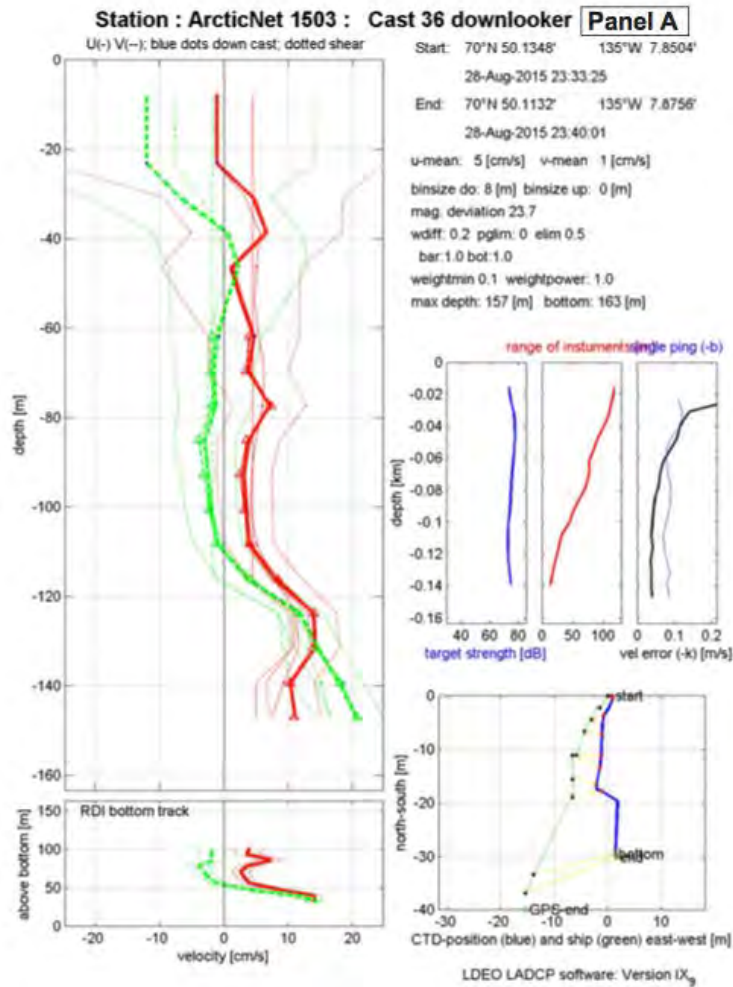


Figure 40-8. CTD and LADCP plots from nearby the shallow Lander station (20158040002). Note the distinct body below 115 m.

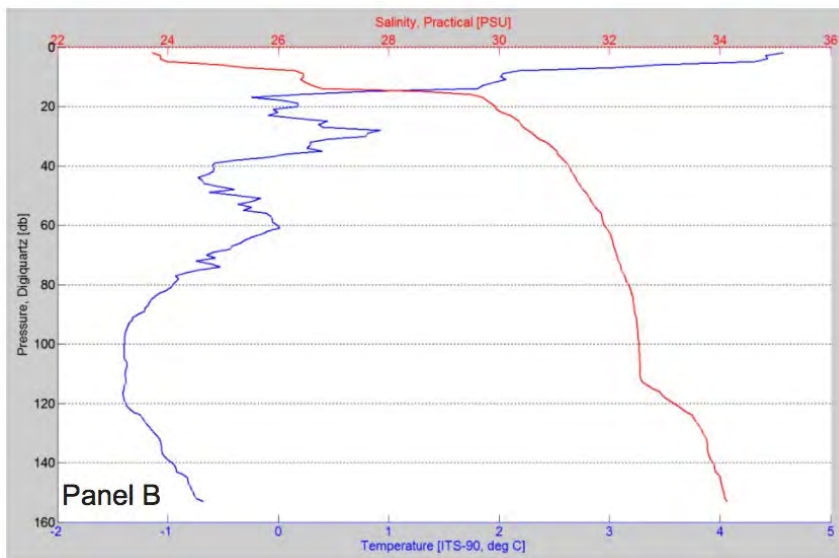
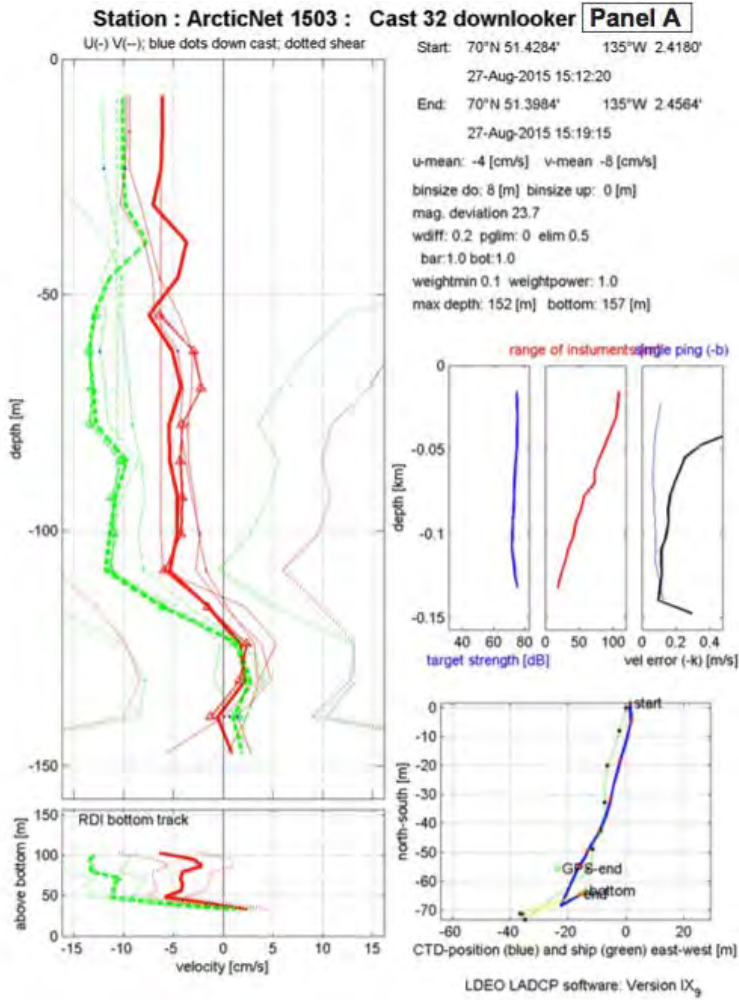


Figure 40-9. CTD and LADCP plots from mooring Site BR-K, 485m east of the deep Lander station (20158040004). Note the distinct body below 115 m.

Box cores

A box core was obtained for each Lander site to provide representative seabed grainsize, texture and sense of possible geo-historical change (GSC Stations 2015804-0001 and -0003).

Amundsen crew assisted the lead deck scientist, Christian Nozais (UQAR), on both recoveries. The box cores are taken primarily for site-specific sediment characterization for future sediment transport modelling from the collected current data. In addition, any sediment column properties related to erodability or evidence of events (such as erosion) may be distinguishable.

A push core was recovered from each box core in addition to a 75 ml vial subsample (0-3 cm depth) and a bagged bulk sample of the upper 20cm amounting to ca. 5 kg. Photographs of the seabed from the recovered box core were also collected from each box core.

Station 2015804-0001, from near the shallow Lander site, yielded an undisturbed seabed with soft brownish mud containing both epi- and in-fauna. Soft coral and brittle starfish on the surface and occasional worm-holes matched numerous filtering worms (in the mud).

Station 2015804-0003, from near the deep Lander site, also yielded an undisturbed seabed and soft coral but the sediment was largely barren below. A grey colour, homogeneous texture and structure, and high cohesivity indicate it likely sampled the targeted eroded glacial mud and little or no post-glacial sediment overlies it here. The glacial origin remains to be proven, likely through foraminiferal examination.

40.2.4 Acoustic Surveys

Formats and Archiving of Sub-bottom profiler data

NRCan, as one of the primary users and beneficiaries of the sub-bottom profiler data, has a commitment to ArcticNet for its archiving and public and scientific user availability. This is accomplished through NRCan databases and portals. Locations of the tracks and stations are available via the Expedition Database (http://ed.gdr.nrcan.gc.ca/index_e.php) via spatial or specific expedition geophysical or sample data queries while the data themselves are on FTP sites in native (generally Konsberg .keb), SEGY and Jpeg 2000 formats, organized by expedition. A SEGY version of the data, concatenated into 24-hour (max.) survey durations (shorter where survey time gaps exist), will also be incorporated into the Polar Data Catalogue (<https://polardata.ca/pdcinput/login.ccin>), along with identifying metadata linking the box core sites to NRCan portals.

Processing of sub-bottom profiler data

The SEGY version of the 3.5 kHz data were converted to JPEG 2000 format using the GSC-Atlantic viewing tool. This has a very effective compression and fidelity as well as nominal value-added interpretation capabilities. These point and horizon interpretations are

embedded in the JP2000 files. This is a format routinely used by GSC staff and enjoys a growing international body of users. Two JP2000 formats were created; an envelope (instantaneous amplitude displaying only the positive waveform but little of the phase information) and a halfwave (though still only a positive waveform display). All four formats are archived.

The JP2 files have a simple navigation export functionality, which creates GIS shapefiles (points, lines or polyline ZMs) and hotlinks from the ESRI ArcMap package. It is this navigation, which becomes archived in the GSC Expedition Database.

Data quality is generally very good and typical of recent ArcticNet cruises. Typically, the sounder images several m to 10s of metres down to horizons representing the latest glacial or low sea-level stand but generally not below. There was only minor degradation of quality with the winds of August 27th.

40.3 Preliminary results

Findings from the lander deployments await successful recovery and data processing after summer 2016. Initial observations from the acoustic profiler and multibeam systems are presented.

40.3.1 Amundsen Gulf

In the narrows of the Dolphin and Union Strait a series of about 25 mounds of till accumulation overlying a relatively planer bedrock surface are identified on the 3.5 kHz data. Till thickness (hill height) ranges from 2 to 15m. The multibeam images indicate both flow-parallel (drumlinoid) and transverse (moraine or moraine-like) features in the size range of 100s to 1000s metres, distributed on bedrock questas and near outcrop.

The new profiler data from outer Amundsen Gulf largely builds on previous coverage, generally surveying adjacent to existing lines. Data quality are generally high, penetrating multiple stacked tills are recognized.

40.3.2 Central Beaufort outermost Shelf and Upper Slope

Sufficient multibeam and sub-bottom coverage is slowly amassing in the area immediately east of the 2009-10 multibeam mosaic (Ajurak/Pokak hydrocarbon exploration areas), near the seaward limit of the oceanographic station transect. These data identify further submarine slides and enough sub-bottom profiler data to allow some reconstruction the canyon and large submarine avalanches. Clearly an old and large sediment slide (likely pre-last glaciation) occurred here, in likeness with the area to the west.

40.3.3 M'Clure Strait Surficial Geology

The first ArcticNet sub-bottom profiler data from outer M'Clure Strait were collected on this cruise apart from a very short 2009 travers at the southern shelf break. The first ArcticNet sub-bottom profiler data from outer M'Clure Strait were collected on this cruise apart from a very short 2010 traverse at the southern shelf break. Some publically accessible 2011 US Coast Guard vessel *Healy* and 2015 *Louis St. Laurent* survey data are also available. This region would have supported a major ice stream draining a large portion of the western Archipelago during the last glacial maximum (England et al. 2009) and may have further fed grounded ice in other parts ringing the Canada Basin (Polyak et al. 2007). The acoustic profiles are characterized by a simple surficial geology; a generally well-defined Glacial Erosion Surface (GES) beneath a sediment cover ranging from 0 to 35 m.

Seismostratigraphic Units in M'Clure Stait

Initial findings show that the shallow geology (upper tens of metres) in M'Clure Strait contrasts strongly with Amundsen Gulf. Three acoustic stratigraphic units can be identified in the upper several metres of sediment in M'Clure Strait. A Glacial Erosion Surface (GES) is expressed as a very smooth horizon, broadly sculpted and often highly reflective. It is generally "acoustic basement" and interpreted as representing the erosional unconformity generated at the base of the last ice sheet. Some deposits below this are locally recognized, with moraine-like or mega-scale lineation character, highlighting the strong glacial imprint of the area. The deposit geometry includes wedges not unlike the depositional and erosional wedges ubiquitous in Amundsen Gulf, but here they are acoustically harder and far fewer.

Overlying the GES is a near ubiquitous sediment blanket which's surface is completely turbated by paleo-iceberg scouring. Only in the deepest basins, below below 690ms (ca. 520m) does the scouring abate. The basin(s) are ideal short sediment coring sites for paleo-environmental and chronological studies.

A further, somewhat enigmatic stratigraphic unit overlies both the GES and iceberg turbate. It has little or no iceberg scour on its surface. It is the thickest of the units (over 40 m) but highly variable. It is mainly comprised of muddy sediments. The stratigraphic position suggests very late stage ice flow with high discharge, possibly meltwater-related.

Outer M'Clure Strait

A very thin, ice scoured blanket covers the GES in outer M'Clure Strait. A notable exception is a constructional (hill-ridge) body about 20km across (lack of seismic coverage precludes defining its length). This is interpreted as a moraine, probably an LGM deposit or one formed immediately following the LGM.

The depth of iceberg scouring across the region shows some variability, despite a very sharp water depth transition between scoured and undisturbed. South-westernmost M'Clure

Strait, near the shelf break, for example is scoured to 520 ms (ca. 390m) fully mixing the originally stratified glacimarine mud cover. The “same” transition in the central Strait is 520 m. This regional variation in scour depth should contribute to an understanding of the nature and pattern of glacial ice retreat.

Lenticular sediment bodies located on the much steeper slope just beyond the shelf break have a vague downhill linearity (on the multibeam image) are interpreted as debris flows. These are less than 2 km across and 5 m thick, constructional.

Submarine slides (headwall scars 50 to 100m relief) and canyon-type features are now recognized across all shelf-slope transects. Some, the larger, are sediment covered and at least glacial age. A surficial scarp recently recognized on the Healy data has the potential for much more recent movement but this remains to be further studied.

Other Seabed Features in M'Clure Strait

In the central M'Clure Strait, the multibeam data revealed a paired hill-hole identical to a newly recognized phenomenon offshore northern Norway (King et al. in press). This pit, 10m deep with an associated 10m high berm on one side is excavated into both the surficial iceberg turbate and into the underlying glacial erosion surface (Figure 40-10). Its genesis is accordingly attributed to direct ice margin calving during glacial retreat whereby a tall and narrow incipient iceberg calves, impacts the seabed, and rotates up- or down-ice (base-out in this example) and scoops a large mud volume to the seabed.

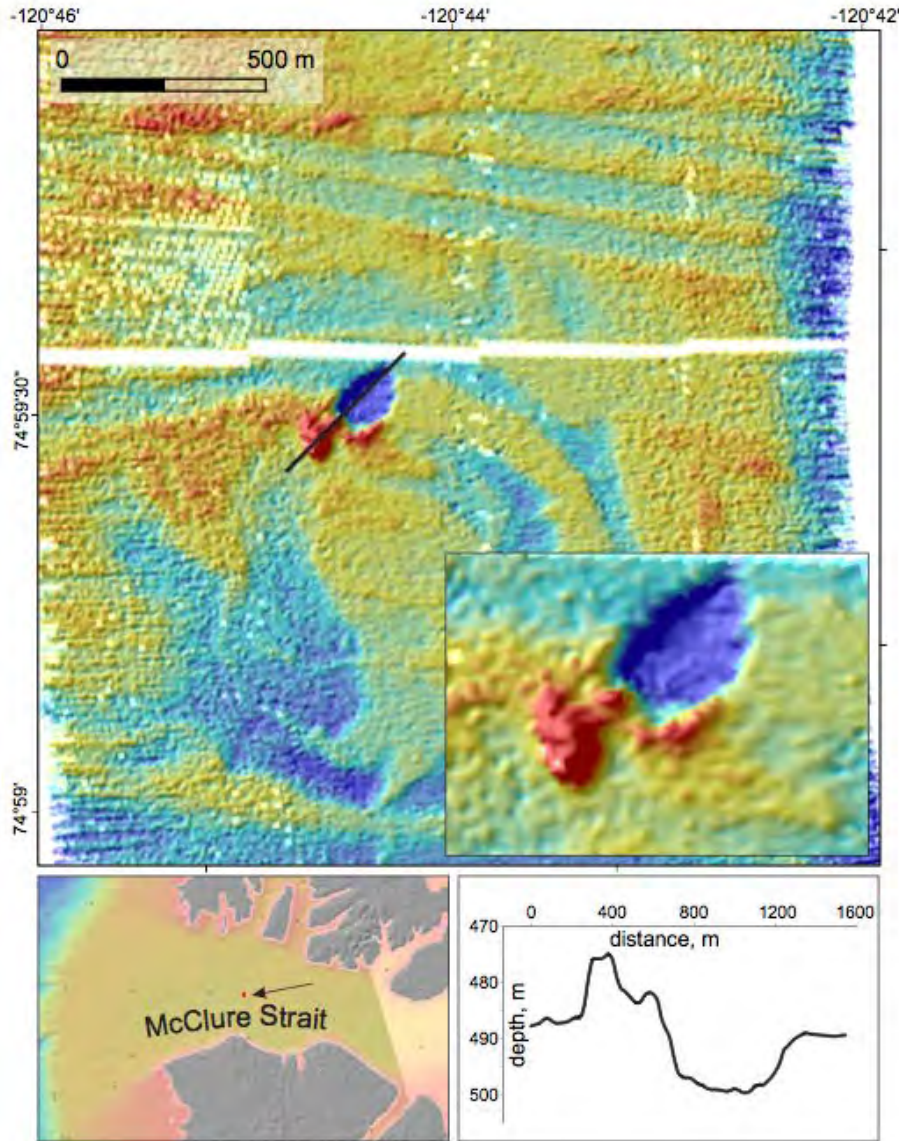


Figure 40-10. Multibeam image across a small hill-hole pair identical to newly identified features off Finnmark, Norway (King et al. in press) and in Lancaster Sound. They are attributed to an iceberg calving from the paleo-glacier's margin whereby the plunge, roll and sediment scoop excavate a large pit (blue) and hill (red) which is generally crescentic. Curvi-linear features are iceberg scours. Depth profile and location shown. Discovery and multibeam rendering, Gabriel Joyal.

A clear correlation of two rivers emerging from northernmost Banks Island and their submarine canyon equivalent into over 200 m water depth (Figure 40-11) was observed (Charles DeGrandpré and Gabriel Joyal). The single multibeam pass does not permit recognition of either a possible low-stand (since submerged) feature, or a deeper fan associated with these simple thalwegs.

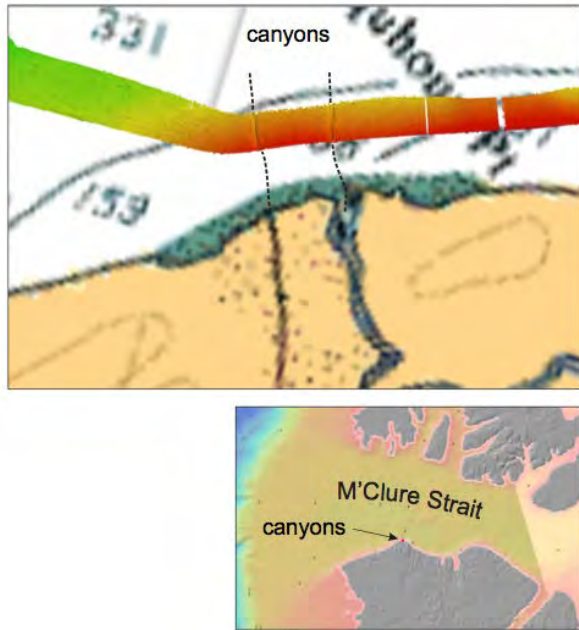


Figure 40-11. Multibeam image from northern Banks Island showing two canyons that are clearly deepwater correlatives with the rivers. Post-glacial uplift caused the river gullies and likely accelerated erosion. The paleo-shoreline is assumed to lie between the survey path and the land. Features identified by Gabriel Joyal and Charles DeGrandpre.

Summary of M'Clure Strait Surficial Geology

All the acoustic survey observations suggest a dominantly erosive ice stream filled the Strait with a very short-lived or sediment starved shelf-break duration. Glacier reconstruction has to account for this seemingly very thin (as little as 400m) ice stream ice.

The calving back to east of Banks Island was a rapid (or sediment starved) retreat, leaving a thin blanket scoured by icebergs. Evidence for fluting (and thus ice direction) has not yet been examined.

The latest, thick glacial deposits in central M'Clure Strait are somewhat enigmatic. More profile data and basic mapping is necessary. The feeding glacier may have emanated from the broad fjord-bays to the north but also possibly as flow-parallel depositional bodies from the main west-flowing ice stream. This suggests very late stage ice flow with high discharge, possibly as meltwater-rich outburst deposits.

40.3.4 Banks Island Shelf

High-resolution coverage of the Banks Island Shelf by ArcticNet has increased nearly three-fold since sparse 2006 and 2009 coverage with the 2014 and -15 surveys—almost four-fold when 2011 American Coast Guard *Healy* data are added. This enables an elevation of the shallow geological understanding immensely. Recognition of a paleo sea-level related terrace (presented at the 2014 ArcticNet conference, King et al. 2014) now has much

greater data support; far more is known of the composition and the extent is confirmed from more than coarse bathymetric data alone. Where only this and a thin surficial iceberg turbated blanket were recognized, the new data indicate substantial marine glacial sedimentation on the mid to outer bank. The source of this material is still in question, suggesting efflux of mud plumes either from adjacent ice-streams or directly from Banks Island based glaciers.

Southern Banks Island Shelf Pingo-Like Features (PLFs)

Multibeam mapping immediately west of southern Banks Island confirmed the presence of a dense network of sediment diapiric mounds, PLFs. Only single passes had been available until now and their identification was not so clear. The survey covers a small part of a long band of PDFs, extending at least 100 km westward. The westernmost are considerably higher (up to 25m) but were not surveyed systematically. They are thought to have some connection with permafrost generation during multiple low-stands across bank areas, leaving the permafrost-free bank edges for sites of gas and fluid migration with associated sediment entrainment. However, much remains to be substantiated. These cannot have survived a Late Wisconsinan ice stream in Amundsen Gulf, suggesting relatively fast growth compared to other PLF fields.

References

- J.H. England, M.F.A. Furze, J.P. Doupé. 2009. Revision of the NW Laurentide Ice Sheet: implications for paleoclimate, the northeast extremity of Beringia, and Arctic Ocean sedimentation. *Quaternary Science Reviews*, 28 1573–1596.
doi.org/10.1016/j.quascirev.2009.04.006
- King, E.L., Rise, L and Bellec, V. in press. Crescentic submarine hills and holes produced by iceberg calving and rotation. *In: Atlas of Submarine Glacial Landforms: Modern, Quaternary and Ancient*. Geological Society of London. xx-xx.
- King, E.L., Lakeman, T.R. & Blasco, S. 2014. The shallow geologic framework of the Banks Island Shelf, eastern Beaufort Sea: Evidence for glaciation of the entire shelf and multiple shelf edge geohazards. (Abstract) *Arctic Change 2014*. 8-12 December, Ottawa, ON, Canada, ESS Contribution number SST: 20140560
- Lakeman, T. R. and England J. H. 2013. Late Wisconsinan glaciation and postglacial relative sea-level change on western Banks Island, Canadian Arctic Archipelago, *Quaternary Research*, 80, 99-112, doi.org/10.1016/j.yqres.2013.02.001.
- Polyak, L., Darby, D.A., Bischof, J.F. and Jakobsson, M. 2007. Stratigraphic constraints on late Pleistocene glacial erosion and deglaciation of the Chukchi margin, Arctic Ocean. *Quaternary Research*, 67, 2, 234-245.

41 GSC piston coring: Geohazard and regional geology studies – Leg 4b

ArcticNet Phase 3 – Marine Biological Hotspots: Ecosystem Services and Susceptibility to Climate Change. <http://www.arcticnet.ulaval.ca/pdf/phase3/marine-ecosystem-services.pdf>
ArcticNet Phase 3 – The Canadian Arctic Seabed: Navigation and Resource Mapping. <http://www.arcticnet.ulaval.ca/pdf/phase3/seabed-mapping.pdf>

Project leader: Robbie Bennett¹ (Robbie.bennett@canada.ca)

Cruise participants Leg 4b: Robbie Bennett¹, Robert Murphy¹, Robert Deering², Jonathan Carter², Gabriel Joyal³ and Étienne Brouard³

¹*Geological Survey of Canada (Atlantic), Bedford Institute of Oceanography, 1 Challenger Drive, Dartmouth, NS, B2Y 4A2, Canada.*

²*Department of Geography, Memorial University of Newfoundland, St. John's, Newfoundland, A1B 3X9, Canada.*

³*Université Laval, Département de géographie, Pavillon Abitibi-Price, 2405 rue de la Terrasse, Québec, QC, G1V 0A6, Canada.*

41.1 Introduction

The objectives of piston coring operations onboard *CCGS Amundsen* during Leg 4b was to collect the longest sediment samples possible at selected piston core sites. The sites selected by the Geological Survey of Canada (GSC) for geohazard and regional geology studies are discussed in this section. See related chapters in this cruise report for information on the scientific goals for cores collected for Memorial University and Laval University projects.

41.2 Methodology

41.2.1 Equipment

The piston corer operated onboard the *Amundsen* was constructed based on blueprints of the Atlantic Geoscience Centre (AGC) Long Coring Facility (LCF) supplied by the Geologic Survey of Canada Atlantic (GSCA). The LCF system obtains a core sample with an ID of 99.2mm. The 10 ft (305cm) long barrels have an OD of 12.71 cm, wall thickness of 0.95325cm and ID of 10.8035cm. The core head is 3m long, 0.6m in diameter and weighs 1800lbs. The core head is connected to the barrel string using a "half" coupling. A maximum of 3 barrels can comprise the barrel string on the *Amundsen* due to the deck layout, and are attached to each other with external couplings. Each coupling has 16 holes drilled and tapped for 3/4" set screws which mate to the grooves on the core barrels.

Core liner, manufactured to meet GSCA specifications, is made of cellulose acetate butyrate (CAB) plastic and contains the recovered sediment. The liner has an I.D. of 9.923cm and an O.D. of 10.523cm. The liner is inserted inside the core barrels and each length is held together with clear tape.

A split piston with two O-rings and a variable orifice size is used to prevent the corer from plugging and results in greater sediment penetration and reduced sample distortion. The split piston is pinned to an Electroline eye socket termination assembly fitting on the end of the 3/4 "cable that is inserted through the core head. A core cutter (I.D. 10.008cm) houses the core catcher and serves as a replaceable nose cone for the corer. The 10-degree taper on the outside guides the cutter into the sediment. The inside bore channels the recovered sediment into the liner where it is retained during recovery. The cutter is fit over the end of the last core barrel and secured with 8 set screws.

The Trigger Weight Core (TWC) has a dual function. It acts as a trip weight and is used in conjunction with the trip arm to set the piston corer up for a predetermined free fall before sediment penetration. The corer and cable is shackled to the end of the trip arm. In addition, the TWC acts as a gravity core, which supplements the data obtained from the piston corer by collecting an undisturbed surface sample. The TWC consists of one barrel, coupling, nose cone, catcher, liner, oneway valve and weight stand. Additional lead weights (donut shaped) may be added around the weight stand. The overall weight of the TWC can vary but it is approximately 300 to 400 lbs (140 to 180 kg). The *Amundsen* TWC had a 213cm long barrel and weighed 250lbs.



Figure 41-1. Piston corer being retrieved on CCGS *Amundsen*.

41.2.2 GSC piston core sites

Two piston core sites (GSC 1 and GSC 2) were selected in Pond Inlet by the Geological Survey of Canada to investigate the paleoseismicity record of Baffin Bay. This region is one of the most seismically active areas in Canada with the largest earthquake north of the Arctic Circle being recorded ~250 km east of Pond Inlet in 1933 (magnitude = 7.3). Earthquakes have only been recorded in Canada for the past ~380 years so the only way to extend this record further into the past is by sediment cores. The evidence of large earthquakes such as the 1933 event are hypothesized to exist as sediment failures on steep slopes such as those present in Baffin Island fiords and inlets. The two cores selected by the GSC in Pond Inlet will hopefully sample sediment failures and improve the understanding of seismicity in the region over the past ~10,000 years.

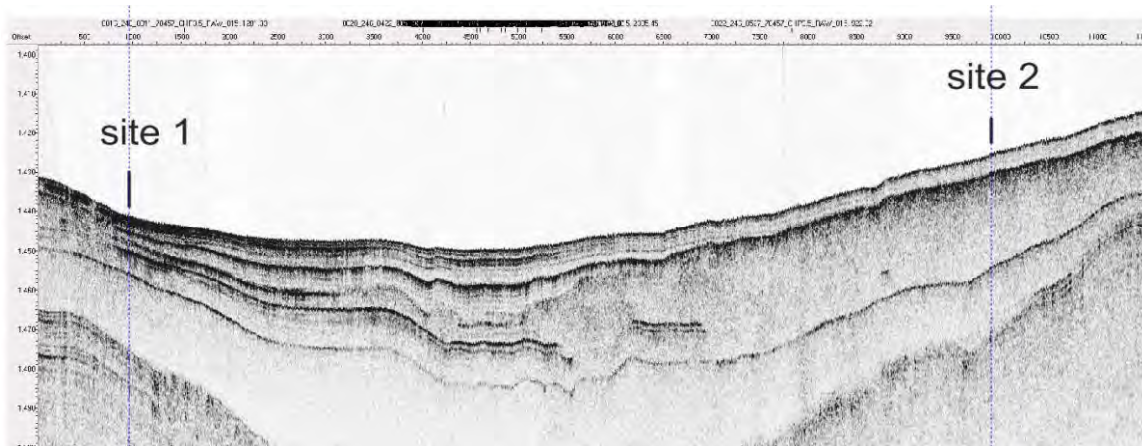


Figure 41-2. 3.5 kHz record in Pond Inlet showing the locations of the two cores collected during Leg 4b.

One other core site (GSC 3) was selected in the outer region of Clyde Trough. Prior to Leg 4b there were no core samples in the area so this core will improve the understanding of the regional geological framework of the Northeast Baffin Shelf and its troughs.

41.3 Preliminary results

Sample recovery was good to excellent considering the sediment types at the selected core locations. All of the cores were collected in areas that have been influenced by glacial sedimentation in the past and therefore the piston corer encountered very stiff silty clay or sand at most locations. These types of sediments are difficult to core as the high cohesion present in these units causes a blockage inside the barrels during the coring process, which prevents additional sediment from entering the corer. Trigger weight core performance was moderate to good considering the hard sediments of the area.

Table 41-1. Collected information for each piston core collected during Leg 4b.

Core #	Expedition #	Sample #	Latitude	Longitude	Water Depth (m)	Location
1 (GSC 1)	2015805	001	72°49.303'	77°33.072'	1058	Pond Inlet
2 (GSC 1)	2015805	002	72°49.320'	77°33.180'	1059	Pond Inlet
3 (GSC 2)	2015805	003	72°48.560'	77°16.690'	1048	Pond Inlet
4	LGM AMU 2015	1	70°42.310'	70°47.750'	781	Sam Ford Fjord
5 (GSC 3)	2015805	004	70°42.374'	67°41.421'	246	Clyde Trough
6	2015805	005	66°56.949'	62°16.636'	71	Big Nose
7	2015805	006	66°57.022'	62°17.289'	95	Big Nose
8	2015805	007	66°53.190'	61°48.560'	147	Akpait Fjord
9	2015805	008	63°38.271'	68°36.670'	125	Frobisher Bay
10	2015805	009	63°38.386'	68°36.705'	115	Frobisher Bay

41.4 Comments and recommendations

The plastic core liner used during Leg 4b was brittle and cracked often during the coring process or during cutting of the sample on deck. The life span of liner is decreased by cold weather and sunlight so care should be taken to store liner in a warm area out of direct sunlight. An inventory of liner and its age would be beneficial for future piston coring operations.

Only two core cutters (or nose cones) were present onboard during Leg 4b. One of these cutters was severely damaged but was made useable again by the engineers of the *Amundsen*. The number and condition of core cutters will need to be assessed prior to future coring operations. It is recommended that there be at least 4 cutters for expeditions similar to Leg 4b.

The jacks that are used to level the core barrels on deck are in poor shape and should be replaced or repaired. There should also be extra bolts for the trip arm (safety bolt and wire guide bolts) put with the piston core equipment for future expeditions.

42 Sediment sampling – Legs 4a, 4b and 4c

ArcticNet Phase 3 – Marine Biological Hotspots: Ecosystem Services and Susceptibility to Climate Change. <http://www.arcticnet.ulaval.ca/pdf/phase3/marine-ecosystem-services.pdf>

ArcticNet Phase 3 – The Canadian Arctic Seabed: Navigation and Resource Mapping. <http://www.arcticnet.ulaval.ca/pdf/phase3/seabed-mapping.pdf>

Project leader: Guillaume Massé¹ (guillaume.masse@takuvik.ulaval.ca)

Cruise participants Leg 4a: Caroline Guilmette¹ and Philippine Campagne^{1,2}

Cruise participants Leg 4b: Caroline Guilmette¹ and Philippine Campagne^{1,2}

Cruise participants Leg 4c: Jacques Giraudeau², Caroline Guilmette¹ and Philippine Campagne^{1,2}

¹ TAKUVIK & Université Laval, Pavillon Alexandre-Vachon, 1045 avenue de la Médecine, Québec, QC, G1V 0A6, Canada.

² EPOC, CNRS/Université de Bordeaux, Allée Geoffroy Saint-Hilaire, CS 50023, 33615 Pessac Cedex, France.

42.1 Introduction

Sediment cores collected during Leg 4a in the Qaanaaq area will be analyzed to provide quantitative and high-resolution climatic records covering the last ca. 10000 years. The data will enable a reconstruction of past changes in sea ice, climate and environment that affected, enabled or constrained past Inuit cultures. This project is in collaboration between ICE-ARC scientists and the Greenedge consortium.

Sediment cores collected during Leg 4b along the Baffin Island coast will complete the set of sediment archives collected in 2014 in the frame of the GREENEDGE project. The objective of this project was to reconstruct the evolution of primary productivity over the last few millennia in relation with past variations of seasonal ice cover in Baffin Bay.

42.2 Methodology

The selection of coring sites for Legs 4a and 4b was based on 3.5 KHz sub-bottom profiles collected during previous ArcticNet campaigns and through mapping during the present cruise with the assistance of the shipboard University Laval mapping group. Coordinates for one CASQ (CALypso SQuare) coring site were also provided by GreenEdge Danish collaborator as part of the ICE-ARC program. A total of 4 sites were selected based on sediment thickness and characteristics observed on the profiles. It was the third time that sediment sampling using the CASQ corer was done onboard the CCGS *Amundsen* following the successful attempts in 2009 during the MALINA sampling campaign.

It was decided to use a 3 section corer (total length: 9m) at two of the four selected coring sites (Table 42-1) during Legs 4a and 4b where sediment thickness was important enough, notably at Stations CASQ1 (ICE-ARC Station) and 3 (Scott Trough) in northern and western

Baffin Bay, respectively. Unfortunately, neither CASQ nor Box coring were attempted at Station CASQ2 due to time constraints (Leg 4a operations started 24 hours behind schedule due to bad weather conditions during crew and scientist shipments). A 2 hours mapping was however conducted at this location followed by a CTD at an appropriate location for future coring operation (ca. 10m sediment thickness from 3.5 Khz profile, coordinates in Table 42-1). A box core was deployed instead of the CASQ core at Station CASQ4 due to time constraints. A 2h mapping however revealed a transparent ~15 m thick layer of possibly Holocene sediment within a small depression in close vicinity to ArcticNet Station 177.

When deployed, each CASQ core was accompanied by a box core and a CTD. Prior to coring a 2hr survey took place to select the most appropriate coring sites.

In each box core, 1 large push cores (15 cm diameter) and 3 small ones (9 cm diameter) were collected, in addition to surface samples for diatoms and dinoflagellate cysts. The large push core was sampled onboard whereas the small ones were sealed and immediately stored in a cold container. For the CASQ cores, up to 6 series of large U-channels (10 cm wide) and 3 series of small U-channels (2 cm wide) were collected at up to 3 different levels along the entire length of the core. Shells, when present, were collected before U-channel sampling and placed in Whirl-pak bags for ¹⁴C dating. All U-channels were labelled, sealed and wrapped in the lab immediately after being extracted from the core, and then stored in a cold container.

Table 42-1. CTD, box and CASQ sampling stations.

Station number	Latitude (N)	Longitude (W)	Location	Water depth (m)	Sampling device	Length
CASQ1	77°17.097	074°23.214	Smith Sound	700	CTD (n°022) Boxcore CASQ	-----
	77°16.746	074°21.428		702		44.5 cm
	73°15.035	064°25.500		692		543 cm
CASQ2	77°01.037	072°08.472	Qaanak Trough	975	CTD (n°023)	-----
CASQ3	71°19.235	070°39.887	Scott trough	818	CTD (n°044) Boxcore CASQ	-----
	71°19.314	070°38.975		832		43 cm
	71°19.321	070°38.748		832		398 cm
CASQ4	67°28.531	063°47.356	Qikiqtarjuaq	379	CTD (n°051) Boxcore	-----
	67°28.980	063°39.280		689		34 cm

42.3 Comments and recommendations

The availability of the geolab for sample holding was really appreciated. We appreciated the professionalism, reactivity and availability of the Chief scientist when handling a very diverse and heavy operation schedule. The deck crew was always concerned and dedicated to ease the deck operations. The CASQ group acknowledges the support of the mapping group (G. Joyal and E. Brouard) and the scientists involved into the box core deployment (most particularly C. Grant) who greatly facilitated the site survey and operations on deck, respectively.

43 Piston coring of shoreline features – Leg 4b

ArcticNet Phase 3 – The Canadian Arctic Seabed: Navigation and Resource Mapping
<http://www.arcticnet.ulaval.ca/pdf/phase3/seabed-mapping.pdf>

Project leaders: Jonathan Carter¹ (jdhc42@mun.ca), Trevor Bell¹ (tbell@mun.ca), Don Forbes^{1,2} (dforbes@nrcan.gc.ca)

Cruise participants Leg 4b: Jonathan Carter¹, Robert Deering¹, James Bennett², Robert Murphy²

¹ *Department of Geography, Memorial University of Newfoundland, St. John's, NL, A1B 3X9, Canada.*

² *Geological Survey of Canada (Atlantic), Bedford Institute of Oceanography, 1 Challenger Drive, Dartmouth, NS, B2Y 4A2, Canada.*

43.1 Introduction

During the Last Glacial Maximum, the Laurentide Ice Sheet covered the majority of the Canadian Arctic Archipelago. As a result of this coverage, most of the archipelago is now experiencing glacio-isostatic uplift following the recession of the Laurentide. However, the Cumberland Peninsula of Baffin Island represents an exception. Situated on the margin of the archipelago, this region is outside of the zone of uplift and has been undergoing shoreline submergence instead. Therefore, a portion of this region's sea level and glacial history can only be interpreted by studying submerged features. Previous bathymetric research in the fjords of the Cumberland Peninsula has resulted in the mapping of multiple submerged deltas. The depth of these deltas increases eastwards at a clearly defined gradient of 0.35m/km, which indicates a relatively synchronous formation. Furthermore, the deltas are observed to lack deeply incised stream channels or terraces, indicating that this synchronous formation occurred during a period of sea-level stability, such as a postglacial lowstand.

The objective of this study was to determine when this lowstand occurred via the radiocarbon dating of its associated features. The samples for radiocarbon analysis were acquired via piston coring. The sites originally targeted for piston coring were the Boas, Big Nose, and Akpait fjords; however, the Boas fjord site had to be cut due to scheduling issues. At the Big Nose site, the bottomset beds of a submerged delta were targeted. Future work on this sediment sample will include the extraction of organic deposits for dating, as well as grain size analysis. At Akpait fjord, the target was a basin up-valley from a sedimentary sill. This basin was targeted in order to obtain a stratigraphic record for interpretation of local conditions prevalent during the lowstand.

43.2 Methodology

For a description of the piston coring operations, see the Methodology section of the report submitted by the Geological Survey of Canada (Section 40).

In regards to the project, a total of three samples were collected from Big Nose and Akpait fjords on October 22 2015, as described in Table 43-1. The initial piston coring attempt at Big Nose fjord (2015805-005) only recovered a very small sample of sand instead of a complete core. This sand sample was bagged, and piston coring was reattempted at a new position. Following piston core extraction, the core samples were sealed and placed in storage for further analysis at the Bedford Institute of Oceanography.

Table 43-1. Locations and timings of piston core retrieval.

Area	Station	Latitude (N)	Longitude (W)	Time	Sample
Big Nose	2015805-005	66°56.949'	62°16.636'	6:19	Coring unsuccessful; 1 small sediment sample bagged.
Big Nose	2015805-006	66°57.022'	62°17.289'	7:36	Piston core.
Akpait	2015805-007	66°53.19'	61°48.56'	12:24	Piston and gravity cores.

43.3 Preliminary results

Analysis of the sediment cores is to be conducted at the Bedford Institute of Oceanography. Thus, only the initial observations of the sediment cores can currently be described; see Table 43-2 below.

Table 43-2. Physical description of recovered samples.

Station	Water depth (m)	Core length (cm)		Preliminary sediment description
		Piston	Gravity	
2015805-005	71	0	0	Sandy, and grey in colour.
2015805-006	95	244	0	Fine and grey, with a pebble deposit occurring near the bottom of the core.
2015805-007	147	501	104	Fine, grey.

44 Schools on Board – Leg 4a

Program coordinator: Michelle Watts¹ (michelle.watts@umanitoba.ca)

Cruise participants Leg 4a: Sonia Saumier, Cheryl Bailey, Tara Warkentin, Grace Osted, Elizabeth McCullum, Camille Daeninck, Carter Lang, Zoe Perkins, Alex Labelle, Gabriel Daveluy Fletcher, Cara Killiktee

¹ *Centre for Earth Observation Science, Department of Environment and Geography, Clayton H. Riddell Faculty of Environment, Earth and Resources, University of Manitoba, 460 Wallace Building, Winnipeg, MB, R3T 2N2.*

44.1 Introduction

As an outreach program of ArcticNet, a Network of Centres of Excellence of Canada that focuses on potential impacts of climate change on the North’s environment and people, Schools on Board’s Arctic Field Program takes a small team of high school students and teachers on board the CCGS *Amundsen* to experience and participate in ArcticNet’s annual scientific expedition. Over the years, the field program has taken participants in the Beaufort Sea, through the famed Northwest Passage, along Baffin Island, and through the spectacular Labrador Fjords.

44.2 Activities on board

While on board the CCGS *Amundsen*, students were involved in a variety of sampling activities and participated in a variety of lectures and workshops delivered by scientists on board (Table 44-1).

Table 44-1. Summary of Schools on board activities provided by scientists on board Leg 4a.

Name	Position/Affiliation	Activity
Philippe Archambault	Chief Scientist – Institut des sciences de la mer de Rimouski	Lecture: Climate Change Arctic Climate Change Benthic Ecosystems
Cindy Grant	Research staff Institut des sciences de la mer de Rimouski	Activity: Agassiz trawl deck operations Benthic lab work – sorting, identifying
Jacques Graudeau Philippine Campagne Caroline Guimette	Researcher/Professor - Université de Bordeaux PhD Student Researcher/Profesor – Université Laval	Lecture: CASQ Coring Activity: viewing from bridge, student helped subsample core
Gabriel Joyal	Research Associate, Université Laval	Lecture: Ocean Mapping Activity: Interpreting maps (corrections)
Patricia DeRepentigny	MSc Student – McGill University	Activity: demonstration of rosette

Name	Position/Affiliation	Activity
Juergen Zier	Professional - ArcticNet	deployment, students assisted with getting the rosette ready
Jonathan Gagnon	Research Associate, Univeristé Laval	Lecture: explanation of rosette profiles Activity: Sampling water from rosette, lab demonstration Water density tank experiment
Virginie Galindo Marjolaine Blais	University of Manitoba Institut des sciences de la mer de Rimouski	Lecture: Phytoplankton/Arctic Food Web Activity: Sampling water from rosette, filtering, measuring chlorophyl a
Anna Crawford	Carlton University	Lecture: Ice Island Research Demonstration of equipment to be deployed
Michelle Kamula	University of Manitoba	Lecture: Sediments as a record Activity: Box core sampling, sectioning of sediment core
Alexis Burt	University of Manitoba	Lecture: Contaminants in the Arctic Activity: Zooplakton tows on deck; sample sorting and identification in labs
Cyril Aubry Thibaud Dezutter Marie Parenteau	Research Staff MSc Student Research Staff Université Laval	Lecture: Zooplankton Community and Sediment Traps (T. Dezutter) Activity: Net tows on deck, sorting and identification in lab
Lantao Geng	PhD Student - Institut des sciences de la mer de Rimouski	Activity: Demonstration of processing of samples for methane. Discussion on the importance of this research.
Rebecca Steinhart	PhD Student – Memorial University	Activity: Subsampling of box core

In addition to the science, students were fully immersed in all aspects of life on the ship and were integrated with the science team. The Canadian Coast Guard crew were instrumental in providing insight on a variety of aspects of working on an icebreaker through informal discussions on the bridge regarding navigation, nature of the job, training and overall mechanical functioning of the ship. The Chief Engineer provided an in-depth tour of the engine room for all participants. Students also had the privilege of having one on one conversations with Captain Alain Gariépy while dinning with him at his table.

Appendix 1 List of Stations							
Leg	Station ID	Station Type	Local Date	Local Time	UTC to local	Latitude (N)	Longitude (W)
2	K1	Full	13/Jul/2015	23:40	UTC -4	56°07.400	053°21.692
2	---	XCTD	15/Jul/2015	18:43	UTC -4	55°25.135	052°18.303
2	---	XCTD	16/Jul/2015	04:46	UTC -4	57°17.653	053°48.958
2	---	XCTD	16/Jul/2015	10:24	UTC -4	58°21.982	054°43.850
2	---	XCTD	16/Jul/2015	15:43	UTC -4	59°25.435	055°37.905
2	LS2	Full	17/Jul/2015	02:06	UTC-4	60°26.960	056°32.643
2	LSINC	Geotrace	19/Jul/2015	22:29	UTC-4	63°57.045	060°07.183
2	BB1	Full	03/Aug/2015	03:44	UTC-4	66°51.461	059°03.789
2	BB3	Full	05/Aug/2015	05:58	UTC-4	71°21.214	065°07.015
2	BB2	Full	07/Aug/2015	04:09	UTC-4	72°45.053	066°59.980
2	CAA1	Full	09/Aug/2015	18:03	UTC-5	74°31.370	080°33.784
2	CAA2	Full	10/Aug/2015	14:52	UTC-5	74°19.132	080°29.676
2	AN323	Nutrient	11/Aug/2015	03:14	UTC-5	74°09.472	080°28.378
2	AN324	Nutrient	11/Aug/2015	05:17	UTC-5	73°58.892	080°27.980
2	CAA3	Full	11/Aug/2015	07:28	UTC-5	73°48.993	080°29.293
2	CAA5	Full	12/Aug/2015	17:15	UTC-6	74°32.353	090°47.055
2	CAA4	Full	13/Aug/2015	13:18	UTC-6	74°07.368	091°30.395
2	CAA6	Full	14/Aug/2015	15:03	UTC-6	74°45.538	097°27.305
2	---	Horizontal Net	15/Aug/2015	13:19	UTC-6	73°49.328	096°33.274
2	CAA7	Full	15/Aug/2015	16:01	UTC-6	73°40.245	096°33.822
2	AN312	Basic	17/Aug/2015	13:34	UTC-7	69°10.167	100°42.466
2	AN314	Basic	18/Aug/2015	11:56	UTC-7	68°58.190	105°27.991
3a	AN405	Basic	22/Aug/2015	17:28	UTC-5	70°36.556	123°02.153
3a	407	Full	23/Aug/2015	04:55	UTC-5	71°00.288	126°04.677
3a	CA08-15	Mooring	23/Aug/2015	15:43	UTC-5	71°00.443	126°04.737
3a	437	Basic	24/Aug/2015	06:00	UTC-5	71°48.181	126°29.774
3a	410	Nutrient	24/Aug/2015	12:06	UTC-5	71°41.000	126°29.000
3a	411	CTD	24/Aug/2015	13:38	UTC-5	71°37.000	126°42.000
3a	CA05-15	Mooring	24/Aug/2015	16:00	UTC-5	71°16.774	127°32.230
3a	Glider	Glider	24/Aug/2015	19:28	UTC-5	71°20.920	126°40.330
3a	412	Nutrient	24/Aug/2015	22:09	UTC-5	71°33.830	126°55.356
3a	413	CTD	24/Aug/2015	23:39	UTC-5	71°29.739	127°07.947
3a	414	Nutrient	25/Aug/2015	00:42	UTC-5	71°25.000	127°21.000
3a	408	Full	25/Aug/2015	02:16	UTC-5	71°18.000	127°34.000
3a	417	CTD	25/Aug/2015	08:03	UTC-5	71°13.395	127°58.664
3a	418	Nutrient	25/Aug/2015	08:49	UTC-5	71°09.755	128°10.221
3a	419	CTD	25/Aug/2015	09:39	UTC-5	71°06.381	128°20.753
3a	420	Basic	25/Aug/2015	11:49	UTC-5	71°03.000	128°30.000
3a	434	Basic	26/Aug/2015	00:03	UTC-5	70°10.000	133°33.000
3a	433	CTD	26/Aug/2015	04:06	UTC-5	70°17.307	133°34.763
3a	432	Nutrient	26/Aug/2015	04:54	UTC-5	70°23.650	133°36.140
3a	BRK-14	Mooring	26/Aug/2015	09:07	UTC-5	70°51.742	135°01.037
3a	BS1-14	Mooring	26/Aug/2015	11:50	UTC-5	70°48.676	134°50.964
3a	BS2-14	Mooring	26/Aug/2015	12:50	UTC-5	70°53.000	135°05.000
3a	BRG-14	Mooring	26/Aug/2015	16:00	UTC-5	71°00.170	135°30.720
3a	423	CTD	26/Aug/2015	20:32	UTC-5	71°16.266	133°51.706
3a	424	Nutrient	26/Aug/2015	21:50	UTC-5	71°10.372	133°49.726

Leg	Station ID	Station Type	Local Date	Local Time	UTC to local	Latitude (N)	Longitude (W)
3a	435	Full	26/Aug/2015	23:41	UTC-5	71°04.756	133°37.907
3a	BRK-15	Mooring	27/Aug/2015	09:24	UTC-5	70°51.785	135°01.624
3a	BS1-14	Mooring	27/Aug/2015	11:55	UTC-5	70°48.711	134°50.835
3a	422	Nutrient	28/Aug/2015	06:30	UTC-5	71°22.810	133°52.940
3a	BRG-15	Mooring	28/Aug/2015	13:48	UTC-5	71°00.000	135°30.000
3a	BS3-14	Mooring	28/Aug/2015	16:24	UTC-5	70°55.660	135°14.030
3a	Lander 2	Lander	28/Aug/2015	19:58	UTC-5	70°50.169	135°07.754
3a	Lander 1	Lander	28/Aug/2015	21:47	UTC-5	70°52.160	135°01.112
3a	431	CTD	29/Aug/2015	01:33	UTC-5	70°29.000	133°37.000
3a	430	Nutrient	29/Aug/2015	02:24	UTC-5	70°35.000	133°38.000
3a	429	CTD	29/Aug/2015	03:21	UTC-5	70°40.000	133°39.000
3a	428	Nutrient	29/Aug/2015	04:05	UTC-5	70°47.430	133°41.240
3a	427	CTD	29/Aug/2015	05:00	UTC-5	70°52.830	133°43.080
3a	426	Nutrient	29/Aug/2015	05:46	UTC-5	70°59.060	133°44.820
3a	---	Horizontal Net	29/Aug/2015	07:12	UTC-5	71°03.530	133°39.530
3a	435	Benthos	29/Aug/2015	09:15	UTC-5	71°12.537	133°41.540
3a	421	Basic	29/Aug/2015	18:00	UTC-5	71°25.710	133°58.510
3a	BR4-14	Mooring	30/Aug/2015	20:49	UTC-5	73°13.200	127°02.828
3a	535	Full	31/Aug/2015	00:58	UTC-5	73°24.778	128°10.560
3a	BR3-14	Mooring	31/Aug/2015	12:11	UTC-5	73°24.583	129°21.608
3a	BR3-15	Mooring	31/Aug/2015	17:59	UTC-5	73°24.550	129°21.410
3a	536/BR3-15	Horizontal Net	01/Sep/2015	02:37	UTC-5	74°10.610	126°20.700
3a	SI_beacon1	Ice	01/Sep/2015	12:47	UTC-5	74°45.425	126°37.136
3a	518	Basic	01/Sep/2015	22:42	UTC-5	74°33.860	121°27.130
3a	518	Mapping	02/Sep/2015	03:45	UTC-5	74°34.450	121°26.330
3a	516	Nutrient	02/Sep/2015	06:57	UTC-5	74°49.690	120°50.290
3a	514	Basic	02/Sep/2015	09:15	UTC-5	75°06.270	120°37.410
3a	512	Nutrient	02/Sep/2015	16:50	UTC-5	75°22.580	120°33.010
3a	510	Nutrient	02/Sep/2015	18:57	UTC-5	75°38.330	120°38.360
3b	CB1	Geotrace	05/Sep/2015	13:32	UTC-5	73°51.643	129°44.595
3b	---	Mapping	06/Sep/2015	02:41	UTC-5	74°22.796	124°37.791
3b	---	MVP	06/Sep/2015	08:21	UTC-5	74°34.940	121°39.760
3b	CB2	Geotrace	08/Sep/2015	18:02	UTC-5	75°49.240	129°13.410
3b	SI_ST1	Ice	09/Sep/2015	14:00	UTC-5	76°02.580	128°42.030
3b	SI_ST2	Ice	09/Sep/2015	19:05	UTC-5	76°07.420	129°18.580
3b	SI_ST3	Ice	10/Sep/2015	12:57	UTC-5	76°21.271	129°03.733
3b	CB3	Geotrace	11/Sep/2015	14:50	UTC-5	76°58.826	140°02.739
3b	SI_contaminant	Ice	12/Sep/2015	12:04	UTC-5	77°00.150	140°05.108
3b	CB3	Pops buoy	Sep 12 2015	16:25	UTC-5	76°59.440	140°05.300
3b	CB4	Geotrace	14/Sep/2015	15:12	UTC-5	74°59.977	149°59.493
3b	CB4.1	Geotrace	16/Sep/2015	17:06	UTC-5	74°42.253	148°46.525
3b	CB4.2	Geotrace	16/Sep/2015	20:17	UTC-5	74°35.578	148°12.713
3b	407	Coring	18/Sep/2015	08:22	UTC-5	71°00.330	126°04.560
3b	314	Basic	20/Sep/2015	11:09	UTC-5	68°58.200	105°28.890
3b	QMG4	Basic	20/Sep/2015	20:19	UTC-5	68°29.000	103°25.480
3b	QMG3	Basic	21/Sep/2015	02:05	UTC-5	68°19.770	102°36.398
3b	WF1-15	Mooring	21/Sep/2015	09:06	UTC-5	68°14.490	101°48.340
3b	QMG/WF1-15	Basic	21/Sep/2015	09:47	UTC-5	68°14.540	101°47.550

Leg	Station ID	Station Type	Local Date	Local Time	UTC to local	Latitude (N)	Longitude (W)
3b	QMG2	Basic	21/Sep/2015	17:44	UTC-5	68°18.820	100°48.010
3b	QMG1	Basic	21/Sep/2015	23:02	UTC-5	68°29.630	099°53.440
3b	312	Basic	22/Sep/2015	09:01	UTC-5	69°10.330	100°41.600
3b	310	Basic	23/Sep/2015	01:41	UTC-5	71°27.411	101°16.734
3b	308 / CAA8	Geotrace	23/Sep/2015	21:36	UTC-5	74°08.320	108°50.080
3b	307	Basic	25/Sep/2015	02:52	UTC-5	74°06.675	103°07.454
3b	342	Basic	25/Sep/2015	08:49	UTC-5	74°47.670	092°46.860
3b	---	MVP	26/Sep/2015	02:38	UTC-5	74°47.208	092°11.635
3b	---	MVP	26/Sep/2015	16:00	UTC-5	75°43.000	095°49.800
3b	CAA9	Basic	26/Sep/2015	22:13	UTC-5	76°19.930	096°44.690
3b	CTD-02	CTD	27/Sep/2015	09:49	UTC-4	76°34.840	096°42.620
3b	PS1	CTD	27/Sep/2015	10:54	UTC-4	76°40.030	096°51.120
3b	PS2	CTD	27/Sep/2015	11:39	UTC-4	76°37.160	096°51.340
3b	PS3	CTD	27/Sep/2015	13:31	UTC-4	76°36.372	097°01.472
3b	PS4	CTD	27/Sep/2015	14:27	UTC-4	76°33.000	097°05.583
3b	PS4	MVP	27/Sep/2015	18:05	UTC-4	76°11.430	096°02.500
3b	PS4	MVP	28/Sep/2015	06:25	UTC-4	75°30.000	093°42.030
3b	WC01	CTD	28/Sep/2015	23:44	UTC-4	75°50.010	093°45.740
3b	WC02	CTD	29/Sep/2015	01:53	UTC-4	75°29.274	093°46.478
3b	WC03	CTD	29/Sep/2015	02:34	UTC-4	75°29.109	093°36.398
3b	WC04	CTD	29/Sep/2015	04:43	UTC-4	75°29.110	093°07.280
3b	WC05	CTD	29/Sep/2015	05:40	UTC-4	75°29.130	092°37.960
3b	WC05.5	CTD	29/Sep/2015	06:10	UTC-4	75°29.130	092°28.310
3b	WC06	CTD	29/Sep/2015	08:03	UTC-4	75°15.720	092°34.360
3b	WC07	CTD	29/Sep/2015	08:44	UTC-4	75°15.730	092°44.350
3b	WC08	CTD	29/Sep/2015	09:22	UTC-4	75°15.730	092°58.050
3b	WC09	CTD	29/Sep/2015	10:05	UTC-4	75°15.700	093°14.510
3b	WC10	CTD	29/Sep/2015	10:47	UTC-4	75°15.620	093°22.540
3b	WC11	MVP	29/Sep/2015	12:22	UTC-4	75°00.772	093°19.902
3b	WC16	CTD	29/Sep/2015	20:03	UTC-4	74°40.760	093°21.360
3b	WC17	CTD	29/Sep/2015	21:07	UTC-4	74°41.010	093°07.460
3b	WC18	CTD	29/Sep/2015	22:23	UTC-4	74°41.420	092°40.950
3b	WC19	CTD	29/Sep/2015	23:37	UTC-4	74°41.840	092°14.200
3b	WC20	CTD	30/Sep/2015	00:22	UTC-4	74°42.193	092°01.019
3b	BS01	CTD	30/Sep/2015	01:23	UTC-4	74°38.029	092°05.361
3b	BS02	CTD	30/Sep/2015	02:19	UTC-4	74°34.211	092°09.780
3b	BS03	CTD	30/Sep/2015	03:49	UTC-4	74°25.401	092°19.606
3b	BS04	CTD	30/Sep/2015	05:22	UTC-4	74°17.320	092°29.450
3b	BS05	CTD	30/Sep/2015	06:15	UTC-4	74°13.600	092°33.640
3b	BS06	CTD	30/Sep/2015	07:05	UTC-4	74°10.000	092°38.150
4a	304	Basic	03/Oct/2015	16:36	UTC-6	74°14.571	091°30.222
4a	346	Nutrient	04/Oct/2015	02:53	UTC-6	74°09.010	091°27.370
4a	343	Nutrient	04/Oct/2015	05:43	UTC-6	74°32.758	091°31.498
4a	301	Basic	04/Oct/2015	17:02	UTC-5	74°07.140	083°19.790
4a	325	Nutrient	05/Oct/2015	04:08	UTC-5	73°48.997	080°29.318
4a	324	Nutrient	05/Oct/2015	06:17	UTC-5	73°58.650	080°28.139
4a	323	Full	05/Oct/2015	08:36	UTC-5	73°09.337	080°27.667
4a	300	Nutrient	06/Oct/2015	00:12	UTC-5	74°19.040	080°29.260

Leg	Station ID	Station Type	Local Date	Local Time	UTC to local	Latitude (N)	Longitude (W)
4a	322	Nutrient	06/Oct/2015	03:03	UTC-5	74°29.620	080°32.170
4a	109	CTD	07/Oct/2015	06:07	UTC-5	76°17.368	074°06.645
4a	110	Nutrient	07/Oct/2015	07:08	UTC-5	76°17.978	072°38.699
4a	111	Basic	07/Oct/2015	08:47	UTC-5	76°18.350	073°12.980
4a	112	CTD	07/Oct/2015	15:00	UTC-5	76°18.900	072°42.160
4a	113	Nutrient	07/Oct/2015	16:07	UTC-5	76°19.290	073°13.200
4a	114	CTD	07/Oct/2015	17:43	UTC-5	76°19.510	071°47.640
4a	115	Basic	07/Oct/2015	19:13	UTC-5	76°20.070	071°12.920
4a	CASQ1	CTD	08/Oct/2015	10:08	UTC-5	77°17.091	074°23.189
4a	CASQ2	Coring	08/Oct/2015	11:16	UTC-5	77°16.751	074°21.262
4a	108	Basic	09/Oct/2015	06:53	UTC-5	76°15.963	074°36.067
4a	107	Nutrient	09/Oct/2015	15:32	UTC-5	76°16.720	074°58.100
4a	106	CTD	09/Oct/2015	17:10	UTC-5	76°18.180	075°20.200
4a	105	Basic	09/Oct/2015	18:53	UTC-5	76°17.318	075°45.237
4a	104	CTD	09/Oct/2015	23:39	UTC-5	76°20.856	076°10.342
4a	103	Nutrient	10/Oct/2015	01:52	UTC-5	76°21.420	076°33.430
4a	102	CTD	10/Oct/2015	04:12	UTC-5	76°22.285	076°59.429
4a	101	Basic	10/Oct/2015	05:53	UTC-5	76°22.095	077°22.514
4b	155	Basic	11/Oct/2015	22:37	UTC-5	76°29.198	078°45.852
4b	Navy Board	ROV	12/Oct/2015	22:58	UTC-5	73°42.885	081°07.393
4b	150	Basic	12/Oct/2015	22:31	UTC-5	72°45.011	079°56.441
4b	GSC1	Coring	13/Oct/2015	08:40	UTC-5	72°49.279	077°33.107
4b	GSC2	Coring	13/Oct/2015	14:03	UTC-5	72°48.540	077°16.650
4b	166	Nutrient	13/Oct/2015	22:07	UTC-5	72°29.422	077°43.909
4b	Sam Ford	Basic	14/Oct/2015	14:09	UTC-5	72°42.380	070°47.920
4b	170	Full	14/Oct/2015	20:33	UTC-5	71°22.811	070°04.017
4b	171	Nutrient	15/Oct/2015	04:41	UTC-5	71°30.901	069°35.357
4b	172	Nutrient	15/Oct/2015	06:53	UTC-5	71°39.470	069°08.274
4b	Scott Inlet	Coring	16/Oct/2015	22:32	UTC-5	71°30.911	070°16.724
4b	Scott Inlet	ROV	17/Oct/2015	06:12	UTC-5	71°30.978	070°16.652
4b	Scott Inlet	ROV	17/Oct/2015	11:52	UTC-5	71°30.970	070°16.660
4b	169	Nutrient	17/Oct/2015	00:03	UTC-5	71°16.380	070°31.730
4b	GSC3	Coring	18/Oct/2015	18:24	UTC-4	70°42.369	067°41.404
4b	173	Nutrient	18/Oct/2015	22:18	UTC-4	70°41.086	066°56.123
4b	176	Nutrient	18/Oct/2015	04:15	UTC-4	69°35.789	065°21.893
4b	178	Nutrient	18/Oct/2015	09:40	UTC-4	68°31.383	064°40.216
4b	177	Full	19/Oct/2015	20:27	UTC-4	67°28.560	063°47.381
4b	177	Lander	20/Oct/2015	18:26	UTC-4	67°29.144	063°48.395
4b	CASQ4	Coring	21/Oct/2015	00:10	UTC-4	67°28.940	063°39.470
4b	179	Nutrient	21/Oct/2015	04:09	UTC-4	67°26.987	061°55.425
4b	180	Basic	21/Oct/2015	05:25	UTC-4	67°28.902	061°40.035
4b	---	Argo Floats	21/Oct/2015	15:37	UTC-4	67°39.420	060°46.890
4b	181	Nutrient	21/Oct/2015	19:40	UTC-4	67°30.097	061°31.648
4b	Big Nose	Coring	22/Oct/2015	06:01	UTC-4	66°56.949	062°16.649
4b	AKPAIT	Coring	22/Oct/2015	12:20	UTC-4	66°53.190	061°48.520
4b	Cape Dyer	ROV	22/Oct/2015	12:25	UTC-4	66°24.820	059°13.200
4b	184	Nutrient	23/Oct/2015	12:30	UTC-4	65°44.420	060°36.670
4b	187	Basic	23/Oct/2015	20:52	UTC-4	64°10.988	060°23.040

Leg	Station ID	Station Type	Local Date	Local Time	UTC to local	Latitude (N)	Longitude (W)
4b	190	Nutrient	24/Oct/2015	11:18	UTC-4	62°27.669	061°55.367
4b	Frobisher Bay	Coring	25/Oct/2015	08:09	UTC-5	63°38.279	068°36.662
4b	Frobisher Bay	ROV	25/Oct/2015	12:25	UTC-5	63°38.350	068°37.520
4c	353	Nutrient	27/Oct/2015	06:33	UTC-5	61°09.299	064°50.129
4c	640	Coring	27/Oct/2015	19:21	UTC-4	58°55.609	062°09.326
4c	650	Nutrient	29/Oct/2015	07:15	UTC-4	53°47.631	055°26.376
4c	Belle Isle	Nutrient	29/Oct/2015	16:22	UTC-4	51°50.887	055°51.079
4c	Belle Isle	MVP	01/Nov/2015	10:00	UTC-5	48°39.700	068°38.800
4c	Belle Isle	MVP	01/Nov/2015	11:00	UTC-5	48°38.900	068°51.000
iBO program							
3	BR2-14	Mooring	29/Sep/2015	08:30		69°59.733	137°58.612
3	BR1-14	Mooring	29/Sep/2015	13:30		70°25.909	139°01.370
3	iBO15-BR1	Mooring	30/Sep/2015	16:30		70°25.944	139°01.235

Appendix 2: Scientif Log

Leg	Station ID	Station Type	Local Date	Local Time	UTC to local	Latitude (N)	Longitude (W)	Activity	Depth (m)	Heading (°)	Wind		Air (°C)	Water (°C)	Pr Baro	Hum (%)	Ice
											Dir	Speed					
1	sx90-001	Statoil	Apr 17 2015	22:41	UTC -5	48°35.500	069°01.100	CTD-Rosette ↓	107	161	310	21	8,3	2,16	1007,45	47	0
1	sx90-001	Statoil	Apr 17 2015	22:51	UTC -5	48°35.600	069°00.100	CTD-Rosette ↑	110	212	320	13	9,5	2,46	1007,9	49	0
1		Statoil	Apr 18 2015	13:12	UTC -5	49°19.600	064°40.120	MVP ↓	388	91	323	122	-1,4	0,29	1016,32	61	0
1		Statoil	Apr 18 2015	13:51	UTC -5	49°19.060	064°34.320	MVP ↑	364	92	327	120	-1,2	0,31	1016,49	58	0
1	sx90-002	Statoil	Apr 18 2015	18:33	UTC -5	48°52.880	063°09.950	CTD-Rosette ↓	392	79	240	2	-0,5	0,56	1016,9	70	0
1	sx90-002	Statoil	Apr 18 2015	18:55	UTC -5	48°52.670	063°09.530	CTD-Rosette ↑	795	259	220	5	0,8	0,37	1017,28	68	0
1	sx90-003	Statoil	Apr 19 2015	08:18	UTC -4	47°21.180	059°06.920	SX90 ↓	423	175	30	13	-1,4	-0,71	1020,77	64	0
1	sx90-003	Statoil	Apr 19 2015	08:22	UTC -4	47°21.200	059°06.970	CTD-Rosette ↓	422	201	30	10	-1,5	-0,75	1020,92	66	0
1	sx90-003	Statoil	Apr 19 2015	08:45	UTC -4	47°21.280	059°07.140	CTD-Rosette ↑	425	185	30	13	-0,3	-0,72	1021,12	59	0
1	sx90-003	Statoil	Apr 19 2015	18:30	UTC -3.5	46°39.690	056°22.980	SX90 ↑	108	110	330	18	-0,1	1,23	1019,98	70	0
1	Station 1	Statoil	Apr 22 2015	14:10	UTC -4	48°29.760	056°29.430	CTD-Rosette ↓	216	182	121	17	-1,5	-0,46	1015,91	91	8/10
1	Station 1	Statoil	Apr 22 2015	14:17	UTC -4	48°29.670	056°29.300	CTD-Rosette ↑	216	180	121	5,7	-0,1	-0,47	1015,96	87	8/10
1		Statoil	Apr 22 2015	15:10	UTC -4	48°29.470	052°30.080	Drifter 1	216	113	141	-1,2	-1,2	-0,52	1015,42	91	8/10
1		Statoil	Apr 22 2015	15:14	UTC -4	48°29.420	052°30.020	Drifter 2	216	84	141	15,5	-1,2	-0,52	1015,42	91	8/10
1		Statoil	Apr 22 2015	16:32	UTC -4	48°28.590	052°23.300	SX90 ↓	206	144	333	15	-1,6	-0,49	1015,03	96	3/10
1	Station 2	Statoil	Apr 22 2015	16:37	UTC -4	48°28.340	052°23.120	CTD-Rosette ↓	204	134	333	15	-1,6	-0,49	1015,03	96	3/10
1	Station 2	Statoil	Apr 22 2015	16:48	UTC -4	48°28.270	052°23.180	CTD-Rosette ↑	205	200	330	14	-1,5	-0,5	1014,94	95	3/10
1		Statoil	Apr 22 2015	17:17	UTC -4	48°28.180	052°23.320	Drifter 1	213	315	340	16	-1	-0,54	1014,66	94	3/10
1		Statoil	Apr 22 2015	17:20	UTC -4	48°28.280	052°23.400	Drifter 2	224	355	340	13	-1,1	-0,55	1014,6	95	3/10
1	Mooring 1	Statoil	Apr 23 2015	10:06	UTC -4	48°59.430	051°02.080	Mooring #1	306	300	Calm	Calm	1,5	-0,75	1012,01	99	7/10
1	Mooring 1	Statoil	Apr 23 2015	11:02	UTC -4	48°59.560	051°02.200	CTD-Rosette ↓	308	250	Calm	Calm	1,1	-0,76	1011,9	99	7/10
1	Mooring 1	Statoil	Apr 23 2015	11:18	UTC -4	48°59.560	051°02.110	CTD-Rosette ↑	312	250	Calm	Calm	1,1	-0,77	1011,83	99	7/10
1	Mooring 1	Statoil	Apr 23 2015	13:20	UTC -4	49°07.790	051°12.770	Acoustic Release check	346	2	Calm	Calm	1,1	0,99	1012,21	99	10/10
1	Mooring 1	Statoil	Apr 23 2015	13:25	UTC -4	49°07.840	051°12.690	Acoustic Release check	346	21	Calm	Calm	1,2	0,95	1012,28	99	10/10
1	Station 3	Statoil	Apr 23 2015	14:49	UTC -4	49°13.500	051°16.200	SX90 ↓	338	67	Calm	Calm	1,4	-0,96	1009,95	98	8/10
1	Station 3	Statoil	Apr 23 2015	15:14	UTC -4	49°13.500	051°15.900	SX90 ↑	334	197	Calm	Calm	1,7	-0,93	1009,95	99	8/10
1	Station 3	Statoil	Apr 23 2015	16:22	UTC -4	49°13.680	051°15.030	CTD-Rosette ↓	328	4	90	3	1,2	-0,9	1012,61	99	8/10
1	Station 3	Statoil	Apr 23 2015	16:10	UTC -4	49°13.500	051°15.180	CTD-Rosette ↑	329	354	Calm	Calm	1,2	-0,9	1012,59	99	8/10
1	Station 3	Statoil	Apr 23 2015	18:47	UTC -4	49°13.390	051°13.530	Drifter 1	331	98	80	4	0,3	-0,83	1012,7	99	9/10
1	Station 4	Statoil	Apr 24 2015	10:53	UTC -4	51°27.770	051°32.630	SX90 ↓	363	38	90	10	1,6	-0,94	1018,48	99	1/10
1	Station 4	Statoil	Apr 24 2015	11:17	UTC -4	51°27.690	051°33.230	Wave Glider ↓	362	243	80	15	1,6	-0,93	1018,69	99	1/10
1	Station 4	Statoil	Apr 24 2015	13:51	UTC -4	51°27.900	051°33.740	CTD-Rosette ↓	365	280	140	17	1,3	-0,9	1016,08	99	0
1	Station 4	Statoil	Apr 24 2015	14:09	UTC -4	51°27.870	051°33.840	CTD-Rosette ↑	363	265	83	12	2,4	-0,89	1016,59	99	0
1	Station 4	Statoil	Apr 24 2015	14:44	UTC -4	51°27.840	051°34.600	CTD-Rosette ↓	371	265	83,5	11,5	1,9	-0,87	1016,64	99	0
1	Station 4	Statoil	Apr 24 2015	15:00	UTC -4	51°27.800	051°34.790	CTD-Rosette ↑	374	268	81,3	15,2	2,1	-0,86	1016,12	99	0
1	Station 4	Statoil	Apr 24 2015	15:30	UTC -4	51°27.880	051°34.570	CTD-Rosette ↓	370	284	73,1	11,3	3	-0,85	1015,9	99	0
1	Station 4	Statoil	Apr 24 2015	15:45	UTC -4	51°27.860	051°34.730	CTD-Rosette ↑	370	306	71,6	13	2,1	-0,85	1016,25	99	0
1	Station 4	Statoil	Apr 24 2015	16:18	UTC -4	51°27.910	051°34.790	CTD-Rosette ↓	369	224	63	18	0,9	-0,86	1015,95	99	0
1	Station 4	Statoil	Apr 24 2015	16:35	UTC -4	51°27.890	051°34.920	CTD-Rosette ↑	369	258	86	21	1,1	-0,85	1016,01	99	0
1	Station 4	Statoil	Apr 24 2015	17:05	UTC -4	51°28.100	051°35.250	CTD-Rosette ↓	380	254	85	19	1	-0,85	1015,79	99	0
1	Station 4	Statoil	Apr 24 2015	17:22	UTC -4	51°28.110	051°35.380	CTD-Rosette ↑	383	260	75	22	1,5	-0,86	1015,64	99	0
1		Statoil	Apr 24 2015	18:01	UTC -4	51°27.830	051°36.400	Barge ↑	384	324	91	20	0,7	-0,86	1015,26	99	0
1		Statoil	Apr 24 2015	18:14	UTC -4	51°27.740	051°36.620	SX90 ↑	388	256	74	22	0,9	-0,86	1015,37	99	0
1		Statoil	Apr 24 2015	18:50	UTC -4	51°27.120	051°37.240	Wave Glider ↑	373	332	112	18	0,7	-0,88	1015,28	99	0
1		Statoil	Apr 24 2015	19:30	UTC -4	51°28.450	051°36.480	Drifter 1	393	59	Calm	Calm	0,7	-0,89	1016,57	99	0
1		Statoil	Apr 24 2015	19:33	UTC -4	51°28.450	051°36.480	Drifter 2	392	50	Calm	Calm	0,7	-0,89	1016,57	99	0
1		Statoil	Apr 24 2015	19:53	UTC -4	51°30.210	051°33.300	Drifter (2x)	388	50	90	18	0,7	-0,87	1016,64	99	0
1		Statoil	Apr 24 2015	20:18	UTC -4	51°32.390	051°29.980	Drifter (2x)	396	45	90	18	0,8	-0,84	1016,74	99	0
1		Statoil	Apr 24 2015	20:40	UTC -4	51°34.570	051°26.460	Drifter (2x)	389	45	90	19	0,8	-0,82	1016,98	99	0

1		Statoil	Apr 25 2015	01:28	UTC -4	51°49.920	051°28.470	Multibeam	323	275	90	18	1	-0,88	1016,62	99	1/10
1	Mooring 3	Statoil	Apr 25 2015	12:55	UTC -4	51°50.090	052°30.630	Mooring # 3	322	300	72	18,3	2,6	-0,77	1016,02	99	1/10
1	Mooring 3	Statoil	Apr 25 2015	13:19	UTC -4	51°50.249	052°30.627	Triangulation # 1	430	310	75	24	2,8	-0,77	1016,07	95	1/10
1	Mooring 3	Statoil	Apr 25 2015	13:25	UTC -4	51°50.221	052°30.230	Triangulation # 2	439	66	85	27	2,7	-0,77	1016,17	94	1/10
1	Mooring 3	Statoil	Apr 25 2015	13:30	UTC -4	51°49.978	052°30.512	Triangulation # 3	450	190	85	24,8	1,9	-0,77	1015,55	98	1/10
1	Mooring 3	Statoil	Apr 25 2015	13:40	UTC -4	51°49.900	052°30.710	CTD-Rosette ↓	323	294	72	22,4	1,7	-0,76	1015,04	98	1/10
1	Mooring 3	Statoil	Apr 25 2015	13:55	UTC -4	51°49.850	052°30.820	CTD-Rosette ↑	321		79	18,4	3,6	-0,73	1014,85	91	1/10
1		Statoil	Apr 25 2015	15:46	UTC -4	51°45.420	052°36.080	SX90 ↑	334	171	69	23,1	1,3	-0,74	1012,89	99	0
1		Statoil	Apr 25 2015	17:50	UTC -4	51°38.950	052°46.020	Coring (Cancelled)	316	4	74	20,4	2,1	-0,89	1011,73	97	9/10
1		Statoil	Apr 25 2015	18:20	UTC -4	51°39.110	052°47.200	Ice Load Panel	320	180	70	22	2,1	-0,9	1012,11	96	8/10
1	Mooring 2	Statoil	Apr 26 2015	09:25	UTC -4	50°16.660	051°50.660	Mooring # 2	285	345	110	23	2,7	-0,74	1011,69	99	2/10
1	Mooring 2	Statoil	Apr 26 2015	10:00	UTC -4	50°16.760	051°50.550	CTD-Rosette ↓	285	295	110	23	2,4	-0,77	1012,01	99	2/10
1	Mooring 2	Statoil	Apr 26 2015	10:17	UTC -4	50°16.720	051°50.610	CTD-Rosette ↑	285	296	110	23	2,6	-0,76	1012,32	99	2/10
1		Statoil	Apr 26 2015	18:55	UTC -4	51°04.330	053°16.460	Ice Load Panel ↓	370	310	90	12	1,7	-1,01	1012,53	99	8/10
1		Statoil	Apr 26 2015	20:00	UTC -4	51°04.530	053°16.860	Ice Load Panel ↑	373	335	80	20	2	-1,01	1012,5	99	8/10
1		Statoil	Apr 27 2015	10:11	UTC -4	52°13.070	055°17.770	Ice Work ↓	161	120	70	17	1,6	-0,94	1015,09	96	8/10
1		Statoil	Apr 27 2015	10:48	UTC -4	51°13.010	055°18.000	Ice Work ↑	182	120	30	15	1,9	-0,89	1015,32	94	8/10
1		Statoil	Apr 27 2015	18:36	UTC -4	52°14.260	055°15.420	Coring	154	276	40	9	2,6	-1	1016,06	95	10/10
1		Statoil	Apr 28 2015	08:18	UTC -4	52°04.000	055°34.610	Coring	99	230	30	25	7,2	-1	1012,98	76	9/10
1		Statoil	Apr 28 2015	08:34	UTC -4	52°03.860	055°34.920	Coring	98	233	30	25	6,2	-0,94	1012,81	81	9/10
1	Station 10	Statoil	Apr 28 2015	18:46	UTC -4	52°00.740	055°40.780	CTD-Rosette ↓	71	233	40	17	3	-0,91	1011,73	99	10/10
1	Station 10	Statoil	Apr 28 2015	18:51	UTC -4	52°00.740	055°40.880	CTD-Rosette ↑	70	228	40	20	4	-0,88	1011,87	98	10/10
1	Station 10	Statoil	Apr 28 2015	18:57	UTC -4	52°00.740	055°40.610	SX90 ↓	70	115	30	18	3,3	-0,88	1011,7	97	10/10
1	Station 10	Statoil	Apr 28 2015	19:19	UTC -4	52°00.750	055°40.360	SX90 ↑	77	49	40	21	1,7	-0,88	1012,08	99	10/10
1		Statoil	Apr 29 2015	12:47	UTC -4	51°43.270	055°58.000	Coring	80	301	90	8	2	-0,98	1011,3	99	10/10
1		Statoil	Apr 29 2015	18:22	UTC -4	52°00.210	055°41.950	Ice Load Panel ↓	70	287	20	21	1,6	-0,92	1012,72	92	9/10
1		Statoil	Apr 29 2015	19:17	UTC -4	51°59.790	055°43.160	Ice Load Panel ↑	67	286	30	8	1,9	-0,91	1013,47	91	9/10
1		Statoil	Apr 30 2015	10:01	UTC -4	50°47.520	058°39.020	SX90 ↓	218	172	40	25	0,7	-0,2	1016,75	90	0
1	Station 13	Statoil	Apr 30 2015	13:33	UTC -4	50°12.300	059°26.720	CTD-Rosette ↓	115	235	170	25	4,4	-0,06	1016,52	74	0
1	Station 13	Statoil	Apr 30 2015	09:36	UTC -4	50°12.300	059°26.790	CTD-Rosette ↑	112	251	163	25	3,1	-0,1	1016,43	78	0
1		Statoil	Apr 30 2015	21:08	UTC -5	50°05.670	062°14.890	Wave Glider ↓	82	240	100	20	2,3	0,42	1018,7	78	0
1		Statoil	Apr 30 2015	21:00	UTC -5	50°05.610	062°14.740	SX90 ↑	76	255	100	20	2,3	0,42	1018,7	78	0
1		Statoil	Apr 30 2015	22:40	UTC -5	50°02.520	062°07.080	Multibeam (Start)	112	91	50	15	2	0,41	1018,7	79	0
1		Statoil	May 01 2015	03:35	UTC -5	50°00.100	062°05.060	Multibeam (End)	108	326	42	21	1,1	0,31	1018,56	82	0
1	Station 14	Statoil	May 01 2015	06:53	UTC -5	50°05.080	062°21.030	CTD-Rosette ↓	121	261	60	6	1,4	0,56	1019,85	80	0
1	Station 14	Statoil	May 01 2015	07:01	UTC -5	50°05.060	062°21.090	CTD-Rosette ↑	122	277	50	5	2,3	0,63	1019,78	76	0
1		Statoil	May 01 2015	07:07	UTC -5	50°05.030	062°21.140	SX90 ↓	122	293	50	5	2,3	0,63	1019,78	76	0
1		Statoil	May 01 2015	08:37	UTC -5	50°03.460	062°20.150	MVP ↓	99	270	Calm	Calm	1,1	0,5	1020	81	0
1		Statoil	May 01 2015	09:34	UTC -5	50°03.030	062°30.500	MVP ↑	126	260	Calm	Calm	1,3	0,55	1019,95	84	0
1		Statoil	May 01 2015	18:24	UTC -5	50°08.450	062°16.630	Wave Glider ↑	96	176	240	2	1,4	1,18	1017,74	87	0
1		Statoil	May 01 2015	18:22	UTC -5	50°08.450	062°16.630	SX90 ↓	96	160	240	1	1,4	1,18	1017,74	87	0
1		Statoil	May 02 2015	06:37	UTC -5	49°47.330	065°28.000	SX90 ↑	306	112	90	23	1,6	2,19	1013,27	92	0
1	Station 15	Statoil	May 02 2015	06:48	UTC -5	49°47.450	065°28.030	CTD-Rosette ↓	304	250	90	23	1,4	2,19	1013,14	95	0
1	Station 15	Statoil	May 02 2015	07:02	UTC -5	49°47.590	065°28.240	CTD-Rosette ↑	295	321	90	18	2,1	1,89	1013,6	93	0
1		Statoil	May 02 2015	09:20	UTC -5	49°40.860	065°52.670	SX90 ↓	343	244	90	10	2,3	2,04	1013,72	96	0
1		Statoil	May 02 2015	10:28	UTC -5	49°41.080	065°54.520	SX90 ↑	343	235	100	8	2,5	2,58	1013,37	98	0
1		Statoil	May 02 2015	14:10	UTC -5	49°24.460	066°50.580	Calibration Camera	288	135	58	5	2,4	2,83	1015,43	90	0
1		Statoil	May 02 2015	14:25	UTC -5	49°24.140	066°50.680	UAV	291	133	56	5	2,3	2,81	1015,43	90	0
1	Station 16	Statoil	May 02 2015	18:25	UTC -5	49°17.710	067°19.620	CTD-Rosette ↓	339	322	40	13	2,4	2,82	1015,78	91	0
1	Station 16	Statoil	May 02 2015	18:26	UTC -5	49°17.710	067°19.620	SX90 ↑	338	320	40	13	2,4	2,82	1015,78	91	0
1	Station 16	Statoil	May 02 2015	18:40	UTC -5	49°17.610	067°19.680	CTD-Rosette ↑	332	218	40	12	2,7	2,65	1015,99	90	0
1		Statoil	May 02 2015	04:31	UTC -5	48°17.580	069°22.170	SX90 ↓	325	218	60	10	3,5	4,86	1017,22	92	0
1		Statoil	May 02 2015	04:41	UTC -5	48°17.310	069°22.620	MVP ↓	327	220	50	8	4,6	4,86	1017,24	86	0
1		Statoil	May 02 2015	05:58	UTC -5	48°11.000	069°32.640	MVP ↑	185	219	350	6	2,5	4,62	1017,49	92	0

1	Station 17	Statoil	May 02 2015	17:25	UTC -5	48°09.080	069°35.550	CTD-Rosette ↓	92	318	50	8	5,3	4,71	1015,6	93	0
1	Station 17	Statoil	May 02 2015	17:31	UTC -5	48°09.060	069°35.590	CTD-Rosette ↑	87	317	60	5	6,1	5,21	1015,6	88	0
1		Statoil	May 03 2015	18:51	UTC -5	47°59.380	069°36.010	SX90 ↑	26	253	350	5	5,8	4,69	1015,58	88	0
2	K1	Full	Jul 13 2015	23:40	UTC -4	56°07.400	053°21.692	TM-Rosette ↓	3309	114	80	17	7,2	6,51	1012,6	99	0
2	K1	Full	Jul 14 2015	01:52	UTC -4	56°07.373	053°22.474	TM-Rosette ↑	3310	103	80	16	7,1	6,93	1011,82	99	0
2	K1	Full	Jul 14 2015	02:37	UTC -4	56°06.727	053°20.671	Horizontal Net Tow ↓	3312	156	70	15	7,1	7,06	1011,9	99	0
2	K1	Full	Jul 14 2015	02:50	UTC -4	56°06.282	053°20.407	Horizontal Net Tow ↑	3307	96	70	13	7	7,07	1012,06	99	0
2	K1	Full	Jul 14 2015	03:27	UTC -4	56°07.094	053°21.823	TM-Rosette ↓	3311	86	80	16	7,2	7,08	1012,01	99	0
2	K1	Full	Jul 14 2015	04:32	UTC -4	56°07.290	053°22.376	TM-Rosette ↑	3312	90	90	17	7,7	7,13	1012,2	99	0
2	K1	Full	Jul 14 2015	05:11	UTC -4	56°07.393	053°22.031	PNF ↓	3311	104	90	14	7,1	7,14	1012,95	99	0
2	K1	Full	Jul 14 2015	05:14	UTC -4	56°07.404	053°22.059	PNF ↑	3313	100	90	14	7,1	7,14	1012,95	99	0
2	K1	Full	Jul 14 2015	05:18	UTC -4	56°07.427	053°22.097	PNF ↓	3315	94	90	14	7,1	7,13	1012,56	99	0
2	K1	Full	Jul 14 2015	05:20	UTC -4	56°07.427	053°22.097	PNF ↑	3317	95	90	14	7,1	7,13	1012,56	99	0
2	K1	Full	Jul 14 2015	05:40	UTC -4	56°07.233	053°22.183	CTD-Rosette ↓	3314	89	90	14	7,1	7,14	1012,05	99	0
2	K1	Full	Jul 14 2015	06:50	UTC -4	56°07.453	053°22.622	CTD-Rosette ↑	3316	92	90	14	7,1	7,13	1012,65	99	0
2	K1	Full	Jul 14 2015	08:08	UTC -4	56°07.207	053°22.002	TM-Rosette ↓	3312	107	80	14	7,1	7,19	1014,08	99	0
2	K1	Full	Jul 14 2015	08:46	UTC -4	56°07.199	053°22.289	TM-Rosette ↑	3315	101	100	14	7,3	7,22	1014,33	99	0
2	K1	Full	Jul 14 2015	09:13	UTC -4	56°07.282	053°22.185	CTD-Rosette ↓	3313	89	90	14	7,2	7,23	1013,04	99	0
2	K1	Full	Jul 14 2015	10:53	UTC -4	56°07.647	053°22.770	CTD-Rosette ↑	3317	76	110	15	7,4	7,29	1012,08	99	0
2	K1	Full	Jul 14 2015	14:39	UTC -4	56°07.252	053°22.157	TM-Rosette ↓	3318	78	110	14	7	7,33	1012,44	99	0
2	K1	Full	Jul 14 2015	16:18	UTC -4	56°07.202	053°23.059	TM-Rosette ↑	3313	105	120	16	7,1	7,39	11012,05	99	0
2	K1	Full	Jul 14 2015	16:32	UTC -4	56°07.050	053°22.922	CTD-Rosette Geochem ↓	3313	120	120	16	7	7,42	1011,76	99	0
2	K1	Full	Jul 14 2015	17:45	UTC -4	56°07.130	053°23.560	CTD-Rosette Geochem ↑	3311	107	120	18	6,9	7,41	1011,37	99	0
2	K1	Full	Jul 14 2015	19:48	UTC -4	56°07.306	053°22.301	CTD-Rosette ↓	3313	122	130	20	6,7	7,17	1011,52	99	0
2	K1	Full	Jul 14 2015	21:19	UTC -4	56°07.659	053°22.353	CTD-Rosette ↑	3315	110	130	25	6,4	7,16	1011,66	99	0
2	---	XCTD	Jul 15 2015	18:43	UTC -4	55°25.135	052°18.303	X-CTD ↓	3211	336	130	16	6,7	6,07	1013,32	99	0
2	---	XCTD	Jul 15 2015	18:49	UTC -4	55°26.315	052°19.072	X-CTD (dropped)	3218	337	130	16	6,7	6,07	1013,45	99	0
2	---	XCTD	Jul 16 2015	04:46	UTC -4	57°17.653	053°48.958	X-CTD ↓	3376	331	125	31	7,9	7,62	1014,11	99	0
2	---	XCTD	Jul 16 2015	04:54	UTC -4	57°18.940	053°50.172	X-CTD (dropped)	3378	333	125	31	7,9	7,63	1014,18	99	0
2	---	XCTD	Jul 16 2015	10:24	UTC -4	58°21.982	054°43.850	X-CTD ↓	3377	341	140	18	8,6	7,5	1013,94	95	0
2	---	XCTD	Jul 16 2015	10:25	UTC -4	58°22.223	054°43.983	X-CTD ↓	3377	341	140	18	8,6	7,5	1013,94	95	0
2	---	XCTD	Jul 16 2015	10:32	UTC -4	58°23.180	054°44.745	X-CTD (dropped)	3382	340	140	20	8,5	7,49	1014,03	96	0
2	---	XCTD	Jul 16 2015	15:43	UTC -4	59°25.435	055°37.905	X-CTD ↓	3216	331	125	23	7,1	6,05	1013,74	98	0
2	---	XCTD	Jul 16 2015	15:49	UTC -4	59°26.555	055°38.957	X-CTD (dropped)	3229	331	125	21	7	5,97	1013,88	98	0
2	LS2	Full	Jul 17 2015	02:06	UTC -4	60°26.960	056°32.643	TM-Rosette ↓	3021	143	45	14	5,4	5,03	1016,01	99	0
2	LS2	Full	Jul 17 2015	03:07	UTC -4	60°27.366	056°32.610	TM-Rosette ↑	3021	129	9	17	5,3	5,03	1017,14	99	0
2	LS2	Full	Jul 17 2015	03:46	UTC -4	60°27.300	056°33.429	PNF + Secchi ↓	3023	128	53	18	5,2	5,11	1017,27	99	0
2	LS2	Full	Jul 17 2015	03:56	UTC -4	60°27.313	056°33.416	PNF + Secchi ↑	3022	160	62	16	5,2	5,11	1017,27	99	0
2	LS2	Full	Jul 17 2015	04:12	UTC -4	60°27.203	056°32.848	CTD-Rosette ↓	3023	112	92	14	5,2	5,1	1017,33	99	0
2	LS2	Full	Jul 17 2015	05:10	UTC -4	60°27.366	056°33.225	CTD-Rosette ↑	3021	112	100	18	5,3	5,35	1018,08	99	0
2	LS2	Full	Jul 17 2015	05:33	UTC -4	60°27.142	056°33.089	TM-Rosette ↓	3031	112	115	17	5,4	5,18	1017,94	99	0
2	LS2	Full	Jul 17 2015	06:48	UTC -4	60°27.370	056°33.799	TM-Rosette ↑	3015	102	103	13	5,5	5,25	1018,69	99	0
2	LS2	Full	Jul 17 2015	11:09	UTC -4	60°27.012	056°32.904	LVP ↓	3023	96	102	14	6,2	5,13	1018,64	99	0
2	LS2	Full	Jul 17 2015	11:37	UTC -4	60°27.012	056°32.904	LVP (Start)	705	112	70	15	6,2	5,14	1018,9	96	0
2	LS2	Full	Jul 17 2015	14:14	UTC -4	60°27.012	056°32.904	LVP (End)	122	90	15	6,3	5,19	1020,26	95	0	
2	LS2	Full	Jul 17 2015	14:50	UTC -4	60°27.654	056°32.877	LVP ↑	3020	122	90	16	6,3	5,2	1020,64	95	0
2	LS2	Full	Jul 17 2015	15:23	UTC -4	60°27.204	056°33.034	TM-Rosette ↓	3022	95	90	13	6,4	5,19	1020,81	95	0
2	LS2	Full	Jul 17 2015	16:10	UTC -4	60°27.637	056°32.049	TM-Rosette ↑	3026	149	65	10	6,3	5,17	1021,24	95	0
2	LS2	Full	Jul 17 2015	18:51	UTC -4	60°27.077	056°32.379	Horizontal Net Tow ↓	3021	318	90	10	6,7	5,19	1022,1	95	0
2	LS2	Full	Jul 17 2015	19:12	UTC -4	60°26.699	056°32.282	Horizontal Net Tow ↑	3021	115	60	10	6,5	5,2	1022,07	94	0
2	LS2	Full	Jul 17 2015	19:26	UTC -4	60°26.576	056°32.183	CTD-Rosette Geochem ↓	3025	80	60	10	6,4	5,2	1022,68	94	0
2	LS2	Full	Jul 17 2015	20:51	UTC -4	60°26.315	056°33.262	CTD-Rosette Geochem ↑	3030	324	80	11	6,5	5,21	1022,75	93	0
2	LS2	Full	Jul 17 2015	21:19	UTC -4	60°26.420	056°33.536	Vertical Net Tow ↓	3030	120	90	12	6,3	5,28	1022,71	93	0
2	LS2	Full	Jul 17 2015	22:21	UTC -4	60°26.952	056°34.400	Vertical Net Tow ↑	3030	120	90	12	6,7	5,21	1022,98	93	0

2	LS2	Full	Jul 18 2015	00:44	UTC-4	60°26.387	056°34.134	CTD-Rosette Geochem ↓	3028	317	70	6	7,7	5,15	1023,33	83	0
2	LS2	Full	Jul 18 2015	01:30	UTC-4	60°26.477	056°34.931	CTD-Rosette Geochem ↑	3022	310	calm	Calm	7,8	5,15	1023,44	81	0
2	LS2	Full	Jul 18 2015	02:52	UTC-4	60°26.994	056°33.513	LVP ↓	3024	142	0	4	8,2	5,17	1023,77	73	0
2	LS2	Full	Jul 18 2015	03:38	UTC-4	60°26.994	056°33.513	LVP (Start)	2800	140	0	6	7,7	5,13	1024,05	77	0
2	LS2	Full	Jul 18 2015	06:33	UTC-4	60°26.600	056°31.527	LVP (End)	3018	152	0	10	7,5	5,11	1024,38	79	0
2	LS2	Full	Jul 18 2015	07:41	UTC-4	60°26.648	056°31.876	LVP ↑	3018	105	5	7	7,9	5,2	1024,38	76	0
2	LS2	Full	Jul 18 2015	09:03	UTC-4	60°26.781	056°32.804	TM-Rosette ↓	3019	298	10	7	7,9	5,4	1024,23	78	0
2	LS2	Full	Jul 18 2015	09:16	UTC-4	60°26.709	056°32.972	TM-Rosette ↑	3027	306	10	10	8	5,33	1024,3	78	0
2	LS2	Full	Jul 18 2015	09:28	UTC-4	60°26.697	056°33.343	CTD-Rosette ↓	3026	316	10	12	8,1	5,28	1024,38	78	0
2	LS2	Full	Jul 18 2015	10:01	UTC-4	60°26.567	056°33.995	CTD-Rosette ↑	3027	294	10	10	8,7	5,32	1024,53	74	0
2	LS2	Full	Jul 18 2015	11:12	UTC-4	60°26.206	056°33.772	LVP ↓	3023	108	10	8	7,9	5,61	1024,61	79	0
2	LS2	Full	Jul 18 2015	12:01	UTC-4	60°26.206	056°33.772	LVP (Start)	2500	102	345	10	7,4	5,66	1024,65	86	0
2	LS2	Full	Jul 18 2015	15:49	UTC-4	60°26.208	056°34.888	LVP (End)	2500	95	340	9	7,3	6,33	1024,76	92	0
2	LS2	Full	Jul 18 2015	16:50	UTC-4	60°26.594	056°35.149	LVP ↑	3025	106	350	10	7,3	6,48	1024,57	91	0
2	LS2	Full	Jul 18 2015	17:30	UTC-4	60°26.908	056°32.969	TM-Rosette ↓	3022	115	0	8	7,1	6,7	1024,51	93	0
2	LS2	Full	Jul 18 2015	18:39	UTC-4	60°26.406	056°33.030	TM-Rosette ↑	3021	123	355	9	7	6,7	1024,41	95	0
2	LS2	Full	Jul 19 2015	01:09	UTC-4	61°43.673	056°59.720	X-CTD ↓	2679	348	330	8	3,7	6,29	1023,76	99	0
2	LS2	Full	Jul 19 2015	07:42	UTC-4	63°01.048	057°29.689	X-CTD ↓	2002	348	calm	Calm	2,3	5,92	1022,67	99	0
2	LS2	Full	Jul 19 2015	14:02	UTC-4	64°19.926	058°00.079	X-CTD ↓	873	350	295	8	3,4	5,83	1021,03	95	0
2	LS2	Full	Jul 19 2015	21:51	UTC-4	63°57.145	060°06.624	CTD-Rosette ↓	482	352	290	6	3,1	4,36	1021,29	95	0
2	LS2	Full	Jul 19 2015	22:16	UTC-4	63°57.085	060°07.031	CTD-Rosette ↑	480	360	280	6	2,9	4,23	1021,27	96	0
2	LSINC	Geotrace	Jul 19 2015	22:29	UTC-4	63°57.045	060°07.183	TM-Rosette ↓	480	5	280	6	2,9	4,21	1021,18	96	0
2	LSINC	Geotrace	Jul 19 2015	22:34	UTC-4	63°57.046	060°07.225	TM-Rosette ↑	478	15	280	7	2,9	4,21	1021,18	96	0
2	LSINC	Geotrace	Jul 19 2015	23:19	UTC-4	63°56.857	060°07.532	TM-Rosette ↓	481	17	310	7	2,8	4,3	1020,72	97	0
2	LSINC	Geotrace	Jul 19 2015	23:23	UTC-4	63°56.843	060°07.520	TM-Rosette ↑	482	19	310	6	2,8	4,3	1020,81	97	0
2	BB1	Full	Aug 03 2015	03:44	UTC-4	66°51.461	059°03.789	TM-Rosette ↓	1040	303	calm	Calm	1,2	2,64	1025,55	99	1/10
2	BB1	Full	Aug 03 2015	04:37	UTC-4	66°51.411	059°03.869	TM-Rosette ↑	1038	342	calm	Calm	1,3	2,96	1025,39	99	1/10
2	BB1	Full	Aug 03 2015	04:52	UTC-4	66°51.427	059°03.784	PNF ↓	1040	183	calm	Calm	1,6	2,96	1025,46	99	1/10
2	BB1	Full	Aug 03 2015	04:59	UTC-4	66°51.429	059°03.746	PNF ↑	1040	185	calm	Calm	1,6	2,96	1025,46	99	1/10
2	BB1	Full	Aug 03 2015	05:10	UTC-4	66°51.416	059°03.674	PNF + Geochem ↓	1038	189	calm	Calm	2	2,72	1025,49	99	1/10
2	BB1	Full	Aug 03 2015	05:56	UTC-4	66°51.299	059°02.889	PNF + Geochem ↑	1038	194	calm	Calm	2,2	2,96	1025,58	99	1/10
2	BB1	Full	Aug 03 2015	06:20	UTC-4	66°51.493	059°03.744	LVP ↓	1041	280	calm	Calm	1,9	2,86	1025,41	99	1/10
2	BB1	Full	Aug 03 2015	06:48	UTC-4	66°51.341	059°03.282	LVP (Start)	1037	240	calm	Calm	1,8	2,87	1025,35	99	1/10
2	BB1	Full	Aug 03 2015	09:15	UTC-4	66°50.529	059°02.141	LVP (End)	1028	339	calm	Calm	1,8	2,16	1025,82	99	1/10
2	BB1	Full	Aug 03 2015	09:34	UTC-4	66°50.552	059°02.170	LVP ↑	1027	341	calm	Calm	1,7	2,13	1025,87	99	1/10
2	BB1	Full	Aug 03 2015	10:00	UTC-4	66°50.723	058°59.153	Horizontal Net Tow ↓	1030	22	280	4	1,8	2,77	1025,96	99	1/10
2	BB1	Full	Aug 03 2015	10:16	UTC-4	66°50.605	058°59.597	Horizontal Net Tow ↑	1029	123	280	4	1,8	3,03	1025,98	99	1/10
2	BB1	Full	Aug 03 2015	10:53	UTC-4	66°51.441	059°03.981	CTD-Rosette ↓	1039	199	260	5	1,7	3,22	1025,94	99	1/10
2	BB1	Full	Aug 03 2015	11:56	UTC-4	66°51.691	059°05.255	CTD-Rosette ↑	1045	204	260	8	2,3	3,07	1026,03	99	1/10
2	BB1	Full	Aug 03 2015	12:40	UTC-4	66°51.467	059°04.298	TM-Rosette ↓	1041	25	260	7	2	3,25	1025,98	99	1/10
2	BB1	Full	Aug 03 2015	12:51	UTC-4	66°51.449	059°04.705	TM-Rosette ↑	1043	283	260	6	1,9	3,18	1025,98	99	1/10
2	BB1	Full	Aug 03 2015	13:12	UTC-4	66°51.481	059°03.800	LVP ↓	1039	125	260	8	2,6	3,24	1025,99	99	1/10
2	BB1	Full	Aug 03 2015	13:34	UTC-4	66°51.535	059°04.338	LVP (Start)	1040	64	260	8	2,8	3,15	1025,98	99	1/10
2	BB1	Full	Aug 03 2015	17:05	UTC-4	66°52.292	059°07.275	LVP (End)	1040	103	285	5	1,4	2,56	1025,87	99	1/10
2	BB1	Full	Aug 03 2015	17:24	UTC-4	66°52.314	059°07.089	LVP ↑	1040	230	290	4	2,3	2,13	1025,72	99	1/10
2	BB1	Full	Aug 03 2015	18:13	UTC-4	66°51.544	059°04.024	Vertical Net Tow ↓	1035	276	290	9	1,6	3,26	1025,62	99	1/10
2	BB1	Full	Aug 03 2015	18:57	UTC-4	66°51.686	059°03.715	Vertical Net Tow ↑	1035	267	290	9	1,4	3,23	1025,5	99	1/10
2	BB1	Full	Aug 03 2015	19:37	UTC-4	66°51.318	059°03.452	Geochem ↓	1030	224	290	9	1,3	3,17	1025,47	99	1/10
2	BB1	Full	Aug 03 2015	20:40	UTC-4	66°51.037	059°02.456	Geochem ↑	1030	197	290	8	1,2	3,31	1025,39	99	1/10
2	BB1	Full	Aug 04 2015	05:06	UTC-4	67°51.400	058°21.500	X-CTD ↓	337	345	0	8	2,3	4,47	1025,92	99	1/10
2	BB1	Full	Aug 04 2015	12:28	UTC-4	69°10.114	059°09.643	X-CTD ↓	1214	0	20	11	4,9	5,1	1024,31	99	1/10
2	BB1	Full	Aug 04 2015	17:29	UTC-4	70°15.500	059°31.800	X-CTD ↓	458	340	320	6	5,1	4,7	1024,3	89	1/10
2	BB1	Full	Aug 04 2015	22:05	UTC-4	71°02.429	061°43.082	X-CTD ↓	1778	295	200	8	0,9	6,34	1023,86	99	1/10
2	BB3	Full	Aug 05 2015	05:58	UTC-4	71°21.214	065°07.015	X-CTD ↓	2237	275	160	17	2,1	5,35	1021,47	99	4/10

2	BB3	Full	Aug 05 2015	07:33	UTC-4	71°22.462	066°23.418	X-CTD ↓	2165	272	140	22	3,8	5,59	1017,78	99	1/10
2	BB3	Full	Aug 05 2015	09:23	UTC-4	71°51.780	067°27.329	X-CTD ↓	1592	202	150	19	1	3,59	1015,45	99	1/10
2	BB3	Full	Aug 05 2015	14:57	UTC-4	71°15.800	068°12.020	X-CTD ↓	813	298	150	17	1,6	2,2	1011,9	97	1/10
2	BB3	Full	Aug 05 2015	16:22	UTC-4	71°24.558	068°35.929	PNF ↓	1250	260	150	15	3	3,07	1010,62	94	1/10
2	BB3	Full	Aug 05 2015	16:30	UTC-4	71°24.629	068°35.804	PNF ↑	1258	267	160	13	3,1	3,64	1010,53	94	1/10
2	BB3	Full	Aug 05 2015	16:45	UTC-4	71°24.529	068°35.737	CTD Rosette Geochem ↓	1243	153	160	16	3,3	4,04	1010,45	94	1/10
2	BB3	Full	Aug 05 2015	17:59	UTC-4	71°24.676	068°33.430	CTD Rosette Geochem ↑	1332	144	170	18	3,4	4,47	1009,67	93	1/10
2	BB3	Full	Aug 05 2015	18:46	UTC-4	71°24.532	068°35.854	TM-Rosette ↓	1247	170	170	12	4	4,53	1009,28	92	1/10
2	BB3	Full	Aug 05 2015	19:10	UTC-4	71°24.610	068°35.179	TM-Rosette ↑	1229	177	170	15	4,5	4,65	1009,07	90	1/10
2	BB3	Full	Aug 05 2015	19:34	UTC-4	71°24.577	068°36.448	LVP ↓	1232	213	180	13	4,3	4,87	1008,8	90	1/10
2	BB3	Full	Aug 05 2015	19:53	UTC-4	71°24.542	068°35.987	LVP (Start)	1241	199	160	14	4,9	4,92	1008,63	88	1/10
2	BB3	Full	Aug 05 2015	22:27	UTC-4	71°24.739	068°31.015	LVP (End)	1396	181	170	12	4,6	5,27	1007,46	91	1/10
2	BB3	Full	Aug 05 2015	22:54	UTC-4	71°24.746	068°30.627	LVP ↑	1393	234	170	12	4,3	5,31	1007,35	92	1/10
2	BB3	Full	Aug 05 2015	23:43	UTC-4	71°24.630	068°36.214	CTD-Rosette ↓	1251	176	160	9	4,5	5,72	1007,09	92	1/10
2	BB3	Full	Aug 06 2015	00:44	UTC-4	71°24.675	068°35.233	CTD-Rosette ↑	1289	178	170	11	5,3	5,8	1006,83	91	1/10
2	BB3	Full	Aug 06 2015	01:05	UTC-4	71°24.499	068°35.943	TM-Rosette ↓	1240	166	215	7	5,6	5,87	1006,91	90	1/10
2	BB3	Full	Aug 06 2015	01:16	UTC-4	71°24.463	068°35.779	TM-Rosette ↑	1238	180	260	4	6	5,74	1006,87	90	1/10
2	BB3	Full	Aug 06 2015	01:33	UTC-4	71°24.448	068°35.557	Horizontal Net Tow ↓	1245	165	260	2	6	5,55	1006,89	93	1/10
2	BB3	Full	Aug 06 2015	01:47	UTC-4	71°24.294	068°34.101	Horizontal Net Tow ↑	1280	30	280	5	6,1	5,62	1006,86	92	1/10
2	BB3	Full	Aug 06 2015	02:18	UTC-4	71°24.440	068°35.613	LVP ↓	1243	178	0	4	6,2	5,64	1006,79	95	1/10
2	BB3	Full	Aug 06 2015	02:39	UTC-4	71°24.429	068°35.356	LVP (Start)	1250	178	calm	Calm	6,9	5,63	1006,52	96	1/10
2	BB3	Full	Aug 06 2015	06:15	UTC-4	71°24.004	068°29.540	LVP (End)	1359	180	320	9	9,4	5,53	1007,71	83	1/10
2	BB3	Full	Aug 06 2015	06:34	UTC-4	71°23.907	068°28.745	LVP ↑	1370	204	320	7	6,7	5,41	1007,88	93	1/10
2	BB3	Full	Aug 06 2015	07:28	UTC-4	71°24.327	068°36.057	TM-Rosette + Incubation ↓	1212	309	330	16	5,5	5,7	1008,41	96	1/10
2	BB3	Full	Aug 06 2015	07:32	UTC-4	71°24.295	068°36.017	TM-Rosette + Incubation ↑	1210	316	330	18	5,4	5,7	1008,49	97	1/10
2	BB3	Full	Aug 06 2015	08:38	UTC-4	71°24.945	068°36.856	CTD-Rosette ↓	1283	331	330	16	5,2	5,61	1008,42	94	1/10
2	BB3	Full	Aug 06 2015	09:22	UTC-4	71°24.611	068°35.868	CTD-Rosette ↑	1261	330	320	16	5,4	5,03	1008,88	91	1/10
2	BB3	Full	Aug 06 2015	10:06	UTC-4	71°20.997	068°46.294	IKMT ↓	492	110	325	15	5,4	5,29	1009,24	92	1/10
2	BB3	Full	Aug 06 2015	11:03	UTC-4	71°20.543	068°38.024	IKMT ↑	644	60	315	15	5,2	4,85	1009,25	90	1/10
2	BB3	Full	Aug 06 2015	11:38	UTC-4	71°24.553	068°35.895	CTD-Rosette ↓	1255	330	320	15	5,1	5,3	1008,76	91	1/10
2	BB3	Full	Aug 06 2015	12:19	UTC-4	71°24.215	068°35.107	CTD-Rosette ↑	1231	277	320	16	5,2	4,49	1008,84	91	1/10
2	BB3	Full	Aug 06 2015	13:39	UTC-4	71°24.577	068°35.934	Moonpool Pumping ↓	1252		340	13	5,3	4,51	1008,98	91	1/10
2	BB3	Full	Aug 06 2015	16:00	UTC-4	71°24.059	068°32.325	Moonpool Pumping ↑	1292	331	330	10	5,2	4,73	1009,11	90	1/10
2	BB3	Full	Aug 06 2015	16:07	UTC-4	71°24.019	068°32.127	Moonpool Pumping ↑	1285	291	330	10	5,2	4,73	1009,11	90	1/10
2	BB3	Full	Aug 06 2015	18:34	UTC-4	71°51.275	068°06.436	X-CTD ↓	2226	14	340	11	4,6	5,96	1008,01	85	1/10
2	BB3	Full	Aug 06 2015	20:52	UTC-4	72°19.772	067°37.789	X-CTD ↓	2333	16	340	16	4,3	6,6	1007,13	82	1/10
2	BB3	Full	Aug 06 2015	23:17	UTC-4	72°45.003	067°00.417	Horizontal Net Tow ↓	2506	141	300	18	4,4	4,75	1006,74	79	0
2	BB3	Full	Aug 06 2015	23:34	UTC-4	72°45.155	066°58.398	Horizontal Net Tow ↑	2369	19	300	17	5	5,91	1006,54	78	0
2	BB2	Full	Aug 07 2015	04:09	UTC-4	72°45.053	066°59.980	PNF ↓	2370	67	270	12	7,7	5,77	1006,2	69	0
2	BB2	Full	Aug 07 2015	04:19	UTC-4	72°44.944	066°59.872	PNF ↑	2368	87	260	16	4,5	5,78	1006,18	85	0
2	BB2	Full	Aug 07 2015	04:44	UTC-4	72°44.970	066°59.204	TM-Rosette ↓	2370	291	270	16	4,6	5,8	1006,27	83	0
2	BB2	Full	Aug 07 2015	05:10	UTC-4	72°44.849	066°58.628	TM-Rosette ↑	2369	291	270	15	4,6	5,6	1006,18	86	0
2	BB2	Full	Aug 07 2015	15:42	UTC-4	72°45.215	066°59.594	CTD-Rosette ↓	2370	127	195	12	5	5,96	1003,98	87	0
2	BB2	Full	Aug 07 2015	17:10	UTC-4	72°45.584	066°58.178	CTD-Rosette ↑	2369	182	190	13	4,5	5,77	1003,38	85	0
2	BB2	Full	Aug 07 2015	17:37	UTC-4	72°45.087	066°59.850	LVP ↓	2370	217	180	13	4,4	5,92	1003,29	86	0
2	BB2	Full	Aug 07 2015	17:52	UTC-4	72°45.129	066°59.778	LVP (Start)	2370	262	180	12	4,3	5,88	1003,35	86	0
2	BB2	Full	Aug 07 2015	20:27	UTC-4	72°45.873	066°57.211	LVP (End)	2367	257	160	15	3,6	5,82	1002,56	89	0
2	BB2	Full	Aug 07 2015	20:37	UTC-4	72°45.927	066°57.136	LVP ↑	2370	271	160	13	3,6	5,89	1002,49	90	0
2	BB2	Full	Aug 07 2015	20:57	UTC-4	72°44.949	067°00.131	CTD-Rosette ↓	2368	175	160	14	3,5	5,92	1002,15	90	0
2	BB2	Full	Aug 07 2015	22:00	UTC-4	72°45.102	066°59.049	CTD-Rosette ↑	2369	173	170	15	3,6	5,85	1002,13	90	0
2	BB2	Full	Aug 07 2015	22:12	UTC-4	72°44.984	066°59.310	TM-Rosette ↓	2371	176	160	15	3,6	5,85	1002,01	90	0
2	BB2	Full	Aug 07 2015	22:37	UTC-4	72°45.093	066°58.209	TM-Rosette ↑	2367	180	160	16	3,6	5,82	1001,88	90	0
2	BB2	Full	Aug 07 2015	23:15	UTC-4	72°45.022	067°00.277	LVP ↓	2371	194	180	18	3,4	5,84	1001,61	89	0
2	BB2	Full	Aug 07 2015	23:45	UTC-4	72°45.120	066°59.859	LVP (Start)	2369	167	170	17	3,3	5,81	1001,57	90	0

2	BB2	Full	Aug 07 2015	02:40	UTC-4	72°46.243	066°57.322	LVP (End)	2370	183	180	18	3,2	5,77	1001,1	91	0
2	BB2	Full	Aug 07 2015	03:37	UTC-4	72°46.297	066°56.647	LVP ↑	2368	196	165	14	3,2	5,84	1001,17	93	0
2	BB2	Full	Aug 08 2015	03:58	UTC-4	72°45.063	067°00.001	TM-Rosette ↓	2368	179	170	16	3,3	5,81	1000,72	92	0
2	BB2	Full	Aug 08 2015	04:51	UTC-4	72°45.296	066°59.373	TM-Rosette ↑	2368	184	190	15	3,5	5,8	1001,12	91	0
2	BB2	Full	Aug 08 2015	06:08	UTC-4	72°45.100	066°59.191	Barge ↓	2369	122	190	13	3,8	5,96	1000,87	94	0
2	BB2	Full	Aug 08 2015	09:03	UTC-4	72°43.846	066°56.895	Barge ↑	2364	90	190	6	4,5	5,96	1000,63	95	0
2	BB2	Full	Aug 08 2015	06:25	UTC-4	72°45.080	066°59.671	CTD-Rosette Geochem ↓	2370	183	200	8	3,8	5,76	1000,81	95	0
2	BB2	Full	Aug 08 2015	07:04	UTC-4	72°45.181	066°59.060	CTD-Rosette Geochem ↑	2368	222	200	10	3,9	5,96	1000,73	91	0
2	BB2	Full	Aug 08 2015	08:09	UTC-4	72°45.059	066°59.916	TM-Rosette ↓	2369	211	190	9	4	5,95	1000,66	92	0
2	BB2	Full	Aug 08 2015	08:17	UTC-4	72°45.108	066°59.742	TM-Rosette ↑	2369	235	200	10	4,1	6	1000,69	93	0
2	BB2	Full	Aug 08 2015	09:41	UTC-4	72°45.056	067°00.020	CTD-Rosette ↓	2370	326	340	14	3,9	6,02	1000,53	93	0
2	BB2	Full	Aug 08 2015	10:13	UTC-4	72°44.936	067°00.347	CTD-Rosette ↑	2370	322	330	12	4,1	6,05	1000,67	89	0
2	BB2	Full	Aug 08 2015	12:44	UTC-4	72°45.022	066°59.233	TM-Rosette ↓	2368	124	305	13	4,1	5,89	1000,75	85	0
2	BB2	Full	Aug 08 2015	13:40	UTC-4	72°44.969	066°59.836	TM-Rosette ↑	2370	300	295	13	4,2	5,78	1000,98	80	0
2	BB2	Full	Aug 08 2015	14:02	UTC-4	72°45.063	067°00.112	LVP ↓	2370	309	300	13	4,3	5,48	1001,05	78	0
2	BB2	Full	Aug 08 2015	14:34	UTC-4	72°45.071	066°59.786	LVP (Start)	2370	260	300	14	4,1	5,73	1001,22	77	0
2	BB2	Full	Aug 08 2015	18:29	UTC-4	72°45.799	066°58.543	LVP (End)	2369	304	290	17	4,2	5,97	1001,33	79	0
2	BB2	Full	Aug 08 2015	19:20	UTC-4	72°45.843	066°58.295	LVP ↑	2371	293	290	20	4,4	5,97	1001,37	73	0
2	BB2	Full	Aug 09 2015	01:13	UTC-5	73°14.516	070°37.723	X-CTD ↓	1444	292	290	23	3,3	4,95	1000,44	88	0
2	BB2	Full	Aug 09 2015	07:13	UTC-5	73°44.086	074°25.331	X-CTD (dropped)	895	295	300	21	3,7	3,38	1003,69	86	icebergs
2	BB2	Full	Aug 09 2015	11:02	UTC-5	74°04.970	076°40.200	X-CTD ↓	815	280	280	26	4	4,58	1003,96	85	0
2	BB2	Full	Aug 09 2015	14:14	UTC-5	74°20.496	078°48.772	X-CTD ↓	690	295	280	14	5,5	4,27	1005,82	76	1/10
2	BB2	Full	Aug 09 2015	14:28	UTC-5	74°21.325	078°52.842	Horizontal Net Tow ↓	684	330	280	17	5,8	4,75	1006,35	72	1/10
2	BB2	Full	Aug 09 2015	15:31	UTC-5	74°21.369	078°50.434	Horizontal Net Tow ↑	688	213	345	12	5,9	4,69	1007,24	78	1/10
2	CAA1	Full	Aug 09 2015	18:03	UTC-5	74°31.370	080°33.784	PNF ↓	633	278	260	8	4,6	3,66	1008,91	79	icebergs
2	CAA1	Full	Aug 09 2015	18:09	UTC-5	74°31.335	080°33.877	PNF ↑	634	283	270	9	4,6	3,66	1008,91	79	icebergs
2	CAA1	Full	Aug 09 2015	18:17	UTC-5	74°31.287	080°34.341	CTD-Rosette ↓	634	268	270	9	5,3	3,3	1008,94	73	icebergs
2	CAA1	Full	Aug 09 2015	18:51	UTC-5	74°31.117	080°35.547	CTD-Rosette ↑	637	334	160	5	4,6	3	1009,32	81	icebergs
2	CAA1	Full	Aug 09 2015	19:22	UTC-5	74°31.285	080°33.723	TM-Rosette ↓	635	345	180	7	4,9	3,39	1009,43	79	icebergs
2	CAA1	Full	Aug 09 2015	19:36	UTC-5	74°31.174	080°34.569	TM-Rosette ↑	636	292	170	7	4,6	3,53	1009,51	80	icebergs
2	CAA1	Full	Aug 09 2015	20:00	UTC-5	74°31.387	080°34.158	LVP ↓	633	255	160	8	5,1	3,74	1009,69	81	icebergs
2	CAA1	Full	Aug 09 2015	20:16	UTC-5	74°31.350	080°34.984	LVP (Start)	634	206	160	6	4,9	3,85	1009,73	82	icebergs
2	CAA1	Full	Aug 09 2015	22:54	UTC-5	74°31.216	080°43.681	LVP (End)	637	157	110	6	5	3,72	1010,84	85	icebergs
2	CAA1	Full	Aug 09 2015	23:08	UTC-5	74°31.190	080°44.117	LVP ↑	633	148	110	5	5	3,66	1010,9	83	icebergs
2	CAA1	Full	Aug 09 2015	23:38	UTC-5	74°31.345	080°33.762	CTD-Rosette ↓	632	64	90	4	5,3	3,18	1011,03	84	icebergs
2	CAA1	Full	Aug 10 2015	00:22	UTC-5	74°31.221	080°36.650	CTD-Rosette ↑	636	18	calm	Calm	4,8	3,02	1011,34	86	icebergs
2	CAA1	Full	Aug 10 2015	00:44	UTC-5	74°31.318	080°34.439	TM-Rosette ↓	633	1	calm	Calm	4,6	3,03	1011,39	87	icebergs
2	CAA1	Full	Aug 10 2015	01:02	UTC-5	74°31.268	080°35.908	TM-Rosette ↑	633	18	calm	Calm	4,5	3,98	1011,51	88	icebergs
2	CAA1	Full	Aug 10 2015	02:45	UTC-5	74°31.328	080°34.674	CTD-Rosette ↓	632	28	calm	Calm	4,5	2,95	1011,91	88	icebergs
2	CAA1	Full	Aug 10 2015	03:15	UTC-5	74°31.368	080°37.421	CTD-Rosette ↑	636	27	calm	Calm	4,5	3,05	1011,86	89	icebergs
2	CAA1	Full	Aug 10 2015	03:45	UTC-5	74°31.339	080°34.117	LVP ↓	634	201	200	5	4,5	3,14	1011,87	91	icebergs
2	CAA1	Full	Aug 10 2015	04:19	UTC-5	74°31.206	080°36.387	LVP (Start)	637	275	180	5	3,9	3,1	1011,75	96	icebergs
2	CAA1	Full	Aug 10 2015	06:33	UTC-5	74°31.261	080°42.692	LVP (End)	636	272	220	4	3,6	2,61	1011,58	99	icebergs
2	CAA1	Full	Aug 10 2015	06:52	UTC-5	74°31.274	080°43.674	LVP ↑	635	261	250	3	3,8	2,55	1011,41	99	icebergs
2	CAA1	Full	Aug 10 2015	08:00	UTC-5	74°31.101	080°33.898	CTD-Rosette ↓	635	263	250	8	3,8	3,32	1011,06	98	icebergs
2	CAA1	Full	Aug 10 2015	08:44	UTC-5	74°31.030	080°37.014	CTD-Rosette ↑	662	282	270	8	3,2	3,57	1011	99	icebergs
2	CAA1	Full	Aug 10 2015	09:14	UTC-5	74°31.426	080°35.192	IKMT ↓	654	251	260	7	3,1	3,61	1011,03	99	icebergs
2	CAA1	Full	Aug 10 2015	10:21	UTC-5	74°30.753	080°41.658	IKMT ↑	642	274	240	8	3,7	2,87	1010,64	88	icebergs
2	CAA1	Full	Aug 10 2015	11:15	UTC-5	74°31.412	080°33.980	CTD-Rosette ↓	634	276	240	7	3,5	2,75	1010,62	87	icebergs
2	CAA1	Full	Aug 10 2015	11:35	UTC-5	74°31.481	080°34.990	CTD-Rosette ↑	633	297	230	7	3,6	2,56	1010,47	86	icebergs
2	CAA1	Full	Aug 10 2015	12:28	UTC-5	74°31.121	080°34.301	Horizontal Net Tow ↓	635	242	250	13	3,5	2,55	1010,14	88	icebergs
2	CAA1	Full	Aug 10 2015	12:43	UTC-5	74°30.575	080°34.272	Horizontal Net Tow ↑	650	33	250	11	3,7	2,53	1010	87	icebergs
2	CAA1	Full	Aug 10 2015	13:00	UTC-5	74°31.258	080°34.148	CTD-Rosette ↓	635	260	260	11	3,4	2,58	1009,98	88	icebergs
2	CAA1	Full	Aug 10 2015	13:44	UTC-5	74°31.181	080°36.222	CTD-Rosette ↑	637	255	260	8	3,5	2,55	1009,94	90	icebergs

2	CAA2	Full	Aug 10 2015	14:52	UTC-5	74°19.132	080°29.676	PNF ↓	711	266	260	15	4,8	5,14	1009,75	90	icebergs
2	CAA2	Full	Aug 10 2015	14:56	UTC-5	74°19.150	080°29.546	PNF ↑	700	288	260	15	4,8	5,14	1009,75	90	icebergs
2	CAA2	Full	Aug 10 2015	15:15	UTC-5	74°19.249	080°29.867	CTD-Rosette ↓	697	264	255	13	4,8	4,47	1009,88	90	icebergs
2	CAA2	Full	Aug 10 2015	15:58	UTC-5	74°19.480	080°28.789	CTD-Rosette ↑	698	254	260	11	5,1	4,52	1010,07	89	icebergs
2	CAA2	Full	Aug 10 2015	16:30	UTC-5	74°19.103	080°30.274	Vertical Net Tow ↓	698	257	260	12	5,1	4,51	1010,01	89	icebergs
2	CAA2	Full	Aug 10 2015	17:15	UTC-5	74°19.383	080°30.007	Vertical Net Tow ↑	703	242	250	8	5,2	4,5	1010,07	91	icebergs
2	CAA2	Full	Aug 10 2015	17:38	UTC-5	74°18.953	080°29.871	CTD-Rosette ↓	701	225	270	12	5	4,56	1010,07	92	icebergs
2	CAA2	Full	Aug 10 2015	18:19	UTC-5	74°18.929	080°29.729	CTD-Rosette ↑	709	245	270	12	4,9	4,77	1010,11	92	icebergs
2	CAA2	Full	Aug 10 2015	18:34	UTC-5	74°19.122	080°30.948	Horizontal Net Tow ↓	725	293	270	13	4,8	4,66	1010,03	92	icebergs
2	CAA2	Full	Aug 10 2015	18:46	UTC-5	74°19.452	080°32.252	Horizontal Net Tow ↑	726	300	270	13	4,7	4,6	1010,07	93	icebergs
2	CAA2	Full	Aug 10 2015	19:04	UTC-5	74°18.919	080°29.958	TM-Rosette ↓	700	230	260	12	4,7	4,49	1011,11	95	icebergs
2	CAA2	Full	Aug 10 2015	19:23	UTC-5	74°18.935	080°30.012	TM-Rosette ↑	703	235	270	10	4,6	4,79	1010,21	95	icebergs
2	CAA2	Full	Aug 10 2015	19:33	UTC-5	74°18.855	080°30.244	CTD-Rosette ↓	701	233	280	10	4,6	4,82	1010,12	95	icebergs
2	CAA2	Full	Aug 10 2015	20:40	UTC-5	74°18.752	080°30.542	CTD-Rosette ↑	701	228	280	8	4,5	4,84	1010,11	94	icebergs
2	CAA2	Full	Aug 10 2015	20:35	UTC-5	74°19.143	080°30.495	LVP ↓	702	218	270	10	4,3	4,72	1009,98	94	icebergs
2	CAA2	Full	Aug 10 2015	20:50	UTC-5	74°19.119	080°30.605	LVP (Start)	703	236	280	6	4,4	4,68	1010,11	94	icebergs
2	CAA2	Full	Aug 10 2015	23:23	UTC-5	74°19.581	080°30.989	LVP (End)	699	246	210	5	4,1	4,6	1009,95	93	icebergs
2	CAA2	Full	Aug 10 2015	23:38	UTC-5	74°19.596	080°31.122	LVP ↑	697	237	210	5	4,2	4,59	1009,92	93	icebergs
2	CAA2	Full	Aug 11 2015	00:01	UTC-5	74°19.071	080°29.742	CTD-Rosette ↓	701	53	215	8	4,5	4,57	1009,9	96	icebergs
2	CAA2	Full	Aug 11 2015	00:34	UTC-5	74°19.151	080°30.135	CTD-Rosette ↑	698	56	205	6	5,3	4,62	1010,05	94	icebergs
2	CAA2	Full	Aug 11 2015	01:43	UTC-5	74°19.212	080°30.280	CTD-Rosette ↓	700	58	190	5	4,8	4,99	1010,36	95	icebergs
2	CAA2	Full	Aug 11 2015	02:14	UTC-5	74°19.240	080°30.799	CTD-Rosette ↑	700	61	190	4	4,9	4,7	1010,28	94	icebergs
2	AN323	Nutrient	Aug 11 2015	03:14	UTC-5	74°09.472	080°28.378	CTD-Rosette ↓	790	220	230	8	4,2	5,37	1010,37	97	icebergs
2	AN323	Nutrient	Aug 11 2015	04:18	UTC-5	74°09.030	080°27.695	CTD-Rosette ↑	802	234	230	9	4,1	5,3	1010,35	97	icebergs
2	AN324	Nutrient	Aug 11 2015	05:17	UTC-5	73°58.892	080°27.980	CTD-Rosette ↓	775	246	240	15	4,3	5,48	1010,23	96	icebergs
2	AN324	Nutrient	Aug 11 2015	06:24	UTC-5	73°58.468	080°26.209	CTD-Rosette ↑	773	256	260	13	4,1	5,46	1010,77	96	icebergs
2	CAA3	Full	Aug 11 2015	07:28	UTC-5	73°48.993	080°29.293	PNF ↓	679	198	250	15	4,3	4	1010,8	93	icebergs
2	CAA3	Full	Aug 11 2015	08:00	UTC-5	73°48.806	080°27.791	PNF ↑	677	83	250	9	6,8	4,08	1011,16	83	icebergs
2	CAA3	Full	Aug 11 2015	08:12	UTC-5	73°48.928	080°29.337	CTD-Rosette ↓	674	252	260	12	5,5	4,06	1011,02	88	icebergs
2	CAA3	Full	Aug 11 2015	08:55	UTC-5	73°48.589	080°25.679	CTD-Rosette ↑	676	277	240	11	4,7	4,07	1010,97	90	icebergs
2	CAA3	Full	Aug 11 2015	09:07	UTC-5	73°48.560	080°24.673	TM-Rosette ↓	679	282	240	9	4,7	4,06	1010,9	89	icebergs
2	CAA3	Full	Aug 11 2015	09:14	UTC-5	73°48.517	080°23.939	TM-Rosette ↑	679	289	240	10	4,6	4,05	1010,89	90	icebergs
2	CAA3	Full	Aug 11 2015	09:52	UTC-5	73°49.104	080°29.950	Helicopter Departure	686	298	240	9	4,5	4,05	1010,66	90	icebergs
2	CAA3	Full	Aug 11 2015	10:21	UTC-5	73°49.149	080°28.993	IKMT ↓	710	21	230	8	4,5	4,11	1010,68	90	icebergs
2	CAA3	Full	Aug 11 2015	11:21	UTC-5	73°49.124	080°21.162	IKMT ↑	826	321	250	9	4,8	4,19	1010,4	87	icebergs
2	CAA3	Full	Aug 11 2015	12:22	UTC-5	73°49.114	080°29.603	CTD-Rosette ↓	688	258	220	3	4,6	4,33	1010,08	91	icebergs
2	CAA3	Full	Aug 11 2015	12:58	UTC-5	73°48.880	080°26.763	CTD-Rosette ↑	687	258	calm	Calm	5	4,29	1009,96	88	icebergs
2	CAA3	Full	Aug 11 2015	14:04	UTC-5	73°49.109	080°29.144	LVP ↓	689	282	calm	Calm	6,5	4,37	1009,72	83	icebergs
2	CAA3	Full	Aug 11 2015	14:27	UTC-5	73°49.047	080°27.777	LVP (Start)	694	281	calm	Calm	6,2	4,28	1009,62	84	icebergs
2	CAA3	Full	Aug 11 2015	16:50	UTC-5	73°48.319	080°19.693	LVP (End)	627	330	230	1	7,3	4,33	1008,54	84	icebergs
2	CAA3	Full	Aug 11 2015	17:08	UTC-5	73°48.287	080°18.767	LVP ↑	658	306	70	5	7	4,35	1008,5	84	icebergs
2	CAA3	Full	Aug 11 2015	18:04	UTC-5	73°49.087	080°28.987	CTD-Rosette ↓	688	269	60	11	4,8	4,37	1008,2	90	icebergs
2	CAA3	Full	Aug 11 2015	18:22	UTC-5	73°48.923	080°28.282	CTD-Rosette ↑	681	266	50	8	7,1	4,32	1008,19	82	icebergs
2	CAA3	Full	Aug 11 2015	18:35	UTC-5	73°49.261	080°29.989	Horizontal Net Tow ↓	695	335	70	5	6,6	4,32	1008,14	84	icebergs
2	CAA3	Full	Aug 11 2015	18:55	UTC-5	73°48.800	080°29.570	Horizontal Net Tow ↑	660	112	50	10	4,4	4,3	1007,99	91	icebergs
2	CAA3	Full	Aug 11 2015	19:06	UTC-5	73°48.973	080°29.588	TM-Rosette ↓	675	277	60	11	4	4,34	1007,8	92	icebergs
2	CAA3	Full	Aug 11 2015	19:22	UTC-5	73°48.895	080°29.341	TM-Rosette ↑	671	330	80	1	5,5	4,36	1007,69	87	icebergs
2	CAA3	Full	Aug 11 2015	19:52	UTC-5	73°49.121	080°29.687	CTD-Rosette ↓	688	255	60	13	4,6	4,34	1007,48	92	icebergs
2	CAA3	Full	Aug 11 2015	20:39	UTC-5	73°48.844	080°28.377	CTD-Rosette ↑	675	268	80	10	6,7	4,37	1007,9	85	icebergs
2	CAA3	Full	Aug 11 2015	20:59	UTC-5	73°49.114	080°30.289	LVP ↓	682	21	80	16	6,7	4,38	1007,41	86	icebergs
2	CAA3	Full	Aug 11 2015	21:12	UTC-5	73°49.095	080°29.950	LVP (Start)	683	30	90	16	4,5	4,33	1007,27	95	icebergs
2	CAA3	Full	Aug 11 2015	23:47	UTC-5	73°48.601	080°27.286	LVP (End)	666	76	80	20	4,2	4,33	1006,19	88	icebergs
2	CAA3	Full	Aug 11 2015	23:59	UTC-5	73°48.592	080°27.024	LVP ↑	668	75	80	20	4,3	4,29	1006,27	86	icebergs
2	CAA3	Full	Aug 12 2015	00:18	UTC-5	73°49.020	080°30.397	CTD-Rosette ↓	674	253	80	18	4,5	4,3	1006,25	85	icebergs

2	CAA3	Full	Aug 12 2015	00:51	UTC-5	73°49.036	080°29.813	CTD-Rosette ↑	680	270	80	15	4,1	4,33	1006,1	85	icebergs
2	CAA3	Full	Aug 12 2015	01:59	UTC-5	73°49.111	080°30.009	CTD-Rosette ↓	686	272	80	18	4,6	4,31	1005,78	85	42644
2	CAA3	Full	Aug 12 2015	02:30	UTC-5	73°48.980	080°29.262	CTD-Rosette ↑	680	266	75	15	7,9	4,28	1005,76	76	1/10
2	CAA5	Full	Aug 12 2015	17:15	UTC-6	74°32.353	090°47.055	PNF ↓	265	285	110	18	5,3	3,94	1008,12	77	0
2	CAA5	Full	Aug 12 2015	17:26	UTC-6	74°32.389	090°46.987	PNF ↑	259	276	110	16	5,7	3,96	1008,21	75	0
2	CAA5	Full	Aug 12 2015	17:39	UTC-6	74°32.361	090°47.591	CTD-Rosette ↓	259	95	110	18	5,2	3,99	1008,42	77	0
2	CAA5	Full	Aug 12 2015	17:59	UTC-6	74°32.409	090°47.347	CTD-Rosette ↑	260	119	110	14	5	4,01	1008,68	78	0
2	CAA5	Full	Aug 12 2015	18:14	UTC-6	74°32.329	090°48.269	TM-Rosette ↓	253	114	120	12	5,1	4,02	1008,7	78	0
2	CAA5	Full	Aug 12 2015	18:28	UTC-6	74°32.384	090°48.255	TM-Rosette ↑	258	116	120	16	5,1	4,03	1008,76	78	0
2	CAA5	Full	Aug 12 2015	18:55	UTC-6	74°32.237	090°48.018	CTD-Rosette Geochem ↓	254	124	100	14	4,8	4,06	1008,86	80	0
2	CAA5	Full	Aug 12 2015	19:29	UTC-6	74°32.233	090°48.075	CTD-Rosette Geochem ↑	254	105	100	17	5	4,1	1008,94	78	0
2	CAA5	Full	Aug 12 2015	19:45	UTC-6	74°32.359	090°47.893	LVP ↓	256	110	110	17	5,3	4,13	1008,93	74	0
2	CAA5	Full	Aug 12 2015	19:57	UTC-6	74°32.263	090°47.908	LVP (Start)	255	120	110	17	5,3	4,13	1008,98	75	0
2	CAA5	Full	Aug 12 2015	22:26	UTC-6	74°32.564	090°47.895	LVP (End)	260	123	110	16	4,9	4,18	1010,16	80	0
2	CAA5	Full	Aug 12 2015	22:35	UTC-6	74°32.546	090°47.916	LVP ↑	263	152	110	16	4,8	4,19	1010,29	80	0
2	CAA5	Full	Aug 12 2015	22:53	UTC-6	74°32.342	090°47.837	CTD-Rosette ↓	259	113	110	15	4,7	4,17	1010,45	81	0
2	CAA5	Full	Aug 12 2015	23:12	UTC-6	74°32.467	090°47.842	CTD-Rosette ↑	262	108	110	17	4,8	4,17	1010,46	81	0
2	CAA5	Full	Aug 12 2015	23:59	UTC-6	74°32.503	090°47.340	Horizontal Net Tow ↓	260	145	110	15	4,5	4,14	1010,7	84	0
2	CAA5	Full	Aug 13 2015	00:15	UTC-6	74°32.632	090°46.628	Horizontal Net Tow ↑	254	110	110	13	4,4	4,14	1010,73	85	0
2	CAA5	Full	Aug 13 2015	00:31	UTC-6	74°32.315	090°48.295	Horizontal Net Tow ↓	197	110	120	14	4,1	4,14	1010,89	86	42645
2	CAA5	Full	Aug 13 2015	01:04	UTC-6	74°32.475	090°49.384	Horizontal Net Tow ↑	175	120	120	14	4,1	4,07	1010,97	87	42645
2	CAA5	Full	Aug 13 2015	01:41	UTC-6	74°32.226	090°48.466	TM-Rosette ↓	179	105	110	14	4	4,13	1011,17	89	42645
2	CAA5	Full	Aug 13 2015	01:49	UTC-6	74°33.273	090°48.659	TM-Rosette ↑	179	87	120	13	4	4,14	1011,25	89	42645
2	CAA5	Full	Aug 13 2015	02:12	UTC-6	74°32.296	090°48.109	LVP ↓	181	114	110	13	4	4,13	1011,44	87	42644
2	CAA5	Full	Aug 13 2015	02:25	UTC-6	74°32.334	090°48.418	LVP (Start)	182	116	110	14	4	4,13	1011,58	88	42644
2	CAA5	Full	Aug 13 2015	04:45	UTC-6	74°32.711	090°51.737	LVP (End)	178	116	110	14	3,9	4,17	1012,73	90	42644
2	CAA5	Full	Aug 13 2015	04:52	UTC-6	74°32.735	090°51.980	LVP ↑	178	112	110	14	3,9	4,17	1012,73	90	42644
2	CAA5	Full	Aug 13 2015	05:18	UTC-6	74°32.196	090°48.018	Beam Trawl ↓	253	150	110	14	3,9	4,13	1012,86	90	42645
2	CAA5	Full	Aug 13 2015	06:03	UTC-6	74°32.239	090°50.628	Beam Trawl ↑	213	211	110	14	3,6	4,05	1013,37	90	42645
2	CAA5	Full	Aug 13 2015	06:38	UTC-6	74°32.430	090°47.863	CTD-Rosette ↓	179	108	120	16	4	4,08	1013,67	89	42644
2	CAA5	Full	Aug 13 2015	06:48	UTC-6	74°32.497	090°47.980	CTD-Rosette ↑	178	90	120	16	3,9	4,07	1013,75	89	42644
2	CAA5	Full	Aug 13 2015	10:13	UTC-6	74°31.949	090°48.105	LVP ↓	164	97	120	13	3,8	4,01	1014,85	84	42644
2	CAA5	Full	Aug 13 2015	10:49	UTC-6	74°32.186	090°48.323	LVP (Start)	188	131	100	8	3,9	3,98	1014,95	83	42644
2	CAA4	Full	Aug 13 2015	13:18	UTC-6	74°07.368	091°30.395	LVP (End)	201	247	60	10	2,2	1,57	1014,83	90	42644
2	CAA4	Full	Aug 13 2015	13:24	UTC-6	74°07.362	091°30.220	LVP ↑	202	250	65	9	2,7	1,56	1014,83	90	42644
2	CAA4	Full	Aug 13 2015	13:38	UTC-6	74°07.353	091°29.984	CTD-Rosette ↓	194	260	60	11	2,5	1,51	1014,89	91	42644
2	CAA4	Full	Aug 13 2015	13:56	UTC-6	74°07.338	091°29.480	CTD-Rosette ↑	182	273	60	10	4,2	1,43	1014,91	85	2/10
2	CAA4	Full	Aug 13 2015	14:06	UTC-6	74°07.576	091°30.076	Horizontal Net Tow ↓	197	291	60	11	3,5	1,43	1014,95	87	2/10
2	CAA4	Full	Aug 13 2015	14:21	UTC-6	74°07.249	091°31.291	Horizontal Net Tow ↑	175	186	60	12	2,6	1,44	1014,85	89	2/10
2	CAA4	Full	Aug 13 2015	14:53	UTC-6	74°07.311	091°30.724	CTD-Rosette ↓	179	63	60	12	2,1	1,33	1014,82	92	2/10
2	CAA4	Full	Aug 13 2015	15:10	UTC-6	74°07.305	091°30.487	CTD-Rosette ↑	179	65	65	12	2,2	1,33	1014,91	92	2/10
2	CAA4	Full	Aug 13 2015	16:03	UTC-6	74°07.380	091°30.811	LVP ↓	181	36	60	9	2,4	1,47	1015,19	91	1/10
2	CAA4	Full	Aug 13 2015	16:18	UTC-6	74°07.393	091°30.392	LVP (Start)	182	36	70	12	2,2	1,39	1015,09	92	1/10
2	CAA4	Full	Aug 13 2015	18:38	UTC-6	74°07.240	091°25.601	LVP (End)	178	32	60	11	2,7	1,3	1015,62	89	1/10
2	CAA4	Full	Aug 13 2015	18:45	UTC-6	74°07.225	091°25.354	LVP ↑	178	32	50	11	2,7	1,31	1015,64	90	1/10
2	CAA4	Full	Aug 13 2015	19:40	UTC-6	74°08.323	091°24.535	Beam Trawl ↓	253	281	90	10	3,9	1,59	1015,71	83	2/10
2	CAA4	Full	Aug 13 2015	20:44	UTC-6	74°07.705	091°21.776	Beam Trawl ↑	213	105	110	9	3,2	1,55	1015,7	87	2/10
2	CAA4	Full	Aug 13 2015	21:17	UTC-6	74°07.250	091°30.678	CTD-Rosette ↓	179	113	80	6	2,7	1,54	1015,7	89	1/10
2	CAA4	Full	Aug 13 2015	21:50	UTC-6	74°07.309	091°29.205	CTD-Rosette ↑	178	130	50	6	2,8	1,41	1015,56	88	1/10
2	CAA4	Full	Aug 13 2015	22:12	UTC-6	74°07.455	091°30.839	LVP ↓	184	100	40	6	2,6	1,43	1015,51	89	1/10
2	CAA4	Full	Aug 13 2015	22:21	UTC-6	74°07.488	091°30.435	LVP (Start)	188	125	40	7	2,9	1,31	1015,61	88	1/10
2	CAA4	Full	Aug 13 2015	00:42	UTC-6	74°07.545	091°23.642	LVP (End)	201	132	50	9	2,4	1,27	1015,33	92	1/10
2	CAA4	Full	Aug 14 2015	00:51	UTC-6	74°07.548	091°23.268	LVP ↑	202	108	40	10	2,4	1,28	1015,34	93	1/10
2	CAA4	Full	Aug 14 2015	01:12	UTC-6	74°07.484	091°29.542	CTD-Rosette ↓	194	148	50	8	2	1,23	1015,43	94	1/10

2	CAA4	Full	Aug 14 2015	01:41	UTC-6	74°07.487	091°28.586	CTD-Rosette ↑	195	121	50	9	2,1	1,23	1015,4	95	1/10
2	CAA4	Full	Aug 14 2015	01:57	UTC-6	74°07.338	091°30.654	TM-Rosette ↓	181	87	50	8	2	1,22	1015,39	95	1/10
2	CAA4	Full	Aug 14 2015	02:04	UTC-6	74°07.355	091°30.415	TM-Rosette ↑	182	74	45	7	1,8	1,16	1015,43	96	1/10
2	CAA4	Full	Aug 14 2015	02:54	UTC-6	74°07.460	091°30.122	CTD-Rosette ↓	187	79	40	8	2	1,28	1015,44	96	1/10
2	CAA4	Full	Aug 14 2015	03:28	UTC-6	74°07.485	091°29.600	CTD-Rosette ↑	193	93	35	7	1,8	1,27	1015,34	96	1/10
2	CAA6	Full	Aug 14 2015	15:03	UTC-6	74°45.538	097°27.305	PNF ↓	260	206	calm	Calm	4,4	1,37	1013,97	90	3/10
2	CAA6	Full	Aug 14 2015	15:14	UTC-6	74°45.529	097°27.326	PNF ↑	259	181	300	2	4,2	1,46	1013,91	90	3/10
2	CAA6	Full	Aug 14 2015	15:24	UTC-6	74°45.530	097°27.429	CTD-Rosette ↓	258	220	330	3	4,9	1,46	1013,89	88	3/10
2	CAA6	Full	Aug 14 2015	15:45	UTC-6	74°45.455	097°27.290	CTD-Rosette ↑	260	198	calm	Calm	4,9	1,45	1013,92	86	3/10
2	CAA6	Full	Aug 14 2015	15:59	UTC-6	74°45.436	097°26.522	Horizontal Net Tow ↓	258	33	260	1	5,1	1,4	1013,85	85	0
2	CAA6	Full	Aug 14 2015	16:16	UTC-6	74°45.767	097°27.910	Horizontal Net Tow ↑	253	231	0	0	4,2	1,62	1013,89	88	0
2	CAA6	Full	Aug 14 2015	16:48	UTC-6	74°45.399	097°27.186	CTD-Rosette ↓	255	240	0	0	4,3	1,71	1013,88	89	0
2	CAA6	Full	Aug 14 2015	17:08	UTC-6	74°45.316	097°27.261	CTD-Rosette ↑	249	249	330	1	4,6	1,31	1013,81	87	0
2	CAA6	Full	Aug 14 2015	17:29	UTC-6	74°45.868	097°27.027	LVP ↓	263	230	320	4	4,4	1,34	1013,77	88	0
2	CAA6	Full	Aug 14 2015	17:44	UTC-6	74°45.829	097°27.076	LVP (Start)	263	223	0	0	5,9	1,97	1013,7	83	0
2	CAA6	Full	Aug 14 2015	20:05	UTC-6	74°45.751	097°26.595	LVP (End)	267	234	0	0	6	1,38	1013,45	82	0
2	CAA6	Full	Aug 14 2015	20:13	UTC-6	74°45.742	097°26.476	LVP ↑	268	249	0	0	6,1	1,45	1013,4	82	0
2	CAA6	Full	Aug 14 2015	20:26	UTC-6	74°45.640	097°25.607	Beam Trawl ↓	268	115	0	0	6,2	1,46	1013,36	82	0
2	CAA6	Full	Aug 14 2015	21:17	UTC-6	74°45.560	097°26.517	Beam Trawl ↑	266	118	0	0	4,8	2,52	1013,07	87	0
2	CAA6	Full	Aug 14 2015	21:37	UTC-6	74°45.576	097°27.194	CTD-Rosette ↓	260	256	340	3	4,1	2,35	1012,97	89	0
2	CAA6	Full	Aug 14 2015	22:16	UTC-6	74°45.322	097°26.480	CTD-Rosette ↑	244	241	330	2	5,4	2,13	1012,73	85	0
2	CAA6	Full	Aug 14 2015	22:36	UTC-6	74°45.829	097°26.765	LVP ↓	267	209	20	6	4,7	2,22	1012,58	87	0
2	CAA6	Full	Aug 14 2015	22:45	UTC-6	74°45.814	097°26.500	LVP (Start)	269	166	20	8	4,4	2,62	1012,58	89	0
2	CAA6	Full	Aug 15 2015	01:09	UTC-6	74°45.336	097°26.586	LVP (End)	250	328	45	11	3,5	1,49	1012,13	92	0
2	CAA6	Full	Aug 15 2015	01:18	UTC-6	74°45.296	097°26.914	LVP ↑	250	326	40	12	3,5	1,49	1012,13	92	0
2	CAA6	Full	Aug 15 2015	01:29	UTC-6	74°45.274	097°27.490	CTD-Rosette ↓	244	318	35	10	3,3	1,5	1012,07	93	0
2	CAA6	Full	Aug 15 2015	02:00	UTC-6	74°45.107	097°28.485	CTD-Rosette ↑	215	293	30	13	3,4	1,47	1011,97	92	0
2	CAA6	Full	Aug 15 2015	04:19	UTC-6	74°45.600	097°27.511	TM-Rosette ↓	256	43	20	11	2,8	1,98	1011,55	94	0
2	CAA6	Full	Aug 15 2015	04:34	UTC-6	74°45.556	097°28.028	TM-Rosette ↑	238	64	20	12	2,8	1,93	1011,39	94	0
2	CAA6	Full	Aug 15 2015	04:48	UTC-6	74°45.457	097°27.230	CTD-Rosette Geochem ↓	259	39	10	11	2,8	1,97	1011,39	94	0
2	CAA6	Full	Aug 15 2015	05:21	UTC-6	74°45.324	097°28.578	CTD-Rosette Geochem ↑	203	67	10	10	2,8	2,03	1011,18	94	0
2	---	Horizontal Net	Aug 15 2015	13:19	UTC-6	73°49.328	096°33.274	Horizontal Net Tow ↓	217	33	320	9	0,6	1,58	1010,22	97	3/10
2	---	Horizontal Net	Aug 15 2015	13:36	UTC-6	73°49.482	096°34.556	Horizontal Net Tow ↑	217	167	340	3	0,8	1,61	1010,04	97	3/10
2	CAA7	Full	Aug 15 2015	16:01	UTC-6	73°40.245	096°33.822	PNF + CTD-Rosette ↓	212	315	0	6	1,3	1,35	1009,76	97	3/10
2	CAA7	Full	Aug 15 2015	16:26	UTC-6	73°40.217	096°34.069	PNF + CTD-Rosette ↑	209	318	30	5	1,3	1,4	1009,88	97	3/10
2	CAA7	Full	Aug 15 2015	17:08	UTC-6	73°39.941	096°33.590	CTD-Rosette ↓	212	352	350	4	1,1	1,26	1009,81	97	3/10
2	CAA7	Full	Aug 15 2015	17:29	UTC-6	73°39.819	096°33.777	CTD-Rosette ↑	211	285	20	5	1,3	1,28	1009,69	97	3/10
2	CAA7	Full	Aug 15 2015	17:51	UTC-6	73°39.913	096°33.358	Vertical Net Tow ↓	215	55	0	4	1,2	1,18	1009,8	97	3/10
2	CAA7	Full	Aug 15 2015	18:06	UTC-6	73°39.831	096°33.401	Vertical Net Tow ↑	214	113	340	4	1,1	1,23	1009,74	97	3/10
2	CAA7	Full	Aug 15 2015	18:27	UTC-6	73°39.989	096°33.493	CTD-Rosette ↓	214	324	350	6	1,3	1,21	1009,7	97	3/10
2	CAA7	Full	Aug 15 2015	18:44	UTC-6	73°39.988	096°33.553	CTD-Rosette ↑	213	33	0	4	1,4	1,61	1009,76	97	3/10
2	CAA7	Full	Aug 15 2015	19:08	UTC-6	73°39.991	096°33.042	LVP ↓	214	42	340	4	1,3	1,48	1009,76	97	3/10
2	CAA7	Full	Aug 15 2015	19:29	UTC-6	73°39.960	096°32.975	LVP (Start)	214	55	340	3	1,3	1,51	1009,77	97	3/10
2	CAA7	Full	Aug 15 2015	21:45	UTC-6	73°39.768	096°31.625	LVP (End)	220	53	290	10	1,5	1,67	1009,04	95	3/10
2	CAA7	Full	Aug 15 2015	21:51	UTC-6	73°39.766	096°31.531	LVP ↑	224	33	280	7	2,4	1,71	1008,93	90	3/10
2	CAA7	Full	Aug 15 2015	22:15	UTC-6	73°40.377	096°31.496	CTD-Rosette ↓	219	274	360	7	2	1,39	1008,94	92	3/10
2	CAA7	Full	Aug 15 2015	22:49	UTC-6	73°40.265	096°31.134	CTD-Rosette ↑	223	226	330	10	2	1,29	1008,76	94	3/10
2	CAA7	Full	Aug 15 2015	22:57	UTC-6	73°40.269	096°31.231	TM-Rosette ↓	218	316	330	10	2,1	1,43	1008,65	93	3/10
2	CAA7	Full	Aug 15 2015	23:10	UTC-6	73°40.230	096°31.093	TM-Rosette ↑	221	310	340	6	1,8	1,46	1008,53	93	3/10
2	CAA7	Full	Aug 16 2015	00:15	UTC-6	73°40.041	096°31.345	LVP ↓	221	243	335	10	2	1,68	1008,18	93	3/10
2	CAA7	Full	Aug 16 2015	00:27	UTC-6	73°40.026	096°31.431	LVP (Start)	223	289	340	12	2,1	1,65	1008,11	92	3/10
2	CAA7	Full	Aug 16 2015	02:51	UTC-6	73°39.691	096°31.887	LVP (End)	220	233	320	10	1,9	1,59	1007,77	95	5/10
2	CAA7	Full	Aug 16 2015	03:03	UTC-6	73°39.651	096°31.832	LVP ↑	220	208	320	13	2	1,6	1007,72	95	5/10
2	CAA7	Full	Aug 16 2015	03:13	UTC-6	73°39.629	096°32.157	CTD-Rosette ↓	219	331	330	11	2,2	1,61	1007,73	95	5/10

3a	407	Full	Aug 23 2015	07:28	UTC-5	71°01.853	126°05.866	Glider ↓	396	358	110	2	7,2	6,15	1014,82	93	0
3a	407	Full	Aug 23 2015	12:58	UTC-5	71°02.000	126°14.000	PNF ↓ ↑	384	210	100	10	7,7	6,9	1017,52	92	0
3a	407	Full	Aug 23 2015	13:10	UTC-5	71°03.000	126°14.000	Secchi ↓ ↑	380	274	110	10	7,7	6,9	1017,53	92	0
3a	407	Full	Aug 23 2015	13:47	UTC-5	71°01.000	126°09.000	CTD-Rosette ↓	382	301	110	10	7,4	6,6	1017,72	93	0
3a	407	Full	Aug 23 2015	14:19	UTC-5	71°01.000	126°09.000	CTD-Rosette ↑	386	342	105	15	9,8	6,4	1018	81	0
3a	CA08-15	Mooring	Aug 23 2015	15:43	UTC-5	71°00.443	126°04.737	Mooring triangulation CA08-15 ↓	391		85	18	7,4	6,13	1017,7	88	0
3a	CA08-15	Mooring	Aug 23 2015	15:47	UTC-5	71°00.666	126°04.710	Triangulation #1 580m	393		100	12	7,9	6,1	1015,66	89	0
3a	CA08-15	Mooring	Aug 23 2015	16:02	UTC-5	71°00.428	126°05.496	Triangulation #2 610m	391		100	12	7,9	6,1	1015,66	89	0
3a	CA08-15	Mooring	Aug 23 2015	16:07	UTC-5	71°00.310	126°04.344	Triangulation #3 533m	391		100	12	7,9	6,1	1015,66	89	0
3a	CA08-15	Mooring	Aug 23 2015	16:30	UTC-5	71°00.601	126°04.602	CTD ↓	392	301	100	16	7,2	6,06	1015,59	91	0
3a	CA08-15	Mooring	Aug 23 2015	16:50	UTC-5	71°00.641	126°04.760	CTD ↑	390	301	100	13	10,4	6,23	1015,77	80	0
3a	407	Full	Aug 23 2015	18:34	UTC-5	71°05.012	126°14.631	Glider ↑	399	398	100	8	8,3	6,99	1015,84	85	0
3a	407	Full	Aug 23 2015	19:47	UTC-5	71°00.285	126°04.459	Hydrobios ↓	390	390	90	23	7	6,44	1015,05	87	0
3a	407	Full	Aug 23 2015	20:15	UTC-5	71°00.464	126°04.198	Hydrobios ↑	392	297	90	15	9,8	6,1	1015,42	78	0
3a	407	Full	Aug 23 2015	20:44	UTC-5	71°00.377	126°04.578	CTD-Rosette ↓	390	258	90	20	7,3	6,15	1015,47	87	0
3a	407	Full	Aug 23 2015	21:09	UTC-5	71°00.587	126°04.848	CTD-Rosette ↑	394	266	90	15	9,5	6,03	1015,66	79	0
3a	407	Full	Aug 23 2015	21:12	UTC-5	71°00.618	126°04.905	CTD-Rosette ↓	390	295	90	15	9,5	6,03	1015,66	79	0
3a	407	Full	Aug 23 2015	21:55	UTC-5	71°00.840	126°04.940	CTD-Rosette ↑	394	298	90	14	11	5,98	1015,69	75	0
3a	407	Full	Aug 23 2015	22:05	UTC-5	71°00.903	126°05.410	Tucker Net ↓	395	255	90	15	10,7	6,19	1015,76	74	0
3a	407	Full	Aug 23 2015	22:30	UTC-5	71°00.469	126°05.917	Tucker Net ↑	390	22	100	19	7,2	6	1015,71	90	0
3a	407	Full	Aug 23 2015	22:46	UTC-5	71°00.576	126°05.997	Box Core ↓	391	298	90	11	7,5	5,96	1015,93	89	0
3a	407	Full	Aug 23 2015		UTC-5	71°00.651	126°06.006	Box Core (bottom)	393	297	100	16	8,4	5,96	1015,92	84	0
3a	407	Full	Aug 23 2015	23:04	UTC-5	71°00.661	126°06.107	Box Core ↑	393	281	90	16	8,4	5,97	1015,95	85	0
3a	407	Full	Aug 23 2015	23:22	UTC-5	71°00.840	126°06.930	Agassiz Trawl ↓	393	243	90	17	7,1	6	1016,08	89	0
3a	407	Full	Aug 23 2015	23:54	UTC-5	71°00.000	126°08.000	Agassiz Trawl ↑	393	237	90	18	6,9	6,5	1018	90	0
3a	407	Full	Aug 24 2015	01:06	UTC-5	71°05.240	126°20.880	Beam Trawl ↓	386	147	70	18	6,7	7,13	1018,5	93	0
3a	407	Full	Aug 24 2015	02:07	UTC-5	71°02.760	126°17.460	Beam Trawl ↑	382	135	80	15	6,9	6,91	1018,33	94	0
3a	437	Basic	Aug 24 2015	06:00	UTC-5	71°48.181	126°29.774	PNF + Secchi ↓	283	239	40	9	5,2	4,41	1018,23	97	0
3a	437	Basic	Aug 24 2015	06:08	UTC-5	71°48.219	126°29.820	PNF + Secchi ↑	279	240	40	9	5,2	4,41	1018,23	97	0
3a	437	Basic	Aug 24 2015	06:30	UTC-5	71°47.844	126°30.148	CTD-Rosette ↓	298	264	70	10	6	4,25	1018,37	94	0
3a	437	Basic	Aug 24 2015	07:27	UTC-5	71°48.039	126°31.129	CTD-Rosette ↑	303	242	40	5	5,7	4,26	1018,65	94	0
3a	437	Basic	Aug 24 2015	07:42	UTC-5	71°48.000	126°31.776	Tucker Net ↓	312	260	50	8	6,7	4,28	1018,53	91	0
3a	437	Basic	Aug 24 2015	07:57	UTC-5	71°47.647	126°31.307	Tucker Net ↑	317	83	60	10	6,1	4,28	1018,52	92	0
3a	437	Basic	Aug 24 2015	08:40	UTC-5	71°48.013	126°29.742	CTD-Rosette ↓	290	273	50	7	6,7	3,77	1018,69	92	0
3a	437	Basic	Aug 24 2015	09:06	UTC-5	71°48.084	126°29.944	CTD-Rosette ↑	293	255	70	7	9,5	4,1	1018,76	79	0
3a	437	Basic	Aug 24 2015	09:25	UTC-5	71°48.104	126°30.267	Monster-Loki Net ↓	291	241	60	10	6,9	4,19	1018,8	90	0
3a	437	Basic	Aug 24 2015	09:47	UTC-5	71°48.155	126°30.251	Monster-Loki Net ↑	287	279	40	5	6,9	4,22	1018,86	88	0
3a	437	Basic	Aug 24 2015	10:12	UTC-5	71°48.260	126°29.791	Box Core ↓	276	250	60	10	6,6	3,99	1018,8	90	0
3a	437	Basic	Aug 24 2015	10:19	UTC-5	71°48.273	126°29.796	Box Core (bottom)	274	279	50	7	7,5	4	1018,84	86	0
3a	437	Basic	Aug 24 2015	10:22	UTC-5	71°48.285	126°29.860	Box Core ↑	275	256	50	7	7,5	4	1018,84	86	0
3a	437	Basic	Aug 24 2015	10:47	UTC-5	71°48.167	126°30.477	Agassiz Trawl ↓	293	186	60	10	7,1	4,02	1018,83	86	0
3a	437	Basic	Aug 24 2015	11:07	UTC-5	71°47.741	126°29.897	Agassiz Trawl ↑	298	101	60	8	6,7	4,16	1018,84	88	0
3a	410	Nutrient	Aug 24 2015	12:06	UTC-5	71°41.000	126°29.000	CTD-Rosette ↓	406	329	73	2	5,5	4,09	1021,4	90	0
3a	410	Nutrient	Aug 24 2015	12:42	UTC-5	71°42.000	126°29.000	CTD-Rosette ↑	405	337		3	6	4,46	1021,22	88	0
3a	411	CTD	Aug 24 2015	13:38	UTC-5	71°37.000	126°42.000	CTD ↓	437	354		5	6,3	4,35	1021,21	89	0
3a	411	CTD	Aug 24 2015	13:53	UTC-5	71°37.000	126°42.000	CTD ↑	439	356		5	6,5	4,24	1021,29	87	0
3a	CA05-15	Mooring	Aug 24 2015	16:00	UTC-5	71°16.774	127°32.230	Mooring CA05-15 ↓	201	233	70	12	6,8	2,79	1021,59	92	0
3a	CA05-15	Mooring	Aug 24 2015			71°16.792	127°32.309	Triangulation #1 (292m)									
3a	CA05-15	Mooring	Aug 24 2015			71°16.667	127°31.374	Triangulation #2 (327m)									
3a	CA05-15	Mooring	Aug 24 2015			71°16.895	127°31.883	Triangulation #3 (330m)									
3a	CA05-15	Mooring	Aug 24 2015	17:31	UTC-5	71°16.706	127°31.021	CTD ↓	206	326	80	3	7,2	2,72	1021,81	91	0
3a	CA05-15	Mooring	Aug 24 2015	17:45	UTC-5	71°16.723	127°31.249	CTD ↑	202	353	100	1	7,3	2,67	1021,85	90	0
3a	Glider	Glider	Aug 24 2015	19:28	UTC-5	71°20.920	126°40.330	Glider ↓	442	96	20	10	8,3	6,97	1022,18	70	0
3a	412	Nutrient	Aug 24 2015	22:09	UTC-5	71°33.830	126°55.356	CTD-Rosette ↓	415	286	50	7	5,9	4,06	1019,75	85	Bergy water

3a	412	Nutrient	Aug 24 2015	22:56	UTC-5	71°33.474	126°55.795	CTD-Rosette ↑	413	341	60	6	6	3,99	1019,72	88	Bergy water
3a	413	CTD	Aug 24 2015	23:39	UTC-5	71°29.739	127°07.947	CTD ↓	375	217	20	5	5,2	3,23	1019,68	89	Bergy water
3a	413	CTD	Aug 24 2015	23:58	UTC-5	71°29.000	127°07.000	CTD ↑	376	257	0	8	6,8	3,39	1022,05	84	Bergy water
3a	414	Nutrient	Aug 25 2015	00:42	UTC-5	71°25.000	127°21.000	CTD-Rosette ↓	306	10	34	10	4,6	3,9	1021,85	96	0
3a	414	Nutrient	Aug 25 2015	01:23	UTC-5	71°24.000	127°21.000	CTD-Rosette ↑	302	249		5	5,1	3,58	1021,84	95	0
3a	408	Full	Aug 25 2015	02:16	UTC-5	71°18.000	127°34.000	CTD-Rosette ↓	204	245	30	15	4,44	2,77	1021,84	95	0
3a	408	Full	Aug 25 2015	02:41	UTC-5	71°18.000	127°34.000	CTD-Rosette ↑	206	224	5	14	6,4	2,48	1021,62	86	0
3a	408	Full	Aug 25 2015	03:00	UTC-5	71°18.000	127°34.000	Tucker Net ↓	204	136	15	15	3,6	2,5	1021,5	96	0
3a	408	Full	Aug 25 2015	03:21	UTC-5	71°17.000	127°33.000	Tucker Net ↑	210	90	0	13	3,6	2,67	1021,36	98	0
3a	408	Full	Aug 25 2015	03:50	UTC-5	71°18.000	127°35.000	Monster-Loki Net ↓	202	172	0	14	3,4	2,6	1021,51	98	0
3a	408	Full	Aug 25 2015	04:05	UTC-5	71°18.666	127°35.662	Monster-Loki Net ↑	202	146	10	14	3,4	2,6	1021,51	98	0
3a	408	Full	Aug 25 2015	04:25	UTC-5	71°18.509	127°35.897	CTD-Rosette ↓	200	224	10	12	3,2	2,49	1021,33	97	0
3a	408	Full	Aug 25 2015	05:06	UTC-5	71°18.386	127°36.341	CTD-Rosette ↑	196	254	0	8	4,5	2,43	1021,21	92	0
3a	408	Full	Aug 25 2015	05:27	UTC-5	71°18.830	127°34.717	Hydrobios ↓	209	170	20	4	4,1	2,5	1021,02	95	0
3a	408	Full	Aug 25 2015	05:41	UTC-5	71°18.760	127°35.083	Hydrobios ↑	205	105	10	11	3,1	2,56	1020,98	97	0
3a	408	Full	Aug 25 2015	06:08	UTC-5	71°18.775	127°35.517	Box Core ↓	202	213	20	12	3,1	2,59	1020,98	98	0
3a	408	Full	Aug 25 2015	06:19	UTC-5	71°18.784	127°35.677	Box Core (bottom)	202	259	20	12	3,1	2,59	1020,98	98	0
3a	408	Full	Aug 25 2015	06:30	UTC-5	71°18.794	127°35.816	Agassiz Trawl ↓	202	222	0	9	4,4	2,53	1020,91	93	0
3a	408	Full	Aug 25 2015	06:47	UTC-5	71°18.514	127°35.968	Agassiz Trawl ↑	200	98	20	11	4	2,5	1020,87	94	0
3a	417	CTD	Aug 25 2015	08:03	UTC-5	71°13.395	127°58.664	CTD ↓	84	241	40	11	4,9	5,12	1020,83	95	0
3a	417	CTD	Aug 25 2015	08:12	UTC-5	71°13.371	127°58.788	CTD ↑	85	253	30	7	6,9	5,08	1020,75	87	0
3a	418	Nutrient	Aug 25 2015	08:49	UTC-5	71°09.755	128°10.221	CTD-Rosette ↓	65	238	40	10	4,8	4,65	1018,38	95	0
3a	418	Nutrient	Aug 25 2015	09:03	UTC-5	71°09.922	128°10.418	CTD-Rosette ↑	66	244	50	9	5,9	5,34	1018,2	91	0
3a	419	CTD	Aug 25 2015	09:39	UTC-5	71°06.381	128°20.753	CTD ↓	56	240	50	12	5,9	6,35	1018,04	93	0
3a	419	CTD	Aug 25 2015	09:51	UTC-5	71°06.413	128°20.815	CTD ↑	56	256	40	10	8,3	6,41	1017,95	85	0
3a	418	Nutrient	Aug 25 2015	10:27	UTC-5	71°09.618	128°10.415	CTD-Rosette ↓	65	307	50	12	5,1	6,54	1017,46	96	0
3a	418	Nutrient	Aug 25 2015	10:43	UTC-5	71°09.692	128°10.600	CTD-Rosette ↑	65	235	40	8	5,7	5,96	1017,84	95	0
3a	420	Basic	Aug 25 2015	11:49	UTC-5	71°03.000	128°30.000	PNF ↓ ↑	41	272	70	10	5,9	6,8	1019,91	97	0
3a	420	Basic	Aug 25 2015	11:54	UTC-5	71°03.000	128°30.000	Secchi ↓ ↑	41	272	70	10	5,9	6,8	1019,91	97	0
3a	420	Basic	Aug 25 2015	12:06	UTC-5	71°03.000	128°30.000	CTD-Rosette ↓	40	269	55	9	6,4	6,79	1019,73	96	0
3a	420	Basic	Aug 25 2015	12:32	UTC-5	71°03.000	128°30.000	CTD-Rosette ↑	41	286	62	8	5,7	6,7	1019,57	97	0
3a	420	Basic	Aug 25 2015	12:51	UTC-5	71°03.000	128°31.000	Tucker Net ↓	42	230	80	8,5	6,6	6,8	1017,5	96	0
3a	420	Basic	Aug 25 2015	12:51	UTC-5	71°03.000	128°32.000	Tucker Net ↑	43	178	103	7	6,2	6,95	1019,42	96	0
3a	420	Basic	Aug 25 2015	13:16	UTC-5	71°03.000	128°32.000	Monster-Loki Net ↓	44	210	138	6	5,8	7,19	1019,34	98	0
3a	420	Basic	Aug 25 2015	13:21	UTC-5	71°03.000	128°33.000	Monster-Loki Net ↑	44	214	140	7	5,8	7,2	1019,27	98	0
3a	420	Basic	Aug 25 2015	13:49	UTC-5	71°03.000	128°31.000	Agassiz Trawl ↓	40	175	90	7	6,2	7,2	1019,1	99	0
3a	420	Basic	Aug 25 2015	14:02	UTC-5	71°02.000	128°31.000	Agassiz Trawl ↑	43	176	60	9	6,3	7,2	1019,05	99	0
3a	434	Basic	Aug 26 2015	00:03	UTC-5	70°10.000	133°33.000	PNF + Secchi ↓ ↑	47	313	120	18	10,1	8,9	1008,4	90	0
3a	434	Basic	Aug 26 2015	00:21	UTC-5	70°10.000	133°33.000	CTD-Rosette ↓	47	353	110	20	11,1	8,55	1008,64	88	0
3a	434	Basic	Aug 26 2015	00:46	UTC-5	70°10.000	133°33.000	CTD-Rosette ↑	47	5	130	20	10,5	8,34	1008,29	89	0
3a	434	Basic	Aug 26 2015	00:48	UTC-5	70°09.000	133°33.000	Tucker Net ↓	47	273	135	20	10,6	8,2	1008,1	88	0
3a	434	Basic	Aug 26 2015	01:06	UTC-5	70°10.000	133°34.000	Tucker Net ↑	45	276	130	21	10,5	8,49	1007,9	85	0
3a	434	Basic	Aug 26 2015	01:39	UTC-5	70°10.000	133°32.000	Monster-Loki Net ↓	47	308	150	21	10,7	8,87	1007,47	81	0
3a	434	Basic	Aug 26 2015	01:44	UTC-5	70°10.000	133°32.000	Monster-Loki Net ↑	46	307	140	22	10,7	8,82	1007,33	80	0
3a	434	Basic	Aug 26 2015	02:10	UTC-5	70°10.650	133°34.000	Agassiz Trawl ↓	46	300	160	23	11,1	8,8	1006,8	81	0
3a	434	Basic	Aug 26 2015	02:24	UTC-5	70°10.900	133°33.200	Agassiz Trawl ↑	47	295	160	22	10,4	9	1006,8	81	0
3a	434	Basic	Aug 26 2015	02:30	UTC-5	70°10.990	133°34.000	Agassiz Trawl ↓	46	290	145	18	10,2	8,9	1006,6	82	0
3a	434	Basic	Aug 26 2015	02:41	UTC-5	70°11.000	133°34.000	Agassiz Trawl ↑	47	298	140	20	10,1	8,91	1006,45	83	0
3a	434	Basic	Aug 26 2015	03:10	UTC-5	70°10.000	133°33.000	Box Core (bottom)	47	17	150	23	11,4	8,77	1006,07	79	0
3a	433	CTD	Aug 26 2015	04:06	UTC-5	70°17.307	133°34.763	CTD ↓	56	2	170	17	11,3	8,75	1005,69	78	0
3a	433	CTD	Aug 26 2015	04:12	UTC-5	70°17.290	133°34.650	CTD ↑	56	345	170	17	11,3	8,75	1005,69	98	0
3a	432	Nutrient	Aug 26 2015	04:54	UTC-5	70°23.650	133°36.140	CTD-Rosette ↓	63	5	170	13	11,5	8,5	1004,8	80	0
3a	432	Nutrient	Aug 26 2015	05:10	UTC-5	70°23.670	133°36.170	CTD-Rosette ↑	62	1	140	11	11	7,55	1004,41	82	0
3a	BRK-14	Mooring	Aug 26 2015	08:43	UTC-5	70°51.541	135°01.473	CTD ↓	152	95	200	7	7,6	5,94	1000,55	96	0

3a	BRK-14	Mooring	Aug 26 2015	08:56	UTC-5	70°51.612	135°01.449	CTD ↑	145	108	230	6	7,3	5,38	1000,45	97	0
3a	BRK-14	Mooring	Aug 26 2015	09:07	UTC-5	70°51.742	135°01.037	Mooring BR-K ↑(triggered, pop-up)	151	26	260	7	10,2	5,07	1000,31	85	0
3a	BRK-14	Mooring	Aug 26 2015	09:37	UTC-5	70°51.808	135°00.823	Mooring BR-K (onboard)	155	359	260	14	5,7	5,44	1000,19	97	0
3a	BS1-14	Mooring	Aug 26 2015	10:29	UTC-5	70°48.470	134°50.309	CTD ↓	79	164	270	6	6,2	6,82	1000,55	93	0
3a	BS1-14	Mooring	Aug 26 2015	10:38	UTC-5	70°48.464	134°50.161	CTD ↑	80	137	270	6	6,2	6,82	1000,55	93	0
3a	BS1-14	Mooring	Aug 26 2015	11:50	UTC-5	70°48.676	134°50.964	Mooring BS-1 not triggered : no pop-up									
3a	BS2-14	Mooring	Aug 26 2015	12:50	UTC-5	70°53.000	135°05.000	CTD ↓ (Mooring BS2-14)	307	132	250	5	5,1	4,56	1000,07	98	0
3a	BS2-14	Mooring	Aug 26 2015	13:10	UTC-5	70°52.000	135°05.000	CTD ↑	308	96	230	8	4,8	3,36	999,95	97	0
3a	BS2-14	Mooring	Aug 26 2015	13:18	UTC-5	70°52.000	135°05.000	ecoverly Mooring BS2-14 + Triangulatio	485	50	230	13	4,8	3,36	999,95	97	0
3a	BRG-14	Mooring	Aug 26 2015	15:19	UTC-5	71°00.000	135°30.000	CTD ↓	721	94	170	10	4,9	1,63	998,86	99	0
3a	BRG-14	Mooring	Aug 26 2015	15:50	UTC-5	71°00.480	135°30.850	CTD ↑	720	102	200	6	4,9	1,42	998,48	99	0
3a	BRG-14	Mooring	Aug 26 2015	16:00	UTC-5	71°00.170	135°30.720	Recovery Mooring BRG-14 triggered	709	94	190	14	5,5	1,37	998,31	99	0
3a	BRG-14	Mooring	Aug 26 2015	17:00	UTC-5	70°59.900	135°30.910	Recovery Mooring BRG-14 onboard	689	75	180	11	6,3	1,18	997,77	99	0
3a	423	CTD	Aug 26 2015	20:32	UTC-5	71°16.266	133°51.706	CTD ↓	794	2	150	10	6,5	3,9	996,85	98	0
3a	423	CTD	Aug 26 2015	21:05	UTC-5	71°16.265	133°52.501	CTD ↑	798	12	140	10	11,8	3,56	996,6	76	0
3a	424	Nutrient	Aug 26 2015	21:50	UTC-5	71°10.372	133°49.726	CTD-Rosette ↓	583	328	150	11	7,2	3,44	996,05	95	0
3a	424	Nutrient	Aug 26 2015	22:52	UTC-5	71°10.302	133°50.188	CTD-Rosette ↑	573	328	110	9	7,7	2,88	995,66	92	0
3a	435	Full	Aug 26 2015	23:41	UTC-5	71°04.756	133°37.907	PNF ↓	301	280	130	13	7,7	4,36	995	99	0
3a	435	Full	Aug 26 2015	23:44	UTC-5	71°04.751	133°37.922	PNF ↑	303	280	130	13	7,7	4,36	995	99	0
3a	435	Full	Aug 26 2015	23:45	UTC-5	71°04.751	133°37.922	Secchi ↓	303	280	130	13	7,7	4,36	995	99	0
3a	435	Full	Aug 26 2015	23:45	UTC-5	71°04.751	133°37.922	Secchi ↑	303	280	130	13	7,7	4,36	995	99	0
3a	435	Full	Aug 26 2015	23:58	UTC-5	71°04.000	133°37.000	CTD-Rosette ↓	299	90	130	16	8	4,55	994,69	98	0
3a	435	Full	Aug 27 2015	00:50	UTC-5	71°04.000	133°38.000	CTD-Rosette ↑	304	90	130	14	8	3,45	994,34	99	0
3a	435	Full	Aug 27 2015	01:08	UTC-5	71°04.000	133°38.000	Tucker Net ↓	295	231	120	14	7,9	4,6	994,26	99	0
3a	435	Full	Aug 27 2015	01:31	UTC-5	71°04.000	133°40.000	Tucker Net ↑	258	147	130	16	8	5,25	994,13	99	0
3a	435	Full	Aug 27 2015	01:59	UTC-5	71°04.000	133°37.000	Monster-Loki Net ↓	329	100	140	12	8,2	5,04	993,79	99	0
3a	435	Full	Aug 27 2015	02:23	UTC-5	71°04.000	133°38.000	Monster-Loki Net ↑	297	89	150	11	10	4,24	993,74	95	0
3a	435	Full	Aug 27 2015	02:37	UTC-5	71°04.000	133°38.000	CTD-Rosette ↓	300	80	165	11	9,4	4,21	993,6	96	0
3a	435	Full	Aug 27 2015	03:06	UTC-5	71°04.000	133°37.000	CTD-Rosette ↑	303	84	170	16	9,7	3,55	993,4	98	0
3a	435	Full	Aug 27 2015	03:27	UTC-5	71°04.000	133°38.000	Hydrobios ↓	295	340	160	17	9,7	3,4	993,3	97	0
3a	435	Full	Aug 27 2015	03:45	UTC-5	71°04.000		Hydrobios ↑	296	82	160	15	9,6	3,98	993,37	98	0
3a	435	Full	Aug 27 2015	04:08	UTC-5	71°04.730	133°38.050	Agassiz Trawl ↓	298	320	170	8	9,9	4,07	991,03	96	0
3a	435	Full	Aug 27 2015	04:45	UTC-5	71°04.500	133°40.320	Agassiz Trawl ↑	300	170	130	11	9,9	5,37	993,08	96	0
3a	435	Full	Aug 27 2015	05:20	UTC-5	71°04.790	133°38.070	Box Core 1 ↓	308	345	130	7	9,8	5,56	992,88	97	0
3a	435	Full	Aug 27 2015	05:28	UTC-5	71°04.770	133°38.150	Box Core 1 (bottom)	302	300	130	7	9,8	5,56	992,88	97	0
3a	435	Full	Aug 27 2015	05:35	UTC-5	71°04.780	133°38.170	Box Core 1 ↑	301	311	130	7	9,8	5,56	992,88	97	0
3a	435	Full	Aug 27 2015	05:50	UTC-5	71°04.750	133°37.980	Box Core 2 ↓	302	86	130	8	9,6	4,54	992,71	98	0
3a	435	Full	Aug 27 2015	05:58	UTC-5	71°04.740	133°37.960	Box Core 2 (bottom)	307	70	130	8	9,4	4,77	992,4	98	0
3a	435	Full	Aug 27 2015	06:06	UTC-5	71°04.740	133°37.940	Box Core 2 ↑	307	80	130	8	9,4	4,77	992,4	98	0
3a	435	Full	Aug 27 2015	06:20	UTC-5	71°04.760	133°37.720	Box Core 3 ↓	302	56	120	7	9,1	4,99	992,56	99	0
3a	435	Full	Aug 27 2015	06:30	UTC-5	71°04.750	133°37.790	Box Core 3 (bottom)	302	82	120	7	9,1	4,99	992,56	99	0
3a	435	Full	Aug 27 2015	06:37	UTC-5	71°04.720	133°37.900	Box Core 3 ↑	302	90	100	6	9	5,14	992,55	99	0
3a	BRK-15	Mooring	Aug 27 2015	09:24	UTC-5	70°51.785	135°01.624	Start deploying Mooring BRK-15	171	293	340	16	3,3	5,22	991,6	99	0
3a	BRK-15	Mooring	Aug 27 2015	09:29	UTC-5	70°51.750	135°01.677	Mooring BRK-15 Deployed	170	352	340	16	3,3	5,22	991,6	99	0
3a	BRK-15	Mooring	Aug 27 2015		UTC-5	70°51.823	135°02.025	Triangulation #1 (274m)									
3a	BRK-15	Mooring	Aug 27 2015		UTC-5	70°51.671	135°01.624	Triangulation #2 (238m)									
3a	BRK-15	Mooring	Aug 27 2015		UTC-5	70°51.850	135°01.376	Triangulation #3 (312m)									
3a	BRK-15	Mooring	Aug 27 2015	10:08	UTC-5	70°51.480	135°02.298	CTD ↓	157	132	340	19	2,4	5,11	992,19	99	0
3a	BRK-15	Mooring	Aug 27 2015	10:21	UTC-5	70°51.390	135°02.449	CTD ↑	153	193	330	17	2,9	4,54	992,76	99	0
3a	BS1-14	Mooring	Aug 27 2015	11:55	UTC-5	70°48.711	134°50.835	Mooring BS1-14 triggered : pop-up	80	280	330	28	2,6	6,3	993,32	99	0
3a	BS1-14	Mooring	Aug 27 2015	14:45	UTC-5	70°47.340	134°52.680	Mooring BS1-14 onboard	76	350	310	30	1,8	6	994,9	99	0
3a	422	Nutrient	Aug 28 2015	06:30	UTC-5	71°22.810	133°52.940	CTD-Rosette ↓	1101	112,2	270	18	0,2	1,98	1001,83	97	2/10
3a	422	Nutrient	Aug 28 2015	07:47	UTC-5	71°22.620	133°51.640	CTD-Rosette ↓	1085	130,9	270	20	1,7	2,11	1002,89	89	2/10
3a	BRG-15	Mooring	Aug 28 2015	12:09	UTC-5	71°00.000	135°30.000	CTD ↓	708	90	270	14	1,5	1,18	1005,46	95	0

3a	BRG-15	Mooring	Aug 28 2015	12:38	UTC-5	71°00.000	135°30.000	CTD ↑	697	102	260	18	4,2	1,22	1006,2	85	0
3a	BRG-15	Mooring	Aug 28 2015	13:48	UTC-5	71°00.000	135°30.000	Mooring BRG-15	702	190	260	15	1,4	1,12	1005,38	93	1/10
3a	BRG-15	Mooring	Aug 28 2015	14:20	UTC-5	70°59.000	135°28.000	Triangulation #1 (1182m)	689	157	250	13	1	1,21	1006,87	95	1/10
3a	BRG-15	Mooring	Aug 28 2015	14:26	UTC-5	71°00.000	135°31.000	Triangulation #2 (1175m)	706	288	250	13	1	1,21	1006,87	95	1/10
3a	BRG-15	Mooring	Aug 28 2015	14:30	UTC-5	71°00.000	135°29.000	Triangulation #3 (1410m)	719	21	250	13	1	1,21	1006,87	95	1/10
3a	BS3-14	Mooring	Aug 28 2015	15:40	UTC-5	70°55.000	135°13.000	CTD ↓	491	72	250	13	2,7	1,9	1008,42	87	1/10
3a	BS3-14	Mooring	Aug 28 2015	16:02	UTC-5	70°55.470	135°13.320	CTD ↑	492	90	270	7	3,5	2,1	1009,01	83	1/10
3a	BS3-14	Mooring	Aug 28 2015	16:24	UTC-5	70°55.660	135°14.030	Mooring BS3-14 triggered, pop-up)	501	140	260	13	1,8	2,11	1009,18	87	1/10
3a	BS3-14	Mooring	Aug 28 2015	16:47	UTC-5	70°55.610	135°14.220	Mooring BS3-14 onboard	502	190	260	4	2,5	1,96	1009,52	85	1/10
3a	Lander 2	Lander	Aug 28 2015	18:30	UTC-5	70°50.150	135°07.800	CTD-Rosette ↓	164	114	280	10	3	2,13	1010,38	77	1/10
3a	Lander 2	Lander	Aug 28 2015	18:40	UTC-5	70°50.100	135°07.860	CTD-Rosette ↑	171	99	260	4	3,7	2,64	1010,25	73	1/10
3a	Lander 2	Lander	Aug 28 2015	18:55	UTC-5	70°50.170	135°07.800	Box Core ↓	175	102	260	6	3,2	2,76	1010,25	76	1/10
3a	Lander 2	Lander	Aug 28 2015	18:58	UTC-5	70°50.140	135°07.830	Box Core (bottom)	167	119	260	6	3,2	2,76	1010,25	76	1/10
3a	Lander 2	Lander	Aug 28 2015	19:03	UTC-5	70°50.110	135°07.850	Box Core ↑	167	125	260	6	3,2	2,76	1010,25	76	1/10
3a	Lander 2	Lander	Aug 28 2015	19:58	UTC-5	70°50.169	135°07.754	Lander 2 deployment	169	1	200	6	3,2	2,84	1010,24	78	1/10
3a	Lander 2	Lander	Aug 28 2015	20:08	UTC-5	70°50.140	135°07.748	Lander 2 (Bottom)	168	353	200	6	3,2	2,84	1010,24	78	0
3a	Lander 2	Lander	Aug 28 2015	20:17	UTC-5	70°50.031	135°07.869	Lander's Anchor deployed	166	77	200	5	3,1	2,85	1008,18	78	0
3a	Lander 2	Lander	Aug 28 2015	20:35	UTC-5	70°50.176	135°07.277	Triangulation #1 (437m)	169								
3a	Lander 2	Lander	Aug 28 2015	20:44	UTC-5	70°50.157	135°08.258	Triangulation #2 (412m)	176								
3a	Lander 2	Lander	Aug 28 2015	20:50	UTC-5	70°50.357	135°07.727	Triangulation #3 (643m)	179								
3a	Lander 1	Lander	Aug 28 2015	21:12	UTC-5	70°52.221	135°01.662	Box Core ↓	205	348	220	5	3	2,97	1008,79	80	0
3a	Lander 1	Lander	Aug 28 2015	21:12	UTC-5	70°52.217	135°01.649	Box Core (bottom)	206	351	190	3	3,3	3,2	1009,03	77	0
3a	Lander 1	Lander	Aug 28 2015	21:17	UTC-5	70°52.222	135°01.595	Box Core ↑	206	350	190	3	3,3	3,2	1009,03	77	0
3a	Lander 1	Lander	Aug 28 2015	21:47	UTC-5	70°52.160	135°01.112	Lander 1 deployment	187	242	200	7	3	3,43	1008,66	77	0
3a	Lander 1	Lander	Aug 28 2015	21:51	UTC-5	70°52.160	135°01.127	Lander 1 (Bottom)	187	211	210	6	3,1	3,37	1008,33	78	0
3a	Lander 1	Lander	Aug 28 2015	22:02	UTC-5	70°52.217	135°00.670	Lander's Anchor Deployed	183	254	210	6	3	3,39	1008,58	78	0
3a	Lander 1	Lander	Aug 28 2015	22:05	UTC-5	70°52.229	135°00.573	Triangulation #1 (205m)	186								
3a	Lander 1	Lander	Aug 28 2015	22:12	UTC-5	70°52.299	135°01.787	Triangulation #2 (735m)	217								
3a	Lander 1	Lander	Aug 28 2015	22:19	UTC-5	70°52.034	135°01.661	Triangulation #3 (692m)	187								
3a	431	CTD	Aug 29 2015	01:33	UTC-5	70°29.000	133°37.000	CTD ↓	67	260	290	5	3,3	5,57	1009,19	76	0
3a	431	CTD	Aug 29 2015	01:41	UTC-5	70°29.000	133°37.000	CTD ↑	67	257	130	3	3,3	5,56	1009,19	76	0
3a	430	Nutrient	Aug 29 2015	02:24	UTC-5	70°35.000	133°38.000	CTD-Rosette ↓	71	260	140	5	3,3	5,64	1009,11	77	0
3a	430	Nutrient	Aug 29 2015	02:42	UTC-5	70°35.000	133°38.000	CTD-Rosette ↑	72	248	130	6	3,2	5,46	1009,02	77	0
3a	429	CTD	Aug 29 2015	03:21	UTC-5	70°40.000	133°39.000	CTD ↓	70	260	130	8	3,3	5,23	1008,82	77	0
3a	429	CTD	Aug 29 2015	03:28	UTC-5	70°40.000	133°39.000	CTD ↑	69	222	130	7	3,3	5,23	1008,82	77	0
3a	428	Nutrient	Aug 29 2015	04:05	UTC-5	70°47.430	133°41.240	CTD-Rosette ↓	75	256	130	7	3,3	5,14	1008,84	76	0
3a	428	Nutrient	Aug 29 2015	04:24	UTC-5	70°47.520	133°40.900	CTD-Rosette ↑	75	4	120	9	3	4,88	1008,86	77	0
3a	427	CTD	Aug 29 2015	05:00	UTC-5	70°52.830	133°43.080	CTD ↓	81	340	140	7	3,3	4,6	1008,79	75	0
3a	427	CTD	Aug 29 2015	05:07	UTC-5	70°52.800	133°42.960	CTD ↑	81	19	120	10	3,2	4,69	1008,8	75	0
3a	426	Nutrient	Aug 29 2015	05:46	UTC-5	70°59.060	133°44.820	CTD-Rosette ↓	100	43	120	9	3	3,15	1008,76	81	0
3a	426	Nutrient	Aug 29 2015	06:13	UTC-5	70°59.050	133°44.980	CTD-Rosette ↑	101	336	120	9	3	3,15	1008,76	81	0
3a	---	Horizontal Net	Aug 29 2015	07:12	UTC-5	71°03.530	133°39.530	Beam Trawl ↓	240	326	110	10	1,8	1,18	1008,53	89	1/10
3a	---	Horizontal Net	Aug 29 2015	07:56	UTC-5	71°02.984	133°42.192	Beam Trawl↑	225	225	110	12	1,9	1,02	1008,41	88	1/10
3a	435	Benthos	Aug 29 2015	09:15	UTC-5	71°12.537	133°41.540	CTD-Rosette ↓	720	339	120	12	1,4	0,49	1007,97	92	eaux berge
3a	435	Benthos	Aug 29 2015	09:48	UTC-5	71°12.511	133°41.643	CTD-Rosette ↑	724	349	120	11	0,8	0,61	1007,92	94	1/10
3a	435	Benthos	Aug 29 2015	09:58	UTC-5	71°12.490	133°41.840	Agassiz Trawl ↓	716	270	110	10	1,5	0,68	1007,85	93	1/10
3a	435	Benthos	Aug 29 2015	11:58	UTC-5	71°11.290	133°44.407	Agassiz Trawl ↑	648	196	80	12	0,8	0,39	1007,34	95	1/10
3a	421	Basic	Aug 29 2015	18:00	UTC-5	71°25.710	133°58.510	PNF + Secchi↓↑	1356	305	80	16	0,9	0,6	1004,87	94	6/10
3a	421	Basic	Aug 29 2015	18:10	UTC-5	71°25.810	133°59.350	CTD-Rosette ↓	1208	316	80	18	1,1	0,4	1005,23	95	6/10
3a	421	Basic	Aug 29 2015	19:10	UTC-5	71°25.880	133°59.950	CTD-Rosette ↑	1211	331	110	15	0,3	0,27	1005,02	96	6/10
3a	421	Basic	Aug 29 2015	19:22	UTC-5	71°25.830	133°59.790	Tucker Net ↓	1209	271	70	15	0,3	0,28	1004,95	96	6/10
3a	421	Basic	Aug 29 2015	19:45	UTC-5	71°25.730	133°59.000	Tucker Net ↑	1209	290	80	17	0	0,23	1004,39	96	6/10
3a	421	Basic	Aug 29 2015	20:12	UTC-5	71°25.790	133°59.930	Monster-Loki Net ↓	1209	209	70	16	-0,6	0,24	1003,88	98	5/10
3a	421	Basic	Aug 29 2015	21:10	UTC-5	71°25.730	134°00.250	Monster-Loki Net ↑	1209	210	60	16	-0,4	0,34	1003,2	98	5/10

3a	421	Basic	Aug 29 2015	21:43	UTC-5	71°25.730	134°00.470	CTD-Rosette ↓	1210	308	70	13	0,8	0,32	1003,49	96	5/10
3a	421	Basic	Aug 29 2015	23:07	UTC-5	71°25.470	134°00.600	CTD-Rosette ↑	1207	268	70	10	2,9	0,28	1003,19	87	5/10
3a	421	Basic	Aug 29 2015	23:28	UTC-5	71°25.620	134°59.880	Box Core ↓	1209	218	60	11	0,8	0,28	1002,78	91	5/10
3a	421	Basic	Aug 29 2015	23:51	UTC-5	71°25.589	134°00.038	Box Core (bottom)	1203	223	60	13	-1	0,31	1001,99	99	5/10
3a	BR4-14	Mooring	Aug 30 2015	20:49	UTC-5	73°13.200	127°02.828	Mooring BR4-14 triggered, pop-up)	160	347	100	5	4,6	0,08	1000,09	92	5/10
3a	BR4-14	Mooring	Aug 30 2015	21:04	UTC-5	73°13.229	127°02.982	Mooring BR4-14 onboard	160	29	110	4	4,3	0,08	1000,01	93	5/10
3a	BR4-14	Mooring	Aug 30 2015	21:12	UTC-5	73°13.370	127°03.000	CTD ↓	158	321	90	11	4	0,08	1000,01	93	5/10
3a	BR4-14	Mooring	Aug 30 2015	21:23	UTC-5	73°13.360	127°03.090	CTD ↑	158	329	90	11	3,7	0,05	1000,08	94	5/10
3a	535	Full	Aug 31 2015	00:58	UTC-5	73°24.778	128°10.560	CTD-Rosette ↓	287	281	90	18	5,7	0,06	999,98	98	2/10
3a	535	Full	Aug 31 2015	01:41	UTC-5	73°24.754	128°11.020	CTD-Rosette ↑	287	251	90	20	2,7	0,1	1000,18	99	2/10
3a	535	Full	Aug 31 2015	02:10	UTC-5	73°24.876	128°09.276	Tucker Net ↓	278	167	85	23	3,1	0,11	1000,29	99	2/10
3a	535	Full	Aug 31 2015	02:30	UTC-5	73°24.115	128°09.881	Tucker Net ↑	282	141	70	20	3,8	0,12	1000,32	99	2/10
3a	535	Full	Aug 31 2015	02:53	UTC-5	73°24.500	128°15.784	Monster-Loki Net ↓	301	256	70	20	4,7	0,11	1000,37	98	2/10
3a	535	Full	Aug 31 2015	03:17	UTC-5	73°24.520	128°13.962	Monster-Loki Net ↑	300	252	70	17	4,6	0,12	1000,24	95	2/10
3a	535	Full	Aug 31 2015	03:35	UTC-5	73°24.937	128°11.870	CTD-Rosette ↓	291	243	85	20	3,1	0,15	1000,11	99	2/10
3a	535	Full	Aug 31 2015	04:13	UTC-5	73°24.910	128°12.330	CTD-Rosette ↑	291	324	70	22	2,9	0,08	1000,41	99	2/10
3a	535	Full	Aug 31 2015	04:31	UTC-5	73°24.960	128°12.280	Hydrobios ↓	291	242	80	23	2,9	0,08	1000,46	99	2/10
3a	535	Full	Aug 31 2015	04:50	UTC-5	73°25.050	128°12.650	Hydrobios ↑	295	247	80	22	2,8	0,1	1000,34	99	2/10
3a	535	Full	Aug 31 2015	05:10	UTC-5	73°25.010	128°11.840	Agassiz Trawl ↓	291	256	80	24	3,1	0,08	1000,46	99	2/10
3a	535	Full	Aug 31 2015	05:50	UTC-5	73°24.220	128°14.000	Agassiz Trawl ↑	304	150	80	22	3,1	0,06	1000,5	99	2/10
3a	535	Full	Aug 31 2015	06:09	UTC-5	73°25.010	128°11.610	Box Core ↓	290	283	70	23	3,2	0,03	1000,15	99	2/10
3a	535	Full	Aug 31 2015	06:17	UTC-5	73°25.010	128°11.760	Box Core (bottom)	291	316	70	23	3,2	0,03	1000,15	99	2/10
3a	535	Full	Aug 31 2015	06:24	UTC-5	73°25.030	128°11.780	Box Core ↑	291	325	70	23	3,2	0,03	1000,15	99	2/10
3a	536/BR3-14	Basic	Aug 31 2015	09:12	UTC-5	73°24.230	129°21.440	CTD ↓	692	308	90	15	2,5	-0,44	1000,73	99	6/10
3a	536/BR3-14	Basic	Aug 31 2015	09:38	UTC-5	73°24.090	129°22.030	CTD ↑	701	298	80	19	2,7	-0,41	1000,76	99	6/10
3a	BR3-14	Mooring	Aug 31 2015	12:11	UTC-5	73°24.583	129°21.608	Mooring BR3-14 triggered, pop-up)	706	89	90	20	2,2	-0,41	1002,76	99	6/10
3a	BR3-14	Mooring	Aug 31 2015	13:15	UTC-5	73°24.790	129°22.741	Mooring BR3-14 onboard	738	345	80	22	2,6	-0,4	1002,2	99	6/10
3a	536/BR3-15	Basic	Aug 31 2015	14:44	UTC-5	73°25.142	129°23.405	CTD ↓	732	274	80	15	4,4	-0,41	1003,62	93	6/10
3a	536/BR3-15	Basic	Aug 31 2015	15:39	UTC-5	73°25.114	129°24.089	CTD ↑	735	278	85	21	4,9	-0,41	1002,72	92	6/10
3a	BR3-15	Mooring	Aug 31 2015	17:59	UTC-5	73°24.550	129°21.410	Mooring BR3-15 deployment	695	99	70	15	3	-0,33	1002,85	99	6/10
3a	536/BR3-15	Basic	Aug 31 2015	18:04	UTC-5	73°25.070	129°21.490	PNF + Secchi ↓↑	723	277	80	18	4,2	-0,3	1003,6	94	6/10
3a	536/BR3-15	Basic	Aug 31 2015	18:15	UTC-5	73°25.010	129°21.650	CTD ↓	725	264	80	15	6,7	-0,29	1003,69	85	6/10
3a	536/BR3-15	Basic	Aug 31 2015	19:02	UTC-5	73°24.910	129°22.110	CTD ↑	730	277	80	17	6	-0,35	1004,07	87	6/10
3a	BR3-15	Mooring	Aug 31 2015		UTC-5	73°24.768	129°20.999	Triangulation #1 (808m)									
3a	BR3-15	Mooring	Aug 31 2015		UTC-5	73°24.604	129°21.549	Triangulation #2 (722m)									
3a	BR3-15	Mooring	Aug 31 2015		UTC-5	73°24.590	129°20.300	Triangulation #3 (851m)									
3a	536/BR3-15	Horizontal Net	Sep 01 2015	02:37	UTC-5	74°10.610	126°20.700	Beam Trawl ↓	230	230	80	18	3,5	0,6	1009,45	95	3/10
3a	536/BR3-15	Horizontal Net	Sep 01 2015	03:22	UTC-5	74°06.745	126°19.919	Beam Trawl ↑		150	65	16	2,5	1,06	1009,49	98	3/10
3a	SI_beacon1	Ice	Sep 01 2015	12:47	UTC-5	74°45.425	126°37.136	Ice work ↓	393	139	100	17	1,5	0,03	1012,88	99	3/10
3a	SI_beacon1	Ice	Sep 01 2015	13:11	UTC-5	74°45.425	126°37.137	Ice work ↑	395	136	98	18	1,5	0,03	1012,88	99	3/10
3a	518	Basic	Sep 01 2015	22:42	UTC-5	74°33.860	121°27.130	PNF ↓	183	315	100	11	2,2	-0,2	1017,02	96	0
3a	518	Basic	Sep 01 2015	22:45	UTC-5	74°33.860	121°27.190	PNF ↑	182	333	100	11	2,2	-0,2	1017,02	96	0
3a	518	Basic	Sep 01 2015	22:46	UTC-5	74°33.850	121°27.210	Secchi ↓	180	321	100	11	2,2	-0,2	1017,02	96	0
3a	518	Basic	Sep 01 2015	22:47	UTC-5	74°33.850	121°27.230	Secchi ↑	179	315	100	11	2,2	-0,2	1017,02	96	0
3a	518	Basic	Sep 01 2015	22:56	UTC-5	74°33.880	121°27.110	CTD-Rosette ↓	185	301	90	14	2,7	-0,23	1017,25	94	0
3a	518	Basic	Sep 01 2015	23:27	UTC-5	74°33.800	121°27.310	CTD-Rosette ↑	170	2	110	10	4,7	-0,3	1017,36	88	0
3a	518	Basic	Sep 01 2015	23:42	UTC-5	74°34.090	121°26.970	Tucker Net ↓	224	283	90	9	2,1	-0,3	1017,36	95	0
3a	518	Basic	Sep 02 2015	00:10	UTC-5	74°33.670	121°27.950	Tucker Net ↑	101	200	92	10	4	-0,4	1017,49	96	0
3a	518	Basic	Sep 02 2015	00:31	UTC-5	74°34.373	121°27.063	Monster-Loki Net ↓	260	300	120	6	2	-0,33	1017,56	96	0
3a	518	Basic	Sep 02 2015	00:54	UTC-5	74°34.366	121°26.496	Monster-Loki Net ↑	283	76	120	5	2,3	-0,25	1017,69	94	0
3a	518	Basic	Sep 02 2015	01:06	UTC-5	74°34.337	121°26.328	CTD-Rosette ↓	280	348	120	7	1,5	-0,24	1017,69	96	0
3a	518	Basic	Sep 02 2015	01:51	UTC-5	74°34.308	121°25.296	CTD-Rosette ↑	316	341	150	11	3,6	-0,13	1017,82	93	0
3a	518	Basic	Sep 02 2015	02:28	UTC-5	74°34.341	121°26.567	Box Core (bottom)	269	30	150	11	4,1	-0,07	1017,89	93	0
3a	518	Basic	Sep 02 2015	02:45	UTC-5	74°34.372	121°25.955	Agassiz Trawl ↓	308	320	150	10	3,1	-0,05	1017,89	94	0

3a	518	Basic	Sep 02 2015	03:23	UTC-5	74°34.200	121°28.700	Agassiz Trawl ↑	227	250	160	15,1	5	-0,17	1017,68	90	0
3a	518	Basic	Sep 02 2015	03:45	UTC-5	74°34.450	121°26.330	Mapping (Start)	200	180	170	17,9	5,5	-0,26	1017,65	89	1/10
3a	518	Basic	Sep 02 2015	05:30	UTC-5	74°33.850	121°11.410	Mapping (End)	420	20	190	13	5,2	-0,11	1017,98	88	1/10
3a	516	Nutrient	Sep 02 2015	06:57	UTC-5	74°49.690	120°50.290	CTD-Rosette ↓	468	333	140	10	1,9	0,79	1018,69	98	1/10
3a	516	Nutrient	Sep 02 2015	07:42	UTC-5	74°49.670	120°50.940	CTD-Rosette ↑	465	317	150	12	2,1	0,93	1018,79	96	1/10
3a	514	Basic	Sep 02 2015	09:15	UTC-5	75°06.270	120°37.410	PNF ↓	456	231	140	12	1,1	0,11	1019,12	98	2/10
3a	514	Basic	Sep 02 2015	09:19	UTC-5	75°06.270	120°37.420	PNF ↑	457	252	140	12	0,9	0,17	1019,09	98	2/10
3a	514	Basic	Sep 02 2015	09:20	UTC-5	75°06.280	120°37.440	Secchi ↓	457	255	130	11	0,9	0,17	1019,09	98	2/10
3a	514	Basic	Sep 02 2015	09:23	UTC-5	75°06.290	120°37.450	Secchi ↑	462	267	130	11	0,9	0,17	1019,09	98	2/10
3a	514	Basic	Sep 02 2015	09:38	UTC-5	75°06.900	120°38.490	CTD-Rosette ↓	467	347	130	11	1,1	0,21	1019,16	99	2/10
3a	514	Basic	Sep 02 2015	10:22	UTC-5	75°06.910	120°39.420	CTD-Rosette ↑	468	14	130	8	4	0,2	1019,28	88	2/10
3a	514	Basic	Sep 02 2015	10:38	UTC-5	75°07.060	120°40.100	Tucker Net ↓	467	275	130	12	1,2	0,17	1019,21	98	2/10
3a	514	Basic	Sep 02 2015	10:56	UTC-5	75°06.990	120°42.410	Tucker Net ↑	468	254	130	12	1,2	0,17	1019,21	98	2/10
3a	514	Basic	Sep 02 2015	11:23	UTC-5	75°07.460	120°41.410	Monster-Loki Net ↓	466	325	150	6	1,8	0,19	1019,15	97	2/10
3a	514	Basic	Sep 02 2015	11:53	UTC-5	75°07.600	120°41.360	Monster-Loki Net ↑	464	308	150	12	1	0,17	1019,33	98	2/10
3a	514	Basic	Sep 02 2015	12:42	UTC-5	75°06.178	120°37.725	CTD-Rosette ↓	457	334	158	13	1,4	0,11	1019,21	99	2/10
3a	514	Basic	Sep 02 2015	13:21	UTC-5	75°06.206	120°37.720	CTD-Rosette ↑	474	28	160	16	2	0,04	1019,4	97	2/10
3a	514	Basic	Sep 02 2015	13:48	UTC-5	75°06.226	120°37.679	Box Core (bottom)	457	27	160	15	2	0,04	1019,42	97	2/10
3a	514	Basic	Sep 02 2015	14:14	UTC-5	75°06.098	120°37.186	Agassiz Trawl ↓	451	273	160	14,6	2	0,06	1019,57	97	2/10
3a	514	Basic	Sep 02 2015	14:59	UTC-5	75°06.110	120°35.427	Agassiz Trawl ↑	440	0,16	160	13	2,6	0,04	1019,77	97	2/10
3a	512	Nutrient	Sep 02 2015	16:50	UTC-5	75°22.580	120°33.010	CTD-Rosette ↓	412	24	180	8	1,8	0,18	1019,99	98	2/10
3a	512	Nutrient	Sep 02 2015	17:26	UTC-5	75°22.680	120°33.400	CTD-Rosette ↑	414	16	160	10	2,6	0,33	1020,21	95	2/10
3a	510	Nutrient	Sep 02 2015	18:57	UTC-5	75°38.330	120°38.360	CTD-Rosette ↓	374	0,23	160	11	1,1	0,21	1020,11	99	3/10
3a	510	Nutrient	Sep 02 2015	19:30	UTC-5	75°38.390	120°38.340	CTD-Rosette ↑	370	0,76	170	12	1,5	0,65	1019,94	98	3/10
3b	CB1	Geotrace	Sep 05 2015	13:32	UTC-5	73°51.643	129°44.595	TM-Rosette ↓	1226	295	20	5	0,2	-0,08	1021,41	99	3/10
3b	CB1	Geotrace	Sep 05 2015	14:16	UTC-5	73°51.567	129°44.555	TM-Rosette ↑	1227	308	32	5	0,1	-0,07	1021,46	99	3/10
3b	CB1	Geotrace	Sep 05 2015	14:50	UTC-5	73°51.494	129°44.665	LVP ↓ (moonpool) (test)	1230	283	30	6	0,3	-0,07	1021,49	99	2/10
3b	CB1	Geotrace	Sep 05 2015	15:03	UTC-5	73°51.447	129°44.694	LVP ↑ (moonpool) (test)	1230	286	30	5	0,4	-0,06	1021,49	99	2/10
3b	---	Mapping	Sep 06 2015	02:41	UTC-5	74°22.796	124°37.791	Mapping 200m	200	60	0	10	-0,5	2,31	1017,53	99	2/10
3b	---	MVP	Sep 06 2015	08:21	UTC-5	74°34.940	121°39.760	MVP ↓	314	60	320	4	-0,7	1,66	1019,39	99	0
3b	---	MVP	Sep 06 2015	13:54	UTC-5	75°00.000	120°06.000	MVP ↑	398		280	5,5	-1,5	1,33	1023,5	99	0
3b	CB1	Geotrace	Sep 06 2015	14:52	UTC-5	75°00.000	120°00.000	CTD-Rosette ↓	413	75	160	8	-2,2	0,97	1017,86	99	0
3b	CB1	Geotrace	Sep 06 2015	15:22	UTC-5	Error		CTD-Rosette ↑									
3b	CB1	Geotrace	Sep 06 2015	16:17	UTC-5	75°07.350	120°38.500	CTD-Rosette ↓	464	98	270	6	-1	1,11	1021,4	99	0
3b	CB1	Geotrace	Sep 06 2015	16:45	UTC-5	75°07.360	120°38.230	CTD-Rosette ↑	465	102	260	6	-1	1,17	1023,29	99	0
3b	CB1	Geotrace	Sep 06 2015	17:08	UTC-5	75°07.179	120°38.063	TM-Rosette ↓ (problem)	464	80	240	7	-1,5	1,16	1023,96	99	1/10
3b	CB1	Geotrace	Sep 06 2015	17:19	UTC-5	75°07.162	120°37.942	TM-Rosette ↑ (problem)	466	61	268	10	-2,5	1,13	1022,07	99	1/10
3b	CB1	Geotrace	Sep 06 2015	17:42	UTC-5	Cancelled		TM-Rosette ↓									
3b	CB1	Geotrace	Sep 06 2015	17:42	UTC-5	Cancelled		TM-Rosette ↑									
3b	CB1	Geotrace	Sep 06 2015	18:42	UTC-5	75°07.080	120°36.890	LVP ↓ (moonpool)	466	308	290	8	-2,1	1,2	1014,43	99	1/10
3b	CB1	Geotrace	Sep 06 2015	22:05	UTC-5	75°06.730	120°35.590	LVP ↑ (moonpool)	457	85	270	8	-2,4	0,98	1010,12	99	1/10
3b	CB1	Geotrace	Sep 06 2015	22:35	UTC-5	75°06.410	120°31.100	CTD-Rosette ↓	432	210	270	9	-2,4	1,04	1010,39	99	1/10
3b	CB1	Geotrace	Sep 06 2015	23:38	UTC-5	75°06.350	120°31.150	CTD-Rosette ↑	430	138	300	8	-1,3	1,11	1009,73	98	1/10
3b	CB1	Geotrace	Sep 06 2015	23:52	UTC-5	75°06.030	120°31.060	Tucker Net ↓	429	158	290	5	-1,5	1,12	1009,42	98	1/10
3b	CB1	Geotrace	Sep 07 2015	00:13	UTC-5	75°05.941	120°28.188	Tucker Net ↑	419	85	280	7,2	-3	1,08	1011,31	99	1/10
3b	CB1	Geotrace	Sep 07 2015	01:15	UTC-5	75°06.110	120°33.842	CTD-Rosette ↓	437	154	280	14	-1,7	1	1013,42	98	1/10
3b	CB1	Geotrace	Sep 07 2015	01:58	UTC-5	75°06.095	120°33.569	CTD-Rosette ↑	435	173	300	11	-0,7	1,07	1014,14	97	1/10
3b	CB1	Geotrace	Sep 07 2015	02:14	UTC-5	75°05.592	120°33.455	LVP ↓	431	157	300	10	-1,6	1,02	1014,23	99	1/10
3b	CB1	Geotrace	Sep 07 2015	06:05	UTC-5	75°05.650	120°33.300	LVP ↑	431	68	260	7	-0,8	1,02	1017,21	99	1/10
3b	CB1	Geotrace	Sep 07 2015	06:42	UTC-5	75°05.600	120°33.160	Monster-Loki Net ↓	431	66	260	6	-0,6	1,01	1017,76	99	1/10
3b	CB1	Geotrace	Sep 07 2015	07:13	UTC-5	75°05.570	120°33.280	Monster-Loki Net ↑	431	110	270	5	-0,4	0,99	1018,11	99	1/10
3b	CB1	Geotrace	Sep 07 2015	08:35	UTC-5	75°05.460	120°33.090	Hydrobios ↓	430	101	290	5	-0,7	1,06	1015,85	99	1/10
3b	CB1	Geotrace	Sep 07 2015	09:01	UTC-5	75°05.400	120°32.850	Hydrobios ↑	430	83	280	6	-0,4	1,06	1016,44	99	1/10
3b	CB1	Geotrace	Sep 07 2015	10:35	UTC-5	75°06.890	120°21.460	TM Rosette ↓ (problem)	409	112	270	2	-0,5	0,94	1015,76	99	1/10

3b	CB1	Geotrace	Sep 07 2015	11:02	UTC-5	75°06.810	120°21.480	TM Rosette ↑ (problem)	408	64	250	1	-0,3	1,19	1014,69	99	1/10
3b	CB1	Geotrace	Sep 07 2015	11:22	UTC-5	75°06.750	120°21.400	Box Core ↓	407	53	240	2	-0,1	1,24	1015,39	99	1/10
3b	CB1	Geotrace	Sep 07 2015	11:32	UTC-5	75°06.730	120°21.340	Box Core (bottom)	409	52	230	1	0,2	1,24	1015,48	99	1/10
3b	CB1	Geotrace	Sep 07 2015	11:42	UTC-5	75°06.710	120°21.260	Box Core ↑	409	74	200	2	0,5	1,23	1015,59	99	1/10
3b	CB1	Geotrace	Sep 07 2015	12:42	UTC-5	75°06.840	120°22.055	Box Core ↓	408	60	255	4,2	-0,6	1,17	1015,11	99	1/10
3b	CB1	Geotrace	Sep 07 2015	12:52	UTC-5	75°06.816	120°21.993	Box Core (bottom)	409	39	240	4	-0,2	1,19	1015,45	99	1/10
3b	CB1	Geotrace	Sep 07 2015	13:01	UTC-5	75°06.818	120°22.013	Box Core ↑	409	3	240	4	-0,4	1,21	1015,41	99	1/10
3b	CB1	Geotrace	Sep 07 2015	13:12	UTC-5	75°06.810	120°21.446	Agassiz Trawl ↓	408	85	268	1,7	-0,6	1,23	1015,25	99	1/10
3b	CB1	Geotrace	Sep 07 2015	13:53	UTC-5	75°07.693	120°20.910	Agassiz Trawl ↑	408	68	255	4	-0,4	1,22	1014,23	99	1/10
3b	CB1	Geotrace	Sep 07 2015	14:19	UTC-5	75°07.151	120°19.627	Beam Trawl ↓	408	159	270	3,1	-0,2	1,23	1013,67	99	1/10
3b	CB1	Geotrace	Sep 07 2015	15:20	UTC-5	75°07.406	120°13.796	Beam Trawl ↑	404	328	265	5,8	-0,5	1,15	1014,56	99	1/10
3b	CB1	Geotrace	Sep 07 2015	16:22	UTC-5	75°06.850	120°38.660	CTD-Rosette ↓ (test)	467	37	220	4	-1	0,74	1012,7	99	1/10
3b	CB1	Geotrace	Sep 07 2015	16:37	UTC-5	75°06.850	120°38.550	CTD-Rosette ↑ (test)	466	74	220	4	-1	0,74	1012,7	99	1/10
3b	CB1	Geotrace	Sep 07 2015	16:52	UTC-5	75°06.800	120°38.510	TM-Rosette ↓	466	57	230	5	-1,1	0,76	1012,61	99	1/10
3b	CB1	Geotrace	Sep 07 2015	17:10	UTC-5	75°06.826	120°38.395	TM-Rosette↑	465	92	235	6,1	0	0,82	1012,53	99	1/10
3b	CB1	Geotrace	Sep 07 2015	22:08	UTC-5	75°07.040	120°37.890	TM-Rosette ↓	466	354	160	4	0,1	0,55	1010,3	99	1/10
3b	CB1	Geotrace	Sep 07 2015	22:25	UTC-5	75°07.070	120°37.700	TM-Rosette↑	466	12	160	9	1,4	0,64	1009,98	97	1/10
3b	CB2	Geotrace	Sep 08 2015	18:02	UTC-5	75°49.240	129°13.410	CTD-Rosette ↓	1373	150	260	9	-0,5	-0,03	1002,32	97	3/10
3b	CB2	Geotrace	Sep 08 2015	18:40	UTC-5	75°49.280	129°13.080	CTD-Rosette ↑	1371	150	270	9	-0,3	0,02	1002,26	95	3/10
3b	CB2	Geotrace	Sep 08 2015	20:27	UTC-5	75°48.880	129°13.160	TM-Rosette ↓	1365	111	270	10	-1,7	0,04	1002,28	97	3/10
3b	CB2	Geotrace	Sep 08 2015	20:56	UTC-5	75°48.810	129°12.920	TM-Rosette↑	1361	126	270	6	-0,4	0,03	1002,46	92	3/10
3b	CB2	Geotrace	Sep 08 2015	21:27	UTC-5	75°49.110	129°14.340	LVP ↓ (moonpool)	1382	125	290	12	-2	-0,02	1002,21	97	3/10
3b	CB2	Geotrace	Sep 09 2015	00:56	UTC-5	75°48.426	129°13.522	LVP ↑ (moonpool)	1356	51	290	7,2	-2,8	0,1	1002,84	93	4/10
3b	CB2	Geotrace	Sep 09 2015	01:22	UTC-5	75°48.466	129°14.073	CTD-Rosette ↓	1356	197	310	10	-2	0,07	1003,09	90	4/10
3b	CB2	Geotrace	Sep 09 2015	02:54	UTC-5	75°48.088	129°14.035	CTD-Rosette ↑	1343	173	300	8	-1,7	0,1	1003,1	90	4/10
3b	CB2	Geotrace	Sep 09 2015	03:15	UTC-5	75°47.913	129°14.821	TM-Rosette ↓	1346	175		0	-2	0,04	1003,08	90	4/10
3b	CB2	Geotrace	Sep 09 2015	04:13	UTC-5	75°47.920	129°14.840	TM-Rosette↑	1346	161	290	5	-1,3	0,06	1003,19	89	4/10
3b	CB2	Geotrace	Sep 09 2015	04:45	UTC-5	75°48.500	129°11.800	CTD-Rosette ↓	1344	105	280	6	-1,8	-0,02	1003,29	90	4/10
3b	CB2	Geotrace	Sep 09 2015	05:53	UTC-5	75°48.350	129°11.520	CTD-Rosette ↑	1335	119	290	7	-2,2	0,07	1003,46	98	4/10
3b	CB2	Geotrace	Sep 09 2015	06:28	UTC-5	75°49.950	129°13.230	LVP ↓ (moonpool)	1383	155	0	9	-1,9	-0,12	1003,46	98	4/10
3b	CB2	Geotrace	Sep 09 2015	10:44	UTC-5	75°49.210	129°14.300	LVP ↑ (moonpool)	1382	199	350	11	0,1	-0,15	1004,61	86	4/10
3b	SI_ST1	Ice	Sep 09 2015	14:00	UTC-5	76°02.580	128°42.030	Ice work (Start)	1774	59	340	13	-3	-0,37	1004,61	94	5/10
3b	SI_ST1	Ice	Sep 09 2015	17:10	UTC-5	76°01.244	128°43.215	Ice work (End)	1774	55	350	15	-3,1	-0,13	1006,29	94	5/10
3b	SI_ST2	Ice	Sep 09 2015	19:05	UTC-5	76°07.420	129°18.580	Ice work (Start)	1800	268	30	18	-2,8	-0,37	1007,8	91	5/10
3b	SI_ST2	Ice	Sep 09 2015	22:48	UTC-5	76°06.610	129°21.500	Ice work (End)	1807	258	10	6	-3,4	-0,37	1009,13	90	5/10
3b	CB2	Geotrace	Sep 09 2015	23:12	UTC-5	75°53.640	129°28.630	Tucker Net ↓	1606	117	330	18	-3,7	-0,32	1009,91	92	5/10
3b	CB2	Geotrace	Sep 09 2015	23:37	UTC-5	75°53.460	129°25.090	Tucker Net ↑	1571	71	340	14	-4,5	-0,23	1010,02	91	5/10
3b	CB2	Geotrace	Sep 10 2015	00:11	UTC-5	75°53.264	129°25.130	Monster-Loki Net ↓	1565	224	320	15	-4,1	-0,26	1010,37	90	5/10
3b	CB2	Geotrace	Sep 10 2015	01:19	UTC-5	75°53.052	129°25.802	Monster-Loki Net ↑	1563	171	0	15	-4,6	-0,29	1011,07	92	5/10
3b	CB2	Geotrace	Sep 10 2015	02:40	UTC-5	75°47.108	129°17.443	CTD-Rosette ↓	1356	199	0	14	-3,4	-0,29	1011,47	86	0
3b	CB2	Geotrace	Sep 10 2015	03:40	UTC-5	75°46.908	129°16.819	CTD-Rosette ↑	1344	191	0	14	-1,7	-0,2	1011,86	83	0
3b	CB2	Geotrace	Sep 10 2015	04:08	UTC-5	75°46.840	129°16.710	Hydrobios ↓	1342	188	10	10	-2	-0,2	1011,93	81	0
3b	CB2	Geotrace	Sep 10 2015	05:23	UTC-5	75°46.660	129°16.920	Hydrobios ↑	1346	180	10	12	-2,9	-0,14	1012,49	85	0
3b	CB2	Geotrace	Sep 10 2015	05:45	UTC-5	75°47.030	129°17.080	Box Core ↓	1350	153	0	14	-2,7	-0,2	1012,6	85	1/10
3b	CB2	Geotrace	Sep 10 2015	06:12	UTC-5	75°47.130	129°17.450	Box Core (bottom)	1355	199	20	11	-3,6	-0,24	1012,9	87	1/10
3b	CB2	Geotrace	Sep 10 2015	06:36	UTC-5	75°47.170	129°17.580	Box Core ↑	1357	202	20	12	-3	-0,24	1013,09	83	1/10
3b	CB2	Geotrace	Sep 10 2015	06:56	UTC-5	75°47.140	129°17.500	Box Core ↓	1357	194	20	9	-2,4	-0,25	1013,21	83	1/10
3b	CB2	Geotrace	Sep 10 2015	07:21	UTC-5	75°47.120	129°17.540	Box Core (bottom)	1356	182	20	10	-1,8	-0,24	1013,43	80	1/10
3b	CB2	Geotrace	Sep 10 2015	07:43	UTC-5	75°47.120	129°17.680	Box Core ↑	1359	193	20	9	-2,4	-0,21	1013,49	85	1/10
3b	SI_ST3	Ice	Sep 10 2015	12:57	UTC-5	76°21.271	129°03.733	Ice work (Start)	2186	63	300	7,2	-2,5	-0,45	1014,35	91	Floe
3b	SI_ST3	Ice	Sep 10 2015		UTC-5	76°20.422	129°03.822	Ice work (End)	2387	65	300	6	-2,3	-0,4	1015	87	Floe
3b	CB3	Geotrace	Sep 11 2015	14:50	UTC-5	76°58.826	140°02.739	CTD-Rosette ↓	3728	167	350	6,2	-4,6	-0,62	1020,33	97	1/10
3b	CB3	Geotrace	Sep 11 2015	15:53	UTC-5	76°58.791	140°02.288	CTD-Rosette ↑	3720	176	0	8	-2,9	-0,55	1020,58	93	1/10
3b	CB3	Geotrace	Sep 11 2015	16:13	UTC-5	76°58.810	140°02.330	TM-Rosette ↓ (problem)	3727	157	0	7	-4,8	-0,55	1020,7	97	1/10

3b	CB3	Geotrace	Sep 11 2015	16:29	UTC-5	76°58.850	140°02.370	TM-Rosette ↑ (problem)	3727	180	0	7	-4,8	-0,55	1020,7	97	1/10
3b	CB3	Geotrace	Sep 11 2015	17:00	UTC-5	76°58.828	140°02.279	TM-Rosette ↓	3931	214	0	8	-3,8	-0,54	1021,04	95	1/10
3b	CB3	Geotrace	Sep 11 2015	17:19	UTC-5	76°58.836	140°02.059	TM-Rosette ↑	3731	246	350	6	-3,6	-0,54	1021,11	95	1/10
3b	CB3	Geotrace	Sep 11 2015	17:34	UTC-5	76°58.830	140°01.830	LVP ↓ (moonpool)	3731	162	340	3	-3,7	-0,53	1021,18	95	1/10
3b	CB3	Geotrace	Sep 11 2015	21:37	UTC-5	76°58.530	140°02.870	LVP ↑ (moonpool)	3729	161	20	7	-5	-0,47	1021,62	98	1/10
3b	CB3	Geotrace	Sep 11 2015	21:57	UTC-5	76°58.510	140°03.090	CTD-Rosette Geochem ↓	3735	207	10	8	-4,9	-0,5	1021,55	98	1/10
3b	CB3	Geotrace	Sep 11 2015	23:15	UTC-5	76°58.400	140°03.240	CTD-Rosette Geochem ↑	3736	213	10	4	-3,5	-0,5	1021,92	97	1/10
3b	CB3	Geotrace	Sep 12 2015	00:11	UTC-5	76°59.475	140°01.970	TM-Rosette ↓ (sensor frozen)	3729		30	6	-4,2	-0,58	1022,17	99	1/10
3b	CB3	Geotrace	Sep 12 2015	00:15	UTC-5			TM-Rosette ↑ (sensor frozen)		225							
3b	CB3	Geotrace	Sep 12 2015	00:21	UTC-5	76°59.477	140°01.901	TM-Rosette ↓	3729	225	30	8	-3,2	-0,57	1022,41	99	1/10
3b	CB3	Geotrace	Sep 12 2015	01:25	UTC-5	76°59.410	140°02.187	TM-Rosette ↑	3729	230	15	8	-2,9	-0,55	1022,87	94	1/10
3b	CB3	Geotrace	Sep 12 2015	01:43	UTC-5	76°59.405	140°02.189	Monster-Loki Net ↓	3729	242	0	10	-2,9	-0,54	1022,94	94	1/10
3b	CB3	Geotrace	Sep 12 2015	02:49	UTC-5	76°59.316	140°02.228	Monster-Loki Net ↑	3729	252	0	7	-3,5	-0,52	1023,51	97	1/10
3b	CB3	Geotrace	Sep 12 2015	03:52	UTC-5	76°59.521	140°02.877	CTD-Rosette Geochem ↓ (cancelled)	3728	214	0	10	-4,6	-0,55	1023,42	99	1/10
3b	CB3	Geotrace	Sep 12 2015	04:10	UTC-5	76°59.420	140°02.890	CTD-Rosette Geochem ↓ (cancelled)	3731	244	20	8	-3,8	-0,58	1023,56	99	1/10
3b	CB3	Geotrace	Sep 12 2015	04:48	UTC-5	76°59.850	139°53.970	Tucker Net ↓	3731	187	0	6	-4,8	-0,61	1023,56	98	3/10
3b	CB3	Geotrace	Sep 12 2015	05:07	UTC-5	76°59.570	139°52.130	Tucker Net ↑	3729	73	340	6	-4,8	-0,61	1023,56	98	3/10
3b	CB3	Geotrace	Sep 12 2015	06:09	UTC-5	76°59.480	139°52.070	LVP ↓ (moonpool)	3729	206	350	7	-4,9	-0,59	1023,7	98	3/10
3b	CB3	Geotrace	Sep 12 2015	11:15	UTC-5	76°58.310	139°52.270	LVP ↑ (moonpool)	3728	203	350	4	-1,2	-0,54	1023,81	96	3/10
3b	SI_contaminant	Ice	Sep 12 2015	12:04	UTC-5	77°00.150	140°05.108	Ice work (start)	3728	232	330	6	-2	-0,63	1023,99	93	3/10
3b	SI_contaminant	Ice	Sep 12 2015	12:32	UTC-5	77°00.250	140°05.795	Ice work (end)	3728	240	332	8	-2	-0,64	1023,98	94	3/10
3b	CB3	Geotrace	Sep 12 2015	12:59	UTC-5	76°59.986	140°05.719	CTD-Rosette Geochem ↓ (frozen)	3731	234	250	10	-1	-0,58	1024,15	89	3/10
3b	CB3	Geotrace	Sep 12 2015		UTC-5	76°59.942	140°05.710	CTD-Rosette Geochem ↑ (frozen)	3732	240	255	10	-1	-0,57	1024,14	89	3/10
3b	CB3	Geotrace	Sep 12 2015	13:11	UTC-5	76°59.938	140°05.702	TM-Rosette ↓	3731	213	354	10	-0,8	-0,56	1024,18	86	3/10
3b	CB3	Geotrace	Sep 12 2015	15:10	UTC-5	76°59.644	140°04.711	TM-Rosette ↑	3751	255	0	9,3	-1	-0,52	1024,33	87	3/10
3b	CB3	Geotrace	Sep 12 2015	16:25	UTC-5	76°59.440	140°05.300	Pops buoy ↓	3732	115	0	9	-2,9	-0,56	1024,23	93	3/10
3b	CB3	Geotrace	Sep 12 2015	18:12	UTC-5	77°01.150	140°02.710	TM-Rosette ↓	3732	152	0	8	-2,9	-0,59	1024,29	94	3/10
3b	CB3	Geotrace	Sep 12 2015	20:22	UTC-5	77°00.860	140°02.580	TM-Rosette ↑	3734	243	5	9	-1,1	-0,54	1023,93	88	3/10
3b	CB3	Geotrace	Sep 12 2015	20:43	UTC-5	77°00.780	140°02.460	LVP ↓	3734	233	5	9	-1	-0,54	1023,95	88	3/10
3b	CB3	Geotrace	Sep 13 2015	01:08	UTC-5	76°59.613	140°04.911	LVP ↑	3733	285	5	8	-3,2	-0,55	1023,7	94	3/10
3b	CB3	Geotrace	Sep 13 2015	01:26	UTC-5	77°00.003	140°07.474	Hydrobios ↓	3733	205	30	10	-3,2	-0,55	1023,7	94	3/10
3b	CB3	Geotrace	Sep 13 2015	03:25	UTC-5	76°59.841	140°09.451	Hydrobios ↑	3734	200	45	10	-3,9	-0,54	1023,73	96	3/10
3b	CB3	Geotrace	Sep 13 2015	04:33	UTC-5	76°59.600	140°04.260	TM-Rosette ↓	3658	245	40	8	-2,9	-0,64	1023,68	91	3/10
3b	CB3	Geotrace	Sep 13 2015	06:43	UTC-5	76°59.240	140°05.750	TM-Rosette ↑	3731	273	40	8	-2,9	-0,57	1023,34	94	3/10
3b	CB3	Geotrace	Sep 13 2015	08:05	UTC-5	76°59.420	140°02.610	CTD-Rosette Geochem ↓	3730	226	70	7	-3,5	-0,63	1023,13	95	3/10
3b	CB3	Geotrace	Sep 13 2015	09:34	UTC-5	76°59.220	140°02.950	CTD-Rosette Geochem ↑	3730	240	50	6	-1,8	-0,58	1022,61	89	3/10
3b	CB4	Geotrace	Sep 14 2015	15:12	UTC-5	74°59.977	149°59.493	CTD-Rosette ↓	3828	223	60	20	1,1	0,2	1015,58	82	0
3b	CB4	Geotrace	Sep 14 2015	16:16	UTC-5	74°59.910	150°00.380	CTD-Rosette ↑	3830	248	50	18	3,6	0,19	1015,76	71	0
3b	CB4	Geotrace	Sep 14 2015	16:33	UTC-5			TM-Rosette ↓ (problem)									
3b	CB4	Geotrace	Sep 14 2015	16:37	UTC-5			TM-Rosette ↑ (problem)									
3b	CB4	Geotrace	Sep 14 2015	16:47	UTC-5	74°59.810	150°00.080	TM-Rosette ↓	3826	253	50	18	4,2	0,2	1015,87	69	0
3b	CB4	Geotrace	Sep 14 2015	17:12	UTC-5	74°59.714	150°01.196	TM-Rosette ↑	3830	253	50	20	4	0,2	1016,06	70	0
3b	CB4	Geotrace	Sep 14 2015	18:07	UTC-5	74°59.620	150°01.830	Monster-Loki Net ↓	3785	252	50	17	2,1	0,21	1016,18	77	0
3b	CB4	Geotrace	Sep 14 2015	19:18	UTC-5	74°59.540	150°02.960	Monster-Loki Net ↑	3829	255	50	15	3,2	0,21	1016,43	73	0
3b	CB4	Geotrace	Sep 14 2015	19:47	UTC-5	75°00.130	150°00.020	CTD-Rosette ↓	3831	256	50	15	-0,8	0,18	1016,09	85	0
3b	CB4	Geotrace	Sep 14 2015	20:53	UTC-5	75°00.000	150°00.360	CTD-Rosette ↑	3829	250	40	7	-0,3	0,21	1016,73	84	0
3b	CB4	Geotrace	Sep 14 2015	21:10	UTC-5	74°59.920	150°01.040	Tucker Net ↓	3830	172	40	9	0,3	0,22	1016,81	83	0
3b	CB4	Geotrace	Sep 14 2015	21:33	UTC-5	74°59.050	150°00.390	Tucker Net ↑	3826	172	20	11	-2,3	0,21	1016,83	90	0
3b	CB4	Geotrace	Sep 14 2015	22:10	UTC-5	75°00.064	150°00.217	TM-Rosette ↓ (problem)	3828	244	25	13	-0,7	0,2	1016,88	84	0
3b	CB4	Geotrace	Sep 14 2015	23:17	UTC-5	74°59.984	149°59.999	TM-Rosette ↑ (problem)	3828	240	15	12	-1,2	0,2	1017,02	85	0
3b	CB4	Geotrace	Sep 15 2015	00:20	UTC-5	74°00.168	150°00.017	TM-Rosette ↓	3828	239	0	14	-1,3	0,2	1017,15	86	0
3b	CB4	Geotrace	Sep 15 2015	04:06	UTC-5	74°59.930	149°59.200	TM-Rosette ↑	3822	230	10	10	-0,7	0,26	1017,25	89	0
3b	CB4	Geotrace	Sep 15 2015	04:45	UTC-5	74°59.990	149°59.430	CTD-Rosette ↓	3830	218	10	10	-0,9	0,26	1017,19	90	0
3b	CB4	Geotrace	Sep 15 2015	06:20	UTC-5	75°00.090	150°00.030	CTD-Rosette ↑	3828	224	340	10	-1	0,26	1017,19	90	0

3b	CB4	Geotrace	Sep 15 2015	07:34	UTC-5	75°00.110	150°00.010	TM-Rosette ↓	3829	220	350	12	-0,9	0,26	1017,09	90	0
3b	CB4	Geotrace	Sep 15 2015	09:51	UTC-5	74°59.940	149°59.630	TM-Rosette ↑	3829	215	340	6	-0,2	0,26	1016,84	84	0
3b	CB4	Geotrace	Sep 15 2015	10:28	UTC-5	75°00.060	150°00.190	LVP ↓	3828	190	340	11	-1,1	0,24	1016,67	87	0
3b	CB4	Geotrace	Sep 15 2015	15:50	UTC-5	74°59.830	150°01.506	LVP ↑	3829	32	340	10	-2,2	0,27	1016,8	93	0
3b	CB4	Geotrace	Sep 15 2015		UTC-5			TM-Rosette ↓ (cancelled)									
3b	CB4	Geotrace	Sep 15 2015		UTC-5			TM-Rosette ↑ (cancelled)									
3b	CB4	Geotrace	Sep 15 2015	17:04	UTC-5	75°00.230	149°59.873	Hydrobios ↓	3830	182	310	10	-2	0,35	1016,85	88	0
3b	CB4	Geotrace	Sep 15 2015	19:00	UTC-5	74°59.880	149°59.040	Hydrobios ↑	3828	121	310	10	-0,2	0,38	1016,48	83	0
3b	CB4	Geotrace	Sep 15 2015	19:21	UTC-5	74°59.980	149°59.450	CTD-Rosette ↓	3830	140	320	13	-2,3	0,39	1016,42	89	0
3b	CB4	Geotrace	Sep 15 2015	19:36	UTC-5	74°59.940	149°59.480	CTD-Rosette ↑	3824	167	320	12	-3,1	0,39	1016,45	90	0
3b	CB4	Geotrace	Sep 15 2015	19:55	UTC-5	74°59.940	149°59.390	LVP ↓ (moonpool)	3829	159	320	14	-1,9	0,4	1016,52	88	0
3b	CB4	Geotrace	Sep 16 2015	00:05	UTC-5	74°59.300	149°59.400	LVP ↑ (moonpool)	3829	290	320	15	-2,2	0,3	1016,5	90	0
3b	CB4	Geotrace	Sep 16 2015	01:08	UTC-5	75°00.215	150°00.091	CTD-Rosette ↓	3824	156	310	10	-3,1	0,22	1016,46	90	0
3b	CB4	Geotrace	Sep 16 2015	01:32	UTC-5	74°59.867	149°59.727	CTD-Rosette ↑	3827	160	300	12	-2,2	0,26	1016,56	88	0
3b	CB4	Geotrace	Sep 16 2015	02:14	UTC-5	75°00.621	150°02.080	LVP ↓	3828	170	300	14	-3,2	0,23	1016,47	93	0
3b	CB4	Geotrace	Sep 16 2015	06:34	UTC-5	75°00.030	150°00.810	LVP ↑	3830	140	310	14	0	0,25	1016,14	84	0
3b	CB4	Geotrace	Sep 16 2015	07:34	UTC-5	75°00.030	149°59.600	TM-Rosette Geochem ↓	3830	142	300	16	-1,9	0,19	1016,07	89	0
3b	CB4	Geotrace	Sep 16 2015	09:37	UTC-5	75°00.240	149°57.650	TM-Rosette Geochem ↑	3830	153	280	9	0,1	0,21	1015,73	87	0
3b	CB4	Geotrace	Sep 16 2015	12:12	UTC-5	75°00.330	150°00.980	TM-Rosette Geochem ↓	3827	131	280	14	0,2	0,15	1015,44	87	0
3b	CB4	Geotrace	Sep 16 2015	14:12	UTC-5	75°00.095	149°59.521	TM-Rosette Geochem ↑	3827	142	280	14	-0,4	0,17	1015,45	90	0
3b	CB4.1	Geotrace	Sep 16 2015	17:06	UTC-5	74°42.253	148°46.525	TM-Rosette Cs ↓	3811	133	275	12	-2	0,38	1015,18	94	0
3b	CB4.1	Geotrace	Sep 16 2015	19:14	UTC-5	74°42.210	148°45.620	TM-Rosette Cs ↑	3811	129	270	14	-0,3	0,48	1014,87	88	0
3b	CB4.2	Geotrace	Sep 16 2015	20:17	UTC-5	74°35.578	148°12.713	TM-Rosette Intercal ↓	3799	100	270	12	-1,8	0,33	1014,51	94	0
3b	CB4.2	Geotrace	Sep 16 2015	21:05	UTC-5	74°35.570	148°12.483	TM-Rosette Intercal ↑	3800	127	270	12	-0,8	0,38	1014,34	90	0
3b	407	Coring	Sep 18 2015	08:22	UTC-5	71°00.330	126°04.560	CTD-Rosette ↓	390	279	90	16	3,4	5,67	1004,26	86	0
3b	407	Coring	Sep 18 2015	09:04	UTC-5	71°00.530	126°05.080	CTD-Rosette ↑	390	331	80	16	5	5,77	1004,14	79	0
3b	407	Coring	Sep 18 2015	09:48	UTC-5	70°59.600	126°03.280	Box Core ↓	398	295	90	22	2,1	5,83	1003,72	87	0
3b	407	Coring	Sep 18 2015	09:58	UTC-5	70°59.620	126°03.390	Box Core (bottom)	395	297	90	17	3,6	5,82	1004,08	78	0
3b	407	Coring	Sep 18 2015	10:09	UTC-5	70°59.640	126°03.560	Box Core ↑	395	290	100	17	4,5	5,88	1004,15	80	0
3b	407	Coring	Sep 18 2015	10:20	UTC-5	70°59.660	126°03.740	Box Core ↓	397	292	90	16	4,5	5,88	1004,11	76	0
3b	407	Coring	Sep 18 2015	10:31	UTC-5	70°59.680	126°03.770	Box Core (bottom)	398	297	90	18	4,3	5,86	1003,96	80	0
3b	407	Coring	Sep 18 2015	10:40	UTC-5	70°59.700	126°03.860	Box Core ↑	394	265	90	17	3,6	5,87	1003,9	82	0
3b	314	Basic	Sep 20 2015	11:09	UTC-5	68°58.200	105°28.890	CTD-Rosette ↓	77	299	80	14	1,9	2,74	1007,69	94	0
3b	314	Basic	Sep 20 2015	11:30	UTC-5	68°58.100	105°28.900	CTD-Rosette ↑	76	270	60	8	4,9	2,67	1008,38	83	0
3b	314	Basic	Sep 20 2015	12:12	UTC-5	68°58.148	105°28.233	Monster-Loki Net ↓	77	235	62	10	4,1	2,64	1008,49	86	0
3b	314	Basic	Sep 20 2015	12:17	UTC-5	68°58.170	105°28.399	Monster-Loki Net ↑	77	223	60	10	4,1	2,64	1008,54	91	0
3b	314	Basic	Sep 20 2015	12:43	UTC-5	68°58.262	105°28.256	Tucker Net ↓	81	177	60	11	3,6	2,62	1008,45	89	0
3b	314	Basic	Sep 20 2015	13:02	UTC-5	68°58.233	105°28.834	Tucker Net ↑	77	236	75	11	3,6	2,71	1008,45	89	0
3b	314	Basic	Sep 20 2015	13:22	UTC-5	68°58.256	105°28.251	Box Core ↓	81	173	58	10	3,8	2,69	1008,39	88	0
3b	314	Basic	Sep 20 2015	13:29	UTC-5	68°58.291	105°28.415	Box Core ↑ (bottom)	78	253	60	10	3,2	2,73	1008,35	91	0
3b	314	Basic	Sep 20 2015	13:41	UTC-5			Box Core ↑									
3b	314	Basic	Sep 20 2015	13:50	UTC-5	68°58.193	105°28.505	Box Core ↓	80	93	60	11	3,9	2,69	1008,28	89	0
3b	314	Basic	Sep 20 2015	13:54	UTC-5	68°58.185	105°28.534	Box Core (bottom)	75	93	60	10	3,9	2,69	1008,28	89	0
3b	314	Basic	Sep 20 2015	14:04	UTC-5	68°58.181	105°28.643	Box Core ↑	73	99	58	10	3,3	2,59	1008,4	90	0
3b	314	Basic	Sep 20 2015	14:11	UTC-5	68°58.208	105°28.348	Box Core ↓	81	63	60	10	3,2	2,68	1008,42	90	0
3b	314	Basic	Sep 20 2015	14:15	UTC-5	68°58.203	105°28.380	Box Core (bottom)	81	127	57	10	3,2	2,68	1008,42	90	0
3b	314	Basic	Sep 20 2015	14:20	UTC-5	68°58.186	105°28.474	Box Core ↑	77	153	45	9,5	3,2	2,78	1008,49	90	0
3b	314	Basic	Sep 20 2015	14:28	UTC-5	68°58.154	105°28.634	Agassiz Trawl ↓	75	159	60	10,4	3,3	2,82	1008,46	90	0
3b	314	Basic	Sep 20 2015	14:50	UTC-5	68°58.366	105°28.886	Agassiz Trawl ↑	74	270	62	10,2	4,2	2,89	1008,63	86	0
3b	314	Basic	Sep 20 2015	15:04	UTC-5	68°58.380	105°29.180	Beam Trawl ↓	75	273	62	8,6	5,6	2,86	1008,66	81	0
3b	314	Basic	Sep 20 2015	15:42	UTC-5	68°58.236	105°29.498	Beam Trawl ↑	81	272	60	8,5	4,3	2,85	1008,81	85	0
3b	QMG4	Basic	Sep 20 2015	20:19	UTC-5	68°29.000	103°25.480	CTD-Rosette ↓	71	278	50	15	2,5	2,87	1009,49	95	0
3b	QMG4	Basic	Sep 20 2015	20:38	UTC-5	68°28.930	103°25.520	CTD-Rosette ↑	69	266	50	8	3,3	2,62	1009,67	92	0
3b	QMG4	Basic	Sep 20 2015	20:52	UTC-5	68°28.950	103°25.560	Monster-Loki Net ↓	69	222	60	12	4,7	2,58	1009,62	86	0

3b	QMG4	Basic	Sep 20 2015	20:58	UTC-5	68°28.980	103°25.630	Monster-Loki Net ↑	69	237	60	12	4,7	2,58	1009,62	86	0
3b	QMG4	Basic	Sep 20 2015	21:21	UTC-5	68°29.090	103°25.750	Tucker Net ↓	71	210	60	10	2,4	2,56	1009,61	94	0
3b	QMG4	Basic	Sep 20 2015	21:45	UTC-5	68°28.060	103°25.610	Tucker Net ↑	66	101	40	10	2,4	2,56	1009,61	94	0
3b	QMG4	Basic	Sep 20 2015	22:14	UTC-5	68°29.060	103°25.660	Box Core ↓	67	199	60	14	2,7	2,56	1009,66	92	0
3b	QMG4	Basic	Sep 20 2015	22:17	UTC-5	68°29.060	103°25.710	Box Core (bottom)	69	205	50	12	2,4	2,51	1009,65	92	0
3b	QMG4	Basic	Sep 20 2015	22:20	UTC-5	68°29.070	103°25.760	Box Core ↑	69	213	50	12	2,4	2,51	1009,65	92	0
3b	QMG4	Basic	Sep 20 2015	22:31	UTC-5	68°29.080	103°25.670	Agassiz Trawl ↓	68	229	60	13	2,6	2,47	1009,73	92	0
3b	QMG4	Basic	Sep 20 2015	22:48	UTC-5	68°28.660	103°26.390	Agassiz Trawl ↑	76	128	60	13	2,6	2,47	1009,73	92	0
3b	QMG4	Basic	Sep 20 2015	23:17	UTC-5	68°29.680	103°23.670	Beam Trawl ↓	77	228	50	12	2,4	2,5	1009,58	94	0
3b	QMG4	Basic	Sep 20 2015	23:58	UTC-5	68°28.032	103°24.536	Beam Trawl ↑	61	149	30	13	2,2	2,48	1009,34	96	0
3b	QMG3	Basic	Sep 21 2015	02:05	UTC-5	68°19.770	102°36.398	CTD-Rosette ↓	64	237	35	16	2,4	3,02	1008,74	96	0
3b	QMG3	Basic	Sep 21 2015	02:26	UTC-5	68°19.675	102°36.402	CTD-Rosette ↑	60	273	30	20	5,3	2,89	1008,63	86	0
3b	QMG3	Basic	Sep 21 2015	02:39	UTC-5	68°19.670	102°36.530	Tucker Net ↓	61	113	30	18	2,6	2,9	1008,7	95	0
3b	QMG3	Basic	Sep 21 2015	02:56	UTC-5	68°19.447	102°34.786	Tucker Net ↑	73	80	50	18	2,3	2,89	1008,73	96	0
3b	QMG3	Basic	Sep 21 2015	03:17	UTC-5	68°39.674	102°36.677	Monster-Loki Net ↓	62	215	55	19	2,6	2,84	1008,86	97	0
3b	QMG3	Basic	Sep 21 2015	03:25	UTC-5	68°19.707	102°36.962	Monster-Loki Net ↑	62	212	45	17	2,1	2,85	1008,86	97	0
3b	QMG3	Basic	Sep 21 2015	03:50	UTC-5	68°19.801	102°36.545	Box Core (bottom)	67	232	45	13,9	2,9	2,86	1008,85	95	0
3b	QMG3	Basic	Sep 21 2015	03:54	UTC-5	68°19.810	102°36.400	Box Core ↑	67	254	45	16	2,9	2,86	1008,55	94	0
3b	QMG3	Basic	Sep 21 2015	04:04	UTC-5	68°19.750	102°36.470	Agassiz Trawl ↓	63	230	40	13	4,1	2,81	1008,99	89	0
3b	QMG3	Basic	Sep 21 2015	04:17	UTC-5	68°19.460	102°36.470	Agassiz Trawl ↑	62	118	40	14	4,1	2,81	1008,99	89	0
3b	QMG3	Basic	Sep 21 2015	04:39	UTC-5	68°19.730	102°36.350	Beam Trawl ↓	63	226	60	18	2,1	2,81	1009,26	94	0
3b	QMG3	Basic	Sep 21 2015	07:17	UTC-5	68°19.020	102°36.410	Beam Trawl ↑	64	102	40	18	1,8	2,71	1009,48	96	0
3b	WF1-15	Mooring	Sep 21 2015	09:06	UTC-5	68°14.490	101°48.340	Mooring deployment	97	205	80	20	1,7	2,73	1009,15	84	0
3b	WF1-15	Mooring	Sep 21 2015	09:15	UTC-5	68°14.460	101°48.350	Mooring WF1-15 deployed	97	304	70	17	1,5	2,73	1009,45	83	0
3b	WF1-15	Mooring	Sep 21 2015		UTC-5	68°14.388	101°48.586	Triangulation #1 240m									
3b	WF1-15	Mooring	Sep 21 2015		UTC-5	68°14.569	101°48.569	Triangulation #2 238m									
3b	WF1-15	Mooring	Sep 21 2015		UTC-5	68°14.435	101°48.099	Triangulation #3 269m									
3b	QMG/WF1-15	Basic	Sep 21 2015	09:47	UTC-5	68°14.540	101°47.550	CTD ↓	107	233	70	20	1,5	2,7	1009,51	80	0
3b	QMG/WF1-15	Basic	Sep 21 2015	09:55	UTC-5	68°14.540	101°47.710	CTD ↑	103	322	70	15	1,5	2,71	1009,61	81	0
3b	QMG/WF1-15	Basic	Sep 21 2015	10:29	UTC-5	68°14.620	101°43.150	Tucker Net ↓	103	252	70	16	1,6	2,73	1009,61	81	0
3b	QMG/WF1-15	Basic	Sep 21 2015	10:45	UTC-5	68°14.210	101°44.380	Tucker Net ↑	101	205	70	16	1,4	2,69	1009,95	82	0
3b	QMG/WF1-15	Basic	Sep 21 2015	11:10	UTC-5	68°14.180	101°44.820	Monster-Loki Net ↓	107	234	70	16	1,4	2,66	1009,97	81	0
3b	QMG/WF1-15	Basic	Sep 21 2015	11:19	UTC-5	68°14.230	101°45.010	Monster-Loki Net ↑	108	227	70	16	1,4	2,69	1009,94	82	0
3b	QMG/WF1-15	Basic	Sep 21 2015	12:47	UTC-5	68°13.759	101°45.722	IKMT ↓	107	130	55	14,2	1,7	2,72	1010,17	86	0
3b	QMG/WF1-15	Basic	Sep 21 2015	13:15	UTC-5	68°13.459	101°44.530	IKMT ↑	97	94	60	17,5	1,9	2,7	1010,2	87	0
3b	QMG/WF1-15	Basic	Sep 21 2015	13:39	UTC-5	68°14.803	101°43.057	CTD-Rosette ↓	107	285	62	18,2	2	2,66	1010,34	86	0
3b	QMG/WF1-15	Basic	Sep 21 2015	14:05	UTC-5	68°14.701	101°43.103	CTD-Rosette ↑	104	264	62	14,5	3,3	2,69	1010,6	78	0
3b	QMG/WF1-15	Basic	Sep 21 2015	14:19	UTC-5	68°14.654	101°43.039	Box Core (bottom)	100	236	60	17,1	4,8	2,55	1010,64	76	0
3b	QMG/WF1-15	Basic	Sep 21 2015	14:24	UTC-5	68°14.633	101°43.043	Box Core ↑	100	223	65	15,1	1,7	2,56	1010,65	85	0
3b	QMG/WF1-15	Basic	Sep 21 2015	14:36	UTC-5	68°14.583	101°43.347	Agassiz Trawl ↓	105	162	45	11,1	1,2	2,55	1010,62	86	0
3b	QMG/WF1-15	Basic	Sep 21 2015	14:54	UTC-5	68°14.176	101°42.732	Agassiz Trawl ↑	98	85	60	14,2	1,3	2,59	1010,84	86	0
3b	QMG/WF1-15	Basic	Sep 21 2015	15:08	UTC-5	68°14.673	101°43.785	Beam Trawl ↓	106	201	45	14,7	1,5	2,59	1010,72	86	0
3b	QMG/WF1-15	Basic	Sep 21 2015	15:51	UTC-5	68°14.069	101°42.668	Beam Trawl ↑	115	138	45	15	1,8	2,58	1011	85	0
3b	QMG2	Basic	Sep 21 2015	17:44	UTC-5	68°18.820	100°48.010	Tucker Net ↓	53	221	50	18	1,6	2,64	1011,11	90	0
3b	QMG2	Basic	Sep 21 2015	18:03	UTC-5	68°18.550	100°48.110	Tucker Net ↑	84	163	50	14	1,6	2,64	1011,11	90	0
3b	QMG2	Basic	Sep 21 2015	18:26	UTC-5	68°18.810	100°47.880	Monster-Loki Net ↓	55	226	50	17	1,4	2,66	1011,11	90	0
3b	QMG2	Basic	Sep 21 2015	18:31	UTC-5	68°18.820	100°47.860	Monster-Loki Net ↑	55	228	60	18	1,6	2,67	1011,82	89	0
3b	QMG2	Basic	Sep 21 2015	18:54	UTC-5	68°18.810	100°47.990	CTD-Rosette ↓	54	247	50	14	1,4	2,69	1011,88	90	0
3b	QMG2	Basic	Sep 21 2015	19:09	UTC-5	68°18.740	100°47.970	CTD-Rosette ↑	59	265	60	14	3,3	2,69	1011,9	81	0
3b	QMG2	Basic	Sep 21 2015	19:23	UTC-5	68°18.720	100°47.890	Box Core ↓	59	228	50	16	2,8	2,69	1011,91	85	0
3b	QMG2	Basic	Sep 21 2015	19:25	UTC-5	68°18.720	100°47.910	Box Core (bottom)	59	225	50	15	2,8	2,69	1011,91	85	0
3b	QMG2	Basic	Sep 21 2015	19:28	UTC-5	68°18.730	100°47.920	Box Core ↑	59	228	50	15	2,8	2,69	1011,91	85	0
3b	QMG2	Basic	Sep 21 2015	19:39	UTC-5	68°18.770	100°47.880	Agassiz Trawl ↓	59	204	50	13	1,4	2,69	1011,95	91	0
3b	QMG2	Basic	Sep 21 2015	19:53	UTC-5	68°18.560	100°47.900	Agassiz Trawl ↑	74	148	50	15	1,4	2,7	1011,95	91	0

3b	QMG2	Basic	Sep 21 2015	20:14	UTC-5	68°18.760	100°48.200	Beam Trawl ↓	63	219	40	15	1,5	2,66	1011,98	91	0
3b	QMG2	Basic	Sep 21 2015	20:58	UTC-5	68°17.080	100°46.770	Beam Trawl ↑	92	144	30	12	1,1	2,62	1012,38	93	0
3b	QMG1	Basic	Sep 21 2015	23:02	UTC-5	68°29.630	099°53.440	CTD-Rosette ↓	35	258	70	9	1	2,34	1012,85	96	0
3b	QMG1	Basic	Sep 21 2015	23:17	UTC-5	68°29.570	099°53.440	CTD-Rosette ↑	36	248	50	7	2,3	2,33	1012,94	91	0
3b	QMG1	Basic	Sep 21 2015	23:31	UTC-5	68°29.520	099°53.540	Monster-Loki Net ↓	39	215	50	7	1,6	2,32	1013,06	90	0
3b	QMG1	Basic	Sep 21 2015	23:35	UTC-5	68°29.520	099°53.620	Monster-Loki Net ↑	42	199	50	7	1,6	2,32	1013,06	90	0
3b	QMG1	Basic	Sep 22 2015	00:12	UTC-5	68°29.469	099°54.091	Box Core ↓	48	213	45	10,4	0,2	2,3	1013,04	96	0
3b	QMG1	Basic	Sep 22 2015	00:14	UTC-5	68°29.497	099°54.276	Box Core (bottom)	45	215	45	10	0,2	2,3	1013,03	96	0
3b	312	Basic	Sep 22 2015	09:01	UTC-5	69°10.330	100°41.600	CTD-Rosette ↓	65	193	330	13	0	1,87	1015,4	92	0
3b	312	Basic	Sep 22 2015	09:25	UTC-5	69°10.320	100°41.430	CTD-Rosette ↑	66	245	330	8	0,9	1,86	1015,56	90	0
3b	312	Basic	Sep 22 2015	09:34	UTC-5	69°10.270	100°41.250	Tucker Net ↓	65	166	330	8	0,6	1,87	1015,65	91	0
3b	312	Basic	Sep 22 2015	09:51	UTC-5	69°09.920	100°39.500	Tucker Net ↑	58	45	345	11	-0,1	1,86	1015,71	91	0
3b	312	Basic	Sep 22 2015	10:11	UTC-5	69°10.110	100°42.110	Monster-Loki Net ↓	65	140	340	10	-0,1	1,82	1015,78	92	0
3b	312	Basic	Sep 22 2015	10:20	UTC-5	69°10.100	100°42.070	Monster-Loki Net ↑	65	158	340	12	-0,3	1,76	1015,68	92	0
3b	312	Basic	Sep 22 2015	10:46	UTC-5	69°10.220	100°41.700	Box Core ↓	64	185	340	14	0,5	1,69	1015,71	92	0
3b	312	Basic	Sep 22 2015	10:50	UTC-5	69°10.230	100°41.590	Box Core (bottom)	63	147	340	11	0,5	1,67	1015,83	92	0
3b	312	Basic	Sep 22 2015	10:53	UTC-5	69°10.230	100°41.560	Box Core ↑	64	156	340	11	0,5	1,67	1015,83	92	0
3b	312	Basic	Sep 22 2015	11:07	UTC-5	69°10.110	100°42.250	Agassiz Trawl ↓	64	166	340	10	0	1,64	1015,83	91	0
3b	312	Basic	Sep 22 2015	11:17	UTC-5	69°09.940	100°41.780	Agassiz Trawl ↑	60	91	340	10	0,4	1,65	1015,83	91	0
3b	312	Basic	Sep 22 2015	11:32	UTC-5	69°10.180	100°41.450	Beam Trawl ↓	64	170	330	17	-0,8	1,65	1015,84	95	0
3b	312	Basic	Sep 22 2015	12:07	UTC-5	69°10.025	100°37.438	Beam Trawl ↑	47	330	16,7	-1	1,73	1016,06	94	0	
3b	312	Basic	Sep 22 2015	12:08	UTC-5	69°10.026	100°37.437	SX90 ↓	47	330	16,7	-1	1,73	1016,07	94	0	
3b	310	Basic	Sep 23 2015	01:41	UTC-5	71°27.411	101°16.734	CTD-Rosette ↓	163	195	0	25	-2,5	0,64	1018,35	94	0
3b	310	Basic	Sep 23 2015	02:15	UTC-5	71°27.142	101°16.756	CTD-Rosette ↑	163	217	0	26,9	0,1	0,52	1018,86	84	0
3b	310	Basic	Sep 23 2015	02:31	UTC-5	71°27.020	101°16.862	Tucker Net ↓	161	137	0	25,2	-0,2	0,51	1018,93	83	0
3b	310	Basic	Sep 23 2015	02:47	UTC-5	71°26.959	101°15.487	Tucker Net ↑	163	20	0	25	-2,7	0,56	1018,87	90	0
3b	310	Basic	Sep 23 2015	03:11	UTC-5	71°27.242	101°17.404	Monster-Loki Net ↓	162	200	0	29,7	-2,7	0,72	1018,95	90	0
3b	310	Basic	Sep 23 2015	03:24	UTC-5	71°27.264	101°17.368	Monster-Loki Net ↑	161	205	0	25	1,2	0,68	1019,63	77	0
3b	310	Basic	Sep 23 2015	04:00	UTC-5	71°26.980	101°17.540	Box Core (bottom)	158	201	0	20	1	0,71	1019,96	76	0
3b	310	Basic	Sep 23 2015	04:05	UTC-5	71°26.950	101°17.580	Box Core ↑	157	208	0	20	1	0,71	1019,96	76	0
3b	310	Basic	Sep 23 2015	04:35	UTC-5	71°27.530	101°16.200	Agassiz Trawl ↓ (cancelled)	166	197	0	25	-2,5	0,74	1019,53	84	0
3b	310	Basic	Sep 23 2015	05:00	UTC-5	71°26.750	101°17.640	Agassiz Trawl ↑ (cancelled)	158	130	0	25	-2,5	0,76	1019,85	84	0
3b	308 / CAA8	Geotrace	Sep 23 2015	21:36	UTC-5	74°08.320	108°50.080	CTD-Rosette ↓ OMICS	565	159	330	7	-3	0,05	1028,12	89	1/10
3b	308 / CAA8	Geotrace	Sep 23 2015	22:08	UTC-5	74°08.340	108°49.610	CTD-Rosette ↑ OMICS	562	196	0	5	-2,7	0,18	1028,13	86	1/10
3b	308 / CAA8	Geotrace	Sep 23 2015	22:28	UTC-5	74°08.310	108°50.390	TM-Rosette ↓	564	168	340	5	-2,6	0,19	1028,1	87	1/10
3b	308 / CAA8	Geotrace	Sep 23 2015	22:48	UTC-5	74°08.330	108°50.270	TM-Rosette ↑	569	141	320	2	-2	0,19	1028,12	84	1/10
3b	308 / CAA8	Geotrace	Sep 23 2015	23:06	UTC-5	74°08.310	108°50.250	LVP ↓	569	90	310	4	-2	0,2	1028,15	84	1/10
3b	308 / CAA8	Geotrace	Sep 24 2015	03:12	UTC-5	74°08.321	108°50.223	LVP ↑	569	156	270	5	-1,9	0,05	1028,49	86	0
3b	308 / CAA8	Geotrace	Sep 24 2015	03:25	UTC-5	74°08.348	108°50.275	CTD-Rosette ↓	563	57	270	4	-2,1	0,07	1028,51	86	0
3b	308 / CAA8	Geotrace	Sep 24 2015	04:21	UTC-5	74°08.370	108°50.250	CTD-Rosette ↑	563	155	260	5	-1,8	0,12	1028,65	89	0
3b	308 / CAA8	Geotrace	Sep 24 2015	04:32	UTC-5	74°08.340	108°50.190	TM-Rosette ↓	563	128	280	5	-1,9	0,12	1028,66	90	0
3b	308 / CAA8	Geotrace	Sep 24 2015	05:06	UTC-5	74°08.380	108°50.130	TM-Rosette ↑	563	188	270	5	-2	0,1	1028,73	86	0
3b	308 / CAA8	Geotrace	Sep 24 2015	05:50	UTC-5	74°08.360	108°50.120	LVP ↓	564	194	270	6	-2,5	0,06	1028,78	88	0
3b	308 / CAA8	Geotrace	Sep 24 2015	09:53	UTC-5	74°08.330	108°50.120	LVP ↑	564	268	240	3	-2,4	0,18	1028,74	91	1/10
3b	308 / CAA8	Geotrace	Sep 24 2015	10:05	UTC-5	74°08.320	108°50.140	CTD-Rosette ↓	563	286	240	3	-2,4	0,17	1028,72	90	1/10
3b	308 / CAA8	Geotrace	Sep 24 2015	10:54	UTC-5	74°08.310	108°50.180	CTD-Rosette ↑	567	76	220	2	-1,2	0,19	1028,68	86	1/10
3b	308 / CAA8	Geotrace	Sep 24 2015	11:00	UTC-5	74°08.520	108°50.030	Tucker Net ↓	565	321	220	3	-1,2	0,19	1028,68	87	1/10
3b	308 / CAA8	Geotrace	Sep 24 2015	11:11	UTC-5	74°08.660	108°51.030	Tucker Net ↑	563	269	220	4	-1,1	0,19	1028,7	90	1/10
3b	308 / CAA8	Geotrace	Sep 24 2015	12:13	UTC-5	74°08.295	108°50.214	Monster-Loki Net ↓	566	72	285	5,1	-1,8	0,15	1028,93	90	0
3b	308 / CAA8	Geotrace	Sep 24 2015	12:51	UTC-5	74°08.327	108°50.150	Monster-Loki Net ↑	570	343	225	7	-2,7	0,18	1029	88	0
3b	308 / CAA8	Geotrace	Sep 24 2015	13:12	UTC-5	74°08.329	108°50.069	Hydrobios ↓	565	345	230	8	-2,6	0,19	1029,04	86	0
3b	308 / CAA8	Geotrace	Sep 24 2015	13:44	UTC-5	74°08.333	108°50.031	Hydrobios ↑	564	323	250	4	-2,6	0,15	1029,17	85	0
3b	308 / CAA8	Geotrace	Sep 24 2015	14:15	UTC-5	74°08.356	108°50.193	Box Core ↓	564	287	225	4,1	-2,4	0,13	1029,38	85	0
3b	308 / CAA8	Geotrace	Sep 24 2015	14:52	UTC-5	74°08.332	108°50.213	Box Core (bottom)	563	8	255	3,9	-2,6	0,23	1029,44	85	0

3b	308 / CAA8	Geotrace	Sep 24 2015	15:30	UTC-5	74°08.352	108°50.429	Box Core ↑	564	34	240	4	-2,6	0,09	1029,39	85	0
3b	308 / CAA8	Geotrace	Sep 24 2015	15:52	UTC-5	74°08.242	108°49.705	Agassiz Trawl ↓	563	110	190	6,1	-1,1	0,13	1029,36	79	0
3b	308 / CAA8	Geotrace	Sep 24 2015	16:42	UTC-5	74°08.890	108°52.480	Agassiz Trawl ↑	561	220	180	10	-2,6	0,06	1026,95	82	0
3b	308 / CAA8	Geotrace	Sep 24 2015	17:07	UTC-5	74°08.400	108°50.049	Beam Trawl ↓	564	5	180	8,3	-2,4	0,06	1029,46	81	0
3b	308 / CAA8	Geotrace	Sep 24 2015	18:24	UTC-5	74°08.250	108°59.020	Beam Trawl ↑	562	170	210	4	-2,7	0,02	1029,47	82	0
3b	307	Basic	Sep 25 2015	02:52	UTC-5	74°06.675	103°07.454	CTD-Rosette ↓	357	72	200	5,5	-4,9	-0,55	1031,02	97	0
3b	307	Basic	Sep 25 2015	03:44	UTC-5	74°02.019	103°07.660	CTD-Rosette ↑	352	308	160	5	-4,3	0,4	1030,92	96	0
3b	307	Basic	Sep 25 2015	04:09	UTC-5	74°06.710	103°06.690	Monster-Loki Net ↓	355	308	200	8	-5	-0,49	1030,86	94	10/10
3b	307	Basic	Sep 25 2015	04:34	UTC-5	74°06.940	103°06.170	Monster-Loki Net ↑	351	21	200	6	-4	-0,38	1030,89	92	10/10
3b	307	Basic	Sep 25 2015	05:00	UTC-5	74°06.980	103°06.000	Box Core ↓	350	334	180	5	-4,6	-0,39	1030,86	94	10/10
3b	307	Basic	Sep 25 2015	05:10	UTC-5	74°07.100	103°05.540	Box Core (bottom)	349	358	180	6	-4,6	-0,39	1030,86	94	10/10
3b	307	Basic	Sep 25 2015	05:20	UTC-5	74°07.120	103°05.450	Box Core ↑	349	4	180	5	-4,5	-0,26	1030,91	94	10/10
3b	342	Basic	Sep 25 2015	08:49	UTC-5	74°47.670	092°46.860	CTD-Rosette ↓	137	193	30	6	-5,5	1,29	1026,3	98	1/10
3b	342	Basic	Sep 25 2015	21:21	UTC-5	74°47.620	092°46.950	CTD-Rosette ↑	138	208	20	8	-5,2	1,15	1025,8	96	1/10
3b	342	Basic	Sep 25 2015	21:33	UTC-5	74°47.630	092°46.860	Tucker Net ↓	137	149	20	7	-5,1	1,1	1025,59	97	1/10
3b	342	Basic	Sep 25 2015	21:57	UTC-5	74°47.580	092°43.490	Tucker Net ↑	128	14	0	8	-5,4	1,07	1025,18	95	1/10
3b	342	Basic	Sep 25 2015	22:25	UTC-5	74°47.660	092°47.300	Monster-Loki Net ↓	137	154	20	8	-5,3	1,02	1024,75	97	1/10
3b	342	Basic	Sep 25 2015	22:36	UTC-5	74°47.660	092°47.630	Monster-Loki Net ↑	140	151	20	8	-5,5	1,06	1024,61	98	1/10
3b	342	Basic	Sep 25 2015	23:04	UTC-5	74°47.650	092°47.160	Box Core ↓	138	200	10	8	-5,1	1,05	1024,04	97	1/10
3b	342	Basic	Sep 25 2015	23:08	UTC-5	74°47.650	092°47.320	Box Core (bottom)	137	165	20	8	-5,2	1	1023,48	98	1/10
3b	342	Basic	Sep 25 2015	23:13	UTC-5	74°47.630	092°47.460	Box Core ↑	138	126	20	8	-5,2	1	1023,48	98	1/10
3b	342	Basic	Sep 25 2015	23:33	UTC-5	74°47.650	092°46.880	Box Core ↓	138	148	350	10	-5,2	0,98	1023,59	98	1/10
3b	342	Basic	Sep 25 2015	23:37	UTC-5	74°47.630	092°47.010	Box Core (bottom)	138	155	350	10	-5,2	0,98	1023,59	98	1/10
3b	342	Basic	Sep 25 2015	23:43	UTC-5	74°47.590	092°47.180	Box Core ↑	137	91	0	9	-5,4	0,97	1023,49	97	1/10
3b	342	Basic	Sep 26 2015	00:10	UTC-5	74°47.558	092°46.632	Beam Trawl ↓	135	97	0	5	-5,5	0,92	1023	97	0
3b	342	Basic	Sep 26 2015	00:50	UTC-5	74°48.000	092°43.500	Beam Trawl ↑	128	0	5	5	-5,6	0,91	1023	97	0
3b	---	MVP	Sep 26 2015	02:38	UTC-5	74°47.208	092°11.635	MVP ↓	78	267	0	10	-6,5	1,67	1020,6	96	0
3b	---	MVP	Sep 26 2015	14:35	UTC-5	75°41.919	095°05.702	MVP ↑	36	276	0	17	-2,4	-0,25	1010,46	98	0
3b	---	MVP	Sep 26 2015	16:00	UTC-5	75°43.000	095°49.800	MVP ↓	103	338	20	12	-3,2	-0,12	1009,13	76	0
3b	---	MVP	Sep 26 2015	21:00	UTC-5	76°14.600	096°16.200	MVP ↑		334							0
3b	CAA9	Basic	Sep 26 2015	22:13	UTC-5	76°19.930	096°44.690	CTD-Rosette ↓	340	191	320	9	-4,9	-0,74	1006,9	85	10/10
3b	CAA9	Basic	Sep 26 2015	22:46	UTC-5	76°19.600	096°43.740	CTD-Rosette ↑	347	190,7	320	2	-5,3	-0,73	1006,68	88	10/10
3b	CAA9	Basic	Sep 26 2015	23:06	UTC-5	76°19.960	096°44.920	TM-Rosette ↓ (cancelled)	339	199,9	350	3	-5	-0,73	1006,26	87	10/10
3b	CAA9	Basic	Sep 26 2015	23:30	UTC-5	76°19.770	096°44.70	TM-Rosette ↑ (cancelled)	344	203	340	3	-4,4	-0,76	1006,04	88	10/10
3b	CAA9	Basic	Sep 27 2015	00:02	UTC-5	76°20.006	096°45.206	TM-Rosette ↓	334	217	30	11	-3,9	-0,76	1005,83	78	10/10
3b	CAA9	Basic	Sep 27 2015	00:16	UTC-5	76°19.981	096°45.376	TM-Rosette ↑	333	155	30	16,2	-3,5	-0,75	1005,73	77	10/10
3b	CAA9	Basic	Sep 27 2015	00:32	UTC-5	76°19.956	096°45.679	CTD-Rosette Geochem ↓	331	246	20	12,3	-3	-0,74	1005,55	76	10/10
3b	CAA9	Basic	Sep 27 2015	01:16	UTC-5	76°19.971	096°46.044	CTD-Rosette Geochem ↑	322	216	0	13	-3,7	-0,74	1005,26	77	10/10
3b	CAA9	Basic	Sep 27 2015	03:11	UTC-4	76°19.912	096°45.161	Monster-Loki Net ↓	337	200	0	16,7	-4,8	-0,82	1004,76	82	10/10
3b	CAA9	Basic	Sep 27 2015	03:36	UTC-4	76°20.027	096°44.856	Monster-Loki Net ↑	336	344	10	16,8	-4,3	-0,76	1004,4	81	10/10
3b	CAA9	Basic	Sep 27 2015	05:00	UTC-4	76°19.820	096°45.400	TM-Rosette ↓	336	199	0	16	-4,4	-0,78	1004,18	82	10/10
3b	CAA9	Basic	Sep 27 2015	05:23	UTC-4	76°19.830	096°45.210	TM-Rosette ↑	336	228	0	11	-1,8	-0,78	1004	74	10/10
3b	CAA9	Basic	Sep 27 2015	05:36	UTC-4	76°19.830	096°45.240	Box Core ↓	338	147	10	9	-3,1	-0,78	1003,94	77	10/10
3b	CAA9	Basic	Sep 27 2015	05:45	UTC-4	76°19.810	096°45.350	Box Core (bottom)	336	127	10	15	-5,2	-0,77	1003,81	82	10/10
3b	CAA9	Basic	Sep 27 2015	05:53	UTC-4	76°19.810	096°45.380	Box Core ↑	336	110	10	15	-5,2	-0,77	1003,81	82	10/10
3b	CAA9	Basic	Sep 27 2015	07:17	UTC-4	76°25.460	096°26.940	CTD-Rosette ↓	278	126	10	11	-5,7	-0,84	1003,53	84	8/10
3b	CAA9	Basic	Sep 27 2015	07:30	UTC-4	76°25.420	096°26.950	CTD-Rosette ↑	276	160	10	14	-5,9	-0,66	1003,44	83	8/10
3b	CTD-02	CTD	Sep 27 2015	09:49	UTC-4	76°34.840	096°42.620	CTD ↓	216	321	10	10	-5,8	-0,76	1003,23	83	1/10
3b	CTD-02	CTD	Sep 27 2015	10:06	UTC-4	76°34.650	096°42.370	CTD ↑	217	248	10	7	-5,5	-0,73	1003,22	82	1/10
3b	PS1	CTD	Sep 27 2015	10:54	UTC-4	76°40.030	096°51.120	CTD ↓	230	277	10	5	-6,7	-0,68	1002,99	89	5/10
3b	PS1	CTD	Sep 27 2015	11:07	UTC-4	76°39.930	096°50.320	CTD ↑	208	333	0	2	-5,5	-0,63	1002,98	85	5/10
3b	PS2	CTD	Sep 27 2015	11:39	UTC-4	76°37.160	096°51.340	CTD ↓	188	159	320	7	-7,7	-0,66	1003,11	86	5/10
3b	PS2	CTD	Sep 27 2015	11:49	UTC-4	76°37.010	096°50.850	CTD ↑	188	167	330	6	-7,4	-0,63	1003,06	85	5/10
3b	PS3	CTD	Sep 27 2015	13:31	UTC-4	76°36.372	097°01.472	CTD ↓	153	176	310	7,8	-6,8	-0,6	1002,63	93	3/10

3b	PS3	CTD	Sep 27 2015	13:41	UTC-4	76°36.318	097°01.028	CTD ↑	149	167	300	6,4	-6,8	-0,6	1002,63	93	3/10
3b	PS4	CTD	Sep 27 2015	14:27	UTC-4	76°33.000	097°05.583	CTD ↓	141	24	270	8,2	-7,4	-0,7	1002,45	93	3/10
3b	PS4	CTD	Sep 27 2015	14:36	UTC-4	76°33.027	097°05.643	CTD ↑	141	32	285	8,8	-7,4	-0,75	1002,46	95	3/10
3b	PS4	MVP	Sep 27 2015	18:05	UTC-4	76°11.430	096°02.500	MVP ↓	224	140	300	7	-5,3	-0,05	1002,2	89	0
3b	PS4	MVP	Sep 28 2015	03:55	UTC-4	75°36.885	094°89.840	MVP ↑	134	301	255	10	-8	0,11	1001,95	91	0
3b	PS4	MVP	Sep 28 2015	06:25	UTC-4	75°30.000	093°42.030	MVP ↓	267	310	300	15	-7,5	0,23	1002,19	91	0
3b	PS4	MVP	Sep 28 2015	22:00	UTC-4	75°35.700	093°59.000	MVP ↑		9							0
3b	WC01	CTD	Sep 28 2015	23:44	UTC-4	75°50.010	093°45.740	CTD ↓	330	156	40	3	-7,2	0,06	1003,95	73	0
3b	WC01	CTD	Sep 29 2015	00:02	UTC-4	75°49.984	093°45.855	CTD ↑	331	160	15	6,2	-6,9	0,15	1003,84	74	0
3b	WC02	CTD	Sep 29 2015	01:53	UTC-4	75°29.274	093°46.478	CTD ↓	249	198	345	12,7	-6,5	-0,01	1003,58	75	0
3b	WC02	CTD	Sep 29 2015	02:08	UTC-4	75°29.174	093°46.070	CTD ↑	253	132	345	8,3	-6,1	-0,03	1003,49	75	0
3b	WC03	CTD	Sep 29 2015	02:34	UTC-4	75°29.109	093°36.398	CTD ↓	231	119	330	8,2	-6,5	-0,05	1003,45	76	0
3b	WC03	CTD	Sep 29 2015	02:47	UTC-4	75°29.271	093°36.325	CTD ↑	232	138	350	-6,2	-6,6	-0,01	1003,49	75	0
3b	WC04	CTD	Sep 29 2015	04:43	UTC-4	75°29.110	093°07.280	CTD ↓	152	260	350	9	-6,5	0,01	1003,7	77	0
3b	WC04	CTD	Sep 29 2015	04:54	UTC-4	75°29.080	093°07.060	CTD ↑	150	177	350	4	-6,5	0,01	1003,7	77	0
3b	WC05	CTD	Sep 29 2015	05:40	UTC-4	75°29.130	092°37.960	CTD ↓	155	254	40	7	-6,4	0,12	1003,56	79	0
3b	WC05	CTD	Sep 29 2015	05:49	UTC-4	75°29.170	092°38.130	CTD ↑	155	182	4	5	-6,4	0,12	1003,56	79	0
3b	WC05.5	CTD	Sep 29 2015	06:10	UTC-4	75°29.130	092°28.310	CTD ↓	100	320	70	6	-6,8	0,48	1003,59	83	0
3b	WC05.5	CTD	Sep 29 2015	06:20	UTC-4	75°29.130	092°28.180	CTD ↑	100	250	70	6	-6,8	0,48	1003,59	83	0
3b	WC06	CTD	Sep 29 2015	08:03	UTC-4	75°15.720	092°34.360	CTD ↓	179	153	30	7	-6,8	0,84	1004,39	76	0
3b	WC06	CTD	Sep 29 2015	08:13	UTC-4	75°15.720	092°34.340	CTD ↑	177	139	30	6	-6,6	0,89	1004,41	75	0
3b	WC07	CTD	Sep 29 2015	08:44	UTC-4	75°15.730	092°44.350	CTD ↓	176	176	340	6	-5,9	0,68	1004,35	73	0
3b	WC07	CTD	Sep 29 2015	08:54	UTC-4	75°15.700	092°44.320	CTD ↑	175	181	330	3	-5,3	0,39	1004,49	72	0
3b	WC08	CTD	Sep 29 2015	09:22	UTC-4	75°15.730	092°58.050	CTD ↓	153	162	340	6	-5,7	0,03	1004,4	75	0
3b	WC08	CTD	Sep 29 2015	09:32	UTC-4	75°15.710	092°58.060	CTD ↑	153	187	340	6	-5,7	0,03	1004,4	75	0
3b	WC09	CTD	Sep 29 2015	10:05	UTC-4	75°15.700	093°14.510	CTD ↓	222	117	300	9	-6,6	0,03	1004,34	86	0
3b	WC09	CTD	Sep 29 2015	10:13	UTC-4	75°15.620	093°14.480	CTD ↑	222	147	290	8	-6,5	-0,06	1004,52	85	0
3b	WC10	CTD	Sep 29 2015	10:47	UTC-4	75°15.620	093°22.540	CTD ↓	226	140	290	11	-7	-0,06	1004,35	86	0
3b	WC10	CTD	Sep 29 2015	10:59	UTC-4	75°15.480	093°22.550	CTD ↑	226	94	280	9	-6,6	-0,01	1004,65	84	0
3b	WC11	MVP	Sep 29 2015	12:22	UTC-4	75°00.772	093°19.902	MVP ↓	263	90	300	11,2	-7,4	-0,03	1004,47	84	0
3b	WC11	MVP	Sep 29 2015	19:05	UTC-4	74°40.950	093°10.710	MVP ↑	144	81	230	6	-7,2	0,85	1006,07	86	0
3b	WC16	CTD	Sep 29 2015	20:03	UTC-4	74°40.760	093°21.360	CTD ↓	102	55	260	5	-7,3	0,78	1006,07	93	0
3b	WC16	CTD	Sep 29 2015	20:11	UTC-4	74°40.730	093°21.360	CTD ↑	102	71	220	2	-6,6	0,95	1006,11	91	0
3b	WC17	CTD	Sep 29 2015	21:07	UTC-4	74°41.010	093°07.460	CTD ↓	143	99	190	5	-6,4	0,31	1006,48	89	1/10
3b	WC17	CTD	Sep 29 2015	21:17	UTC-4	74°41.020	093°07.590	CTD ↑	142	87	180	7	-6,3	0,15	1006,33	89	1/10
3b	WC18	CTD	Sep 29 2015	22:23	UTC-4	74°41.420	092°40.950	CTD ↓	144	44	170	6	-6	0,53	1006,14	87	1/10
3b	WC18	CTD	Sep 29 2015	22:34	UTC-4	74°41.430	092°41.100	CTD ↑	139	45	160	2	-5,3	0,56	1006,21	84	1/10
3b	WC19	CTD	Sep 29 2015	23:37	UTC-4	74°41.840	092°14.200	CTD ↓	91	13	170	9	-5,9	0,45	1006,09	84	0
3b	WC19	CTD	Sep 29 2015	23:45	UTC-4	74°41.900	092°14.400	CTD ↑	91	32	160	4	-5,4	0,67	1006,23	83	0
3b	WC20	CTD	Sep 30 2015	00:22	UTC-4	74°42.193	092°01.019	CTD ↓	115	36	160	12	-5,7	0,71	1006,28	83	0
3b	WC20	CTD	Sep 30 2015	00:30	UTC-4	74°42.229	092°01.177	CTD ↑	116	28	150	12	-5,2	0,7	1006,34	82	0
3b	BS01	CTD	Sep 30 2015	01:23	UTC-4	74°38.029	092°05.361	CTD ↓	125	30	165	11	-5,7	0,18	1006,13	86	0
3b	BS01	CTD	Sep 30 2015	01:34	UTC-4	74°28.178	092°05.699	CTD ↑	124	118	165	14,5	-4	0,56	1006,48	82	0
3b	BS02	CTD	Sep 30 2015	02:19	UTC-4	74°34.211	092°09.780	CTD ↓	171	138	160	18,1	-6,6	0,63	1006,15	89	0
3b	BS02	CTD	Sep 30 2015	02:28	UTC-4	74°34.266	092°09.824	CTD ↑	171	137	160	17,8	-6,3	0,69	1006,31	88	0
3b	BS03	CTD	Sep 30 2015	03:49	UTC-4	74°25.401	092°19.606	CTD ↓	302	167	160	16	-5	-0,45	1005,92	79	0
3b	BS03	CTD	Sep 30 2015	04:04	UTC-4	74°25.420	092°19.480	CTD ↑	267	130	170	17	-5,1	-0,3	1006,2	80	0
3b	BS04	CTD	Sep 30 2015	05:22	UTC-4	74°17.320	092°29.450	CTD ↓	177	0	170	19	-4,4	-0,24	1005,55	83	0
3b	BS04	CTD	Sep 30 2015	05:32	UTC-4	74°17.340	092°29.370	CTD ↑	177	30	170	20	-4,4	-0,24	1005,55	83	0
3b	BS05	CTD	Sep 30 2015	06:15	UTC-4	74°13.600	092°33.640	CTD ↓	164	0	140	18	-3,8	-0,47	1005,39	84	0
3b	BS05	CTD	Sep 30 2015	06:23	UTC-4	74°13.670	092°33.680	CTD ↑	164	13	140	19	-3,8	-0,47	1006,39	84	0
3b	BS06	CTD	Sep 30 2015	07:05	UTC-4	74°10.000	092°38.150	CTD ↓	152	23	160	18	-3	-0,68	1005,36	84	0
3b	BS06	CTD	Sep 30 2015	07:15	UTC-4	74°10.010	092°38.120	CTD ↑	152	34	160	18	-3	-0,68	1005,36	84	0
4a	304	Basic	Oct 03 2015	16:36	UTC-6	74°14.571	091°30.222	PNF + Secchi ↓	315	228	200	21	-1,8	0,54	1015,4	88	0

4a	304	Basic	Oct 03 2015	16:44	UTC-6	74°14.599	091°30.257	PNF + Secchi ↑	317	226	210	20	-2,1	0,55	1015,35	92	0
4a	304	Basic	Oct 03 2015	17:46	UTC-6	74°14.600	091°31.300	Tucker Net ↓	315	230	225	18	-1,5	0,54	1014,99	90	0
4a	304	Basic	Oct 03 2015	18:13	UTC-6	74°14.858	091°29.319	Tucker Net ↑	317	350	230	14	-1,1	0,55	1015,01	92	0
4a	304	Basic	Oct 03 2015	18:31	UTC-6	74°14.807	091°30.945	CTD-Rosette ↓	315	234	230	19	-1,4	0,56	1014,79	91	0
4a	304	Basic	Oct 03 2015	19:10	UTC-6	74°14.724	091°29.721	CTD-Rosette ↑	314	235	250	19	-1,2	0,58	1015,02	87	0
4a	304	Basic	Oct 03 2015	19:30	UTC-6	74°14.874	091°30.596	Monster-Loki Net ↓	315	251	250	18	-1,3	0,57	1015,05	88	0
4a	304	Basic	Oct 03 2015	19:51	UTC-6	74°15.019	091°30.369	Monster-Loki Net ↑	316	235	235	18	-1,3	0,58	1015,14	88	0
4a	304	Basic	Oct 03 2015	20:24	UTC-6	74°14.799	091°31.086	Hydrobios ↓	314	235	240	20	-1,5	0,56	1015,22	86	0
4a	304	Basic	Oct 03 2015	20:44	UTC-6	74°14.938	091°30.907	Hydrobios ↑	315	259	240	20	-1,6	0,56	1015,28	87	0
4a	304	Basic	Oct 03 2015	21:13	UTC-6	74°14.759	091°31.492	Box Core ↓	314	243	250	19	-1,6	0,54	1015,36	87	0
4a	304	Basic	Oct 03 2015	21:21	UTC-6	74°14.795	091°31.181	Box Core (bottom)	313	268	250	18	-1,6	0,54	1015,35	85	0
4a	304	Basic	Oct 03 2015	21:27	UTC-6	74°14.859	091°31.207	Box Core ↑	313	272	250	18	-1,6	0,54	1015,35	85	0
4a	304	Basic	Oct 03 2015	21:44	UTC-6	74°14.993	091°31.891	Agassiz Trawl ↓	314	238	230	15	-1,7	0,55	1015,29	85	0
4a	304	Basic	Oct 03 2015	22:10	UTC-6	74°15.185	091°28.947	Agassiz Trawl ↑	321	299	230	18	-0,7	0,54	1015,23	80	0
4a	304	Basic	Oct 03 2015	22:15	UTC-6	74°15.282	091°28.848	Agassiz Trawl ↓	321	300	230	18	-0,7	0,54	1015,23	80	0
4a	304	Basic	Oct 03 2015	22:46	UTC-6	74°15.644	091°27.888	Agassiz Trawl ↑	322	335	230	16	-1,6	0,57	1015,28	82	0
4a	304	Basic	Oct 03 2015	23:15	UTC-6	74°14.824	091°30.461	Beam Trawl ↓	313	338	220	17	-1,7	0,58	1015,02	83	0
4a	304	Basic	Oct 04 2015	00:20	UTC-6	74°15.660	091°32.020	Beam Trawl ↑	318	153	200	18	-1,8	0,6	1015,07	86	0
4a	304	Basic	Oct 04 2015	01:01	UTC-6	74°14.800	091°29.580	CTD-Rosette ↓	316	204	220	19	-1,6	0,61	1014,97	88	0
4a	304	Basic	Oct 04 2015	01:42	UTC-6	74°14.640	091°26.180	CTD-Rosette ↑	319	125	220	18	-1,3	0,62	1014,98	84	0
4a	346	Nutrient	Oct 04 2015	02:53	UTC-6	74°09.010	091°27.370	CTD-Rosette ↓	280	209	220	18	-1,8	0,26	1015,1	86	0
4a	346	Nutrient	Oct 04 2015	03:32	UTC-6	74°08.990	091°22.570	CTD-Rosette ↑	280	225	220	16	-1,9	0,03	1014,95	85	0
4a	343	Nutrient	Oct 04 2015	05:43	UTC-6	74°32.758	091°31.498	CTD-Rosette ↓	151	218	240	22	-1,9	0,15	1014,21	89	0
4a	343	Nutrient	Oct 04 2015	06:17	UTC-6	74°32.676	091°31.358	CTD-Rosette ↑	153	209	220	16	-1,7	0,17	1014,27	88	0
4a	301	Basic	Oct 04 2015	17:02	UTC-5	74°07.140	083°19.790	PNF + Secchi ↓	672	204	240	15	-1,5	0,35	1015,47	78	0
4a	301	Basic	Oct 04 2015	17:10	UTC-5	74°06.960	083°19.940	PNF + Secchi ↑	677	217	240	15	-1,7	0,38	1015,31	78	0
4a	301	Basic	Oct 04 2015	18:10	UTC-5	74°07.312	083°18.889	CTD-Rosette ↓	679	235	240	15	-1,5	0,4	1014,94	76	1/10
4a	301	Basic	Oct 04 2015	19:09	UTC-5	74°06.919	083°19.133	CTD-Rosette ↑	676	254	240	15	-1,4	0,42	1014,64	77	1/10
4a	301	Basic	Oct 04 2015	19:27	UTC-5	74°06.758	083°18.769	Tucker Net ↓	675	22	240	13	-1,3	0,42	1014,52	78	1/10
4a	301	Basic	Oct 04 2015	19:43	UTC-5	74°07.321	083°18.854	Tucker Net ↑	680	345	210	14	-1,6	0,37	1014,48	77	1/10
4a	301	Basic	Oct 04 2015	20:13	UTC-5	74°07.091	083°19.542	Monster-Loki Net ↓	674	257	230	12	-0,8	0,38	1014,42	77	1/10
4a	301	Basic	Oct 04 2015	20:57	UTC-5	74°07.107	083°19.221	Monster-Loki Net ↑	672	258	230	14	-1,4	0,42	1014,07	80	1/10
4a	301	Basic	Oct 04 2015	21:28	UTC-5	74°07.079	083°17.952	Box Core ↓	676	248	230	16	-0,3	0,38	1013,93	77	1/10
4a	301	Basic	Oct 04 2015	21:38	UTC-5	74°07.127	083°18.136	Box Core (bottom)	677	259	230	16	-1,2	0,39	1013,7	78	1/10
4a	301	Basic	Oct 04 2015	21:49	UTC-5	74°07.178	083°18.248	Box Core ↑	681	253	220	15	-1,5	0,39	1013,71	79	1/10
4a	301	Basic	Oct 04 2015	22:07	UTC-5	74°07.189	083°18.808	Agassiz Trawl ↓	676	2	230	17	-1,3	0,4	1013,5	78	1/10
4a	301	Basic	Oct 04 2015	22:51	UTC-5	74°08.235	083°18.485	Agassiz Trawl ↑	678	345	230	16	-1,5	0,39	1013,11	81	1/10
4a	301	Basic	Oct 04 2015	23:16	UTC-5	74°07.256	083°19.374	CTD-Rosette ↓	676	222	230	17	-1,3	0,41	1012,6	79	1/10
4a	301	Basic	Oct 05 2015	00:02	UTC-5	74°06.89	083°18.290	CTD-Rosette ↑	676	252	220	17	-1,4	0,47	1012,65	79	1/10
4a	325	Nutrient	Oct 05 2015	04:08	UTC-5	73°48.997	080°29.318	CTD-Rosette ↓	679	226	240	13	-1,4	-0,08	1012,19	68	1/10
4a	325	Nutrient	Oct 05 2015	05:03	UTC-5	73°49.012	080°25.883	CTD-Rosette ↑	706	258	200	14	-1,3	-0,02	1011,81	65	1/10
4a	324	Nutrient	Oct 05 2015	06:17	UTC-5	73°58.650	080°28.139	CTD-Rosette ↓	773	230	230	14	-1,4	-0,16	1011,2	69	1/10
4a	324	Nutrient	Oct 05 2015	07:30	UTC-5	73°58.335	080°26.223	CTD-Rosette ↑	773	66	240	17	-1,4	-0,18	1010,74	68	1/10
4a	323	Full	Oct 05 2015	08:36	UTC-5	73°09.337	080°27.667	PNF + Secchi ↓	792	69	240	19	-1,5	0,34	1010,19	81	1/10
4a	323	Full	Oct 05 2015	08:42	UTC-5	73°09.360	080°27.456	PNF + Secchi ↑	796	72	250	19	-1,6	0,36	1010,08	83	1/10
4a	323	Full	Oct 05 2015	08:58	UTC-5	73°09.386	080°28.547	CTD-Rosette ↓	790	249	250	19	-1,4	0,38	1009,85	82	1/10
4a	323	Full	Oct 05 2015	09:54	UTC-5	73°09.531	080°25.909	CTD-Rosette ↑	782	265	240	19	-1,4	0,41	1009,58	78	1/10
4a	323	Full	Oct 05 2015	10:12	UTC-5	73°09.583	080°27.989	Tucker Net ↓	784	49	240	18	-1,6	0,39	1009,23	80	1/10
4a	323	Full	Oct 05 2015	10:25	UTC-5	73°10.208	080°25.593	Tucker Net ↑	786	360	240	18	-0,8	0,35	1009,04	77	1/10
4a	323	Full	Oct 05 2015	11:02	UTC-5	73°09.438	080°28.306	CTD-Rosette ↓	788	249	240	21	-1,4	0,38	1008,58	78	1/10
4a	323	Full	Oct 05 2015	12:12	UTC-5	73°09.480	080°25.990	CTD-Rosette ↑	785	253	250	17	-0,8	0,27	1008,2	72	1/10
4a	323	Full	Oct 05 2015	12:55	UTC-5	73°09.360	080°27.570	Monster-Loki Net ↓	790	239	240	17	-0,9	0,14	1008	71	1/10
4a	323	Full	Oct 05 2015	13:45	UTC-5	73°09.780	080°27.210	Monster-Loki Net ↑	794	272	230	16	-1,3	0,14	1007,71	73	1/10
4a	323	Full	Oct 05 2015	14:13	UTC-5	73°09.300	080°27.750	Hydrobios ↓	798	238	230	17	-1,3	0,1	1007,43	70	1/10

4a	323	Full	Oct 05 2015	14:58	UTC-5	73°09.620	080°27.240	Hydrobios ↑	808	244	220	18	-1,9	0,11	1007,32	75	1/10
4a	323	Full	Oct 05 2015	16:24	UTC-5	73°09.487	080°27.702	Agassiz Trawl ↓	789	14	230	19	-1,7	0,16	1006,23	72	1/10
4a	323	Full	Oct 05 2015	17:10	UTC-5	73°10.840	080°28.065	Agassiz Trawl ↑	789	280	220	18	-1,8	0,16	1006,48	69	1/10
4a	323	Full	Oct 05 2015	17:35	UTC-5	74°09.48	080°28.220	Box Core ↓	791	219	210	19	-1,6	0,26	1006	69	1/10
4a	323	Full	Oct 05 2015		UTC-5			Box Core (bottom)									1/10
4a	323	Full	Oct 05 2015	18:00	UTC-5	74°09.549	080°28.597	Box Core ↑	792	228	200	21	-1,6	0,17	1006,13	72	1/10
4a	323	Full	Oct 05 2015	18:14	UTC-5	74°09.491	080°28.747	Box Core ↓	797	212	215	18	-1,6	0,18	1006,05	71	1/10
4a	323	Full	Oct 05 2015	18:26	UTC-5	74°09.450	080°28.588	Box Core (bottom)	794	228	215	20	-1,7	0,18	1005,94	73	1/10
4a	323	Full	Oct 05 2015	18:37	UTC-5	74°09.490	080°28.505	Box Core ↑	791	211	205	17	-1,7	0,18	1005,91	74	1/10
4a	323	Full	Oct 05 2015	19:06	UTC-5	74°09.585	080°28.305	Beam Trawl ↓	783	307	190	19	-1,7	0,14	1005,63	72	1/10
4a	323	Full	Oct 05 2015	20:40	UTC-5	74°11.500	080°35.487	Beam Trawl ↑	765	182	160	14	-1,3	0,11	1004,92	67	1/10
4a	323	Full	Oct 05 2015	21:48	UTC-5	74°08.104	080°25.914	IKMT ↓	804	281	140	10	-1,1	0,11	1004,77	72	1/10
4a	323	Full	Oct 05 2015	22:53	UTC-5	74°08.498	080°28.357	IKMT ↑	790	330	140	7	-1,1	0,18	1004,73	72	1/10
4a	300	Nutrient	Oct 06 2015	00:12	UTC-5	74°19.040	080°29.260	CTD-Rosette ↓	703	345	170	10	-1,9	-0,43	1004,68	76	1/10
4a	300	Nutrient	Oct 06 2015	01:08	UTC-5	74°19.510	080°28.880	CTD-Rosette ↑	700	34	140	10	-1,9	-0,42	1004,52	89	1/10
4a	322	Nutrient	Oct 06 2015	03:03	UTC-5	74°29.620	080°32.170	CTD-Rosette ↓	661	348	150	12	-2,4	-0,62	1004,56	97	2/10
4a	322	Nutrient	Oct 06 2015	04:10	UTC-5	74°29.397	080°37.147	CTD-Rosette ↑	662	49	180	16	-1,5	-0,5	1004,54	99	2/10
4a	109	CTD	Oct 07 2015	06:07	UTC-5	76°17.368	074°06.645	CTD ↓	453	129	0	5	-2,6	-0,55	1003,78	78	1/10
4a	109	CTD	Oct 07 2015	06:24	UTC-5	76°17.374	074°06.420	CTD ↑	456	135	10	2	-2,9	-0,57	1003,61	80	1/10
4a	110	Nutrient	Oct 07 2015	07:08	UTC-5	76°17.978	072°38.699	CTD-Rosette ↓	533	126	310	3	-2,6	-0,59	1003,46	76	1/10
4a	110	Nutrient	Oct 07 2015	08:01	UTC-5	76°18.073	073°37.755	CTD-Rosette ↑	535	102	320	5	-3,3	-0,5	1002,5	78	1/10
4a	111	Basic	Oct 07 2015	08:47	UTC-5	76°18.350	073°12.980	CTD-Rosette ↓	595	119	310	4	-2,8	-0,54	1002,45	77	1/10
4a	111	Basic	Oct 07 2015	09:33	UTC-5	76°18.235	073°12.269	CTD-Rosette ↑	598	110	310	6	-2,3	-0,29	1002,06	81	1/10
4a	111	Basic	Oct 07 2015	09:41	UTC-5	76°18.376	073°11.827	Tucker Net ↓	592	339	310	5	-3,1	-0,25	1001,88	84	1/10
4a	111	Basic	Oct 07 2015	09:58	UTC-5	76°18.164	073°13.382	Tucker Net ↑	597	139	310	6	-3,1	-0,33	1001,8	85	Icebergs
4a	111	Basic	Oct 07 2015	10:23	UTC-5	76°18.514	073°12.785	Monster-Loki Net ↓	595	122	300	4	-3	-0,4	1001,75	84	Icebergs
4a	111	Basic	Oct 07 2015	11:03	UTC-5	76°18.335	073°12.349	Monster-Loki Net ↑	596	120	298	5	-2,2	-0,42	1001,58	80	Icebergs
4a	111	Basic	Oct 07 2015	12:03	UTC-5	76°18.280	073°12.550	CTD-Rosette ↓	598	137	Calm	Calm	-2,4	-0,4	1001,36	80	Icebergs
4a	111	Basic	Oct 07 2015	12:55	UTC-5	76°18.250	073°11.420	CTD-Rosette ↑	594	137	Calm	Calm	-1,7	-0,25	1001,39	77	Icebergs
4a	111	Basic	Oct 07 2015	11:20	UTC-5	76°18.257	073°12.185	PNF + Secchi ↓	594	174	290	4	-2,5	-0,38	1001,57	81	Icebergs
4a	111	Basic	Oct 07 2015	11:26	UTC-5	76°18.267	073°12.160	PNF + Secchi ↑	594	174	290	2	-1,6	-0,36	1001,52	78	Icebergs
4a	111	Basic	Oct 07 2015	13:10	UTC-5	76°18.410	073°12.970	Box Core ↓	597	349	280	5	-2,6	-0,24	1001,26	81	Icebergs
4a	111	Basic	Oct 07 2015	13:28	UTC-5	76°18.410	073°12.920	Box Core ↑	595	312	280	5	-3,3	-0,35	1001,29	84	Icebergs
4a	111	Basic	Oct 07 2015	13:40	UTC-5	76°18.530	073°13.270	Agassiz Trawl ↓	590	293	250	5	-3,3	-0,4	1001,14	85	1/10
4a	111	Basic	Oct 07 2015	14:13	UTC-5	76°18.340	073°12.890	Agassiz Trawl ↑	592	238	240	7	-2,9	-0,4	1001,03	83	1/10
4a	112	CTD	Oct 07 2015	15:00	UTC-5	76°18.900	072°42.160	CTD ↓	561	187	Calm	Calm	-3,7	-0,53	1001,31	88	1/10
4a	112	CTD	Oct 07 2015	15:21	UTC-5	76°18.940	072°42.030	CTD ↑	562	169	Calm	Calm	-2,8	-0,33	1001,36	85	1/10
4a	113	Nutrient	Oct 07 2015	16:07	UTC-5	76°19.290	073°13.200	CTD-Rosette ↓	554	104	180	8	-2,9	-0,56	1001,51	82	1/10
4a	113	Nutrient	Oct 07 2015	17:01	UTC-5	76°19.450	072°11.120	CTD-Rosette ↑	564	103	165	9	-2,9	-0,2	1001,62	82	1/10
4a	114	CTD	Oct 07 2015	17:43	UTC-5	76°19.510	071°47.640	CTD ↓	610	130	140	13	-3,3	-0,38	1002,4	85	1/10
4a	114	CTD	Oct 07 2015	18:10	UTC-5	76°18.620	071°46.970	CTD ↑	616	179	140	14	-3,5	-0,29	1002,29	86	1/10
4a	115	Basic	Oct 07 2015	19:13	UTC-5	76°20.070	071°12.920	Tucker Net ↓	674	287	60	14	-3,5	-0,21	1002,43	84	1/10
4a	115	Basic	Oct 07 2015	19:28	UTC-5	76°19.810	071°14.860	Tucker Net ↑	671	185	60	17	-3,5	-0,17	1002,51	82	1/10
4a	115	Basic	Oct 07 2015	20:31	UTC-5	76°19.888	071°12.407	Hydrobios ↓	655	129	120	18	-3,8	-0,15	1002,81	81	1/10
4a	115	Basic	Oct 07 2015	21:18	UTC-5	76°20.083	071°12.574	Hydrobios ↑	671	174	120	20	-3,7	-0,06	1003,06	81	1/10
4a	115	Basic	Oct 07 2015	21:44	UTC-5	76°19.971	071°12.029	CTD-Rosette ↓	674	105	120	20	-3,7	-0,1	1002,93	85	1/10
4a	115	Basic	Oct 07 2015	22:45	UTC-5	76°20.279	071°12.019	CTD-Rosette ↑	656	115	120	20	-3,5	-0,05	1003,14	85	1/10
4a	115	Basic	Oct 07 2015	23:09	UTC-5	76°20.017	071°11.941	Monster-Loki Net ↓	667	114	120	19	-3,3	-0,08	1003,06	86	Icebergs
4a	115	Basic	Oct 07 2015	23:51	UTC-5	76°19.980	071°13.033	Monster-Loki Net ↑	675	132	130	22	-2,8	-0,07	1003,1	89	Icebergs
4a	115	Basic	Oct 08 2015	00:12	UTC-5	76°20.510	071°14.020	Agassiz Trawl ↓	664	227	110	20	-2,1	-0,09	1003,29	88	Icebergs
4a	115	Basic	Oct 08 2015	00:46	UTC-5	76°20.370	071°18.140	Agassiz Trawl ↑	676	209	130	24	-3	-0,08	1003,4	91	Icebergs
4a	115	Basic	Oct 08 2015	01:44	UTC-5	76°20.190	071°14.010	Beam Trawl ↓	668	231	120	19	-1,9	-0,1	1003,62	88	Icebergs
4a	115	Basic	Oct 08 2015	03:03	UTC-5	76°19.820	071°27.440	Beam Trawl ↑	673	184	120	23	-2,7	-0,28	1003,94	88	Icebergs
4a	115	Basic	Oct 08 2015	03:38	UTC-5	76°20.130	071°14.110	CTD-Rosette ↓	669	322	130	22	-2,7	-0,28	1003,86	88	Icebergs

4a	115	Basic	Oct 08 2015	04:36	UTC-5	76°20.340	071°15.440	CTD-Rosette ↑	667	314	120	18	-0,4	-0,09	1004,49	83	Icebergs
4a	CASQ1	CTD	Oct 08 2015	10:08	UTC-5	77°17.091	074°23.189	CTD ↓	701	140	200	15	-3	-0,73	1006,06	89	Icebergs
4a	CASQ1	CTD	Oct 08 2015	10:38	UTC-5	77°17.066	074°23.149	CTD ↑	702	104	210	8	-2,8	-0,78	1006,43	90	Icebergs
4a	CASQ2	Coring	Oct 08 2015	11:16	UTC-5	77°16.751	074°21.262	Box Core ↓	702	233	210	9	-3,5	-0,87	1006,63	91	Icebergs
4a	CASQ2	Coring	Oct 08 2015	11:25	UTC-5	77°16.746	074°21.428	Box Core (bottom)	702	282	220	8	-3,6	-0,88	1006,82	91	Icebergs
4a	CASQ2	Coring	Oct 08 2015	11:36	UTC-5	77°16.736	074°21.654	Box Core ↑	702	226	210	8	-3,9	-0,86	1006,88	91	Icebergs
4a	CASQ2	Coring	Oct 08 2015	15:40	UTC-5	77°15.015	074°25.644	CASQ ↓	692	58	320	5	-5	-0,79	1008,92	94	Icebergs
4a	CASQ2	Coring	Oct 08 2015	15:49	UTC-5	77°15.035	074°25.500	CASQ (bottom)	692	74	320	8	-4,9	-0,8	1009,02	94	Icebergs
4a	CASQ2	Coring	Oct 08 2015	16:02	UTC-5	77°14.903	074°25.949	CASQ ↑	694	148	320	6	-5,1	-0,81	1009,06	94	Icebergs
4a	CASQ2	Coring	Oct 08 2015	22:20	UTC-5	77°01.037	072°81.472	CTD ↓	976	82	40	14	-2,3	-0,05	1009,11	73	1/10
4a	CASQ2	Coring	Oct 08 2015	22:59	UTC-5	77°00.932	072°81.904	CTD ↑	974	37	30	15	-2,7	0	1008,88	69	1/10
4a	108	Basic	Oct 09 2015	06:53	UTC-5	76°15.963	074°36.067	Monster-Loki Net ↓	450	98	330	16	-3,5	-0,89	1007,17	89	9/10
4a	108	Basic	Oct 09 2015	07:25	UTC-5	76°15.587	074°36.442	Monster-Loki Net ↑	447	70	340	19	-3,3	-0,87	1006,91	90	9/10
4a	108	Basic	Oct 09 2015	08:14	UTC-5	76°16.300	074°36.376	PNF + Secchi ↓	448	67	360	22	-3,6	-0,88	1006,24	86	9/10
4a	108	Basic	Oct 09 2015	08:18	UTC-5	76°16.207	074°36.556	PNF + Secchi ↓	450	76	360	22	-3,6	-0,88	1006,24	86	9/10
4a	108	Basic	Oct 09 2015	08:27	UTC-5	76°16.103	074°37.398	PNF + Secchi ↑	450	188	340	17	-3,7	-0,88	1006,3	87	9/10
4a	108	Basic	Oct 09 2015	08:36	UTC-5	76°15.939	074°38.707	CTD-Rosette ↓	450	342	350	16	-3,5	-0,88	1006,24	87	9/10
4a	108	Basic	Oct 09 2015	09:20	UTC-5	76°15.410	074°40.391	CTD-Rosette ↑	445	32	350	14	-4,1	-0,87	1006,3	91	9/10
4a	108	Basic	Oct 09 2015	09:46	UTC-5	76°15.841	074°37.133	Hydrobios ↓	453	1	350	17	-3,9	-0,88	1006,08	93	9/10
4a	108	Basic	Oct 09 2015	10:13	UTC-5	76°15.604	074°37.103	Hydrobios ↑	448	20	350	17	-4	-0,87	1005,92	92	9/10
4a	108	Basic	Oct 09 2015	10:39	UTC-5	76°16.115	074°35.068	CTD-Rosette ↓	447	360	350	20	-0,39	-0,88	1005,68	92	9/10
4a	108	Basic	Oct 09 2015	11:31	UTC-5	76°15.746	074°36.336	CTD-Rosette ↑	450	334	350	17	-3,6	-0,86	1005,64	92	9/10
4a	108	Basic	Oct 09 2015	12:17	UTC-5	76°15.930	074°36.740	Box Core ↓	449	23	330	9	-3,4	-0,82	1005,9	93	9/10
4a	108	Basic	Oct 09 2015	12:31	UTC-5	76°15.880	074°36.740	Box Core ↑	448	29	330	4	-3	-0,81	1006,05	91	9/10
4a	108	Basic	Oct 09 2015	12:44	UTC-5	76°15.830	074°47.410	Agassiz Trawl ↓	449	302	Calm	Calm	-2,8	-0,81	1006,15	89	9/10
4a	108	Basic	Oct 09 2015	13:15	UTC-5	76°15.510	074°38.700	Agassiz Trawl ↑	445	298	150	7	-2,1	-0,82	1006,57	86	9/10
4a	108	Basic	Oct 09 2015	13:37	UTC-5	76°15.370	074°39.300	Beam Trawl ↓	446	193	160	9	-2,4	-0,82	1006,71	85	9/10
4a	108	Basic	Oct 09 2015	14:37	UTC-5	76°13.690	074°44.150	Beam Trawl ↑	451	186	150	8	-2,9	-0,83	1007,33	89	9/10
4a	107	Nutrient	Oct 09 2015	15:32	UTC-5	76°16.720	074°58.100	CTD-Rosette ↓	440	300	Calm	Calm	-3	-0,82	1007,77	89	9/10
4a	107	Nutrient	Oct 09 2015	16:22	UTC-5	76°16.585	074°59.421	CTD-Rosette ↑	438	329	100	14	-1,5	-0,76	1008,14	85	9/10
4a	106	CTD	Oct 09 2015	17:10	UTC-5	76°18.180	075°20.200	CTD ↓	384	29	120	6	-2,9	-0,85	1008,56	95	4/10
4a	106	CTD	Oct 09 2015	17:27	UTC-5	76°18.190	075°20.610	CTD ↑	382	319	110	5	-2,5	-0,84	1008,54	95	4/10
4a	105	Basic	Oct 09 2015	18:53	UTC-5	76°17.318	075°45.237	CTD-Rosette ↓	315	81	100	13	-3	-0,86	1008,76	90	9/10
4a	105	Basic	Oct 09 2015	19:29	UTC-5	76°17.599	075°46.512	CTD-Rosette ↑	311	90	85	12	-3	-0,8	1008,94	94	9/10
4a	105	Basic	Oct 09 2015	19:47	UTC-5	76°17.532	075°45.970	Monster-Loki Net ↓	313	97	70	14	-3,1	-0,81	1008,93	95	9/10
4a	105	Basic	Oct 09 2015	20:09	UTC-5	76°17.569	075°46.897	Monster-Loki Net ↑	314	114	60	11	-3,4	-0,81	1009,14	94	9/10
4a	105	Basic	Oct 09 2015	20:35	UTC-5	76°17.707	075°47.906	CTD-Rosette ↓	321	25	50	11	-3,4	-0,82	1009,12	95	9/10
4a	105	Basic	Oct 09 2015	21:12	UTC-5	76°17.702	075°49.850	CTD-Rosette ↑	332	305	50	12	-3,1	-0,78	1009,04	96	9/10
4a	105	Basic	Oct 09 2015	21:26	UTC-5	76°17.657	075°50.368	Box Core ↓	331	49	40	14	-2,9	-0,8	1009,04	96	9/10
4a	105	Basic	Oct 09 2015	21:32	UTC-5	76°17.655	075°50.482	Box Core (bottom)	330	68	40	12	-3,1	-0,81	1009,03	96	9/10
4a	105	Basic	Oct 09 2015	21:40	UTC-5	76°17.620	075°50.740	Box Core ↑	336	93	40	12	-3,1	-0,81	1009,03	96	9/10
4a	104	CTD	Oct 09 2015	23:39	UTC-5	76°20.856	076°10.342	CTD ↓	183	330	100	5	-1,9	-0,87	1009,38	99	9/10
4a	104	CTD	Oct 09 2015	23:50	UTC-5	76°20.873	076°10.631	CTD ↑	182	340	110	2	-1,9	-0,87	1009,38	99	9/10
4a	103	Nutrient	Oct 10 2015	01:52	UTC-5	76°21.420	076°33.430	CTD-Rosette ↓	152	313	100	5	-1,9	-0,89	1010,25	97	9/10
4a	103	Nutrient	Oct 10 2015	02:18	UTC-5	76°21.700	076°34.030	CTD-Rosette ↑	151	334	90	3	-1,8	-0,86	1010,39	96	9/10
4a	102	CTD	Oct 10 2015	04:12	UTC-5	76°22.285	076°59.429	CTD ↓	254	314	0	18	-4,8	-0,89	1011,24	96	6/10
4a	102	CTD	Oct 10 2015	04:25	UTC-5	76°22.289	076°59.785	CTD ↑	257	265	0	11	-4,8	-0,86	1011,37	96	6/10
4a	101	Basic	Oct 10 2015	05:53	UTC-5	76°22.095	077°22.514	CTD-Rosette ↓	373	293	20	11	-4,5	-0,91	1012,07	96	9/10
4a	101	Basic	Oct 10 2015	06:36	UTC-5	76°22.102	077°23.261	CTD-Rosette ↑	365	286	20	14	-4,4	-0,85	1012,46	95	9/10
4a	101	Basic	Oct 10 2015	07:05	UTC-5	76°21.677	077°22.773	Monster-Loki Net ↓	378	143	20	16	-5	-0,88	1012,6	96	9/10
4a	101	Basic	Oct 10 2015	07:30	UTC-5	76°21.402	077°23.288	Monster-Loki Net ↑	385	106	20	16	-5	-0,88	1012,7	96	9/10
4a	101	Basic	Oct 10 2015	08:34	UTC-5	76°22.736	077°25.686	Hydrobios ↓	390	23	30	15	-4,9	-0,84	1012,8	96	7/10
4a	101	Basic	Oct 10 2015	08:57	UTC-5	76°22.759	077°26.158	Hydrobios ↑	395	86	30	15	-4,8	-0,84	1012,95	96	7/10
4a	101	Basic	Oct 10 2015	09:13	UTC-5	76°22.674	077°26.616	PNF + Secchi ↓	394	133	20	14	-4,9	-0,84	1012,97	96	7/10

4a	101	Basic	Oct 10 2015	09:19	UTC-5	76°22.631	077°26.914	PNF + Secchi ↑	392	135	20	14	-4,9	-0,84	1012,96	96	7/10
4a	101	Basic	Oct 10 2015	09:30	UTC-5	76°22.593	077°26.947	CTD-Rosette ↓	390	356	20	15	-4,8	-0,86	1012,92	96	7/10
4a	101	Basic	Oct 10 2015	10:09	UTC-5	76°22.280	077°27.874	CTD-Rosette ↑	378	99	30	14	-4,6	-0,81	1013,05	96	7/10
4a	101	Basic	Oct 10 2015	10:21	UTC-5	76°22.431	077°26.476	Box Core ↓	396	40	20	13	-4,5	-0,86	1013,1	95	7/10
4a	101	Basic	Oct 10 2015	10:28	UTC-5	76°22.435	077°26.468	Box Core (bottom)	399	41	20	13	-4,5	-0,86	1013,1	95	7/10
4a	101	Basic	Oct 10 2015	10:33	UTC-5	76°22.404	077°26.591	Box Core ↑	397	33	20	12	-4,6	-0,88	1013,23	95	7/10
4b	155	Basic	Oct 11 2015	22:37	UTC-5	76°29.198	078°45.852	CTD-Rosette ↓	309	166	240	3	-2,7	1,08	1005,56	88	1/10
4b	155	Basic	Oct 11 2015	23:15	UTC-5	76°29.174	078°45.616	CTD-Rosette ↑	270	222	250	2	-2,6	1,14	1005,44	88	1/10
4b	155	Basic	Oct 11 2015	23:24	UTC-5	76°29.191	078°46.000	Tucker Net ↓	321	287	250	2	-2,6	1,17	1005,35	88	1/10
4b	155	Basic	Oct 11 2015	23:42	UTC-5	76°28.762	078°46.728	Tucker Net ↑	380	128	220	2	-2,7	0,93	1005,24	88	1/10
4b	155	Basic	Oct 12 2015	00:02	UTC-5	76°29.250	078°45.990	Monster-Loki Net ↓	308	185	270	3	-2,6	1,05	1005,12	88	1/10
4b	155	Basic	Oct 12 2015	00:22	UTC-5	76°29.260	078°45.610	Monster-Loki Net ↑	299	205	300	3	-1,5	1,11	1004,99	82	1/10
4b	155	Basic	Oct 12 2015	00:41	UTC-5	76°29.260	078°45.240	CTD-Rosette ↓	288	222	300	3	-1,9	1,2	1004,96	85	1/10
4b	155	Basic	Oct 12 2015	01:17	UTC-5	76°29.220	078°44.840	CTD-Rosette ↑	279	260	Calm	Calm	-2,5	1,23	1004,76	86	1/10
4b	155	Basic	Oct 12 2015	01:59	UTC-5	76°29.270	078°46.990	Box Core ↓	386	354	Calm	Calm	-2,5	0,62	1004,6	86	1/10
4b	155	Basic	Oct 12 2015	02:07	UTC-5	76°29.390	078°46.860	Box Core (bottom)	376	318	Calm	Calm	-2,5	0,62	1004,6	86	1/10
4b	155	Basic	Oct 12 2015	02:15	UTC-5	76°29.310	078°46.720	Box Core ↑	366	314	Calm	Calm	-2,3	0,61	1004,53	85	1/10
4b	155	Basic	Oct 12 2015	02:23	UTC-5	76°29.410	078°46.600	Agassiz Trawl ↓	346	0	Calm	Calm	-2,3	0,61	1004,53	85	1/10
4b	155	Basic	Oct 12 2015	02:49	UTC-5	72°29.640	078°47.450	Agassiz Trawl ↑	397	168	Calm	Calm	-2,3	0,52	1004,44	85	1/10
4b	Navy Board	ROV	Oct 12 2015	22:58	UTC-5	73°42.885	081°07.393	CTD-Rosette ↓	451	16	150	5	-3,7	-0,28	1002,29	89	1/10
4b	Navy Board	ROV	Oct 12 2015	11:31	UTC-5	73°42.939	081°07.185	CTD-Rosette ↑	440	87	160	3	-3,3	-0,11	1002,11	89	1/10
4b	Navy Board	ROV	Oct 12 2015	12:57	UTC-5	73°42.890	081°07.480	ROV ↓	440	187	150	3	-4	-0,13	1001,69	91	1/10
4b	Navy Board	ROV	Oct 12 2015	20:17	UTC-5	73°43.196	081°07.471	ROV ↑	257	51	70	20	-3	-0,07	1000,51	95	1/10
4b	150	Basic	Oct 12 2015	22:31	UTC-5	72°45.011	079°56.441	CTD-Rosette ↓	126	339	330	12	-2,9	0,02	998,35	92	1/10
4b	150	Basic	Oct 12 2015	22:57	UTC-5	72°44.896	079°56.528	CTD-Rosette ↑	126	22	360	12	-2,8	0,06	998,29	93	1/10
4b	150	Basic	Oct 12 2015	23:08	UTC-5	72°44.958	079°56.869	Tucker Net ↓	127	179	360	13	-2,7	0,07	998,2	92	1/10
4b	150	Basic	Oct 12 2015	23:23	UTC-5	72°44.516	079°55.454	Tucker Net ↑	136	41	330	12	-4,8	0,05	997,98	91	1/10
4b	150	Basic	Oct 12 2015	23:47	UTC-5	72°44.983	079°56.280	Monster-Loki Net ↓	128	349	350	14	-2,9	0,06	997,76	92	1/10
4b	150	Basic	Oct 12 2015	23:58	UTC-5	72°44.940	079°56.160	Monster-Loki Net ↑	128	347	340	16	-2,9	0,05	997,78	92	1/10
4b	150	Basic	Oct 13 2015	01:12	UTC-5	72°44.960	079°56.290	Agassiz Trawl ↓	127	8	340	15	-2,5	0,05	997,46	91	1/10
4b	150	Basic	Oct 13 2015	01:26	UTC-5	72°45.020	079°56.630	Agassiz Trawl ↑	126	189	340	15	-2,7	0,05	997,41	90	1/10
4b	150	Basic	Oct 13 2015	01:45	UTC-5	72°44.430	079°56.340	Beam Trawl ↓	133	96	330	10	-2,1	0,04	997,43	89	1/10
4b	150	Basic	Oct 13 2015	02:12	UTC-5	72°43.980	079°53.050	Beam Trawl ↑	147	9	340	11	-2,4	0,09	997,37	86	1/10
4b	GSC1	Coring	Oct 13 2015	08:40	UTC-5	72°49.279	077°33.107	Piston Core ↓	1058	111	80	18	-1,2	0,75	997,05	80	1/10
4b	GSC1	Coring	Oct 13 2015	09:05	UTC-5	72°49.303	077°33.720	Piston Core (bottom)	1058	89	90	19	-1,3	0,77	997,04	80	1/10
4b	GSC1	Coring	Oct 13 2015	09:20	UTC-5	72°49.250	077°33.267	Piston Core ↑	1058	107	80	19	-1,3	0,78	996,98	79	1/10
4b	GSC1	Coring	Oct 13 2015	11:18	UTC-5	72°49.285	077°33.135	Piston Core ↓	1059	103	90	20	-1,7	0,82	996,92	80	1/10
4b	GSC1	Coring	Oct 13 2015	11:52	UTC-5	72°49.320	077°33.180	Piston Core (bottom)	1058	107	80	21	-1,8	0,81	996,93	82	0
4b	GSC1	Coring	Oct 13 2015	12:05	UTC-5	72°49.330	077°33.590	Piston Core ↑	1058	95	90	22	-2	0,81	996,95	84	0
4b	GSC2	Coring	Oct 13 2015	14:03	UTC-5	72°48.540	077°16.650	Piston Core ↓	1048	115	90	22	-2,4	1,05	997,29	88	0
4b	GSC2	Coring	Oct 13 2015	14:53	UTC-5	72°48.560	077°16.690	Piston Core (bottom)	1049	102	80	21	-2,4	1,02	997,41	88	0
4b	GSC2	Coring	Oct 13 2015	15:08	UTC-5	72°48.550	077°16.750	Piston Core ↑	1049	109	80	21	-2,4	1,02	997,39	88	0
4b	166	Nutrient	Oct 13 2015	22:07	UTC-5	72°29.422	077°43.909	CTD-Rosette ↓	336	348	14	14	-3,2	1,02	997,96	87	0
4b	166	Nutrient	Oct 14 2015	22:52	UTC-5	72°29.369	077°43.021	CTD-Rosette ↑	340	352	15	15	-3	1,11	997,75	84	0
4b	Sam Ford	Basic	Oct 14 2015	14:09	UTC-5	72°42.380	070°47.920	Piston Core ↓	781	180	14	14	-2,6	1,91	988,31	88	1/10
4b	Sam Ford	Basic	Oct 14 2015	14:25	UTC-5	72°42.310	070°47.750	Piston Core (bottom)	780	221	18	18	-2,3	1,92	988,11	83	1/10
4b	Sam Ford	Basic	Oct 14 2015	14:37	UTC-5	72°42.290	070°47.670	Piston Core ↑	780	225	21	21	-2	1,92	988,05	78	1/10
4b	Sam Ford	Basic	Oct 14 2015	16:56	UTC-5	70°53.489	070°24.521	PNF ↓	392	29	210	14	-2,2	1,95	987,36	82	1/10
4b	Sam Ford	Basic	Oct 14 2015	17:00	UTC-5	72°53.480	070°24.520	PNF ↑	391	13	200	17	-2,1	2,03	987,11	80	1/10
4b	Sam Ford	Basic	Oct 14 2015	17:01	UTC-5	72°53.480	070°24.520	Secchi ↓	391	37	200	17	-2,1	2,03	987,11	80	1/10
4b	Sam Ford	Basic	Oct 14 2015	17:03	UTC-5	72°53.480	070°24.520	Secchi ↑	389	34	200	18	-2,1	2,03	987,11	80	1/10
4b	170	Full	Oct 14 2015	20:33	UTC-5	71°22.811	070°04.017	CTD-Rosette ↓	255	121	140	8	-2,3	1,11	987,08	89	1/10
4b	170	Full	Oct 14 2015	21:13	UTC-5	71°23.052	070°03.380	CTD-Rosette ↑	254	102	90	6	-2,1	1,13	987,33	86	1/10
4b	170	Full	Oct 14 2015	21:24	UTC-5	71°22.815	070°04.017	Tucker Net ↓	258	260	100	5	-2,2	1,12	987,27	84	1/10

4b	170	Full	Oct 14 2015	21:40	UTC-5	71°22.560	070°03.686	Tucker Net ↑	242	35	100	4	-2,1	1,09	987,22	82	1/10
4b	170	Full	Oct 14 2015	22:04	UTC-5	71°22.782	070°04.123	Monster-Loki Net ↓	258	258	120	3	-1,8	1,04	987,97	82	1/10
4b	170	Full	Oct 14 2015	22:21	UTC-5	71°22.778	070°04.034	Monster-Loki Net ↑	261	270	110	3	-1,7	1,04	986,96	78	1/10
4b	170	Full	Oct 14 2015	22:45	UTC-5	71°22.767	070°04.150	Box Core ↓	259	268	270	2	-1,5	1,17	986,59	77	0
4b	170	Full	Oct 14 2015	22:50	UTC-5	71°22.756	070°04.168	Box Core (bottom)	257	273	280	3	-1,7	1,2	986,52	80	0
4b	170	Full	Oct 14 2015	22:56	UTC-5	71°22.744	070°04.099	Box Core ↑	256	273	280	3	-1,7	1,2	986,52	80	0
4b	170	Full	Oct 14 2015	23:13	UTC-5	71°22.781	070°04.165	Box Core ↓	260	279	310	5	-1,8	1,24	986,33	79	0
4b	170	Full	Oct 14 2015	23:18	UTC-5	71°22.761	070°04.153	Box Core (bottom)	259	285	310	5	-1,8	1,24	986,33	79	0
4b	170	Full	Oct 14 2015	23,24	UTC-5	71°22.732	070°04.127	Box Core ↑	264	294	310	6	-1,8	1,25	986,23	80	0
4b	170	Full	Oct 14 2015	23:33	UTC-5	71°22.816	070°04.265	Agassiz Trawl ↓	264	342	300	5	-1,9	1,26	986,14	79	0
4b	170	Full	Oct 14 2015	23,54	UTC-5	71°22.648	070°03.631	Agassiz Trawl ↑	245	63	270	4	-1,3	1,07	985,83	77	0
4b	170	Full	Oct 15 2015	01:40	UTC-5	71°22.500	070°05.930	Beam Trawl ↓	265	89	265	8	-2,3	1,09	983,91	83	0
4b	170	Full	Oct 15 2015	02:26	UTC-5	71°23.660	070°03.260	Beam Trawl ↑	271	257	271	12	-2,2	1,07	983,82	82	0
4b	170	Full	Oct 15 2015	00:56	UTC-5	71°22.840	070°07.430	Hydrobios ↓	348	305	348	10	-1,7	1,13	984,93	82	0
4b	170	Full	Oct 15 2015	01:16	UTC-5	71°22.840	070°07.070	Hydrobios ↑	331	320	331	9	-2,1	1,16	984,68	82	0
4b	170	Full	Oct 15 2015	02:46	UTC-5	71°23.450	070°07.420	CTD-Rosette ↓	385	200	385	11	-2	1,07	983,44	80	0
4b	170	Full	Oct 15 2015	03:33	UTC-5	71°23.330	070°06.220	CTD-Rosette ↑	334	209	334	14	-2	1,13	983,11	81	0
4b	171	Nutrient	Oct 15 2015	04:41	UTC-5	71°30.901	069°35.357	CTD-Rosette ↓	693	220	693	14	-1,5	1,22	982,41	77	1/10
4b	171	Nutrient	Oct 15 2015	05:42	UTC-5	71°30.773	069°33.941	CTD-Rosette ↑	688	238	688	13	-1,5	1,23	982,3	76	1/10
4b	172	Nutrient	Oct 15 2015	06:53	UTC-5	71°39.470	069°08.274	CTD-Rosette ↓	1633	232	1633	15	-2,5	1,03	982,06	96	1/10
4b	172	Nutrient	Oct 15 2015	08:18	UTC-5	71°39.215	069°06.800	CTD-Rosette ↑	1640	47	1640	20	-0,8	1,1	982,26	99	1/10
4b	Scott Inlet	Coring	Oct 16 2015	22:32	UTC-5	71°30.911	070°16.724	Elevator deployment ↓	600	306	600	20	-4,9	1,11	1000,83	77	1/10
4b	Scott Inlet	Coring	Oct 16 2015	23:12	UTC-5	71°30.968	070°16.700	Elevator deployment ↑	520	327	520	23	-5	1,12	1001,13	78	1/10
4b	Scott Inlet	Coring	Oct 16 2015	21:22	UTC-5	71°19.347	070°39.110	CTD-Rosette ↓	831	19	831	9	-5,2	1,15	1002,27	76	1/10
4b	Scott Inlet	Coring	Oct 16 2015	21:56	UTC-5	71°19.235	070°39.887	CTD-Rosette ↓	818	28	818	6	-5,2	1,13	1002,48	75	1/10
4b	Scott Inlet	Coring	Oct 16 2015	22:11	UTC-5	71°19.353	070°38.928	Box Core ↓	832	24	832	4	-5,4	1,13	1002,51	73	1/10
4b	Scott Inlet	Coring	Oct 16 2015	22:23	UTC-5	71°19.314	070°38.975	Box Core (bottom)	832	37	832	5	-5,3	1,12	1002,61	75	1/10
4b	Scott Inlet	Coring	Oct 16 2015	22:34	UTC-5	71°19.309	070°39.016	Box Core ↑	832	30	832	8	-5,5	1,13	1002,56	75	1/10
4b	Scott Inlet	Coring	Oct 16 2015	22:47	UTC-5	71°19.342	070°38.911	Box Core ↓	832	38	230	12	-5,8	1,13	1002,47	73	1/10
4b	Scott Inlet	Coring	Oct 16 2015	23:01	UTC-5	71°19.316	070°38.966	Box Core (bottom)	833	23	240	10	-5,7	1,15	1002,64	74	1/10
4b	Scott Inlet	Coring	Oct 16 2015	23:12	UTC-5	71°19.326	070°38.955	Box Core ↑	832	40	240	11	-6	1,16	1002,62	74	1/10
4b	169	Nutrient	Oct 17 2015	00:03	UTC-5	71°16.380	070°31.730	CTD-Rosette ↓	771	195	250	16	-5,7	1,08	1002,71	73	1/10
4b	169	Nutrient	Oct 17 2015	01:07	UTC-5	71°16.220	070°30.500	CTD-Rosette ↑	766	157	240	9	-5,4	0,94	1002,88	72	1/10
4b	Scott Inlet	Coring	Oct 17 2015	04:20	UTC-5	71°30.726	070°16.787	CTD-Rosette ↓	602	288	295	20	-5,9	1,02	1003,02	86	1/10
4b	Scott Inlet	Coring	Oct 17 2015	04:45	UTC-5	71°30.510	070°16.131	CTD-Rosette ↑	588	293	295	15	-5,8	0,96	1002,98	87	1/10
4b	Scott Inlet	Coring	Oct 17 2015	06:12	UTC-5	71°30.978	070°16.652	ROV ↓	520	303	290	18	-5,2	0,91	1003,04	87	1/10
4b	Scott Inlet	Coring	Oct 17 2015	08:03	UTC-5	71°30.977	070°16.631	ROV ↑	520	301	310	21	-4,8	0,97	1002,89	91	1/10
4b	Scott Inlet	Coring	Oct 17 2015	09:16	UTC-5	71°30.967	070°16.259	CTD-Rosette ↓	492	349	20	12	-3,8	0,97	1003,26	91	0
4b	Scott Inlet	Coring	Oct 17 2015	09:38	UTC-5	71°30.840	070°15.657	CTD-Rosette ↑	498	326	360	11	-3,4	0,98	1003,24	83	0
4b	Scott Inlet	Coring	Oct 17 2015	10:41	UTC-5	71°30.801	070°16.401	Box Core ↓	606	329	360	12	-3,2	0,98	1002,93	89	0
4b	Scott Inlet	Coring	Oct 17 2015	11:15	UTC-5	71°30.786	070°16.327	Box Core (bottom)	607	314	20	14	-2,8	0,98	1002,78	89	0
4b	Scott Inlet	Coring	Oct 17 2015	11:24	UTC-5	71°30.755	070°16.319	Box Core ↑	604	335	20	13	-3,2	0,98	1002,77	90	0
4b	Scott Inlet	Coring	Oct 17 2015	11:52	UTC-5	71°30.970	070°16.660	ROV ↓	519	331	20	20	-3,2	0,98	1002,56	90	0
4b	Scott Inlet	Coring	Oct 17 2015	14:31	UTC-5	71°30.990	070°16.730	ROV ↑	519	328	30	17	-2,6	1,01	1002,8	79	0
4b	Scott Inlet	Coring	Oct 17 2015	15:24	UTC-5	71°30.740	070°15.900	Elevator deployment ↑	519	335	30	16	-2,6	1	1003,14	72	1/10
4b	Scott Inlet	Coring	Oct 18 2015	09:31	UTC-5	71°19.358	070°38.795	CASQ-3	832	271	260	8	-4,4	1,09	1007,28	91	1/10
4b	Scott Inlet	Coring	Oct 18 2015	09:55	UTC-5	71°19.321	070°38.748	CASQ-3	832	5	240	8	-4,4	1,09	1007,4	92	1/10
4b	GSC3	Coring	Oct 18 2015	18:24	UTC-4	70°42.369	067°41.404	Piston Core ↓	246	320	160	7	-5,3	1,52	1008,96	67	1/10
4b	GSC3	Coring	Oct 18 2015	18:29	UTC-4	70°42.374	067°41.421	Piston Core (bottom)	246	252	160	11	-5,3	0,152	1008,96	67	1/10
4b	GSC3	Coring	Oct 18 2015	18:35	UTC-4	70°42.401	067°41.433	Piston Core ↑	245	323	160	10	-5,3	1,54	1008,99	66	1/10
4b	173	Nutrient	Oct 18 2015	22:18	UTC-4	70°41.086	066°56.123	CTD-Rosette ↓	399	173	140	6	-3,4	1,63	1009,38	73	1/10
4b	173	Nutrient	Oct 18 2015	23:05	UTC-4	70°41.085	066°55.998	CTD-Rosette ↑	401	237	120	5	-3,5	1,76	1009,57	78	1/10
4b	176	Nutrient	Oct 18 2015	04:15	UTC-4	69°35.789	065°21.893	CTD-Rosette ↓	359	344	340	6	-3	1,12	1008,09	91	1/10
4b	176	Nutrient	Oct 18 2015	05:00	UTC-4	69°35.563	065°22.542	CTD-Rosette ↑	321	34	N	3	-2,5	1,15	1008,2	87	1/10

4b	178	Nutrient	Oct 18 2015	09:40	UTC-4	68°31.383	064°40.216	CTD-Rosette ↓	378	320	300	14	-3,7	0,52	1007,73	85	1/10
4b	178	Nutrient	Oct 18 2015	10:31	UTC-4	68°31.046	064°40.056	CTD-Rosette ↑	352	333	352	13	-3,6	0,69	1007,77	85	1/10
4b	177	Full	Oct 19 2015	20:27	UTC-4	67°28.560	063°47.381	CTD-Rosette ↓	369	314	Calm	Calm	-4	-0,28	1008,28	64	1/10
4b	177	Full	Oct 19 2015	21:15	UTC-4	67°28.568	063°47.388	CTD-Rosette ↑	370	266	Calm	Calm	-4,1	-0,25	1008,24	63	1/10
4b	177	Full	Oct 19 2015	21:23	UTC-4	67°28.565	063°47.469	Tucker Net ↓	373	270	Calm	Calm	-4	-0,24	1008,21	63	1/10
4b	177	Full	Oct 19 2015	21:35	UTC-4	67°28.315	063°47.572	Tucker Net ↑	429	88	Calm	Calm	-4	-0,25	1008,2	64	1/10
4b	177	Full	Oct 19 2015	21:59	UTC-4	67°28.574	063°47.346	Monster-Loki Net ↓	371	259	Calm	Calm	-4	-0,28	1008,22	64	1/10
4b	177	Full	Oct 19 2015	22:25	UTC-4	67°28.603	063°47.379	Monster-Loki Net ↑	370	279	Calm	Calm	-3,9	-0,2	1008,14	62	1/10
4b	177	Full	Oct 19 2015	22:53	UTC-4	67°28.577	063°47.366	Box Core ↓	368	244	Calm	Calm	-4,1	-0,24	1008,16	65	1/10
4b	177	Full	Oct 19 2015	23:00	UTC-4	67°28.590	063°47.389	Box Core (bottom)	371	213	Calm	Calm	-4,1	-0,2	1008,15	64	1/10
4b	177	Full	Oct 19 2015	23:07	UTC-4	67°28.604	063°47.390	Box Core ↑	369	248	Calm	Calm	-4,1	-0,2	1008,15	64	1/10
4b	177	Full	Oct 19 2015	23:18	UTC-4	67°28.584	063°47.399	Box Core ↓	369	187	Calm	Calm	-4,2	-0,24	1008,2	62	1/10
4b	177	Full	Oct 19 2015	23:25	UTC-4	67°28.580	063°47.388	Box Core (bottom)	373	212	Calm	Calm	-4,2	-0,25	1008,17	61	1/10
4b	177	Full	Oct 19 2015	23:33	UTC-4	67°28.587	063°47.412	Box Core ↑	372	216	160	6	-4,3	-0,23	1008,11	60	1/10
4b	177	Full	Oct 19 2015	23:44	UTC-4	67°28.584	063°47.414	Box Core ↓	372	168	160	6	-4,2	-0,19	1008,08	60	1/10
4b	177	Full	Oct 19 2015	23:51	UTC-4	67°28.579	063°47.407	Box Core (bottom)	373	178	160	5	-4,2	-0,15	1008,05	59	1/10
4b	177	Full	Oct 19 2015	23:57	UTC-4	67°28.572	063°47.419	Box Core ↑	374	197	160	5	-4,1	-0,15	1008,05	59	1/10
4b	177	Full	Oct 20 2015	00:10	UTC-4	67°28.560	063°47.470	Box Core ↓	376	186	170	4	-4,1	-0,14	1007,96	58	1/10
4b	177	Full	Oct 20 2015	00:17	UTC-4	67°28.580	063°47.510	Box Core (bottom)	374	157	180	5	-4,1	-0,14	1007,96	58	1/10
4b	177	Full	Oct 20 2015	00:23	UTC-4	67°28.570	063°47.520	Box Core ↑	374	123	170	6	-4,1	-0,14	1007,93	58	1/10
4b	177	Full	Oct 20 2015	01:23	UTC-4	67°28.310	063°46.750	Beam Trawl ↓	417	153	170	9	-3,8	-0,2	1007,81	61	1/10
4b	177	Full	Oct 20 2015	02:20	UTC-4	67°28.300	063°46.930	Beam Trawl ↑	422	185	Calm	Calm	-3,8	-0,23	1008,06	63	1/10
4b	177	Full	Oct 20 2015	02:59	UTC-4	67°28.470	063°41.550	ROV ↓	677	205	190	13	-3,5	-0,16	1008,11	61	1/10
4b	177	Full	Oct 20 2015	06:27	UTC-4	67°28.733	063°40.548	ROV ↑		204	200	9	-3,7	-0,14	1009,17	61	1/10
4b	177	Full	Oct 20 2015	09:40	UTC-4	67°28.542	063°47.482	PNF + Secchi ↓	381	116	Calm	Calm	-3,5	0	1010,4	58	1/10
4b	177	Full	Oct 20 2015	09:46	UTC-4	67°28.525	063°47.463	PNF + Secchi ↑	381	119	290	3	-3,6	-0,03	1010,43	57	1/10
4b	177	Full	Oct 20 2015	09:59	UTC-4	67°28.531	063°47.356	CTD-Rosette ↓	379	285	Calm	Calm	-2,2	-0,11	1010,44	53	1/10
4b	177	Full	Oct 20 2015	10:44	UTC-4	67°28.525	063°47.229	CTD-Rosette ↑	379	308	Calm	Calm	-3,4	0,04	1010,73	60	1/10
4b	177	Full	Oct 20 2015	18:26	UTC-4	67°29.144	063°48.395	Lander ↓	282	306	330	13	-4,1	0,01	1013,74	79	1/10
4b	177	Full	Oct 20 2015	18:50	UTC-4	67°29.138	063°48.393	Lander ↑	281	307	330	14	-4,1	0,04	1013,77	78	1/10
4b	177	Full	Oct 20 2015	19:24	UTC-4	67°28.606	063°47.272	Hydrobios ↓	369	306	305	11	-4,3	0	1013,9	82	1/10
4b	177	Full	Oct 20 2015	19:45	UTC-4	67°28.625	063°47.047	Hydrobios ↑	368	306	310	13	-4,2	0,1	1014,04	80	1/10
4b	177	Full	Oct 20 2015	20:19	UTC-4	67°28.522	063°45.836	IKMT ↓	403	70	300	9	-4,3	0,02	1014,23	80	1/10
4b	177	Full	Oct 20 2015	21:06	UTC-4	67°30.098	063°42.566	IKMT ↑	80	257	260	6	-2,7	-0,14	1014,12	68	1/10
4b	177	Full	Oct 20 2015	21:34	UTC-4	67°28.049	063°45.099	Agassiz Trawl ↓	493	136	280	12	-3,5	-0,22	1013,93	77	1/10
4b	177	Full	Oct 20 2015	21:45	UTC-4	67°27.968	063°44.371	Agassiz Trawl ↑	599	74	280	8	-3,1	-0,08	1014,35	71	1/10
4b	177	Full	Oct 20 2015	21:49	UTC-4	67°27.934	063°44.082	Agassiz Trawl ↓	653	121	280	8	-3,1	-0,08	1014,35	71	1/10
4b	177	Full	Oct 20 2015	22:32	UTC-4	67°28.381	063°41.631	Agassiz Trawl ↑	677	356	280	10	-4,3	-0,02	1014,24	81	1/10
4b	177	Full	Oct 20 2015	22:56	UTC-4	67°28.431	063°41.494	Box Core ↓	679	309	280	9	-4	-0,18	1014,27	80	1/10
4b	177	Full	Oct 20 2015	23:06	UTC-4	67°28.430	063°41.526	Box Core (bottom)	680	324	280	8	-4,1	-0,21	1014,23	78	1/10
4b	177	Full	Oct 20 2015	23:15	UTC-4	67°28.455	063°41.470	Box Core ↑	670	322	270	8	-4,2	-0,19	1014,25	78	1/10
4b	177	Full	Oct 20 2015	23:31	UTC-4	67°28.437	063°41.604	Box Core ↓	674	295	270	8	-4,1	-0,16	1014,19	78	1/10
4b	177	Full	Oct 20 2015	23:39	UTC-4	67°28.441	063°41.555	Box Core (bottom)	679	335	270	7	-4	-0,22	1014,12	77	1/10
4b	177	Full	Oct 20 2015	23:48	UTC-4	67°28.454	063°41.532	Box Core ↑	678	331	270	7	-4,1	-0,21	1014,04	76	1/10
4b	CASQ4	Coring	Oct 21 2015	00:10	UTC-4	67°28.940	063°39.470	Box Core ↓	688	29	270	6	-3,9	-0,3	1013,93	74	1/10
4b	CASQ4	Coring	Oct 21 2015	00:18	UTC-4	67°28.980	063°39.280	Box Core (bottom)	689	355	270	6	-3,9	-0,3	1013,93	74	1/10
4b	CASQ4	Coring	Oct 21 2015	00:26	UTC-4	67°28.980	063°39.190	Box Core ↑	690	349	250	4	-3,9	-0,2	1013,95	75	1/10
4b	179	Nutrient	Oct 21 2015	04:09	UTC-4	67°26.987	061°55.425	CTD-Rosette ↓	189	351	340	7	-2,6	-0,07	1013,16	76	1/10
4b	179	Nutrient	Oct 21 2015	04:37	UTC-4	67°26.822	061°55.486	CTD-Rosette ↑	186	4	330	8	-2,5	-0,02	1013,21	75	1/10
4b	180	Basic	Oct 21 2015	05:25	UTC-4	67°28.902	061°40.035	CTD-Rosette ↓	337	322	325	7	-2,6	0,02	1013,02	76	1/10
4b	180	Basic	Oct 21 2015	05:55	UTC-4	67°28.616	061°39.921	CTD-Rosette ↑	311	1	325	6	-2,5	0,12	1012,96	75	1/10
4b	180	Basic	Oct 21 2015	06:11	UTC-4	67°28.654	061°39.152	Tucker Net ↓	349	53	330	7	-2,5	0,13	1012,88	75	1/10
4b	180	Basic	Oct 21 2015	06:28	UTC-4	67°28.785	061°39.990	Tucker Net ↑	316	169	315	5	-2,4	0,08	1012,76	76	1/10
4b	180	Basic	Oct 21 2015	07:01	UTC-4	67°28.889	061°39.739	Monster-Loki Net ↓	357	5	295	5	-2,6	0,08	1012,72	76	1/10

4b	180	Basic	Oct 21 2015	07:24	UTC-4	67°28.681	061°39.534	Monster-Loki Net ↑	329	51	280	5	-2,7	0,13	1012,74	75	1/10
4b	180	Basic	Oct 21 2015	08:19	UTC-4	67°28.958	061°39.953	CTD-Rosette ↓	352	327	280	11	-2,6	0,07	1012,38	80	1/10
4b	180	Basic	Oct 21 2015	09:09	UTC-4	67°28.801	061°39.826	CTD-Rosette ↑	332	318	280	9	-2,9	0,09	1012,13	83	1/10
4b	180	Basic	Oct 21 2015	09:23	UTC-4	67°29.027	061°40.099	Box Core ↓	359	332	280	8	-3	0,06	1011,96	81	1/10
4b	180	Basic	Oct 21 2015	09:32	UTC-4	67°28.986	061°39.996	Box Core (bottom)	360	342	280	8	-3	0,05	1011,93	80	1/10
4b	180	Basic	Oct 21 2015	09:41	UTC-4	67°28.978	061°39.923	Box Core ↑	359	336	280	7	-3	0,1	1011,87	79	1/10
4b	180	Basic	Oct 21 2015	10:31	UTC-4	67°28.812	061°39.726	Agassiz Trawl ↓	345	82	290	7	-2,4	0,07	1011,45	74	1/10
4b	180	Basic	Oct 21 2015	10:58	UTC-4	67°28.937	061°39.756	Agassiz Trawl ↑	361	126	300	6	-2,5	0,03	1011,27	74	1/10
4b	180	Basic	Oct 21 2015	12:18	UTC-4	67°28.810	061°39.670	Beam Trawl ↓	340	30	270	8	-3	0,02	1010,81	72	1/10
4b	180	Basic	Oct 21 2015	13:17	UTC-4	67°29.280	061°41.170	Beam Trawl ↑	338	218	260	9	-2,5	-0,01	1010,23	72	1/10
4b	---	Argos Floats	Oct 21 2015	15:37	UTC-4	67°39.420	060°46.890	Argos Float ↓	1538	216	300	7	-2,5	0,23	1009,73	70	0
4b	---	Argos Floats	Oct 21 2015	16:00	UTC-4	67°39.548	060°47.016	Argos Float ↑	1541	236	300	6	-2,3	0,3	1009,61	71	0
4b	---	Argos Floats	Oct 21 2015	16:13	UTC-4	67°39.610	060°47.050	CTD ↓	1543	204	290	5	-2,5	0,32	1099,57	72	0
4b	---	Argos Floats	Oct 21 2015	16:24	UTC-4	67°39.655	060°47.103	CTD ↑	1542	209	290	5	-2,3	0,29	1009,52	72	0
4b	181	Nutrient	Oct 21 2015	19:40	UTC-4	67°30.097	061°31.648	CTD-Rosette ↓	935	337	270	7	-3,8	0,13	1008,62	70	0
4b	181	Nutrient	Oct 21 2015	20:51	UTC-4	67°29.595	061°30.845	CTD-Rosette ↑	893	344	260	7	-3,9	0,07	1008,16	68	0
4b	Big Nose	Coring	Oct 22 2015	06:01	UTC-4	66°56.949	062°16.649	Piston Core ↓	71	14	130	6	-7,5	-0,52	1007,39	72	1/10
4b	Big Nose	Coring	Oct 22 2015	06:03	UTC-4	66°56.949	062°16.636	Piston Core (bottom)	71	122	130	6	-7,5	-0,52	1007,39	72	1/10
4b	Big Nose	Coring	Oct 22 2015	06:06	UTC-4	66°56.950	062°16.635	Piston Core ↑	71	135	120	5	-7,5	-0,52	1007,39	72	1/10
4b	Big Nose	Coring	Oct 22 2015	07:34	UTC-4	66°57.022	062°17.287	Piston Core ↓	93	196	Calm	Calm	-6,7	-0,46	1007,59	68	1/10
4b	Big Nose	Coring	Oct 22 2015	07:37	UTC-4	66°57.022	062°17.289	Piston Core (bottom)	93	202	Calm	Calm	-6,7	-0,46	1007,59	68	1/10
4b	Big Nose	Coring	Oct 22 2015	07:40	UTC-4	66°57.022	062°17.291	Piston Core ↑	92	207	Calm	Calm	-6,2	-0,44	1007,63	68	1/10
4b	AKPAIT	Coring	Oct 22 2015	12:20	UTC-4	66°53.190	061°48.520	Piston Core ↓	145	283	260	5	-6,2	-0,16	1007,06	62	0
4b	AKPAIT	Coring	Oct 22 2015	12:27	UTC-4	66°53.190	061°48.560	Piston Core (bottom)	147	290	270	5	-6	-0,12	1007,12	56	0
4b	AKPAIT	Coring	Oct 22 2015	12:32	UTC-4	66°53.190	061°48.550	Piston Core ↑	146	305	Calm	Calm	-5,8	-0,09	1007,08	56	0
4b	Cape Dyer	ROV	Oct 22 2015	12:25	UTC-4	66°24.820	059°13.200	ROV ↓	742	314	310	10	-3,7	0,27	1010,41	80	0
4b	Cape Dyer	ROV	Oct 23 2015	04:23	UTC-4	66°24.611	059°13.387	ROV ↑	740	12	330	8	-3,4	0,3	1011,53	71	0
4b	Cape Dyer	ROV	Oct 23 2015	07:13	UTC-4	66°25.161	059°09.469	CTD ↓	729	299	350	3	-3,1	0,19	1012,39	68	0
4b	Cape Dyer	ROV	Oct 23 2015	07:41	UTC-4	66°25.075	059°09.458	CTD ↑	728	323	Calm	Calm	-3,5	0,23	1012,5	68	0
4b	184	Nutrient	Oct 23 2015	12:30	UTC-4	65°44.420	060°36.670	CTD-Rosette ↓	357	177	170	6	-1,9	0,26	1012,38	71	1/10
4b	184	Nutrient	Oct 23 2015	13:15	UTC-4	65°44.380	060°36.630	CTD-Rosette ↑	357	168	180	7	-2,4	0,23	1012,46	73	1/10
4b	187	Basic	Oct 23 2015	20:52	UTC-4	64°10.988	060°23.040	CTD-Rosette ↓	353	289	270	18	-3,2	0,45	1012,7	78	1/10
4b	187	Basic	Oct 23 2015	21:28	UTC-4	64°10.901	060°22.771	CTD-Rosette ↑	353	346	270	21	-3,5	0,69	1012,89	78	1/10
4b	187	Basic	Oct 23 2015	21:45	UTC-4	64°10.900	060°23.067	Tucker Net ↓	352	104	270	20	-3,5	0,5	1012,58	77	1/10
4b	187	Basic	Oct 23 2015	22:06	UTC-4	64°11.225	060°21.699	Tucker Net ↑	355	41	260	17	-3,8	0,49	1012,54	79	1/10
4b	187	Basic	Oct 23 2015	22:35	UTC-4	64°10.972	060°23.136	Monster-Loki Net ↓	353	234	270	18	-3,7	0,49	1012,34	78	1/10
4b	187	Basic	Oct 23 2015	22:59	UTC-4	64°10.896	060°23.179	Monster-Loki Net ↑	353	268	270	18	-3,9	0,51	1012,44	76	1/10
4b	187	Basic	Oct 23 2015	23:35	UTC-4	64°11.486	060°21.444	CTD-Rosette ↓	355	284	260	15	-3,9	0,49	1012,18	76	1/10
4b	187	Basic	Oct 24 2015	00:19	UTC-4	64°11.230	060°21.440	CTD-Rosette ↑	356	281	240	11	-4	0,5	1011,82	76	1/10
4b	187	Basic	Oct 24 2015	01:07	UTC-4	64°10.380	060°24.020	Agassiz Trawl ↓	350	327	240	11	-4,1	0,49	1011,4	77	1/10
4b	187	Basic	Oct 24 2015	01:35	UTC-4	64°10.970	060°24.090	Agassiz Trawl ↑	352	349	230	10	-4	0,49	1011,02	75	1/10
4b	187	Basic	Oct 24 2015	01:47	UTC-4	64°11.370	060°24.030	Beam Trawl ↓	357	350	230	10	-4	0,48	1010,99	74	1/10
4b	187	Basic	Oct 24 2015	02:40	UTC-4	64°12.170	060°25.790	Beam Trawl ↑	356	95	200	16	-3,6	0,48	1010,41	73	1/10
4b	190	Nutrient	Oct 24 2015	11:18	UTC-4	62°27.669	061°55.367	CTD-Rosette ↓	351	166	180	25	-1,8	1,69	1004,57	94	0
4b	190	Nutrient	Oct 24 2015	12:04	UTC-4	62°27.520	061°55.110	CTD-Rosette ↑	354	195	180	21	-1,4	2,25	1003,66	89	0
4b	Frobisher Bay	Coring	Oct 25 2015	08:09	UTC-5	63°38.279	068°36.662	Piston Core ↓	126	313	310	26	-5,2	0,03	989,05	82	0
4b	Frobisher Bay	Coring	Oct 25 2015	08:12	UTC-5	63°38.271	068°36.670	Piston Core (bottom)	126	323	310	26	-5,2	0,03	989,26	84	0
4b	Frobisher Bay	Coring	Oct 25 2015	08:17	UTC-5	63°38.294	068°36.656	Piston Core ↑	127	317	310	26	-5,2	0,03	989,26	84	0
4b	Frobisher Bay	Coring	Oct 25 2015	10:25	UTC-5	63°38.380	068°36.724	Piston Core ↓	116	336	320	22	-5,2	-0,12	992,04	76	0
4b	Frobisher Bay	Coring	Oct 25 2015	10:29	UTC-5	63°38.386	068°36.705	Piston Core (bottom)	115	319	320	22	-5,2	-0,12	992,04	76	0
4b	Frobisher Bay	Coring	Oct 25 2015	10:32	UTC-5	63°38.389	068°36.694	Piston Core ↑	114	317	315	18	-6,3	-0,13	992,03	76	0
4b	Frobisher Bay	Coring	Oct 25 2015	12:25	UTC-5	63°38.350	068°37.520	ROV ↓	136	325	320	16	-6,4	-0,2	993,2	72	0
4b	Frobisher Bay	Coring	Oct 25 2015	17:00	UTC-5	63°38.300	068°37.780	ROV ↑		323	310	18	-7,5	-0,19	994,74	71	0
4b	Frobisher Bay	Coring	Oct 25 2015	18:50	UTC-5	63°38.412	068°36.775	CTD ↓	122	272	270	14	-8,3	-0,02	995,9	67	0

Appendix 3: CTD Logbook

Cast number	Station ID	Station Type	Date start UTC	Time UTC	Latitude (N)	Longitude (W)	Bottom depth (m)	Cast depth (db)	Comments	Init
001	sx90-001	CTD	17/4/15	22:42	48°35.537	069°10.000	95	93	altimètre et isus h/s	SB
002	sx90-002	CTD	18/4/15	21:37	48°52.867	063°09.935	393	381		SB
003	sx90-003	CTD	19/4/15	11:25	47°21.234	059°07.002	427	408	installé altimètre Benthos	SB
004	Station 1	CTD	22/4/15	17:09	48°29.703	052°29.365	212	200		SB
005	Station 2	CTD	22/4/15	19:40	48°28.344	052°23.111	204	196		SB
006	Mooring 1	CTD	23/4/15	14:05	48°59.563	051°02.164	312	305		SB
007	Station 3	CTD	23/4/15	19:08	49°13.640	051°15.137	333	322		SB
008	Station 4	CTD	24/4/15	16:55	51°27.893	051°33.782	366	354	pompe allumée à 354m	SB
009	Station 4	CTD	24/4/15	17:47	51°27.845	051°34.672	372	364		SB
010	Station 4	CTD	24/4/15	18:32	51°27.864	051°34.613	373	364		SB
011	Station 4	CTD	24/4/15	19:21	51°27.931	051°34.801	369	362		SB
012	Station 4	CTD	24/4/15	20:08	51°28.118	051°35.263	382	377		SB
013	Mooring 3	CTD	25/4/15	16:43	51°49.889	052°30.716	323	313		SB
014	Mooring 2	CTD	26/4/15	13:02	50°16.752	051°50.567	285	277		SB
015	Station 10	CTD	28/4/15	21:47	52°00.743	055°40.808	71	65	installé altimètre Valport	SB
016	Station 13	CTD	30/4/15	16:37	50°12.263	059°26.730	112	104		SB
017	Station 14	CTD	1/5/15	10:56	50°05.072	062°21.051	122	114	changé nom de station pour 14	SB
018	Station 15	CTD	2/5/15	10:50	49°47.495	065°28.070	304	293	changé nom de station pour 15	SB
019	Station 16	CTD	2/5/15	22:27	49°17.674	067°19.691	339	330	altimètre fonctionne mal	SB
020	Station 17	CTD	3/5/15	21:27	48°09.066	069°35.543	92	82	installé altimètre benthos	SB

Cast number	Station ID	Station Type	Date start UTC	Time UTC	Latitude (N)	Longitude (W)	Bottom depth (m)	Cast depth (db)	Comments	Init
001	K1	Full	14/7/15	09:58	56°07.271	053°22.300	3310	500	btl 2 did not close	PG
002	K1	Full	14/7/15	13:14	56°07.290	053°22.211	3309	990	CTD off at 1000 m. cast 3 to finish. No bottles	CTS
003	K1	Full	14/7/15	13:35	56°07.399	053°22.264	3309	1600	End of the cast 002	CTS
004	K1	Full	14/7/15	20:33	56°07.060	053°22.915	3312	1500		PG
005	K1	Full	14/7/15	23:48	56°07.313	053°22.313	3312	1600		CTS
006	LS2	Full	17/7/15	08:15	60°27.216	056°32.884	3023	700		CTS
007	LS2	Full	17/7/15	23:26	60°26.575	056°32.201	3016	1506	Large swell (>5 m)	PG
008	LS2	Full	18/7/15	04:44	60°25.370	056°34.063	3028	700		CTS
009	LS2	Full	18/7/15	13:25	60°26.686	056°33.346	3028	200		PG
010	Incubation	Full	20/7/15	01:51	63°57.126	060°06.618	480	203		CTS
011	BB1	Full	3/8/15	09:11	66°51.435	059°03.701	1040	500		CTS
012	BB1	Full	3/8/15	14:52	66°51.457	059°03.995	1039	1000		PG
013	BB1	Full	3/8/15	23:34	66°51.332	059°03.438	1038	1000		CTS
014	BB3	Full	5/8/15	20:45	71°24.544	068°35.761	1243	1000	Winch cable read out malfunction	PG
015	BB3	Full	6/8/15	03:44	71°24.653	068°36.205	1251	1000	Winch cable read out malfunction.	CTS
016	BB3	Full	6/8/15	12:39	71°24.918	068°36.791	1272	500		PG
017	BB3	Full	6/8/15	15:39	71°24.539	068°35.864	1252	300		CTS
018	BB2	Full	7/8/15	19:43	72°45.224	066°59.599	2371	1500	Light swell	PG
019	BB2	Full	8/8/15	00:58	72°44.964	067°00.131	2346	1000		CTS
020	BB2	Full	8/8/15	10:24	72°45.097	066°59.665	2369	300	Light swell	CTS
021	BB2	Full	8/8/15	13:42	72°45.040	066°59.988	2369	300		PG
022	CAA1	Full	9/8/15	22:17	74°31.280	080°34.292	635	625		PG
023	CAA1	Full	10/8/15	03:37	74°31.333	080°33.841	632	600	Light swell. fast current	CTS
024	CAA1	Full	10/8/15	06:47	74°31.316	080°34.834	633	613	Fast current	CTS
025	CAA1	Full	10/8/15	12:01	74°31.094	080°33.880	636	300	Light swell	PG
026	CAA1	Full	10/8/15	15:15	74°31.411	080°33.980	634	200		PG
027	CAA1	Full	10/8/15	17:00	74°31.258	080°34.073	636	300		CTS
028	CAA2	Full	10/8/15	19:15	74°19.254	080°29.743	698	250		PG
029	CAA2	Full	10/8/15	21:39	74°18.956	080°29.836	1464	300		PG
030	CAA2	Full	10/8/15	23:33	74°18.860	080°30.191	702	600		PG
031	CAA2	Full	11/8/15	04:00	74°19.074	080°29.755	700	690	Seasave.exe failed to initialize	CTS
032	CAA2	Full	11/8/15	05:44	74°19.207	080°30.358	700	685		CTS
033	AN323	Nutrient	11/8/15	07:14	74°09.482	080°28.327	785	780	Salinity samples taken	CTS
034	AN324	Nutrient	11/8/15	09:17	73°58.892	080°27.924	769	760		PG
035	CAA3	Full	11/8/15	12:13	73°48.928	080°29.249	674	300		PG
036	CAA3	Full	11/8/15	16:22	73°49.114	080°29.536	687	300		PG
037	CAA3	Full	11/8/15	22:04	73°49.086	080°28.933	690	200		CTS

038	CAA3	Full	11/8/15	23:53	73°49.120	080°29.635	690	600	Pb with fluorescence sensor	PG
039	CAA3	Full	12/8/15	04:21	73°49.031	080°30.325	673	665		CTS
040	CAA3	Full	12/8/15	05:59	73°49.106	080°29.944	682	663		CTS
041	CAA5	Full	12/8/15	21:40	74°32.374	090°47.652	259	239		PG
042	CAA5	Full	12/8/15	22:55	74°32.251	090°48.108	254	243		CTS
043	CAA5	Full	13/8/15	02:54	74°32.350	090°47.899	259	250		CTS
044	CAA5	Full	13/8/15	04:32	74°32.324	090°48.386	257	250		CTS
045	CAA5	Full	13/8/15	14:13	74°31.955	090°48.145	241	231	LADCP off	PG
046	CAA4	Full	13/8/15	17:38	74°07.354	091°29.941	181	160		PG
047	CAA4	Full	13/8/15	18:53	74°07.306	091°30.775	178	168		PG
048	CAA4	Full	14/8/15	01:18	74°07.260	091°30.707	177	167	Seasave.exe failed to initialize; btl 2 does not fire	PG
049	CAA4	Full	14/8/15	05:12	74°07.500	091°29.600	193	150	Btl 2 did not fire	CTS
050	CAA4	Full	14/8/15	06:54	74°07.460	091°30.174	186	176		CTS
051	CAA6	Full	14/8/15	19:25	74°45.539	097°27.384	253	243		PG
052	CAA6	Full	14/8/15	20:48	74°45.404	097°27.131	249	242		PG
053	CAA6	Full	15/8/15	01:37	74°45.576	097°27.134	260	250		PG
054	CAA6	Full	15/8/15	05:29	74°45.260	097°27.448	246	190		CTS
055	CAA6	Full	15/8/15	08:48	74°45.444	097°27.281	253	250		CTS
056	CAA7	Full	15/8/15	21:09	73°39.920	096°35.590	214	204		PG
057	CAA7	Full	15/8/15	22:26	73°39.973	096°33.463	211	192		PG
058	CAA7	Full	16/8/15	02:16	73°40.373	096°31.429	219	200		CTS
059	CAA7	Full	16/8/15	07:14	73°39.610	096°32.131	218	210		CTS
060	CAA7	Full	16/8/15	09:22	73°39.832	096°32.173	217	190	Ice conditions	CTS
061	VS	Full	17/8/15	10:49	69°52.607	099°32.416	138	129		PG
062	AN312	Basic	17/8/15	18:12	69°09.886	100°41.395	59	50		CTS
063	AN312	Basic	17/8/15	19:23	69°09.794	100°41.963	59	40		PG
064	AN312	Basic	17/8/15	20:41	69°09.892	100°41.801	60	50	Btl 2 did not fire	CTS
065	AN314	Basic	18/8/15	16:13	68°58.133	105°27.788	79	69		CTS
066	AN314	Basic	18/8/15	17:43	68°58.049	105°27.260	79	69	Btl 2 did not fire	CTS
067	AN314	Basic	18/8/15	19:09	68°58.267	105°27.554	83	58		CTS

Cast number	Station ID	Station Type	Date start UTC	Time UTC	Latitude (N)	Longitude (W)	Bottom depth (m)	Cast depth (db)	Comments	Init
001	405	Basic	22/8/15	22:56	70°36.581	123°02.014	604	594		CM
002	405	Basic	23/8/15	01:41	70°36.490	123°02.060	610	600		OA
003	407	Full	23/8/15	18:45	71°01.150	126°09.170	382	369		OA
004	CA-08	Mooring	23/8/15	21:33	71°00.600	126°04.000	392	378		OA
005	407	Full	23/8/15	02:11	71°00.609	126°04.853	394	378		CM
006	437	Basic	24/8/15	11:32	71°47.848	126°30.140	298	287		CM
007	437	Basic	24/8/15	13:40	71°48.000	126°29.000	290	280		OA
008	410	Nutrient	24/8/15	17:05	71°41.972	126°29.415	409	392		OA
009	CA-05	Mooring	24/8/15	22:33	71°16.703	127°31.029	206	192		OA
011	412	Nutrient	25/8/15	03:10	71°33.852	126°55.328	417	403		CM
012	413	CTD	25/8/15	04:35	71°29.730	127°07.933	373	361		CM
013	414	Nutrient	25/8/15	05:41	71°25.041	127°21.452	304	294		CM
014	408	Full	25/8/15	07:18	71°18.735	127°34.908	204	195		CM
015	408	Full	25/8/15	09:25	71°18.534	127°35.892	197	187		CM
016	417	CTD	25/8/15	13:06	71°13.399	127°58.607	85	71		CM
017	418	Nutrient	25/8/15	13:49	71°09.765	128°10.253	65	55	not sampled	OA
018	419	CTD	25/8/15	14:40	71°06.388	128°20.593	56	46		OA
019	418	Nutrient	25/8/15	15:29	71°09.615	128°10.439	65	55	Went back for more samples	OA
020	420	Basic	25/8/15	17:08	71°03.058	128°30.662	43	31	Bottles 3 and 23 didn't fire	OA
021	434	Basic	26/8/15	05:25	70°10.614	133°33.233	47	35		CM
022	433	CTD	26/8/15	09:05	70°17.303	133°34.769	56	44	LADCP not enough data	CM
023	432	Nutrient	26/8/15	09:55	70°23.665	133°36.130	63	50		CM
024	BR-K	Mooring	26/8/15	13:43	70°51.542	135°01.482	152	137		OA
025	BS-1	Mooring	26/8/15	15:31	70°48.465	134°50.288	81	68		OA
026	BS-2	Mooring	26/8/15	17:52	70°53.038	135°05.809	306	296		OA
027	BR-G	Mooring	26/8/15	20:20	71°00.467	135°30.937	721	708		OA
028	423	CTD	27/8/15	01:32	71°16.265	133°51.718	794	778		OA
029	424	Nutrient	27/8/15	02:52	71°10.371	133°49.729	576	564	LADCP processing problem	CM
030	435	Full	27/8/15	05:00	71°04.745	133°37.859	299	287		CM
031	435	Full	27/8/15	07:38	71°04.727	133°37.824	300	287		CM
032	BR-K	Mooring	27/8/15	15:10	70°51.469	135°02.349	157	151		OA
033	422	Nutrient	28/8/15	11:30	71°22.815	133°52.948	1100	1080	Bottle 2 didn't fire	CM
034	BR-G	Mooring	28/8/15	17:10	71°00.130	135°30.427	708	683		OA
035	BS-3	Mooring	28/8/15	20:41	70°55.474	135°13.503	491	479		OA
036	Lander 2	Lander	28/8/15	23:31	70°50.145	135°07.824	164	156		OA

037	431	CTD	29/8/15	06:31	70°29.711	133°37.615	68	56		CM
038	430	Nutrient	29/8/15	07:22	70°35.906	133°38.706	71	58	Bottle 2 didn't fire	CM
039	429	CTD	29/8/15	08:20	70°41.685	133°39.930	70	56	Bottle 2 fired successfully	CM
040	428	Nutrient	29/8/15	09:05	70°47.425	133°41.155	75	63		CM
041	427	CTD	29/8/15	10:00	70°52.835	133°43.026	80	68		CM
042	426	Nutrient	29/8/15	10:44	70°59.069	133°44.818	100	88		CM
043	435	Benthos	29/8/15	14:16	71°12.533	133°41.537	720	707		OA
044	421	Basic	29/8/15	23:11	71°25.819	133°59.393	1207	1195		OA
045	421	Basic	30/8/15	02:44	71°25.730	134°00.461	1210	1194		CM
046	BR-4	Mooring	31/8/15	02:11	73°13.355	127°03.047	156	148		CM
047	535	Full	31/8/15	06:00	73°24.808	128°10.482	287	272		CM
048	535	Full	31/8/15	08:35	73°24.939	128°11.799	291	277		CM
049	BR-3	Mooring	31/8/15	14:08	73°24.222	129°21.437	692	680		OA
050	536	Basic	31/8/15	19:44	73°25.138	129°23.350	732	722		OA
051	536	Basic	31/8/15	23:16	73°25.012	129°21.677	727	717		OA
052	518	Basic	2/9/15	03:55	74°33.880	121°27.104	186	170		CM
053	518	Basic	2/9/15	06:05	74°34.331	121°26.338	281	267		CM
054	516	Nutrient	2/9/15	11:56	74°49.697	120°50.294	469	454		CM
055	514	Basic	2/9/15	14:39	75°06.899	120°38.504	468	456		OA
056	514	Basic	2/9/15	17:42	75°06.183	120°37.704	457	447		OA
057	512	Nutrient	2/9/15	21:51	75°22.569	120°33.024	412	402		OA
058	510	Nutrient	2/9/15	23:58	75°38.332	120°38.381	374	364		OA
059	CB1	Geotrace	6/9/15	19:53	75°07.563	120°23.740	413	401	Pump cable broken: bad data. No sampling done.	OA
060	CB1	Geotrace	6/9/15	21:18	75°07.350	120°38.466	463	453	Problem fixed. Correct data	OA
061	CB1	Geotrace	7/9/15	03:30	75°06.414	120°31.103	430	418		CM
062	CB1	Geotrace	7/9/15	06:20	75°06.113	120°33.790	437	425		CM
063	CB1	Geotrace	7/9/15	15:37	75°06.886	120°21.474	409	398	4 miles east of CB-1: CB-1*	OA
064	CB1	Geotrace	7/9/15	21:23	75°06.856	120°38.680	468	100	Looking at transmission min	OA
065	CB2	Geotrace	8/9/15	23:03	75°49.252	129°13.415	1374	700		OA
066	CB2	Geotrace	9/9/15	06:20	75°48.383	129°14.050	1356	1338	Bottle 3 did not close	CM
067	CB2	Geotrace	9/9/15	09:45	75°48.109	129°11.683	1346	1325		CM
068	CB2	Geotrace	10/9/15	07:40	75°47.123	129°17.417	1354	1340	Bottle 2 did not close	OA
069	CB3	Geotrace	11/9/15	19:51	76°58.840	140°02.750	3728	1400		OA
070	CB3	Geotrace	12/9/15	03:00	76°58.508	140°03.108	3736	1600	Bottle 5 didn't close	OA
071	CB3	Geotrace	12/9/15	08:10	76°59.535	140°02.830	3728	1600	Comms error with SBE	CM
072	CB3	Geotrace	13/9/15	13:07	76°59.423	140°02.609	3697	1500	Cable fixed	OA
073	CB4	Geotrace	14/9/15	20:13	75°00.015	149°59.655	3828	1400		OA

074	CB4	Geotrace	15/9/15	00:47	75°00.145	150°00.048	3829	1400	OA
075	CB4	Geotrace	15/9/15	09:44	74°59.996	149°59.482	3829	1500	CM
076	CB4	Geotrace	16/9/15	00:21	74°59.975	149°59.495	3828	220	OA/CM
077	CB4	Geotrace	16/9/15	05:48	74°59.929	150°00.135	3828	1000	OA/CM
078	407	Coring	18/9/15	13:24	71°00.351	126°04.526	390	388	OA
079	314	Basic	20/9/15	16:10	68°58.191	105°28.889	77	66	OA
080	QMG4	Basic	21/9/15	01:20	68°28.995	103°25.477	71	60	OA
081	QMG3	Basic	21/9/15	07:05	68°19.774	102°36.340	64	53	CM
082	WF1	Mooring	21/9/15	14:47	68°14.517	101°47.570	103	91	CM
083	QMG	Basic	21/9/15	18:40	68°14.796	101°43.014	107	93	OA
084	QMG2	Basic	21/9/15	23:54	68°18.810	100°48.008	54	42	OA
085	QMG1	Basic	22/9/15	04:00	68°29.631	099°53.430	34	24	CM
086	312	Basic	22/9/15	14:03	69°10.337	100°41.577	65	55	OA
087	310	Basic	23/9/15	06:42	71°27.408	101°16.924	163	153	CM
088	308/CAA8	Geotrace	24/9/15	02:26	74°08.325	108°50.079	565	554	OA
089	308/CAA8	Geotrace	24/9/15	08:27	74°08.333	108°50.309	562	551	CM
090	308/CAA8	Geotrace	24/9/15	15:07	74°08.323	108°50.130	566	553	OA
091	307	Basic	25/9/15	07:55	74°06.660	103°07.517	355	345	CM
092	342	Basic	26/9/15	01:49	74°47.671	092°46.857	137	128	OA
093	CAA9	Basic	27/9/15	03:14	76°19.930	096°44.688	340	333	OA/CM
094	CAA9	Basic	27/9/15	05:30	76°19.971	096°45.598	331	319	CM
095	J1	CTD	27/9/15	11:16	76°25.472	096°26.907	280	265	CM
096	J2	CTD	27/9/15	12:54	76°34.836	096°42.625	217	207	OA
097	J3	CTD	27/9/15	14:53	76°40.042	096°51.156	231	207	OA
098	J4	CTD	27/9/15	15:38	76°37.170	096°51.350	187	176	OA
099	J5	CTD	27/9/15	17:30	76°36.380	097°01.456	148	143	OA
100	J6	CTD	27/9/15	18:29	76°33.004	097°05.564	141	129	OA
101	WC01	CTD	29/9/15	03:44	75°50.013	093°45.750	331	319	OA
102	WC02	CTD	29/9/15	05:54	75°29.249	093°46.235	250	240	OA
103	WC03	CTD	29/9/15	06:35	75°29.113	093°36.438	232	221	OA
104	WC04	CTD	29/9/15	08:42	75°29.107	093°07.276	152	140	CM
105	WC05	CTD	29/9/15	09:38	75°29.170	92°38.0213	159	145	CM
106	WC05.5	CTD	29/9/15	10:10	75°29.128	092°28.219	100	88	CM
107	WC06	CTD	29/9/15	12:03	75°15.733	092°34.278	176	166	CM
108	WC07	CTD	29/9/15	12:43	75°15.732	092°44.347	175	164	OA
109	WC08	CTD	29/9/15	13:22	75°15.731	092°58.061	153	142	OA
110	WC09	CTD	29/9/15	14:05	75°15.703	093°14.520	222	212	OA

Bottle 3 didn't fire

111	WC10	CTD	29/9/15	14:46	75°15.610	093°22.550	226	214	OA
112	WC16	CTD	30/9/15	00:03	74°40.765	093°21.369	103	90	OA
113	WC17	CTD	30/9/15	01:08	74°41.012	093°07.481	143	131	OA
114	WC18	CTD	30/9/15	02:24	74°41.414	092°40.949	145	133	OA
115	WC19	CTD	30/9/15	03:37	74°41.833	092°14.120	91	80	OA
116	WC20	CTD	30/9/15	04:23	74°42.175	092°01.045	116	106	OA
117	BS1	CTD	30/9/15	05:24	74°38.017	092°05.448	124	112	CM
118	BS2	CTD	30/9/15	06:18	74°34.227	092°09.803	170	158	CM
119	BS3	CTD	30/9/15	07:48	74°25.426	092°19.583	266	253	CM
120	BS4	CTD	30/9/15	09:21	74°17.323	092°29.442	177	164	CM
121	BS5	CTD	30/9/15	10:12	74°13.649	092°33.657	165	153	CM
122	BS6	CTD	30/9/15	11:06	74°09.996	092°38.166	152	141	CM

Cast number	Station ID	Station Type	Date start UTC	Time UTC	Latitude (N)	Longitude (W)	Bottom depth (m)	Cast depth (db)	Comments	Init
001	304	Basic	3/10/15	22:31	74°14.819	091°30.881	314	304	Altimeter only working at 30m from bottom	JZ
002	304	Basic	4/10/15	05:02	74°14.779	091°29.418	314	304		PDR
003	346	Nutrient	4/10/15	06:51	74°09.004	091°27.036	282	272	Acquisition Screen blacked out for a sec close to bottom	JZ
004	343	Nutrient	4/10/15	09:43	74°32.771	091°31.450	151	140		JZ
005	301	Basic	4/10/15	22:13	74°07.277	083°18.899	679	669	Bottle #23 did not fire, Sal samples	PDR
006	301	Basic	5/10/15	03:16	74°07.268	083°19.324	673	667		JZ
007	325	Nutrient	5/10/15	08:08	73°49.000	080°29.221	678	668		JZ
008	324	Nutrient	5/10/15	10:19	73°58.607	080°28.036	772	762	Still no scm	PDR
009	323	Full	5/10/15	13:00	74°09.410	080°28.409	784	774	No scm	PDR
010	323	Full	5/10/15	15:04	74°09.474	080°28.228	790	780	Bottle #3 did not fire	PDR
011	300	Nutrient	6/10/15	04:12	74°19.037	080°29.255	698	690		JZ
012	322	Nutrient	6/10/15	07:03	74°29.620	080°32.154	662	650	encountered ice during cast, cable pinched, skipped 3 sampling depths	JZ
013	109	CTD	7/10/15	10:08	76°17.381	074°06.693	453	443	No scm	PDR
014	110	Nutrient	7/10/15	11:11	76°18.000	073°38.721	530	520	Screen blacked out for a sec	PDR
015	111	Basic	7/10/15	12:50	76°18.352	073°12.980	591	585	Valve of bottle #4 open	PDR
016	111	Basic	7/10/15	16:04	76°18.276	073°12.489	590	582		PDR
017	112	CTD	7/10/15	19:00	76°18.908	072°42.160	560	554	Ox samples	PDR
018	113	Nutrient	7/10/15	20:09	76°19.299	072°13.105	552	542	Still no scm	PDR
019	114	CTD	7/10/15	21:43	76°19.511	071°47.639	610	600		JZ
020	115	Basic	8/10/15	01:43	76°19.979	071°12.097	660	650		JZ
021	115	Basic	8/10/15	07:37	76°20.125	071°14.083	665	656		JZ
022	CASQ1	CTD	8/10/15	14:11	77°17.097	074°23.214	700	690	Problems with the radio	PDR
023	CASQ2	Coring	9/10/15	02:21	77°01.034	072°08.556	975	965	Ox blanks	JZ
024	108	Basic	9/10/15	12:38	76°15.912	074°38.826	450	440		PDR
025	108	Basic	9/10/15	14:41	76°16.079	074°35.144	447	437		PDR
026	107	Nutrient	9/10/15	19:34	76°16.715	074°58.113	439	429		PDR
027	106	CTD	9/10/15	21:12	76°18.191	075°20.254	380	376		PDR
028	105	Basic	9/10/15	22:53	76°17.380	075°45.318	315	304		JZ
029	105	Basic	10/10/15	00:36	76°17.692	075°47.968	321	310	Sal samples	JZ
030	104	CTD	10/10/15	03:40	76°20.855	076°10.352	185	175		JZ
031	103	Nutrient	10/10/15	05:51	76°21.491	076°33.412	153	143		JZ
032	102	CTD	10/10/15	08:11	76°22.266	076°59.369	252	243		JZ
033	101	Basic	10/10/15	09:54	76°22.088	077°22.459	372	360		JZ
034	101	Basic	10/10/15	13:32	76°22.572	077°27.040	382	373		PDR
035	155	Basic	12/10/15	02:38	72°29.213	078°45.856	298	295		JZ
036	155	Basic	12/10/15	04:40	72°29.258	078°45.239	284	274	Sal samples	JZ
037	Navy Board	ROV	12/10/15	15:01	73°42.886	081°07.339	459	449	Ox samples, no downcast recorded	PDR
038	150	Basic	13/10/15	02:31	72°44.993	079°56.430	128	117	extra station in Pond Inlet	JZ
039	166	Nutrient	14/10/15	02:07	72°29.400	073°43.894	332	322		JZ
040	170	Full	15/10/15	00:34	71°22.832	070°03.997	252	243		JZ
041	170	Full	15/10/15	06:46	71°23.447	070°07.418	370	360		JZ
042	171	Nutrient	15/10/15	08:41	71°30.812	069°35.306	692	680		JZ

043	172	Nutrient	15/10/15	10:55	71°39.472	069°08.110	1632	1242	Maximum cable length (1250m)	PDR
044	Scott Inlet	Coring	17/10/15	01:23	71°19.332	070°39.166	825	818		JZ
045	169	Nutrient	17/10/15	04:03	71°16.384	070°31.726	770	760	Sal samples	JZ
046	Scott Inlet RO	Benthos	17/10/15	08:21	71°30.714	070°16.727	591	585		JZ
047	Scott Inlet RO	Benthos	17/10/15	13:18	71°30.945	070°16.154	490	488		PDR
048	173	Nutrient	19/10/15	02:18	70°41.100	066°56.119	400	390		JZ
049	176	Nutrient	19/10/15	08:15	69°35.772	065°21.895	352	343		JZ
050	178	Nutrient	19/10/15	13:42	68°31.384	064°40.216	373	363	Ox samples	PDR
051	177	Full	20/10/15	00:27	67°28.547	063°47.356	372	363		JZ
052	177	Full	20/10/15	14:02	67°28.525	063°47.336	376	366		PDR
053	179	Nutrient	21/10/15	08:10	67°26.966	061°55.421	185	177		JZ
054	180	Basic	21/10/15	09:25	67°28.884	061°40.009	325	318		JZ
055	180	Basic	21/10/15	12:21	67°28.939	061°39.901	352	342		PDR
056	Argo Floats	CTD	21/10/15	20:15	67°39.637	060°47.040	1541	200		PDR
057	181	Nutrient	21/10/15	23:40	67°30.084	061°31.640	915	902	Sal samples	JZ
058	Cape Dyer	CTD	23/10/15	11:15	66°25.138	059°09.444	728	718		PDR
059	184	Nutrient	23/10/15	16:31	65°44.413	060°36.677	357	347		PDR
060	187	Basic	24/10/15	00:53	64°10.98	060°23.005	350	340		JZ
061	187	Basic	24/10/15	03:35	64°11.477	060°21.404	354	344		JZ
062	190	Nutrient	24/10/15	15:22	62°27.671	061°55.284	349	339		PDR
063	Frobisher Bay	Coring	25/10/15	22:50	63°38.408	068°36.736	120	110		JZ
064	Frobisher Bay	Coring	26/10/15	00:23	63°38.279	068°36.695	125	115		PDR
065	353	Nutrient	27/10/15	10:35	61°09.304	064°50.342	397	396	Rosette hit the bottom	PDR
066	640	Coring	28/10/15	01:10	58°55.543	062°09.014	142	132		JZ
067	650	Nutrient	29/10/15	11:17	53°47.577	055°26.372	204	194		PDR
068	Belle Isle	Nutrient	29/10/15	20:24	51°50.912	055°51.062	123	113	Last Cast of the leg!!!	PDR

Appendix 4: List of Participants

Leg	Name	Position	Affiliation	Network Investigator/supervisor	Embark date	Disembark date
Leg 1	Andersson, Leif Erik	Iceberg data collection - student	NTNU	NTNU	17-Apr-15	4-May-15
Leg 4a - Leg 4b	Archambault, Philippe	Chief Scientist	Institut des Sciences de la Mer - UQAR	Archambault, Philippe	01-oct-15	26-oct-15
Leg 3a - Leg 3b	Asselin, Olivier	PhD Student	McGill University	Tremblay, Bruno	20-août-15	01-oct-15
Leg 3b - Leg 4c	Aubry, Cyril	Research Staff	Université Laval	Fortier, Louis	04-sept-15	01-nov-15
Leg 4b	Auger, Vincent	Professional	Canadian Scientific Submersible Facility	CSSF	11-oct-15	26-oct-15
Leg 3b	Baconnais, Isabelle	PhD Student	University of Saskatoon	Holmden, Chris	04-sept-15	01-oct-15
Leg 4a	Bailey, Cheryl	Professional	School on Board	ArcticNet	01-oct-15	11-oct-15
Leg 1	Barber, David	Chief Scientist	University of Manitoba	Barber, Dave	20-Apr-15	4-May-15
Leg 1	Bartlett, James	Mooring Technician	ASL	ASL	17-Apr-15	4-May-15
Leg 4b	Bennett, Robbie	Professional	Geological Survey of Canada	Bennett, Robbie	11-oct-15	26-oct-15
Leg 2	Blais, Marjolaine	Research Staff	Institut des Sciences de la Mer - UQAR	Gosselin, Michel	10-juil-15	20-août-15
Leg 4a	Blais, Marjolaine	Research Staff	Institut des Sciences de la Mer - UQAR	Gosselin, Michel	01-oct-15	11-oct-15
Leg 3b	Blanken, Hauke	PhD Student	McGill University	Klymak, Jody	26-sept-15	01-oct-15
Leg 1	Blondeau, Sylvain	Ocean instrumentation Tech/CTD Op	ArcticNet	Levesque, Keith	17-Apr-15	4-May-15
Leg 2	Bouchard, Caroline	Research Staff	Université Laval	Fortier, Louis	10-juil-15	20-août-15
Leg 3a - Leg 3b	Bourgeois, Solveig	Postdoctoral Fellow	University of Aberdeen	Archambault, Philippe	20-août-15	01-oct-15
Leg 2	Brouard, Étienne	Professional	Université Laval	Lajeunesse, Patrick	10-juil-15	20-août-15
Leg 4a - Leg 4c	Brouard, Étienne	Professional	Université Laval	Lajeunesse, Patrick	01-oct-15	01-nov-15
Leg 1	Brown, Jeff	Ice Management Specialist	AKAC	AKAC	20-Apr-15	4-May-15
Leg 2	Brown, Kristina	Postdoctoral Fellow	WHOI	Brown, Kristina	10-juil-15	20-août-15
Leg 3a	Burt, Alexis	Professional	University of Manitoba	Stern, Gary	20-août-15	04-sept-15
Leg 4a - Leg 4c	Burt, Alexis	Research Staff	University of Manitoba	Stern, Gary	01-oct-15	01-nov-15
Leg 1	Bylsma, Jason	SWIR Sensor Application Specialist	UTAS	UTAS	17-Apr-15	20-Apr-15
Leg 4a - Leg 4c	Campagne, Philippine	PhD Student	Université Laval	Massé, Guillaume	01-oct-15	01-nov-15
Leg 1	Candlish, Lauren	Sea Ice Research Associate	University of Manitoba	Barber, Dave	17-Apr-15	4-May-15
Leg 3a - Leg 3b	Candlish, Lauren	Research Staff	University of Manitoba	Barber, David	20-août-15	01-oct-15
Leg 3a	Carpenter, Jeff	Researcher/Professor	Helmholtz-Zentrum Geesthacht Centre for Materials and Coastal Research (Germany)	Waterman, Stephanie	20-août-15	04-sept-15
Leg 4a - Leg 4c	Carrier, Vincent	MSc Student	Université Laval	Lovejoy, Connie	01-oct-15	01-nov-15
Leg 4b - Leg 4c	Carter, Jonathan	MSc Student	Memorial University	Bell, Trevor	11-oct-15	01-nov-15
Leg 2	Chandan, Priyanka	PhD Student	University of Toronto	Bergquist, Bridget	10-juil-15	20-août-15
Leg 3b	Chandan, Priyanka	PhD Student	University of Toronto	Bergquist, Bridget	04-sept-15	01-oct-15
Leg 3a	Charette, Joannie	MSc Student	ISMER/UQAR	Gosselin, Michel	20-août-15	04-sept-15
Leg 1	Clark, Erin	Ice Observer	Canadian Ice Service	Vaillant, Eric	17-Apr-15	4-May-15
Leg 1	Collin-Hansen, Christian	Statoil WP3 Lead/MMO	Statoil ASA	Statoil	17-Apr-15	4-May-15
Leg 2	Colombo, Manuel	PhD Student	University of British Columbia	Orians, Kristin	10-juil-15	20-août-15

Leg 3b	Colombo, Manuel	PhD Student	ArcticNet	Orians, Kristin	04-sept-15	01-oct-15
Leg 1	Connors, Shawn	Dual-polarized radar tech/operator	Rutter	Rutter	17-Apr-15	4-May-15
Leg 2	Courchesne, Isabelle	MSc Student	Université Laval	Tremblay, Jean-Éric	10-juil-15	20-août-15
Leg 4b - Leg 4c	Cramm, Margaret	Research Staff	University of Calgary	Hubert, Casey	11-oct-15	01-nov-15
Leg 1	Crawford, Anna	Iceberg Drift Researcher	Carleton University	Mueller, Derek	17-Apr-15	4-May-15
Leg 4a - Leg 4c	Crawford, Anna	PhD Student	Carleton University	Mueller, Derek	01-oct-15	01-nov-15
Leg 2	Cullen, Jay	Researcher/Professor	University of Victoria	Cullen, Jay	10-juil-15	20-août-15
Leg 4a	Daeninck, Camille	High School Student	School on Board	ArcticNet	01-oct-15	11-oct-15
Leg 4a	Daveluy Fletcher, Gabriel	High School Student	School on Board	ArcticNet	01-oct-15	11-oct-15
Leg 3b	De Montety, Laure	Research Staff	Institut des Sciences de la Mer - UQAR	Archambault, Philippe	04-sept-15	01-oct-15
Leg 4b - Leg 4c	de Moura Neves, Barbara	PhD Student	Memorial University	Edinger, Evan	11-oct-15	01-nov-15
Leg 4b	Deering, Robert	MSc Student	Memorial University	Bell, Trevor	11-oct-15	26-oct-15
Sea Trial	DeGrandpré, Charles	Research Staff	Université Laval	Lajeunesse, Patrick	21-Jun-15	25-Jun-15
Leg 3a - Leg 3b	DeGrandpré, Charles	Professional	Université Laval	Lajeunesse, Patrick	20-août-15	01-oct-15
Leg 4a - Leg 4c	DeRepentigny, Patricia	MSc Student	McGill University	Tremblay, Bruno	01-oct-15	01-nov-15
Leg 2	Deslongchamps, Gabrièle	Professional	Université Laval	Tremblay, Jean-Éric	10-juil-15	20-août-15
Leg 3b	Deslongchamps, Gabrièle	Professional	Université Laval	Tremblay, Jean-Éric	04-sept-15	01-oct-15
Leg 3b - Leg 4c	Dezutter, Thibaud	MSc Student	Université Laval	Fortier, Louis	04-sept-15	01-nov-15
Leg 1	Divine, John	SWIR Sensor Operator	UTAS	UTAS	20-Apr-15	4-May-15
Leg 4b	Dufour, Suzanne	Researcher/Professor	Memorial University	Dufour, Suzanne	11-oct-15	26-oct-15
Leg 1	Durinck, Jan	Lead Marine Observer	Marine Observers	Marine Observers	17-Apr-15	4-May-15
Leg 3b	Elliott, Ashley	MSc Student	University of Manitoba - CEOS	Wang, Feiyue	04-sept-15	01-oct-15
Leg 1	Elliott, Bradley James	Statoil Data Manager	Statoil Canada	Statoil	17-Apr-15	4-May-15
Leg 3a	Forest, Alexandre	Professional	Golder Associates Ltd	Osborne, Phil	20-août-15	04-sept-15
Leg 1	Fournier, Nicolas	Sea Ice Research Associate	Shell	Shell	17-Apr-15	4-May-15
Leg 3b	Fox, Rowan	Professional	University of Victoria	Cullen, Jay and Klymak, Jody	04-sept-15	01-oct-15
Leg 2	François, Roger	Chief Scientist	University of British Columbia	François, Roger	10-juil-15	20-août-15
Leg 3b	François, Roger	Chief Scientist	University of British Columbia	François, Roger	04-sept-15	01-oct-15
Leg 3a	Gagnon, Jonathan	Professional	Université Laval	Tremblay, Jean-Éric	20-août-15	04-sept-15
Leg 4a - Leg 4c	Gagnon, Jonathan	Professional	Université Laval	Tremblay, Jean Eric	01-oct-15	01-nov-15
Leg 3a	Galand, Pierre	Researcher/Professor	Université Laval	Lovejoy, Connie	20-août-15	04-sept-15
Leg 4a - Leg 4b	Galindo, Virginie	Postdoctoral Fellow	University of Manitoba - CEOS	Gosselin, Michel	01-oct-15	26-oct-15
Leg 2	Gao, Jeff (Zhiyuan)	MSc Student	Trent University	Gueguen, Celine	10-juil-15	20-août-15
Leg 1	Garvin, Matthew	Ice Properties Researcher	National Research Council		20-Apr-15	4-May-15
Leg 3a - Leg 4c	Geng, Lantao	PhD Student	Institut des Sciences de la Mer - UQAR	Xie, Huixiang	20-août-15	01-nov-15
Leg 1	Geoffroy, Maxime	EK60/SX90 Operator/Researcher	Université Laval	Fortier, Louis	17-Apr-15	4-May-15
Leg 3b	Geoffroy, Maxime	PhD Student	Université Laval	Fortier, Louis	19-sept-15	01-oct-15
Leg 2	Giesbrecht, Karina	PhD Student	University of Victoria	Varela, Diana	10-juil-15	20-août-15

Leg 4c	Giraudeau, Jacques	Researcher/Professor	Université de Bordeaux	Massé, Guillaume	01-oct-15	01-nov-15
Leg 4b	Graham, Clark	BSc Student	Carleton University	Mueller, Derek	11-oct-15	26-oct-15
Leg 4a - Leg 4c	Grant, Cindy	Research Staff	Institut des Sciences de la Mer - UQAR	Archambault, Philippe	01-oct-15	01-nov-15
Leg 2	Grenier, Mélanie	Postdoctoral Fellow	University of British Columbia	François, Roger	10-juil-15	20-août-15
Leg 2	Guignard, Constance	Research Staff	McGill University	Mucci, Al	10-juil-15	01-oct-15
Leg 3a - Leg 3b	Guignard, Constance	Research Staff	McGill University	Mucci, Al	10-juil-15	01-oct-15
Leg 2	Guillot, Pascal	Professional	Quebec-Ocean	Tremblay, Jean-Eric	10-juil-15	20-août-15
Leg 4a - Leg 4c	Guilmette, Caroline	Researcher/Professor	Université Laval	Massé, Guillaume	01-oct-15	01-nov-15
Leg 1	Gunn, Geoffrey	Sea Ice Research Associate	University of Manitoba	Barber, Dave	17-Apr-15	4-May-15
Leg 2	Hegmans, Alyse	Professional	Environment Canada	Jantunen, Liisa	10-juil-15	29-juil-15
Leg 1	Heyn, Hans-Martin	Sea ice data collection - student	NTNU	NTNU	17-Apr-15	4-May-15
Leg 1	Hinse, Philipp	Ice Pressure Panel Tech	HSVA	HSVA	17-Apr-15	4-May-15
Leg 2	Hoppe, Clara	Postdoctoral Fellow	Alfred Wegener Institute	Tortell, Philippe	10-juil-15	20-août-15
Leg 3b	Hughes, Ken	PhD Student	University of Victoria	Klymak, Jody	26-sept-15	01-oct-15
Leg 2	Hussherr, Rachel	MSc Student	Université Laval	Levasseur, Maurice	10-juil-15	20-août-15
Leg 4b	Jackson, Keith	Research Staff	University of Aberdeen	Archambault, Philippe	11-oct-15	26-oct-15
Leg 3b	Jackson, Sarah Louise	MSc Student	University of Victoria	Cullen, Jay	04-sept-15	01-oct-15
Leg 1	Jafarikhasragh, Shabnam	Sea Ice Research Associate	University of Manitoba	Barber, Dave	17-Apr-15	4-May-15
Leg 2	Janssen, David	PhD Student	University of Victoria	Cullen, Jay	10-juil-15	20-août-15
Leg 2	Jarnikova, Tereza	PhD Student	University of British Columbia	Tortell, Philippe	10-juil-15	20-août-15
Leg 1	Jones, Tim	Wave Glider Operator	Liquid Robotics	Liquid Robotics	17-Apr-15	4-May-15
Leg 1	Joyal, Gabriel	Multibeam Surveyor/MVP	Université Laval	Lajeunesse, Patrick	17-Apr-15	4-May-15
Leg 3a	Joyal, Gabriel	Research Staff	Université Laval	Lajeunesse, Patrick	20-août-15	04-sept-15
Leg 4a - Leg 4c	Joyal, Gabriel	Professional	Université Laval	Lajeunesse, Patrick	01-oct-15	01-nov-15
Leg 4a - Leg 4c	Kalenitchenko, Dimitri	PhD Student	Université Laval	Lovejoy, Connie	01-oct-15	01-nov-15
Leg 4a	Kamula, Michelle	Research Staff	University of Manitoba	Kuzyk, ZouZou	01-oct-15	11-oct-15
Leg 4a	Killiktee, Cara	High School Student	School on Board	ArcticNet	01-oct-15	11-oct-15
Leg 3a	King, Edward	Research Staff	Geological Survey of Canada	King, Edward	20-août-15	04-sept-15
Leg 3b	Klymak, Jody	Researcher/Professor	University of Victoria	Klymak, Jody	26-sept-15	01-oct-15
Leg 2	Kuang, Cheng	MSc Student	University of British Columbia	Soon, Maureen	10-juil-15	20-août-15
Leg 4a	Labeelle, Alex	High School Student	School on Board	ArcticNet	01-oct-15	11-oct-15
Leg 3a	Lafleur, Charlotte	BSc Student	Universtié Laval	Louis Fortier	20-août-15	04-sept-15
Leg 2	Lagunas, Jose Luis	Professional	Takuvik	Babin, Marcel	05-août-15	15-août-15
Leg 4b	Lagunas, Jose Luis	Professional	Takuvik	Babin, Marcel	11-oct-15	26-oct-15
Leg 4a	Lang, Carter	High School Student	School on Board	ArcticNet	01-oct-15	11-oct-15
Leg 2 - Leg 3a	Leblanc, Mathieu	MSc Student	Université Laval	Fortier, Louis	10-juil-15	04-sept-15
Leg 2	Lehmann, Nadine	PhD Student	Dalhousie University	Kienast, Markus	10-juil-15	20-août-15
Leg 1	Levesque, Keith	Research Manager	ArcticNet	Fortier, Martin	17-Apr-15	20-Apr-15

Leg 3a	Levesque, Keith	Chief Scientist	ArcticNet	Fortier, Martin	20-août-15	04-sept-15
Leg 2	Li, Jingxuan	MSc Student	University of British Columbia	Maldonado, Maite	10-juil-15	20-août-15
Leg 3b	Li, Jingxuan	MSc Student	University of British Columbia	Maldonado, Maite	04-sept-15	01-oct-15
Leg 3a	Lim, Rangyn	Professional	Kavik-Stantec	Beckett, Janine	20-août-15	04-sept-15
Leg 2	Linkowski, Thomas	Professional	ArcticNet	Levesque, Keith	10-juil-15	20-août-15
Leg 4a - Leg 4c	Linkowski, Thomas	Professional	ArcticNet	Levesque, Keith	01-oct-15	01-nov-15
Leg 2	Lizotte, Martine	Research Staff	Université Laval	Levasseur, Maurice	10-juil-15	20-août-15
Leg 4b	Lockhart, Peter	Professional	Canadian Scientific Submersible Facility	CSSF	11-oct-15	26-oct-15
Leg 2	Lovejoy, Connie	Researcher/Professor	Université Laval	Lovejoy, Connie	05-août-15	15-août-15
Leg 3a	Lucas, Trevor	Professional	Kavik-Stantec	Beckett, Janine	20-août-15	04-sept-15
Leg 1	Lundy, Jim	Field Service Technician	Rutter Inc	Rutter Inc	17-Apr-15	4-May-15
Leg 4a - Leg 4b	Luque, Sebastian	Research Staff	University of Manitoba - CEOS	Papakyriakou, Tim	01-oct-15	26-oct-15
Leg 1	MacTavish, Bruce	Marine Observer	LGL	LGL	20-Apr-15	4-May-15
Leg 1	McCullough, Greg	Sea Ice Research Associate	University of Manitoba	Barber, Dave	17-Apr-15	4-May-15
Leg 4a	McCullum, Elizabeth	High School Student	School on Board	ArcticNet	01-oct-15	11-oct-15
Leg 1	McKeever, Thomas Jonathai	Statoil Project Manager / Party Chief	Statoil Canada	Statoil	17-Apr-15	4-May-15
Leg 1	Meadus, Chris	Ice Properties Researcher	National Research Council		17-Apr-15	4-May-15
Leg 1	Meredyk, Shawn	Mooring Professional	ArcticNet	Levesque, Keith	17-Apr-15	4-May-15
Leg 3a	Meredyk, Shawn	Professional	ArcticNet	Levesque, Keith	20-août-15	04-sept-15
Leg 3b	Meredyk, Shawn	Professional	ArcticNet	Levesque, Keith	19-sept-15	01-oct-15
Leg 1	Michaud, Luc	Mooring Professional	ArcticNet	Levesque, Keith	17-Apr-15	4-May-15
Leg 3a	Michaud, Luc	Professional	ArcticNet	Levesque, Keith	20-août-15	04-sept-15
Leg 3a - Leg 3b	Mireault, Callum	Professional	ArcticNet	Levesque, Keith	20-août-15	01-oct-15
Leg 2 - Leg 3b	Mol, Jacoba	MSc Student	Dalhousie University	Helmuth Thomas / Papakyriakou, Tim	10-juil-15	01-oct-15
Leg 3a	Montoya, Oscar	MSc Student	University of Calgary	Hubert, Casey	20-août-15	04-sept-15
Leg 1	Morisset, Simon	Ocean instrumentation Tech/CTD Op	ArcticNet	Levesque, Keith	17-Apr-15	20-Apr-15
Leg 3a - Leg 3b	Morisset, Simon	Professional	ArcticNet	Levesque, Keith	20-août-15	01-oct-15
Leg 1	Mueller, Derek	Iceberg Drift Researcher	Carleton University	Mueller, Derek	17-Apr-15	4-May-15
Leg 2	Munson, Kathleen	Postdoctoral Fellow	University of Manitoba - CEOS	Wang, Feiyue	10-juil-15	23-juil-15
Leg 4b	Murphy, Robert	Professional	Geological Survey of Canada	Bennett, Robbie	11-oct-15	26-oct-15
Leg 3a	Nadaï, Gabrielle	BSc Student	Université Laval	Louis Fortier	20-août-15	04-sept-15
Leg 1	Nistad, Jean-Guy	Multibeam Surveyor/MVP	Université Laval	Lajeunesse, Patrick	17-Apr-15	4-May-15
Leg 3b	Nixon, Richard	MSc Student	University of Victoria	Ross, Andrew	04-sept-15	01-oct-15
Leg 3a - Leg 3b	Noël, Amy	MSc Student	University of Calgary	Hubert, Casey	20-août-15	01-oct-15
Leg 2	Noël, Laura	BSc Student	Institut des Sciences de la Mer - UQAR	Xie, Huixiang	10-juil-15	20-août-15
Leg 4a - Leg 4c	Noël, Laura	BSc Student	Institut des Sciences de la Mer - UQAR	Xie, Huixiang	01-oct-15	01-nov-15
Leg 3a	Nozais, Christian	Researcher/Professor	UQAR	Nozais, Christian	20-août-15	04-sept-15
Leg 4b	Olivier, Frédéric	Researcher/Professor	Museum d'Histoire Naturelle de Paris	Archambault, Philippe	11-oct-15	26-oct-15

Leg 3b	Orians, Kristin	Researcher/Professor	University of British Columbia	Orians, Kristin	04-sept-15	01-oct-15
Leg 4a	Osted, Grace	High School Student	School on Board	ArcticNet	01-oct-15	11-oct-15
Leg 3b	Pangun, Preston	Professional	ArcticNet	Levesque, Keith	19-sept-15	01-oct-15
Leg 3b - Leg 4c	Parenteau, Marie	Research Staff	Université Laval	Fortier, Louis	04-sept-15	01-nov-15
Leg 4c	Peck, Liam	Professional	Environment Canada	Gjerdrum, Carina	26-oct-15	01-nov-15
Leg 3a	Pelletier-Rousseau, Michèle	Research Staff	ISMER/UQAR	Gosselin, Michel	20-août-15	04-sept-15
Leg 4a	Perkins, Zoe	High School Student	School on Board	ArcticNet	01-oct-15	11-oct-15
Leg 1	Pind, Meredith	Ice Survey Specialist trainee	Canadian Ice Service	Vaillant, Eric	17-Apr-15	4-May-15
Leg 1	Pritchett, Robert	Sea Ice Research Associate	CARD	CARD	20-Apr-15	4-May-15
Leg 3b	Provost, Roger	Professional	Canadian Ice Service	Vaillant, Eric	04-sept-15	01-oct-15
Leg 3b	Purdon, Kathryn	BSc Student	University of Victoria	Cullen, Jay	04-sept-15	01-oct-15
Leg 3a	Robertson, Angus	Research Staff	Geological Survey of Canada	King, Edward	20-août-15	04-sept-15
Leg 1	Roth, Jens Christian	Statoil WP1 Researcher	Statoil ASA	Statoil	17-Apr-15	4-May-15
Leg 3b	Sabourin, Clément	Media/Artist	Agence France-Presse	Sabourin, Clément	19-sept-15	01-oct-15
Leg 4a	Saumier, Sonia	Professional	School on Board	ArcticNet	01-oct-15	11-oct-15
Leg 3b	Sauve, Daniel	MSc Student	University of Ottawa	Cornett, J and Smith, J	04-sept-15	01-oct-15
Leg 3a	Scheifele, Benjamin	PhD Student	University of British Columbia	Waterman, Stephanie	20-août-15	04-sept-15
Leg 2	Schuback, Nina	PhD Student	University of British Columbia	Tortell, Philippe	10-juil-15	20-août-15
Leg 1	Scibilia, Francesco	Statoil WP2 Lead	Statoil ASA	Statoil	17-Apr-15	4-May-15
Leg 2	Seaton, Cris	Professional	ArcticNet	Levesque, Keith	10-juil-15	20-août-15
Leg 2	Semienuk, David	Postdoctoral Fellow	University of British Columbia	Maldonado, Maite	10-juil-15	20-août-15
Leg 4b	Snelgrove, Paul	Researcher/Professor	Memorial University	Snelgrove, Paul	11-oct-15	26-oct-15
Leg 2	Soon, Maureen	Researcher/Professor	University of British Columbia	François, Roger	10-juil-15	20-août-15
Leg 3b	Soon, Maureen	Professional	University of British Columbia	Francois, Roger	04-sept-15	01-oct-15
Leg 4a - Leg 4c	Steinhart, Rebecca	PhD Student	Memorial University	Snelgrove, Paul	01-oct-15	01-nov-15
Leg 3b	Sun, Xiaoxu	PhD Student	Georgia Tech	Hubert, Casey	04-sept-15	01-oct-15
Leg 1	Teigen, Sigurd	Statoil WP1 Lead: Mooring specialist	Statoil ASA	Statoil	17-Apr-15	4-May-15
Leg 3a - Leg 3b	Theriault, Nathalie	Research Staff	University of Manitoba	Barber, David	20-août-15	01-oct-15
Leg 2	Thomas, Helmuth	Researcher/Professor	Dalhousie University	Thomas, Helmuth	05-août-15	20-août-15
Leg 2	Timmerman, Amanda	PhD Student	University of Victoria	Hamme, Roberta	10-juil-15	20-août-15
Leg 2	Toldi, Glenn	Professional	Canadian Hydrographic Service	Youngblut, Scott	10-juil-15	20-août-15
Leg 2	Tortell, Philippe	Researcher/Professor	University of British Columbia	Tortell, Philippe	10-juil-15	20-août-15
Leg 1	Trottier, Annie-Pier	Multibeam Surveyor/Iceberg work	Université Laval	Lajeunesse, Patrick	17-Apr-15	4-May-15
Leg 1	Turnbull, Ian David	Sea Ice Research Associate	CARD	CARD	20-Apr-15	4-May-15
Leg 4b - Leg 4c	Verhoeven, Joost	PhD Student	Memorial University	Dufour, Suzanne	11-oct-15	01-nov-15
Leg 2	Wang, Kang	PhD Student	University of Manitoba	Wang, Feiyue	10-juil-15	20-août-15
Leg 3b	Wang, Kang	PhD Student	University of Manitoba - CEOS	Wang, Feiyue	04-sept-15	01-oct-15
Leg 4b - Leg 4c	Wareham, Vonda	Professional	Department of Fisheries and Oceans	Gilkinson, Kent	11-oct-15	01-nov-15

Leg 4a	Warkentin, Tara	High School Student	School on Board	ArcticNet
Leg 1	Warner, Kerri	Sea Ice Research Associate	University of Manitoba	Barber, Dave
Leg 4a	Watts, Michelle	Professional	School on Board	ArcticNet
Leg 1	Wollvik, Roy	Statoil HSE Lead	Statoil ASA	Statoil
Leg 2 - Leg 3a	Xu, Wen	MSc Student	University of Manitoba - CEOS	Wang, Feiyue
Leg 3b	Yu, Heidi	Professional	Canadian Hydrographic Service	Youngblut, Scott
Leg 4a - Leg 4c	Zier, Juergen	Professional	ArcticNet	Levesque, Keith

01-oct-15	11-oct-15
17-Apr-15	4-May-15
01-oct-15	11-oct-15
17-Apr-15	4-May-15
05-août-15	04-sept-15
04-sept-15	01-oct-15
01-oct-15	01-nov-15